

Table of Contents.

Summary.....	viii
Declaration.....	xi
Acknowledgements.....	xii
Publications arising from this thesis.....	xiv
Activated Immune Cells: 1H-NMR Spectroscopy and Flow Cytometry Studies	xv
List of Figures.....	xvi
List of Tables.....	xx
List of Abbreviations.....	xxi
Chapter 1..... Margaret Fiona Veale, B.Sc.(Hons.)	1
General Introduction.....	1
1.1. Introduction to the immune response.....	1
1.1.1. Innate immunity.....	3
1.1.2. Acquired immunity.....	4
1.2. Cells and tissues of the immune system.....	5
1.2.1. T cells.....	5
1.2.2. B cells.....	9
1.2.3. Monocytes/Macrophages.....	10
1.2.4. Dendritic cells.....	10
A Thesis submitted for the Degree of Doctor of Philosophy	11
1.3. Immune cell activation.....	14
1.3.1. T cell activation.....	15
1.4. Molecular aspects of the immune system. I. Cell surface receptors.....	15
1.4.1. The T cell receptor complex.....	16
1.4.2. Major Histocompatibility Complex (MHC II).....	18
1.4.3. CD28.....	21
1.4.4. CD44.....	21
1.4.5. LFA-1.....	22
1.4.6. CD45 isoforms.....	22
1.4.7. Complement Receptor type 2 (CD21).....	22
1.4.8. 175 antigen.....	23
1.5. Molecular aspects of the immune system. II. Protein kinase C isoenzymes in T cell activation.....	23
1.5.1. The diversity of protein kinase C isoenzymes.....	24
1.5.2. Differential expression of protein kinase C isoenzymes in T lymphocyte activation.....	24
1.6. Molecular aspects of the immune system. III. Lipid structure and metabolism.....	26

October, 1996

Table of Contents

Summary	1
Declaration	2
Acknowledgements	3
Introduction	4
Activated Immune Cells: ¹H-NMR Spectroscopy and Flow Cytometry Studies	
1.1 Introduction	5
1.2 Objectives	6

Margaret Fiona Veale, B.Sc.(Hons.)

I dedicate this thesis to Greg for his love and unending support throughout these studies,

to the memory of Nathan, always in search of the answers to the questions of life,

and to Andrew, Shelley, Hamish, Ross, David, Racquelle, Dhenai and Sarah.

Department of Pathology,
Faculty of Medicine,
The University of Sydney

October, 1996

Table of Contents.

Summary.....	viii
Declaration.....	xi
Acknowledgements.....	xii
Publications arising from this Thesis.....	xiv
Publications arising from previous research.....	xvi
List of Figures.....	xvii
List of Tables.....	xx
List of Abbreviations.....	xxi
Chapter 1.....	1
General Introduction.....	1
1.1. Introduction to the immune response.....	1
1.1.1. Innate immunity.....	3
1.1.2. Acquired immunity.....	4
1.2. Cells and tissues of the immune system.....	5
1.2.1. T cells.....	5
1.2.2. B cells.....	9
1.2.3. Monocytes/Macrophages.....	10
1.2.4. Dendritic cells.....	10
1.2.5. Immune cell recirculation.....	11
1.3. Immune cell activation.....	14
1.3.1. T cell activation.....	15
1.4. Molecular aspects of the immune system. I. Cell surface receptors.....	15
1.4.1. The T cell receptor-CD3 (TCR/CD3) complex.....	16
1.4.2. Major Histocompatibility Complex II (MHC II).....	18
1.4.3. CD2.....	21
1.4.4. CD44.....	21
1.4.5. LFA-1.....	22
1.4.6. CD45 isoforms.....	22
1.4.7. Complement Receptor type 2 (CD21).....	22
1.4.8. 175 antigen.....	23
1.5. Molecular aspects of the immune system. II. Protein kinase C isoenzymes in T cell activation.....	23
1.5.1. The diversity of protein kinase C isoenzymes.....	24
1.5.2. Differential expression of protein kinase C isoenzymes in T lymphocyte activation.....	24
1.6. Molecular aspects of the immune system. III. Lipid structure and metabolism.....	26

Chapter 2	1.6.1. Lipid structural arrangements.....	28
Materials and Methods	1.6.2. Fatty acids.....	28
2.1. Isolation and culture of splenic T cells	1.6.3. Triglycerides and diacylglycerols.	29
	1.6.4. Phospholipids.	29
	1.6.5. Sterols.	34
	1.6.6. Diacylglycerol and triglyceride biosynthesis.....	34
	1.6.7. Phospholipid biosynthesis.....	35
	1.6.8. The Effects of phospholipid-derived metabolites on protein kinase C in T cell activation.	37
2.2. Hydrolysis of phospholipids	1.6.9. The effects of metabolites of phospholipase C, D and A ₂ activity in immune cell activation.	39
2.3. Triclyclodecan-9-yl-xanthogenate (D609)	1.6.10. PC-specific phospholipase C inhibition using the xanthate triclyclodecan-9-yl-xanthogenate (D609).....	41
2.5. Phospholipid metabolism	1.7. NMR studies of phospholipid metabolism and mobile lipids in cells.	42
	1.7.1. NMR studies of phospholipid metabolism in cells.....	43
	1.7.2. ¹ H-NMR studies of mobile lipids in cells.	47
	1.7.3. ¹ H-NMR for the detection of mobile lipid in activated immune cells.	49
2.6. NMR analysis of mobile lipids	1.8. Previously proposed models for the role and origin of ¹ H-NMR-detectable mobile lipids.	54
	1.8.1. Lipoproteins in the membrane.....	54
	1.8.2. Membrane fluidity.....	55
	1.8.3. Summary of previous models.	56
	1.9. A new model for the origin and function of mobile lipid: relationship between mobile lipid, phosphatidylcholine metabolism and the cell cycle.....	56
	1.9.1. Overview of the cell cycle.....	57
	1.9.2. Relationship between phosphatidylcholine metabolism and the cell cycle.....	58
	1.9.3. Regulation of phosphatidylcholine in the cell cycle.....	58
	1.9.4. The generation of mobile lipid in G ₀ /G ₁ of the cell cycle.....	62
	1.9.5. The importance of PC catabolism for cell cycle progression.....	62
	1.9.6. Summary.....	64
	1.10. NMR evidence supporting the proposed model: the effect of the extracellular environment on cell cycle status and its relationship to mobile lipid.	64
Chapter 3	1.10.1. Growth factor and cytokine effects.....	64
Comparative NMR analysis	1.10.2. Cell adhesion effects.	68
3.1. In vitro analysis of splenic T cells for	1.10.3. Serum factor effects.....	70
3.2. Receptor regulation	1.10.4. Contributions by lipoprotein receptor regulation to mobile lipid.	71
	1.10.5. Summary.....	73
	1.11. Concluding remarks.	73
	3.2.4. ¹ H-NMR analysis of isolated splenic T cells.....	107

Chapter 2	75
Materials and Methods	75
2.1. Isolation of splenic and thymic T lymphocytes.....	75
2.1.1. Animals.....	75
2.1.2. Materials for cell culture.....	75
2.1.3. Isolation of splenocytes and thymocytes.....	75
2.1.4. Separation of splenic T cells.....	77
2.1.5. Culture conditions for thymic and splenic T cells.....	84
2.2. Hybridoma cell culture.....	85
2.2.1. Maintenance of cell cultures.....	85
2.2.2. Cryopreservation of hybridoma cell lines.....	85
2.3. Tritiated thymidine assays.....	85
2.4. Measurement of cell diameter.....	86
2.5. Flow cytometric analysis.....	86
2.5.1. Antibodies.....	86
2.5.2. Flow cytometry labelling procedure.....	86
2.6. NMR spectroscopy.....	87
2.6.1. NMR materials.....	87
2.6.2. Cell preparation for NMR analysis.....	87
2.6.3. ¹ H-NMR spectroscopy.....	89
2.6.4. Calculation of mobile lipid concentrations.....	90
2.7. Sheep studies.....	92
2.7.1. Animals.....	92
2.7.2. Surgery and lymph collection.....	92
2.7.3. Immunisations and antigen challenge.....	95
2.7.4. Lymph node cell preparation.....	95
2.7.5. Monoclonal antibodies for flow cytometry.....	95
2.7.6. Immunofluorescence staining and flow cytometry.....	95
2.7.7. Preparation of the afferent and efferent cells for NMR analysis.....	97
2.7.8. ¹ H-NMR analysis of sheep lymph and lymph node cells.....	97
Chapter 3	98
Comparative methods for large scale isolation of splenic T cells for NMR analysis	98
3.1. Introduction.....	98
3.2. Results.....	99
3.2.1. Characterisation of the purified sheep α mouse antibody.....	99
3.2.2. Flow cytometric analysis of splenic T cell fractions using nylon wool and SRBC-S α Mi γ separation procedures.....	101
3.2.3. Proliferation of isolated splenic T cells.....	107
3.2.4. ¹ H-NMR analysis of isolated splenic T cells.....	107

3.3. Discussion.....	110
Chapter 4.....	112
¹H-NMR-visible mobile lipids in activated splenic and thymic T lymphocytes: relationship to phosphatidylcholine cycling.....	112
4.1. Introduction.....	112
4.2. Results.....	113
4.2.1. Flow cytometric histogram analysis of separated splenic T cells.....	113
4.2.2. Proliferation of separated splenic T cells.....	116
4.2.3. Proliferation of splenic and thymic T cells in response to PMA and ionomycin.....	116
4.2.4. 1D ¹ H-NMR spectra of activated thymic T cells.....	119
4.2.5. 2D ¹ H-NMR spectra of activated splenic T cells.....	119
4.2.6. Changes in mobile lipid, PCCho, Cho, and GPC during activation of thymic and splenic T cells.....	122
4.2.7. Changes in cell size during T cell activation.....	122
4.3. Discussion.....	125
Chapter 5.....	131
The role of phosphatidylcholine-specific phospholipase C in the generation of mobile lipid in T cells.....	131
5.1. Introduction.....	131
5.2 Results.....	134
5.2.1 FCM histogram analysis of IL-2R α expression in stimulated thymocytes.....	134
5.2.2. FCM histogram analysis of Thy 1.2 expression in stimulated thymocytes.....	135
5.2.3. Proliferation of treated thymocytes.....	139
5.2.4. 1D ¹ H-NMR spectra of treated thymocytes.....	142
5.2.5. 2D COSY ¹ H-NMR spectra of treated thymocytes.....	142
5.2.6. Inhibition of splenocyte proliferation using the inhibitor D609.....	147
5.2.7. Viability of thymocytes and splenocytes incubated with the inhibitor D609.....	149
5.2.8. ¹ H-NMR analysis of thymocytes and splenocytes incubated with the inhibitor D609 and α CD3.....	149
5.2.9. Summary of results.....	156
5.3. Discussion.....	158
5.3.1. Relationship between cell surface antigen expression and immune cell activation status.....	158
5.3.2. The role of the PC cycle in the generation of the mobile lipid spectrum and its relationship to signalling in T lymphocytes.....	160
5.3.3. Inhibition of the PC-specific PLC with D609.....	162
5.3.4. Conclusions.....	165

Chapter 6	166
¹H-NMR and FCM studies of immune cell activation in an in vivo sheep model	166
6.1. Introduction.....	166
6.2. Results.....	169
6.2.1. Total cells collected per hour from afferent and efferent vessels of immunised prefemoral lymph nodes.....	169
6.2.2. Afferent input and efferent output per hour of T cells through prefemoral lymph nodes of antigen-challenged sheep.....	171
6.2.3. Cell surface expression of the adhesion molecules CD2, CD44 and LFA-1, and of CD45R, prior to antigen challenge.....	177
6.2.4. Cell surface expression of the adhesion molecules CD2, CD44 and LFA-1, and of CD45R, after antigen challenge.....	181
6.2.5. The expression of Major Histocompatibility Complex Class II (MHC II).....	188
6.2.6. Expression of CD21, a B cell surface receptor.....	190
6.2.7. Expression of the surface antigen detected using 175 MAb.....	195
6.2.8. ¹ H-NMR studies of isolated immune cells.....	197
6.2.9. Summary of results.....	208
6.3. Discussion.....	213
6.3.1. Total cell output and input through an antigen-challenged lymph node.....	214
6.3.2. Recirculation of T cells through lymph node before and after antigen challenge.....	215
6.3.3. Differential cell surface expression of CD2, CD44, CD45R and LFA-1 in afferent and efferent lymph vessels and lymph node, before and after antigen challenge.....	216
6.3.4. ¹ H-NMR studies of lymph nodes and afferent and efferent lymph.....	223
6.3.5. Conclusions.....	225
Chapter 7	227
General Discussion	227
7.1. Mobile lipid in activated immune cells.....	228
7.2. Model for the origin of mobile lipid in activated immune cells.....	235
References	237
Appendix 1	A1
The theory of nuclear magnetic resonance (NMR) spectroscopy	A1
A1.1. Introduction.....	A1
A1.2. Theory of Fourier transform NMR spectroscopy.....	A3
A1.3. The NMR spectrum.....	A7
A1.4. Two-dimensional NMR spectroscopy.....	A9
A1.5. Water suppression.....	A12

Appendix 2.....	A14
The theory of flow cytometry.....	A14
A2.1. Introduction.....	A14
A2.2. The flow cytometer.....	A15
A2.3. Light scatter.....	A15
A2.4. Fluorescence.....	A17
A2.5. Quantitation using flow cytometry.....	A17

NMR-visible) mobile lipid. An increase in the level of mobile lipid compared with that seen in resting cells has been observed in a variety of activated immune cells. The appearance of the mobile lipid is associated with activation and can be induced by a variety of stimuli. However, the origin and function of the neutral lipid resonances in ¹H-NMR spectra of activated immune and other cell types has been unresolved. I propose that the mobile lipids arise from phosphatidylcholine (PC) cycling.

Two-dimensional ¹H-NMR spectroscopy was used to compare changes in the concentration of isotropically-tumbling neutral lipid during the activation of splenic and thymic T cells. Splenic T cells were isolated from the mouse spleen using a two-step purification procedure. The concentration of mobile lipid was similar in splenic and thymic T cells after 72 h of activation using the calcium ionophore, ionomycin and the phorbol ester, phorbol myristate acetate (PMA). However, after 120 h of activation, mobile lipid concentrations in splenic T cells were more than 3-fold higher than in thymic T cells. An increase in choline (Cho), phosphocholine (PCho), and glycerophosphocholine (GPC) levels was also observed in both thymic and splenic T cells after 24 h of activation. However after 72 h of stimulation, Cho and PCho levels had decreased and continued to decline at 96-120 h, while GPC continued to be maintained at elevated levels. The simultaneous increase in mobile lipid and GPC and the decline in Cho and PCho leads us to propose that the synthesis of NMR-visible mobile lipid in activated lymphocytes is linked to the PC cycle.

The mobile lipid spectrum was investigated using different activation methods to stimulate murine T cells via different biochemical pathways. Stimulation was carried out via the CD3/TCR complex, using ionomycin and/or PMA. ¹H-NMR-detectable mobile lipid levels increased after treatment of thymocytes with PMA and ionomycin. These spectral experiments indicate that levels of mobile lipid were increased using ¹H-NMR.

Summary

Proton nuclear magnetic resonance ($^1\text{H-NMR}$) spectroscopy has been used to study immune cell activation. One-dimensional and two-dimensional $^1\text{H-NMR}$ spectra of activated immune cells are dominated by signals arising from elevated levels of isotropically tumbling (i.e., NMR-visible) mobile lipid. An increase in the level of mobile lipid compared with that seen in resting cells has been observed in a variety of activated immune cells. The appearance of the mobile lipid is associated with activation and can be induced by a variety of stimuli. However, the origin and function of the neutral lipid resonances in $^1\text{H-NMR}$ spectra of activated immune and other cell types has been unresolved. I propose that the mobile lipids arise from phosphatidylcholine (PC) cycling.

Two-dimensional $^1\text{H-NMR}$ spectroscopy was used to compare changes in the concentration of isotropically-tumbling neutral lipid during the activation of splenic and thymic T cells. Splenic T cells were isolated from the mouse spleen using a two-step purification procedure. The concentration of mobile lipid was similar in splenic and thymic T cells after 72 h of activation using the calcium ionophore, ionomycin and the phorbol ester, phorbol myristate acetate (PMA). However, after 120 h of activation, mobile lipid concentrations in splenic T cells were more than 3-fold higher than in thymic T cells. An increase in choline (Cho), phosphocholine (PCho), and glycerophosphocholine (GPC) levels was also observed in both thymic and splenic T cells after 24 h of activation. However after 72 h of stimulation, Cho and PCho levels had decreased and continued to decline at 96–120 h, while GPC continued to be maintained at elevated levels. The simultaneous increase in mobile lipid and GPC and the decline in Cho and PCho leads us to propose that the synthesis of NMR-visible mobile lipid in activated lymphocytes is linked to the PC cycle.

The mobile lipid spectrum was investigated using different activation methods to stimulate murine T cells via different biochemical pathways. Stimulation was carried out via the CD3/TCR complex, using ionomycin and/or PMA. $^1\text{H-NMR}$ -detectable mobile lipid levels increased after treatment of thymocytes with PMA and ionomycin. These spectral

changes were correlated with changes in IL-2 receptor (IL-2R α) expression detected using flow cytometry (FCM), and with proliferation detected using ^3H -thymidine incorporation, as indicators of the activation status. PMA and ionomycin in combination induced an increase in IL-2R α expression, thymocyte proliferation and a mobile lipid spectrum, consistent with full activation. PMA stimulation alone induced a small increase in IL-2R α expression and a mobile lipid signal. Ionomycin alone induced a smaller but significant increase in IL-2R α expression and a marginal mobile lipid spectrum. αCD3 induced no increase in IL-2R α expression but, in contrast, induced a distinct mobile lipid spectrum. No proliferation was found in thymocytes stimulated with any of PMA, ionomycin or αCD3 antibody alone.

D609, a PC-specific phospholipase C (PLC) inhibitor, was used to inhibit the mobile lipid spectrum in αCD3 -stimulated thymic T cells. This showed that the ^1H -NMR detectable mobile lipid can be generated in αCD3 -stimulated thymic T cells by the action of PC-specific PLC activity. However, an increased mobile lipid spectrum, associated with inhibition of ^3H -thymidine incorporation, was seen in αCD3 -stimulated splenocytes. This may have been due to the additional co-stimulation of the splenic lymphocytes from other accessory cells present in the splenocyte cell suspension. This could have resulted in the stimulation of receptor agonist-mediated phospholipase D and phospholipase A $_2$ activity, which may have resulted in the generation and accumulation of the mobile lipid despite the treatment of the splenocytes using D609.

Most previous studies of the mobile lipid spectrum in activated immune cells have been restricted to using isolated cells activated *in vitro*. Therefore, in this thesis *Bacillus-Calmette-Guerin*-primed (BCG-primed) sheep were used to monitor the immune response to subsequent antigen challenge with purified protein derivative (PPD) *in vivo*. The efferent and pseudoafferent lymphatic vessels of the prefemoral lymph node were cannulated. Lymph was collected for 0-4 days after antigen challenge and the cells isolated. Cells were also isolated from lymph nodes which were removed at day 1 and 3 after antigen challenge. The immune cells were analysed using FCM for cell surface markers using a panel of monoclonal antibodies. Levels of mobile lipid were monitored using ^1H -NMR.

The total input of cells/h via the afferent lymphatic vessel increases approximately 7-fold within the first 24 h after antigen challenge. This increase in the cellular input into the lymph node decreased between 48 and 72 h but remained above the pre-challenge level. The cell/h output via the efferent lymphatic vessel decreased initially after antigen-challenge and then increased from 24-72 h. An increase in T cell subsets, particularly CD4 and CD8, occurred in afferent and efferent lymph after antigen-challenge. Increases in the proportion of cells expressing other cell surface molecules were also observed, including Major Histocompatibility Complex II (MHC II) and Cluster of Differentiation 2 (CD2). $^1\text{H-NMR}$ studies on the isolated cells collected from afferent or efferent lymph did not show significant mobile lipid levels after challenge. However, mobile lipid levels were detectable in cells isolated from the lymph node at day 1 and 3 days post-challenge. These results suggest that the mobile lipid from immune cells *in vivo* may be detected at sites where cellular proliferation is occurring in response to antigen challenge.

This study strongly suggests that increases in levels of $^1\text{H-NMR}$ -detectable mobile lipid were closely related to the simultaneously observed changes in the choline and phosphocholine metabolites in these activated immune cells. The mobile lipid may result from phosphatidylcholine cycling in stimulated cells. The inhibition of the mobile lipid in αCD3 stimulated thymocytes using a PC-specific phospholipase C inhibitor demonstrates that the mobile lipid in these stimulated cells may arise from PC catabolism. The *in vivo* stimulation of lymph and lymph node cells from immunised and antigen challenged sheep showed that mobile lipids were only significantly present in isolated antigen-challenged lymph node cells. These results suggest that the mobile lipid is detectable in rapidly proliferating immune cells but not necessarily as a result of proliferation.

Acknowledgments.

Declaration

I would like to thank my Supervisor, Dr. Nicholas J.C. King, for his help and I, Margaret Fiona Veale, certify that this thesis does not include any material previously submitted for a degree or diploma in any University. Moreover, to the best of my knowledge it does not contain any material previously written or published by another person unless duly referenced.

This thesis describes original research work carried out in the Departments of Pathology and Biochemistry, University of Sydney, between November, 1992 and October 1996. The data presented in this thesis was obtained from experiments performed by myself unless otherwise acknowledged in the text.

I also acknowledge the financial support by way of a generous Postgraduate Scholarship and acknowledge the support of the University of Sydney Cancer Research Fund and the Leo and Jersey Leukemia and Cancer Foundation.

[Redaction]

Margaret Fiona Veale

31st October, 1996

Thanks also to all the people in Glenn King's laboratory, especially Andrew Dingley who helped me enormously and Keith Jervis for solving my computer problems.

Thank you to the staff in the Department of Pathology for their support, and a special thanks to Dr Jillian Kril and Dr Gheta Chaudhri.

I also acknowledge the staff of the Blackburn Animal House, especially Kelly O'Sullivan, and of the CSIRO McMaster Laboratory Animal House for their expert technical advice and support.

Thank you to Dr Susan McClure and Dr David Emery for their expertise and encouragement.

Acknowledgements.

I would like to thank my Supervisor, Dr. Nicholas J.C. King, for his help and enthusiasm during my studies, and my Associate Supervisor, Dr. Glenn F. King, for his assistance with the NMR spectroscopy and encouragement throughout this project. I also thank Professors Nicholas Hunt and Clive Harper for the opportunity to study in the Department of Pathology and for the use of the Departmental facilities throughout my studies. I am also grateful to Professor Philip Kuchel for the use of the NMR spectrometers and other facilities in the Department of Biochemistry. I thank Dr Bill Bubb for his expert assistance in the maintenance of the NMR spectrometers. I also acknowledge the Faculty of Medicine for their financial support by way of a generous Postgraduate Scholarship and acknowledge the support of the University of Sydney Cancer Research Fund and the Leo and Jenny Leukaemia and Cancer Foundation.

There are many people I would like to acknowledge all of the Postgraduates in Nicholas King's laboratory, Lina Tian, Jenny Bao, Li Wen, David Lu, and especially Linda Johnston for her help, support and friendship throughout. A special thanks to Ana Manthey and Wendy Crabb.

Thanks also to all the people in Glenn King's laboratory, especially Andrew Dingley who helped me enormously and Keith Junius for solving my computer problems.

Thank you to the staff in the Department of Pathology for their support, and a special thanks to Dr Jillian Kril and Dr Gheeta Chaudhri.

I also acknowledge the staff of the Blackburn Animal House, especially Kelly O'Sullivan, and of the CSIRO McMaster Laboratory Animal House for their expert technical advice and support.

Thank you to Dr Susan McClure and Dr David Emery for their expertise and encouragement.

Publications arising from this Thesis.

Thank you to all of my Postgraduate colleagues in the Department of Pathology, especially Isabelle Medana, Robert Pack, Alan Watts, Bill Huang, Sontaya Simasathiansophon, Latifu Sanni, Naili Ma, Lawrence Li, Jian Lin Yin, Jenny Harasty and David van Reyk, for their support and friendship. Thanks also to colleagues and friends Andrew Lucas, Liz Cooper, Rachel Cameron and Ray Chan.

I am also grateful to Dr David Liu and Dr Zehra Kaymakcalan who encouraged me in my PhD studies and for introducing me to the sticky world of adhesion. A special thanks to David for his continued career support. Also, thank you to Rhonda Holdsworth for introducing me to Immunology and for her continued support.

A very special thank you to Greg, for his inspiration, support, love, patience and encouragement throughout our life together.

Abstracts:

Veale, M.F., Dingley, A.J., King, G.F., & King, N.J.C. (1993). Membrane Changes in Nylon Wool-Isolated Splenic T Cells. *Journal of Leukocyte Biology Supplement*: 58.

Veale, M.F., Dingley, A.J., King, G.F., & King, N.J.C. (1993). Membrane Triglyceride Changes in Activated Thymocytes and Splenic T cells. *Journal of Leukocyte Biology Supplement*: 64.

Veale, M.F., Dingley, A.J., King, G.F. & King, N.J.C. (1994). Activation of thymic and splenic T cells: $^1\text{H-NMR}$ Studies. *Proceedings of The Australian Society for Medical Research (NSW), Scientific Meeting*.

Veale, M.F., Dingley, A.J., King, G.F. & King, N.J.C. (1994). Changes in Membrane Triglyceride Levels in Activated Thymic and Splenic T Cells. *Keystone Symposium, Biology of Physicochemical Interactions at the Cell Surface, Journal of Cellular Biochemistry, Supplement 18C*, 263.

Veale, M.F., Dingley, A.J., King, G.F. & King, N.J.C. (1994). Activation of thymic and splenic T cells: $^1\text{H-NMR}$ Studies. *Proceedings of The Australian Society for Medical Research (NSW), Scientific Meeting*.

Publications arising from this Thesis.

Veale, M.F., Dingley, A.J., King, G.F. & King, N.J.C. (1994). Activation of thymic and splenic T cells: $^1\text{H-NMR}$ Studies. *Proceedings of The Australian Society for Medical Research (NSW) Scientific Meeting*.

Refereed Papers:

Dingley, A.J., Veale, M.F., King, G.F., and King, N.J.C. (1994). Two-Dimensional $^1\text{H-NMR}$ studies of membrane changes during the activation of primary T lymphocytes. *Immunomethods* **4**, 127-138.

Veale, M.F., Dingley, A.J., King, G.F., and King, N.J.C. (1996). Neutral lipid synthesis and its relationship to phosphatidylcholine cycling: $^1\text{H-NMR}$ studies. *Biochimica et Biophysica Acta* **1303**, 215-221.

Veale, M.F., Dingley, A.J., Roberts, N., King, G.F. and King, N.J.C. (1995). $^1\text{H-NMR}$ Studies of Activated Immune Cells. *Proceedings of The Australian Society for Medical Research, 34th National Scientific Conference*.

Papers in Preparation:

Veale, M.F., Roberts, N.J., King, G.F., and King, N.J.C. (In preparation). The role of phosphatidylcholine-specific phospholipase C in the generation of the $^1\text{H-NMR}$ detectable mobile lipid.

Veale, M.F., McClure, S.J., Wilson, G.J., King, G.F., and King, N.J.C. (In preparation). Activation of sheep immune cells *in vivo*: $^1\text{H-NMR}$ and flow cytometry studies.

Dingley, A.J., Veale, M.F., King, N.J.C. and King, G.F. (In preparation). Metabolite changes in activated splenic and thymic T cells: $^1\text{H-NMR}$ studies.

Veale, M.F., Dingley, A.J., King, G.F. & King, N.J.C. (1996). The immune response after *in vivo* antigen challenge: $^1\text{H-NMR}$ and flow cytometry studies. *The University of Sydney Faculty of Medicine Second Faculty Research Conference, N.S.W. Abstract 112*.

Abstracts:

Veale, M.F., Dingley, A.J., King, G.F., & King, N.J.C. (1993). Membrane Changes in Nylon Wool-Isolated Splenic T Cells. *Journal of Leukocyte Biology Supplement*: 58.

Veale, M.F., Dingley, A.J., King, G.F., & King, N.J.C. (1993). Membrane Triglyceride Changes in Activated Thymocytes and Splenic T cells. *Journal of Leukocyte Biology Supplement*: 64.

Veale, M.F., Dingley, A.J., King, G.F. & King, N.J.C. (1994). Activation of thymic and splenic T cells: $^1\text{H-NMR}$ Studies. *Proceedings of The Australian Society for Medical Research (NSW), Scientific Meeting*.

Veale, M.F., Dingley, A.J., King, G.F. & King, N.J.C. (1994). Changes in Membrane Triglyceride Levels in Activated Thymic and Splenic T Cells. Keystone Symposium, Biology of Physicochemical Interactions at the Cell Surface. *Journal of Cellular Biochemistry, Supplement 18C*, 263.

Veale, M.F., Dingley, A.J., King, G.F. & King, N.J.C. (1994). Activation of thymic and splenic T cells: $^1\text{H-NMR}$ Studies. *Proceedings of The Australian Society for Medical Research (NSW), Scientific Meeting*.

Veale, M.F., Dingley, A.J., King, G. F. & King, N.J.C. (1994). Activation of thymic and splenic T cells: $^1\text{H-NMR}$ Studies. *Proceedings of The Australian Society for Medical Research (NSW), Scientific Meeting.*

Veale, M.F., Dingley, A.J., Roberts, N., King, G.F. and King, N.J.C. (1994). $^1\text{H-NMR}$ Studies of Immune Cell Activation. *Proceedings of the University of Sydney Faculty of Medicine Research Conference.*

Veale, M.F., N. Roberts & King, N.J.C. (1994). $^1\text{H-NMR}$ and Flow Cytometry Studies of Activated Thymocytes. *Proceedings of The Australian Society for Medical Research, 33rd National Scientific Conference.*

Veale, M.F., Dingley, A.J., Roberts, N., King, G.F. and King, N.J.C. (1995). $^1\text{H-NMR}$ and Flow Cytometry Studies of Activated Immune Cells. *Proceedings of The Australian Society for Medical Research, 34th National Scientific Conference.*

Veale, M.F., N. Roberts, King, G.F. & King, N.J.C. (1995). $^1\text{H-NMR}$ and Flow Cytometry Studies of Activated Thymocytes. *Proceedings of the 7th Federation of Asian and Oceanic Biochemistry and Molecular Biology Congress, 27.*

Veale, M.F., McClure, S.J., King, G.F. and King, N.J.C. (1996). Faculty conference (1996). Activation of immune cells *in vivo*: $^1\text{H-NMR}$ and flow cytometry studies. *First Congress of the Federation of Immunological Societies of Asia-Oceania, Adelaide, S.A. Abstract 62.*

Veale, M.F., McClure, S.J., King, G.F. and King, N.J.C. (1996). The immune response after *in vivo* antigen challenge: $^1\text{H-NMR}$ and flow cytometry studies. *The University of Sydney Faculty of Medicine Second Faculty Research Conference, Wollongong, N.S.W. Abstract 112.*

Holdsworth, R., Veale, M.F. & McGrath, K. (1985). Relative sensitivity of platelet bindable immunoglobulin assays for the detection of HLA antibodies. *Proceedings of the International Society of Haematology.*

Holdsworth, R., Veale, M.F. & McGrath, K. (1985). HLA antigens on platelets: a comparison of three methods of detection. *Proceedings of the Australian and South East Asian Tissue Typing Association Annual Scientific Meeting.*

McGrath, K., Bishop, J., Wolf, M., Holdsworth, R., Veale, M.F., De Luise, T., Matthews, J. & Whiteside, M. (1985). Aetiology of refractory platelet transfusions in marrow suppressive states. *Proceedings of the Haematology Society of Australia* 1, 10.

Veale, M.F. & Barr, I. (May, 1988). An improved bioassay for the detection of murine γ -interferon. *Proceedings of the Australian Society for Microbiology.*

Veale, M.F., Holdsworth, R., Cunningham, I., Langley, J., McGrath, K. & Clarke, S. (1985). HLA and platelet crossmatching for platelet transfusions. *Proceedings of the Australian and South East Asian Tissue Typing Association Annual Scientific Meeting.*

Publications arising from previous research.

Refereed Papers :

Bishop, J.F., McGrath, K., Wolf, M.M., Mathews, J.P., De Luise, T., Holdsworth, R., Yuen, K., **Veale, M.**, Whiteside, M.G., Cooper, I.A. & Szer, J. (1988). Clinical factors influencing the efficacy of pooled platelet transfusions. *Blood* **71**, 383-7.

Coulepis, A.G., **Veale, M.F.**, MacGregor, A., Kornitschuk, M. & Gust, I.D. (1985). Detection of Hepatitis A virus and antibody by solid phase radioimmunoassay and enzyme-linked immunosorbent assay with monoclonal antibodies. *Journal of Clinical Microbiology* **22**, 119-24.

McGrath, K., Holdsworth, R., **Veale, M.F.**, Bishop, J. & Wolf, M. (1988). Detection of HLA antibodies by platelet crossmatching techniques. *Transfusion* **28**, 214-6.

McGrath, K., Wolf, M., Bishop, J., **Veale, M.**, Ayberk, H., Szer, J., Cooper, I. & Whiteside, M. (1988). Transient platelet and HLA antibody formation in multitransfused patients with malignancy. *British Journal of Haematology* **68**, 345-50.

Abstracts:

Bishop, J.F., McGrath, K., Wolf, M., Matthews, J., De Luise, T., Holdsworth, R., **Veale, M.F.**, Yuen, K. & Szer, J. (1985). Clinical factors influencing increments following pooled platelet transfusions from random donors. *Proceedings of the International Society of Haematology*.

Holdsworth, R., **Veale, M.F.** & McGrath, K. (1985). Relative sensitivity of platelet bindable immunoglobulin assays for the detection of HLA antibodies. *Proceedings of the International Society of Haematology*.

Holdsworth, R., **Veale, M.F.** & McGrath, K. (1985). HLA antigens on platelets: a comparison of three methods of detection. *Proceedings of the Australian and South East Asian Tissue Typing Association Annual Scientific Meeting*.

McGrath, K., Bishop, J., Wolf, M., Holdsworth, R., **Veale, M.F.**, De Luise, T., Matthews, J. & Whiteside, M. (1985). Aetiology of refractory platelet transfusions in marrow suppressive states. *Proceedings of the Haematology Society of Australia* **1**, 10.

Veale, M.F. & Barr, I. (May, 1988). An improved bioassay for the detection of murine γ -interferon. *Proceedings of the Australian Society for Microbiology*.

Veale, M.F., Holdsworth, R., Cunningham, I., Langley, J., McGrath, K. & Clarke, S. (1985). HLA and platelet crossmatching for platelet transfusions. *Proceedings of the Australian and South East Asian Tissue Typing Association Annual Scientific Meeting*.

Figure 3.5.	Stimulation to proliferation of splenic T cells with Con A and α CD3.....	106
Figure 3.6.	One-Dimensional NMR spectra of SRBC-S α MIg-separated T cells and nylon wool-separated T cells.....	108
List of Figures.		
Figure 1.1.	The role of lymphocytes in cellular and humoral immunity.....	2
Figure 1.2.	Maturation of lymphocytes.	6
Figure 1.3.	Systemic pathway of lymphocyte recirculation.....	12
Figure 1.4.	Pathway of lymphocyte recirculation through the lymph node.....	13
Figure 1.5.	CD4 T cell receptor and CD3 complex.	17
Figure 1.6.	T lymphocyte receptor for antigen.	19
Figure 1.7.	T lymphocyte receptors involved in T cell activation via interactions with cytokines and accessory cell receptors.	20
Figure 1.8.	Model for the T cell receptor/CD3 induced signal transduction pathways in the plasma membrane.....	27
Figure 1.9.	The arrangements of phospholipids within the cell membrane and some typical phospholipid structures.....	31
Figure 1.10.	Phospholipids with different alcohol headgroups.....	33
Figure 1.11.	The sites of action of different phospholipase isoenzymes upon phosphatidylcholine.	36
Figure 1.12.	Interactions among lipid biosynthetic pathways.....	38
Figure 1.13.	1D 1 H-NMR spectra of PMA- and ionomycin-stimulated thymocytes at various times after activation (lower three spectra) and of rat adenocarcinoma cells (upper spectrum).	50
Figure 1.14.	Aspects of the cell cycle.....	59
Figure 1.15.	The cell cycle and its relationship to phosphatidylcholine cycling.	61
Figure 2.1.	Anatomy of the mouse, showing the location of the spleen and thymus.	76
Figure 2.2.	Procedure for isolation and culture of thymic and splenic T cells.....	78
Figure 2.3.	Procedures for separation of splenic T cells using nylon wool column.	79
Figure 2.4.	Procedures for separation of splenic T cells using sheep α mouse Ig-coupled sheep red blood cell adherence technique.....	83
Figure 2.5.	Representative FCM dot plots and resultant histograms.	88
Figure 2.6.	Two-Dimensional 1 H-NMR spectrum of thymic T cells 72 h after activation with PMA and ionomycin.....	91
Figure 2.7.	The sheep lymphatic system.....	93
Figure 2.8.	The cannulation of the sheep lymph nodes.	94
Figure 3.1.	Sodium dodecyl sulphate polyacrylamide gel electrophoresis of purified sheep α mouse Ig.....	100
Figure 3.2.	Ouchterlony plate diffusion of sheep amouse antibody.	102
Figure 3.3.	Flow cytometric histogram analysis of SRBC-S α MIg-separated and nylon wool-separated splenic T cells.	104
Figure 3.4.	Summary of flow cytometric analysis of SRBC-S α MIg and nylon wool separated splenic T cells.....	105

Figure 3.5.	Stimulation to proliferation of splenic T cells with Con A and α CD3.....	106
Figure 3.6.	One-Dimensional and Two-Dimensional $^1\text{H-NMR}$ spectra of SRBC- α MiG-separated T cells and nylon wool-separated T cells.....	108
Figure 4.1.	The relationship between neutral lipid synthesis and the PC cycle.....	114
Figure 4.2.	FCM analysis of separated splenic T cells.	115
Figure 4.3.	Proliferation of separated splenic T cells and unseparated splenocytes.	117
Figure 4.4.	Determination of optimal stimulating doses of PMA and ionomycin for thymic and splenic T cells.	118
Figure 4.5.	One-Dimensional $^1\text{H-NMR}$ spectra of cultured thymic T lymphocytes at various stages after the onset of activation with PMA and ionomycin.....	120
Figure 4.6.	Two-Dimensional $^1\text{H-NMR}$ COSY spectrum of splenic T lymphocytes after 120 h of stimulation with PMA/ionomycin.	121
Figure 4.7.	The relative changes in phosphatidylcholine metabolites and mobile lipid in activated splenic and thymic T lymphocytes.....	123
Figure 5.1.	Phosphatidylcholine cycling and its relationship to cellular signalling.....	133
Figure 5.2.	Flow cytometric histogram analysis of IL-2R α expression on murine thymocytes.....	136
Figure 5.3.	FCM histogram analysis of IL-2R α expression of thymocytes treated as described for 18-24 h.....	137
Figure 5.4.	Representative FCM histogram analysis of Thy 1.2 expression in thymocytes treated as described for 18-24 h.....	138
Figure 5.5.	FCM analysis of Thy 1.2 expression in thymocytes treated as described for 18-24 h.....	140
Figure 5.6.	One-dimensional $^1\text{H-NMR}$ spectra from control thymocytes and splenocytes, and α CD3-stimulated thymocytes.	143
Figure 5.7.	Symmetrised 2D COSY spectra of thymocytes treated for 18-24 h with different stimulating agents.	144
Figure 5.8.	Proliferation of spleen cells stimulated with α CD3 for 72 h in the presence of increasing doses of the inhibitor D609.....	148
Figure 5.9.	The effect of inhibitor D609 on proliferation of splenocytes stimulated using α CD3.....	150
Figure 5.10.	Cell viability of cultured thymocytes and splenocytes after α CD3 and D609 treatment.	151
Figure 5.11.	1D $^1\text{H-NMR}$ spectra of thymocytes showing effects of D609 on α CD3-stimulation.....	152
Figure 5.12.	1D $^1\text{H-NMR}$ spectra of splenocytes showing effects of D609 on α CD3-stimulation.....	153
Figure 5.13.	2D $^1\text{H-NMR}$ spectra of thymocytes showing effects of D609 on α CD3-stimulation.....	154
Figure 5.14.	2D $^1\text{H-NMR}$ spectra of splenocytes showing effects of D609 on α CD3-stimulation.....	155
Figure 6.1.	Total cell output from the afferent and efferent lymph of antigen-challenged sheep.....	170

Figure 6.2.	Changes in T cell subsets in afferent and efferent lymph and lymph node after antigen challenge.	172
Figure 6.3.	FCM analysis of CD2, CD44, CD45R and LFA-1 expression.	179
Figure 6.4.	Isotype control staining for sheep T lymphocyte surface antigens.	182
Figure 6.5.	CD2 expression on afferent and efferent lymph and lymph node cells.	183
Figure 6.6.	CD44 expression on sheep afferent and efferent lymph and lymph node cells.	184
Figure 6.7.	CD45R expression on sheep afferent and efferent lymph and lymph node cells.	185
Figure 6.8.	LFA-1 expression on sheep afferent and efferent lymph and lymph node cells.	186
Figure 6.9.	MHC II expression on sheep afferent and efferent lymph cells.	189
Figure 6.10.	FCM analysis of CD21 expression.	191
Figure 6.11.	Percentage of B cells expressing CD21 using MAb DU74.	193
Figure 6.12.	Percentage of B cells expressing CD21 using MAb DU104.	194
Figure 6.13.	The percentage of cells expressing the 175 antigen.	196
Figure 6.14.	1D ¹ H-NMR spectra from sheep lymph and lymph node cells.	198
Figure 6.15.	2D ¹ H-NMR spectra of sheep afferent and efferent lymph cells.	199
Figure 6.16.	2D ¹ H-NMR spectra of sheep lymph node cells.	204
Figure 6.17.	Summary of effects of antigen challenge upon total numbers of cells and T cell subsets.	209
Figure 6.18.	Summary of effects of antigen challenge upon cell surface molecule expression and ¹ H-NMR-detectable mobile lipid.	211
Figure A1.1.	Thermal population of energy levels and spin-lattice relaxation from the excited energy level.	A2
Figure A1.2.	Proton spin and angular momentum.	A4
Figure A1.3.	The general philosophy of 2D COSY NMR spectroscopy.	A10
Figure A1.4.	Schematic representation of the general 2D NMR experiment.	A11
Figure A2.1.	The flow cytometer.	A16
Figure A2.2.	Flow cytometry dot plot of a lysed whole blood sample.	A18

List of Tables.

Table 1.1.	Common fatty acids.	30
Table 2.1.	Monoclonal antibodies used in the sheep immune challenge studies.	96
Table 4.1.	Changes in mean cell diameter and membrane surface area during the activation of cultured thymic and splenic T Lymphocytes with PMA/ionomycin.....	124
Table 5.1.	³ H-thymidine incorporation of thymocytes and spleen cells treated with PMA, ionomycin and αCD3.....	141
Table 5.2.	Summary of results for Chapter 5.	157
Table 6.1.	Relative cross-peak intensities of mobile lipid resonances from two-dimensional ¹ H-NMR spectra of isolated sheep lymph node cells, before and after antigen challenge.....	207

AU	arbitrary units
ATP	adenosine 5'-triphosphate
B ₀	magnetic field strength
B ₁	strength of applied magnetic field
BCG	Bacillus-Calmette-Guérin
BrdU	Hoechst 33342 dye
BSA	bovine serum albumin
B ₂ -cAMP	dibutyryl cyclic adenosine 5'-monophosphate
C	constant (hemoglobin gene segment)
¹³ C	carbon-13 isotope
¹⁴ C	carbon-14 isotope
Ca ²⁺	calcium ion
CD	cluster of differentiation (antigen, eg. CD3, CD4, CD8, CD45R)
CDP	cytidine 5'-diphosphate
CDP-choline	cytidine 5'-diphosphate-choline
CEM	human leukemic cell line
Cho	Choline
Cho cells	Chinese hamster ovary cells
cis	"on this side" geometric configuration
CM	chylomicra
CoA	cofactor A
ConA	concanavalin A
CCSY	correlated spectroscopy
cPKC	calcium-dependent protein kinase C
cpm	counts per minute
CR	Complement receptor
Cr(acac) ₃	chromium acetyl acetonate

List of Abbreviations.

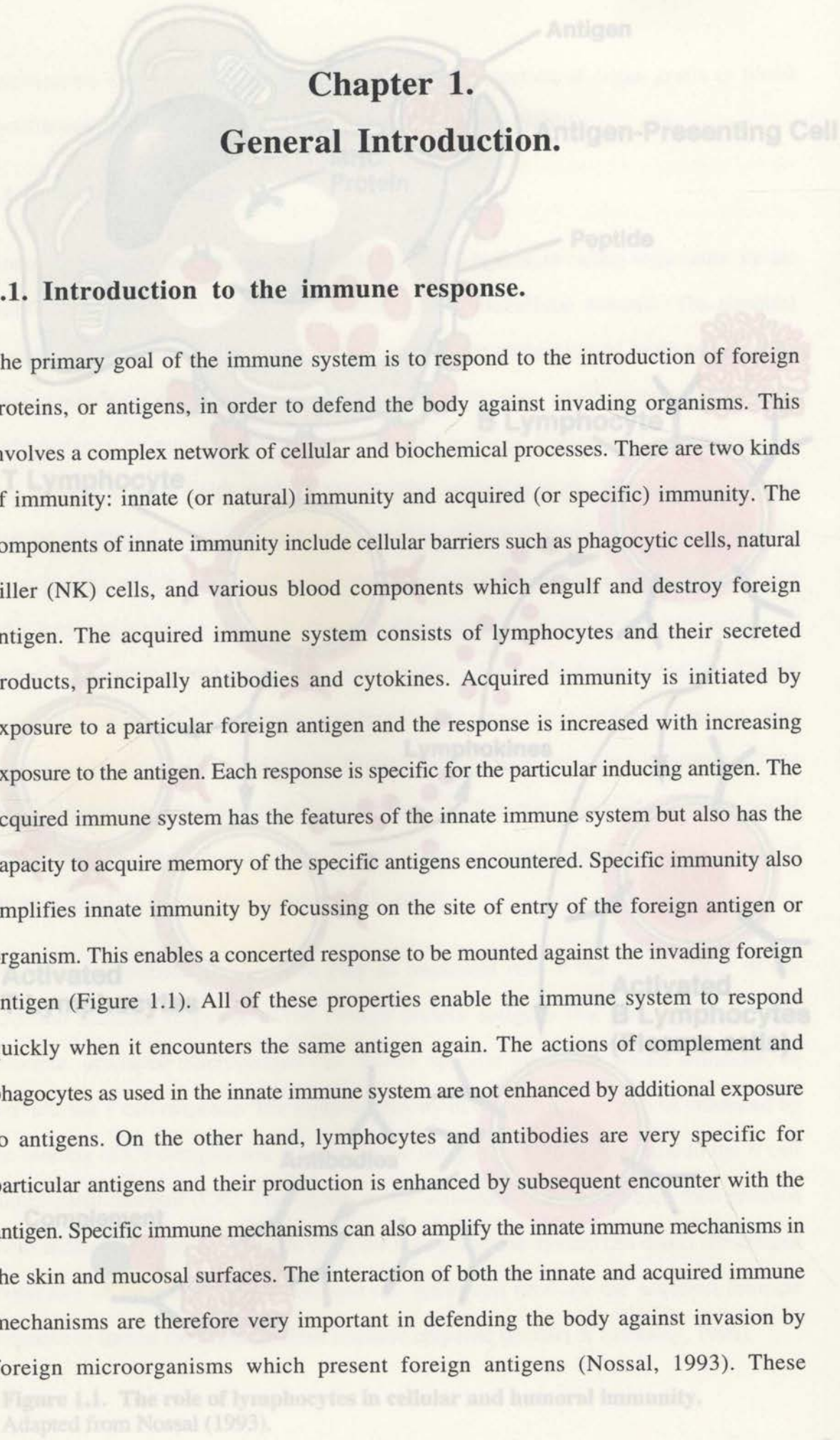
AA	arachidonic acid
α CD3	anti-CD3 antibody
acyl-CoA	acyl-cofactor A
1-Acyl-G3P	1-acyl-glycerol-3-phosphate
APC	antigen presenting cell
A _t	acquisition time
aPKC	atypical protein kinase C
ARAM	antigen recognition activation motif
AU	arbitrary units
ATP	adenosine 5'-triphosphate
B ₀	magnetic field strength
B ₁	strength of applied magnetic field
BCG	Bacillus-Calmette-Guerin
BrdU	Hoechst 33342 dye
BSA	bovine serum albumin
Bt ₂ -cAMP	dibutyryl cyclic adenosine 5'-monophosphate
C	constant (immunoglobulin gene segment)
¹³ C	carbon-13 isotope
¹⁴ C	carbon-14 isotope
Ca ²⁺	calcium ion
CD	cluster of differentiation (antigen, eg. CD3, CD4, CD8, CD45R)
CDP	cytidine 5'-diphosphate
CDP-choline	cytidine 5'-diphosphate-choline
CEM	human leukaemic cell line
Cho	Choline
Cho cells	Chinese hamster ovary cells
cis	"on this side" geometric configuration
CM	chylomicra
CoA	cofactor A
ConA	concanavalin A
COSY	correlated spectroscopy
cPKC	calcium-dependent protein kinase C
cpm	counts per minute
CR	Complement receptor
Cr(acac) ₃	chromium acetyl acetonate

CSF	colony stimulating factor
CT	CTP-phosphocholine cytidyltransferase
CTL	cytotoxic T lymphocytes
CTP	cytidine 5'-triphosphate
D IV	diversity (immunoglobulin gene segment)
1D	one dimensional
2D	two dimensional
D ₂ O	deuterium oxide (deuterated water)
D609	xanthate tricyclodecan-9-yl-xanthogenate
DAG	diacylglycerol
DES	desferrioxamine
DGAT	diacylglycerol acyltransferase
DMEM	Dulbecco's Modified Eagle's Medium
DMSO	dimethyl sulphoxide
DNA	deoxyribonucleic acid
DTT	dithiothreitol
E	difference between the two nuclear energy levels
emf	electromotive force
EGF	epidermal growth factor
ER	endoplasmic reticulum
F1	frequency domain 1
F2	frequency domain 2
Fab'	monovalent IgG fragment, antigen binding
F(ab') ₂	divalent IgG fragment, antigen binding
FCM	flow cytometry
FCS	foetal calf serum
FID	free induction decay
FITC	fluorescein isothiocyanate
fMLP	formyl-Methionyl-Leucyl-Phenylalanine
FSC	forward scatter
FT	Fourier transform
γ	magnetogyric ratio
GB	fraction of A _t at which LG function reaches a maximum
GM-CSF	granulocyte/macrophage colony stimulating factor
GMP-140	P-selectin
G3P	glycerol-3-phosphate
GPC	glycerophosphocholine
GPCCho	glycerophosphocholine
GPE	glycerophosphoethanolamine

^2H cells	deuterium isotope
^3H	tritium isotope
HDL	high density lipoprotein
HEPES	N-[2-hydroxyhydroxyethyl]piperazine-N'-[2-ethanesulfonic acid]
HIV	human immunodeficiency virus
^1H -NMR	proton nuclear magnetic resonance
HPLC	high pressure liquid chromatography
HU	hydroxyurea
ICAM-1	intercellular adhesion molecule-1
IFN- γ	interferon- γ
Ig	immunoglobulin
IGF-1	insulin-like growth factor-1
IgG	immunoglobulin G
IL	interleukin (eg. IL-1 β , IL-2, IL-3, IL-6, IL-2R α)
IL-2R α	interleukin-2 receptor α
InsP $_3$	inositol triphosphate
IUPAC	International Union of Pure and Applied Chemistry
JH	joining (immunoglobulin gene segment)
K	degrees Kelvin
k	Boltzman's constant
LAT	lysophosphatidylcholine acyl transferase
LB	line broadening if positive or line narrowing if negative
LFA-1	lymphocyte functional antigen 1
LFA-3	lymphocyte functional antigen 3
LG	Lorentz-Gauss
LPS	lipopolysaccharide
Lyso-PC	lysophosphatidylcholine
M_0	equilibrium magnetization vector
M_p	magnetization vector immediately after pulse
MAb	monoclonal antibody
2-ME	2-mercaptoethanol
MHC I	major histocompatibility complex class I
MHC II	major histocompatibility complex class II
MR	magnetic resonance
mRNA	messenger ribonucleic acid
n	number of energy transients
η_h	Boltzmann distribution number of nuclei in high energy states
η_l	Boltzmann distribution number of nuclei in low energy states
SRBC- α Mg	sheep red blood cell-coupled anti-mouse immunoglobulin

NK cells	Natural killer cells
NMR	nuclear magnetic resonance
NOESY	nuclear Overhauser effect and exchange spectroscopy
nPKC	novel protein kinase C
ω	angular frequency of precession
ω_0	Larmor frequency
^{31}P	phosphorus-31 isotope
^{32}P	phosphorus-32 isotope
PA	phosphatidic acid
PAF	platelet activating factor
PBMC	peripheral blood mononuclear cells
PBS	phosphate buffered saline
PC	phosphatidylcholine
PCho	phosphocholine
PDGF	platelet-derived growth factor
PE	phosphatidylethanolamine
pH	$-\log_{10}[\text{H}^+]$
PHA	phytohaemagglutinin
PKC	protein kinase C (with α , β , γ and ζ isoforms)
PLA ₂	phospholipase (A ₂ isoform)
PLC	phospholipase (C isoform)
PLD	phospholipase (D isoform)
PMA	phorbol myristate acetate
PMN	polymorphonuclear leukocytes
^{31}P -NMR	^{31}P nuclear magnetic resonance
PPD	purified protein derivative
ppm	parts per million (chemical shift)
PS	phosphatidyl serine
Ptd-Ins	phosphatidylinositol
Ptd-Ins(3,4,5)P ₃	phosphatidylinositol 3,4,5-trisphosphate
Ptd-Ins(4,5)P ₂	phosphatidylinositol 4,5-bisphosphate
rf	radio frequency
RNA	ribonucleic acid
SCC	standard culturing conditions
SDS-PAGE	sodium dodecyl sulphate polyacrylamide gel electrophoresis
sheep α MIgFab'	sheep anti-mouse IgG Fab'
S/N	signal to noise ratio
SRBC	sheep red blood cell
SRBC- α MIg	sheep red blood cell-coupled anti-mouse immunoglobulin

SSC	side scatter
τ	time after rf pulse
t_1	evolution time
t_2	acquisition time
T_1	longitudinal relaxation time
T_2	transverse relaxation time
TAG	triacylglycerol
TCR	T cell receptor
TFR	transferrin receptor
TG	triglyceride
TGF- β	transforming growth factor- β
TLC	thin layer chromatography
TNF	tumour necrosis factor
TPA	12-O-tetradecanoylphorbol-13-acetate
triolein	1,2,3-tri- <i>cis</i> -9-octadecenoylglycerol
Tris	tris[hydroxymethyl]aminomethane
TSP	3-trimethylsilyl[2,2,3,3- ^2H] propionate
ν	resonance frequency of a nucleus
UV	ultraviolet
V	variable (immunoglobulin gene segment)
VLDL	very low density lipoprotein



Chapter 1.

General Introduction.

1.1. Introduction to the immune response.

The primary goal of the immune system is to respond to the introduction of foreign proteins, or antigens, in order to defend the body against invading organisms. This involves a complex network of cellular and biochemical processes. There are two kinds of immunity: innate (or natural) immunity and acquired (or specific) immunity. The components of innate immunity include cellular barriers such as phagocytic cells, natural killer (NK) cells, and various blood components which engulf and destroy foreign antigen. The acquired immune system consists of lymphocytes and their secreted products, principally antibodies and cytokines. Acquired immunity is initiated by exposure to a particular foreign antigen and the response is increased with increasing exposure to the antigen. Each response is specific for the particular inducing antigen. The acquired immune system has the features of the innate immune system but also has the capacity to acquire memory of the specific antigens encountered. Specific immunity also amplifies innate immunity by focussing on the site of entry of the foreign antigen or organism. This enables a concerted response to be mounted against the invading foreign antigen (Figure 1.1). All of these properties enable the immune system to respond quickly when it encounters the same antigen again. The actions of complement and phagocytes as used in the innate immune system are not enhanced by additional exposure to antigens. On the other hand, lymphocytes and antibodies are very specific for particular antigens and their production is enhanced by subsequent encounter with the antigen. Specific immune mechanisms can also amplify the innate immune mechanisms in the skin and mucosal surfaces. The interaction of both the innate and acquired immune mechanisms are therefore very important in defending the body against invasion by foreign microorganisms which present foreign antigens (Nossal, 1993). These

Figure 1.1. The role of lymphocytes in cellular and humoral immunity.
Adapted from Nossal (1993).

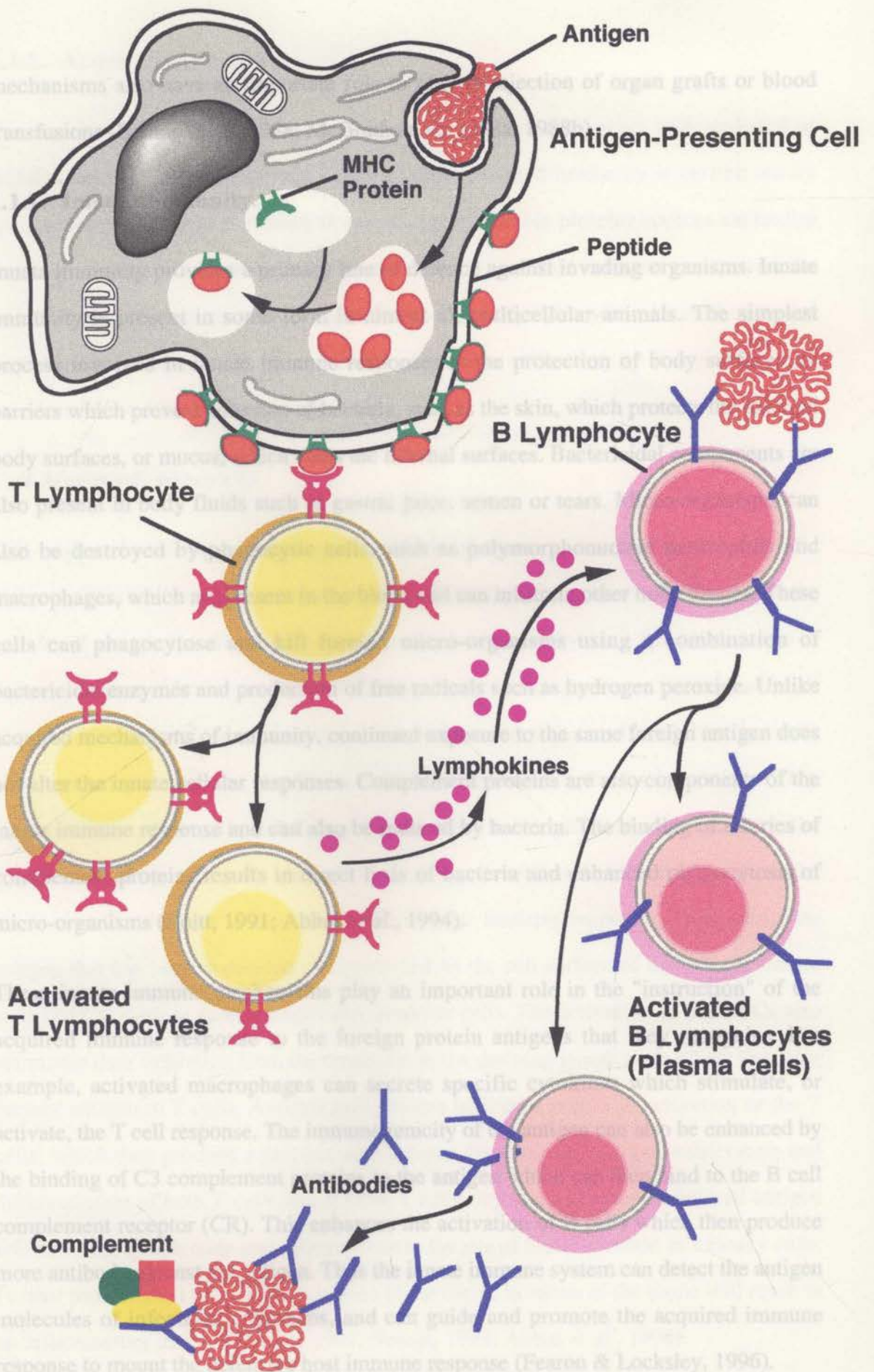


Figure 1.1. The role of lymphocytes in cellular and humoral immunity.
Adapted from Nossal (1993).

1.1.2. Acquired Immunity.

mechanisms also have an important role to play in rejection of organ grafts or blood transfusions (Bishop *et al.*, 1988; McGrath *et al.*, 1988a, 1988b).

1.1.1. Innate immunity.

Innate immunity provides a primary line of defence against invading organisms. Innate immunity is present in some form in almost all multicellular animals. The simplest process involved in innate immune responses is the protection of body surfaces by barriers which prevent adhesion of bacteria, such as the skin, which protects the external body surfaces, or mucus, which coats the internal surfaces. Bactericidal components are also present in body fluids such as gastric juice, semen or tears. Micro-organisms can also be destroyed by phagocytic cells, such as polymorphonuclear neutrophils and macrophages, which are present in the blood and can infiltrate other body tissues. These cells can phagocytose and kill foreign micro-organisms using a combination of bactericidal enzymes and production of free radicals such as hydrogen peroxide. Unlike acquired mechanisms of immunity, continued exposure to the same foreign antigen does not alter the innate cellular responses. Complement proteins are also components of the innate immune response and can also be induced by bacteria. The binding of a series of complement proteins results in direct lysis of bacteria and enhanced phagocytosis of micro-organisms (Roitt, 1991; Abbas *et al.*, 1994).

These innate immune mechanisms play an important role in the "instruction" of the acquired immune response to the foreign protein antigens that they recognise. For example, activated macrophages can secrete specific cytokines which stimulate, or activate, the T cell response. The immunogenicity of the antigen can also be enhanced by the binding of C3 complement proteins to the antigen which can then bind to the B cell complement receptor (CR). This enhances the activation of B cells which then produce more antibody against the antigen. Thus the innate immune system can detect the antigen molecules of infectious organisms, and can guide and promote the acquired immune response to mount the defensive host immune response (Fearon & Locksley, 1996).

1.1.2. Acquired immunity.

The acquired immune response can be divided into two categories: cell-mediated or cellular immunity, and humoral immunity. Cell-mediated immunity is carried out by lymphocytes. Humoral immunity is carried out by soluble proteins such as antibodies and complement. The interaction between the cell-mediated immune system and the humoral immune response, involving the interaction of lymphocytes with antibodies and complement, is important in the prevention of invasion of the body by foreign antigen or parasites (Roitt, 1991; Abbas *et al.*, 1994).

1.2. Cells and tissues of the immune system.

Cell-Mediated immunity

The cells of the immune system are derived from bone marrow stem cells. T cells and B cells. Cell-mediated immunity is dependent upon the response of immune cells to specific antigens. This is illustrated by the acquisition of immunity by a naive individual after the transfer of antigen specific lymphocytes from an immune individual. The primary line of defence against infection in the cell-mediated immune responses is the migration of phagocytic cells, such as macrophages and polymorphonuclear cells (PMNs), from the blood stream into the tissue site. These cells engulf and destroy the foreign antigen. They also produce cellular chemical messengers known as cytokines which induce the migration of phagocytic cells and other lymphocytes, such as T cells and B cells, to the tissue site. T cells play a key role in the cellular immune response. They recognize antigen that has been processed and presented on the cell surface of antigen presenting cells (APCs) such as macrophages and dendritic cells. The activation of the APCs also stimulates their migration from the tissue site to the draining lymph node where they also present antigen to T cells. Antigen presentation to T cells results in activation of the T cells, which then produce a number of cytokines that can regulate the proliferation and differentiation of both T cells and B cells. Lymphocytes that have encountered antigen will leave the lymph node and migrate back to the site of tissue invasion as memory cells. Further proliferation and cytokine release at the site of invasion of the tissue will result in an inflammatory response (Roitt, 1991; Nossal, 1993; Abbas *et al.*, 1994).

T cells are identified by the possession of a T cell receptor (TCR) on the cell surface, which functions to recognise and bind to processed antigen together with "self" major histocompatibility complex (MHC) II presented on the surface of the APC (Frelinger *et al.*, 1975; Swain, 1983). The TCR usually comprises the $\alpha\beta$ subunits, but on $\gamma\delta$ T cells

Humoral immunity

The humoral immune response also plays a role in the removal of invading organisms. The binding of specific antibody, either on to the surface of B cells or secreted by plasma cells, to an antigen will result in the initiation of the binding of a number of complement proteins in a cascade of events that results in the destruction of the particular antigen and ultimately in the lysis of the invading organism (Roitt, 1991; Janeway, 1993; Abbas *et al.*, 1994).

1.2. Cells and tissues of the immune system.

The cells of the immune system are derived from bone marrow stem cells. T cells and B cells, which are important in the acquired immune response, differentiate and mature in the bone marrow and thymus. The mature cells are released to circulate through the peripheral lymphoid organs, such as the lymph nodes and spleen, and recirculate back into the blood and lymph (Figure 1.2). At peripheral tissue sites the cells encounter antigen which initiates a specific immune response, resulting in cellular proliferation and the production of specific lymphokines. A number of other immune cells, such as dendritic cells, polymorphonuclear cells, and monocytes/macrophages, are involved in a coordinated network of interactions which collectively constitute the immune response.

1.2.1. T cells.

T cells play an essential part in the regulation and generation of a cellular immune response to foreign antigens. T helper cell responses are particularly important for an adequate immune response. For example, a decrease in the numbers of CD4⁺ T helper cells can result in severe immune deficiency, as illustrated by the effects of human immunodeficiency virus (HIV) infection (Schnittman *et al.*, 1987).

T cells are identified by the possession of a T cell receptor (TCR) on the cell surface, which functions to recognise and bind to processed antigen together with "self" major histocompatibility complex (MHC) II presented on the surface of the APC (Frelinger *et al.*, 1975; Swain, 1983). The TCR usually comprises the $\alpha\beta$ subunits, but on $\gamma\delta$ T cells

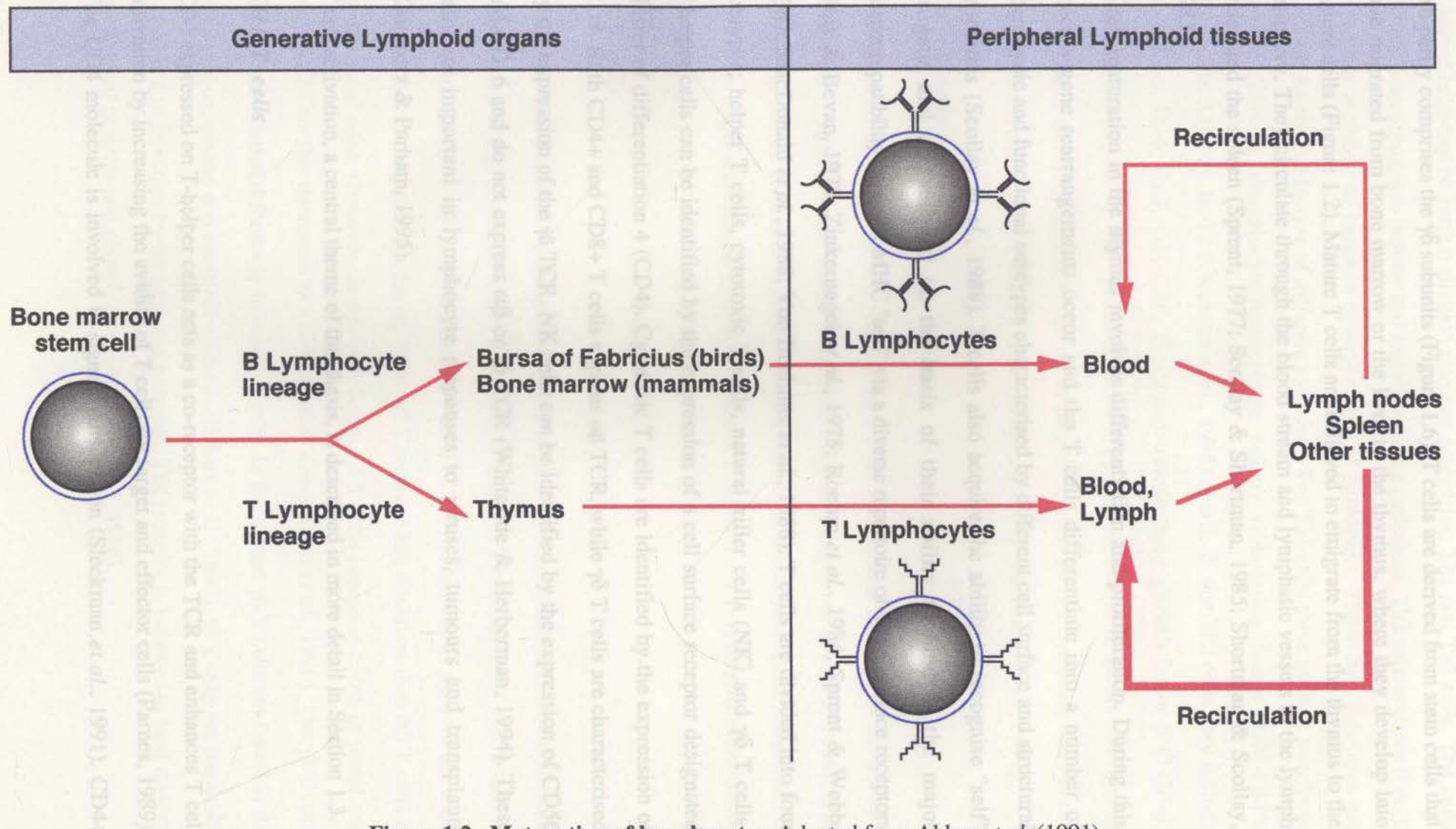


Figure 1.2. Maturation of lymphocytes. Adapted from Abbas *et al.* (1991).

also partly comprises the $\gamma\delta$ subunits (Figure 1.6). T cells are derived from stem cells that have migrated from bone marrow or the liver to the thymus, where they develop into mature cells (Figure 1.2). Mature T cells are believed to emigrate from the thymus to the periphery. They circulate through the blood stream and lymphatic vessels to the lymph nodes and the spleen (Sprent, 1977; Scollay & Shortman, 1985; Shortman & Scollay, 1985).

T cell maturation in the thymus involves differentiation and proliferation. During this process gene rearrangements occur and the T cells differentiate into a number of phenotypic and functional subtypes characterised by different cell surface and structural properties (Scollay *et al.*, 1988). T cells also acquire the ability to recognise "self" antigens and are selected on the basis of their ability to bind to the major histocompatibility complex MHC "self" via a diverse repertoire of T cell surface receptors (Fink & Bevan, 1978; Zinkernagel *et al.*, 1978; Roehm *et al.*, 1984; Sprent & Webb, 1987; MacDonald *et al.*, 1988; Von Boehmer *et al.*, 1988). T cells are divided into four subtypes; helper T cells, cytotoxic T cells, natural killer cells (NK) and $\gamma\delta$ T cells. T helper cells can be identified by the expression of a cell surface receptor designated cluster of differentiation 4 (CD4). Cytotoxic T cells are identified by the expression of CD8. Both CD4+ and CD8+ T cells express $\alpha\beta$ TCR, while $\gamma\delta$ T cells are characterised by the expression of the $\gamma\delta$ TCR. NK cells can be identified by the expression of CD56 and CD16 and do not express $\alpha\beta$ or $\gamma\delta$ TCR (Whiteside & Herberman, 1994). These cells are important in lymphocyte responses to viruses, tumours and transplants (Gumperz & Parham, 1995).

T cell activation, a central theme of this thesis, is described in more detail in Section 1.3.

CD4 T cells

CD4 expressed on T-helper cells acts as a co-receptor with the TCR and enhances T cell activation by increasing the avidity of T cells for target and effector cells (Parnes, 1989). The CD4 molecule is involved in signal transduction (Sleckman *et al.*, 1991). CD4+

T-helper cells can be further divided into two categories: Th1 and Th2 cells. Th1 cells activate macrophages to destroy and engulf invading pathogens. Th2 cells activate B cells to secrete antibody to enhance neutralisation of pathogens. These two functions are achieved by the production of different cytokines. For Th1 cells these include interferon gamma (IFN- γ), granulocyte/macrophage colony stimulating factor (GM-CSF), interleukin-3 (IL-3), IL-12 (Okamura *et al.*, 1995) and IL-2. For Th2 cells they include IL-4, IL-5, IL-6, IL-3, GM-CSF, IL-10 and transforming growth factor- β (TGF- β) (Mosmann *et al.*, 1991). The cytokines secreted by Th1 cells serve to attract neutrophils, macrophages and lymphocytes to the site of infection, whereas Th2 cytokines drive B cell differentiation and immunoglobulin class isotype switching (Mosmann *et al.*, 1991).

The antibody repertoire is so diverse because the Ig consists of separate domains which are generated by the rearrangement of V, D and J genes. This allows the detection of a

CD8 T cells

CD8 is found on cytotoxic and suppressor T cells and natural killer cells. It acts as a co-receptor together with MHC I in TCR antigen recognition (Parnes, 1989). The function of CD8 T cells is to kill cells infected with intracellular pathogens. CD8 binds to MHC I on target and effector cells and enhances T cell activation via signal transduction (Salter *et al.*, 1990).

$\gamma\delta$ T cells

$\gamma\delta$ T cells are identified by the possession of a $\gamma\delta$ TCR which contains chains distinct from the $\alpha\beta$ chains found on CD4+ and CD8+ T cells. $\gamma\delta$ T cells are CD4-, CD8- and in sheep express the T-19 antigen (McClure *et al.*, 1989). These cells possess the CD3 complex but are negative for the $\alpha\beta$ TCR. $\gamma\delta$ T cells are less abundant than $\alpha\beta$ T cells in humans and mice. However, in newborn lambs, $\gamma\delta$ T cells comprise $\geq 50\%$ of peripheral blood cells but this decreases to $\sim 30\%$ in adult sheep (Hein *et al.*, 1990). The $\gamma\delta$ T cells are also distributed differently from $\alpha\beta$ T cells. In the mouse $\gamma\delta$ T cells are found in the skin, tongue, uterine and intestinal epithelia (Itohara *et al.*, 1990). $\gamma\delta$ T cells are important in defence of infection by bacteria and parasites. The receptor is believed to bind directly to bacterial proteins and phosphoproteins (Kaufmann, 1996).

1.2.2. B cells.

B cells synthesise immunoglobulins (Igs). Therefore they form the basis for the humoral immune response to foreign antigen. Membrane-bound Ig on the surface of B cells can bind to free antigen, such as small peptides, which can then be presented to T helper cells (Chestnut & Grey, 1981; Hodgkin & Kehry, 1992). Membrane-bound Ig is also involved in signal transduction (Pleiman *et al.*, 1994). Antigen can be processed and presented by B cells in association with MHC II (Pernis & Weber, 1989). Antigen recognition activates B cells, whereupon they can differentiate into antibody-secreting plasma cells.

The antibody repertoire is so diverse because the Ig consists of separate domains which are generated by the rearrangement of V, D and J genes. This allows the detection of a vast array of antigens. The immunoglobulin receptor consists of 2 heavy and light chains covalently linked by disulphide bonds. The antigen binding site of the Ig chains consists of variable regions in both the heavy and light chains. The remainder of the chain consists of conserved constant regions which provide sites for complement protein binding. Different isotypes of antibodies can be identified by their heavy chain class, γ , α , μ , δ or ϵ , which occur in IgG, IgA, IgM, IgD and IgE respectively. Within the IgG class a number of different isotypes can be identified IgG₁, IgG₂, IgG₃, IgG₄. IgM antibodies consist of a pentamer of immunoglobulin molecules and IgA can exist as a monomer, dimer or trimer. IgG isotypes exist in monomer form only (Davies & Metzger, 1983).

IgG molecules can be structurally modified in the laboratory to generate monovalent or divalent subfragments for either preparative or diagnostic purposes. IgG molecules can be divided into fragments by the proteolytic enzymes papain and pepsin, separating the antigen binding Fab portions from the Fc constant region of the molecule. Papain separates the constant Fc region from the antigen binding portion Fab, and two single fragments are generated (monovalent forms). Pepsin, on the other hand, cleaves the Ig molecule at the hinge area, separating F(ab')₂ (divalent) fragments from the Fc portion (Abbas *et al.*, 1991).

1.2.3. Monocytes/Macrophages.

Monocytes are derived from myeloid stem cell precursors and are found in the circulation. They can migrate into the tissue areas and become macrophages (Nauseef, 1989). Along with phagocytic neutrophils, tissue macrophages contribute to the first line of defence against invading pathogens, and recruit other monocytes into the tissue site. Macrophages differ from monocytes in the expression of different cell surface molecules and the performance of different cellular functions. The macrophage can bind to specific ligands via its receptors. These include immunoglobulins and complement components, bacterial peptides, polysaccharides such as N-formylated peptides (fMLP), endotoxin such as LPS, extracellular matrix proteins including fibrin and fibronectin, cytokines and growth factors including colony-stimulating factor (CSF), insulin, interleukin-1 (IL-1), interferons- α , β and γ and lipoprotein receptors (Ho, 1989). Monocytes and phagocytic neutrophils move from the blood stream to the site of inflammation after chemotactic attraction to cellular and bacterial metabolites. At the tissue site the macrophages can be activated by cytokines and microbial and lipid-derived products such as tumour necrosis factor (TNF), GM-CSF, IL-1, IFN- γ , platelet-derived growth factor (PDGF), platelet activating factor (PAF) (1-alkyl-2-acetyl-*sn*-glycero-3-phosphocholine), fMLP and LPS. Ingestion of the invading organism is mediated by complement receptors and immunoglobulin binding. The macrophage then becomes fully activated and the organism is destroyed by an oxidative burst from superoxide production and cytokine production (Ho, 1989). Macrophages can also function as antigen presenting cells and present processed endocytosed antigen to the T helper cells in association with MHC class II (Unanue & Allen, 1987).

1.2.4. Dendritic cells.

Dendritic cells are antigen presenting cells which present antigen to T cells in an MHC II-restricted manner. Dendritic cells are found in non-lymphoid organs, such as skin epidermis (as Langerhans cells) (Schuler & Steinman, 1985), heart (Spencer & Fabre, 1990), lung (Holt *et al.*, 1990), gut (Pavli *et al.*, 1990), in the circulation as afferent

lymph veiled cells (Bujdoso *et al.*, 1989a) and blood dendritic cells (Freudenthal & Steinman, 1990), in lymphoid organs as lymphoid dendritic cells and interdigitating cells in tonsil (Hart & McKenzie, 1988), thymus (Barclay & Mayrhofer, 1981) and spleen (Crowley *et al.*, 1990). Dendritic cells can also be identified by the expression of the cell surface marker CD1. These cells also express high levels of MHC I and II molecules and other adhesion molecules such as intercellular adhesion molecule-1 (ICAM-1) and lymphocyte functional antigen-3 (LFA-3) which mediate T cell interactions (Steinman, 1991). Dendritic cells serve several functions. They acquire antigen in tissues and can migrate to lymphoid organs and present antigen to specific T cells.

1.2.5. Immune cell recirculation.

Recirculation of lymphocytes enables a large number of cells to encounter antigen and for the antigen-specific lymphocytes to be selected for accumulation at the tissue site where the antigen is located. Mature naive lymphocytes move from the blood into peripheral lymphoid organs, spleen, lymph nodes and Peyer's patches, and return back to the blood either directly or via efferent lymph (Gowans & Knight, 1964). The lymphocytes leave the blood at particular sites in the lymph nodes via the endothelial cells of the post-capillary venules (Figures 1.3, 1.4).

These endothelial-lymphocyte interactions are mediated by specific cell surface molecules (Chin *et al.*, 1982; Gallatin *et al.*, 1983). A large majority of the lymphocytes entering the lymph node (~85-90%) are derived from blood. A small proportion are derived from the afferent lymph (~10%) (Hall & Morris, 1965b). Afferent lymph has been shown to carry antigen to the lymph node in addition to the cell-associated antigen on antigen presenting cells also present in afferent lymph. In addition to lymphocytes, the afferent lymph contains dendritic cells, macrophages and, during inflammation, granulocytes and erythrocytes (Hall & Morris, 1965b; Smith *et al.*, 1970). Afferent lymph contains fewer B cells than blood or efferent lymph (Scollay *et al.*, 1976). More recently, several studies have shown distinct differences between the cells in afferent and efferent lymph, lymph node and blood using monoclonal antibodies to specific cell surface markers to

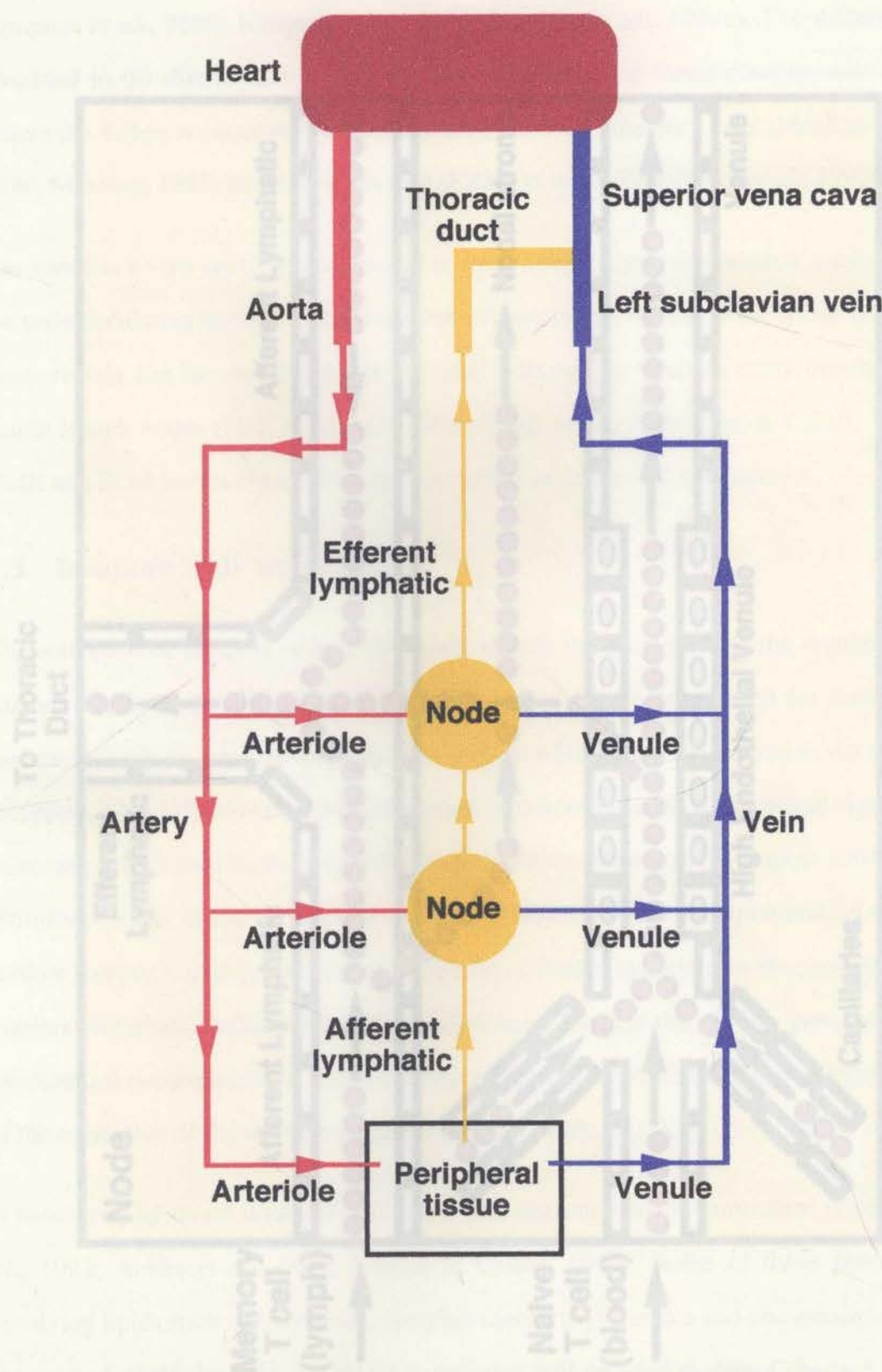


Figure 1.3. Systemic pathway of lymphocyte recirculation.

Figure 1.4. Pathway of lymphocyte recirculation through the lymph node. Adapted from Abbas et al. (1991).

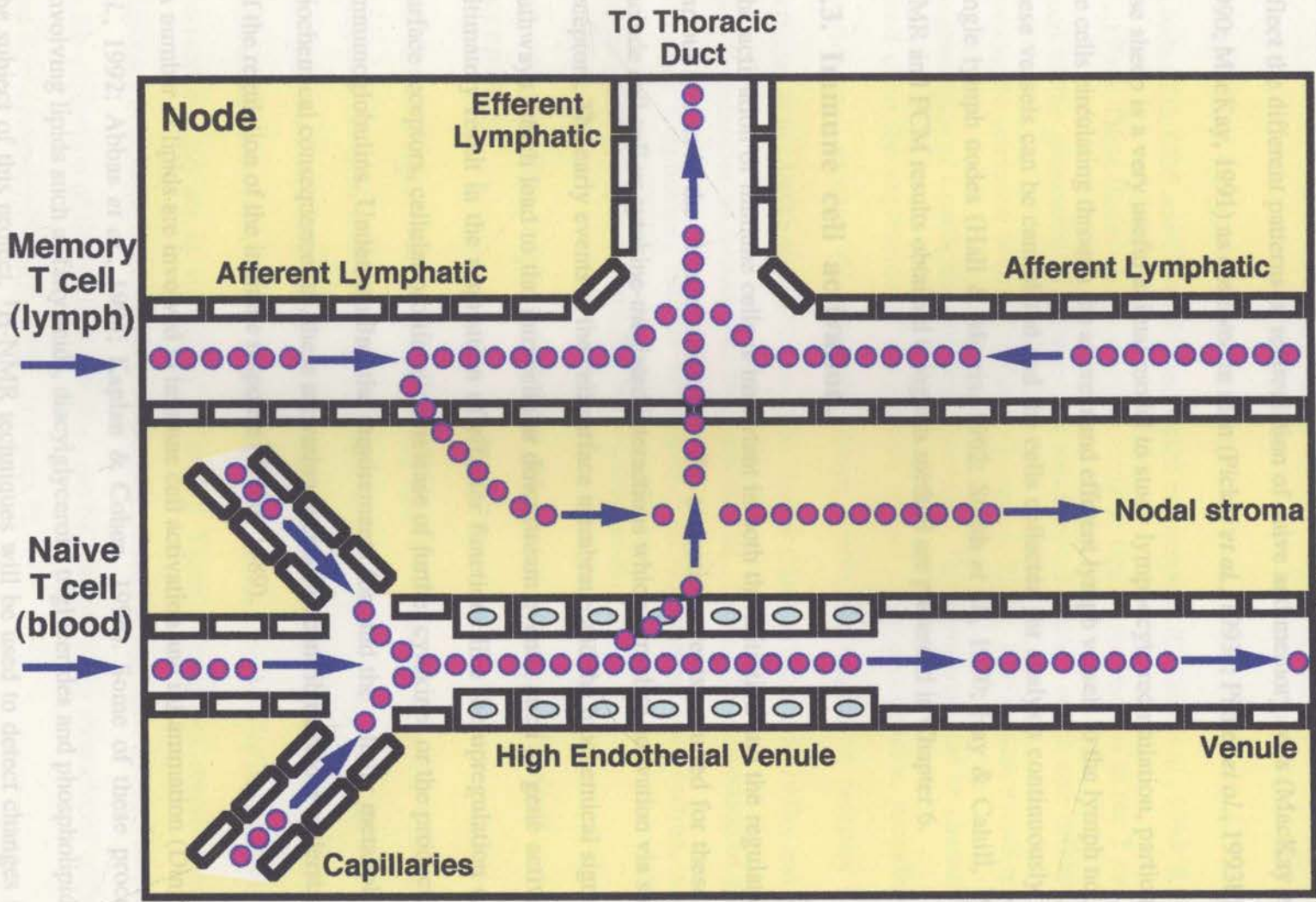


Figure 1.4. Pathway of lymphocyte recirculation through the lymph node. Adapted from Abbas et al. (1991).

1.3.1. T-cell activation.

distinguish between different cell populations. These include differences both before and after antigen challenge of the lymph node (Hein *et al.*, 1987; MacKay *et al.*, 1988; Kimpton *et al.*, 1989; Kimpton *et al.*, 1990; MacKay *et al.*, 1992a). The differences observed in the distribution of cell types in different sheep tissue compartments may reflect the different patterns of recirculation of naive and memory cells (MacKay *et al.*, 1990; MacKay, 1991) as observed in man (Picker *et al.*, 1993a; Picker *et al.*, 1993b).

The sheep is a very useful animal model to study lymphocyte recirculation, particularly the cells circulating through the afferent and efferent lymph vessels to the lymph node, as these vessels can be cannulated and the cells collected for analysis continuously from single lymph nodes (Hall & Morris, 1962; Smith *et al.*, 1970; Hay & Cahill, 1982). NMR and FCM results obtained using this method are presented in Chapter 6.

1.3. Immune cell activation.

The activation of immune cells is important in both the initiation and the regulation of various events in the immune response. The activation events required for these cells include cell-cell or cytokine-mediated interactions which stimulate activation via surface receptors. The early events at the cell surface membrane and the biochemical signalling pathways which lead to the intracellular downstream events, such as gene activation, ultimately result in the acquisition of effector functions like the upregulation of cell surface receptors, cellular proliferation, release of further cytokines or the production of immunoglobulins. Understanding the requirements for, and the cellular metabolic and biochemical consequences of, these activation events can contribute to our understanding of the regulation of the immune response (Weiss, 1989).

A number of lipids are involved in immune cell activation and inflammation (Dingley *et al.*, 1992; Abbas *et al.*, 1994; Kaplan & Cohen, 1994). Some of these processes, involving lipids such as fatty acids, diacylglycerols, triglycerides and phospholipids, are the subject of this project. ¹H-NMR techniques will be used to detect changes in the properties of these lipid species in response to immune cell activation.

1.3.1. T cell activation.

T cell activation requires the simultaneous engagement of the TCR and specific cell ligand-receptor interactions that occur between antigen presenting cells and antigen specific T cells (Inaba & Steinman, 1984; Kupfer & Singer, 1989; Weiss, 1989). Recently a number of accessory cell-surface molecule interactions have been identified as having a role in the optimal activation of the T cell, via the interaction with APCs. These include CD2, CD5 and CD4/CD8 and CD28 co-receptors (Collins *et al.*, 1994; Rudd *et al.*, 1994). These ligand-receptor events result in signal transduction in the T cell as a result of the generation of intracellular biochemical signals which can influence or promote the activation of over 100 genes (Szamel & Resch, 1995). These events result in the generation of a particular activated phenotype. The phenotypes can be characterised based upon the expression of a repertoire of cell surface molecules, including the interleukin-2 receptor (IL-2R α) (Waldman, 1989), the transferrin receptor (TFR) (Jefferies *et al.*, 1984), the early activation marker CD69 (Testi *et al.*, 1990), and MHC class II molecules on human T cells (Sanders *et al.*, 1988). The production of growth factors or lymphokines such as interleukin-2 (IL-2), cellular proliferation, and the acquisition of cytolytic activity also occur (Abbas *et al.*, 1994).

1.4. Molecular aspects of the immune system. I. Cell surface receptors.

Cell surface receptors bind to complimentary ligands on adjacent cells. The binding of the TCR/CD3 complex with an antigen presenting cell is the first step in T cell activation. This promotes the engagement of other cell surface accessory molecules which further enhance the activation of the T cell. These cell surface molecules promote cell-cell interactions and act as signalling molecules. These interactions result in effector responses in immune cells (Geppert *et al.*, 1990; Dustin & Springer, 1991). The changes in the expression of cell surface receptors can be detected using monoclonal antibodies and flow cytometry (Shapiro, 1995; Appendix 2).

A number of cell surface adhesion molecules are up-regulated on memory T cells which have encountered antigen previously, or on recently activated cells. These include CD2, CD44, LFA-1, LFA-3 and MHC II (Sanders *et al.*, 1988). These cell adhesion molecules promote cell-cell interactions and enhance T cell activation by increasing the activity of accessory molecules, some of which have enzymatic activity (Sanders *et al.*, 1989).

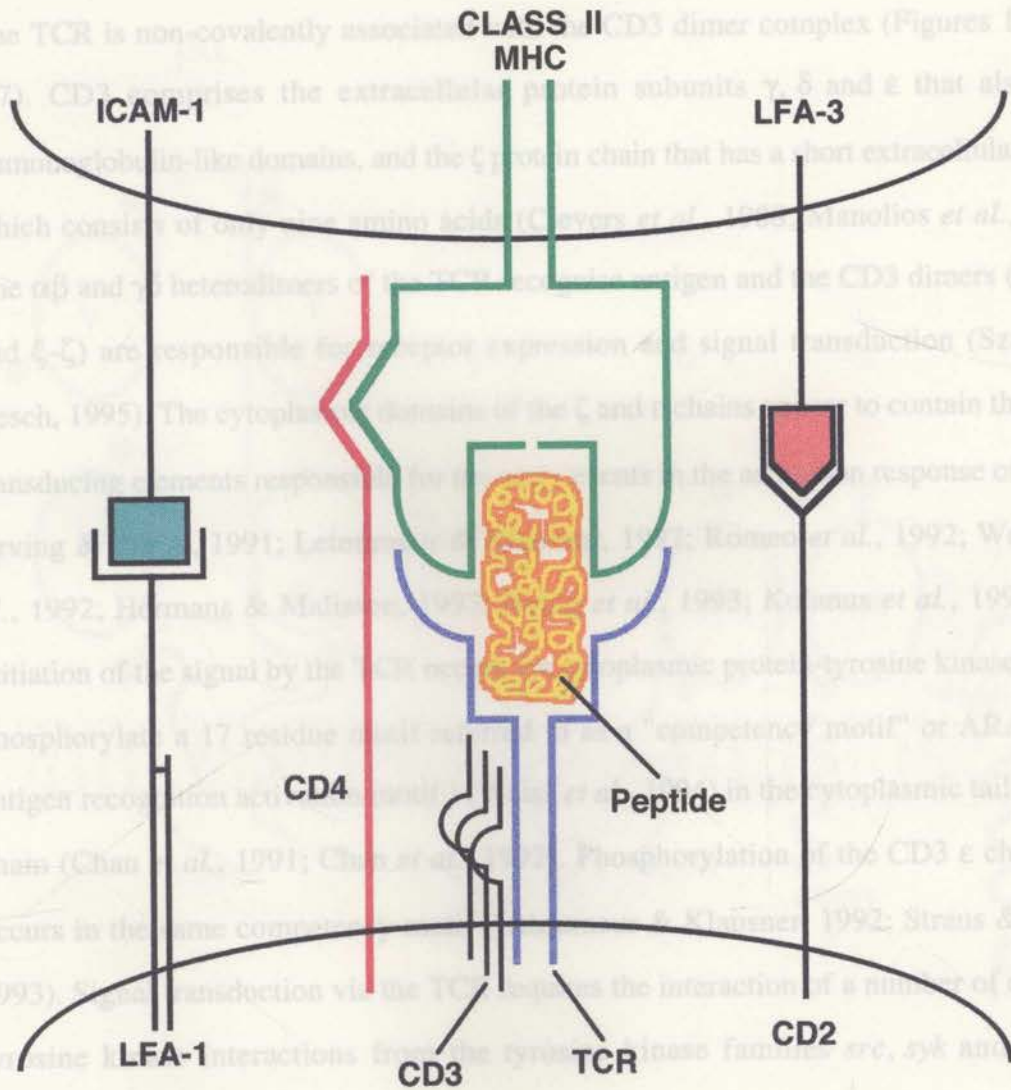
1.4.1. The T cell receptor-CD3 (TCR/CD3) complex.

A T cell is activated by an antigen via the binding of the TCR with antigen presented on the antigen-presenting cell (APC) in association with the Major Histocompatibility Complex (MHC). Two events are important in this interaction: (i) the recognition of specific antigen in combination with the MHC molecules via the TCR, and (ii) the acquisition of effector function which occurs as a result of a signal which is transmitted across the plasma membrane by the CD3 complex to the interior of the cell (Weiss, 1989) (Figures 1.1, 1.5, 1.7).

Structure and molecular features of the T cell receptor-CD3 complex

The T cell receptor (TCR) is a transmembrane heterodimer multi-subunit complex with a diverse specificity repertoire that binds to antigen peptides in combination with MHC (Marrack & Kappler, 1987). The diversity of the T cell repertoire can be accounted for by the combinatorial and permutational arrangements of the gene segments expressing different ligand binding chains, as well as the different chain combinations (Siu *et al.*, 1984; Yoshikai *et al.*, 1985; Davis, 1988). It consists of two glycoprotein binding chains comprising either the $\alpha\beta$ pair, which are mostly linked through disulphide bonds, or the $\gamma\delta$ pair which are usually linked non-covalently. The $\alpha\beta$ and $\gamma\delta$ glycoproteins belong to the immunoglobulin superfamily and resemble immunoglobulins in that they contain variable and constant domains (Acuto *et al.*, 1983; Kappler *et al.*, 1983; Reinherz *et al.*, 1983). The TCR is able to recognise a large number of antigens due to the gene rearrangements (Royer *et al.*, 1984; Raulet *et al.*, 1985; Royer *et al.*, 1985; Yoshikai *et al.*, 1985; Townsend *et al.*, 1986). As with immunoglobulin genes, the two forms of the

**ANTIGEN
PRESENTING CELL
EXPRESSING
CLASS II MHC**



**HELPER T
LYMPHOCYTE
EXPRESSING CD4**

Figure 1.5. CD4 T-cell receptor and CD3 complex.

TCR, $\alpha\beta$ and $\gamma\delta$, arise from recombination of variable (V), diversity (D) (in some cases), joining (J) and constant (C) gene segments (Siu *et al.*, 1984).

The TCR is non-covalently associated with the CD3 dimer complex (Figures 1.5, 1.6, 1.7). CD3 comprises the extracellular protein subunits γ , δ and ϵ that also have immunoglobulin-like domains, and the ζ protein chain that has a short extracellular region which consists of only nine amino acids (Clevers *et al.*, 1988; Manolios *et al.*, 1991). The $\alpha\beta$ and $\gamma\delta$ heterodimers of the TCR recognise antigen and the CD3 dimers ($\gamma\epsilon$, $\delta\epsilon$ and $\zeta\zeta$) are responsible for receptor expression and signal transduction (Szamel & Resch, 1995). The cytoplasmic domains of the ζ and ϵ chains appear to contain the signal transducing elements responsible for the early events in the activation response of T cells (Irving & Weiss, 1991; Letourneur & Klausner, 1992; Romeo *et al.*, 1992; Wegner *et al.*, 1992; Hermans & Malissen, 1993; Irving *et al.*, 1993; Kolanus *et al.*, 1993). The initiation of the signal by the TCR occurs via cytoplasmic protein-tyrosine kinases which phosphorylate a 17 residue motif referred to as a "competency motif" or ARAM (for antigen recognition activation motif) (Weiss *et al.*, 1994) in the cytoplasmic tail of the ζ chain (Chan *et al.*, 1991; Chan *et al.*, 1992). Phosphorylation of the CD3 ϵ chain also occurs in the same competency motif (Letourneur & Klausner, 1992; Straus & Weiss, 1993). Signal transduction via the TCR requires the interaction of a number of different tyrosine kinase interactions from the tyrosine kinase families *src*, *syk* and ZAP70 (Burgess *et al.*, 1991; Chan *et al.*, 1991; Chan *et al.*, 1992; Ravichandran *et al.*, 1993).

1.4.2. Major Histocompatibility Complex II (MHC II).

MHC II is important in cell-cell interactions and in antigen presentation (Buus *et al.*, 1987). MHC II molecules are heterodimers consisting of α and β chains which are highly polymorphic. The α and β chains have immunoglobulin-like extracellular domains, transmembrane domains and short cytoplasmic domains (Brown *et al.*, 1988).

MHC II expression can be influenced by various cell mediated and cytokine responses associated with immune cell activation (Geppert *et al.*, 1990). MHC II is expressed on

TcR

CD3

$\beta\alpha$

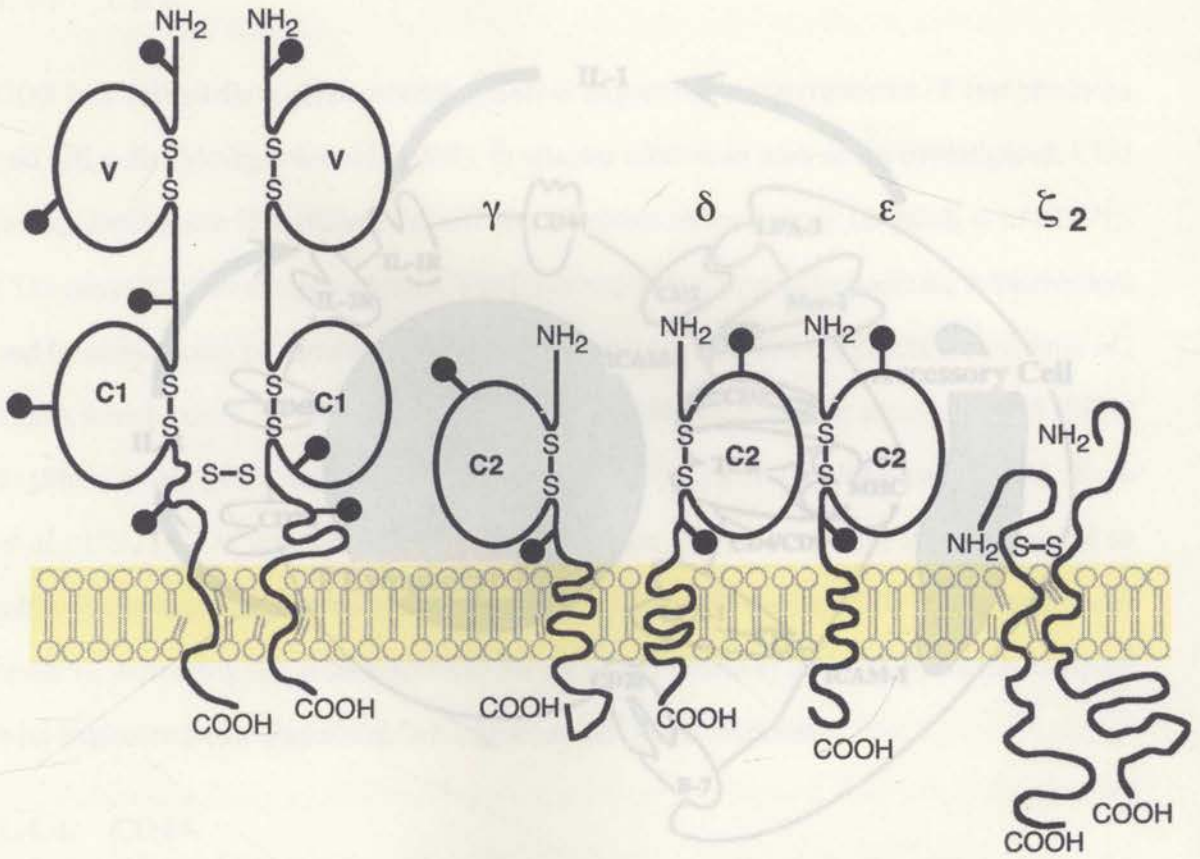


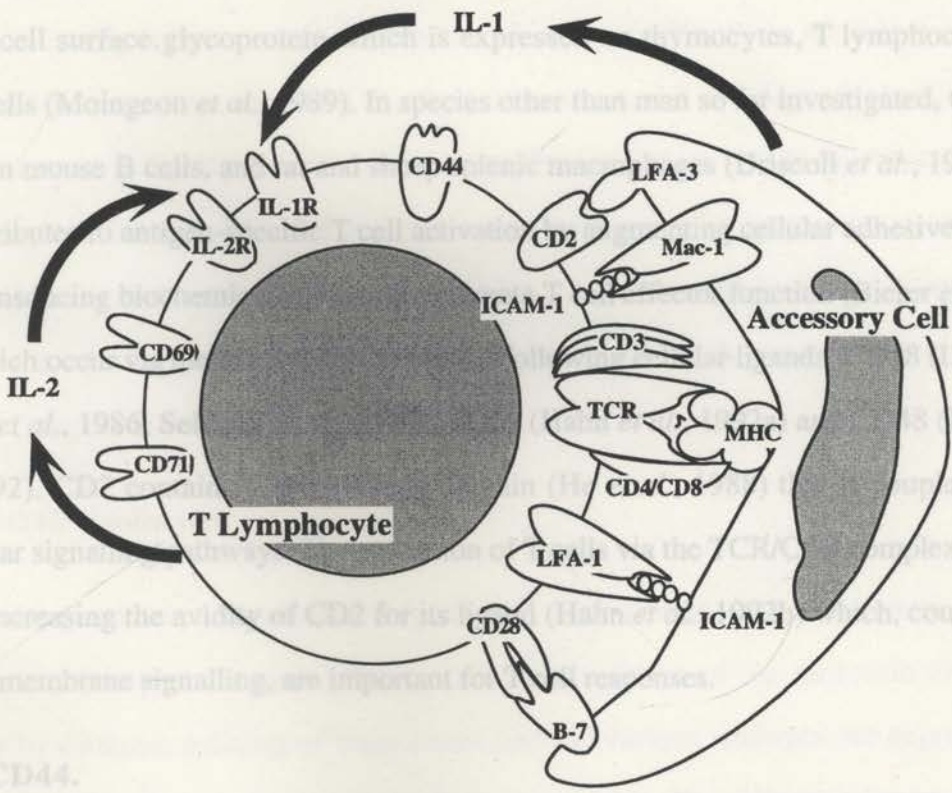
Figure 1.6. T-lymphocyte receptor for antigen. Adapted from Hudson & Hay (1989) and Malissen & Malissen (1996).

involved in T cell activation via interactions with cytokines and accessory cell (APC) receptors.

Langerhans' cells, dendritic cells, B cells, monocytes, macrophages, myeloid and erythroid precursors and some epithelial cells. Expression can be induced on endothelium, fibroblasts, macrophages and T lymphocytes (Korman *et al.*, 1985). MHC Class II molecules usually present antigens to CD4⁺ T cells (Yewdell & Bennink, 1990).

1.4.3. CD2.

CD2 is a cell surface glycoprotein which is expressed on T lymphocytes and NK cells (Moingeon *et al.*, 1989). In species other than man investigated, CD2 is found on mouse B cells, and on T cells of several mammalian species (Kato *et al.*, 1991). CD2 contributes to T cell activation by interacting with LFA-3 on accessory cells and by transducing biological signals to T cells (Kato *et al.*, 1991). CD2 is also involved in the regulation of T cell adhesion to endothelial cells (Shaw *et al.*, 1986; Seaman & Shaw, 1987; Shaw & Seaman, 1988; Kato *et al.*, 1992). CD2 is also involved in the regulation of T cell adhesion to endothelial cells (intracellular signalling pathways). The interaction of CD2 with LFA-3 is coupled to intracellular signalling pathways. The interaction of CD2 with LFA-3 can result in increasing the avidity of CD2 for its ligand (Hain *et al.*, 1991). CD2, coupled with transmembrane signalling, are important for T cell activation.



1.4.4. CD44.

CD44 is expressed in man on T cells, B cells, monocytes, granulocytes and medullary thymocytes and on most erythrocytes (Stamenkovic *et al.*, 1989) but not in the mouse (Hughes *et al.*, 1989). It has also been shown to be expressed on epithelial cells, brain white matter, fibroblasts, skeletal muscle and tumour cells (Stamenkovic *et al.*, 1989).

CD44 binds principally to hyaluronate and this mediates the binding of the cells to the high endothelial venules (Aryffo *et al.*, 1990). The structure of CD44 is similar to

Figure 1.7. T lymphocyte receptors involved in T cell activation via interactions with cytokines and accessory cell (APC) receptors.

1.4.5. LFA-1

Langerhans' cells, dendritic cells, B cells, monocytes, macrophages, myeloid and erythroid precursors and some epithelial cells. Expression can be induced on endothelium, fibroblasts, macrophages and T lymphocytes (Korman *et al.*, 1985). MHC Class II molecules usually present antigen to CD4⁺ T cells (Yewdell & Bennink, 1990).

1989) and ICAM-3 (de Fougerolles & Springer, 1992). LFA-1 is involved in homotypic and heterotypic T and B cell interactions. These include the binding of leukocytes to the

1.4.3. CD2.

CD2 is a cell surface glycoprotein which is expressed on thymocytes, T lymphocytes and NK cells (Moingeon *et al.*, 1989). In species other than man so far investigated, CD2 is found on mouse B cells, and rat and sheep splenic macrophages (Driscoll *et al.*, 1991). CD2 contributes to antigen-specific T cell activation by augmenting cellular adhesiveness and by transducing biochemical signals that promote T cell effector function (Bierer *et al.*, 1989), which occur via the binding of CD2 to the following cellular ligands; CD58 (LFA-3) (Shaw *et al.*, 1986; Selvaraj *et al.*, 1987), CD59 (Hahn *et al.*, 1992a) and CD48 (Kato *et al.*, 1992). CD2 contains a cytoplasmic domain (He *et al.*, 1988) that is coupled to intracellular signalling pathways. The activation of T cells via the TCR/CD3 complex can result in increasing the avidity of CD2 for its ligand (Hahn *et al.*, 1992b) which, coupled with transmembrane signalling, are important for T cell responses.

1.4.6. CD45 Isoforms.

The activation of T cells via the TCR/CD3 complex can result in increasing the avidity of CD2 for its ligand (Hahn *et al.*, 1992b) which, coupled with transmembrane signalling, are important for T cell responses.

1.4.4. CD44.

CD44 is expressed in man on T cells, B cells, monocytes, granulocytes and medullary thymocytes and on most erythrocytes (Stamenkovic *et al.*, 1989) but not in the mouse (Hughes *et al.*, 1989). It has also been shown to be expressed on epithelial cells, brain white matter, fibroblasts, skeletal muscle and tumour cells (Stamenkovic *et al.*, 1989). CD44 binds principally to hyaluronate and this mediates the binding of the cells to the high endothelial venules (Aruffo *et al.*, 1990). The structure of CD44 is similar to

1.4.7. Complement Receptor Type 2 (CD21).

Human CD21 is expressed on mature B cells, follicular dendritic cells, pharyngeal cells,

cervical epithelial cells and some thymocytes (Ahearn & Fearon, 1989). It is the ligand for C3d complement fragment and Epstein Barr virus. It is involved in B cell activation

1.4.5. LFA-1.

associates with surface Ig (Tanner *et al.*, 1987) and complexes with CD35 (Complement receptor 1) and CD19 (regulates proliferation of B cells) (Tuveson *et al.*, 1991). The CD21 gene is one member of the complement activation gene cluster that encodes complement proteins C3b/iC3b (Hourcade *et al.*, 1989). The cytoplasmic domain has protein kinase C and tyrosine kinase sites (Ahearn & Fearon, 1989). LFA-1 mediates cell-cell and cell-matrix adhesion through the binding to its ligands ICAM-1 (Marlin & Springer, 1987), ICAM-2 (Staunton *et al.*, 1989) and ICAM-3 (de Fougerolles & Springer, 1992). LFA-1 is involved in homotypic and heterotypic T and B cell interactions. These include the binding of leukocytes to the endothelium during inflammation, the binding of cytotoxic T cells to the target cells, antigen-specific and mitogen-induced T cell proliferation, and T cell-dependent antibody responses (Larson & Springer, 1990). Signal transduction occurs via the $\beta 2$ subunit and cross-linking of LFA-1 or ICAM-1 in combination with anti-CD3 antibodies results in increased IL-2 production and DNA synthesis. LFA-1 is constitutively expressed and the affinity of the adhesion is changed upon activation of the cell with phorbol ester via the TCR/CD3 complex (Dustin & Springer, 1989).

1.4.6. CD45 isoforms.

expressed on ovine cells of myeloid or erythroid origin during differentiation and is associated with serine protease activity (Deane *et al.*, 1995). The cell surface antigen is present on >80% of ovine nucleated bone marrow cells. CD45 is known as leucocyte common antigen and is expressed on all haematopoietic cells except for erythrocytes (Thomas, 1989). Different isoforms of the molecule can be generated by different splicing of three exons and the various isoforms are expressed differently on different lymphoid cells (Streuli *et al.*, 1990). The differential expression of different isoforms of CD45 are useful in distinguishing naive from memory T cells (Thomas, 1989). The expression of CD45 is necessary for signalling through the T cell receptor via tyrosine phosphatase activity (Pingel & Thomas, 1989). Naive cells may be characterised by the expression of the CD45R isoform while memory cells show a reduced expression of this isoform (MacKay *et al.*, 1990).

1.4.7. Complement Receptor type 2 (CD21).

Human CD21 is expressed on mature B cells, follicular dendritic cells, pharyngeal cells, cervical epithelial cells and some thymocytes (Ahearn & Fearon, 1989). It is the ligand for C3d complement fragment and Epstein Barr virus. It is involved in B cell activation and proliferation (Furtak *et al.*, 1990).

and proliferation, associates with surface Ig (Tanner *et al.*, 1987) and complexes with CD35 (Complement receptor 1) and CD19 (regulates proliferation of B cells) (Tuveson *et al.*, 1991). The CD21 gene is one member of the complement activation gene cluster that encodes complement proteins C3/C4 (Hourcade *et al.*, 1989). The cytoplasmic domain has protein kinase C and tyrosine kinase sites (Ahearn & Fearon, 1989).

Two monoclonal antibodies, 2-74 and 2-104, used in this study (Chapter 6) recognise sheep CD21. They recognise two different isoforms of CR-2, one of which is ubiquitinated in the cytoplasmic domain. Differential expression of these two surface isoforms changes during the life of the B cell, possibly regulated by ubiquitylation of the cytoplasmic region of the protein (Hein, 1995).

1.4.8. 175 antigen.

The 175 antigen (detected with MAb 175) is expressed on ovine cells of myeloid or erythroid origin during differentiation and is associated with serine protease activity (Deane *et al.*, 1995). The cell surface antigen is present on >80% of ovine nucleated bone marrow cells and the level of expression increases on individual bone marrow cells upon differentiation. The antigen is not expressed on basophils, mast cells, or bone marrow lymphocytes. The antigen has been detected in cell surface studies (Miyasaka *et al.*, 1985; Miyasaka & Morris, 1988; Haig *et al.*, 1991; Haig *et al.*, 1992) but has also been detected in the cytoplasm (Deane *et al.*, 1995). The 175 antigen is part of the family of cell-surface proteases identified in man, associated with haemopoietic cell differentiation (Shipp & Look, 1993; Deane *et al.*, 1995).

1.5. Molecular aspects of the immune system. II. Protein kinase C isoenzymes in T cell activation.

The activation of protein kinase C is one of the early essential steps in T cell activation. In T lymphocyte primary cultures all of the recognised PKC isoenzymes have been detected except PKC- δ (Kochs & Reich, 1995). It has been recently shown that the activation of human T cells by the stimulation of the TCR results in a "transient" activation of PKC. Immediately after stimulation the activation of the PKC α

1.5.1. The diversity of protein kinase C isoenzymes.

Protein kinase C was first recognised as a cytoplasmic serine/threonine protein kinase (Takai *et al.*, 1977). It was later recognised as being activated by Ca^{2+} , phospholipids and lipids (specifically diacylglycerol), or phorbol esters (Castagna *et al.*, 1982; Kikkawa *et al.*, 1983; Nishizuka, 1984; Isakov & Altman, 1987). The protein kinase C family is currently known to consist of at least 12 isoenzymes (Azzi *et al.*, 1992; Nishizuka, 1992; Dekker & Parker, 1994). They are divided into three groups: the conventional or calcium-dependent protein kinase Cs (cPKCs), the calcium-independent or novel protein kinase Cs (nPKCs), and the atypical protein kinases Cs (aPKCs) (Knopf *et al.*, 1986; Parker *et al.*, 1986). Within the cPKCs fall the isoforms α , $\beta 1$, $\beta 2$, and γ . The nPKC isoforms are designated δ , ϵ , η , θ and μ . The aPKC isoforms comprise the ζ , π , and τ forms which are calcium independent (Hug & Sarre, 1993; Dekker & Parker, 1994).

Protein kinase C isoforms possess distinctive enzyme specificity and are differentially expressed and distributed in tissues. Phosphatidylserine is a requirement for all isoenzymes. The activities of the isoforms show different sensitivities to Ca^{2+} , fatty acids and phosphatidylinositols. cPKCs are activated by Ca^{2+} and 1,2-diacylglycerols but their activity is also enhanced by *cis*-polyunsaturated fatty acids and lysophosphatidylcholine. The nPKC group are Ca^{2+} insensitive and respond to 1,2-diacylglycerol and to phorbol esters. The ϵ and δ isoforms will respond to free fatty acids from phosphatidylcholine hydrolysis (Nishizuka, 1992; Ha & Exton, 1993b). The ζ isoform can be activated by phosphoinositol phosphates ($\text{PtdIns}(3,4,5)\text{P}_3$) and can be slightly activated by arachidonic acid, phosphatidylserine and γ -linoleic acid (Kochs *et al.*, 1993).

1.5.2. Differential expression of protein kinase C isoenzymes in T lymphocyte activation.

In T lymphocyte primary cultures and cell lines all of the recognised PKC isoenzymes have been detected except for PKC- γ (Szamel & Resch, 1995). It has been recently shown that the activation of human T cells via the stimulation of the TCR results in a "bimodal" activation of PKC. Immediately after stimulation the activation of the PKC α

isoform was observed. This was followed by the activation of PKC β . If the activation of PKC β was inhibited the production of IL-2 was inhibited but not expression of IL-2R α (Szamel *et al.*, 1993). PMA and ionomycin has also been shown to exert differential effects upon the induction of different protein kinase C isoenzymes in human T cells. PMA and ionomycin-stimulated T cells expressed PKC α , β and γ proteins, expressed the IL-2R α , and the transferrin receptor, and proliferated. Unstimulated resting T cells showed mRNA levels for α and β isoforms but very low levels of γ . The use of PMA alone for activation resulted in the expression of the IL-2R α , a 2-3-fold increase in the mRNA level of PKC α and β but not γ , 12 h after stimulation, whereas the use of ionomycin alone resulted in only minimal effects (Altman *et al.*, 1992). These reports imply that the PKC isoforms α and β play a role in the activation of human T lymphocytes. Similar results have also been reported in unstimulated murine CD4 and CD8 thymocyte subsets where the expression of mRNA for PKC- α , β , ϵ and ζ were detected. This implies that there is no relationship between the state of differentiation of the cell and the expression of PKC isoenzymes. However, stimulation of unfractionated thymocytes with PMA and ionomycin, in combination or alone, resulted in differential expression of PKC isoenzymes. PKC- α , β and ζ mRNA were down regulated while PKC- ϵ expression remained unaltered after the stimulation of unfractionated thymocytes with PMA and ionomycin (Freire-Moar *et al.*, 1991; Strulovici *et al.*, 1991). PKC- δ was induced after stimulation with PMA or Concanavalin A (ConA), but was inhibited by the addition of ionomycin (Freire-Moar *et al.*, 1991).

The subcellular distribution of isoenzymes of PKC is different in T cells with different modes of action. The distribution and localisation of PKC in the cell in turn can influence the enzyme activity (Keenan *et al.*, 1995). In a human T cell line K4, PKC- ζ was stained using specific antibodies after stimulation using OKT3 antibody which stimulates via the TCR. Enzyme distribution changed from a diffuse pattern in unstimulated cells to spike like protrusions after stimulation. No change in the expression of the PKC- ζ isoform was evident when the cells were stimulated with PMA. This isoform is independent of

phorbol esters and Ca^{2+} but has been activated by *cis*-polyunsaturated fatty acids and lysophosphatidylcholine (which would arise from phosphatidylcholine catabolism).

Collectively these results show that the expression and activation of different PKC isoforms are crucial for activation, are cell type specific and are dependent upon the mode of cell stimulation. The Ca^{2+} -independent PKC isoforms also locate to specific cellular locations after activation. These observations suggest that there are a number of ways in which PKC activation in T cells can be regulated (Keenan *et al.*, 1995) (Figure 1.8).

1.6. Molecular aspects of the immune system. III. Lipid structure and metabolism.

Lipids are organic, water-insoluble molecules. They are amphipathic molecules with polar and non-polar regions. The presence of a polar head group and fatty acid non-polar chains can dictate the formation of bilayers as found in biological membranes (Petty, 1993). These properties lend themselves to the formation of organised structures such as cellular membranes, which form impermeant barriers at the cell surface. The relative lipid composition of membranes can vary widely between 30-80% by weight. Lipids are composed of three main groups: glycerophosphatides, sphingolipids and sterols. As well as having important structural functions, lipids and their metabolites are involved in cell signalling processes (Pelech & Vance, 1989; Mathews & van Holde, 1990; Petty, 1993).

A variety of lipids, such as fatty acids, diacylglycerols, triglycerides, phospholipids, sterols, leukotrienes and prostaglandins, are involved in activation and inflammatory responses in a variety of immune cells. Since lipids are largely hydrophobic, there are a number of constraints upon their arrangement, diffusion and mobility within the hydrophilic environment of the cytoplasm (Singer, 1972). When these lipids have some degree of isotropic molecular motion- that is, they are mobile to some degree- they can be detected using $^1\text{H-NMR}$ spectroscopy (see Appendix 1). Therefore, from this section onwards, $^1\text{H-NMR}$ -detectable lipids will be described as mobile lipids. Previous studies

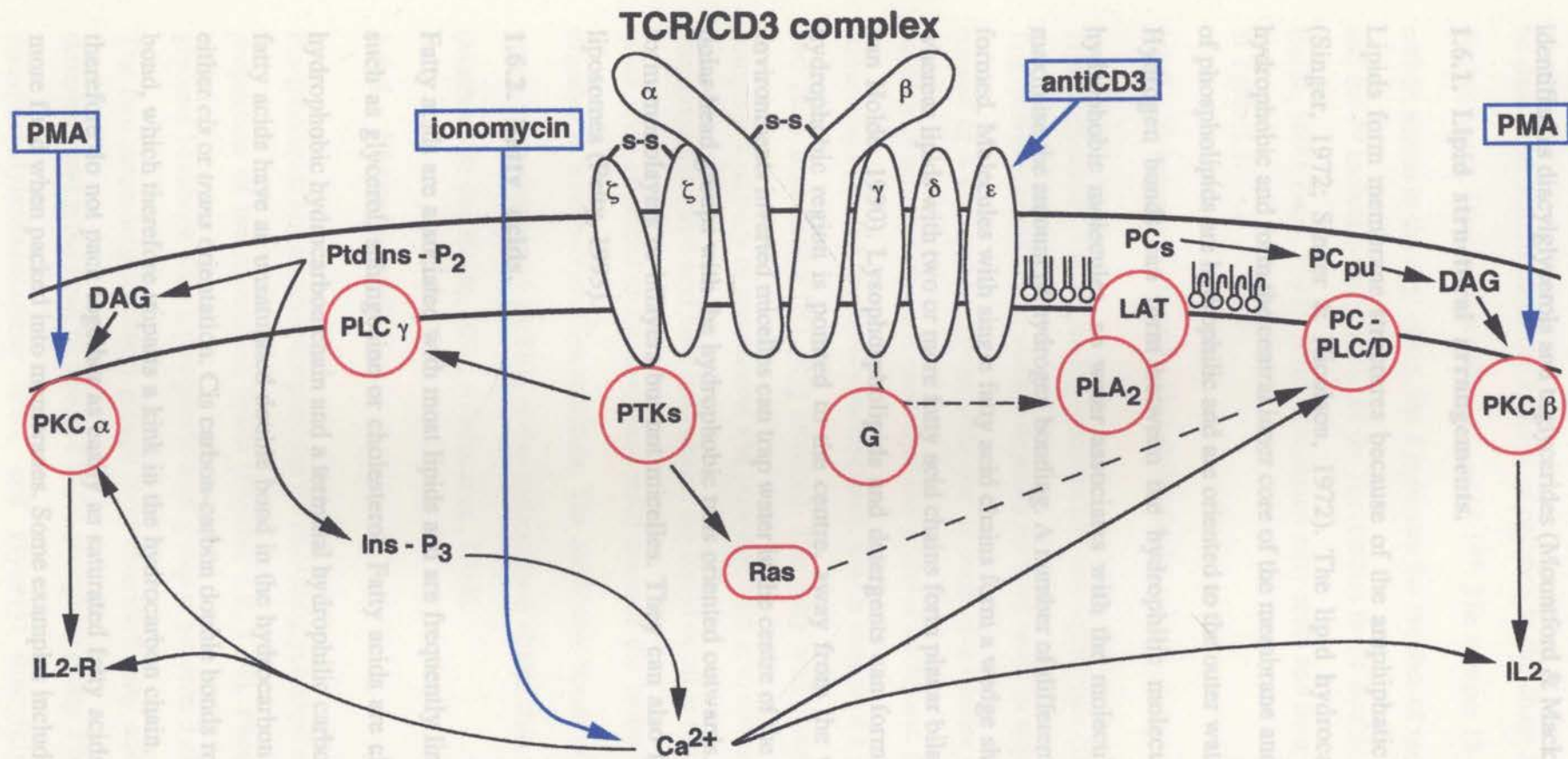


Figure 1.8. Model for the T cell receptor/CD3-induced signal transduction pathways in the plasma membrane. The modes by which PMA, ionomycin and antiCD3 antibody effect signal transduction are indicated. anti-CD3, anti-CD3 antibody; Ca²⁺, calcium ion; CD3, cluster of differentiation 3; DAG, diacylglycerol; G, G-protein; IL2, interleukin-2; IL2-R, interleukin-2 receptor; InsP₃, inositol triphosphate; LAT, lysophosphatidylcholine acyl transferase; PC-PLC/D, phosphatidylcholine-phospholipase C or D isoform; PC_{pu}, phosphatidylcholine with unsaturated acyl chains; PC_s, phosphatidylcholine with saturated acyl chains; PKC α , protein kinase C α isoform; PKC β , protein kinase C β isoform; PLA₂, phospholipase A₂ isoform; PLC γ , phospholipase C γ isoform; PMA, phorbol myristate acetate; PtdIns-P₂, phosphatidylinositol 4,5-bisphosphate; PTKs, protein tyrosine kinases; Ras, Ras oncogene; TCR, T cell receptor. Some of the subunits of the TCR/CD3 complex are covalently bound by disulphide bridges. Adapted from Szamel and Resch (1995).

acid and linoleic acid. The numbering of the carbons begins at the carboxyl end. of cells have used $^1\text{H-NMR}$ spectroscopy to detect mobile lipids which have been identified as diacylglycerols and triglycerides (Mountford & Mackinnon, 1994).

1.6.1. Lipid structural arrangements.

Lipids form membrane structures because of the amphiphatic features of the lipids (Singer, 1972; Singer & Nicolson, 1972). The lipid hydrocarbon side chains are hydrophobic and form the central inner core of the membrane and the polar head groups of phospholipids are hydrophilic and are oriented to the outer water membrane interface. Hydrogen bonds can form between the hydrophilic molecules but not with the hydrophobic molecules, so water associates with the molecules at the interface to maximise the amount of hydrogen bonding. A number of different lipid structures can be formed. Molecules with single fatty acid chains form a wedge shape and form micelles, whereas lipids with two or more fatty acid chains form planar bilayer sheets (Mathews & van Holde, 1990). Lysophospholipids and detergents can form micelles in which the hydrophobic region is pointed to the centre, away from the water. In hydrophobic environments inverted micelles can trap water in the centre of the micelle associated with polar head groups with the hydrophobic tails oriented outwards. Glycerophospholipids form monolayers or bilayers but not micelles. They can also form lipid vesicles and liposomes (Petty, 1993).

1.6.2. Fatty acids.

Fatty acids are associated with most lipids and are frequently linked to other molecules such as glycerol, sphingosine or cholesterol. Fatty acids are characterised by a long, hydrophobic hydrocarbon chain and a terminal hydrophilic carboxylic acid group. Some fatty acids have an unsaturated double bond in the hydrocarbon chain, which can be of either *cis* or *trans* orientation. *Cis* carbon-carbon double bonds restrict rotation about the bond, which therefore imparts a kink in the hydrocarbon chain. Unsaturated fatty acids therefore do not pack together as easily as saturated fatty acids, and are consequently more fluid when packed into membranes. Some examples include oleic acid, palmitoleic

acid and linoleic acid. The numbering of the carbons begins at the carboxyl end. Unsaturated double bonds are usually found between carbons 9 and 12. Fatty acids can be described according to the number of carbons in the chain and the position of the double bonds. Oleic acid is referred to as 18:1 Δ^9 . The number 18 refers to the number of carbon atoms in the acyl chain, the 1 indicates the number of unsaturated double bonds and the Δ^9 indicates the position of the first carbon in the double bond (Mathews & van Holde, 1990; Petty, 1993). A list of common fatty acids and their nomenclature is shown in Table 1.1.

1.6.3. Triglycerides and diacylglycerols.

Triacylglycerols (TAGs) are triglycerides and diacylglycerols (DAGs) are diglycerides. Triglycerides are efficient storage deposits for fatty acids in animal cells. Triglycerides consist of a glycerol backbone with one of each of a triester of fatty acids (R1-R3) covalently attached to each carbon of the glycerol backbone. DAGs activate PKC in stimulated cells and are rapidly metabolised. DAGs consist of a glycerol backbone with two fatty acid chains (R1, R2) attached. The fatty acid chains R1, R2 and R3 can comprise a mixture of unsaturated and saturated fatty acid chains. The triglycerides that contain unsaturated acyl fatty acid chains are liquid or oil at room temperature whereas those with saturated chains are more solid because the hydrocarbon chains can pack together in a semi-crystalline structure. The *cis*-double bonds of unsaturated fatty acids cause more disordered packing of the hydrocarbon chains than the *trans* configuration (Mathews & van Holde, 1990; Alberts *et al.*, 1994).

1.6.4. Phospholipids.

Phospholipids are glycerophosphatides (or phosphoglycerides) and comprise the largest proportion of the membrane lipids (Figures 1.9, 1.10). Phospholipids consist of a glycerol backbone with a phosphoric acid group at position 3 of the glycerol molecule. The two remaining hydroxyl groups have esterified fatty acid chains. A number of different head groups can be attached to the phosphate group. Phosphatidylcholine (PC), phosphatidylethanolamine (PE), and glycosyl diacylglycerols (glycosylated

Notation	Name	IUPAC Name
14 : 0	Myristic acid	<i>n</i> -tetradecanoic
16 : 0	Palmitic acid	<i>n</i> -hexadecanoic
16 : 1 Δ^9	Palmitoleic acid	<i>cis</i> -9-hexadecenoic
18 : 0	Stearic acid	<i>n</i> -octadecanoic
18 : 1 Δ^9	Oleic acid	<i>cis</i> -9-octadecenoic
18 : 1 Δ^9trans	Elaidic acid	<i>trans</i> -9-octadecenoic
18 : 1 Δ^{11}	Vaccenic acid	<i>cis</i> -11-octadecenoic
18 : 2 $\Delta^{9,12}$	Linoleic acid	<i>cis-cis</i> -9,12,15-octadecatrienoic
18 : 3 : 2 $\Delta^{9,12,15}$	α -Linoleic acid	all- <i>cis</i> -9,12,15-octadecatrienoic
20 : 0	Arachidic acid	<i>n</i> -eicosanoic
20 : 4 $\Delta^{5,8,11,14}$	Arachidonic acid	all- <i>cis</i> -5,-8,-11,-14-eicosatetraenoic
22 : 0	Behenic acid	<i>n</i> -docosanoic
24 : 0	Lignoceric acid	<i>n</i> -tetracosanoic

Table 1.1. Common Fatty Acids.

Taken from Petty (1993).

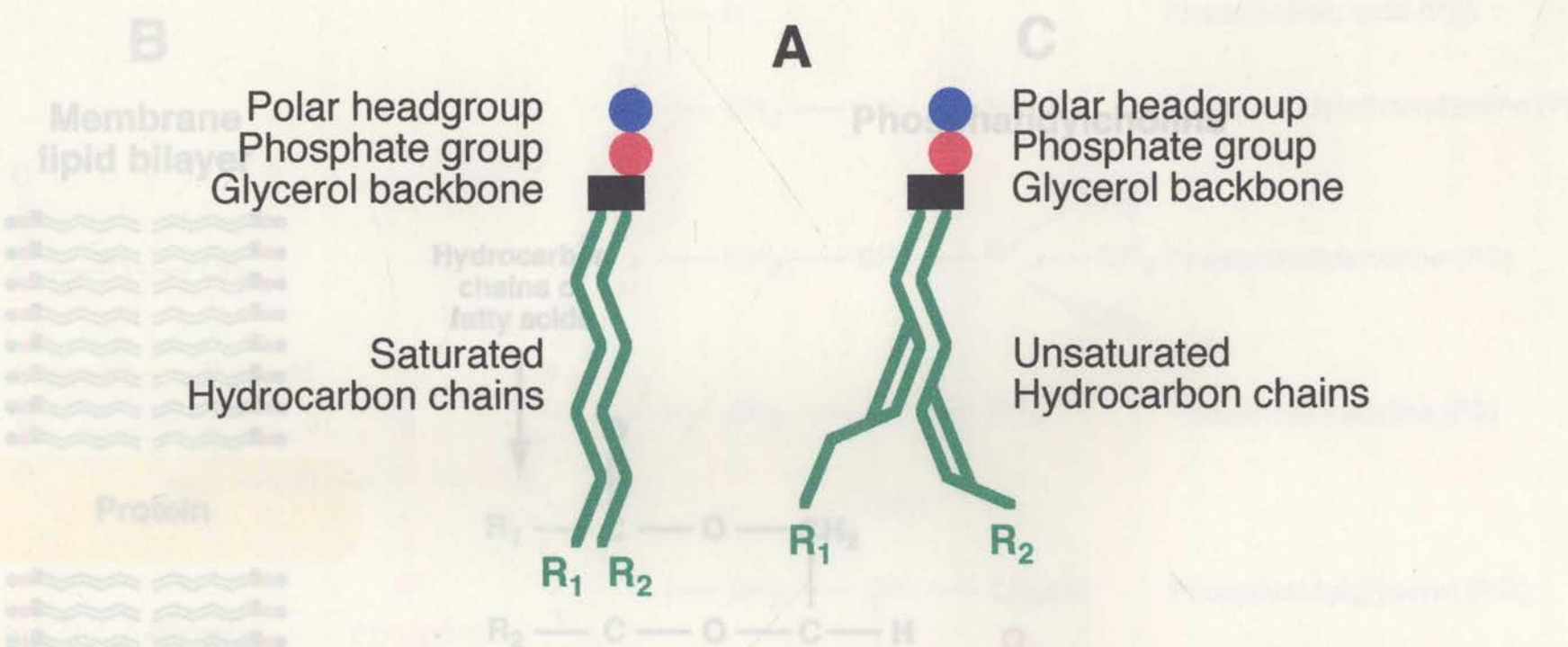
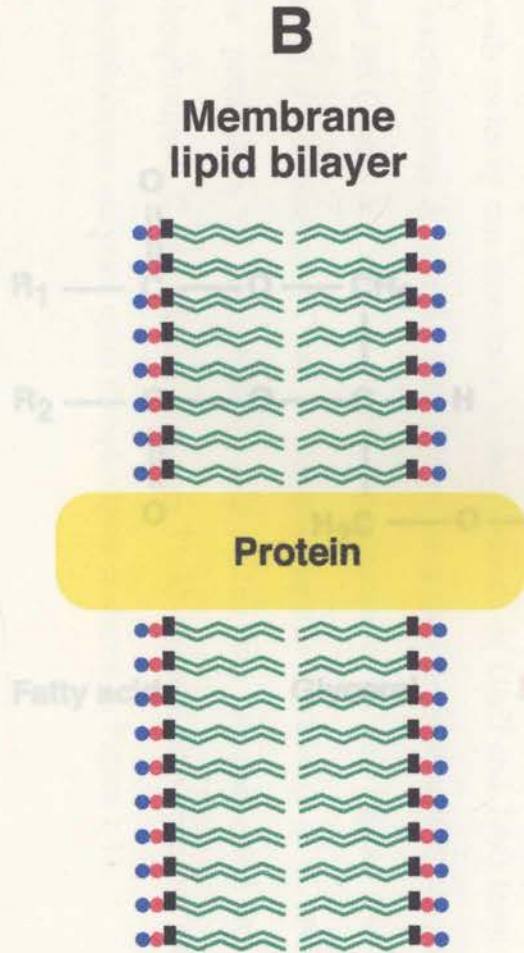


Figure 1.9. The structure and arrangement of phospholipids within the cell membrane and a typical phospholipid.

- A. The general structure of phospholipids containing saturated or unsaturated hydrocarbon chains.
- B. Polar headgroups align towards solution, while hydrophobic hydrocarbon chains align towards each other in the interior of the membrane. Proteins are incorporated into the membrane according the same principles, with hydrophilic residues generally pointing out and hydrophobic residues generally associated within the membrane bilayer with the hydrophobic moieties of the phospholipids. The colours of the different moieties correspond with the colours in Panel A.
- C. The structure of Phosphatidylcholine. The colours of the different moieties correspond with the colours in Panel A.



Hydrocarbon chains of fatty acids

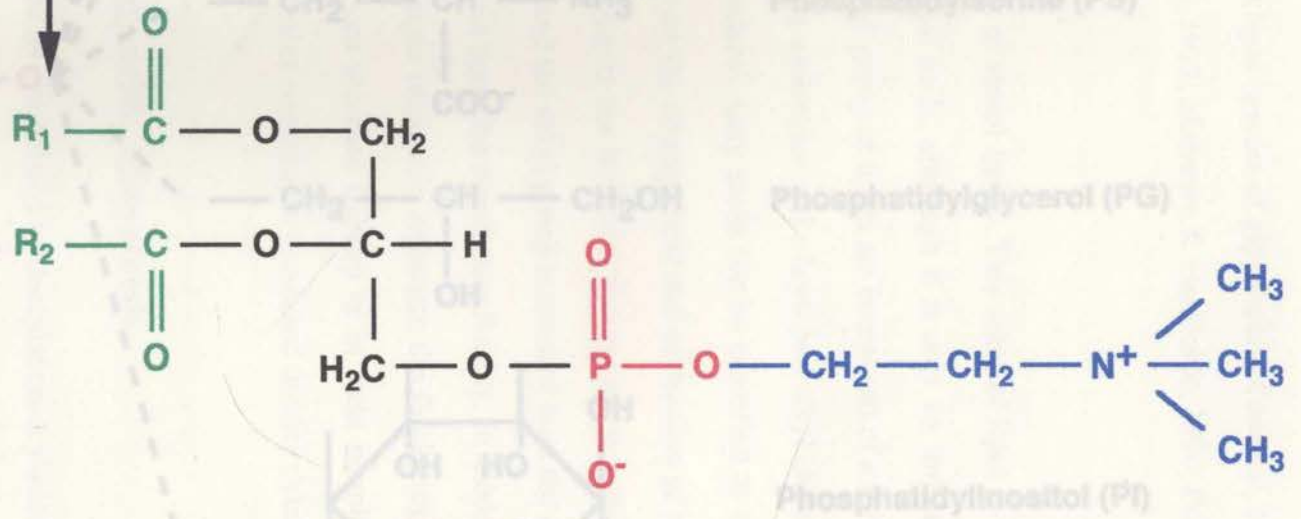


Figure 1.9 continued.

Figure 1.10. Phospholipids with different headgroups.

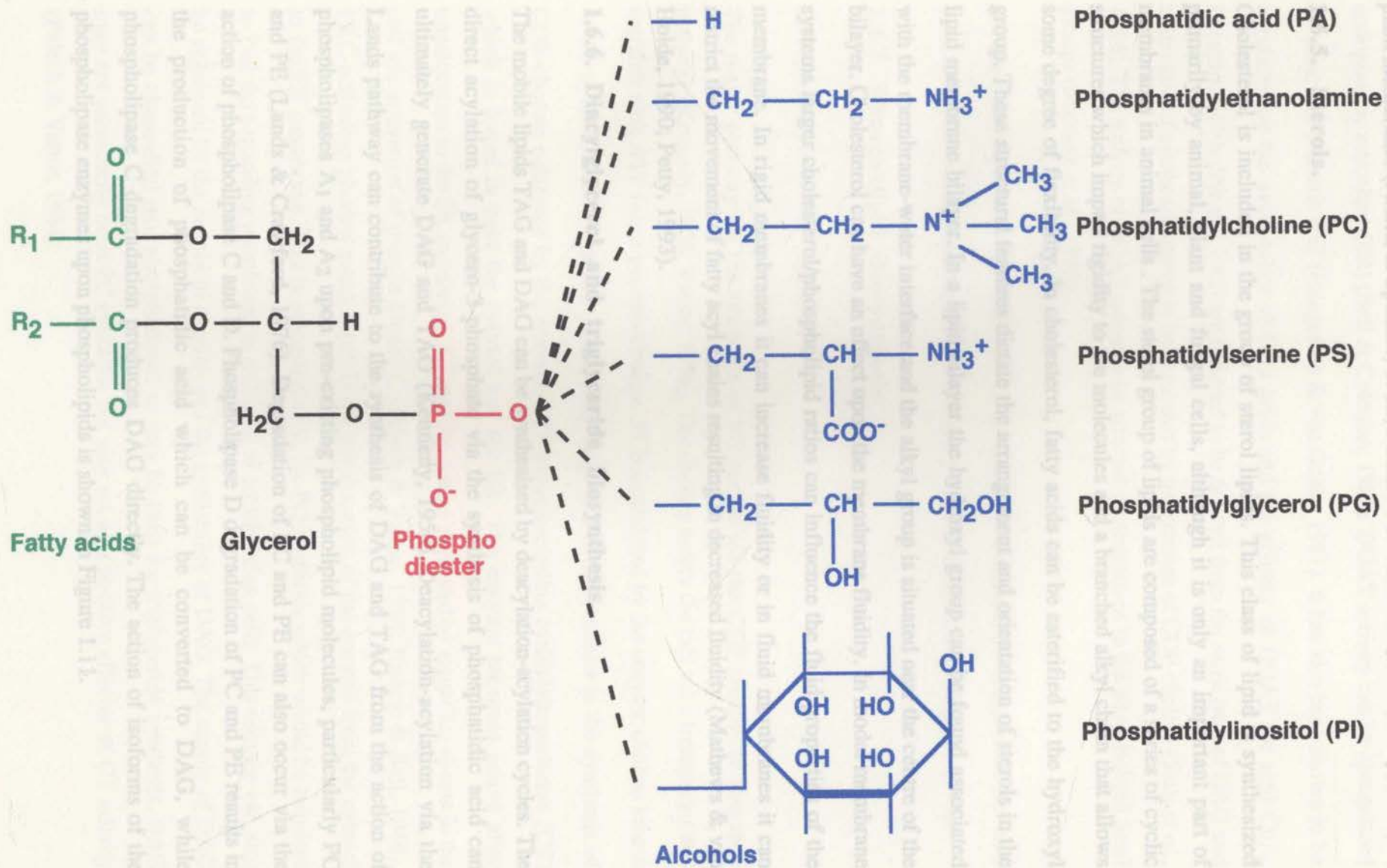


Figure 1.10. Phospholipids with different headgroups.

diacylglycerols) are the predominant lipid species of glycolipids of animal, bacterial and plant membranes (Ansell & Spanner, 1982; Mathews & van Holde, 1990; Petty, 1993).

1.6.5. Sterols.

Cholesterol is included in the group of sterol lipids. This class of lipid is synthesized primarily by animal, plant and fungal cells, although it is only an important part of membranes in animal cells. The sterol group of lipids are composed of a series of cyclic structures which impart rigidity to the molecules and a branched alkyl chain that allows some degree of flexibility. In cholesterol, fatty acids can be esterified to the hydroxyl group. These structural features dictate the arrangement and orientation of sterols in the lipid membrane bilayer. In a lipid bilayer the hydroxyl group can be found associated with the membrane-water interface and the alkyl group is situated near the centre of the bilayer. Cholesterol can have an effect upon the membrane fluidity. In model membrane systems larger cholesterol/phospholipid ratios can influence the fluid properties of the membrane. In rigid membranes it can increase fluidity or in fluid membranes it can restrict the movement of fatty acyl chains resulting in decreased fluidity (Mathews & van Holde, 1990; Petty, 1993).

1.6.6. Diacylglycerol and triglyceride biosynthesis.

The mobile lipids TAG and DAG can be synthesised by deacylation-acylation cycles. The direct acylation of glycerol-3-phosphate via the synthesis of phosphatidic acid can ultimately generate DAG and TAG (Kennedy, 1956). Deacylation-acylation via the Lands pathway can contribute to the synthesis of DAG and TAG from the action of phospholipases A₁ and A₂ upon pre-existing phospholipid molecules, particularly PC and PE (Lands & Crawford, 1976). Degradation of PC and PE can also occur via the action of phospholipase C and D. Phospholipase D degradation of PC and PE results in the production of phosphatidic acid which can be converted to DAG, while phospholipase C degradation produces DAG directly. The action of isoforms of the phospholipase enzymes upon phospholipids is shown in Figure 1.11.

Triglycerides (TAG) are also synthesised from diacylglycerol (DAG) via the activity of the enzyme diacylglycerol acyltransferase (DGAT) at the cytosolic surface of the endoplasmic reticulum (ER) (Bell & Coleman, 1983). DGAT activity can be upregulated by oleic and palmitic acid (Haagsman & van Golde, 1981). It has also been shown to be regulated by the availability of fatty acids and the affinity of DGAT for acyl-CoA. Phosphatidylcholine and TAG are believed to be derived from the same pool of DAG and their rates of synthesis appear to be regulated by the amount of CDP-choline (Stals *et al.*, 1994). The activity of DGAT can also be affected by alterations in the phospholipid head groups (Maziere *et al.*, 1990).

An alternative pathway for TAG and DAG synthesis via monoacyltransferase has also been demonstrated in hepatocytes of developing animals (Coleman & Haynes, 1984).

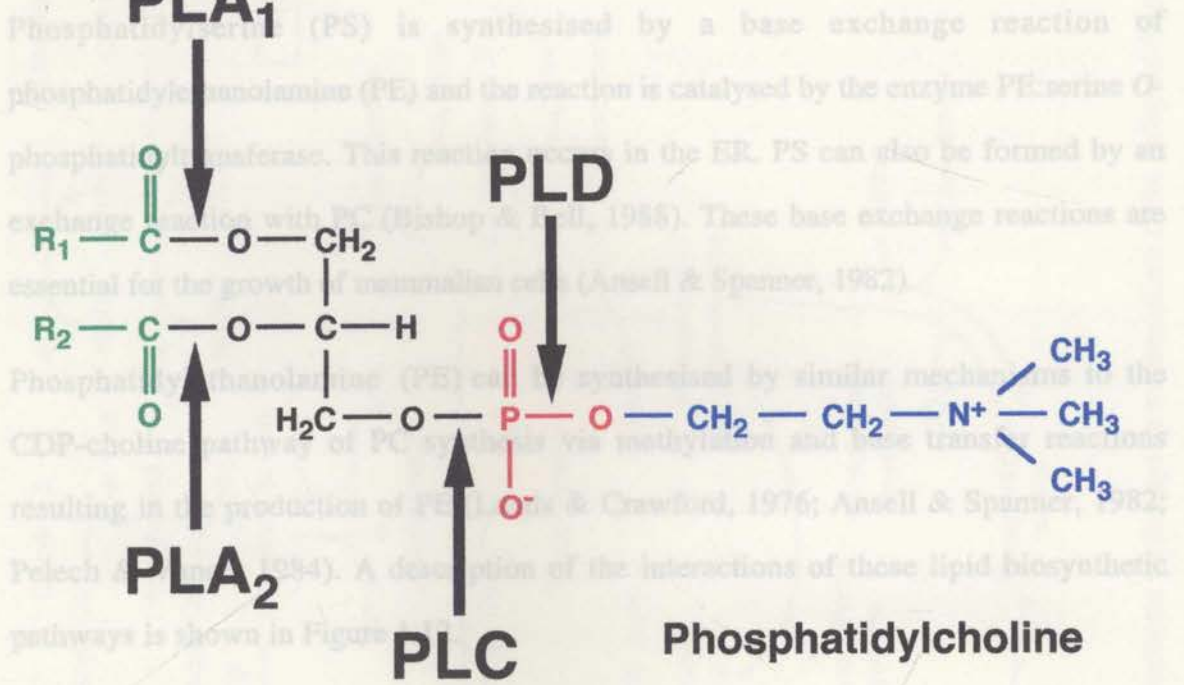
1.6.7. Phospholipid biosynthesis.

Phosphatidylcholine synthesis

The major pathway for the synthesis of PC occurs via the CDP-choline or Kennedy pathway (Kennedy, 1956; Vance, 1986). The choline enters the cell via a transporter and together with ATP forms phosphocholine (PCho) catalysed by the enzyme choline kinase in the cytosol. One of the rate controlling steps in PC biosynthesis is the synthesis of CDP-choline catalysed by the enzyme CTP-phosphocholine cytidylyltransferase (CT) which is found in both the cytosol and the ER. The enzyme becomes active after translocation to the ER membrane. CT activity can be regulated by signalling events in the cell via activation of protein kinase C (Pelech & Vance, 1984; Bishop & Bell, 1988). PKC-activating phorbol esters result in the translocation of the enzyme from the cytosol to the ER membrane. This is consistent with the PC synthesis which would be required to fuel the expanding membrane in activated or proliferating cells. This enzyme can also be regulated by the supply of choline and the availability of DAG. The supply of DAG can be channelled into phospholipids or may be used for triglyceride synthesis. DAG may not necessarily limit PC synthesis but may act as a positive effector of CT activity (Pelech & Vance, 1984).

The final step in PC synthesis is the incorporation of the CDP-choline to DAG which is catalysed by the enzyme CDP-choline:1,2-diacylglycerol phosphocholine transferase (Patty, 1993).

Phosphatidylethanolamine and phosphatidylserine metabolism



1.6.8. The Effects of phospholipid-derived metabolites on protein kinase C in T cell activation.

The proposed "bimodal model" for the activation of T cells (Figure 1.8) suggests that there are two phases of PKC stimulation. After the stimulation of the TCR 1,2-diacylglycerol (DAG) is produced via the hydrolysis of a series of inositol

Figure 1.11. Chemical bond specificity of cleavage sites on Phosphatidylcholine for various Phospholipases. PLA₁, Phospholipase A₁; PLA₂, Phospholipase A₂; PLC, Phospholipase C; PLD, Phospholipase D. Adapted from Liscovitch (1992) and Cheng (1994).

are necessary. The sustained production of DAG in the second phase of activation is thought to occur via the metabolism of phospholipids, particularly phosphatidylcholine in stimulated cells (van Blitterswijk *et al.*, 1991b; van Blitterswijk *et al.*, 1991a; Chen *et al.*, 1992; Liscovitch, 1992; Nishizuka, 1992; Boarder, 1994). The extended or prolonged activation of PKC is essential for cellular differentiation and

The final step in PC synthesis is the incorporation of the CDP-choline to DAG which is catalysed by the enzyme CDP-choline:1,2-diacylglycerol phosphocholine transferase (Petty, 1993).

Phosphatidylethanolamine and phosphatidylserine metabolism

Phosphatidylserine (PS) is synthesised by a base exchange reaction of phosphatidylethanolamine (PE) and the reaction is catalysed by the enzyme PE:serine *O*-phosphatidyltransferase. This reaction occurs in the ER. PS can also be formed by an exchange reaction with PC (Bishop & Bell, 1988). These base exchange reactions are essential for the growth of mammalian cells (Ansell & Spanner, 1982).

Phosphatidylethanolamine (PE) can be synthesised by similar mechanisms to the CDP-choline pathway of PC synthesis via methylation and base transfer reactions resulting in the production of PE (Lands & Crawford, 1976; Ansell & Spanner, 1982; Pelech & Vance, 1984). A description of the interactions of these lipid biosynthetic pathways is shown in Figure 1.12.

1.6.8. The Effects of phospholipid-derived metabolites on protein kinase C in T cell activation.

The proposed "bimodal model" for the activation of T cells (Figure 1.8) suggests that there are two phases of PKC stimulation. After the stimulation of the TCR 1,2-diacylglycerol (DAG) is produced via the hydrolysis of a series of inositol phospholipids such as PtdIns(4,5)P₂. This results in the production of InsP₃ and the subsequent release of intracellular stores of Ca²⁺ from the endoplasmic reticulum. This production of DAG is relatively transient. For long-term stimulation of PKC, sustained increases in DAG are necessary. The sustained production of DAG in the second phase of activation is thought to occur via the catabolism of phospholipids, particularly phosphatidylcholine in stimulated cells (van Blitterswijk *et al.*, 1991b; van Blitterswijk *et al.*, 1991a; Chen *et al.*, 1992; Liscovitch, 1992; Nishizuka, 1992; Boarder, 1994). The extended or prolonged activation of PKC is essential for cellular differentiation and

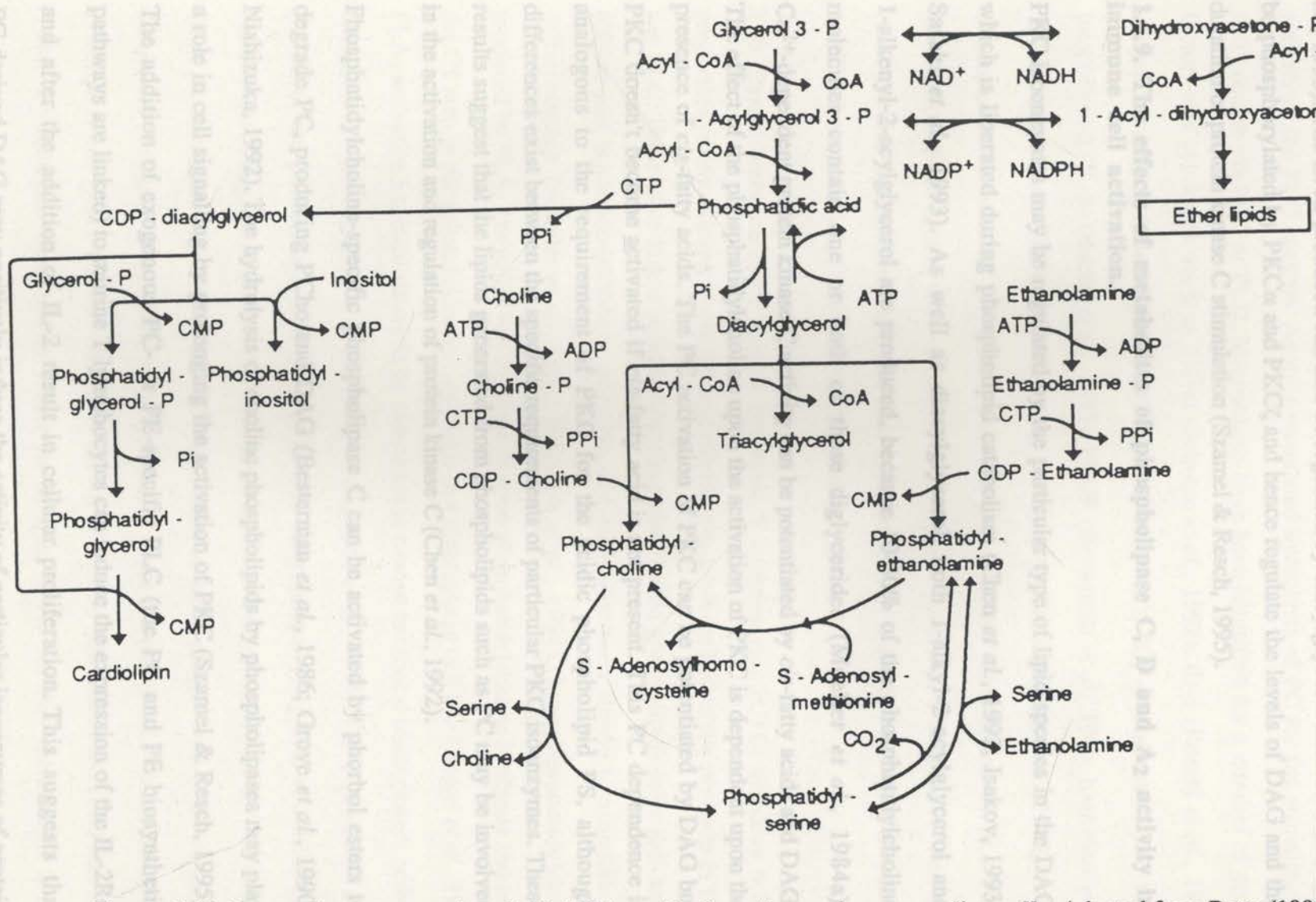


Figure 1.12. Interactions among phospholipid biosynthetic pathways in mammalian cells. Adapted from Petty (1993).

proliferation (Berry *et al.*, 1990; Nishizuka, 1992). In T cells it is necessary for IL-2 production (Davis & Lipsky, 1989; Szamel *et al.*, 1989; Szamel *et al.*, 1990; Szamel *et al.*, 1993). The DAG produced can also be regulated by diacylglycerol kinases which can be phosphorylated by PKC α and PKC ζ and hence regulate the levels of DAG and the duration of protein kinase C stimulation (Szamel & Resch, 1995).

1.6.9. The effects of metabolites of phospholipase C, D and A₂ activity in immune cell activation.

PKC isoenzymes may be regulated by the particular type of lipid species in the DAG which is liberated during phospholipid catabolism (Chen *et al.*, 1992; Isakov, 1993; Sasaki *et al.*, 1993). As well as diacylglycerol, both 1-alkyl-2-acylglycerol and 1-alkenyl-2-acylglycerol are produced, because 10-50% of the phosphatidylcholine molecules contain one or both of these diglycerides (Mueller *et al.*, 1984a). Ca²⁺-dependent protein kinase C activity can be potentiated by *cis*-fatty acids and DAG. The effect of the phosphatidylcholine upon the activation of PKC is dependent upon the presence of *cis*-fatty acids. The PC activation of PKC can be potentiated by DAG but PKC doesn't become activated if *cis*-fatty acid is not present. This PC dependence is analogous to the requirement of PKC for the acidic phospholipid PS, although differences exist between the specific requirements of particular PKC isoenzymes. These results suggest that the lipids generated from phospholipids such as PC may be involved in the activation and regulation of protein kinase C (Chen *et al.*, 1992).

Phosphatidylcholine-specific phospholipase C can be activated by phorbol esters to degrade PC, producing PCho and DAG (Besterman *et al.*, 1986; Grove *et al.*, 1990; Nishizuka, 1992). The hydrolysis of choline phospholipids by phospholipases may play a role in cell signalling by prolonging the activation of PKC (Szamel & Resch, 1995). The addition of exogenous PC- or PE-specific PLC (the PC and PE biosynthetic pathways are linked) to murine T lymphocytes can induce the expression of the IL-2R α and after the addition of IL-2 result in cellular proliferation. This suggests that PC-derived DAG may positively induce the activity of particular isoenzymes of protein

kinase C (Isakov, 1993). The increases in IL-2R α expression shown in PMA or PMA and ionomycin-stimulated cells may be a result of the activation of PLC (Figure 5.2). This may be due to the combined effect of the phorbol ester PMA on the activation of PKC and on the activity of the PLC enzyme. Agonist-stimulated hydrolysis of PC for the stimulation of PKC occurs via PLC or PLD. Mechanisms have been identified for a number of growth factors and cytokines, such as TNF α (Schutze *et al.*, 1992), IL-1 (Rosoff *et al.*, 1988), colony stimulating factor-1 (CSF-1) (Tessner *et al.*, 1991), TGF- β (Halstead *et al.*, 1995), interleukin-8 (IL-8) (Bacon *et al.*, 1995), PDGF (Besterman *et al.*, 1986; Larrodera *et al.*, 1990), interferon- α (INF α) (Pfeffer *et al.*, 1990), epinephrine (Slivka *et al.*, 1988) and the chemotactic microbial peptide, f-met-leu-phe (fMLP) (Tronchere *et al.*, 1995). Pharmacological agents such as phorbol esters and synthetic DAGs have also been demonstrated to stimulate PC hydrolysis and can directly activate PKC (Guy & Murray, 1982; Besterman *et al.*, 1986; Kolesnick & Paley, 1987).

The plasma membranes of murine cytotoxic T lymphocytes (CTL) contains a large proportion of ether-linked glycerophospholipids which are the hydrolytic products of PLA₂ and PLC. These ether-linked phospholipids and ether-linked glycerolipids show anti-tumour effects and immunomodulatory activities and have also been shown to stimulate cell differentiation (Asaoka *et al.*, 1991; Nishihira *et al.*, 1994). Lysophosphatidylcholine produced by PLA₂ can negatively regulate *de novo* phosphatidylcholine synthesis and acts at the CT step in phosphatidylcholine synthesis in a macrophage cell line (Boggs *et al.*, 1995). PLA₂ activation has been shown to be stimulated in murine peritoneal macrophages activated with LPS or zymosan (Grove *et al.*, 1990; de Carvalho *et al.*, 1995). The degradation of PC via PLA₂ can produce arachidonic acid (AA) in macrophages (Triggiani *et al.*, 1994) and neutrophils (Triggiani *et al.*, 1991). TAG can function as a reacylation pool for AA released from phospholipid degradation after the activation of macrophages with PMA or calcium ionophore (Triggiani *et al.*, 1994) or in zymosan or f-met-leu-phe (f-MLP) stimulated PMNs (Phillips *et al.*, 1986). AA has also been shown to directly stimulate PKC (McPhail *et al.*, 1984). Cytoplasmic lipid bodies which act as lipid stores for AA metabolism in PMN

cells have also been shown to be induced by PKC or *cis*-fatty acids in neutrophils (Weller *et al.*, 1991).

Phosphatidic acid (PA), the metabolic product of phosphatidylcholine hydrolysis by PLD, and lysophosphatidic acid, the product of PLA₂ action on PA, have been shown to have cellular biological activity, such as mitogenic effects, in a variety of cells (Eichholtz *et al.*, 1992; Ha & Exton, 1993a; Exton, 1994a). IL-2 responses in the T lymphocyte clone CTLL-2 can be regulated by phosphatidic acid (Cano *et al.*, 1992). The expression of the IL-2R α (CD25) and the RNA transcription of *c-myc* can be induced by the addition of PA to CTLL cells (Cano *et al.*, 1992). IL-2 binding to its receptor in T lymphocytes results in the production of phosphatidic acid which can be converted to DAG by PA phosphohydrolase. IL-2 dependent cell growth can be effected by the inhibition of the alpha isoform of DG kinase which converts DAG to PA. IL-2 induced PA can cause the arrest of IL-2 dependent T lymphocytes in the late G₁ phase of the cell cycle (See section 1.9). PA is therefore an important product which is linked to IL-2 dependent cell growth via the activation of DG kinase alpha isoform (Flores *et al.*, 1996). Phosphatidylcholine cycling has also been recently shown to occur in PMA or f-MLP activation of human neutrophils via agonist-mediated stimulation of phospholipase D (Tronchere *et al.*, 1995).

1.6.10. PC-specific phospholipase C inhibition using the xanthate tricyclodecan-9-yl-xanthogenate (D609).

The compound D609 has been identified as an anti-tumour and anti-viral agent (Mueller-Decker *et al.*, 1988; Music *et al.*, 1989) and has been shown to specifically inhibit the enzyme phospholipase C, thereby preventing PC catabolism (Mueller-Decker *et al.*, 1988; Mueller-Decker, 1989; Arenzana-Seisdedos *et al.*, 1993). This inhibitor has also been used to inhibit tumour necrosis factor (TNF) signalling via the PC-specific phospholipase C pathway in U937 monocyte cell line and the leukaemia cell line Jurkat (Schutze *et al.*, 1992). The anti-viral nature of the D609 in human immunodeficiency virus (HIV) infection has been shown to be mediated by the inhibition of the up-regulation of the nuclear transcription factor NF- κ B. This transcription factor can be

induced via receptor-mediated PC-specific phospholipase C catabolism of PC. The production of DAG via PC catabolism results in sustained activation of protein kinase C (PKC) which is necessary for IL-2R α gene induction and proliferation in T lymphocytes. PKC is also important for monocyte activation. NF- κ B can also be induced by influenza virus haemagglutinin (Pahl & Baeuerle, 1995). Influenza virus also causes changes in the ¹H-NMR-detectable mobile lipids and the choline/phosphocholine groups detectable in infected chicken fibroblasts (Mountford *et al.*, 1981). Similar changes have also been observed in HIV infected T cell lines indicating that infection with these viruses has caused an alteration to the PC and lipid metabolism in infected cells (Luciani *et al.*, 1991) which would be consistent with the relationship between PC catabolism and signal transduction in these cells. A recent report has also shown that the compound D609 can inhibit phorbol ester- or nucleotide-induced phospholipase D activity and PLC-mediated PE hydrolysis in NIH 3T3 fibroblasts, although, it was only possible to inhibit the activity of PLD in membrane fractions but not in intact cells. It was thought that the inhibitory activity may be dependent upon the type of activator which may induce specific D609 resistant forms of PLD (Kiss & Tomono, 1995).

1.7. NMR studies of phospholipid metabolism and mobile lipids in cells.

Nuclear magnetic resonance (NMR) spectroscopy is a useful non-invasive tool to study cellular metabolism of lipids and phospholipids *in vitro* in normal cells (Sze & Jardetzky, 1990b; Kaplan & Cohen, 1991; Dingley *et al.*, 1992; Bental & Deutsch, 1994) or cancer cells (Mountford *et al.*, 1982; Mountford *et al.*, 1984; Daly *et al.*, 1987; Daly & Cohen, 1989; Kuesel *et al.*, 1990; Merchant *et al.*, 1991; Lean *et al.*, 1992; Delikatny *et al.*, 1993), and *in vivo* (Levy & Craik, 1981). ¹H-NMR and ³¹P-NMR can be readily used to study cellular metabolism as these nuclides are abundant in biological tissues and cells. One dimensional (1D) experiments have been used to monitor changes in metabolites, but two-dimensional (2D) experiments can be used to clearly differentiate between particular metabolite peaks due to increased resolution of this technique (Appendix A1) (King & Kuchel, 1994).

1.7.1. NMR studies of phospholipid metabolism in cells.

$^1\text{H-NMR}$ -detected mobile lipid was shown to correlate with the increased concentration of triglyceride in activated murine lymphocytes (Holmes *et al.*, 1988). Previously the mobile lipid was thought to be primarily associated with the plasma membrane (Mountford *et al.*, 1982; Mountford & Wright, 1988; MacKinnon *et al.*, 1989; Holmes *et al.*, 1990; May *et al.*, 1991; Dingley *et al.*, 1992). However, this remains controversial and will be discussed further in Section 1.9. These studies did show that the mobile lipid is associated with the cancer cells or the activation of immune cells but the function and origin of the $^1\text{H-NMR}$ detectable mobile lipid is undetermined, and it is a major aim of this thesis to investigate these phenomena.

A comprehensive $^1\text{H-NMR}$ study of normal lymphocyte metabolism was performed on ConA activated human lymphocytes by Sze and Jardetzky (1990b). Human peripheral lymphocytes were stimulated with mitogens in culture. At various time points after activation, cellular extracts of the intracellular metabolites were prepared for analysis in $^1\text{H-NMR}$ studies. Metabolites were quantitated using the peak intensity of 1D $^1\text{H-NMR}$ spectra, the wet weight of the cell pellets and the signal from the $^1\text{H-NMR}$ intensity standard TSP. These concentrations were compared to HPLC analysis of metabolites. 2D $^1\text{H-NMR}$ experiments were performed on the extracts to clearly identify and assign the particular metabolite cross peaks but were not used in the calculation of the metabolite concentrations. This caused some problems with the degree of spectral overlap between particular metabolite peaks, such as some amino acids, which were difficult to quantitate. Although there were some discrepancies between estimation of some metabolite concentrations using $^1\text{H-NMR}$ and HPLC, most showed good agreement when single assays of known mixtures of substances were compared. Of particular interest was the change observed in the concentrations of the membrane phospholipid precursors. Substantial changes were observed in inositol which increased 3-fold during the activation period. In lymphocytes stimulated using phytohaemagglutinin (PHA), total concentration of choline-containing phospholipids decreased over the activation period, particularly in the first 48 h after stimulation. However, an increase in phosphorylcholine

was observed, suggesting an increased turnover of phosphatidylcholine (Sze & Jardetzky, 1990b).

^{31}P -NMR has been used to detect glycerophosphoethanolamine (GPE) which corresponded with an accumulation of DAG in rapidly regenerating rat liver cells with altered phosphatidylethanolamine (PE) metabolism. This may indicate a possible role for PE-specific phospholipase C in cellular proliferation. These phospholipid metabolite changes are also observed in neoplastic cells undergoing rapid proliferation (Murphy *et al.*, 1992). ^{31}P -NMR and ^1H -NMR studies in Friend leukemia cells have also found that alterations in the peaks corresponding to phosphomonoester and phosphodiester such as phosphocholine (PCho) and glycerophosphocholine (GPCho) occur in erythroid differentiation from a highly proliferating state (proerythroblastic) to a more mature state (normoblastic). These alterations in phosphocholine precursors and catabolites in the differentiation of Friend erythroleukemia cells suggests a role for phosphatidylcholine specific-phospholipase C in the PC catabolism and anabolism in these cells (Podo *et al.*, 1992; Ferretti *et al.*, 1993). It has also been suggested that alterations in the phospholipid metabolism in cancer cells may be associated with the accumulation of fatty acids and diacylglycerols (Ferretti *et al.*, 1993).

Phorbol esters can stimulate the synthesis and catabolism of choline-containing phospholipids and the hydrolysis and synthesis of PE (Hii *et al.*, 1990). ^1H -NMR and ^{31}P -NMR studies of PMA-treated human lymphocytes showed an increase in phosphoethanolamine (PEth) which can be derived from the catabolism of phosphatidylethanolamine (Ricciolini *et al.*, 1991) via the action of phospholipases C and D (Kiss & Anderson, 1989). The concentration of ethanolamine in the extracellular medium used to culture stimulated lymphocytes was found to influence the relative rates of synthesis and catabolism of PE (Sze & Jardetzky, 1990b; Ricciolini *et al.*, 1991). Phosphatidylethanolamine synthesis was stimulated after the addition of ethanolamine via the Kennedy pathway (Tijburg *et al.*, 1989). The concentration of ethanolamine can also regulate the metabolism of choline-containing phospholipids (Daly *et al.*, 1987). Concentrations of PE, ethanolamine and glycerophosphoethanolamine (GPE), and of the

choline-containing phospholipid metabolites choline (Cho), phosphocholine (PCho) and glycerophosphocholine (GPC), were also shown to be elevated in PMA- and ionomycin-stimulated murine thymic T lymphocytes (Dingley *et al.*, 1992, 1994).

³¹P-NMR has been used to study *in vitro* energy and phospholipid metabolic pathways in human lymphocytes. Immobilised cells were perfused in alginate capsules with interleukin-2, PMA or PHA (Kaplan & Cohen, 1991, 1994). The phospholipid degradation products GPE and GPC were apparent after 12-24 h of stimulation. The accumulation of GPC and GPE was postulated to be due accelerated phospholipid turnover in these cells and was not dependent upon the growth medium conditions. Phosphatidylcholine and phosphatidylethanolamine turnover in lymphocytes is considered an integral part of the activation process (Kaplan & Cohen, 1994).

Similar findings were reported by Bental and Deutsch using perfused human peripheral lymphocytes trapped within alginate beads and stimulated with PMA and ionomycin (Bental & Deutsch, 1993, 1994). However, there were inconsistencies in the studies conducted by Bental and Deutsch (1993, 1994). Firstly, contrary to the authors' statements, the PMA- and ionomycin-treated human lymphocytes trapped within alginate beads do not show either similar kinetics nor a similar magnitude of response to the stimulus when compared to control-treated lymphocytes in suspension cultures. ³H-thymidine incorporation in T lymphocytes trapped in alginate beads was 60,000 cpm on day 3 compared with 10,000 cpm for control suspension cultures. This contrasts with the statement made by the authors that both sets of results were similar. The numbers of cells entrapped in the agarose beads are substantially higher than the number in the suspension control cultures, as mentioned by the authors. Therefore one would expect a greater incorporation of ³H-thymidine due to the large cell numbers in the agarose beads. Although this is apparent from the increased ³H-thymidine counts in the agarose cultures, the absolute counts for both cultures should be substantially greater given the stimulus with PMA and ionomycin (compare with Figure 4.4).

The second inconsistency was that the doses of PMA and ionomycin used in the ^3H -thymidine incorporation experiments (PMA 1 ng/ml and ionomycin 100 ng/ml) and for the stimulation of IL-2 production (PMA 5 ng/ml and ionomycin 100 ng/ml) are clearly different (Bental & Deutsch, 1993, 1994). These differences in the doses of PMA would substantially affect the proliferation and activation kinetics of the T lymphocytes. If the lower dose of PMA, which would be sub-optimal for human T lymphocytes, was used in the ^{31}P -NMR experiments, it may explain why phospholipid turnover was not observed at early activation time points. Finally, if the T lymphocytes had been sufficiently purified they would not have responded to stimulation using PHA because the accessory cells necessary for proliferation of the T lymphocytes would not be present in sufficient numbers to generate a proliferative response (See Figure 3.5). This may explain the poor proliferative response shown when the cells were stimulated with PHA for 3 days in suspension culture and the complete lack of proliferation in the cells entrapped in the beads (Bental & Deutsch, 1993, 1994).

Of particular interest is the observation that there is an increase in the PCho peak in the spectra of PMA-stimulated lymphocytes (Kaplan & Cohen, 1991, 1994). These results are consistent with those found with murine lymphocytes presented in this thesis (Chapters 4 and 5) and would be consistent with the ability of PMA to activate both CT and phospholipases C and D, with resultant increased catabolic products from PC. This need not necessarily only relate to the specific enzyme activity of choline kinase as suggested by the authors. An increase and accumulation of PCho was also observed in lymphocytes perfused with dapsone, an inhibitor of the CT enzyme, while PCho levels did not appear to change when cells were perfused with high concentrations of Cho. These results suggested to the authors that choline kinase was the rate limiting enzyme of phospholipid synthesis in human lymphocytes (Kaplan & Cohen, 1991, 1994). However, while this explanation may be correct, the evidence presented does not exclude the possibility that the rate of reaction of the enzyme choline kinase is similar to the rate of CT, and that therefore either or both steps could be rate limiting. In most other

mammalian cells CT has been shown to be the rate-limiting enzyme in phospholipid metabolism (Pelech & Vance, 1984).

Activated or proliferating normal cells show some similar changes in phospholipid turnover compared with cancer cell metabolism. In human CEM leukaemic cell lines, significant differences in the levels of phosphocholine (PC) and phosphoethanolamine (PE) were found between different cell lines (Adebodun & Post, 1994). High levels of PE and PC have previously been found to correlate with the rate of cellular proliferation (Daly *et al.*, 1987; Adebodun & Post, 1994).

1.7.2. $^1\text{H-NMR}$ studies of mobile lipids in cells.

Proton nuclear magnetic resonance ($^1\text{H-NMR}$) spectroscopy is a technique which can be used to study lipid composition non-invasively in living cells (Mountford & Mackinnon, 1994). Certain cells, including malignant and embryonic cells (Mountford *et al.*, 1984; Santini *et al.*, 1992), exhibit $^1\text{H-NMR}$ spectra dominated by signals which arise from elevated levels of isotropically tumbling (i.e. NMR-visible) mobile lipid. Mobile lipids have also been observed in a variety of malignant tissues associated with changes in phospholipid metabolites (Lean *et al.*, 1992; Kuesel *et al.*, 1994a; Kuesel *et al.*, 1994b; Sivaraja *et al.*, 1994).

In myeloma cells grown to high density an accumulation of $^1\text{H-NMR}$ -detectable high resolution lipid resonances occurred with a subsequent decrease in the phosphorylcholine peak at 3.25 ppm (Callies *et al.*, 1993). Interestingly, similar observations were made in this thesis (Chapter 4 & 5): high levels of triglycerides were correlated with a decline in the intensity of the phosphorylcholine peak in normal murine T cells activated with PMA and ionomycin. Similar intensity changes in this phosphorylcholine peak have also been associated with corresponding changes in mobile lipid peak intensity in HIV-1-infected lymphoblastoid cells (Luciani *et al.*, 1991). A peak in the phosphodiester region of the ^{31}P spectra of human colon adenocarcinoma cells corroborates the presence of mobile phospholipids, as does the $^1\text{H-NMR}$ spectrum corroborate the presence of highly mobile lipid (Guidoni *et al.*, 1987). One dimensional $^1\text{H-NMR}$ spectra of chick embryo

myoblast cells show lipid resonances at 0.9 ppm and 1.26 ppm corresponding to the lipid groups CH_3 and $(\text{CH}_2)_n$ and a phosphorylcholine peak at 3.2 ppm corresponding to the choline-based metabolites $\text{N}(\text{CH}_3)^+$. During further cell differentiation and fusion, changes in the relaxation times of these resonances point towards an increase in molecular motion of the molecules. One explanation for these changes may be that there is a difference in the structural organisation of the lipids associated with differentiation and membrane fusion in myoblast cultures (Santini *et al.*, 1992).

Cell culture conditions have also been reported to influence the occurrence of mobile lipids in a transformed murine fibroblast cell line (Delikatny *et al.*, 1996a). NMR detectable resonances arising from triglycerides and cholesteryl esters increased significantly in intensity when the cells were grown to confluence, exposed to extremes of pH (6.0-9.0) or grown to high density in the absence of serum (Delikatny *et al.*, 1996a). The chemotactic response in these cells grown at high density decreased but was not found to be associated with changes in the lipid signal. The lipid signal did not correlate with any particular phase of the cell cycle as measured using flow cytometry. Alterations in the phosphatidylcholine metabolites choline, phosphocholine and glycerophosphocholine were observed in 2D NMR experiments, suggesting that the mobile lipids may result from the catabolism of phospholipids. In particular, PCho cross peaks were attenuated under all of the experimental conditions when mobile lipid was detectable. This implies that the catabolism of phosphatidylcholine may be generating the fatty acids which can be synthesised into triglycerides (Delikatny *et al.*, 1996a). One of the important features of this study as shown by the authors, is that the mobile lipid can be regulated by the culture conditions, which suggests that the changes in the metabolic state of the cells has a direct influence on the development of the mobile lipids. This work supports a previous study in which ^{31}P NMR was used to investigate the effects of pH of the culture medium upon the phospholipid metabolites in tumour cell lines (Kuesel *et al.*, 1990). Growth rates and cell adhesion of the cells was decreased as the pH of the medium was lowered below neutral, but the viability of the cells or the detection of diphosphates, triphosphates or phosphocreatine and phosphate did not change with pH.

When the cells in the exponential phase of growth were exposed to pH 7.0 and then to pH 6.0 the PCho levels decreased and PE levels increased. GPC levels increased when the pH was dropped from 7.2 to 6.3 and CDP-Choline was detectable at a pH >6.3. However, this was not evident in confluent cells (Kuesel *et al.*, 1990). These results suggest that phospholipid turnover can be manipulated by extreme pH changes.

1.7.3. $^1\text{H-NMR}$ for the detection of mobile lipid in activated immune cells.

The $^1\text{H-NMR}$ detectable mobile lipid appears in a variety of immune cells after activating stimuli (Figure 1.13). These include macrophages (King *et al.*, 1991), B cells, T cells (Holmes *et al.*, 1988; Dingley *et al.*, 1992; Dingley *et al.*, 1994) and polymorphonuclear leukocytes (PMNs) (May *et al.*, 1991; May *et al.*, 1992). PMNs stimulated *in vivo* and *in vitro* also give rise to the production of $^1\text{H-NMR}$ detectable mobile lipids. PMNs isolated from patients with serious bacterial infections and analysed using 2D COSY showed significantly higher volumes of the triglyceride cross peak F, indicating mobile lipid generation in these cells. These spectra were compared to PMNs stimulated with LPS *in vitro* and found to be similar but less intense than the PMNs isolated from patients with sepsis (May *et al.*, 1993) (Figure 1.13).

Previously it was shown that cellular proliferation was not necessary for the development of the mobile lipid spectrum. In macrophages stimulated with γ -interferon *in vitro* and by *Listeria monocytogenes in vivo*, the characteristic mobile lipid resonances were present in activated but not resting macrophages. Flow cytometric analysis using the quenching of the fluorescent dye Hoechst 33342 dye (also known as BrdU), which incorporates into the DNA of dividing or proliferating cells, failed to detect a change in the staining profiles for resting and activated macrophages (King *et al.*, 1991). In murine T and B cells, evidence using cell cycle blocking agents also suggests that a $^1\text{H-NMR}$ mobile lipid spectrum can occur independently of cellular proliferation (Holmes *et al.*, 1990). In this study, murine lymphocytes stimulated with lipopolysaccharide (LPS) or Concanavalin A and treated with the agents hydroxyurea (HU) and desferrioxamine (DES) were inhibited from further progression through the cell cycle and resulted in >95% inhibition of

R13762 Adenocarcinoma Cells

Mitogen-stimulated T lymphocytes

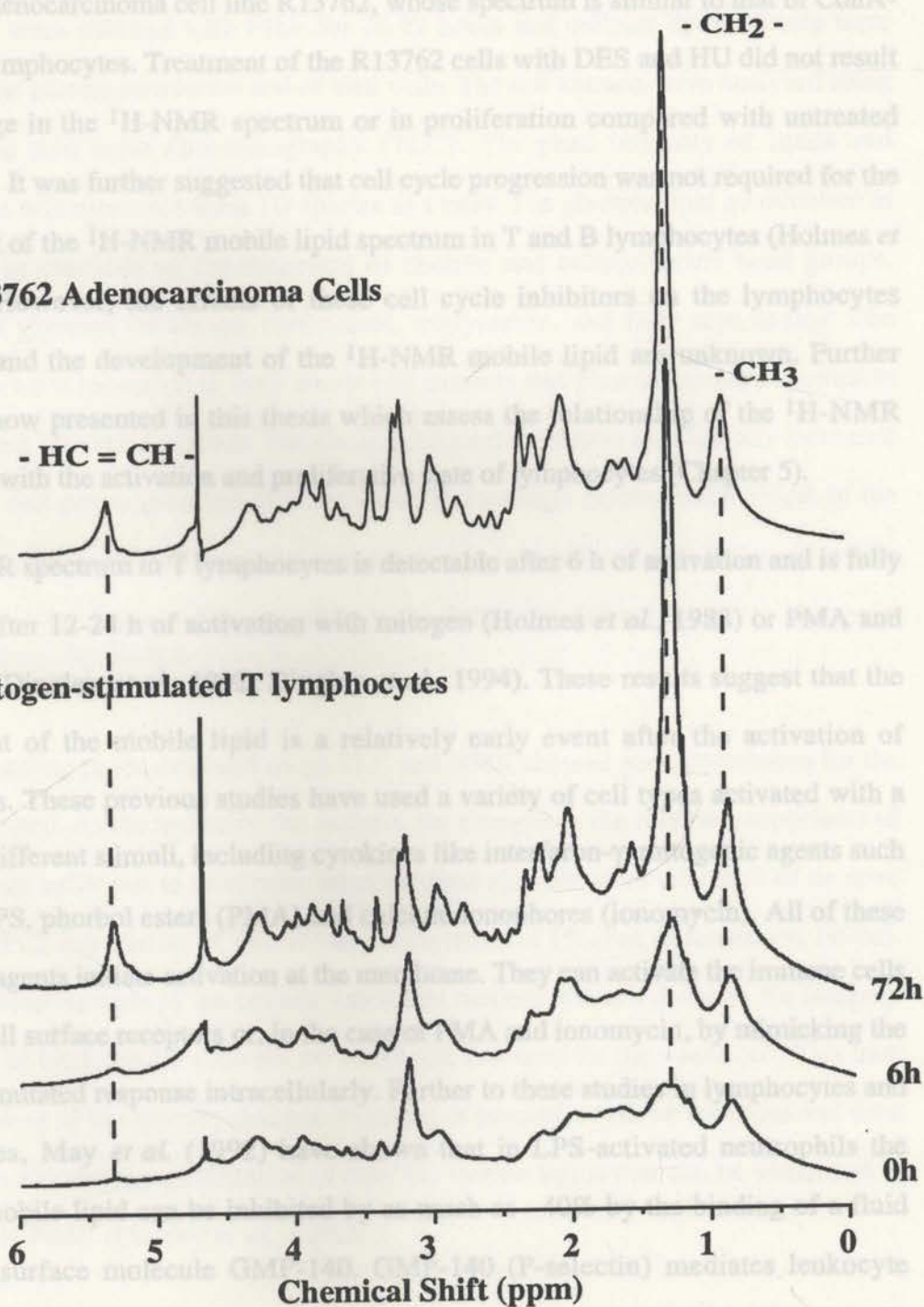


Figure 1.13. 1D $^1\text{H-NMR}$ spectra of PMA and ionomycin stimulated thymocytes at various times after activation (lower three spectra) and of rat adenocarcinoma cells (upper spectrum). PMA and ionomycin stimulated thymocytes from Dingley *et al.* (1992). R13762, rat adenocarcinoma cells, from Wright *et al.* (1988).

A comprehensive study of the total lipid content of PHA-activated human lymphocytes proliferation (Holmes *et al.*, 1990). A similar comparison was also made with the rat mammary adenocarcinoma cell line R13762, whose spectrum is similar to that of ConA-stimulated lymphocytes. Treatment of the R13762 cells with DES and HU did not result in any change in the $^1\text{H-NMR}$ spectrum or in proliferation compared with untreated control cells. It was further suggested that cell cycle progression was not required for the development of the $^1\text{H-NMR}$ mobile lipid spectrum in T and B lymphocytes (Holmes *et al.*, 1990). However, the effects of these cell cycle inhibitors on the lymphocytes themselves and the development of the $^1\text{H-NMR}$ mobile lipid are unknown. Further studies are now presented in this thesis which assess the relationship of the $^1\text{H-NMR}$ mobile lipid with the activation and proliferative state of lymphocytes (Chapter 5).

The $^1\text{H-NMR}$ spectrum in T lymphocytes is detectable after 6 h of activation and is fully developed after 12-24 h of activation with mitogen (Holmes *et al.*, 1988) or PMA and ionomycin (Dingley *et al.*, 1992; Dingley *et al.*, 1994). These results suggest that the development of the mobile lipid is a relatively early event after the activation of lymphocytes. These previous studies have used a variety of cell types activated with a number of different stimuli, including cytokines like interferon- γ , mitogenic agents such as ConA, LPS, phorbol esters (PMA) and calcium ionophores (ionomycin). All of these stimulating agents initiate activation at the membrane. They can activate the immune cells either via cell surface receptors or, in the case of PMA and ionomycin, by mimicking the receptor stimulated response intracellularly. Further to these studies in lymphocytes and macrophages, May *et al.* (1992) have shown that in LPS-activated neutrophils the $^1\text{H-NMR}$ mobile lipid can be inhibited by as much as ~40% by the binding of a fluid phase cell surface molecule GMP-140. GMP-140 (P-selectin) mediates leukocyte attachment such as the adhesion of neutrophils to activated endothelium (Geng *et al.*, 1990). These results imply that cell surface membrane events may influence or modulate the generation of the mobile lipid in neutrophils. These data suggests that, as in activated lymphocytes, the acquisition of the $^1\text{H-NMR}$ spectrum may be associated with early activation or signalling events (Chapters 4 & 5).

A comprehensive study of the total lipid content of PHA-activated human lymphocytes was performed from prepared lipid cell extracts (Sze & Jardetzky, 1990a). The lymphocytes were cultured with PHA for 24-72 hours and cellular lipid extracts were prepared of the plasma membrane and of total cells. The cell extracts were analysed using $^1\text{H-NMR}$ and thin layer chromatography (TLC). The peak intensity of lipids and phospholipids was measured from 1D spectra as a ratio. The phospholipid quantitation in this study was confined to the detection of choline and ethanolamine head groups, phospholipid glycerol backbone, cholesterol, triglyceride, and fatty acid chains. The PC:PE ratios were increased in both whole cell extracts and plasma membrane extracts over increasing activation periods. The cholesterol:total lipid ratio also initially increased in the whole cell preparation but then declined. The average carbon chain length of the fatty acids also increased in stimulated lymphocytes in both plasma membrane and whole cells. However, the degree of unsaturation of the fatty acids did not appear to change in whole cell or plasma membrane extracts.

The corresponding ratios obtained using TLC and NMR showed good correlation for the lipids quantitated. As discussed by the authors, the changes in the relative proportions of PC:PE was not sufficient to determine whether these changes were the result of *de novo* synthesis of PC, degradation of PE, or transmethylation of PE (Sze & Jardetzky, 1990a). One of the disadvantages of the cellular extraction method is that it destroys the integrity of the cell. The total cellular contents are tested and averaged for the whole cell. This may not be indicative of the specific changes occurring at particular cellular locations and does not take into account the quantitation of only the mobile lipids that can be visualised in whole cell $^1\text{H-NMR}$ (Dingley *et al.*, 1992).

Two-dimensional (2D) $^1\text{H-NMR}$ techniques were used previously in this laboratory to quantitate the increases in mobile lipid levels observed in T lymphocytes with increasing time after activation with PMA and ionomycin (Dingley *et al.*, 1992). This study was the first to quantitate mobile lipid using 2D $^1\text{H-NMR}$ experiments. The kinetics of development of the mobile lipid were investigated in activated thymic T lymphocytes. The mobile lipid levels were found to increase in activated thymic T lymphocytes for

activation periods up to 72 h. Previous studies of thymic T cells indicated that the levels of phospholipid precursors of phosphatidylcholine and phosphatidylethanolamine were increased in T cells activated with PMA and ionomycin compared with levels in unstimulated cells over this time period (Dingley *et al.*, 1992). These results showed that the mobile lipid increased in T lymphocytes with increasing activation periods in culture and that there was an associated increase in the intracellular water soluble phospholipid precursors phosphocholine, choline, glycerophosphocholine, phosphoethanolamine, ethanolamine, and glycerophosphoethanolamine detected using 2D $^1\text{H-NMR}$ experiments of perchloric acid cellular extracts (Dingley *et al.*, 1992). The increase in choline phospholipid metabolites, including GPC, reported in murine lymphocytes by Dingley *et al.* (1992) and in this thesis, contrasts with the previous report in PHA-stimulated human lymphocytes extracted using perchloric acid, which shows a decrease in choline-containing metabolites but not in GPC (Sze & Jardetzky, 1990a). The different sources of lymphocytes, i.e., human peripheral lymphocytes compared with immature murine thymocytes, and the different modes of activation, may also contribute to the differences between the metabolite changes observed in the studies by Dingley *et al.* (1992) and by Sze and Jardetzky (1990a).

However, in chloroform/methanol lipid extracts by the same authors Sze and Jardetzky (1990a), the PC:PE ratio increased in the same cells over the same time period. PC and PE in this instance refers to choline and ethanolamine headgroups, which would include all of the related phospholipid precursors (Sze & Jardetzky, 1990b). These differences may have arisen from the different extraction methods used to isolate the phospholipids. Differences in the method of quantitation of 1D spectra may also have led to the discrepancies shown in these studies, because peak overlap of metabolites in $^1\text{H-NMR}$ spectra can give rise to inaccuracies (Sze & Jardetzky, 1990a; Dingley *et al.*, 1992).

This work has been extended in this thesis to include longer periods of activation of murine lymphocytes from two different tissue sources and monitoring of the associated relative changes in the phosphatidylcholine metabolites from whole intact cells (Chapter 4).

1.8. Previously proposed models for the role and origin of $^1\text{H-NMR}$ -detectable mobile lipids.

At present there is no satisfactory unifying model to fully account for the characteristics of freely mobile lipids in cells. Mobile lipids, detectable using $^1\text{H-NMR}$, have been found in a number of cell types undergoing different cellular processes, including activated immune cells, cancer cells, embryonic cells and virally-infected cells (see Section 1.7). Previous models have proposed that the main reason for the appearance of the $^1\text{H-NMR}$ mobile lipid spectrum is that it is associated with alterations in the biophysical properties of mobile lipids in the plasma membranes, specifically that the mobile lipid enters the cell incorporated as lipoproteins and is deposited directly and exclusively into the plasma membrane (Mountford & Wright, 1988). Other explanations extend this model to propose that membrane fluidity is also important.

1.8.1. Lipoproteins in the membrane.

The mobile lipid associated with activated immune cells and malignant cancer cells has been identified as a triglyceride and was shown to be associated with the membrane (Cross *et al.*, 1984; May *et al.*, 1986; Holmes *et al.*, 1987; Holmes & Mountford, 1991). Mountford and colleagues proposed that mobile lipids are embedded in the membrane bilayer in lipoprotein domains. Triglycerides in this configuration can tumble freely to generate the narrow linewidths observed in $^1\text{H-NMR}$ spectra (Mountford & Wright, 1988). This is supported by $^1\text{H-NMR}$ studies of chylomicra (CM) and very low density lipoproteins (VLDL) isolated from lymph (Hamilton *et al.*, 1983; Wright *et al.*, 1986), where spectra are similar to those of activated immune and cancer cells. $^{31}\text{P-NMR}$ studies in adenocarcinoma cells have shown that the phospholipid changes seen in these cells are due to an increase in the mobility of phospholipids and their association with lipids in the vesicles released from cancer cells (Guidoni *et al.*, 1987).

However, although the mobile lipid may appear to be consistent with the triglyceride structure, the resonances of the acyl and glycerol backbone chains might also arise from a mixture of other lipid species such as diacylglycerol (Mountford & MacKinnon, 1994)

which may contribute to the $^1\text{H-NMR}$ resonances observed. Although the lipoprotein structure may contribute to the $^1\text{H-NMR}$ resonances detected in these cells, it is not the only possible source of mobile lipid $^1\text{H-NMR}$ spectra. Although it has been established that lipoproteins can be membrane-associated (Mountford & Wright, 1988), it has also been shown that the appearance of mobile lipid signals in the $^1\text{H-NMR}$ can be correlated with the formation of cytoplasmic lipid droplets (Callies *et al.*, 1993). Therefore, it is unlikely that lipoprotein embedded in the plasma membrane is the only source of the $^1\text{H-NMR}$ mobile lipid in whole cells.

1.8.2. Membrane fluidity.

It has previously been proposed that the mobile lipid may serve to enhance the fluidity of the plasma membrane in activated immune cells (King *et al.*, 1991) and cancer cells (Mountford & Wright, 1988). Certainly, differences in cell membrane fluidity do occur. Fluorescence polarization showed that chicken thymic lymphocytes had greater membrane fluidity than lymphocytes from spleen and peripheral blood (Traill & Wick, 1984). Changes in fatty acid content have pronounced effects upon the lipid fluidity of the plasma membrane. Fluidity is augmented by increases in unsaturated/saturated fatty acid and phospholipid/cholesterol ratios (Traill & Wick, 1984), strongly suggesting that increases in triglyceride in activating T cells could be associated with an increase in membrane fluidity. Incorporation of triglycerides into cell membranes promotes destabilisation of the bilayer phospholipid phases to form hexagonal phases (Epanand *et al.*, 1988). This increases the separation of phospholipid headgroups, causing deeper penetration of water molecules into the membrane, thus decreasing membrane hydrophobicity (Epanand & Leon, 1992) and altering permeability properties. Functionally, increases in membrane fluidity critically influence the activity of membrane-bound enzymes (Anderson, 1980), and can alter the expression of several immune system-associated transmembrane molecules. These include Thy 1.2, and major histocompatibility complex antigen on murine lymphocytes (Knowles *et al.*, 1976), and Fc-receptors on phagocytic cells (Kyoizumi *et al.*, 1981). It follows that changes in membrane surface properties must profoundly influence cell-cell and receptor-ligand

interactions in activated immune cells (Schaeffer & Curtiss, 1977). Thus, as a means of altering function, changes in cell membrane lipid composition may be a crucial immunoregulatory mechanism (Traill & Wick, 1984). Triglyceride molecules form a major part of the numerous plasma membrane projections which begin to appear during the first few hours of lymphocyte activation (Patarroyo *et al.*, 1982). Rapid translational diffusion along the outer edges of the narrowest of these projections may provide the necessary reorientational motions to average out the dipolar interactions and lead to a narrow-line $^1\text{H-NMR}$ spectrum (Dingley *et al.*, 1994). However, this is not the only source of narrow $^1\text{H-NMR}$ mobile lipid linewidths. Cytoplasmic triglyceride lipid droplets can also give rise to narrow linewidths (Callies *et al.*, 1993). Therefore, membrane fluidity is probably partly responsible for the $^1\text{H-NMR}$ mobile lipid spectrum, but it is most unlikely that this explanation is sufficient to explain all of the effects observed.

1.8.3. Summary of previous models.

In conclusion, while it is established that activation of normal immune cells is invariably associated with the appearance of $^1\text{H-NMR}$ -detectable mobile lipid, the origin and possible role of the mobile lipid in immunoregulation are as yet not known. While I think that the effects described above contribute to the $^1\text{H-NMR}$ mobile lipid spectrum, I would like to propose a model which does account for the results observed in different cell types in different metabolic states.

1.9. A new model for the origin and function of mobile lipid: relationship between mobile lipid, phosphatidylcholine metabolism and the cell cycle.

I would like to propose a model in which the $^1\text{H-NMR}$ -detectable mobile lipid spectrum in activated immune cells is due to phospholipid turnover during the cell cycle. The model has been devised partly from the work of others (described in this section) and partly from results obtained from this project. I believe this model can explain the $^1\text{H-NMR}$ -visible mobile lipid spectra in a range of different cell types, experimental

conditions and disease states. This new model is not dependent upon the mobile lipid being associated with any particular subcellular location or organelle, which was a limitation in the lipoprotein model described above (Mountford & Wright, 1988). It can also explain the link between simultaneous changes in mobile lipids and phospholipids observed in activated immune and other cells.

Cellular phospholipid metabolism is influenced by cell cycle status. In rapidly dividing cells, a number of changes occur in phospholipid turnover because of the need for phospholipid in the expanding cell membrane and for signal transduction (Jackowski, 1994). Signal transduction via phospholipase mechanisms also augments phospholipid turnover, which is important in the activation in immune cells (Szamel & Resch, 1995).

Therefore, increases in phospholipid turnover correlate with activation processes which in turn correlate with the appearance of the $^1\text{H-NMR}$ -visible mobile lipid spectra.

The unifying themes in this model are the relationship with the cell cycle and the regulation of phosphatidylcholine metabolism. These are fundamental cellular processes that can influence not only lipids, but also the overall metabolism of the cell. All of these processes are essential for cell cycle progression and relate to cell cycle status. Further evidence for this model will appear throughout this thesis and will be discussed in Chapter 7 in the context of the results obtained.

1.9.1. Overview of the cell cycle.

Cells can be stimulated to progress from the G_0 phase of the cell cycle by stimulation with a range of mitogenic activating stimuli in the presence of optimal growth conditions (Figure 1.14). Passage through G_1 results in the induction of a number of nuclear activating genes, such as *jun*, *fos*, *c-myc* and *ras*, which can induce the transcription from a number of cytokine growth factor and other genes necessary for progression to the S phase. In the presence of sub-optimal growth conditions, such as altered pH, serum deprivation or amino acid depletion, cells will be induced to go into the quiescent G_0 phase (Pardee, 1989; Figure 1.14). Under optimal conditions and once the appropriate

mitogenic signals are received, cells will re-enter G_1 from G_0 via the G_{1a} , G_{1b} and G_{1c} steps (Lloyd *et al.*, 1982; Pardee, 1989; Furuya *et al.*, 1994; Pardee & Wang, 1995).

However, if the cell cycle is specifically blocked by blocking particular events outside G_0 , the cells will eventually undergo cell death, either by the programmed pathway to cellular fragmentation (apoptosis) or by the non-programmed (necrotic) pathway (Kim *et al.*, 1995). For example, metastatic prostate cancer cells can be blocked at different points in the proliferative cell cycle (G_1 , S or G_2) by chemotherapeutic drugs. This makes the cells bypass the G_0 quiescent phase and go into apoptosis (Furuya *et al.*, 1994).

1.9.2. Relationship between phosphatidylcholine metabolism and the cell cycle.

The cell cycle is associated with phospholipid turnover, particularly turnover of phosphatidylcholine. In a macrophage cell line dependent upon colony-stimulating factor-1 (CSF-1) (Jackowski, 1994) and in fibroblast cultures (Terce *et al.*, 1994), phospholipid accumulation occurs in S phase of the cell cycle as a result of oscillations in phosphatidylcholine biosynthesis and degradation. Increased phosphatidylcholine degradation resulted in the dephosphorylation of cytidylyltransferase (CT), which increased phosphatidylcholine synthesis. This balance between synthesis and degradation maintains the mass of membrane phosphatidylcholine in G_1 . The cessation of degradation of phosphatidylcholine in S phase results in the accumulation of phospholipid in preparation for cell division (Jackowski, 1994; Figure 1.15).

1.9.3. Regulation of phosphatidylcholine in the cell cycle.

Figure 1.14. Aspects of the cell cycle.

The activity of CT, the rate-controlling enzyme in phosphatidylcholine biosynthesis, oscillates throughout the cell cycle, attaining a maximum at mid- G_1 , when the rate of phosphatidylcholine synthesis is also maximal (Jackowski, 1994). In eukaryotic cells, growth-factor-stimulated synthesis of phosphatidylcholine in G_1 is associated with enhanced PC turnover (Exton, 1990; Larrodera *et al.*, 1990). However, in continuously proliferating cells the levels of CT protein and mRNA remain constant, suggesting that

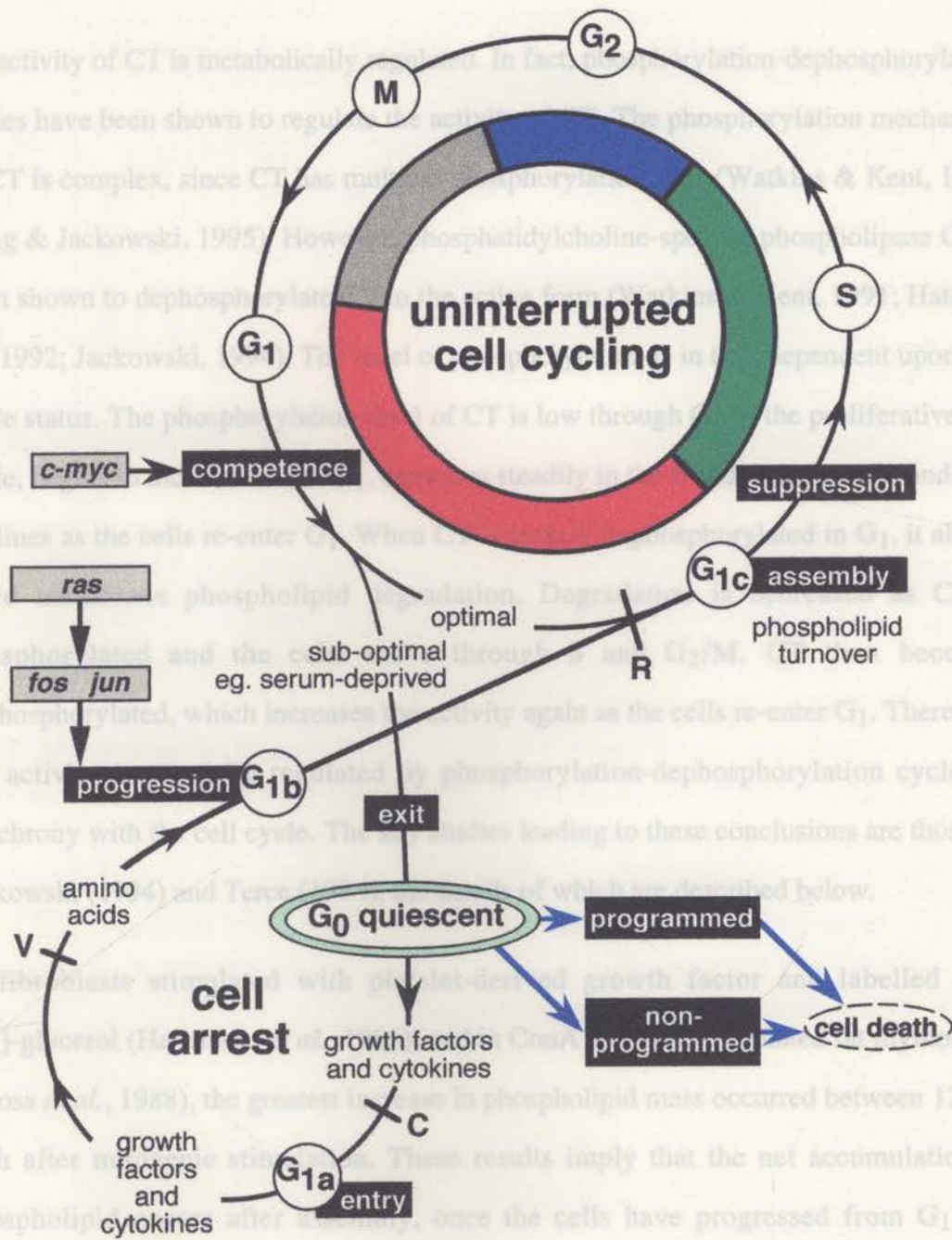


Figure 1.14. Aspects of the cell cycle.

Major phases, stages and requirements. Upper cycle represents cells in uninterrupted cell cycle under optimal growth conditions. Although distinct boundaries are represented between G₁, S, G₂ and M, overlap does exist in cellular processes between these phases. Lower cycle represents exit from G₁ into G₀ due to sub-optimal growth conditions. C, V and R are boundary points between G₀:G_{1a}, G_{1a}:G_{1b}, G₁/G_{1b}:G_{1c}, respectively. Alternate pathways to cell death from G₀ are also shown. Adapted from Pardee (1989), Roitt (1991), Furuya *et al.* (1994).

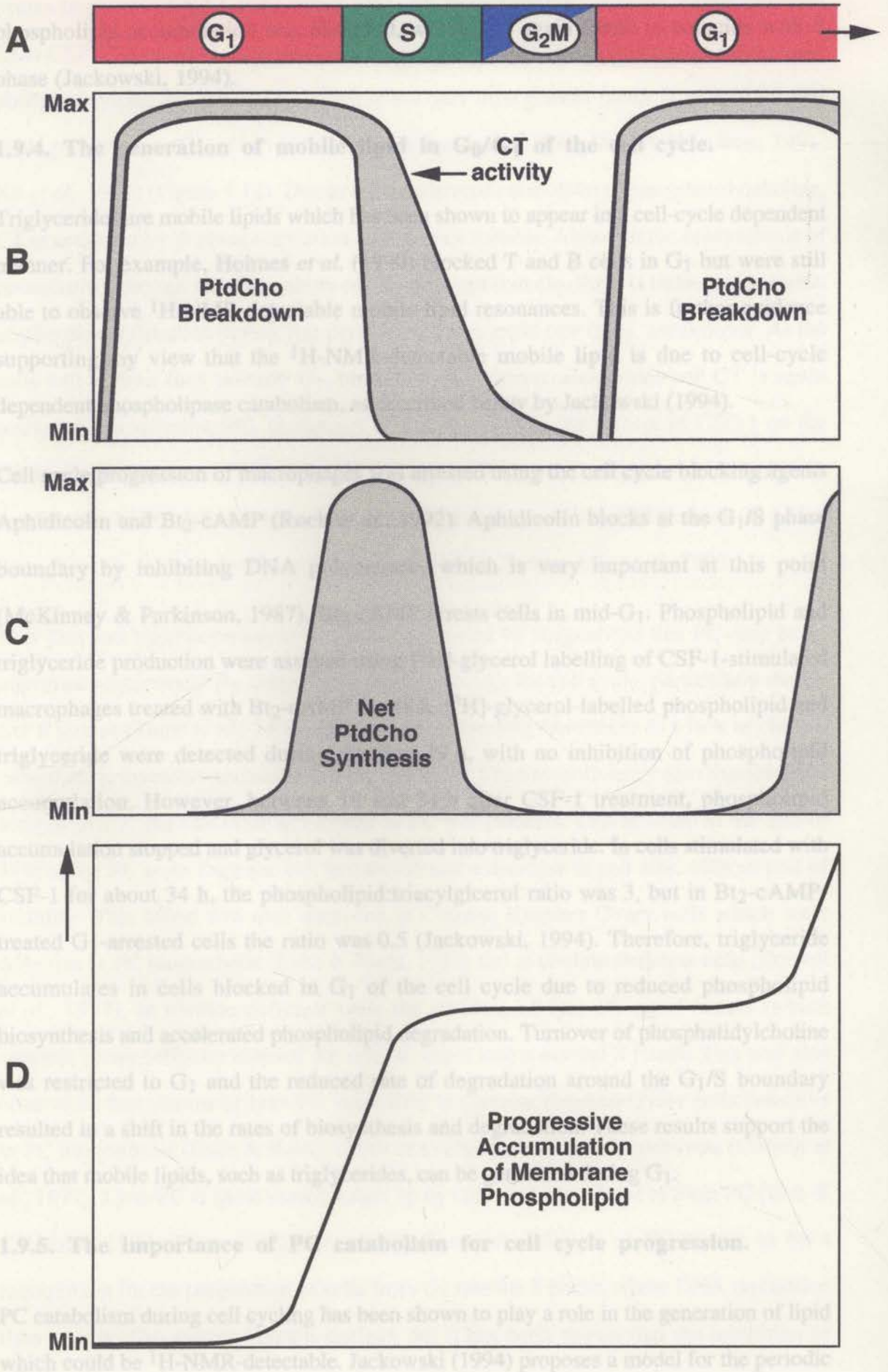
the activity of CT is metabolically regulated. In fact, phosphorylation-dephosphorylation cycles have been shown to regulate the activity of CT. The phosphorylation mechanism of CT is complex, since CT has multiple phosphorylation sites (Watkins & Kent, 1991; Yang & Jackowski, 1995). However, phosphatidylcholine-specific phospholipase C has been shown to dephosphorylate CT to the active form (Watkins & Kent, 1991; Hatch *et al.*, 1992; Jackowski, 1994). The level of phosphorylation is in turn dependent upon cell cycle status. The phosphorylation level of CT is low through G₁ of the proliferative cell cycle, begins to increase in late G₁, increases steadily in the S and G₂/M phases and then declines as the cells re-enter G₁. When CT is largely unphosphorylated in G₁, it allows rapid membrane phospholipid degradation. Degradation is decreased as CT is phosphorylated and the cells move through S and G₂/M. CT then becomes dephosphorylated, which increases the activity again as the cells re-enter G₁. Therefore, CT activity is carefully regulated by phosphorylation-dephosphorylation cycles in synchrony with the cell cycle. The key studies leading to these conclusions are those by Jackowski (1994) and Terce (1994), the details of which are described below.

In fibroblasts stimulated with platelet-derived growth factor and labelled with [³H]-glycerol (Habenicht *et al.*, 1985), and in ConA and IL-2-stimulated rat thymocytes (Gross *et al.*, 1988), the greatest increase in phospholipid mass occurred between 12 and 24 h after mitogenic stimulation. These results imply that the net accumulation of phospholipid occurs after assembly, once the cells have progressed from G₁ to S (Jackowski, 1994; Figures 1.14, 1.15). In the CSF-1-dependent murine macrophage cell line BAC1.2F5, cells were arrested in early G₁ by CSF-1 starvation for 18 h. After the re-addition of CSF-1 the cells entered the proliferative cell cycle synchronously (Tessner *et al.*, 1991; Rock *et al.*, 1992). Cells were monitored at various times over two cell cycles to determine the amounts of [³²P] incorporation into phospholipid. Upon entry into G₁ there was a small increase in the phospholipid mass which was followed by a significant increase during S phase (approximately 10-19 h after entry into G₁). Cell division occurred after about 20 h, and a lag period was observed before the next

Figure 1.15. The cell cycle and its relationship to phosphatidylcholine cycling.

Changes in cytidylyltransferase (CT) activity affect phosphatidylcholine (PtdCho) catabolism at different phases of the cell cycle. (A) The cell cycle, depicting continuous, unarrested progression through G_1 . The stages of the cell cycle project onto each of the three panels below. (B) In G_1 , CT is dephosphorylated and PtdCho turnover is maximal. After the G_1/S boundary, CT becomes progressively phosphorylated and inactivated, leading to decreased PtdCho catabolism. In G_2/M , maximal CT phosphorylation coincides with minimal PtdCho catabolic activity. (C) The rates of PtdCho synthesis and degradation result in the net accumulation of PtdCho for the newly formed membrane of the daughter cells. The combination of the increasing CT activity and decreased PtdCho catabolism at the G_1/S boundary results in S phase phospholipid synthesis. (D) This results in the periodic accumulation of phospholipid during the S phase of the cell cycle. Adapted from Jackowski (1994).

Time →



phospholipid accumulation was observed, which was again found to coincide with S phase (Jackowski, 1994).

1.9.4. The generation of mobile lipid in G₀/G₁ of the cell cycle.

Triglycerides are mobile lipids which has been shown to appear in a cell-cycle dependent manner. For example, Holmes *et al.* (1990) blocked T and B cells in G₁ but were still able to observe ¹H-NMR-detectable mobile lipid resonances. This is further evidence supporting my view that the ¹H-NMR-detectable mobile lipid is due to cell-cycle dependent phospholipase catabolism, as described below by Jackowski (1994).

Cell cycle progression of macrophages was arrested using the cell cycle blocking agents Aphidicolin and Bt₂-cAMP (Rock *et al.*, 1992). Aphidicolin blocks at the G₁/S phase boundary by inhibiting DNA polymerase, which is very important at this point (McKinney & Parkinson, 1987). Bt₂-cAMP arrests cells in mid-G₁. Phospholipid and triglyceride production were assayed using [³H]-glycerol labelling of CSF-1-stimulated macrophages treated with Bt₂-cAMP for 48 h. [³H]-glycerol-labelled phospholipid and triglyceride were detected during the first 19 h, with no inhibition of phospholipid accumulation. However, between 19 and 34 h after CSF-1 treatment, phospholipid accumulation stopped and glycerol was diverted into triglyceride. In cells stimulated with CSF-1 for about 34 h, the phospholipid:triacylglycerol ratio was 3, but in Bt₂-cAMP-treated G₁-arrested cells the ratio was 0.5 (Jackowski, 1994). Therefore, triglyceride accumulates in cells blocked in G₁ of the cell cycle due to reduced phospholipid biosynthesis and accelerated phospholipid degradation. Turnover of phosphatidylcholine was restricted to G₁ and the reduced rate of degradation around the G₁/S boundary resulted in a shift in the rates of biosynthesis and degradation. These results support the idea that mobile lipids, such as triglycerides, can be generated during G₁.

1.9.5. The importance of PC catabolism for cell cycle progression.

PC catabolism during cell cycling has been shown to play a role in the generation of lipid which could be ¹H-NMR-detectable. Jackowski (1994) proposes a model for the periodic

events in phospholipid metabolism during cell cycle progression using results obtained from CSF-1-stimulated macrophages (Figure 1.15). CSF-1 stimulates rapid turnover of phosphatidylcholine during G_1 , which is the only time growth factor is needed for cell cycle progression (G_{1a} , G_{1b}) (McKinney & Parkinson, 1987; Veis & Hamilton, 1991; Xu *et al.*, 1993) (Figure 1.14). Due to the accelerated catabolism of phosphatidylcholine, CT is activated by dephosphorylation as cells exit mitosis. Although the biosynthesis of phosphatidylcholine and the activity of CT are highest in G_1 , there is little accumulation of phosphatidylcholine during this period due to the rapid rate of PC breakdown. As the cells exit mitosis they re-enter G_1 , phospholipid turnover accelerates and CT is again activated to synthesise PC. In support of this hypothesis, the effects of CSF-1 on the macrophages can be mimicked by the addition of PC-specific PLC, which causes the degradation of PC. It has also been shown that this enzyme, like CSF-1, must be added throughout G_1 in order for the cells to progress to the S phase (Xu *et al.*, 1993).

This data and hypothesis has been further supported by suggestions that PC may be an important requirement for normal progression through the cell cycle, particularly the G_1 and S phases (Terce *et al.*, 1994) (Chapter 4). Subjecting fibroblasts to a lack of choline caused the progressive accumulation of cells in G_1 . Choline-deficiency also regulated the activity of CT, the rate limiting enzyme in PC biosynthesis. This resulted in the loss of 35% of the PC mass from the cell membrane and a decrease in cell size, without loss of viability. This effect was also observed in Chinese Hamster Ovary cells which were defective in PC biosynthesis (Esko & Raetz, 1980) and in choline-deficient cells (Cornell *et al.*, 1977). In choline-deficient cells the addition of lyso-PC or of serum (which contains phospholipids) enabled the cells to move into a normal S phase. This was also observed when choline or lyso-PC was added to Chinese Hamster Ovary cells defective in PC biosynthesis (Esko & Raetz, 1980) or to choline deficient hepatocytes (Cornell *et al.*, 1977). Lyso-PC is more readily taken up by cells and is acylated to form PC (Bell & Coleman, 1980; Choy & Arthur, 1989). The accumulation of PC seems to be a requirement for the progression of cells from G_1 into the S phase, where DNA replication then occurs. The reasons remain unclear, but it has been shown that the inhibition of

DNA synthesis does not affect the accumulation of PC (Jackowski, 1994). In contrast, a block in PC synthesis can arrest cells in G₁ and prevent DNA synthesis (Terce *et al.*, 1994).

1.9.6. Summary.

These results show that the degradation of PC by phospholipases in G₁ may be necessary for cell cycle progression. These events may be responsible for the appearance of the mobile lipid spectrum detectable using ¹H-NMR.

1.10. NMR evidence supporting the proposed model: the effect of the extracellular environment on cell cycle status and its relationship to mobile lipid.

Cell cycle status can be influenced by a number of factors such as availability of serum, the availability of particular growth factors, pH, cell density and cell adhesion, or the application of specific cell cycle blockers. These factors can have metabolic or gene regulatory effects which favour arrest of the cells in G₀/G₁ (Taylor & Hodson, 1984; Musgrove *et al.*, 1987; Pardee, 1989; DiSalvo *et al.*, 1995; Coats *et al.*, 1996; Kuzumaki *et al.*, 1996). In some situations this leads ultimately to apoptosis or necrosis (Furuya *et al.*, 1994) (Figure 1.14). All of these effects can result in increased turnover of PC and the generation of ¹H-NMR-detectable mobile lipid. I am proposing that there is a link between these two effects.

1.10.1. Growth factor and cytokine effects.

Growth factors have differential biochemical effects upon cells. These effects occur in a particular sequence during the stimulation of quiescent cells to proliferate. Fibroblasts grown in serum-free but hormone supplemented media, containing insulin, transferrin, epidermal growth factor (EGF) and selenium, were shown to have increased levels of ¹H-NMR-visible mobile lipids (Delikatny *et al.*, 1996a). EGF and a large variety of other growth factors have been shown previously to stimulate the hydrolysis of PC and PE via the action of PLC, PLD and PLA₂ (Billah & Anthes, 1990; Exton, 1994b). PDGF has

been shown to stimulate arachidonic acid incorporation into triglycerols 4-6 hours after stimulation in Swiss 3T3 fibroblasts. At 6 h the accumulation of triglyceride far exceeded the incorporation of arachidonic acid into phosphatidylcholine and phosphatidylethanolamine and this continued until 12 h after stimulation. The major synthesis of PE and PC only occurred during S phase of the cell cycle and it was concluded that synthesis of PE or PC were not influenced by stimulation by PDGF during G₁ (Habenicht *et al.*, 1985). These results imply that PDGF stimulated the degradation of PE and PC in the G₁ phase, resulting in accumulation of triglyceride. In the study by Delikatny *et al.* (1996), a high proportion of fibroblasts grown in serum-free supplemented medium were in G₁. Increased levels of ¹H-NMR mobile lipids were also seen. This is also consistent with an increased phospholipid turnover as a result of agonist-stimulation of phospholipases.

A decrease in the viability of fibroblasts grown in growth factor-supplemented medium (PDGF, EGF, insulin etc.) was also associated with an increase in ¹H-NMR-detectable mobile lipids (Delikatny *et al.*, 1996a), indicating an increase in cell death due either to apoptosis or necrosis. Growth factors such as PDGF, EGF, and insulin have been shown to have differential effects upon the cell cycle kinetics of fibroblasts (Chen & Rabinovitch, 1989; Pardee, 1989). It has previously been shown that PDGF and EGF, but not insulin-like growth factor-1 (IGF-1), stimulate the expression of the *c-fos*, *c-myc* and other early G₁ genes (Kruijer *et al.*, 1984; Mueller *et al.*, 1984b). This is consistent with the finding that EGF and PDGF influence the early G₁ phase, while IGF-1 influences the transition of cells through the G₁/S boundary (Campisi & Pardee, 1984). Combinations of these factors can have differential effects and may influence the relative proportions of cells found in the different stages of the cell cycle. Fibroblasts that have been growth-arrested by serum deprivation fail to progress past G₁ phase when PDGF-stimulated, resulting in apoptosis. This effect can be accelerated by the additive effect of EGF (Chen & Rabinovitch, 1990). A similar response is seen with treatment of serum deprived cells treated with EGF alone. However, these factors can exert a positive effect upon the progression of cells through the cell cycle under exponential growth conditions.

These results indicate that growth factors such as PDGF and EGF can exert a positive or negative effect upon the control of the cells through the G₁ phase, resulting in progression or arrest of the cell cycle resulting in increased apoptosis or necrosis (Kim *et al.*, 1995). These results may explain the decrease in the viability shown in fibroblast cultures in serum-free, growth factor supplemented cultures and the increase in ¹H-NMR detectable lipid signals shown in these cultures (Delikatny *et al.*, 1996a).

The fibroblast cells grown in serum-free medium in the study by Delikatny *et al.* (1996a) showed a larger proportion of cells in the G₀/G₁ phase of the cell cycle and an increased doubling time compared with serum-supplemented cells (Delikatny *et al.*, 1996a). This finding is not surprising as the defined serum-free supplemented medium used in this study contained a large variety of other growth factor sources such as bovine pituitary extract, in addition to EGF and insulin. The influence and interaction of these other growth factors would have had an effect upon the distribution of cells in the cell cycle. Therefore, the explanation for the increase in the mobile lipid in the serum-free, growth factor supplemented cells in the study of Delikatny *et al.* (1996a) is likely to be explained by the stimulation of phospholipases, via growth factor receptor binding. The increased phospholipid degradation would result in the generation of mobile lipids. A large proportion of the cells were also shown to be in the G₁ phase of the cell cycle, suggesting cell cycle arrest. This would correlate with increased degradation of phospholipids.

A similar situation can occur when mitogens are added to cells which are arrested in G₀/G₁. In normal human T lymphocytes cultured in serum-free conditions and stimulated with phorbol dibutyrate and ionomycin, the T cells entered the cell cycle but were arrested in the G₁ phase of the cell cycle. Supplementation of the cultures with the mitogenic factors linoleic acid (a fatty acid) and iron allowed progression of the cells through the cell cycle and DNA synthesis. The analysis of various phosphoproteins during this type of stimulation is consistent with what is found in T cells stimulated with serum-containing medium. Iron added alone to serum-free cultures did not result in the stimulation of cell cycle progression, but linoleic acid when added alone had a substantial effect on cell cycle progression, although it did not result in DNA synthesis. The cells

appeared to be blocked in the G₁/S boundary (Terada *et al.*, 1993). Therefore the inclusion of a fatty acid appears to be necessary for cells to pass through G_{1c} (Figure 1.14). This timing correlates with the appearance of the ¹H-NMR-detectable mobile lipid spectrum (Holmes *et al.*, 1990).

A correlation between cell cycle-dependent cell adhesion and the generation of the IGF-1 is required in the late phase of G₁ in fibroblasts when the proto-oncogene *c-Ha-ras* is maximally expressed. PDGF and EGF induce *c-fos* mRNA and this is unaffected by the treatment of the cells with an anti-*ras* antibody that blocked the ability of IGF to initiate DNA synthesis (Lu & Campisi, 1992). In a *ras*-transfected human keratinocyte cell line, the *ras* oncogene has been shown to have activating effects upon CT, the rate limiting enzyme in phosphatidylcholine biosynthesis. This resulted in a 3-fold increase in incorporation of choline into phosphatidylcholine (Geilen *et al.*, 1996). Increases in choline kinase activity have also been observed in murine fibroblast cell lines upon the induction of the *H-ras* oncogene (Ratnam & Kent, 1995). Previously, it has been suggested that *ras* may also stimulate the activity of phospholipases, but that this occurs indirectly via oscillations in the intracellular Ca²⁺ concentration (Fu *et al.*, 1992). Massive accumulation of mobile lipids, consisting of cholesterol esters, triglycerides and glycerol ethers have also been shown in growth-arrested cells transformed by an activated *ras* gene (Hirakawa *et al.*, 1991). Even though the effects of *ras* are not clearly resolved it is clear that the expression of *ras* can have effects upon cell lipid metabolism.

The ¹H-NMR-detectable mobile lipid in T cells appears very early after activation. This is strong evidence to suggest that the resonances are appearing in G₁ (Pardee, 1989). Previous ¹H-NMR studies of the development of the mobile lipid in murine T and B cells, stimulated by ConA or LPS and arrested in G₁ using cell cycle blockers, indicate that mobile lipid is detectable in these cells (Holmes *et al.*, 1990). The mobile lipid resonances were detectable 6 h after stimulation and were fully developed in activated cells 12 h after stimulation (Holmes *et al.*, 1990; Dingley *et al.*, 1992). This is further supported by the development of the mobile lipid in murine macrophages stimulated with IFN- γ . A lack of BrdU incorporation indicated that the cells did not pass through G₁ and did not proliferate and were therefore thought to be arrested in G₁ (King *et al.*, 1991). An

increase in the mobile lipid has also been shown to correlate with the G₀/G₁ phase of the cell cycle in fibroblast cell lines (Delikatny *et al.*, 1996a).

1.10.2. Cell adhesion effects.

A correlation between cell cycle-dependent cell adhesion and the generation of the ¹H-NMR-detectable mobile lipid spectrum would be consistent with the model. For example, normal human keratinocytes from post-confluent cultures have 10-fold higher triglyceride levels than pre-confluent or confluent cultures (Ponec, 1991). Cell adhesion to substratum is important for G₁/S phase transition through the cell cycle in monocytes. Adhesion plays a role in the generation of mobile lipid in peripheral blood monocytes (PBMCs) and macrophages (King *et al.*, 1991; King *et al.*, 1994), and is necessary to "prime" monocytes for further activation (Haskill *et al.*, 1988) - that is, in the G₁ phase of the cell cycle. Adhesion is also important in other cell types. For example, in murine fibroblasts, adhesion activates tyrosine kinases, such as growth factor receptor-linked tyrosine kinases, which ultimately result in the transduction of a signal to the nucleus (Rosales *et al.*, 1995; Kuzumaki *et al.*, 1996). During adhesion of PBMCs to plastic tissue culture surfaces or onto substrata coated with fibronectin, collagen, or laminin, there is a significant induction of a number of early genes such as *c-fos*, *c-jun* and *IκB*, as well as cytokines such as IL-1β, IL-8 and TNF-α. Many of the genes induced by the ligation of integrins can activate the nuclear transcription factor NF-κβ which is necessary for the transcription of cytokine genes (Haskill *et al.*, 1988; Haskill *et al.*, 1991). However, the secretion of cytokines was not evident in cell culture supernatant until an additional signal, such as LPS, was provided to further stimulate the cells.

Specific cell adhesion between CD63, a cell surface molecule, and VLA-3 or VLA-6

Cell density can positively or negatively regulate both the rate of progression to the G₁/S phase and the duration of the G₁ phase, by mechanisms involving both soluble factors and cell-cell contact. The length of G₁ during the exponential phase of cell proliferation can increase as a result of increasing cell density. This negative regulation can be inhibited if the serum concentration is increased (see section 1.10.4), which causes the

et al., 1992).

rate of cellular proliferation and cell cycling to increase, thereby decreasing G₁ phase time (DiSalvo *et al.*, 1995).

These results may shed some light on the ¹H-NMR studies showing that the mobile lipid is detectable in unstimulated PBMCs after culture in serum-containing medium for 16 h (King *et al.*, 1991; King *et al.*, 1994). The induction of the mobile lipid may be due to the interaction via cell adhesion receptors between monocytes that have adhered to the bottom of the tissue culture flask, and the T and B cells. This cell receptor interaction may also be enough to initiate the release of cytokines by the adherent monocytes. This would stimulate the T cells to develop mobile lipid in response to cytokine receptor stimulation, although cell to cell contact may be sufficient for the receptor-ligand mediated stimulation of phospholipases. Adhesion of cells has been shown to alter the expression and affinity of integrin molecules on the surface of the adherent cell.

1.10.3. Serum factor effects.

Integrin molecules can regulate cell cycle status (Meridith *et al.*, 1995), and therefore may play a role in the timing of the appearance of the ¹H-NMR-detectable mobile lipid. For instance, in fibroblasts growth-arrested by either serum deprivation or cell density growth arrest, differential expression of the cell-surface integrin molecules VLA-1 (Very Late Antigen-1), VLA-2 and VLA-3 was found (Fingerman & Hemler, 1988). VLA-1 and VLA-2 are detected on T cells and their expression can be altered by activation or culture conditions (Hemler & Jacobson, 1987). Resting T cells express VLA-4 and VLA-6, amongst other integrins. B cells express VLA-2, VLA-3, VLA-4, while monocytes express VLA-2, VLA-4 and VLA-6 (Hemler, 1990; Pigott & Power, 1993).

Specific cell adhesion between CD63, a cell surface molecule, and VLA-3 or VLA-6 integrins, has been recognised (Berditchevski *et al.*, 1995). Macrophages and monocytes express CD63, particularly after adhesion, which is believed to be involved in the adhesion of monocytes to serum coated plates (Toothill *et al.*, 1990). Some weak CD63 expression has also been shown on T cells and B cells (Barclay *et al.*, 1993). VLA-2 and VLA-4 have been shown to be involved in homotypic cell-cell adhesion (Campanero *et al.*, 1992).

Increased homotypic binding and cellular aggregation via LFA-1 has also been shown in G_1 growth arrested T lymphoma cells (Dumont *et al.*, 1995). Collectively, the homotypic and heterotypic binding that exists between T cells, B cells, monocytes and adherent macrophages, causing the cells to enter G_1 , may explain the development of the mobile lipid in the adherent and non-adherent cells observed in co-culturing experiments (King *et al.*, 1994). These interactions may be sufficient to stimulate resting cells to move into the G_1 phase where they may remain arrested until they receive an additional specific stimulating signal to move them into the S phase of the cell cycle, resulting in cellular proliferation. In late G_1 the degradation of PC via phospholipases is maximal and this may result in the accumulation of the mobile lipid in these cells. Thus the stimulation via cell surface receptors may also result in the direct activation of phospholipases, which may also contribute to the development of the $^1\text{H-NMR}$ -detectable mobile lipid.

1.10.3. Serum factor effects.

Serum contains a wide variety of growth factors and mitogenic agents necessary for the initiation of cell cycle progression. The proliferative rate of mammalian cells is regulated during the G_1 phase of the cell cycle. Mitogenic factors contained in serum can positively stimulate cells to progress into S phase. Increased percentages of human serum or foetal calf serum increased the $^1\text{H-NMR}$ mobile lipid signal in cultured PBMCs. The $-\text{N}(\text{CH}_3)^+$ peak corresponding to the choline head group of choline-containing phospholipid metabolites was also observed to increase with increasing amounts of serum supplementation, indicating some turnover of these metabolites (King *et al.*, 1994). This suggests that there is a relationship between the development of the mobile lipid and phosphatidylcholine metabolism.

Serum deprivation can arrest cells in the G_0/G_1 phase of the cell cycle, or the cells can complete mitosis and arrest in the next cell cycle. The commitment of cells to progress from G_1 to S phase occurs in mid to late G_1 . In murine fibroblasts which have been serum deprived there is an accumulation of a cyclin-dependent kinase inhibitor p27Kip1 which has been correlated with cell cycle arrest in these cells. p27 was down-regulated by

the addition of specific mitogens. This correlation links progression through the cell cycle with mitogenic signals at the restriction or commitment point in the cell cycle (Coats *et al.*, 1996).

Serum-deprivation of density-inhibited quiescent Swiss 3T3 fibroblasts caused the cells to undergo rapid cell death similar to apoptosis. All of the early G₁ genes, c-myc, c-fos, and c-jun, are induced by serum deprivation. Cells have fragmented DNA and have been shown to incorporate BrdU, which may indicate DNA repair activity rather than cell cycle progression. These results suggest that apoptosis and cell death involve events that are also typical of the G₁ phase or G₁/S boundary of the cell cycle. Therefore, failure to progress through the cell cycle after serum deprivation results in cell death (Pardee, 1989; Pardee & Wang, 1995). This may explain the increases in the mobile lipid observed in serum deprived fibroblasts (Delikatny *et al.*, 1996a) and the increase in the mobile lipid after the addition of serum to previously deprived PBMCs (King *et al.*, 1994).

1.10.4. Contributions by lipoprotein receptor regulation to mobile lipid.

Expression of lipoprotein receptors increases in mitogenically activated T lymphocytes (Cuthbert & Lipsky, 1984; Traill & Wick, 1984; Cuthbert & Lipsky, 1986; Traill *et al.*, 1987; Cuthbert & Lipsky, 1989; Traill *et al.*, 1990). The extra lipoprotein subsequently taken up may supply the cholesterol necessary for cellular proliferation and the unsaturated fatty acids necessary for incorporation into the phospholipids of the expanding membrane after activation (Cuthbert & Lipsky, 1986; Cuthbert & Lipsky, 1989). In fact, murine T cells and B cells depend upon fatty acid and lipoprotein uptake because they have been shown to be deficient in unsaturated fatty acid synthesis (Buttke *et al.*, 1989). Lipoproteins are also important for the supply of arachidonic acid for prostaglandin and leukotriene synthesis in cells stimulated by PDGF (Habenicht *et al.*, 1990). Lipoprotein receptor mRNA is detectable in PMA and ionomycin-stimulated Jurkat T cells and can be regulated by the transcription of early or immediate genes (Makar *et al.*, 1994). The lipoprotein receptors are present in G₁. Cells such as lymphocytes or fibroblasts can be stimulated to proliferate by the addition of lipoproteins

(Cuthbert & Lipsky, 1989; Yamaguchi *et al.*, 1993). These results suggest that while lipoproteins can be membrane associated, uptake and release of these molecules from within the cell may also contribute to the mobile lipids detected using $^1\text{H-NMR}$ in activated immune cells and cancer cells (Wright *et al.*, 1986; Mountford & Wright, 1988).

It may be important for triglycerides to act as intracellular storage pools of long chain unsaturated fatty acids in normal murine T and B cells, because these cells are deficient in unsaturated fatty acid synthesis (Buttke *et al.*, 1989). Mitogen-stimulated T and B cells obtain fatty acids from exogenous sources, such as lipoproteins, for incorporation into triglycerides (Goppelt *et al.*, 1985; Goppelt-Strube & Resch, 1987; Ricciolini *et al.*, 1991). Triglycerides can be incorporated into plasma membrane phospholipids upon mitogenic stimulation. However, there is some evidence for the presence of intracellular triglyceride in small amounts intercalated within the membrane in model phospholipid bilayers and in the phospholipid-rich surface monolayers of plasma lipoproteins (Hamilton & Small, 1981; Smaby & Brockman, 1987). NMR studies have shown that the molecular mobility of triglyceride increases dramatically after incorporation into the fluid bilayer (Hamilton, 1989). However, increases in mobile plasma membrane triglycerides during cell activation may also be partly a result of increased incorporation of lipoproteins into the membrane from exogenous serum sources. High affinity lipoprotein receptors are expressed at high levels on activated T lymphocytes, with low levels occurring on resting cells (Traill *et al.*, 1987; Jurgens *et al.*, 1989). Lipoproteins are believed to provide an exogenous source of fatty acids for optimal cell growth via these receptors (Cuthbert & Lipsky, 1986). This phenomenon may perhaps be explained by the incorporation of mobile lipids into phospholipid vesicles (Callies *et al.*, 1993) as suggested earlier (Hamilton & Small, 1981), further reducing the intracellular phospholipid precursors in cells already growing in a relatively effete medium (Hamilton & Small, 1981).

Cellular defects in lipid metabolism that occur in monocytes and macrophages, such as Tangier's disease, can give us information about the normal metabolism of these cells. In Tangier's disease there is an accumulation of lipids in cells due to increased turnover of

phospholipids (sphingomyelin, phosphatidylcholine, phosphatidylserine, phosphatidylethanolamine). Overproduction of triacylglycerols and esterified cholesterol is associated with the absence of HDL in the plasma, as detected using the incorporation of radioactive labels (^{32}P i, ^3H -serine, ^3H -choline, ^{14}C -acetate and ^{14}C -oleic acid) in normal and Tangier mononuclear phagocytes. The binding of HDL to its cellular receptor results in the removal of cholesterol esters from normal cells, but in Tangier's disease the binding of HDL to the cells causes an increase in the levels of cholesterol esters (Schmitz *et al.*, 1990). It was also shown by these authors that defects in signal transduction pathways from the HDL receptor occur in patients with Tangier's disease, which may explain the impaired regulation of lipid metabolism in these cells (Drobnik *et al.*, 1995). These findings show that in cells which are not transformed or stimulated, an accumulation of triglycerides is associated with increased phospholipid anabolism and catabolism in cells with impaired lipid regulation. These results add further weight to the argument that the expression of lipoprotein receptors and regulation of lipoprotein metabolism may play a role in the ^1H -NMR mobile lipid accumulation.

1.10.5. Summary.

Collectively, this evidence indicates that the accumulation of mobile lipids may be a consequence of the cell cycle status induced by the extracellular environment. Mobile lipid has been shown to accumulate in serum-deprived cells, in cells activated using growth factors, mitogens or cytokines, and during cell adhesion. Cell cycle-associated lipoprotein uptake may also contribute to the accumulation of mobile lipid.

1.11. Concluding remarks.

The principle point of this project was to determine the nature and the origin of the mobile lipid resonances detectable using ^1H -NMR in activated immune cells. These resonances are also present in metastatic cancer cells and a variety of other cells which are undergoing cellular processes associated with activation, proliferation, necrosis or possibly even apoptosis. The mobile lipid was previously identified as primarily triglyceride which existed in a lipoprotein structure in cells that display the mobile lipid

resonances. However, although these lipoprotein structures, abundant in plasma, can give rise to these resonances, it is also possible that other structural configurations occurring in vesicles or membranes which can be associated with the activated cells give rise to similar high resolution $^1\text{H-NMR}$ spectra. There may also be a combination of different lipid species which exhibit associated acyl chain resonances that overlap with the $^1\text{H-NMR}$ resonances detected for triglycerides. These include the acyl fatty acid chains associated with phospholipids.

Previously it was thought that the mobile lipid spectrum was exclusively associated with the plasma membrane of the cell. It has been confirmed that the plasma membrane contributes, but it has also been shown that mobile lipid can be associated with lipid droplets and vesicles within cells. Thus, this issue remains controversial. However, if phospholipid synthesis and catabolism, associated with a number of cellular activation processes, does play a role in the generation of the mobile lipid, it would be expected that the processes involved would occur both within the cell and associated with the plasma membrane.

The mobile lipid resonances are present in immune cells such as neutrophils, macrophages, T cells and B cells after activation by a variety of stimuli, both *in vivo* and *in vitro*. These observations imply that a common mechanism may be involved in the generation of the mobile lipid in all of these cells. At the start of this study very little was known about the origin of these resonances. It had been established that the $^1\text{H-NMR}$ detectable mobile lipid was associated with activated immune cells and that it could appear early in the activation of T cells. Various antioxidant and protein kinase C inhibitors were unable to block the generation of the development of the mobile lipid. Blocking lymphocytes in the G_1 phase of the cell cycle, thereby inhibiting proliferation, did not inhibit the appearance of the mobile lipid resonances.

Chapter 2.

Materials and Methods.

2.1. Isolation of splenic and thymic T lymphocytes.

2.1.1. Animals.

The mice used in the experiments described were the strain C57BL/6 mice (*Mus musculus*), 5-9 weeks old, housed under standard conditions, with free access to food and water, in the Blackburn Building Animal House, University of Sydney. Animals in this age group were used so that maximal yields of thymocytes could be isolated.

2.1.2. Materials for cell culture.

Bovine foetal calf serum (FCS), penicillin, streptomycin and L-glutamine were obtained from the Commonwealth Serum Laboratories (Melbourne, Australia). Dulbecco's Modified Eagle's Medium (DMEM) was obtained from Cytosystems (Castle Hill, NSW, Australia). 2-Mercaptoethanol (2-ME) was obtained from Sigma (St. Louis, MO, USA). Ionomycin, phorbol myristate acetate (PMA) and [methyl-³H]thymidine were purchased from Calbiochem (La Jolla, CA, USA) or ICN Biomedicals Inc. (Irvine, CA, USA). Tricyclodecan-9-yl-xanthogenate (D609) was purchased from Biomol Inc. (PA, USA).

2.1.3. Isolation of splenocytes and thymocytes.

Mice were killed by cervical dislocation. The thymus and spleen (Figure 2.1) were removed under sterile conditions (Gelman BH120 biohazard hood; Gelman Sciences, Ann Arbor, MI) and placed in sterile disposable petri dishes (Sarstedt, Germany) containing a small volume of DMEM supplemented with 10% FCS, L-glutamine (2 mM), HEPES (20 mM), NaHCO₃ (44 mM), penicillin (50 units mL⁻¹), streptomycin (50 µg mL⁻¹), and 0.1 mM 2-mercaptoethanol. The thymus was excised carefully to avoid

the parathymic nodes, which would contaminate the thymocyte suspension with peripheral B and T lymphocytes (Mishell *et al.*, 1980). Thymocyte and splenocyte cell suspensions were prepared by forcing the tissue through a sterile 70 µm nylon mesh cell strainer (Falcon-Becton Dickinson, Mountainview, CA USA) using a sterile 5 mL disposable syringe plunger (Terumo, Melbourne, Australia) into a sterile petri dish containing supplemented medium. Splenocytes were enriched for T cells using two separation procedures, nylon wool separation and sheep α-Mouse Ig coupled SRBCs (Figure 2.2 and Section 2.1.4).

2.1.4. Separation of splenocytes

Nylon Wool

Splenic T lymphocytes were used for cell suspensions using a nylon wool separation procedure. The nylon wool column (Pharmacia, Polysciences, PA, USA) was teased into a plastic syringe barrel fitted with a plastic stopcock. The nylon wool column was incubated with media (DMEM/10% FCS) with gentle tapping to ensure that the wool was wet and free of air bubbles. The column was then equilibrated for 1 h at 37°C. Prior to separation on the nylon wool column, splenocytes were separated over Ficoll [9.8% w/v Ficoll 400 (Pharmacia Biotech, Uppsala, Sweden), 5% w/v metrizoic acid (Sigma, St. Louis, MO, USA)], washed, and resuspended in DMEM/5% FCS. The column was drained of media to the top of the nylon wool and $1-2 \times 10^6$ splenocytes were added per column in a volume of 2 mL of supplemented media. A further 2 mL of media was added to the top of the column and this was allowed to run into the column to allow the cell suspension to penetrate the nylon wool. Another 2-5 mL of media was added to the top to cover the top of the column. The column was incubated for 1 h at 37°C. The non-adherent T cells were collected by using two 50 mL washes. The collected cells were

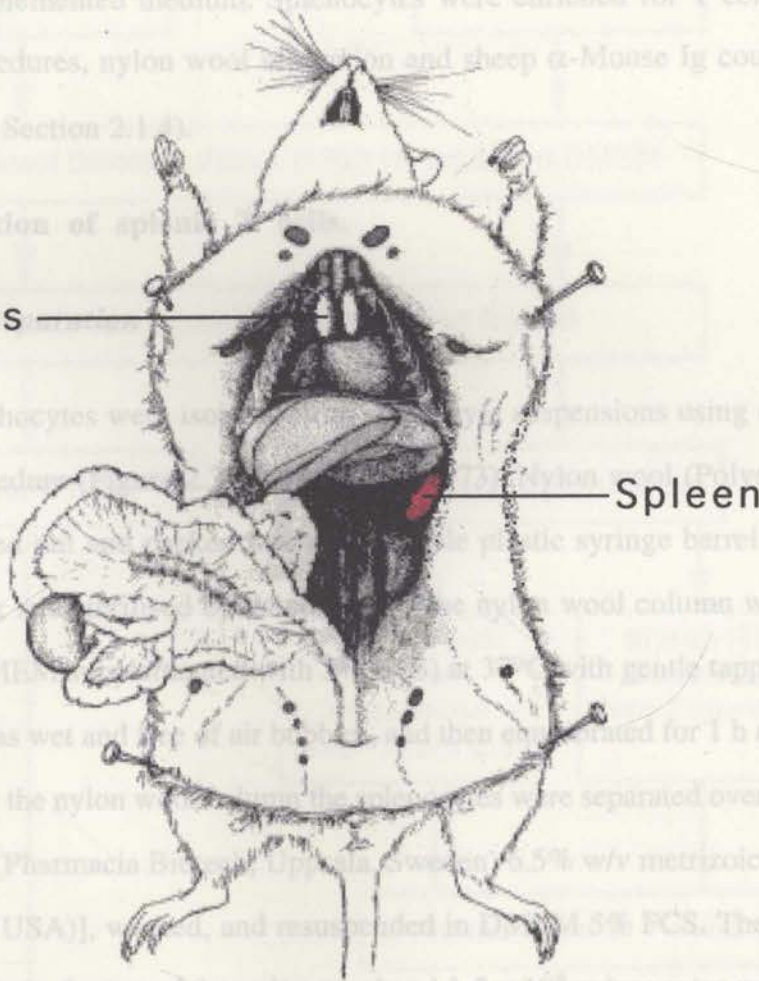


Figure 2.1. The anatomy of the mouse showing the location of the thymus and spleen. Adapted from Mishell *et al.* (1980).

supernatant discarded. The cell pellet was resuspended in approximately 10 mL of medium. Cells were suspended in DMEM/10% FCS and incubated for 2 h in FCS-coated

the parathymic nodes, which would contaminate the thymocyte suspension with peripheral B and T lymphocytes (Mishell *et al.*, 1980). Thymocyte and splenocyte cell suspensions were prepared by forcing the tissue through a sterile 70 μm nylon mesh cell strainer (Falcon Becton Dickinson, Mountainview, CA USA) using a sterile 5 mL disposable syringe plunger (Terumo, Melbourne, Australia) into a sterile petri dish containing supplemented medium. Splenocytes were enriched for T cells using two separation procedures, nylon wool separation and sheep α -Mouse Ig coupled SRBCs (Figure 2.2 and Section 2.1.4).

2.1.4. Separation of splenic T cells.

Nylon wool separation

Splenic T lymphocytes were isolated from splenocyte suspensions using a nylon wool separation procedure (Figure 2.3) (Julius *et al.*, 1973). Nylon wool (Polysciences, PA, USA) was teased out and packed into a disposable plastic syringe barrel fitted with a plastic stopcock and sterilised by autoclaving. The nylon wool column was incubated with media (DMEM supplemented with 5% FCS) at 37°C with gentle tapping to ensure that the wool was wet and free of air bubbles, and then equilibrated for 1 h at 37°C. Prior to separation on the nylon wool column the splenocytes were separated over Ficoll [9.8% w/v Ficoll 400 (Pharmacia Biotech, Uppsala, Sweden) 6.5% w/v metrizoic acid (Sigma, St. Louis, MO, USA)], washed, and resuspended in DMEM 5% FCS. The column was drained of media to the top of the nylon wool and $1-2 \times 10^8$ splenocytes were added per column in a volume of 2 mL of supplemented media. A further 2 mL of media was added to the top of the column and this was allowed to run into the column to allow the cell suspension to penetrate the nylon wool. Another 2-5 mL of media was added to the top to cover the top of the column. The column was incubated for 1 h at 37°C. The non-adherent T cells were collected by using two 50 mL washes. The collected cells were centrifuged at 1000 g for 10 min (Heraeus, 2250 Rotor, Osterode, Germany) and the supernatant discarded. The cell pellet was resuspended in approximately 10 mL of medium. Cells were suspended in DMEM/10% FCS and incubated for 2 h in FCS-coated

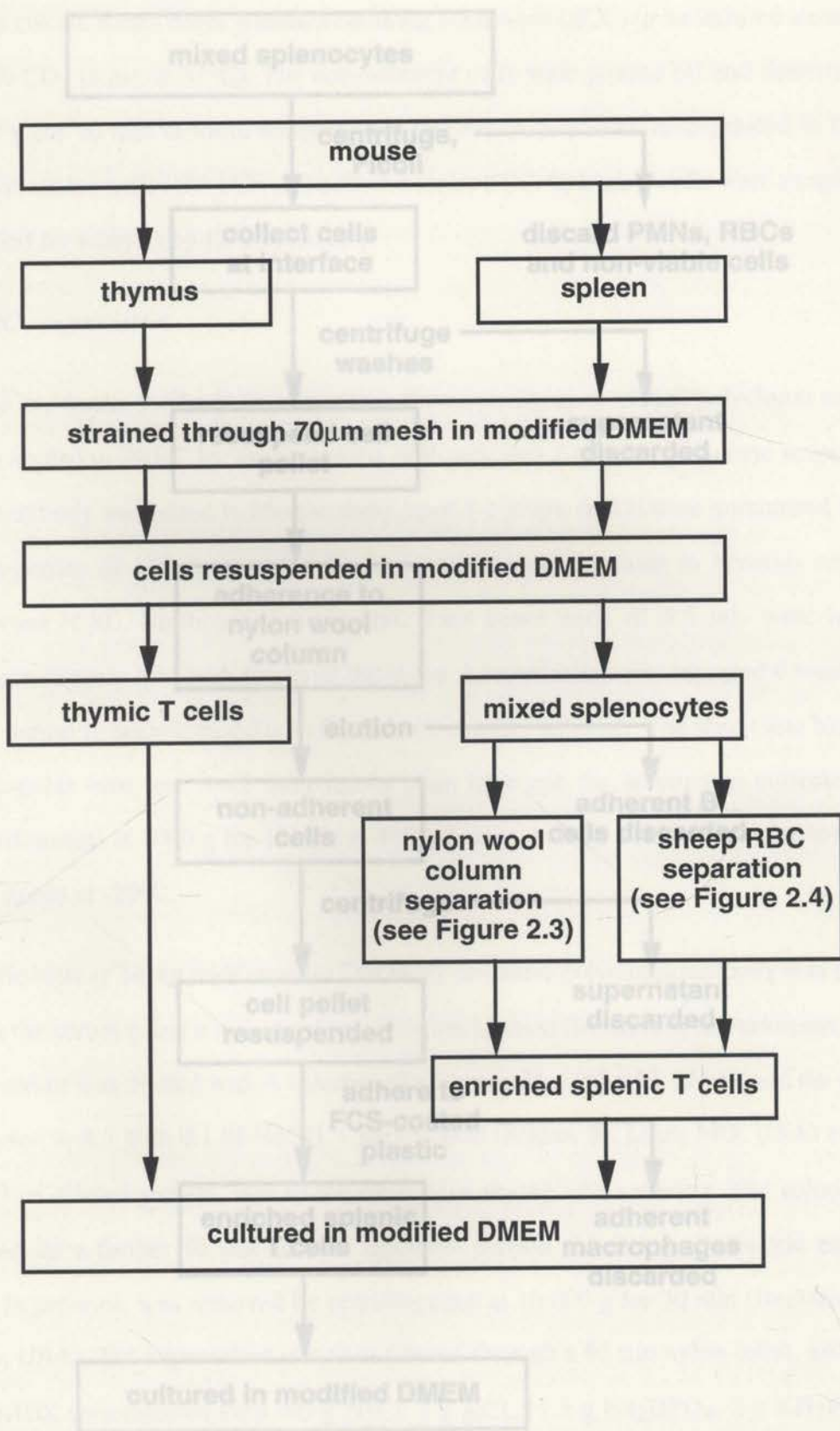


Figure 2.2. Procedure for isolation and culture of thymic and splenic T cells.

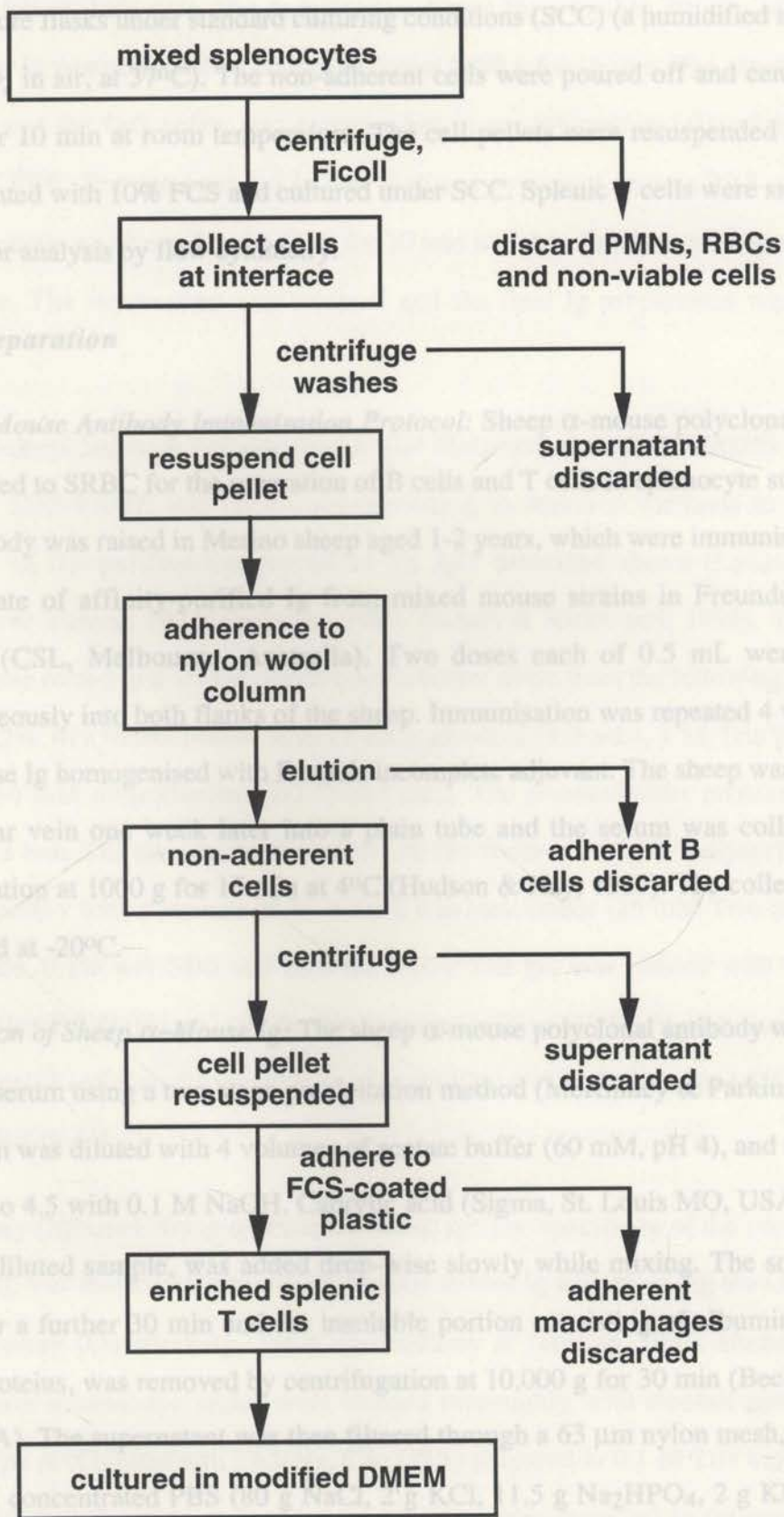


Figure 2.3. Procedures for separation of splenic T cells using nylon wool column.

tissue culture flasks under standard culturing conditions (SCC) (a humidified atmosphere of 5% CO₂ in air, at 37°C). The non-adherent cells were poured off and centrifuged at 1000 g for 10 min at room temperature. The cell pellets were resuspended in DMEM supplemented with 10% FCS and cultured under SCC. Splenic T cells were sampled and labelled for analysis by flow cytometry.

SRBC separation

Sheep α -Mouse Antibody Immunisation Protocol: Sheep α -mouse polyclonal antibody was coupled to SRBC for the separation of B cells and T cells in splenocyte suspensions. The antibody was raised in Merino sheep aged 1-2 years, which were immunised with an homogenate of affinity-purified Ig from mixed mouse strains in Freund's complete adjuvant (CSL, Melbourne, Australia). Two doses each of 0.5 mL were injected sub-cutaneously into both flanks of the sheep. Immunisation was repeated 4 weeks later with mouse Ig homogenised with Freund's incomplete adjuvant. The sheep was bled from the jugular vein one week later into a plain tube and the serum was collected after centrifugation at 1000 g for 15 min at 4°C (Hudson & Hay, 1989). The collected serum was stored at -20°C.

Purification of Sheep α -Mouse Ig: The sheep α -mouse polyclonal antibody was purified from the serum using a two-stage precipitation method (McKinney & Parkinson, 1987). The serum was diluted with 4 volumes of acetate buffer (60 mM, pH 4), and the pH was adjusted to 4.5 with 0.1 M NaOH. Caprylic acid (Sigma, St. Louis MO, USA) at 25 μ L mL⁻¹ of diluted sample, was added drop-wise slowly while mixing. The solution was stirred for a further 30 min and the insoluble portion consisting of albumin and other non-Ig proteins, was removed by centrifugation at 10,000 g for 30 min (Beckman, Palo Alto, USA). The supernatant was then filtered through a 63 μ m nylon mesh, and mixed with 10X concentrated PBS (80 g NaCl, 2 g KCl, 11.5 g Na₂HPO₄, 2 g KH₂PO₄ and 20 mL of 100 mM EDTA, pH 7.4 and made up to 1 L) at a ratio of 1:9 (PBS:supernatant). The pH was then adjusted to 7.4 with 1.0 M NaOH. The supernatant was cooled to 4°C and ammonium sulphate (BDH, Australia) was added to give a

concentration of 45% w/v. The sample was stirred for a further 30 min and then the precipitated Ig was collected by centrifugation at 5000 g for 15 min. The supernatant was discarded and the IgG pellet was resuspended in approximately 1/10 of the original volume of PBS. The resuspended Ig was dialyzed overnight against PBS at 4°C. The dialyzed sample was heated to 50-55°C for 20 min and then finally centrifuged at 5000 g for 20 min. The supernatant was retained and the final Ig preparation was stored at -20°C.

Sodium Dodecyl Sulphate Polyacrylamide Gel Electrophoresis (SDS-PAGE) of Purified Sheep Ig: SDS-PAGE was performed according to standard methods to assess the efficiency of the purification procedure for IgG described above (Laemmli, 1970; Stanworth & Turner, 1978; Springer, 1980; Hames & Rickwood, 1994). The protein samples were mixed in a 1:1 ratio with sample buffer made from the following: 10% SDS (1 mL), 0.2% w/v bromophenol blue (1 mL), glycerol (1.5 mL), 1 M Tris pH 6.8 (0.5 mL) and 50 mM dithiothreitol (DTT) (0.8 mL). The protein/buffer mixture was then boiled for 2 min. The samples were loaded into the wells of a 12.5% polyacrylamide gel and run at 200 v with a current of 25 A for 2 h in tank buffer (25 mM Tris, pH 8.3, 192 mM glycine, 0.1% w/v SDS and distilled H₂O). The gel was stained with Coomassie Brilliant Blue R250 (Sigma) (0.5% w/v Coomassie Blue, 10% v/v methanol, and 25% v/v acetic acid) and then destained in methanol (10% v/v) and acetic acid (25% v/v) and finally in distilled H₂O.

Ouchterlony Diffusion Assay of Purified Sheep Ig: The specificity of the purified sheep α -mouse Ig was assessed for reactivity against mouse Ig antigen using the Ouchterlony diffusion assay (Ouchterlony, 1968; Ouchterlony & Nilsson, 1986; Hudson & Hay, 1989). Glass microscope slides were cleaned thoroughly with alcohol and 1% (w/v) agarose type A (Calbiochem, La Jolla, CA, USA) prepared in 0.1 M Tris buffer pH 8.0, was poured over the slide surface (~10 mL). The slides were left to set overnight in a humidified box prepared using paper towels saturated with Tris buffer at 4°C. Wells were cut out of the gel when dry. The antigen, mouse Ig, was added to the centre well and dilutions of the sheep anti-mouse purified antibody and unpurified immune serum

were added to the surrounding wells. Antigen and antibody diffuse out of the wells into the surrounding agar and precipitin lines form when the antibody and antigen bind at equimolar concentrations. The plates were stored in a humidified box as described above for at least 24 h before precipitin lines were observed.

Sheep α -Mouse-Coupled SRBC (SRBC-S α MIg) Separation Procedure: Splenic T lymphocytes were isolated from splenocyte suspensions using a two-stage method modified from Parish *et al.* (1974) (Figure 2.4). Whole blood was collected aseptically from a sheep into heparinised tubes and mixed at a ratio of 3 parts of whole blood to 4 parts of Alsever's solution (2.05% D-glucose, 0.42% NaCl, 0.8% trisodium citrate) and stored at 4°C. Sheep red blood cells (SRBCs) were washed in normal saline and centrifuged for 10 min at 1650 g (Heraeus Omnifuge 2.0RS, Osterode, Germany) to remove the Alsever's solution. 0.25 mL of packed SRBCs were resuspended in 4 mL of normal saline and were coupled with 40 μ L of sheep anti-mouse antibody (S α MIg) using 300 μ L of 0.1% CrCl₃ (Poston, 1974; Van der Giessen *et al.*, 1985) (the concentration was determined by previous titration) diluted in normal saline. The cell suspension was mixed and incubated at room temperature for 5 min. The coupling process was stopped by the addition of 7 mL of PBS. The cell suspension was then centrifuged for 10 min at 825 g and washed once with 20 mL of PBS. The final cell pellet was resuspended in 2.5 mL of RPMI supplemented with 1% FCS and stored at 4°C. S α MIg-coupled SRBCs were normally used within 24 h of preparation.

Splenocytes isolated from each spleen were resuspended in 2.5 mL of DMEM-supplemented medium and added to 2.5 mL of SRBC-S α MIg. The splenocytes and SRBC-S α MIgs were centrifuged for 3 min at 1230 g and 4°C to mix the two cell types. They were then incubated on ice for 30 min to facilitate adherence of the B cells to the S α MIg. Following this incubation, 25 μ L of 25% NaN₃ was added to fix the rosettes, consisting of SRBC-S α MIgs and B-cells, and the cell pellet was resuspended. The cells were layered onto Ficoll (9.8% Ficoll 400 w/v and 6.5% w/v metrizoic acid) and centrifuged for 20 min at 2500 g and 20°C, to remove the SRBC-S α MIg and adhered B cells. The mononuclear layer of cells containing the T cells was removed,

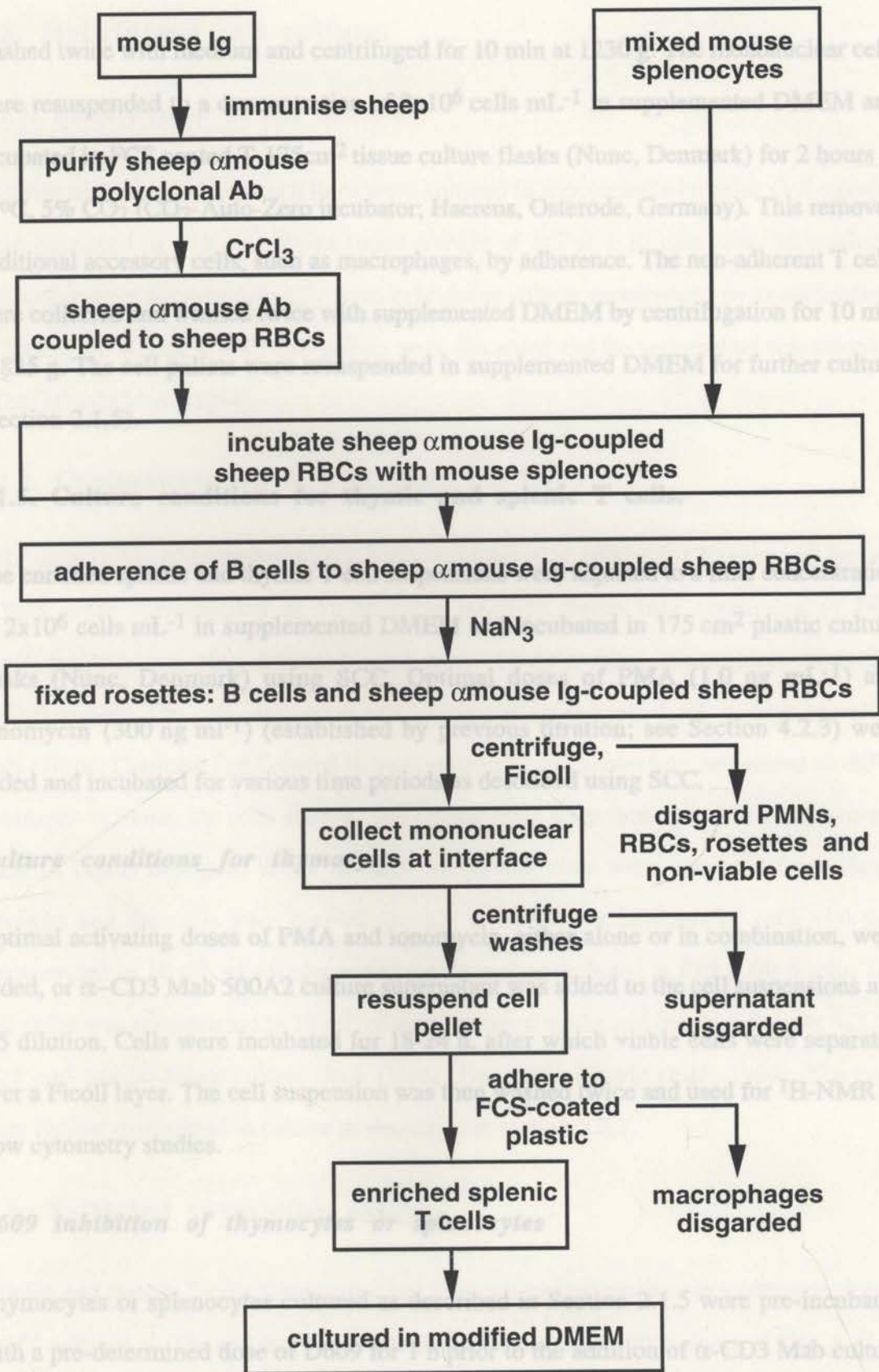


Figure 2.4. Procedures for separation of splenic T cells using sheep α mouse Ig-coupled sheep red blood cell adherence technique.

washed twice with medium and centrifuged for 10 min at 1230 g. The mononuclear cells were resuspended to a concentration of 2×10^6 cells mL^{-1} in supplemented DMEM and incubated in FCS coated T-175 cm^2 tissue culture flasks (Nunc, Denmark) for 2 hours at 37°C, 5% CO_2 (CO_2 -Auto-Zero incubator; Haereus, Osterode, Germany). This removed additional accessory cells, such as macrophages, by adherence. The non-adherent T cells were collected and washed twice with supplemented DMEM by centrifugation for 10 min at 825 g. The cell pellets were resuspended in supplemented DMEM for further culture (Section 2.1.5).

2.1.5. Culture conditions for thymic and splenic T cells.

The enriched splenic and thymic T cell suspensions were adjusted to a final concentration of 2×10^6 cells mL^{-1} in supplemented DMEM and incubated in 175 cm^2 plastic culture flasks (Nunc, Denmark) using SCC. Optimal doses of PMA (1.0 ng mL^{-1}) and ionomycin (300 ng mL^{-1}) (established by previous titration; see Section 4.2.3) were added and incubated for various time periods as described using SCC.

Culture conditions for thymocytes

Optimal activating doses of PMA and ionomycin, either alone or in combination, were added, or α -CD3 Mab 500A2 culture supernatant was added to the cell suspensions at a 1:5 dilution. Cells were incubated for 18-24 h, after which viable cells were separated over a Ficoll layer. The cell suspension was then washed twice and used for $^1\text{H-NMR}$ or flow cytometry studies.

D609 inhibition of thymocytes or splenocytes

Thymocytes or splenocytes cultured as described in Section 2.1.5 were pre-incubated with a pre-determined dose of D609 for 1 h prior to the addition of α -CD3 Mab culture supernatant. All other procedures were performed as described (Section 2.1.5).

A final volume of 200 μl was added to each well of a sterile 96-well microtiter flat-bottomed plate (Nunc, Denmark) and incubated using SCC for 72 h. Culture wells were pulsed with 1 μCi of [methyl- ^3H] thymidine in PBS and

2.2. Hybridoma cell culture.

2.2.1. Maintenance of cell cultures.

Hamster and rat hybridoma cell lines were cultured in supplemented media. Cell cultures were passaged in 175 cm² flasks twice weekly at 1:5 or 1:10 dilutions. Monoclonal antibodies were harvested weekly from hybridoma culture supernatants by centrifugation at 2500 g for 10 min at 4°C. Cell pellets were discarded and the supernatant was stored at -20°C (Doyle *et al.*, 1994).

2.2.2. Cryopreservation of hybridoma cell lines.

Cell suspensions of hybridoma cells were centrifuged at 1000 g for 10 min and the cell pellets were resuspended at 1×10^7 cells mL⁻¹ in freeze mix consisting of FCS supplemented with 10% dimethyl sulphoxide (DMSO; Ajax, Melbourne, Australia) chilled to 4°C. The cell suspension was quickly aliquoted into 1 mL cryopreservation vials (Nunc, Denmark) and placed in a polystyrene foam cooler box and stored at -80°C overnight to freeze the cells slowly. The frozen vials were then stored in a cell storage bank in liquid nitrogen. When needed, individual vials were removed from liquid nitrogen and the cells were thawed quickly at 37°C. The contents of each vial was resuspended in 10 mL of supplemented media and centrifuged at 825 g for 5 min. The cell pellet was resuspended in 20 mL of supplemented media and incubated under SCC in a 25 cm² plastic tissue culture flask (Nunc, Denmark) (Doyle *et al.*, 1994). The cells were further maintained in culture as described in section 2.2.1.

2.3. Tritiated thymidine assays.

Splenic and thymic T cells were suspended in supplemented medium at a concentration of 2×10^6 cells mL⁻¹. The cell suspensions were activated with optimal doses of Con A ($2 \mu\text{g mL}^{-1}$), PMA (1 ng mL^{-1}) and ionomycin (300 ng mL^{-1} , or Mab 500A2 (α -CD3) (1:5 dilution of culture supernatant). A final volume of 200 μL was added to each well of a sterile 96-well microtiter flat-bottomed plate (Nunc, Denmark) and incubated using SCC for 72 h. Culture wells were pulsed with 1 μCi of [methyl-³H] thymidine in PBS and

incubated for 6 h under SCC. Well contents were harvested (Pharmacia LKB, Uppsala, Sweden) onto filter mats which were allowed to dry for 4 h or overnight before being sealed in a sample plastic bag with 10 mL of scintillant. Thymidine incorporation was measured using a 1205 Betaplate liquid scintillation counter (Pharmacia LKB, Uppsala, Sweden). The results were expressed as counts per minute (CPM) (Mishell *et al.*, 1980).

2.4. Measurement of cell diameter.

Splenic and thymic T cells were removed from culture after activation with PMA/ionomycin at designated time points and transferred to a haemocytometer grid. The diameters of 100 cells were measured at each stage of activation using a calibrated ocular grid, and the mean diameter \pm SE was calculated.

2.5. Flow cytometric analysis.

2.5.1. Antibodies.

Anti-mouse Thy 1.2 conjugated to biotin was obtained from Becton Dickinson (CA, USA). Avidin fluorescein isothiocyanate (FITC) was obtained from Tago (Burlingame, CA, USA), while affinity purified sheep anti-mouse Ig-FITC F(ab')₂ and isotype control antibodies were obtained from Silenus Laboratories (Melbourne, Australia). Anti-mouse IL-2R monoclonal antibody (7D4) (Ortega *et al.*, 1984), α -CD3 (500A2) (Havran *et al.*, 1987) was a gift from Dr Barbara Fazekis De St Groth (Centenary Institute for Cell Biology and Cancer Medicine, Camperdown, Sydney).

2.5.2. Flow cytometry labelling procedure.

Samples of 10⁶ cells from unseparated splenocytes and isolated splenic T cells were incubated with biotin labelled anti-mouse Thy 1.2 antibody, at a dilution previously titrated for maximal binding, or incubated with supplemented medium for 1 h at 4°C. After the first antibody incubation the cells were centrifuged through a FCS bed and incubated with either avidin-FITC or affinity purified sheep anti-mouse Ig-FITC F(ab')₂ at a dilution for maximum specific fluorescence for 1 h at 4°C. After this time cells were

at a dilution for maximum specific fluorescence for 1 h at 4°C. After this time cells were again centrifuged through FCS, then the cell pellets were resuspended in PBS and filtered through a 63- μ m nylon mesh for flow cytometry. The fluorescence was measured using a FACScan (Becton Dickinson, Mountainview, CA) with an argon ion laser set at 488 nm for excitation of FITC (maximum excitation 495 nm, peak emission 525 nm). The cells were gated based on low forward scatter and low side scatter (see Appendix 2). In each gated region 10^4 events were counted. A representative dot plot of the gated region for activated murine thymocytes is shown in Figure 2.5. This gated region can be represented using a histogram where fluorescence intensity is plotted as a function of the number of events or number of cells.

Statistical analysis was used to monitor the changes in fluorescence intensity by setting region markers, as shown on the dot plots and histograms from mouse thymocytes (Figure 2.5). These markers were set relative to control antibody staining.

2.6. NMR spectroscopy.

2.6.1. NMR materials.

Deuterium oxide (D_2O ; 99.97%) was supplied by the Australian Nuclear Science and Technology Organization (Lucas Heights, NSW, Australia), while 3-(trimethylsilyl)[2,2,3,3- 2H] propionate (TSP- d_4) was from Fluka A.G. (Buchs, Switzerland). Triolein (1,2,3-tri-*cis*-9-octadecenoylglycerol) was supplied by Sigma (St Louis, MO, USA).

2.6.2. Cell preparation for NMR analysis.

Thymocytes, splenocytes, and isolated splenic T cells were prepared for 1H -NMR analysis as described by Dingley *et al.* (1992). The cells were removed from culture at the end of the incubation period and centrifuged in two tubes at 1230 g for 15 min at 21°C. The two cell pellets were combined and resuspended in 10 mL of supernatant. To separate viable from dead T cells the resuspended cells were layered onto a Ficoll bed and centrifuged at 2500 g for 20 min at 21°C. The live T lymphocytes were removed from

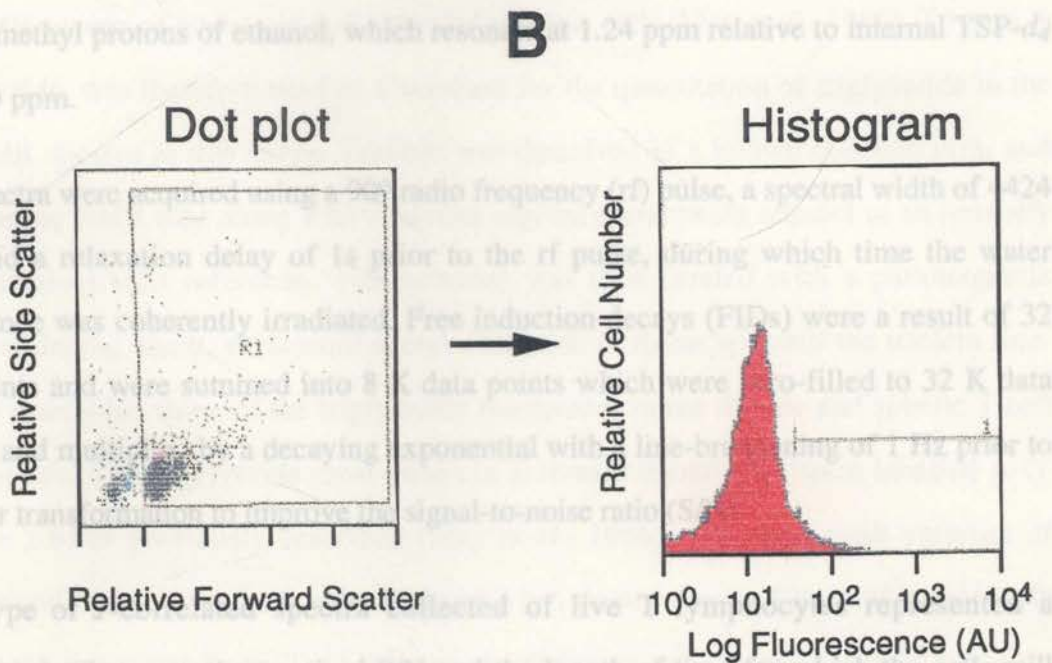
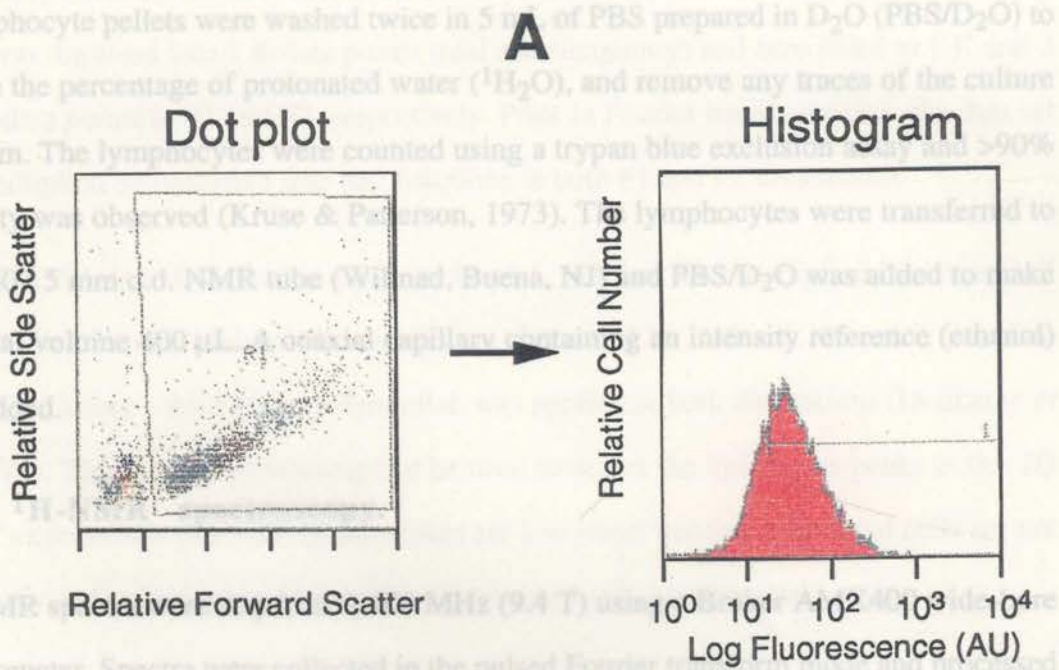


Figure 2.5. Representative flow cytometry dot plots and resultant histograms. Flow cytometric analysis of IL-2R α expression on thymocytes treated with (A) PMA and ionomycin, or (B) α CD3 antibody.

FIDs were collected after 8 unwritten dummy transients and each FID consisted of 32 T lymphocyte pellets were washed twice in 5 mL of PBS prepared in D₂O (PBS/D₂O) to reduce the percentage of protonated water (¹H₂O), and remove any traces of the culture medium. The lymphocytes were counted using a trypan blue exclusion assay and >90% viability was observed (Kruse & Patterson, 1973). The lymphocytes were transferred to a PP-507 5 mm o.d. NMR tube (Wilmad, Buena, NJ) and PBS/D₂O was added to make the final volume 400 μL. A coaxial capillary containing an intensity reference (ethanol) was added.

2.6.3. ¹H-NMR spectroscopy.

¹H-NMR spectra were acquired at 400 MHz (9.4 T) using a Bruker AMX400 wide-bore spectrometer. Spectra were collected in the pulsed Fourier transform mode and processed on Aspect X32 computers using UXNMR software (Bruker A. G., Karlsruhe, Germany). The temperature was controlled at 310 K. Chemical shifts (δ) were referenced to the methyl protons of ethanol, which resonate at 1.24 ppm relative to internal TSP-*d*₄ at 0.00 ppm.

1D spectra were acquired using a 90° radio frequency (rf) pulse, a spectral width of 4424 Hz, and a relaxation delay of 1 s prior to the rf pulse, during which time the water resonance was coherently irradiated. Free induction decays (FIDs) were a result of 32 transients and were summed into 8 K data points which were zero-filled to 32 K data points and multiplied by a decaying exponential with a line-broadening of 1 Hz prior to Fourier transformation to improve the signal-to-noise ratio (S/N).

The type of *J*-correlated spectra collected of live T lymphocytes represented a compromise between the required S/N and the length of time for which the cells will survive in the NMR tube (~85% viability as assessed by trypan blue exclusion after 3 h in the NMR probe). Non-phase-sensitive COSY spectra were acquired in 2.75 h using a spectral width of 4424 Hz in both F2 and F1, with 256 incremented values of the evolution time (*t*₁). Acquisition incorporated a relaxation delay of 1 s prior to the first radio frequency pulse, during which time the water resonance was coherently irradiated.

FIDs were collected after 8 unwritten dummy transients and each FID consisted of 32 transients digitised into 2 K data points (real and imaginary) and zero filled to 1 K and 2 K real data points in F1 and F2, respectively. Prior to Fourier transformation, the data set was multiplied by unshifted sine bell functions in both F1 and F2 dimensions.

For $^1\text{H-NMR}$ data described in Chapter 5 and 6, the data was multiplied by a sine bell function in F1 and a Lorentz-Gauss function (LB = -30 Hz, GB = 0.12) in F2. Baseline correction, using a third-order polynomial, was applied in both dimensions (Delikatny *et al.*, 1991). This type of processing can be used to detect the lipid cross-peaks in the 2D COSY experiments when signal intensities are low either because individual cells are not fully activated or because only a small percentage of cells are activated.

2.6.4. Calculation of mobile lipid concentrations.

Triglyceride was identified as the major source of the mobile lipid resonances in $^1\text{H-NMR}$ spectra of malignant and activated immune cells (May *et al.*, 1986). Triolein, a triglyceride, was therefore used as a standard for the quantitation of triglyceride in the $^1\text{H-NMR}$ spectra in this study. Triolein was dissolved at a known concentration and added to an NMR tube along with a coaxial capillary containing ethanol as an intensity and chemical shift reference. This solution was then titrated with a paramagnetic line-broadening agent, chromium acetyl acetonate ($\text{Cr}(\text{acac})_3$), until the triolein line-widths resembled those of the triglyceride resonances in the thymic and splenic T cell suspensions. The triglyceride cross-peaks in activated thymocytes were labelled A-G' (Figure 2.6) as previously described (May *et al.*, 1986). The cross-peak volumes of triolein and ethanol standards were integrated and these were used in combination with cross-peak intensities from 2D COSY spectra of thymic and splenic T cells to calculate the triglyceride concentrations in the lymphocyte suspensions ($[\text{T}]_{\text{cell}}$) using the following equation.

$$[\text{T}]_{\text{cell}} = \frac{\text{CE}_s(10^6x)}{\text{EC}_s\text{N}} \pm \frac{\text{CE}_s(10^6x)}{\text{EC}_s\text{N}} \times \sqrt{(\delta\text{E}/\text{E})^2 + (\delta\text{C}/\text{C})^2 + (\delta\text{E}_s/\text{E}_s)^2 + (\delta\text{C}_s/\text{C}_s)^2 + (\delta\text{N}/\text{N})^2 + (\delta x/x)^2}$$

Figure 2.6. Two-Dimensional ^1H -NMR spectrum of thymic T cells 72 h after activation with PMA and ionomycin.

The cross-peaks A-G' correspond to the triglyceride structure. Other labelled cross-peaks are as follows:

l	lactate
h	hepes
t	taurine
Cho	choline
PCho	phosphocholine
GPC	glycerophosphocholine

where $[T]_{\text{cell}}$ is the concentration of the triglyceride in nmoles/ 10^6 cells; C and C_s are the integrals of the triglyceride cross-peaks in the T lymphocyte suspension and appropriately line-broadened triolein standard solution, respectively; E and E_s are the integrals of the ethanol cross-peak in the T lymphocyte suspension and the line-broadened triolein standard solution, respectively; N is the cell count; and x is the number of moles (nmoles) of triolein in the triolein standard. $\delta E/E$, $\delta E_s/E_s$, $\delta C/C$, $\delta C_s/C_s$, $\delta N/N$, and $\delta x/x$ are the respective percentage errors of the measured parameters, where $\delta E/E$, $\delta E_s/E_s$, $\delta C/C$, and $\delta C_s/C_s$ were 5%, and $\delta N/N$ and $\delta x/x$ were 1 % of the measured parameter values.

The relative peak intensity of the choline (Cho), phosphocholine (PCho), and glycerophosphocholine (GPC) cross-peaks were normalized relative to the cell number and the intensity reference ethanol.

2.7. Sheep studies.

2.7.1. Animals.

Sheep were used for the *in vivo* studies because a large animal model was required for the cannulation of lymph nodes (Hurn & Chantler, 1980). Merino sheep one year of age were housed in pens and fed a standard pelleted ration and water *ad libitum*.

2.7.2. Surgery and lymph collection.

The surgery for the cannulations and the removal of the lymph nodes from the sheep was performed by Dr. Susan McClure, CSIRO Mc Master Laboratory, Division of Animal Health, Glebe, NSW. The prefemoral lymph nodes were removed on the left side of the sheep and the node area was allowed to re-anastomose for ~6 weeks to form a pseudoafferent vessel. The pseudoafferent vessel on the left side of the sheep and the efferent vessel on the right side were cannulated as previously described (Lascelles & Morris, 1961; Hall & Morris, 1963) (Figure 2.7 and 2.8). The animals were maintained in metabolism cages with free access to food and water. Lymph was collected continuously into sterile bottles containing heparin as an anticoagulant and antibiotics

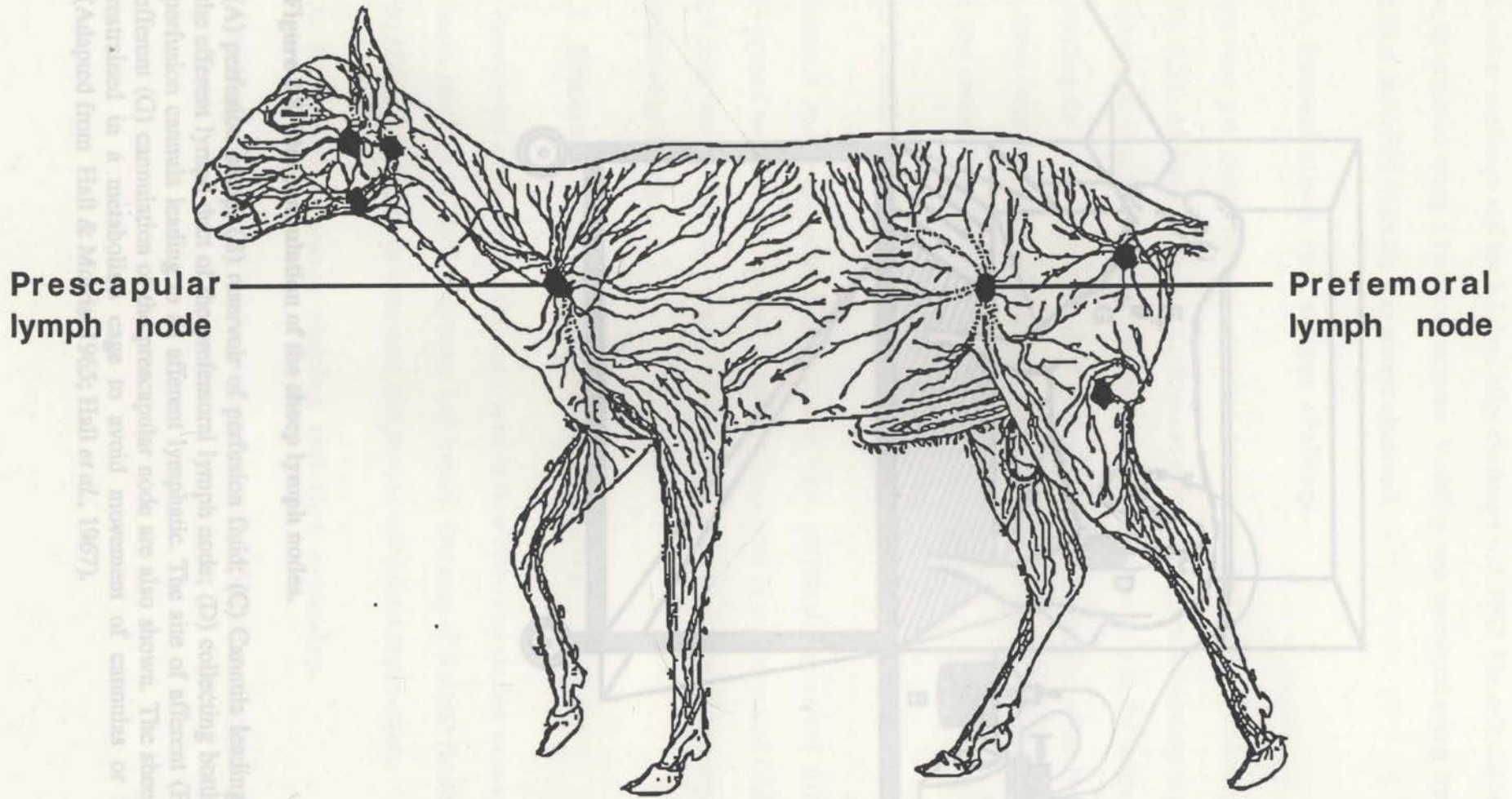


Figure 2.7. The sheep lymphatic system. Adapted from Hecker (1983).

both before challenge and for 2-3 days after challenge with PPD. The cell concentrations were determined using a haemocytometer. Viability was measured using trypan blue exclusion and >90% viability was always observed.

2.7.3. Immunisation and antigen challenge.

Sheep were pre-anaesthetised with xylazine (Rhone-Mérieux) and anaesthesia was maintained with sodium pentothal (Eli Lilly-Calmette-Gueirin (BCG) (CSL, Melbourne) and a derivative (Gibco) in the collecting area surrounding the lymph node. Lymph nodes were removed 7-10 days post challenge. The sheep were restrained in a metabolism cage to avoid movement of cannulas or injury.

2.7.4. Lymph node cannulation
 Prefemoral and prescapular lymph nodes were aseptically removed from killed BCG-primed and untreated control sheep, suspended in supplemented DMEM. The lymph node was cut into pieces and forced through a cell strainer with a syringe plunger as described in Section 2.5.2.

2.7.5. Monoclonal antibodies for flow cytometry.

The monoclonal antibodies (MAbs) used in these flow cytometry studies were a gift from Dr Susan McClure (CSIRO McMaster Laboratory, Division of Animal Health, Glebe, NSW) (Table 2.1). All MAb were used undiluted as cell culture supernatants.

2.7.6. Immunofluorescence staining and flow cytometry.

Figure 2.8. The cannulation of the sheep lymph nodes.

(A) perfusion pump; (B) reservoir of perfusion fluid; (C) Cannula leading from the efferent lymph duct of the prefemoral lymph node; (D) collecting bottle; (E) perfusion cannula leading to an afferent lymphatic. The site of afferent (F) and efferent (G) cannulation of the prescapular node are also shown. The sheep was restrained in a metabolism cage to avoid movement of cannulas or injury (Adapted from Hall & Morris, 1965; Hall *et al.*, 1967).

both before challenge and for 2-3 days after challenge with PPD. The cell concentrations were determined using a haemocytometer. Viability was measured using trypan blue exclusion and >90% viability was always observed.

2.7.3. Immunisations and antigen challenge.

Sheep were previously immunised with 6 human doses of Bacillus-Calmette-Guerin (BCG) (CSL, Melbourne, Australia). Immune sheep were given a boosting dose of 200 µg soluble purified BCG protein derivative (PPD) intra-dermally in the collecting area surrounding the draining lymph node 7-10 days prior to the collection of the lymph cells. The sheep were also given a challenging dose of 200 µg of soluble PPD approximately 2 days post cannulation (Emery & Davey, 1995).

2.7.4. Lymph node cell preparation.

Prefemoral and prescapular lymph nodes were aseptically removed from killed BCG-primed and untreated control sheep and suspended in supplemented DMEM. The lymph node was cut into pieces and forced through a cell strainer with a syringe plunger as described in Section 2.5.2.

2.7.5. Monoclonal antibodies for flow cytometry.

The monoclonal antibodies (MAbs) used in these flow cytometry studies were a gift from Dr Susan McClure (CSIRO McMaster Laboratory, Division of Animal Health, Glebe, NSW) (Table 2.1). All MAb were used undiluted as cell culture supernatants.

2.7.6. Immunofluorescence staining and flow cytometry.

The labelling procedure and the flow cytometry was performed as described in Section 2.5.2.

2.7.7. Preparation of the afferent and efferent cells for NMR analysis.

Table 2.1. Monoclonal antibodies used in the sheep immune challenge studies.

washed twice in PBS. The cell pellet was resuspended and washed twice in 5 mL of

Sheep Antigens	Ig Isotype	MAb clone	Tissue Distribution	Reference
CD21	IgG _{2a}	DU 74	B cells	Hein (1995)
CD21	IgM	DU 104	B cells	Hein (1995)
CD4	IgG ₁	17D	T cells	Mackay <i>et al.</i> (1988b)
CD8	IgG _{2a}	7C2	T cells	Mackay <i>et al.</i> (1988b)
TCR $\gamma\delta$	IgG ₁	86D	$\gamma\delta$ T cells	Hunig <i>et al.</i> (1985)
CD2	IgG ₁	135A	$\alpha\beta$ T cells	Giegerich <i>et al.</i> (1989)
CD44	IgG ₁	25-32	T cells, B cells, monocytes, granulocytes, most erythrocytes	Mackay <i>et al.</i> (1988c)
CD45R	IgG ₁	73B	isoform of CD45, expressed on B cells and some T cells	Mackay <i>et al.</i> (1987)
MHC II	IgG _{2a}	SW73.2	B cells and activated T cells, dendritic cells	Hopkins <i>et al.</i> (1986)
LFA-1	IgG ₁	F10-150	all leukocytes	Mackay <i>et al.</i> (1990)
175	IgM	175	reacts with ~90% of nucleated adult ovine bone marrow cells	Deane <i>et al.</i> (1995)

2.7.7. Preparation of the afferent and efferent cells for NMR analysis.

Lymph samples were centrifuged at 1000 g for 10 min at 21°C and the cell pellets were washed twice in PBS. The cell pellet was resuspended and washed twice in 5 mL of PBS/D₂O as described in Section 2.6.2.

2.7.8. ¹H-NMR analysis of sheep lymph and lymph node cells

1D and 2D ¹H-NMR COSY experiments were performed on sheep cells as described in Section 2.7.4. 2D ¹H-NMR spectra were processed using the parameters described for mouse cells in Section 2.6.3.

Comparative studies were performed to investigate the kinetics of development of the mobile lipid in immature thymic and mature splenic peripheral T cells. It was necessary to enrich the spleen cell suspension for T cells for comparison with the cells isolated from the thymus. The splenocyte cell suspensions contain a smaller proportion of T cells and a greater proportion of macrophages, B cells, dendritic cells and red blood cells than the thymus (Roitt, 1991). The additional accessory cells in the spleen such as B cells and macrophages might be activated by the mitogens used in this study, which might in turn provide co-stimulation to activate the T cells (Roitt, 1991). Thus the presence of accessory cells in the splenocyte suspension makes it difficult to compare with T cells derived from the thymus which contains a much smaller proportion of accessory cells.

A variety of simple T cell separation procedures are available to remove accessory cells from mixed spleen cell suspensions (Hunt, 1986). However, few methods are suitable for the large-scale isolation of splenic T cells required for ¹H-NMR studies (~10⁸ cells for each experiment). The requirement of large cell numbers and a method that minimized disruption to the cell membrane restricted the number of available methods that could be employed. The limitations of cost and the use of minimal steps in the procedure resulted in the selection of two methods for evaluation: (i) the nylon wool separation procedure (Julius *et al.*, 1973); (ii) a two-step method using sheep α-mouse antibody coupled to sheep red blood cells (SRBC-SoxMIg) to remove the B cells and some macrophages

Chapter 3.

Comparative methods for large scale isolation of splenic T cells for NMR analysis.

3.1. Introduction.

Comparative studies were performed to investigate the kinetics of development of the mobile lipid in immature thymic and mature splenic peripheral T cells. It was necessary to enrich the spleen cell suspension for T cells for comparison with the cells isolated from the thymus. The splenocyte cell suspensions contain a smaller proportion of T cells and a greater proportion of macrophages, B cells, dendritic cells and red blood cells than the thymus (Roitt, 1991). The additional accessory cells in the spleen such as B cells and macrophages might be activated by the mitogens used in this study, which might in turn provide co-stimulation to activate the T cells (Roitt, 1991). Thus the presence of accessory cells in the splenocyte suspension makes it difficult to compare with T cells derived from the thymus which contains a much smaller proportion of accessory cells.

A variety of simple T cell separation procedures are available to remove accessory cells from mixed spleen cell suspensions (Hunt, 1986). However, few methods are suitable for the large-scale isolation of splenic T cells required for $^1\text{H-NMR}$ studies ($\sim 10^8$ cells for each experiment). The requirement of large cell numbers and a method that minimized disruption to the cell membrane restricted the number of available methods that could be employed. The limitations of cost and the use of minimal steps in the procedure resulted in the selection of two methods for evaluation: (i) the nylon wool separation procedure (Julius *et al.*, 1973); (ii) a two-step method using sheep α -mouse antibody coupled to sheep red blood cells (SRBC- $\text{S}\alpha\text{MIg}$) to remove the B cells and some macrophages

(Julius *et al.*, 1973; Goding, 1976) followed by an adherence step to remove additional accessory cells such as macrophages (Kumagai *et al.*, 1979). Both of these methods use negative selection of the T cells involving little or no interaction with the T cell membrane.

In this Chapter the isolation, characterisation and purification of the sheep α -mouse antibody, used in the SRBC separation procedure, is described, together with the comparative results of the T cell enrichment procedures. The separation procedures were monitored using flow cytometry (FCM) to assess the relative proportions of cells in the fractionated samples, and functional purity was assessed using proliferation assays. Finally, $^1\text{H-NMR}$ analysis was used to compare fractionated cells with those freshly isolated from the spleen to ensure that the procedure had not resulted in the development of mobile lipid in the isolated, untreated T cells.

3.2. Results.

3.2.1. Characterisation of the purified sheep α -mouse antibody.

SDS-PAGE of purified sheep α -mouse antibody

The sheep α -mouse antibody was purified from sheep whole serum using the two step precipitation method described in Section 2.1.4. The purified antibody and the whole serum sample were compared using SDS-PAGE under reducing conditions as described in Section 2.1.4. β -mercaptoethanol, a potent reducing agent, was used to cleave the disulphide bridges between the Ig heavy chains (Ig HC) and Ig light chains (Ig LC), liberating the Ig HC and Ig LC monomers (Stanworth & Turner, 1978). Bovine serum albumin (BSA) was used as a control. The BSA in lane one has a prominent band as expected at ~ 68 kDa, with a small amount of contaminating Ig HC and Ig LC running at 51 kDa and 24 kDa respectively (Figure 3.1). A commercially available sheep α -mouse IgG₁ was run without further purification in lane 2, and contained more prominent bands corresponding to Ig HC and Ig LC, but some contaminating serum albumin. The whole sheep serum sample containing sheep α -mouse Ig raised by me is shown at two dilutions in lanes 3 and 4. The sample showed very similar bands to those in the commercial

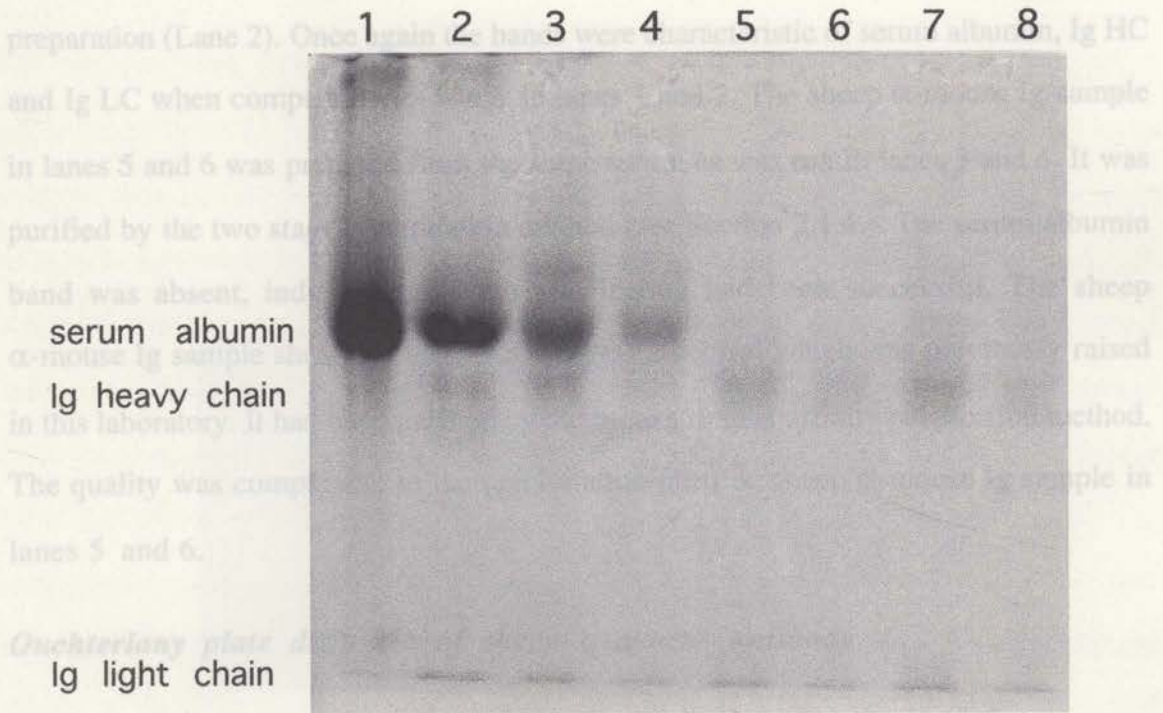


Figure 3.1. Sodium dodecyl sulphate polyacrylamide gel electrophoresis of purified sheep α -mouse Ig.

- Lane 1. bovine serum albumin (BSA) (Sigma, USA) control
- Lane 2. commercial preparation of sheep α MIgG₁ (Silenus, Melbourne, Australia)
- Lane 3. unpurified, undiluted sheep serum
- Lane 4. unpurified sheep serum diluted 1:2
- Lane 5. purified, undiluted sheep α -mouse Ig
- Lane 6. purified sheep α -mouse Ig diluted 1:2
- Lane 7. affinity-purified sheep α -mouse Ig control undiluted
- Lane 8. affinity-purified sheep α -mouse Ig control diluted 1:2

3.2.2. Flow cytometric analysis of splenic T cell fractions using nylon
 Serum albumin, Ig heavy chains and Ig light chains have the molecular weights 68 kDa, 51 kDa and 24 kDa respectively.

The FCM results of the SRBC-S α MIg technique presented in this Chapter represent small scale isolation of splenic T cells. The large scale FCM results will be presented and discussed in Chapter 4, Section 4.2.1, Figure 4.2. Spleen cells were isolated and the T

preparation (Lane 2). Once again the bands were characteristic of serum albumin, Ig HC and Ig LC when compared with bands in lanes 1 and 2. The sheep α -mouse Ig sample in lanes 5 and 6 was prepared from the same serum as was run in lanes 3 and 4. It was purified by the two stage precipitation method (see Section 2.1.4.). The serum albumin band was absent, indicating that the purification had been successful. The sheep α -mouse Ig sample shown in lanes 7 and 8 was a control which was previously raised in this laboratory. It had been purified by the more stringent affinity purification method. The quality was comparable to the precipitation-purified sheep α -mouse Ig sample in lanes 5 and 6.

Ouchterlony plate diffusion of sheep α -mouse antibody

The specificity of the purified sheep α mouse Ig was assessed using Ouchterlony agarose plate diffusion (Ouchterlony, 1968; Ouchterlony & Nilsson, 1986). Panel A in Figure 3.2, shows the control affinity-purified sheep α mouse Ig and Panel B shows the purified sheep α mouse Ig. The samples were diluted in 0.1 M Tris pH 8 at 1:2, 1:4, 1:8 and 1:16 and placed in the wells in a clockwise direction from the top of the gel and an undiluted mixture of mouse Ig was added to the centre well. The control affinity-purified sheep α mouse Ig (Panel A), shows precipitin lines in wells corresponding to 1:2 and 1:4 dilutions. A precipitin line seen in Panel B (containing the purified sheep α -mouse Ig) from the 1:2 dilution, and a faint line is visible at a 1:4 dilution, but not at higher dilutions. These results indicate that the purified sheep α mouse Ig specifically binds to mouse Ig and was therefore suitable for use in separation procedures. This also indicates that the purified sheep α mouse Ig was comparable to the affinity-isolated control sheep α mouse Ig.

3.2.2. Flow cytometric analysis of splenic T cell fractions using nylon wool and SRBC-S α MIg separation procedures.

The FCM results of the SRBC-S α MIg technique presented in this Chapter represent small scale isolation of splenic T cells. The large scale FCM results will be presented and discussed in Chapter 4, Section 4.2.1, Figure 4.2. Spleen cells were isolated and the T

cell fractions were separated either using nylon wool or using SRBC-ScMlg separation procedures followed by adherence of the fractionated cell suspensions to plastic tissue culture flasks as described in Section 2.1.4. The amount of T cell enrichment and the level of B cell contamination in the fractionated T cell suspensions was quantitated using FCM. Aliquots of cells were obtained using three different procedures. In the first, unseparated spleen cells were used. The second technique obtained cells using nylon wool. The third technique separated cells using SRBC-ScMlg. The results of the SRBC-ScMlg separation procedure are shown in Panels A and B. Panels C and D show the results of the nylon wool purification procedure. Thy 1.2 labelling for T cells is shown in Panels A and C. SRBC-ScMlg separation resulted in a 2.4-fold enrichment for T cells from unseparated spleen compared with a 2.8-fold increase for nylon-wool-separated cells. In Panel B and D the cell suspensions were incubated with sheep α -mouse Ig. To detect the surface expression of Ig on B cells, SRBC-ScMlg-separated T cells show a 63-fold enrichment for B cells compared with unseparated spleen cells. Purified sheep α -mouse Ig was added to the outer wells of each plate, diluted in a clockwise direction from the top well at 1:2, 1:4, 1:8 and 1:16 in 0.1 M Tris (pH 8.0).

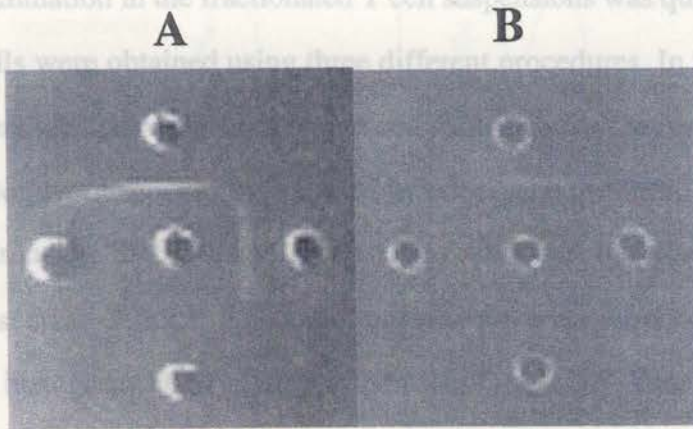


Figure 3.2. Ouchterlony plate diffusion of sheep α -mouse antibody.

Panel A: sheep α -mouse Ig control raised previously in this laboratory and affinity-purified. Panel B: sheep α -mouse Ig raised in this project and purified by two-step precipitation procedure. An undiluted mixture of mouse Ig was added to the centre well of each plate. Purified sheep α -mouse Ig was added to the outer wells of each plate, diluted in a clockwise direction from the top well at 1:2, 1:4, 1:8 and 1:16 in 0.1 M Tris (pH 8.0).

Figure 3.4, Panel A shows that the SRBC-ScMlg separation procedure increased the proportion of T cells in the cell suspension from 35% in unseparated spleen cells to 84%, while the proportion of B cells decreased from 50% to 0.8% in the separated cell fraction. Panel B shows that using the nylon wool separation procedure increased the proportion of T cells in the unseparated fraction from 24% to 67%, while the proportion of B cells has decreased from 40% to 11% in the separated fraction.

These results indicate that both of the separation procedures successfully enriched for T cells and depleted the cell fraction of B cells. However, the SRBC-ScMlg separation

cell fractions were separated either using nylon wool or using SRBC-S α MIg separation procedures followed by adherence of the fractionated cell suspensions to plastic tissue culture flasks as described in Section 2.1.4. The amount of T cell enrichment and the level of B cell contamination in the fractionated T cell suspensions was quantitated using FCM. Aliquots of cells were obtained using three different procedures. In the first, unseparated spleen cells were taken directly from spleen cell suspensions. A second technique obtained cells using nylon wool separation followed by adherence to plastic. The third technique separated cells using SRBC-S α MIg separation followed by adherence to plastic (as described in section 2.5.2.). The cell suspensions were analysed using FCM and representative histogram FCM plots are shown in Figure 3.3. Panels A and B show the results of the SRBC-S α MIg separation procedure and Panels C and D show the results of the nylon wool purification procedure. Thy 1.2 labelling for T cells is shown in Panels A and C. SRBC-S α MIg separation resulted in a 2.4-fold enrichment for T cells from unseparated spleen compared with a 2.8-fold increase for nylon-wool-separated cells. In Panel B and D the cell suspensions are labelled with sheep α MIg(Fab')₂ to detect the surface expression of Ig on B cells. SRBC-S α MIg-separated T cells show a 63-fold depletion of B cells when compared to unseparated cells, while nylon-wool-separated T cells show a 3.6-fold depletion which is significantly less than the SRBC-S α MIg procedure. A summary of the FCM showing the proportion of cells staining positively for α Thy 1.2, to detect T cells, and S α MIg(Fab')₂ for the detection of B cells, is shown in Figure 3.4. Panel A shows that the SRBC-S α MIg separation procedure increased the proportion of T cells in the cell suspension from 35% in unseparated spleen cells to 84%, while the proportion of B cells decreased from 50% to 0.8% in the separated cell fraction. Panel B shows that using the nylon wool separation procedure increased the proportion of T cells in the unseparated fraction from 24% to 67%, while the proportion of B cells has decreased from 40% to 11% in the separated fraction.

These results indicate that both of the separation procedures successfully enriched for T cells and depleted the cell fraction of B cells. However, the SRBC-S α MIg separation

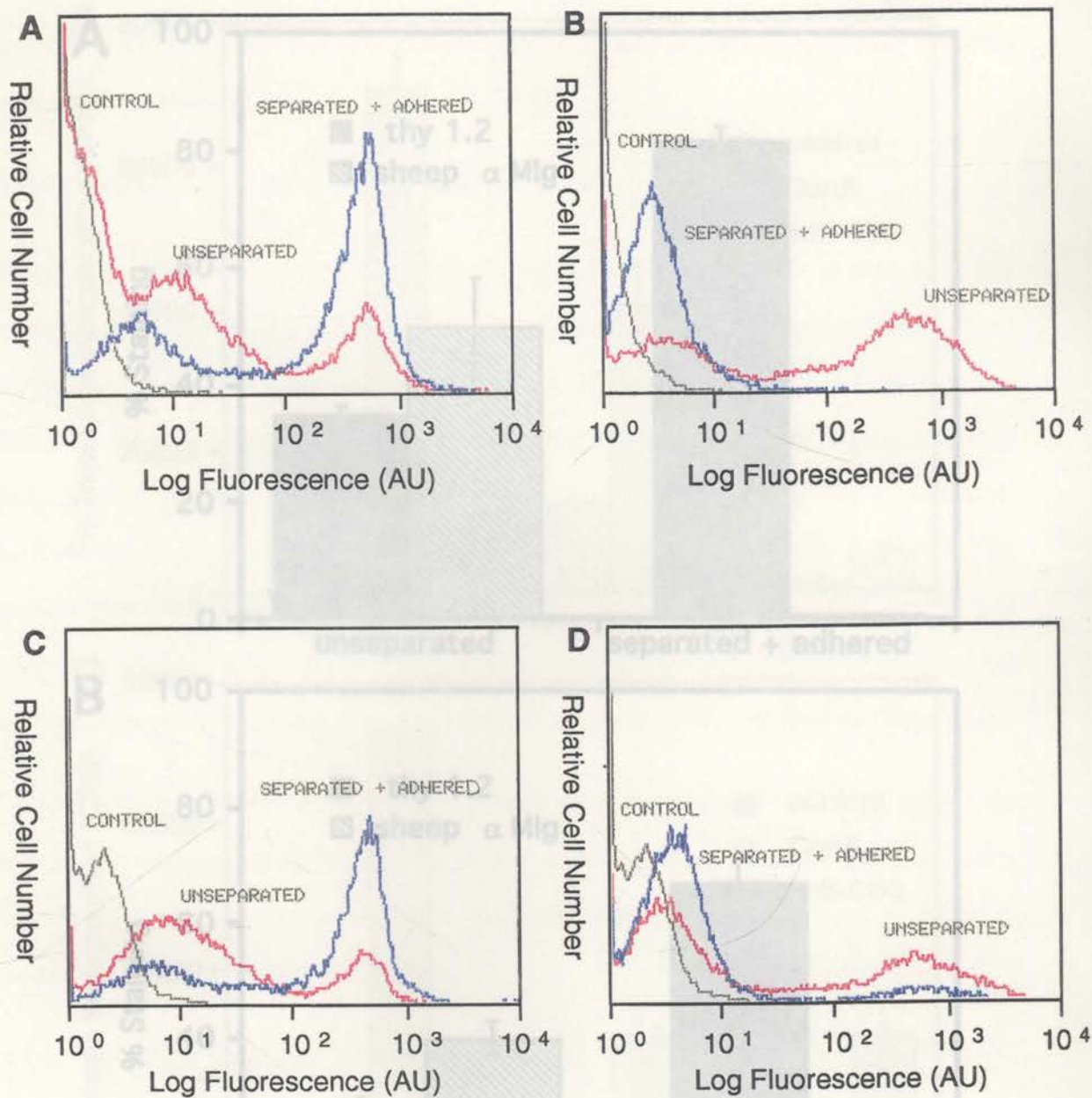


Figure 3.3. Flow cytometric histogram analysis of SRBC-S α MIg-separated and nylon wool-separated splenic T cells.

Panels A and C show the staining for T cells with α Thy 1.2 FITC and the panels B and D show staining with sheep α MIg to detect B cells. The non-specific control staining is shown by the grey histogram, the unseparated cell staining is shown in red and the separated and adhered cells are shown in blue.

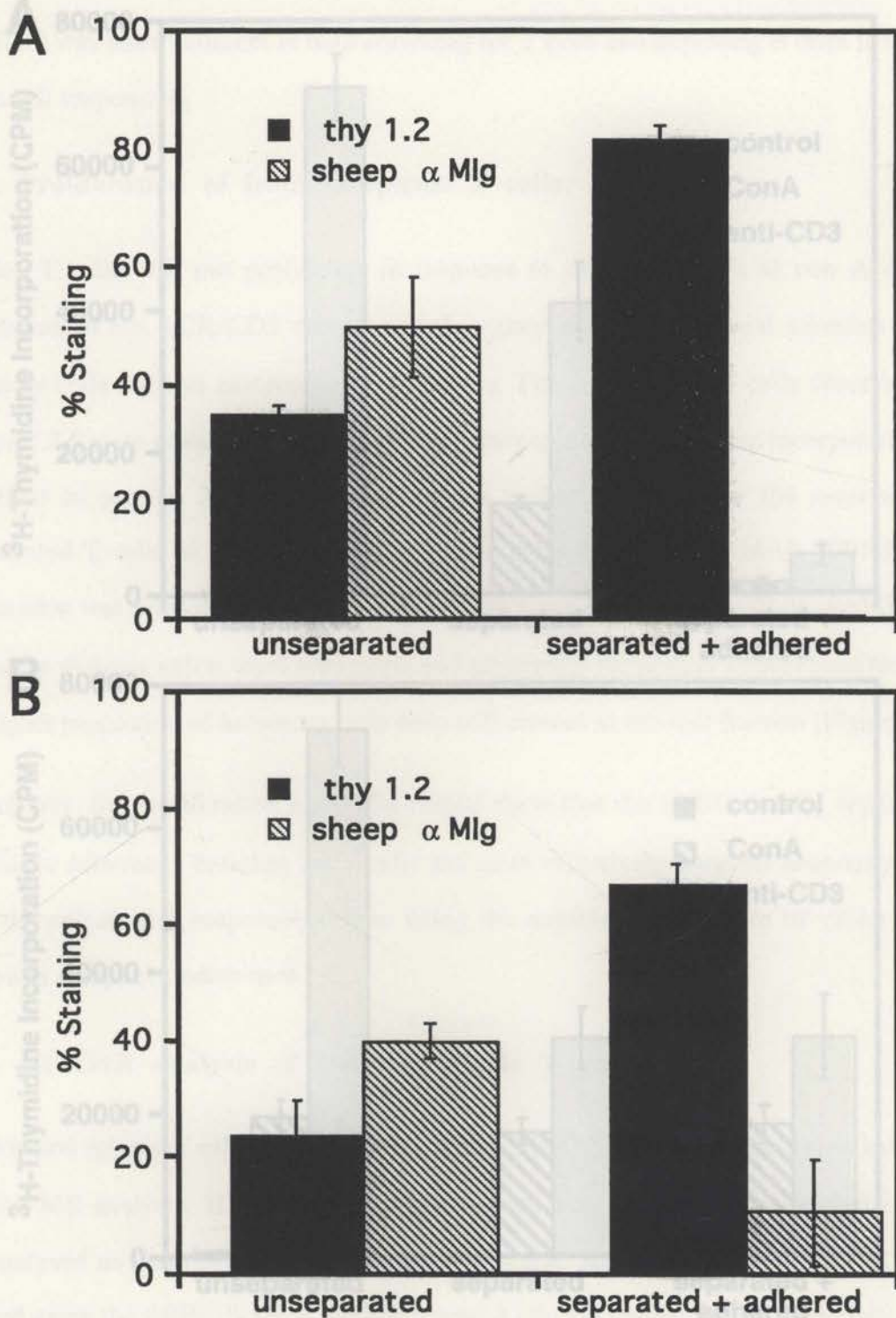


Figure 3.4. Summary of flow cytometric analysis of SRBC-S α MIg and nylon wool-separated splenic T cells.

Panel A, SRBC-S α MIg. Panel B, nylon-wool-separated. Cell aliquots from unseparated spleen cells and separated fractions and were labelled with a Thy1.2 FITC and α MIg FITC. The proportion of positively staining cells in each fraction is shown.

Ability to proliferate in response to mitogens was assessed by 3 H-thymidine incorporation, measured in CPM.

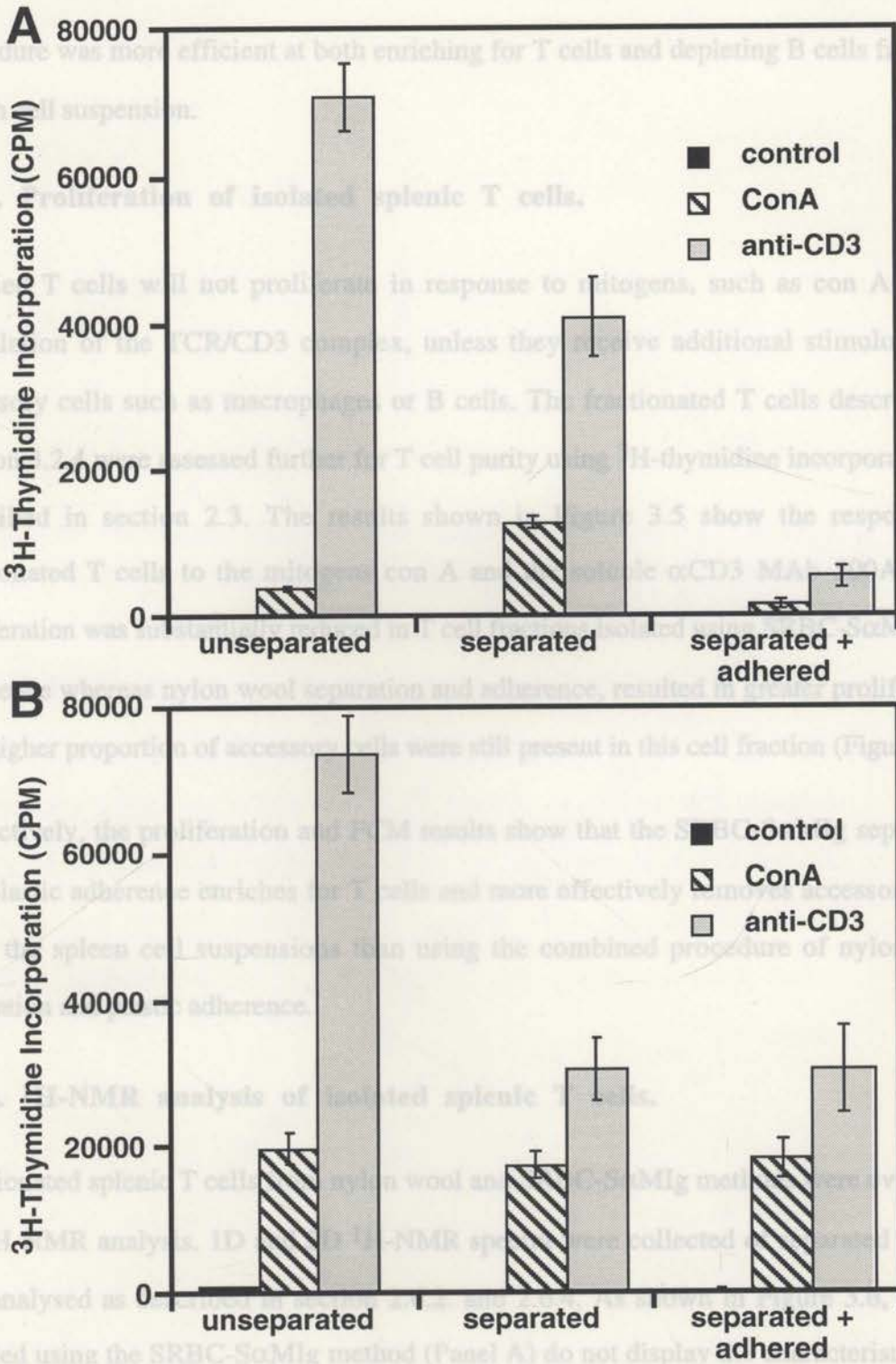


Figure 3.5. Stimulation to proliferation of splenic T cells with Con A and α CD3.

SRBC- α MIg (A) and nylon wool (B) separation methods for splenic T cells. Aliquots of unseparated spleen cells, spleen cells separated but not adhered, and spleen cells separated and adhered to plastic were assessed for relative T cell purity. Ability to proliferate in response to mitogens was assessed by ^3H -thymidine incorporation, measured in CPM.

procedure was more efficient at both enriching for T cells and depleting B cells from the spleen cell suspension.

3.2.3. Proliferation of isolated splenic T cells.

Purified T cells will not proliferate in response to mitogens, such as con A or via stimulation of the TCR/CD3 complex, unless they receive additional stimulus from accessory cells such as macrophages or B cells. The fractionated T cells described in Section 3.2.4 were assessed further for T cell purity using ^3H -thymidine incorporation as described in section 2.3. The results shown in Figure 3.5 show the response of fractionated T cells to the mitogens con A and the soluble αCD3 MAb 500A2. The proliferation was substantially reduced in T cell fractions isolated using SRBC-S α MIg and adherence whereas nylon wool separation and adherence, resulted in greater proliferation as a higher proportion of accessory cells were still present in this cell fraction (Figure 3.5).

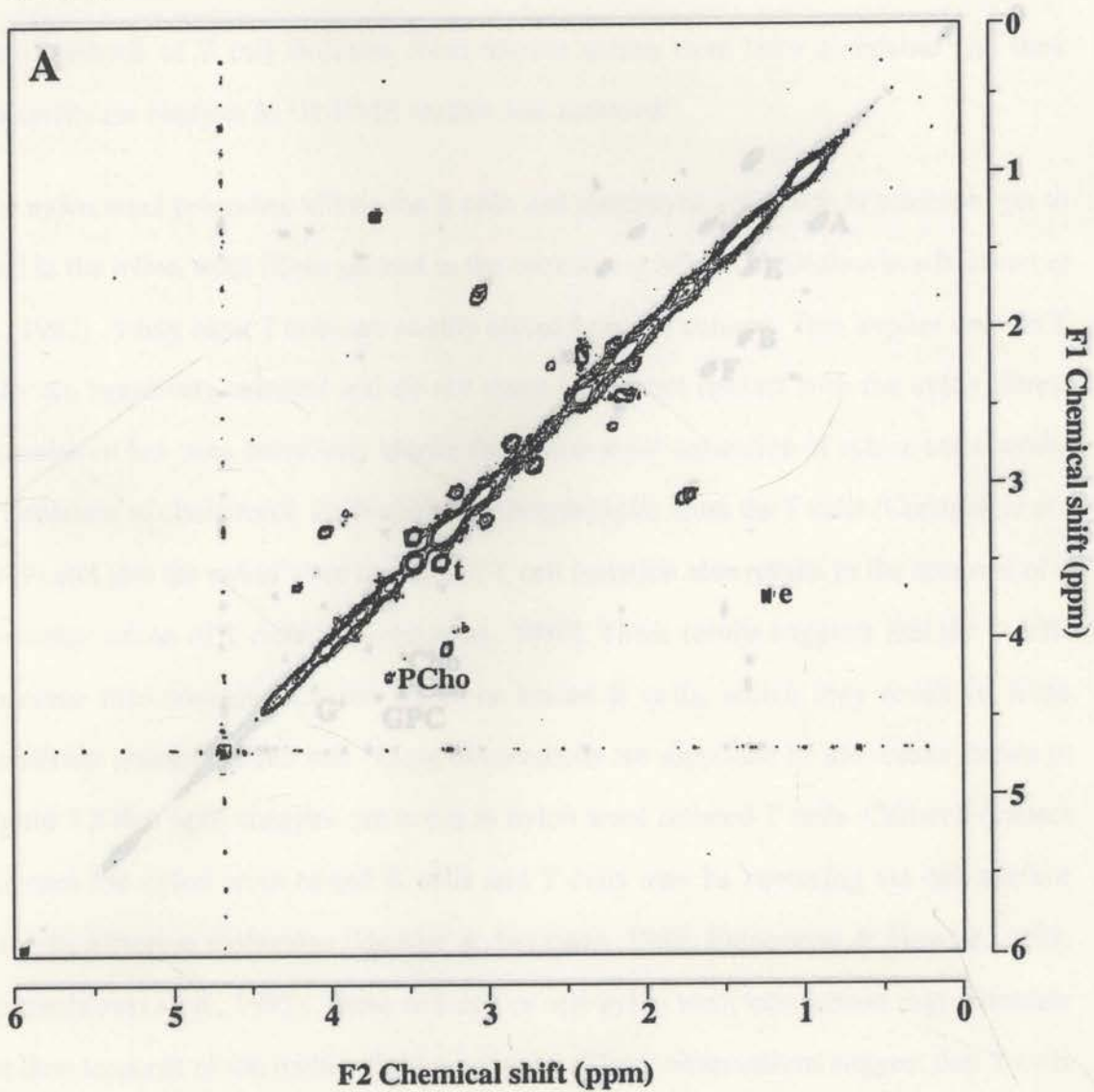
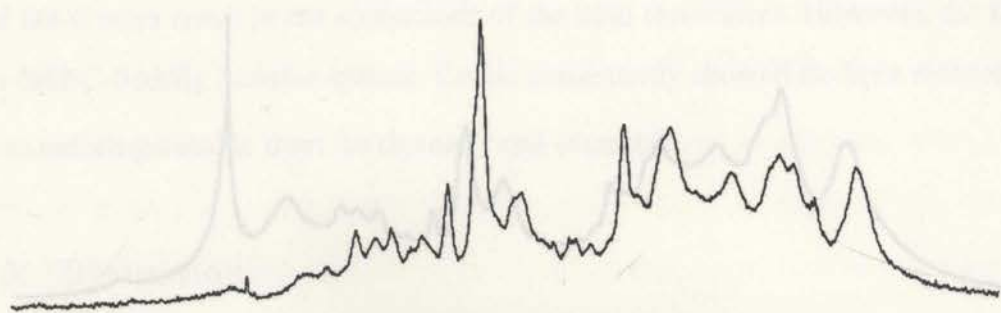
Collectively, the proliferation and FCM results show that the SRBC-S α MIg separation and plastic adherence enriches for T cells and more effectively removes accessory cells from the spleen cell suspensions than using the combined procedure of nylon wool separation and plastic adherence.

3.2.4. ^1H -NMR analysis of isolated splenic T cells.

Fractionated splenic T cells from nylon wool and SRBC-S α MIg methods were evaluated for ^1H -NMR analysis. 1D and 2D ^1H -NMR spectra were collected of separated T cells and analysed as described in section 2.6.2. and 2.6.4. As shown in Figure 3.6, T cells isolated using the SRBC-S α MIg method (Panel A) do not display the characteristic lipid acyl chain resonances in the 2D or 1D spectra. In nylon wool isolated splenic T cells these resonances are visible in the 1D spectrum and are more clearly shown in the 2D spectrum labelled A-F and G' (Panel B). The nylon-wool-isolated T cells show several of these cross peaks (section 2.6.5.) suggesting that unlike the SRBC-S α MIg isolated splenic T cells the nylon wool isolation procedure may "activate" the T cells

Figure 3.6. One-Dimensional and Two-Dimensional ^1H -NMR spectra of SRBC-S α MiG-separated T cells and nylon wool-separated T cells.

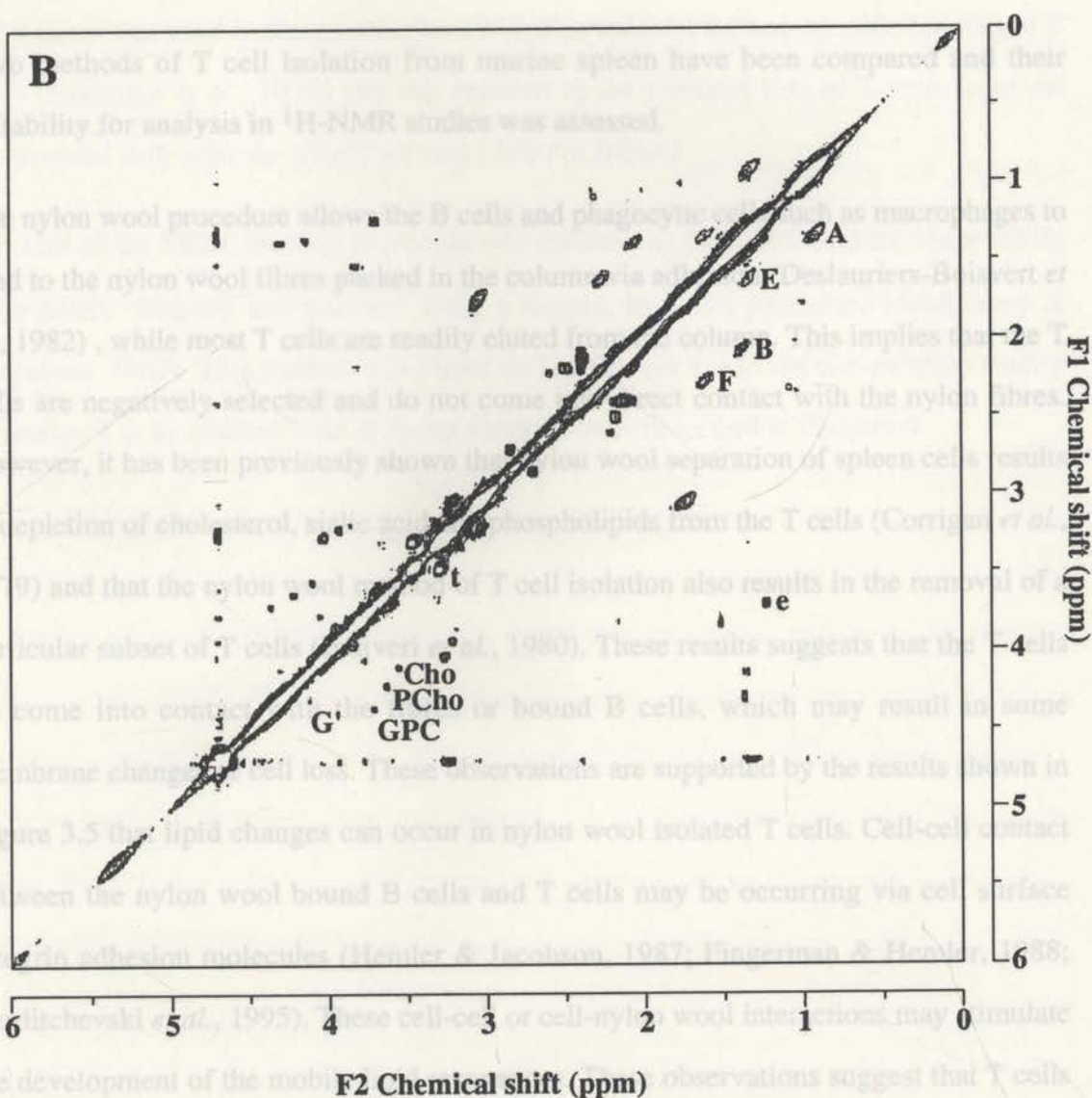
Both (A) SRBC-S α MiG separated T cells fractions and (B) nylon wool separated T cell fractions were also adhered to plastic before ^1H -NMR analysis. The resonances labelled A, B, E, F and G' in panel B arise from the acyl fatty acid chains of triglyceride as described in Section 2.6.5. Other labelled crosspeaks were assigned to phosphocholine (PCho), choline (Cho), glycerophosphocholine (GPC), taurine (t) and the intensity standard ethanol (e).



resulting in lipid changes in the cells. The spectrum shows from the SRBC-ScMig was indistinguishable from that obtained from the control thymic T cells.

The $^1\text{H-NMR}$ spectra from nylon wool separated splenic T cells were not consistent and did not always result in the appearance of the lipid resonances. However, the results of the SRBC-ScMig isolated splenic T cells consistently showed no lipid resonances and were indistinguishable from the thymic T cell controls.

3.3. Discussion.



splenic T cells. The SRBC-S α MIg procedure negatively selected for the T cells by resulting in lipid changes in the cells. The spectrum shown from the SRBC-S α MIg was indistinguishable from that obtained from the control thymic T cells.

The $^1\text{H-NMR}$ spectra from nylon wool separated splenic T cells were not consistent and did not always result in the appearance of the lipid resonances. However, the results of the SRBC-S α MIg isolated splenic T cells consistently showed no lipid resonances and were indistinguishable from the thymic T cell controls.

3.3. Discussion.

Two methods of T cell isolation from murine spleen have been compared and their suitability for analysis in $^1\text{H-NMR}$ studies was assessed.

The nylon wool procedure allows the B cells and phagocytic cells such as macrophages to bind to the nylon wool fibres packed in the column via adhesion (Deslauriers-Boisvert *et al.*, 1982), while most T cells are readily eluted from the column. This implies that the T cells are negatively selected and do not come into direct contact with the nylon fibres. However, it has been previously shown that nylon wool separation of spleen cells results in depletion of cholesterol, sialic acid and phospholipids from the T cells (Corrigan *et al.*, 1979) and that the nylon wool method of T cell isolation also results in the removal of a particular subset of T cells (Indiveri *et al.*, 1980). These results suggest that the T cells do come into contact with the fibres or bound B cells, which may result in some membrane changes or cell loss. These observations are supported by the results shown in Figure 3.5 that lipid changes can occur in nylon wool isolated T cells. Cell-cell contact between the nylon wool bound B cells and T cells may be occurring via cell surface integrin adhesion molecules (Hemler & Jacobson, 1987; Fingerman & Hemler, 1988; Berditchevski *et al.*, 1995). These cell-cell or cell-nylon wool interactions may stimulate the development of the mobile lipid resonances. These observations suggest that T cells isolated using the nylon wool method were unsuitable for biochemical studies (Corrigan *et al.*, 1979). The observations by myself and others suggest that this method of T cell isolation is unsuitable for the comparative $^1\text{H-NMR}$ studies between thymic and isolated

splenic T cells. The SRBC-S α MIg procedure negatively selected for the T cells by binding to the Ig on the B cells. This method was efficient and easy to perform with a single incubation with the spleen cells followed by a ficoll plaque separation step to isolate the T cells (Parish *et al.*, 1974). Although a one-step procedure would be preferred for T cell isolation the results shown in Figure 3.5 illustrate that the second step in the purification procedure of adherence to plastic is necessary for the successful removal of additional accessory cells. The property of macrophages to adhere to plastic or glass surfaces is well recognised (Koller *et al.*, 1973; Pierce & Kapp, 1976), however a modification of this method based on the ability of macrophages to bind to serum-coated substratum was used in these procedures as it also reduced the non-specific binding of T cells (Kumagai *et al.*, 1979) and this resulted in the minimal loss of T cells from the fractionated cells after the adherence step (data not shown).

The cost of the SRBC-S α MIg procedure was minimal as the SRBC and the sheep α MIg were easily obtained and purified using a simple, low-cost procedure (McKinney & Parkinson, 1987). This method was therefore suitable for use in the comparative studies of murine T cells isolated from different tissue sources described in Chapter 4.

Activation of lymphocytes, which leads to cell expansion and proliferation, requires sustained stimulation of protein kinase C (PKC) and a source of intracellular calcium (Davis & Lipsky, 1988). Prolonged stimulation of PKC can occur via phosphatidylcholine (PC) cycles that generate second messengers such as diacylglycerol (DAG) (Pelech & Vance, 1989) (see Figure 4.1). This process can be mimicked by the use of phorbol esters and calcium ionophores.

Neutral lipid synthesis is closely linked to PC cycling (see Fig.4.1) and may play a role in signal transduction (Besterman *et al.*, 1986; Pelech & Vance, 1989; Florin-Christensen *et al.*, 1992). Thus, in this study, I have used two-dimensional (2D) $^1\text{H-NMR}$ spectroscopy (Dingley *et al.*, 1992; Dingley *et al.*, 1994) to investigate the relationship between PC cycling and mobile lipid synthesis in activated T cells.

Chapter 4.

¹H-NMR-visible mobile lipids in activated splenic and thymic T lymphocytes: relationship to phosphatidylcholine cycling.

4.1. Introduction.

Increased levels of ¹H-NMR-visible mobile lipid have been observed in activated thymocytes (Dingley *et al.*, 1992), neutrophils (May *et al.*, 1994), macrophages (King *et al.*, 1991; King *et al.*, 1994) and B cells (Holmes *et al.*, 1990). However, the origin and function of the lipid resonances in ¹H-NMR spectra of activated cells still remains unresolved. The mobile lipid has previously been shown to contain triglyceride (May *et al.*, 1986; Holmes *et al.*, 1987; Holmes & Mountford, 1991). Diglycerides, such as diacylglycerol (DAG), are virtually indistinguishable from triglycerides, such as triacylglycerol (TAG), using 2D ¹H-NMR techniques. However, once generated, DAG is rapidly metabolised and can be converted to quickly to TAG.

Activation of lymphocytes, which leads to cell expansion and proliferation, requires sustained stimulation of protein kinase C (PKC) and a source of intracellular calcium (Davis & Lipsky, 1989). Prolonged stimulation of PKC can occur via phosphatidylcholine (PC) cycles that generate second messengers such as diacylglycerol (DAG) (Pelech & Vance, 1989) (see Figure 4.1). This process can be mimicked by the use of phorbol esters and calcium ionophores.

Neutral lipid synthesis is closely linked to PC cycling (see Fig.4.1) and may play a role in signal transduction (Besterman *et al.*, 1986; Pelech & Vance, 1989; Florin-Christensen *et al.*, 1992). Thus, in this study, I have used two-dimensional (2D) ¹H-NMR spectroscopy (Dingley *et al.*, 1992; Dingley *et al.*, 1994) to investigate the relationship between PC cycling and mobile lipid synthesis in activated T cells.

The kinetics of development of the $^1\text{H-NMR}$ -detectable mobile lipid was monitored in T cells from two different tissue sources in this study; in immature thymic and mature splenic T cells. The cells were stimulated with a PKC activator, phorbol myristate acetate (PMA), and with the calcium ionophore ionomycin. When used in combination, this method generates fully activated T cells.

Phosphatidylcholine plays an important role in the activation process in T cells (Szamel & Resch, 1995). The results obtained in this study show a simultaneous decrease in the levels of phosphatidylcholine metabolites and an increase mobile lipid in T lymphocytes following PMA and ionomycin activation. It is therefore proposed that the appearance of NMR-visible mobile lipid in activated T cells may result from DAG and free fatty-acids generated during phospholipid cycling.

4.2. Results.

4.2.1. Flow cytometric histogram analysis of separated splenic T cells.

Highly enriched suspensions of splenic T cells were isolated and analysed for T cell purity using FCM as described in Section 2.5. The spleen contains a mixed population of cells which includes T cells, B cells, macrophages, dendritic cells, and red cells (Roitt, 1991). It was therefore necessary to isolate T cells from the spleen to obtain the highly enriched population of T cells for comparison with thymic T cells. Splenic T cells, isolated by a two-step purification procedure using SRBC-SaMIg (Section 2.1.5 and Chapter 3), were compared with unpurified splenocytes using flow cytometry. T cells were detected by specific fluorescent-antibody labelling of their cell surface immunoglobulin. The relative proportions of T and B cells present in each population were compared and the T cell enrichment determined. Figure 4.2 (histogram A) shows the profile of unpurified splenocytes labelled with anti-Thy 1.2 antibody. This population contained 22% Thy 1.2 positive cells. After the separation and adherence steps this proportion increased to 78% (histogram B). The mean fluorescence of the non-specifically labelled cell populations (histogram C) was <10% of that of the Thy 1.2

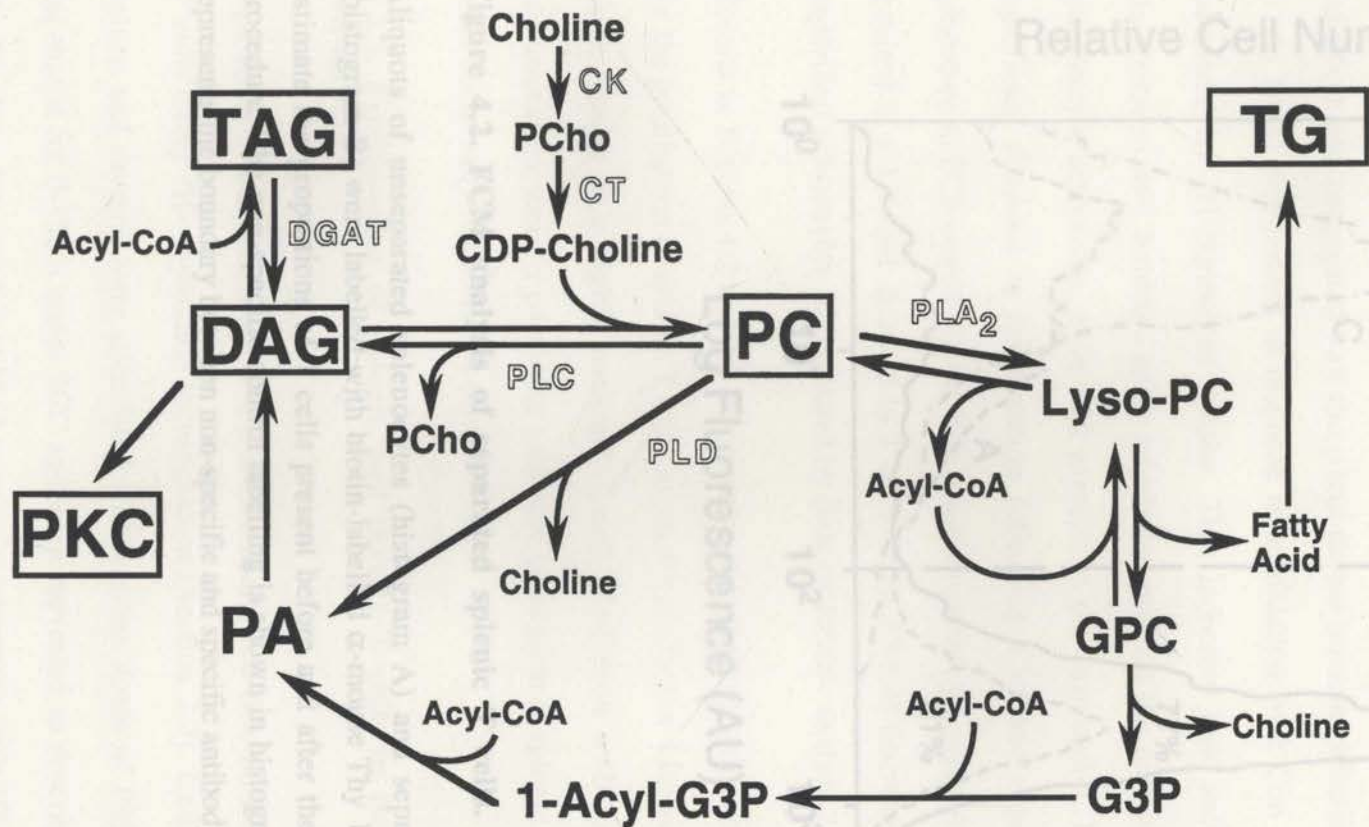


Figure 4.1. The relationship between neutral lipid synthesis and the PC cycle.

Abbreviations: Acyl-CoA, acyl-Coenzyme A; 1-Acyl-G3P, 1-acyl-glycerol 3-phosphate; CDP-choline, cytidine 5'-diphosphate-choline; CK, choline kinase; CT, cytidyldyltransferase; DAG, diacylglycerol; DGAT, diacylglycerol acyltransferase; G3P, glycerol 3-phosphate; GPC, glycerophosphocholine; Lyso-PC, lysophosphatidylcholine; PA, phosphatidic acid; PC, phosphatidylcholine; PCho, phosphocholine; PLA₂, phospholipase A₂; PLC, phospholipase C; PLD, phospholipase D; PKC; protein kinase C; TAG, triacylglycerol; TG, triglyceride. Adapted from Pelech & Vance (1989).

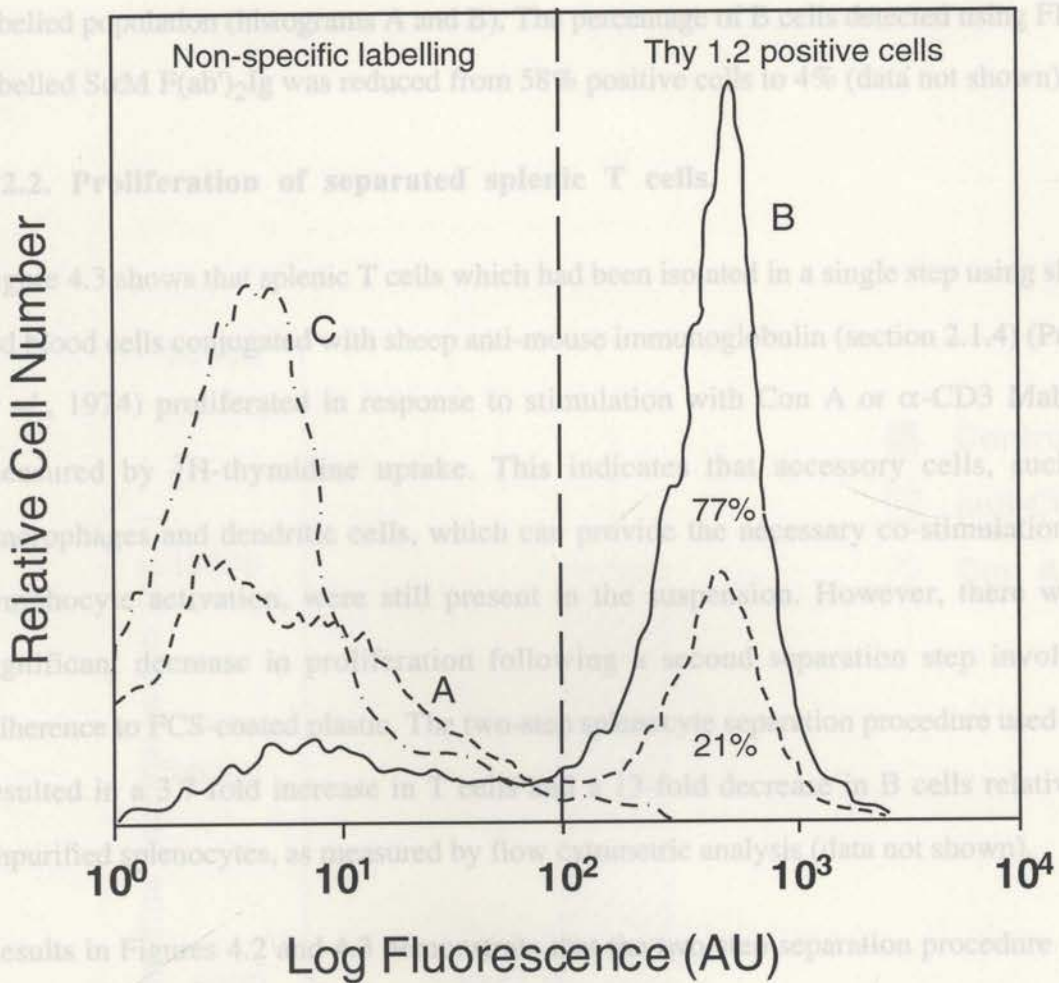


Figure 4.2. FCM analysis of separated splenic T cells.

Aliquots of unseparated splenocytes (histogram A) and separated splenic T cells (histogram B) were labelled with biotin-labelled α -mouse Thy 1.2 and avidin-FITC to estimate the proportions of T cells present before and after the two-step purification procedure. The non-specific control labelling is shown in histogram C. The broken line represents the boundary between non-specific and specific antibody staining.

T cells using ^3H -thymidine incorporation (Section 2.3). Cell suspensions from the spleen and thymus were stimulated with various doses of PMA and ionomycin and incubated for 0-120 h under SCC and were harvested as described in Section 2.3. The results show that 1 ng/ml of PMA used in combination with 300 ng/ml of ionomycin is the optimal dose to stimulate maximum proliferation, which occurs at 96 h of incubation (Figure 4.4).

labelled population (histograms A and B). The percentage of B cells detected using FITC-labelled $S\alpha M F(ab')_2 Ig$ was reduced from 58% positive cells to 4% (data not shown).

4.2.2. Proliferation of separated splenic T cells.

Figure 4.3 shows that splenic T cells which had been isolated in a single step using sheep red blood cells conjugated with sheep anti-mouse immunoglobulin (section 2.1.4) (Parish *et al.*, 1974) proliferated in response to stimulation with Con A or α -CD3 Mab, as measured by 3H -thymidine uptake. This indicates that accessory cells, such as macrophages and dendritic cells, which can provide the necessary co-stimulation for lymphocyte activation, were still present in the suspension. However, there was a significant decrease in proliferation following a second separation step involving adherence to FCS-coated plastic. The two-step splenocyte separation procedure used here resulted in a 3.7-fold increase in T cells and a 13-fold decrease in B cells relative to unpurified splenocytes, as measured by flow cytometric analysis (data not shown).

Results in Figures 4.2 and 4.3 demonstrate that the two-step separation procedure used for the purification of splenic T cells, as shown in Chapter 3 for small scale isolation of T cells, results in a highly enriched T cell population with minimal accessory cell contamination, thereby providing a suitable population of splenic T cells for use in large scale comparative studies with thymic T cells.

4.2.3. Proliferation of splenic and thymic T cells in response to PMA and ionomycin.

Optimal activating doses of PMA and ionomycin were determined for splenic and thymic T cells using 3H -thymidine incorporation (Section 2.3). Cell suspensions from the spleen and thymus were stimulated with various doses of PMA and ionomycin and incubated for 0-120 h under SCC and were harvested as described in Section 2.3. The results show that 1 ng/ml of PMA used in combination with 300 ng/ml of ionomycin is the optimal dose to stimulate maximum proliferation, which occurs at 96 h of incubation (Figure 4.4).

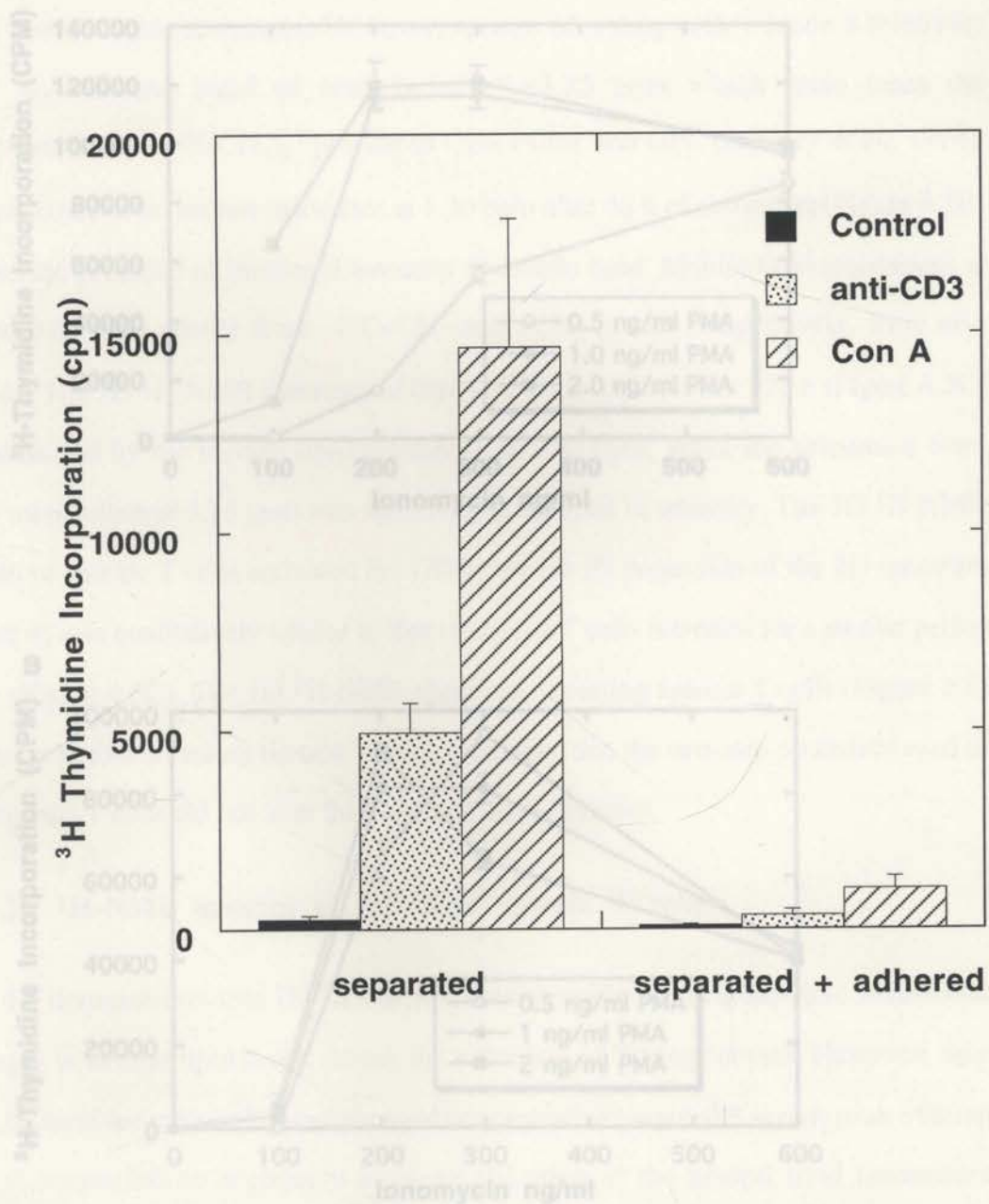


Figure 4.3. Proliferation of separated splenic T cells and unseparated splenocytes.

Determination of optimal stimulating doses of PMA and ionomycin for thymic and splenic T cells.

Proliferation of splenic T cells was measured using ^3H -thymidine incorporation. After each stage of the two-step purification procedure, cells were stimulated for 72 h with Con A ($2 \mu\text{g mL}^{-1}$), MAb 500A2 (α -CD3) supernatant, or medium only (control).

(mean \pm SD, $n=12$ replicates).

4.2.4. 1D $^1\text{H-NMR}$ spectra of activated thymic T cells.

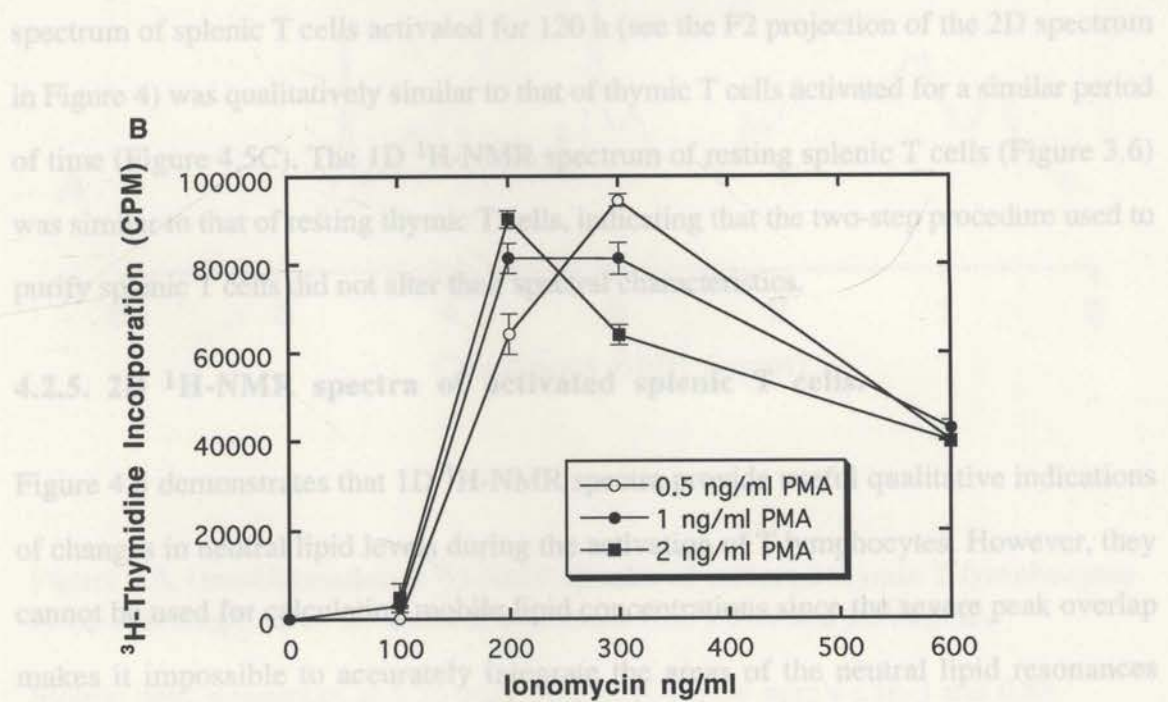
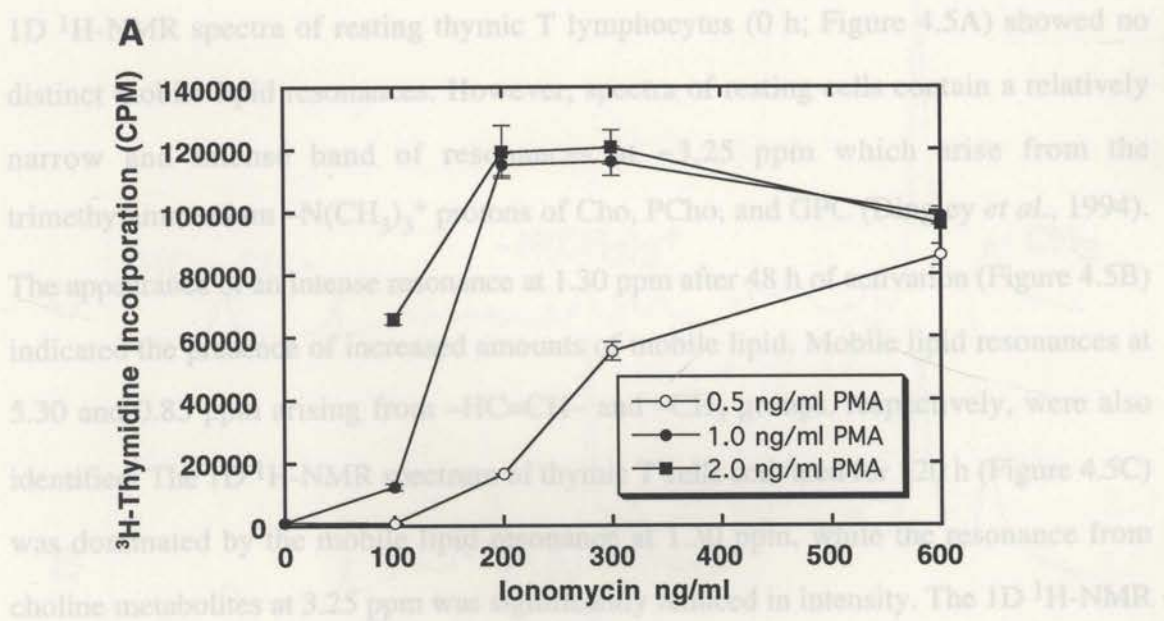


Figure 4.4. Determination of optimal stimulating doses of PMA and ionomycin for thymic and splenic T cells.

Optimal stimulating doses of PMA and ionomycin for thymic (A) and splenic (B) T cells were determined using ^3H -thymidine incorporation at 72 h of incubation under SCC (mean \pm SD, n=12 replicates). (May *et al.*, 1986). Peaks A-F denote the acyl chains of

4.2.4. 1D $^1\text{H-NMR}$ spectra of activated thymic T cells.

1D $^1\text{H-NMR}$ spectra of resting thymic T lymphocytes (0 h; Figure 4.5A) showed no distinct mobile lipid resonances. However, spectra of resting cells contain a relatively narrow and intense band of resonances at ~ 3.25 ppm which arise from the trimethylammonium $-\text{N}(\text{CH}_3)_3^+$ protons of Cho, PCho, and GPC (Dingley *et al.*, 1994). The appearance of an intense resonance at 1.30 ppm after 48 h of activation (Figure 4.5B) indicated the presence of increased amounts of mobile lipid. Mobile lipid resonances at 5.30 and 0.85 ppm arising from $-\text{HC}=\text{CH}-$ and $-\text{CH}_3$ groups, respectively, were also identified. The 1D $^1\text{H-NMR}$ spectrum of thymic T cells activated for 120 h (Figure 4.5C) was dominated by the mobile lipid resonance at 1.30 ppm, while the resonance from choline metabolites at 3.25 ppm was significantly reduced in intensity. The 1D $^1\text{H-NMR}$ spectrum of splenic T cells activated for 120 h (see the F2 projection of the 2D spectrum in Figure 4) was qualitatively similar to that of thymic T cells activated for a similar period of time (Figure 4.5C). The 1D $^1\text{H-NMR}$ spectrum of resting splenic T cells (Figure 3.6) was similar to that of resting thymic T cells, indicating that the two-step procedure used to purify splenic T cells did not alter their spectral characteristics.

4.2.5. 2D $^1\text{H-NMR}$ spectra of activated splenic T cells.

Figure 4.5 demonstrates that 1D $^1\text{H-NMR}$ spectra provide useful qualitative indications of changes in neutral lipid levels during the activation of T lymphocytes. However, they cannot be used for calculating mobile lipid concentrations since the severe peak overlap makes it impossible to accurately integrate the areas of the neutral lipid resonances (Dingley *et al.*, 1992). It has been recently shown in this laboratory that the increased resolution afforded by introducing a second dimension in the NMR experiment allows quantitation of mobile lipid from the 2D cross peaks (Dingley *et al.*, 1992). Figure 4.6 shows a 2D COSY spectrum of splenic T cells activated with PMA/ionomycin for 120 h. The spectrum is dominated by cross peaks arising from mobile lipid, which are labelled A–G' as previously described (May *et al.*, 1986). Peaks A–F denote the acyl chains of

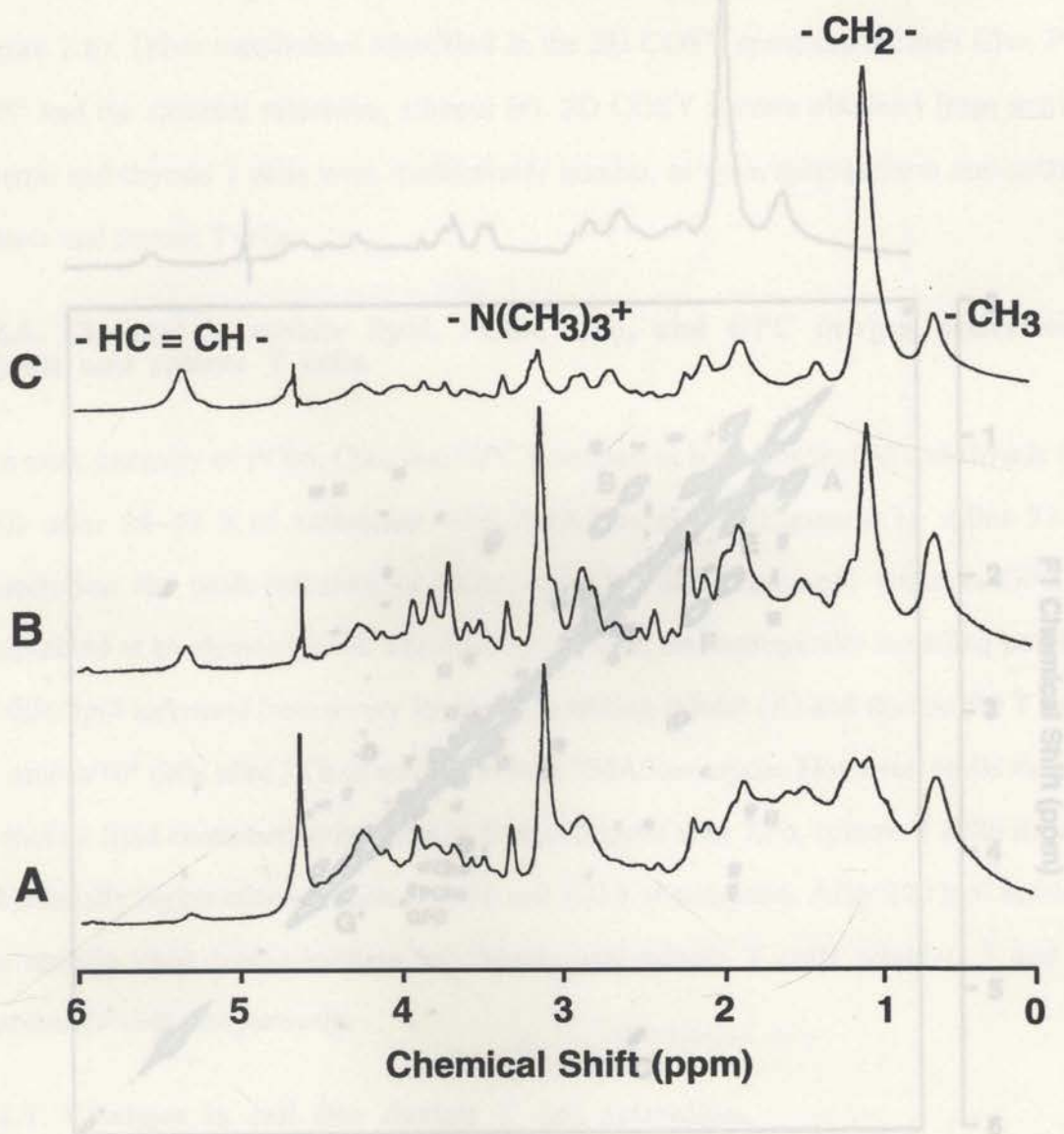


Figure 4.5. One-Dimensional ^1H -NMR spectra of cultured thymic T lymphocytes at various stages after the onset of activation with PMA and ionomycin.

Mobile lipid resonances at 5.30 ppm ($-\text{HC}=\text{CH}-$), 1.30 ppm ($-\text{CH}_2-$) and 0.85 ppm ($-\text{CH}_3$) are visible in the spectrum of non-activated thymic T lymphocytes (Panel A), but are clearly evident after 48 hours of activation (Panel B), and dominate the NMR spectrum after 120 hours (Panel C). The resonance at 3.25 ppm, which arises from the $\text{N}(\text{CH}_3)_3^+$ groups of choline metabolites, is markedly reduced in intensity after 120 hours of activation (Panel C). The 1D ^1H -NMR spectra of thymic and splenic T lymphocytes activated for 120 hours are very similar (compare Panel C with the F2 projection in Figure 4.6).

mobile lipids, while G' arises from the protons on the glycerol backbone (Section 2.6.4, Figure 2.6). Other metabolites identified in the 2D COSY spectrum include Cho, PCho, GPC and the external reference, ethanol (e). 2D COSY spectra obtained from activated splenic and thymic T cells were qualitatively similar, as were spectra from non-activated splenic and thymic T cells.

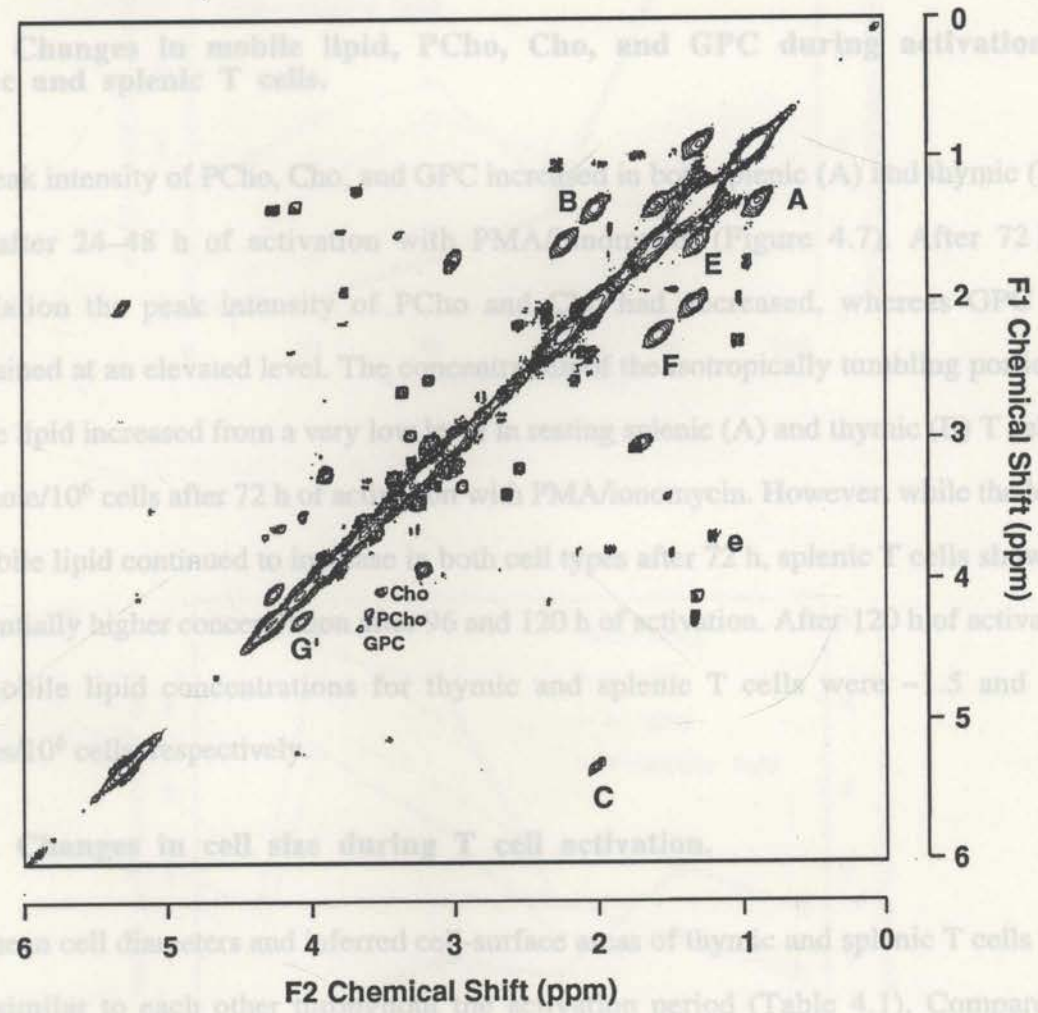


Figure 4.6. Two-Dimensional $^1\text{H-NMR}$ COSY spectrum of splenic T lymphocytes after 120 h of stimulation with PMA/ionomycin.

Cross peaks arising from mobile lipid are labelled A-G' as described in Section 2.6.1 and shown in Figure 2.2. Other labelled cross peaks arise from Cho, PCho, GPC and ethanol (e). The spectrum was symmetrized and the F2 projection is represented in the upper panel.

mobile lipids, while G' arises from the protons on the glycerol backbone (Section 2.6.4, Figure 2.6). Other metabolites identified in the 2D COSY spectrum include Cho, PCho, GPC and the external reference, ethanol (e). 2D COSY spectra obtained from activated splenic and thymic T cells were qualitatively similar, as were spectra from non-activated splenic and thymic T cells.

4.2.6. Changes in mobile lipid, PCho, Cho, and GPC during activation of thymic and splenic T cells.

The peak intensity of PCho, Cho, and GPC increased in both splenic (A) and thymic (B) T cells after 24–48 h of activation with PMA/ionomycin (Figure 4.7). After 72 h of stimulation the peak intensity of PCho and Cho had decreased, whereas GPC was maintained at an elevated level. The concentration of the isotropically tumbling portion of mobile lipid increased from a very low level in resting splenic (A) and thymic (B) T cells to ~ 1 nmole/ 10^6 cells after 72 h of activation with PMA/ionomycin. However, while the levels of mobile lipid continued to increase in both cell types after 72 h, splenic T cells showed a substantially higher concentration after 96 and 120 h of activation. After 120 h of activation, the mobile lipid concentrations for thymic and splenic T cells were ~ 1.5 and ~ 4.9 nmoles/ 10^6 cells, respectively.

4.2.7. Changes in cell size during T cell activation.

The mean cell diameters and inferred cell-surface areas of thymic and splenic T cells were very similar to each other throughout the activation period (Table 4.1). Compared to unstimulated cells (0 h), the membrane surface area of activated cells had increased by ~ 3 -fold by 72 h. However, by 120 h the area had decreased in size to be only 2.3-fold larger than in unstimulated cells. In contrast, mobile lipid levels increased substantially for both thymic and splenic T cells between 72 h and 120 h of activation (Figure 4.7). Therefore, increases in mobile lipid levels are not due simply to increases in plasma membrane surface area during T cell activation. Nor can differences between splenic and thymic T cell size explain the marked differences in mobile lipid levels seen in these cells after 96–120 h of activation.

Table 4.1. Changes in mean cell diameter and membrane surface area during the activation of cultured thymic and splenic T Lymphocytes with PMA/ionomycin.

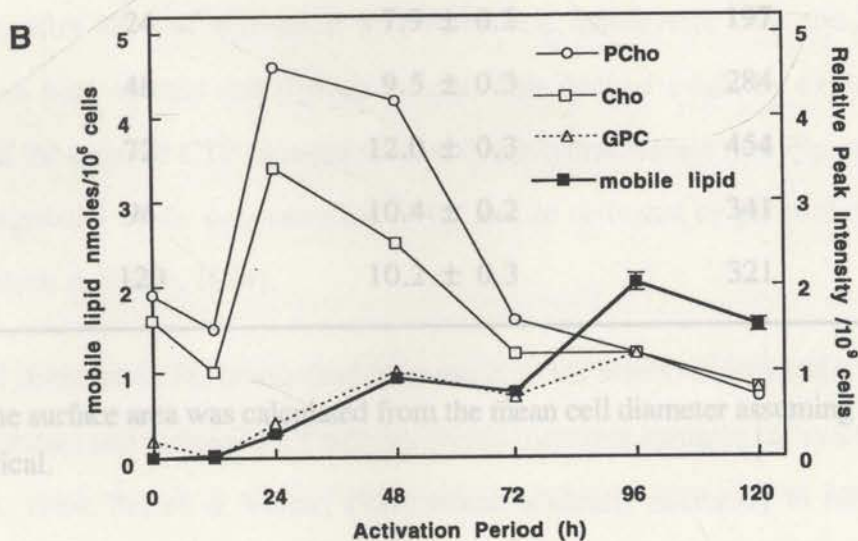
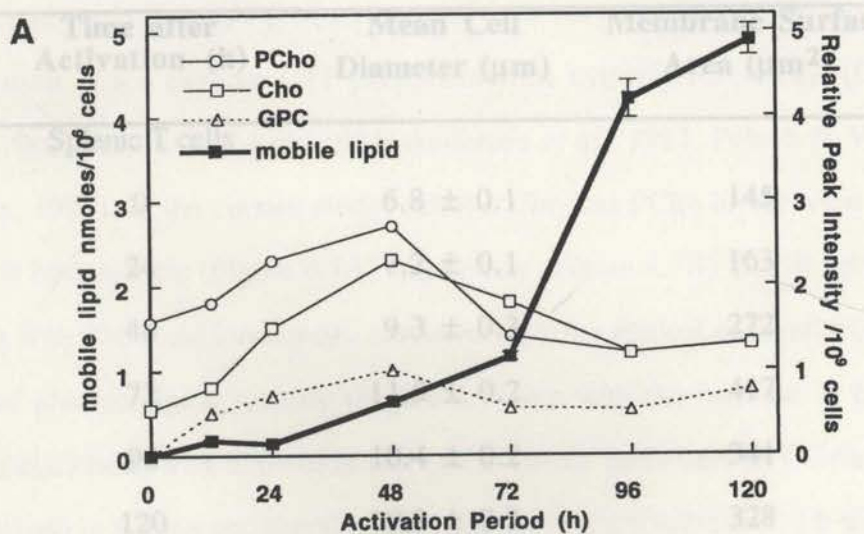


Figure 4.7. The relative changes in phosphatidylcholine metabolites and mobile lipid in activated splenic and thymic T lymphocytes.

Changes in the relative intensity of the PCho, Cho, and GPC cross peaks (right ordinate axis) and the concentration of mobile lipid (left ordinate axis) during the stimulation of splenic (A) and thymic (B) T lymphocytes with PMA/ionomycin. The values given are the mean of two experiments which varied by no more than $\pm 15\%$ for any time point.

Table 4.1. Changes in mean cell diameter and membrane surface area during the activation of cultured thymic and splenic T Lymphocytes with PMA/ionomycin.

Time after Activation (h)	Mean Cell Diameter (μm)	Membrane Surface Area (μm^2)
Splenic T cells		
0	6.8 \pm 0.1	145
24	7.2 \pm 0.1	163
48	9.3 \pm 0.3	272
72	11.5 \pm 0.2	417
96	10.4 \pm 0.2	341
120	10.2 \pm 0.3	328
Thymic T cells		
0	6.6 \pm 0.1	137
24	7.9 \pm 0.2	197
48	9.5 \pm 0.3	284
72	12.0 \pm 0.3	454
96	10.4 \pm 0.2	341
120	10.2 \pm 0.3	321

An initial decrease in PC levels (and increase in DAG levels) due to PMA activation of splenic and thymic T lymphocytes and increased CT activity would therefore enhance PC synthesis (Pelech & Vance, 1984; Pelech & Vance, 1989) which is clearly necessary to fuel the rapidly expanding plasma membrane in the early stages of activation (Figure 1.14), as shown by the increased cell diameters in Table 4.1.

The gradual depletion of Cho from the medium and intracellular stores after 48 h of activation would be expected to result in decreased PC synthesis, since choline kinase may be a rate-limiting enzyme (Kaplan & Cohen, 1994) and CDP-choline a rate-limiting substrate (Pelech & Vance, 1984; Stals *et al.*, 1994) in PC synthesis. Since PC and

4.3. Discussion.

It is well established that phorbol esters and calcium ionophores stimulate both the synthesis and catabolism of PC in a variety of cells via activation of phospholipases and the activation of the enzyme CTP-phosphocholine cytidyltransferase (CT) (Guy & Murray, 1982; Pelech & Vance, 1984; Anderson *et al.*, 1985; Pelech & Vance, 1989; Nishizuka, 1992). In the current study, cellular Cho and PCho levels were observed to increase in both splenic (Figure 4.7A) and thymic (Figure 4.7B) T cells up to 48 h after activation with PMA and ionomycin, consistent with the gradual accumulation of GPC as a result of phospholipase activity (Figure 4.7) and with the increase in phospholipid synthesis associated with activation and cell division. Increased GPC levels have also been observed in human peripheral blood lymphocytes activated for 12 h with IL-2, and it was proposed that this resulted from increased PC turnover associated with activation (Kaplan & Cohen, 1994).

However, after 48 h of activation with PMA and ionomycin, Cho and PCho levels declined in both splenic and thymic T cells. This decline might be explained by the activity of the enzyme CTP-phosphocholine cytidyltransferase (see Figure 4.1), which may be regulated by the concentration of PC and be activated by phorbol esters such as PMA (Pelech & Vance, 1984).

An initial decrease in PC levels (and increase in DAG levels) due to PMA activation of phospholipases and increased CT activity would therefore enhance PC synthesis (Pelech & Vance, 1984; Pelech & Vance, 1989) which is clearly necessary to fuel the rapidly expanding plasma membrane in the early stages of activation (Figure 1.14), as shown by the increased cell diameters in Table 4.1.

The gradual depletion of Cho from the medium and intracellular stores after 48 h of activation would be expected to result in decreased PC synthesis, since choline kinase may be a rate-limiting enzyme (Kaplan & Cohen, 1994) and CDP-choline a rate-limiting substrate (Pelech & Vance, 1984; Stals *et al.*, 1994) in PC synthesis. Since PC and

triacylglycerols (TAGs) are believed to be derived from the same pool of DAGs, then a decrease in PC synthesis will result in the accumulation of DAGs and increased TAG synthesis. Therefore, after 120 h activation, DAG and fatty acids would be converted to storage pools of triglyceride and this may account for the dramatic increase in mobile lipid which we observed during the latter stages of T cell activation (Figures 4.6, 4.7). Clearly, since DAG is a potent second messenger which stimulates PKC (Nishizuka, 1992), the conversion of DAG and fatty acids to storage pools of triglyceride may be important in signal attenuation (Florin-Christensen *et al.*, 1992) in the early stages of T cell activation and later as a source of fatty acids for incorporation into synthesised phosphatidylcholine (Goppelt-Strube & Resch, 1987; Szamel & Resch, 1995).

These observations and conclusions are supported by recent studies that show the relationship of PC cycling with the progression of cells through the cell cycle (Jackowski, 1994; Terce *et al.*, 1994). Cyclic oscillations of PC catabolism and biosynthesis occur in the G₁/S phase of the cell cycle. PC catabolism via phospholipase degradation occurs in the G₁ phase. PC biosynthesis is regulated by the activity of CT. Enzyme activity of CT is maximal in G₁/S phase, resulting in the accumulation of phospholipids in S phase in preparation for cell division (Section 1.9.2, Figure 1.14) (Jackowski, 1994). These proposals are consistent with the observations shown in this study in activated murine lymphocytes that are rapidly proliferating. Oscillations in Cho, PCho and an elevated level of GPC indicate that degradation and biosynthesis of PC are occurring, resulting in the net accumulation of mobile lipid after multiple cell cycles. Murine T cells activated with PMA and ionomycin for 96-120 h showed increased accumulation of mobile lipid. This was associated with a simultaneous decrease in phosphatidylcholine metabolites and cell size (Figure 4.7, Table 4.1). These observations may be explained by changes in the cell cycle status and the phosphatidylcholine cycle due to choline deficiency (Terce *et al.*, 1994). The cell mass of fibroblast 3T3 cells was reduced by up to 35% in cells growth arrested by the removal of choline from the culture medium. Viability remained high in these cells, but they were prevented from progressing through the cell cycle because choline, an essential metabolite for PC synthesis, was not available (Terce *et al.*, 1994).

The decrease in the phospholipid mass of the cells was due to PC catabolism in the G_0/G_1 phase of the cell cycle. These observations are consistent with the results obtained in this study in murine T cells at 96-120 h after activation with PMA and ionomycin, which showed a reduction in cell size without the loss of cell viability, with a corresponding increase in the mobile lipid when Cho levels were reduced (Figure 4.7, Table 4.1.).

The lipid accumulation observed in T cells in this study is also consistent with the changes that occur as a consequence of membrane signalling events. Activation of lymphocytes results in changes in the lipid composition of the plasma membranes. Upon mitogen stimulation of rabbit and calf thymocytes, exogenous polyunsaturated long-chain fatty acids are incorporated into plasma membrane phospholipids. Similar changes were observed when serum-free culture conditions were used, indicating that there is an internal storage pool of polyunsaturated fatty acids (Goppelt *et al.*, 1985; Goppelt-Strube & Resch, 1987). Transfer of unsaturated fatty acids from triglycerides to phospholipids has also been observed, suggesting that the triglycerides may act as an intracellular storage pool for long-chain fatty acids which can be transferred to membrane phospholipids (Goppelt *et al.*, 1985). An increase in polyunsaturated fatty acid incorporation in PC with a smaller increase in incorporation into phosphatidylethanolamine (PE) was also observed in thymocytes after four hours of stimulation with ConA (Rode *et al.*, 1982). This observation was supported by results showing that during differentiation in murine leukemia cells, exogenous fatty acids are incorporated into PC and are transferred to PE where they are stored as a metabolically stable pool of polyunsaturated fatty acids (Kannagi *et al.*, 1982). In further support, triglycerides exchange poorly in biological systems, whereas phospholipids are easily able to exchange fatty acids (Bell & Coleman, 1980). We have also observed PE increases in activated murine thymocytes over a 72 h incubation with PMA and ionomycin (Dingley *et al.*, 1992).

PC and PE consist of a mixture of 1,2-diacyl-, 1-alkyl-2-acyl-, and 1-alkenyl-2-acyl acyl chain subspecies (Hii *et al.*, 1990). In neutrophils it has been demonstrated that the relative proportions of these acyl chain subspecies determines the rate of phospholipid

catabolism. The catabolic rate of 1-acyl-2-acetyl-GPC is approximately 2-fold higher than 1-alkyl-2-acetyl-GPC, and the removal of the acyl group during catabolism results in the long acyl chain being incorporated into triglyceride or PC (Triggiani *et al.*, 1991) (see Figure 4.1). *cis*-unsaturated fatty acids have been shown to activate CT in bovine lymphocytes and enhance the pathway leading to PC synthesis by 1.5-7.0-fold. Unsaturated fatty acids with chain lengths of 16-20 carbons and at least one *cis* double bond near the middle of the chain were particularly active, while *trans*-isomers were inactive (Anderson *et al.*, 1985; Whitlon *et al.*, 1985). This fatty acid structure is consistent with the lipid structure obtained in the $^1\text{H-NMR}$ -visible mobile lipid spectrum (see Figure 4.6), with unsaturated bonds at carbon 9 and 12 of the 18-carbon acyl chains. Thus, deacetylation and deacylation-acylation cycles, which are enhanced in activated neutrophils (Triggiani *et al.*, 1991; Triggiani *et al.*, 1994) and lymphocytes (Goppelt-Strube & Resch, 1987; Szamel & Resch, 1995), may also be a source of triglyceride (Lerique *et al.*, 1994).

The pathways involved in PC cycling are complex and may be regulated in a number of ways (Pelech & Vance, 1984; Pelech & Vance, 1989; Jackowski, 1994; Terce *et al.*, 1994). I have attempted to explain the associated changes in light of known T cell activation events and our observations about the development of the mobile lipid in these cells. Other recent studies in human neutrophils stimulated with PMA or the chemotactic peptide fMLP have shown that PC cyclic turnover can be stimulated via agonist-induced phospholipase D activation (Tronchere *et al.*, 1994; Tronchere *et al.*, 1995). Similar models have been proposed to explain rapid PC turnover in Friend leukemia cells via PC-specific phospholipase C hydrolysis (Podo *et al.*, 1992; Ferretti *et al.*, 1993). Ferretti and colleagues propose that this may be the mechanism for the observed increases in the accumulation of mobile lipids in tumour cells or in immature or transformed cells (Ferretti *et al.*, 1993). Phospholipid catabolism has also recently been proposed as the possible mechanism for the generation of mobile lipid in fibroblast cell lines (Delikatny *et al.*, 1996a) and breast cancer cell lines treated with the cytotoxic drug TPP (Delikatny *et al.*, 1996b).

Although at present there is no consensus model to account for the appearance of $^1\text{H-NMR}$ -visible mobile lipid in malignant cells and activated immune cells, two explanations have been put forward. Mountford and colleagues have proposed that the mobile lipid may be associated with the plasma membrane in the form of lipoprotein domains intercalated within the bilayer (Mountford & Wright, 1988). High affinity lipoprotein receptors have also been demonstrated on T lymphocytes. Low levels of expression are seen on resting cells and high levels on activated T cells (Traill *et al.*, 1987; Jurgens *et al.*, 1989). It is believed that lipoproteins can provide an exogenous source of fatty acids via these receptors for optimal T cell growth (Cuthbert & Lipsky, 1986). Therefore, it is possible that mobile lipids incorporated into lipoproteins from exogenous serum sources can provide a source of fatty acids that can be incorporated into membrane phospholipids during cell activation. Lipoproteins would also contribute to the mobile lipid spectra obtained from activated cells.

An alternative proposal is that mobile lipids accrue within intracellular lipid droplets. These have been shown to accumulate in the cytoplasm of myeloma cells (Callies *et al.*, 1993) and murine splenocytes grown to high density (Stubbs *et al.*, 1980). The accumulation of cytoplasmic lipid droplets and their correlation with an increase in $^1\text{H-NMR}$ -detectable mobile lipid remains controversial (Mountford *et al.*, 1982; Mackinnon *et al.*, 1989; Holmes *et al.*, 1990; Callies *et al.*, 1993; May *et al.*, 1994). It has been suggested that both explanations may be possible and that the two may be interrelated (Callies *et al.*, 1993). The results of this study suggest that interrelation is likely, based on the cellular location of the various enzymes involved in neutral lipid and PC cycling and their role in cell-signal attenuation.

This study represents the first demonstration of a significant difference in the kinetics of appearance of mobile lipid in activated immune cells of the same origin and lineage, but isolated from different cell sources. At this stage, we cannot explain the larger accumulation of mobile lipid in activated splenic compared to thymic T cells (3-fold higher after 120 h of activation). Although, recent evidence has shown that activated spleen cells are the only tissue to express high levels of mRNA for both the cell surface

molecule Fas and its ligand FasL (Suda *et al.*, 1993). The binding of Fas to its ligand can induce activated T cells to undergo apoptosis via the binding of T cells to each other (Crispe, 1994). This may have implications for the increased accumulation of mobile lipids in activated splenic T cells. However, the difference may simply result from different proportions of various phospholipids, particularly their acyl chain composition, in the two cell types, since this is known to depend on tissue source (Ansell & Spanner, 1982), cell type, and/or the state of differentiation (Dulbecco *et al.*, 1980; Kannagi *et al.*, 1982). However, the concomitant accumulation of mobile lipids and decline in Cho/PCho levels in both cell-types suggest that, in activated T cells at least, the accumulation of $^1\text{H-NMR}$ -visible mobile lipid may be dependent on the status of the PC cycle, which in turn can be regulated by cell cycle status.

The aim was to investigate the activation pathways required for the generation of the NMR-visible mobile lipid and to correlate this with the activation state of the cells.

The increase in mobile lipid observed in thymic and splenic T cells activated with PMA and ionomycin has been shown in the previous chapter to be associated with changes in phospholipid levels, particularly during PC cycling, which occurs in activated cells. It has also been previously shown that the appearance of the $^1\text{H-NMR}$ -visible mobile lipid can be induced by different stimuli in a variety of activated immune cells (Mountford *et al.*, 1984; Holmes *et al.*, 1990; King *et al.*, 1991; Dingley *et al.*, 1992; Dingley *et al.*, 1994; King *et al.*, 1994; May *et al.*, 1994), and is independent of proliferation and cell cycle progression (King *et al.*, 1991). In activated thymocytes, mobile lipid can be detected as early as six hours after stimulation with PMA and ionomycin (Dingley *et al.*, 1992). A reduction of the $^1\text{H-NMR}$ -visible mobile lipid was observed in activated neutrophils which are inhibited by the binding of an antibody to cell surface adhesion receptors (May *et al.*, 1991).

Collectively, these results suggest that the induction of the $^1\text{H-NMR}$ -visible mobile lipid is an early event in the activation of thymocytes and may be influenced by the activation of distinct biochemical pathways which may be important in the acquisition of the mobile

Chapter 5.

The role of phosphatidylcholine-specific phospholipase C in the generation of mobile lipid in T cells.

5.1. Introduction.

In this study, T lymphocytes have been stimulated using an antibody against the TCR/CD3 complex. This was compared to the action of PMA and ionomycin used separately or in combination. The aim was to investigate the activation pathways required for the generation of the NMR-visible mobile lipid and to correlate this with the activation state of the cells.

The increase in mobile lipid observed in thymic and splenic T cells activated with PMA and ionomycin has been shown in the previous chapter to be associated with changes in phospholipid levels, particularly during PC cycling, which occurs in activated cells. It has also been previously shown that the appearance of the $^1\text{H-NMR}$ -visible mobile lipid can be induced by different stimuli in a variety of activated immune cells (Mountford *et al.*, 1984; Holmes *et al.*, 1990; King *et al.*, 1991; Dingley *et al.*, 1992; Dingley *et al.*, 1994; King *et al.*, 1994; May *et al.*, 1994), and is independent of proliferation and cell cycle progression (King *et al.*, 1991). In activated thymocytes, mobile lipid can be detected as early as six hours after stimulation with PMA and ionomycin (Dingley *et al.*, 1992). A reduction of the $^1\text{H-NMR}$ -visible mobile lipid was observed in activated neutrophils which are inhibited by the binding of an antibody to cell surface adhesion receptors (May *et al.*, 1991).

Collectively, these results suggest that the induction of the $^1\text{H-NMR}$ -visible mobile lipid is an early event in the activation of thymocytes and may be influenced by the activation of distinct biochemical pathways which may be important in the acquisition of the mobile

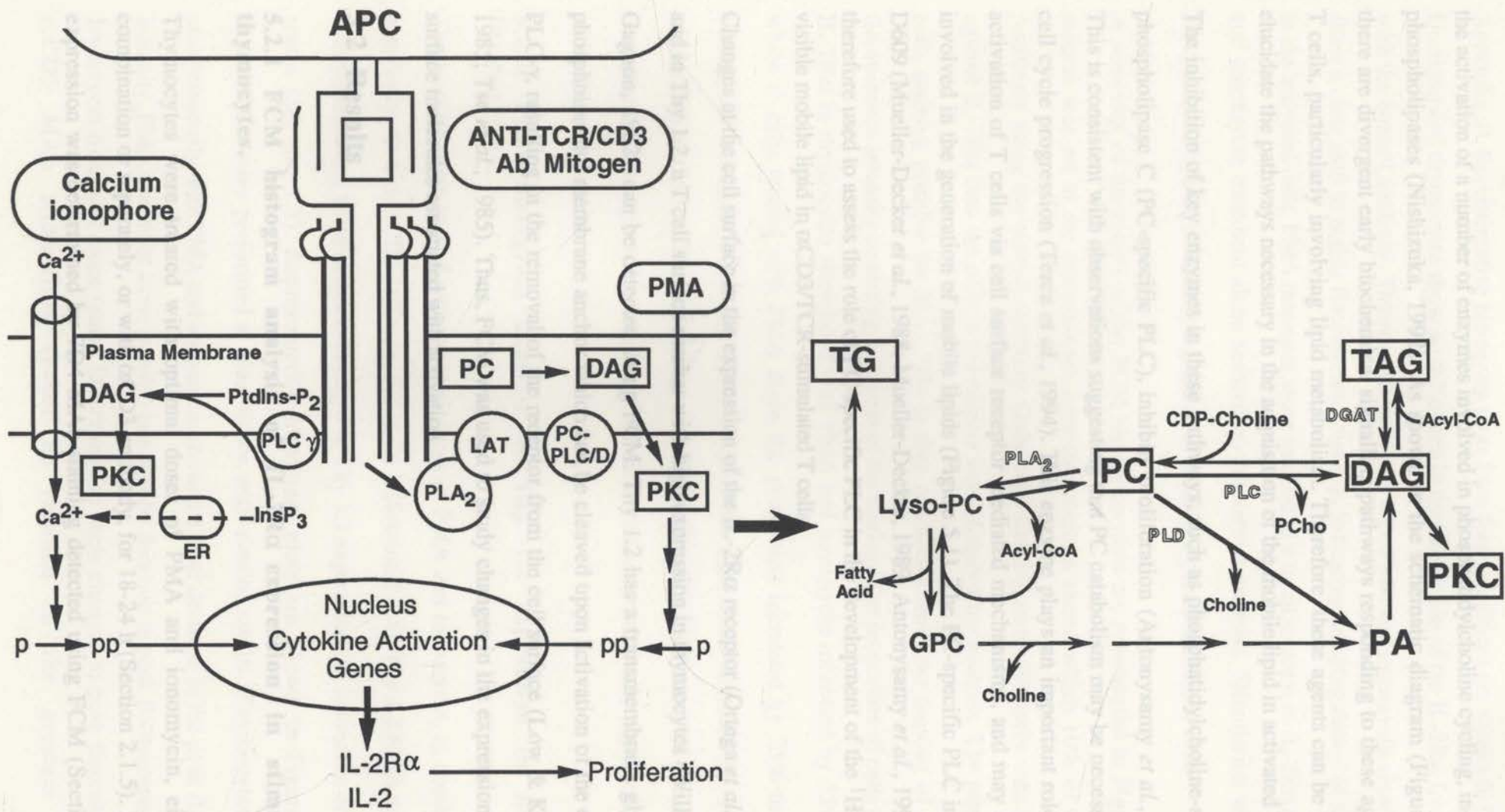
lipid spectrum. These observations are also consistent with oscillations in phospholipid metabolism during the cell cycle and the generation of lipids in the G₁ phase of the cell cycle (Jackowski, 1994).

The activation of T cells results in the expression of cell surface receptors and then in the production of cytokines. Firstly, the interleukin-2 receptor α (IL-2R α) is expressed on the cell surface, which may indicate that the cells have progressed into the G₁ phase of the cell cycle. This is followed by the production of the cytokine IL-2 which binds to the receptor, IL-2R α resulting in cellular cell cycle progression and proliferation (Cantrell & Smith, 1984; Ortega *et al.*, 1984). T cells can be activated by treatment with phorbol esters, such as PMA, and the calcium ionophore ionomycin, or an α CD3/TCR antibody. These agents activate T cells via different signalling pathways (Szamel & Resch, 1995). As suggested in Section 4.3, the accumulation of the mobile lipid in activated T lymphocytes may result from anabolic and catabolic pathways involving phosphatidylcholine cycling and may also contribute to signal attenuation in the early part of activation (Florin-Christensen *et al.*, 1992). Stimulation of the TCR/CD3 is believed to result in the activation of a number of enzymes which include lysophosphatidylcholine transferase (LAT) (which incorporates unsaturated fatty acids into membrane phosphatidylcholine upon activation), phospholipase A₂ (PLA₂) (which degrades PC to produce lysophosphatidylcholine and leads to GPC and fatty acid liberation), phosphatidylcholine-specific phospholipase C and D (hydrolyse phosphatidylcholine, liberating DAG which can activate particular isoforms of PKC), and PLC- γ (which catalyses the catabolism of phosphatidylinositol 4,5-*bis*phosphate to yield inositol 1,4,5-*tris*phosphate (IP₃) and DAG). The DAG can cause short-term stimulation of PKC isoforms and the release of inositol phospholipids can release Ca²⁺ from the endoplasmic reticulum (ER) (Figure 5.1; Szamel & Resch, 1995).

PMA and ionomycin when used in combination mimic the action of inositol phospholipid-derived second messengers normally generated by stimulation of the TCR/CD3 complex (Altman *et al.*, 1992). As discussed in Chapter 4, PMA directly activates PKC and ionomycin can cause a calcium influx into the cell which can potentiate

Figure 5.1. Phosphatidylcholine cycling and its relationship to cellular signalling.

APC	antigen presenting cell
TCR/CD3	T cell receptor/ CD3 complex
PtdIns-P ₂	phosphatidylinositol 4,5 bisphosphate
InsP ₃	inositol-1,4,5-triphosphate
LAT	lysophosphatidylcholine acyltransferase
PKC	protein kinase C
(p)p	(phosphorylated) protein
CDP-choline	cytidine 5'-diphosphate-choline
PCho	phosphocholine
DAG	diacylglycerol
G3P	glycerol-3-phosphate
GPC	glycerophosphocholine
Lyso-PC	lysophosphatidylcholine
PLA ₂	phospholipase A ₂
PC	phosphatidylcholine
PLC	phospholipase C
PLC γ	phospholipase C- γ
PLD	phospholipase D
PA	phosphatidic acid
TAG	triacylglycerol
TG	triglyceride



the activation of a number of enzymes involved in phosphatidylcholine cycling, including phospholipases (Nishizuka, 1992). As shown in the schematic diagram (Figure 5.1), there are divergent early biochemical signalling pathways responding to these agents in T cells, particularly involving lipid metabolism. Therefore, these agents can be used to elucidate the pathways necessary in the acquisition of the mobile lipid in activated T cells.

The inhibition of key enzymes in these pathways, such as phosphatidylcholine-specific phospholipase C (PC-specific PLC), inhibits proliferation (Antonysamy *et al.*, 1995). This is consistent with observations suggesting that PC catabolism may be necessary for cell cycle progression (Terce *et al.*, 1994). This enzyme plays an important role in the activation of T cells via cell surface receptor mediated mechanisms, and may also be involved in the generation of mobile lipids (Figure 5.1). The PC-specific PLC inhibitor D609 (Mueller-Decker *et al.*, 1988; Mueller-Decker, 1989; Antonysamy *et al.*, 1995) was therefore used to assess the role of PC-specific PLC in the development of the ¹H-NMR-visible mobile lipid in α CD3/TCR-stimulated T cells.

Changes at the cell surface in the expression of the IL-2R α receptor (Ortega *et al.*, 1984) and in Thy 1.2, a T cell surface marker with high expression in thymocytes (Williams & Gagnon, 1982), can be detected using FCM. Thy 1.2 has a transmembrane glycosylphosphoinositol membrane anchor which can be cleaved upon activation of the enzyme PLC- γ , resulting in the removal of the receptor from the cell surface (Low & Kincade, 1985; Tse *et al.*, 1985). Thus, FCM was used to study changes in the expression of cell surface molecules associated with activation.

5.2 Results

5.2.1 FCM histogram analysis of IL-2R α expression in stimulated thymocytes.

Thymocytes were treated with optimal doses of PMA and ionomycin, either in combination or separately, or with α CD3 antibody, for 18-24 h (Section 2.1.5). IL-2R α expression was determined by 7D4 MAb staining detected using FCM (Section 2.5,

Appendix 2). Representative histogram plots from four repetitions are shown in Figure 5.2. Unstimulated thymocytes show no difference in the expression of the IL-2R α from staining with the control antibody. Thymocytes activated with PMA and ionomycin simultaneously show a clear shift to higher fluorescence intensity, indicating an upregulation of the IL-2R α in the activated cells. PMA treatment alone resulted in a small increase in IL-2R α expression and ionomycin treatment alone showed no substantial increase. Stimulation with α CD3 MAb resulted in a significant upregulation of IL-2R α expression in these cells.

A summary of the results of the FCM histogram plots are represented in Figure 5.3. A marker was set at the fluorescence intensity position above which 10% of cells stain positively using the control antibody. Only cells staining more intensely with MAb 7D4 against IL-2R α than the cells at the marker were included for analysis. The percentage of cells staining positive for MAb 7D4 is then calculated from the number of cells with fluorescence intensity occurring in excess of the marker. The proportion of cells expressing IL-2R α in thymocytes stimulated with PMA and ionomycin increased by 35% to 45%, while in cells treated with PMA alone the proportion increased by 25% to 35% and ionomycin treatment alone did show a small but significant increase by 12% in the expression of the IL-2R α , indicating a change in the activation status of the thymocytes treated with these agents. In contrast, α CD3 alone did not result in any significant increases in IL-2R α expression.

5.2.2. FCM histogram analysis of Thy 1.2 expression in stimulated thymocytes.

Thymocytes were treated with optimal doses of PMA and ionomycin, in combination or separately, or with α CD3 antibody, for 18-24 h (Section 2.1.5). Thy 1.2 MAb staining was determined using FCM to detect changes in Thy 1.2 expression, an indication of activation status (Section 2.5). Representative histogram plots are shown in Figure 5.4. All experiments were performed at least thrice with similar results. Thymocytes activated simultaneously with PMA and ionomycin showed a clear decrease in the peak fluorescence intensity. PMA treatment alone resulted in a smaller decrease in peak fluorescence intensity. Ionomycin treatment alone (panel D) resulted in some changes in peak fluorescence, and α CD3 MAb stimulation (panel E) resulted in the greatest decrease

Figure 5.2. Flow cytometric histogram analysis of IL-2R α expression on murine thymocytes.

Representative histograms of (A) untreated thymocytes, or of thymocytes treated (stimulated) with (B) PMA and ionomycin in combination, (C) PMA alone, (D) ionomycin alone or (E) α CD3 Mab, 500A2. The red, solid histogram represents control antibody staining and the blue histogram represents staining with α IL-2R α Mab, 7D4. The relative cell numbers are plotted against the logarithm of the fluorescence intensity measured in arbitrary units (AU).

Flow Cytometric Analysis of IL-2R Expression on Murine Thymocytes

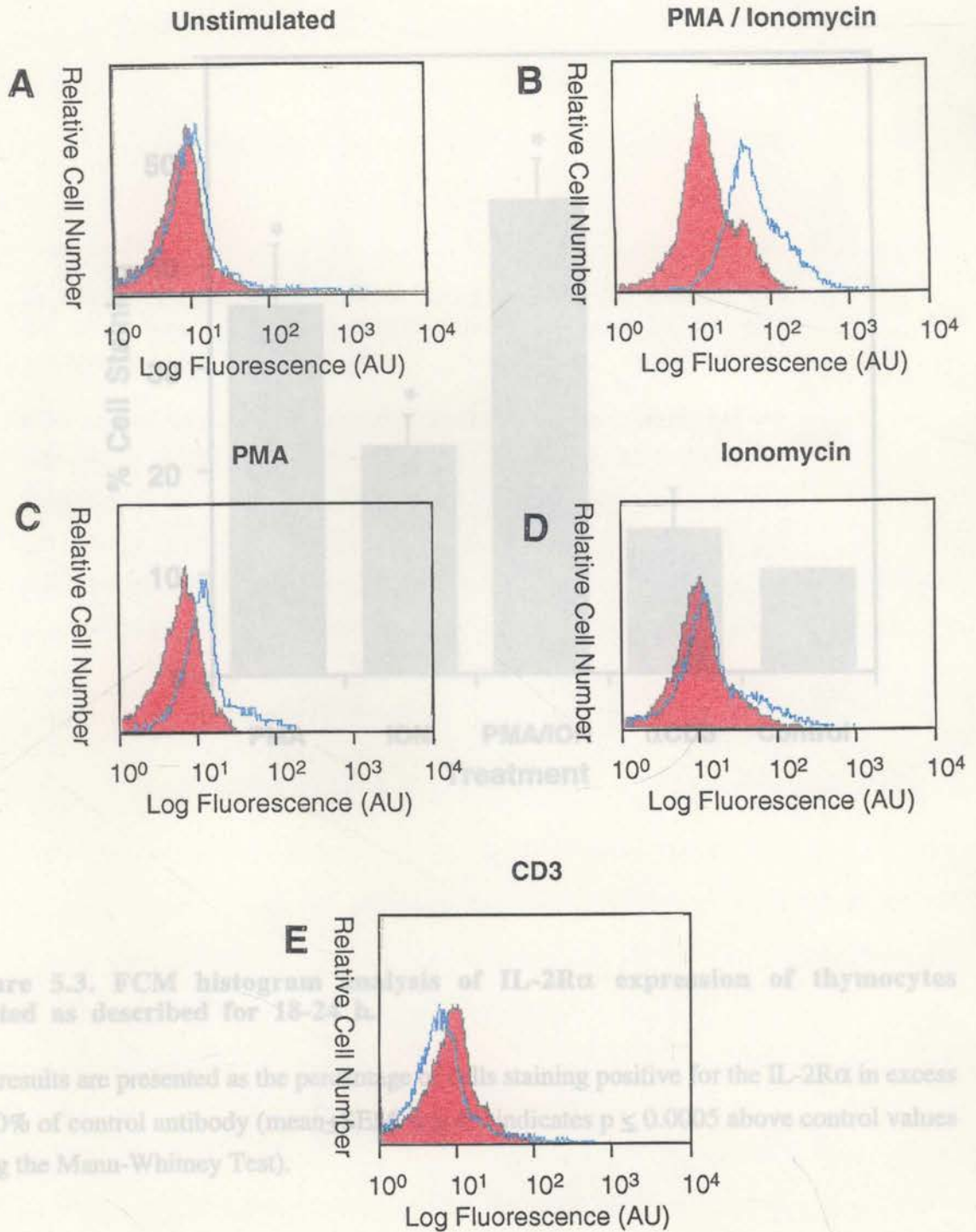


Figure 5.3. FCM histogram analysis of IL-2R α expression of thymocytes treated as described for 18-24 h. The results are presented as the percentage of cells staining positive for the IL-2R α in excess of 10% of control antibody (mean \pm SEM). * indicates $p \leq 0.0005$ above control values using the Mann-Whitney Test.

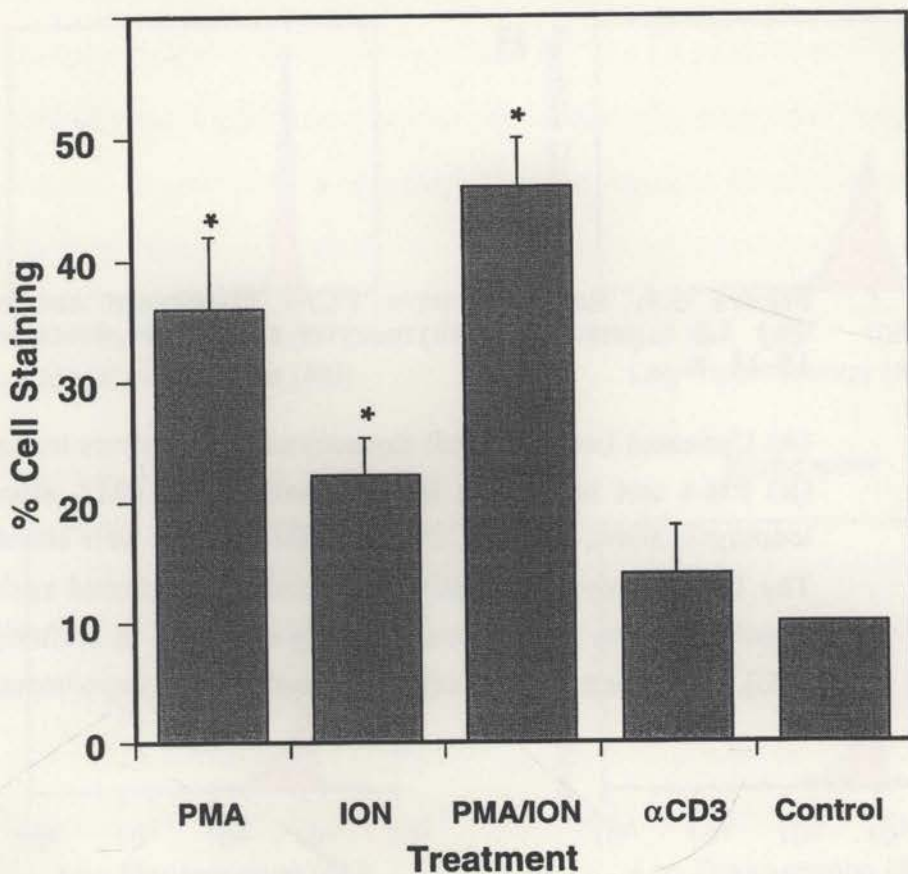


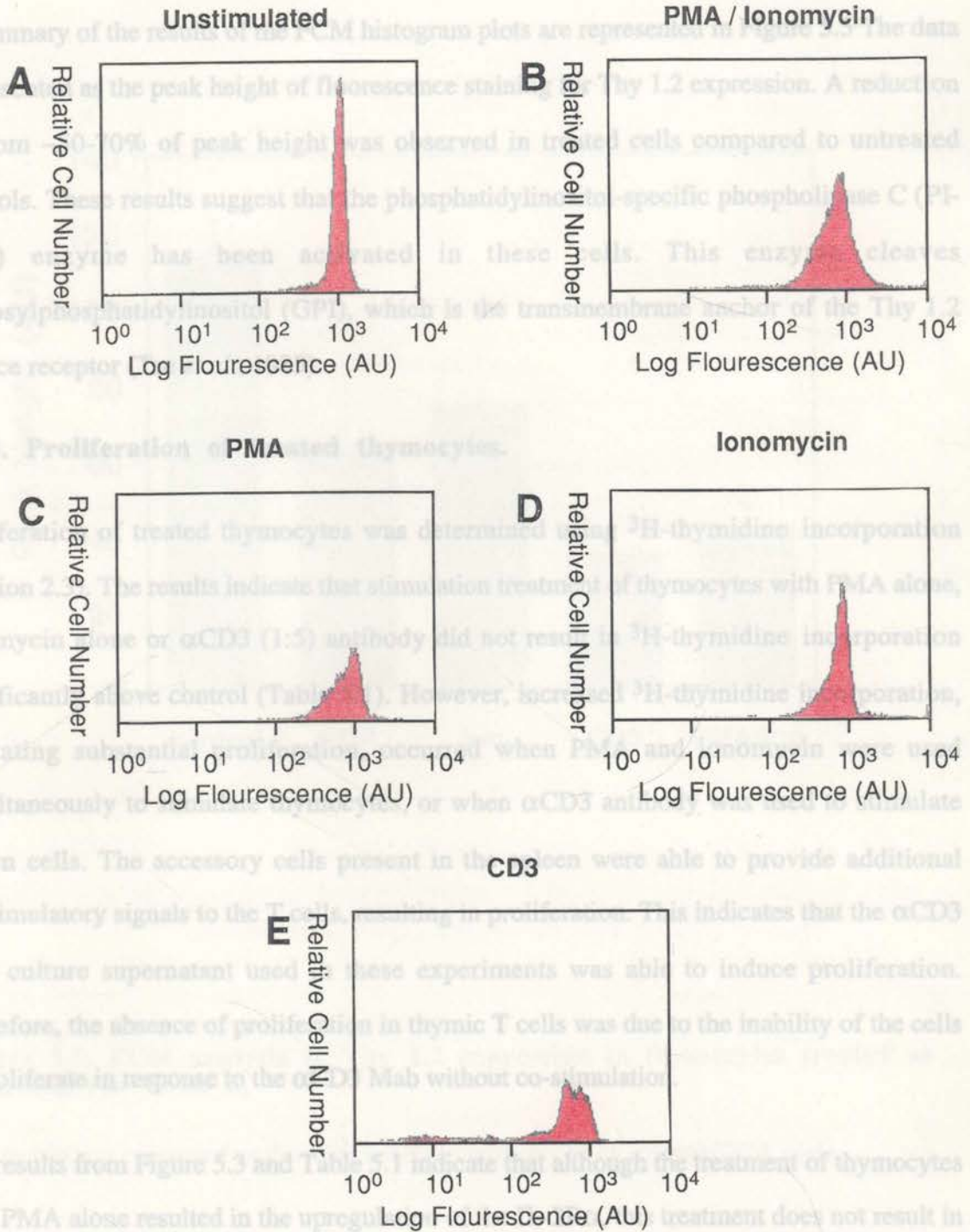
Figure 5.3. FCM histogram analysis of IL-2R α expression of thymocytes treated as described for 18-24 h.

The results are presented as the percentage of cells staining positive for the IL-2R α in excess of 10% of control antibody (mean \pm SEM, $n \geq 4$, *indicates $p \leq 0.0005$ above control values using the Mann-Whitney Test).

Figure 5.4. Representative FCM histogram analysis of Thy 1.2 expression in thymocytes treated as described for 18-24 h.

(A) Untreated (unstimulated) thymocytes. Thymocytes treated with (B) PMA and ionomycin in combination; (C) PMA alone; (D) ionomycin alone; or (E) α CD3, Mab 500A2. Cells were stained with Thy 1.2 antibody. The relative cell numbers are plotted against the logarithm of the fluorescence intensity measured in arbitrary units (AU). The same number of cells were used for each experiment.

Flow Cytometric Analysis of Thy 1.2 Expression on Murine Thymocytes



in peak fluorescence intensity. These results indicate that all of the treatments resulted in some change in the expression of Thy 1.2 in thymocytes.

A summary of the results of the FCM histogram plots are represented in Figure 5.5 The data is presented as the peak height of fluorescence staining for Thy 1.2 expression. A reduction of from ~50-70% of peak height was observed in treated cells compared to untreated controls. These results suggest that the phosphatidylinositol-specific phospholipase C (PI-PLC) enzyme has been activated in these cells. This enzyme cleaves glycosylphosphatidylinositol (GPI), which is the transmembrane anchor of the Thy 1.2 surface receptor (Tse *et al.*, 1985).

5.2.3. Proliferation of treated thymocytes.

Proliferation of treated thymocytes was determined using ^3H -thymidine incorporation (Section 2.3). The results indicate that stimulation treatment of thymocytes with PMA alone, ionomycin alone or αCD3 (1:5) antibody did not result in ^3H -thymidine incorporation significantly above control (Table 5.1). However, increased ^3H -thymidine incorporation, indicating substantial proliferation, occurred when PMA and ionomycin were used simultaneously to stimulate thymocytes, or when αCD3 antibody was used to stimulate spleen cells. The accessory cells present in the spleen were able to provide additional co-stimulatory signals to the T cells, resulting in proliferation. This indicates that the αCD3 Mab culture supernatant used in these experiments was able to induce proliferation. Therefore, the absence of proliferation in thymic T cells was due to the inability of the cells to proliferate in response to the αCD3 Mab without co-stimulation.

The results from Figure 5.3 and Table 5.1 indicate that although the treatment of thymocytes with PMA alone resulted in the upregulation of the $\text{IL-2R}\alpha$, this treatment does not result in the proliferation of the thymocytes. Proliferation of thymocytes using higher doses of PMA or ionomycin were also tested to assess whether the optimal doses, normally used in combination, were sufficient to induce proliferation when used alone to

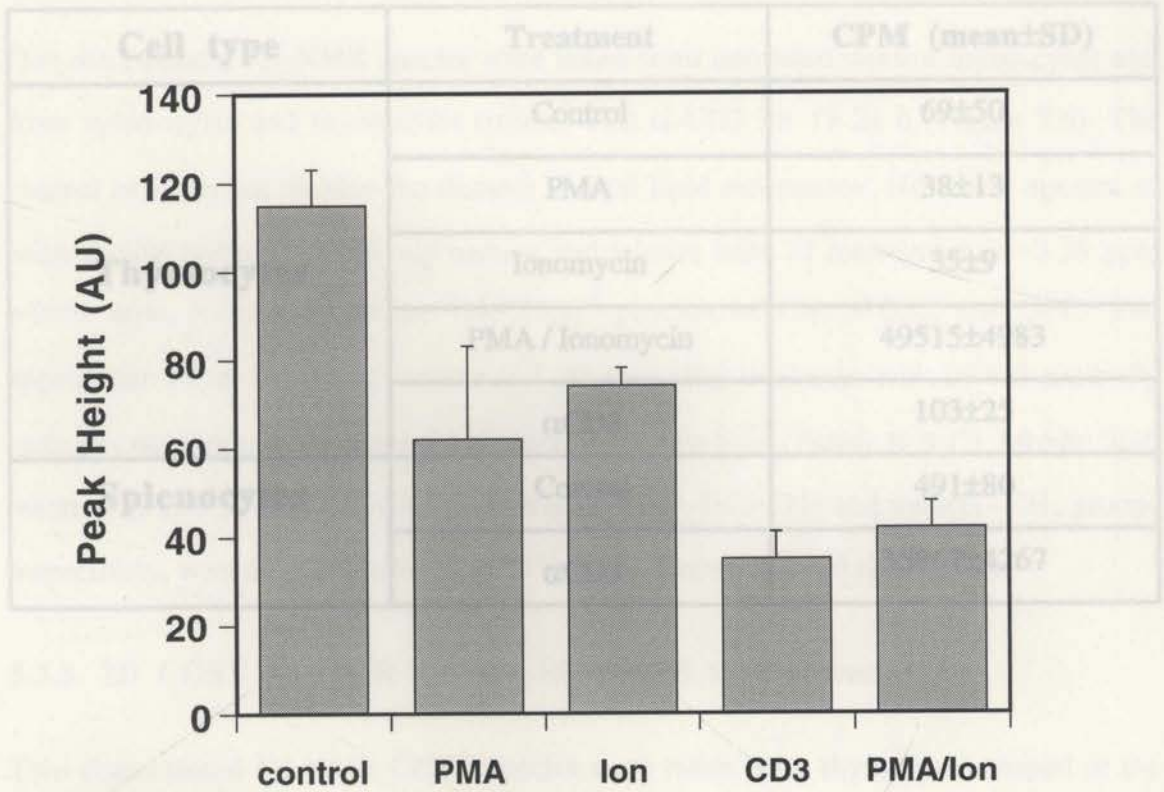


Table 5.1. ³H-thymidine incorporation of thymocytes and spleen cells treated with PMA, ionomycin and αCD3.

The thymocytes were stimulated with optimal doses of PMA (1 ng ml⁻¹) and ionomycin (300 ng ml⁻¹) and incubated for 48 h (representative experiment n=12 replicates).

Figure 5.5. FCM analysis of Thy 1.2 expression in thymocytes treated as described for 18-24 h.

The results are expressed as the peak height in arbitrary units (mean±SEM, n≥4).

treat cells. These experiments showed that higher doses did not induce proliferation in thymocytes either (data not shown).

5.2.4. 1D ¹H-NMR spectra of treated thymocytes.

Cell type	Treatment	CPM (mean±SD)
Thymocytes	Control	69±50
	PMA	38±13
	Ionomycin	35±9
	PMA / Ionomycin	49515±4983
	αCD3	103±25
Splenocytes	Control	491±80
	αCD3	35967±4267

5.2.5. 2D COSY ¹H-NMR spectra of treated thymocytes.

Two-dimensional ¹H-NMR COSY spectra were taken from thymocytes treated in the following ways (Figure 5.7): untreated thymocytes; thymocytes which had been treated for 24 h with PMA and ionomycin simultaneously; thymocytes which had been treated for

Table 5.1. ³H-thymidine incorporation of thymocytes and spleen cells treated with PMA, ionomycin and αCD3.

The thymocytes were stimulated with optimal doses of PMA (1 ng ml⁻¹) and ionomycin (300 ng ml⁻¹) and incubated for 48 h (representative experiment n=12 replicates).

thymocytes which had been treated with isotype control Ab; thymocytes which had been stimulated with optimal doses of PMA (1 ng ml⁻¹) and ionomycin in combination show distinct cross-peaks arising from mobile lipid, denoted A-G (Figure 5.7A). However, ionomycin treatment alone induced some weak mobile lipid cross-peaks (A, E, B and F) but other mobile lipid cross-peaks (G, C or D) were not observed. Untreated control thymocytes (Figure 5.7D) showed small amounts of the cross-peak A and the isotype control Ab-treated cells showed small amounts of cross-peaks A, E, and B (Figure 5.7E). These results show that mobile lipid can be generated by thymocytes treated with PMA alone, PMA and ionomycin in combination, or αCD3 antibody. This corresponds to the generation of triglyceride in these cells upon

treat cells. These experiments showed that higher doses did not induce proliferation in thymocytes either (data not shown).

5.2.4. 1D $^1\text{H-NMR}$ spectra of treated thymocytes.

One-dimensional $^1\text{H-NMR}$ spectra were taken from untreated control thymocytes and from splenocytes and thymocytes treated with $\alpha\text{-CD3}$ for 18-24 h (Figure 5.6). The control cells do not display the distinct neutral lipid resonances. However, spectra of control cells contain a relatively narrow and intense band of resonances at ~ 3.25 ppm which arise from the choline $-\text{N}(\text{CH}_3)_3^+$ protons of Cho, PCho, and GPC. The appearance of an intense resonance at 1.30 ppm after treatment with αCD3 antibody indicates the presence of increased amounts of mobile lipid (Panels B & C). Mobile lipid resonances at 5.30 ppm and 0.85 ppm, arising from $-\text{HC}=\text{CH}-$ and methyl $-\text{CH}_3$ groups respectively, were also identified in αCD3 treated thymocytes and splenocytes.

5.2.5. 2D COSY $^1\text{H-NMR}$ spectra of treated thymocytes.

Two-dimensional $^1\text{H-NMR}$ COSY spectra were taken from thymocytes treated in the following ways (Figure 5.7): untreated thymocytes; thymocytes which had been treated for 24 h with PMA and ionomycin simultaneously; thymocytes which had been treated for 24 h with PMA alone; thymocytes which had been treated for 24 h with ionomycin alone; thymocytes which had been treated with isotype control-Ab; thymocytes which had been treated for 24 h with αCD3 . Thymocytes treated with PMA, αCD3 , or PMA and ionomycin in combination show distinct cross-peaks arising from mobile lipid, denoted A-G' (Figure 5.7A). However, ionomycin treatment alone induced some weak mobile lipid cross-peaks (A, E, B and F) but other mobile lipid cross-peaks (G', C or D) were not observed. Untreated control thymocytes (Figure 5.7D) showed small amounts of the cross-peak A and the isotype control Ab-treated cells showed small amounts of cross-peaks A, E, and B (Figure 5.7E). These results show that mobile lipid can be generated by thymocytes treated with PMA alone, PMA and ionomycin in combination, or αCD3 antibody. This corresponds to the generation of triglyceride in these cells upon

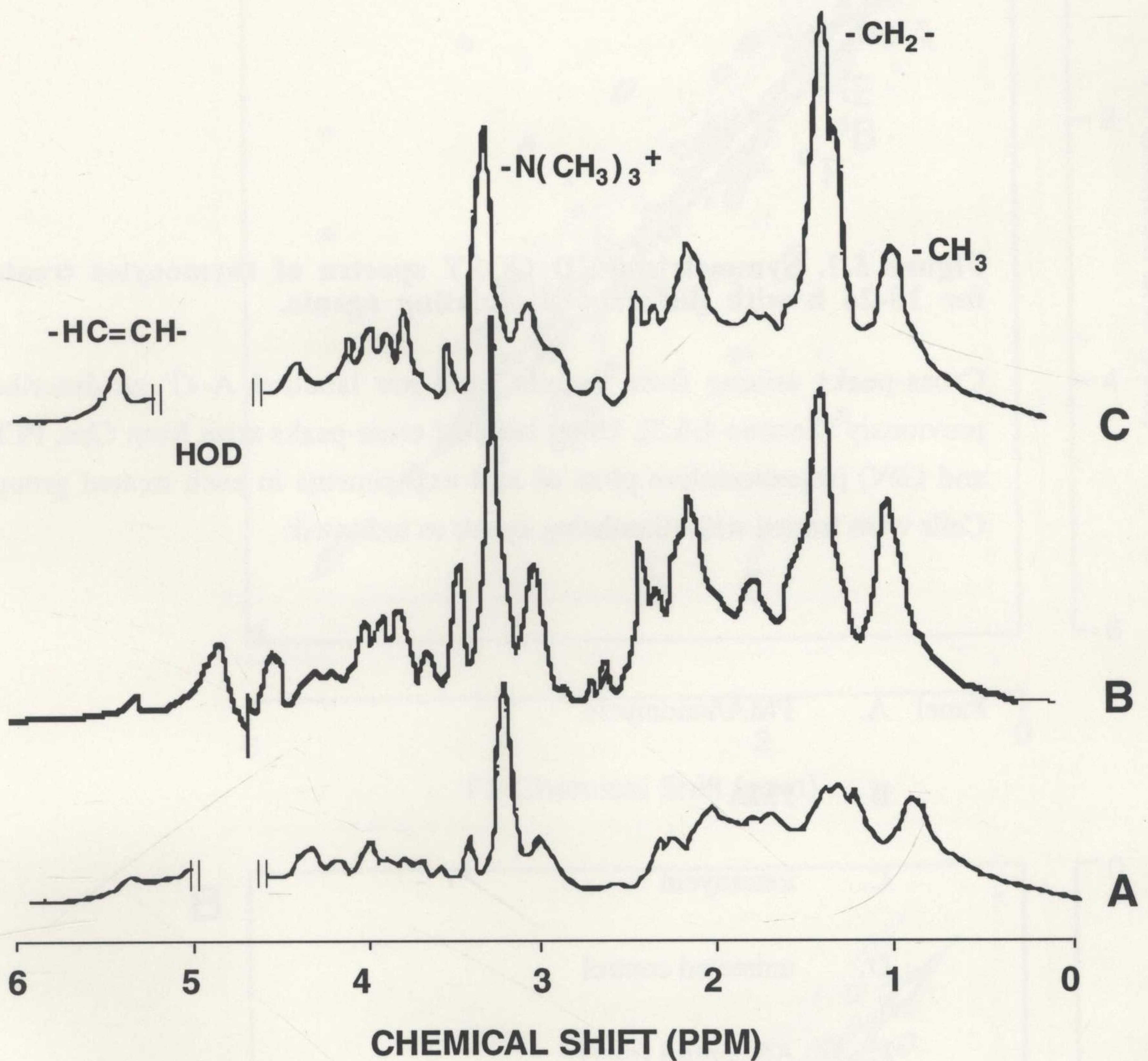


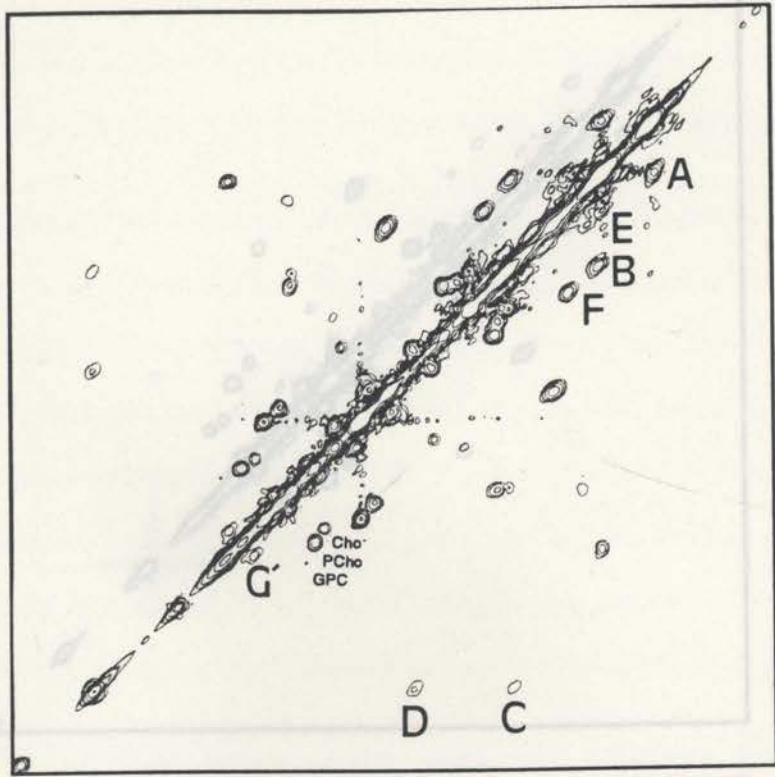
Figure 5.6. One-dimensional ^1H -NMR spectra from control thymocytes and splenocytes, and αCD3 -stimulated thymocytes.

Representative spectra of untreated control thymocytes ($n \geq 4$) (A). Splenocytes ($n=2$) (B) and thymocytes ($n \geq 4$) (C) treated for 18-24 h with αCD3 . Mobile lipid resonances at 5.30 ppm ($-\text{HC}=\text{CH}-$), 1.30 ppm ($-\text{CH}_2-$), and 0.85 ppm ($-\text{CH}_3$) are shown. The resonance at ~ 3.25 ppm arises from the choline $-\text{N}(\text{CH}_3)_3^+$ protons of Cho, PCho, and GPC. HOD indicates the position of the water resonance.

Figure 5.7. Symmetrised 2D COSY spectra of thymocytes treated for 18-24 h with different stimulating agents.

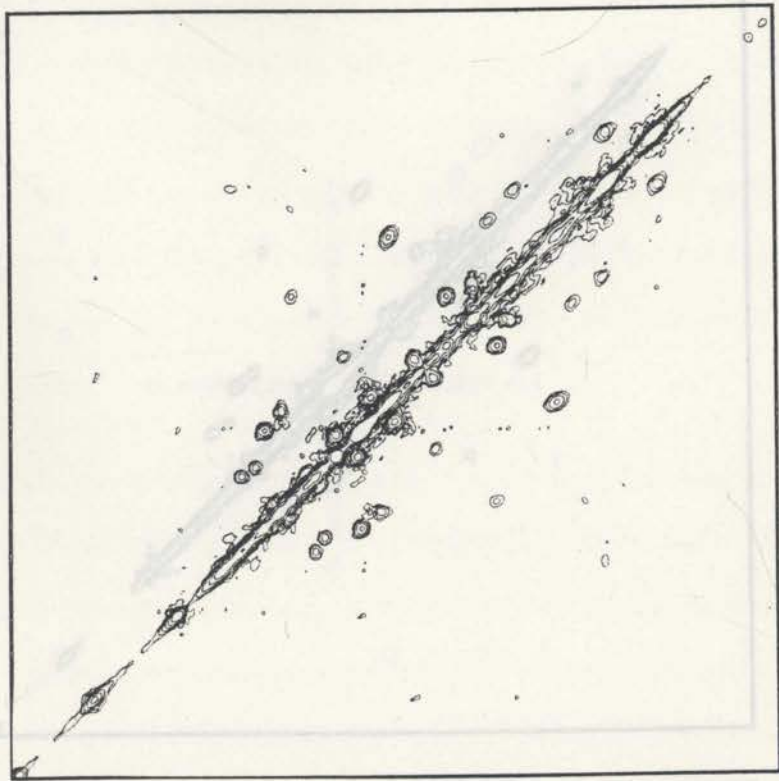
Cross-peaks arising from mobile lipid are labelled A-G' as described previously (Section 2.6.5). Other labelled cross-peaks arise from Cho, PCho and GPC (representative plots of $n \geq 4$ experiments in each treated group). Cells were treated with stimulating agents as indicated:

- Panel A. PMA/ionomycin
- B. PMA
- C. ionomycin
- D. untreated control
- E. Ab control (n=2)
- F. α CD3

A

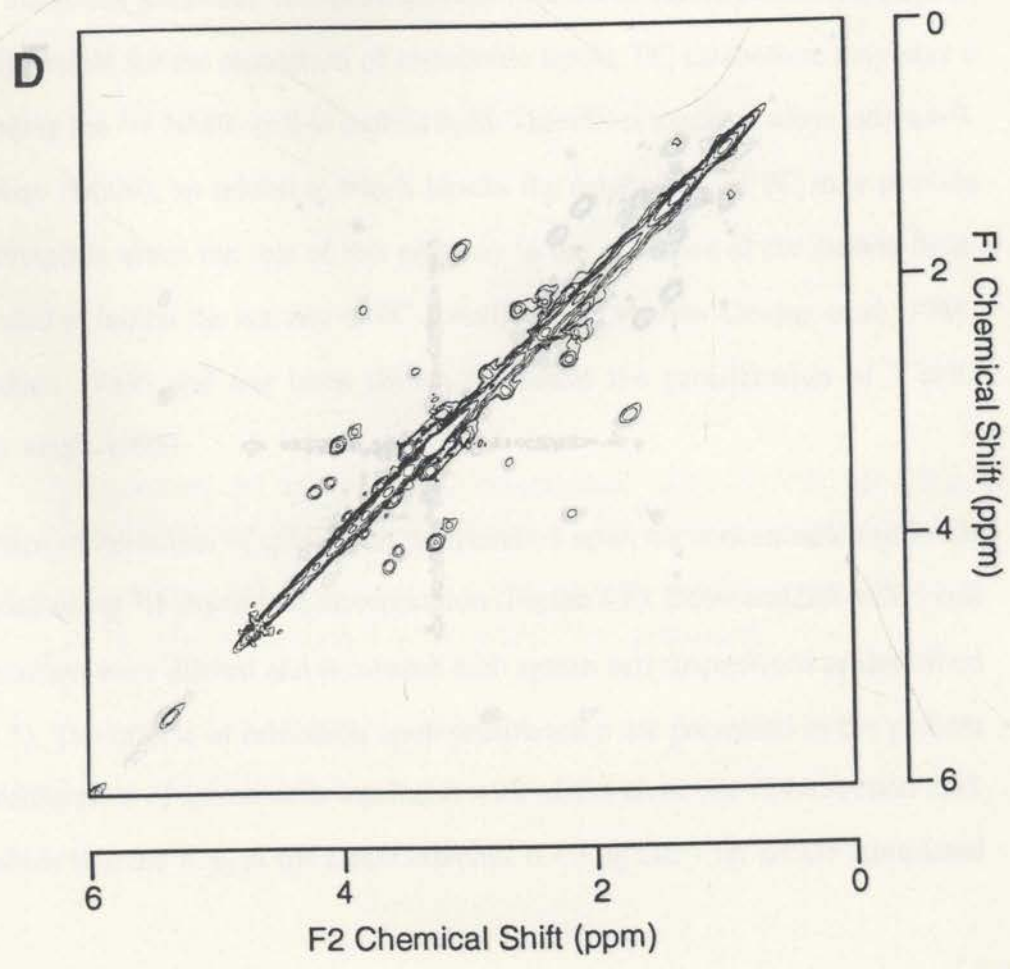
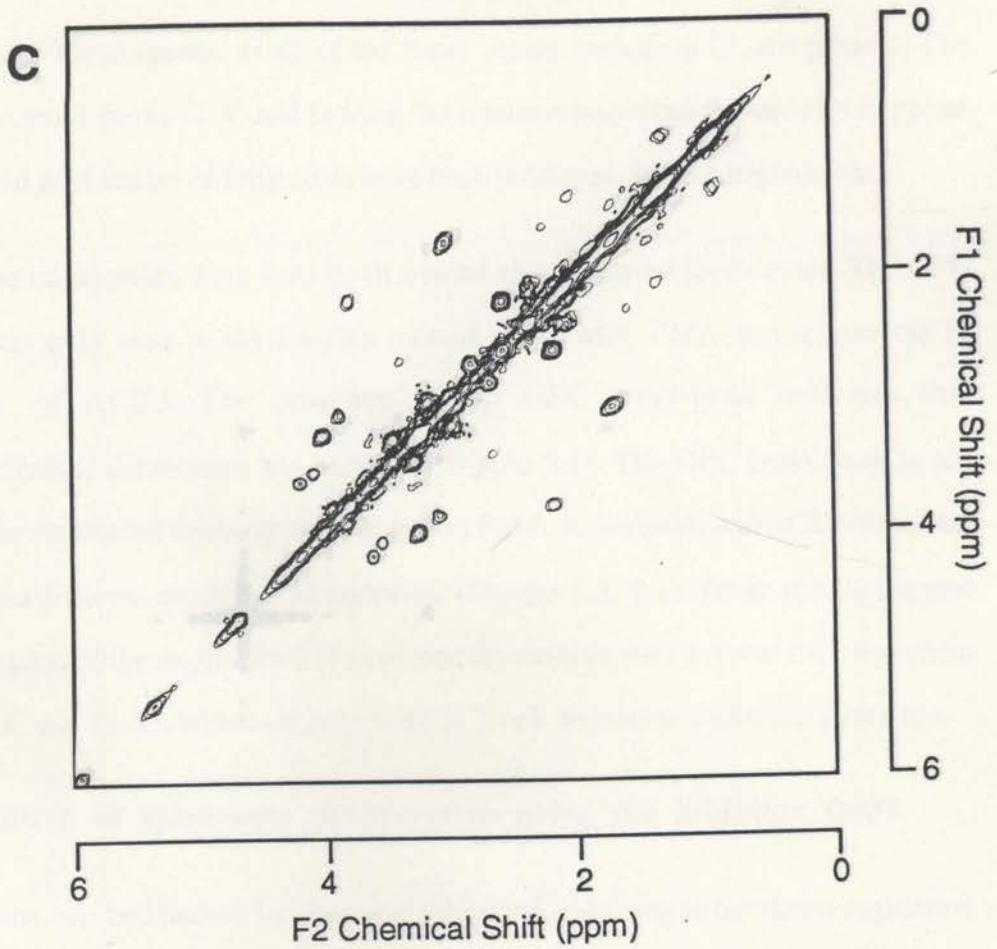
F1 Chemical Shift (ppm)

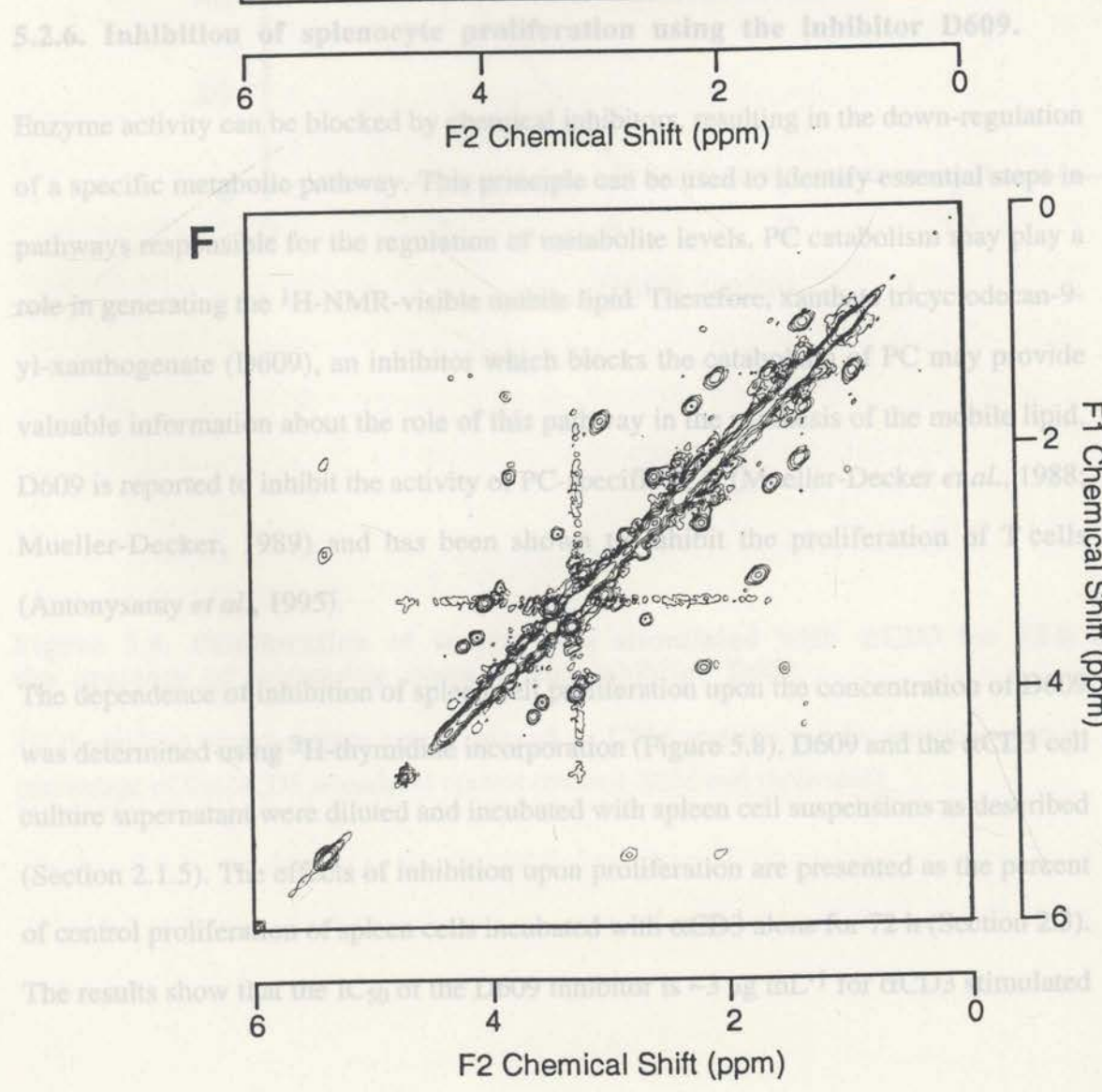
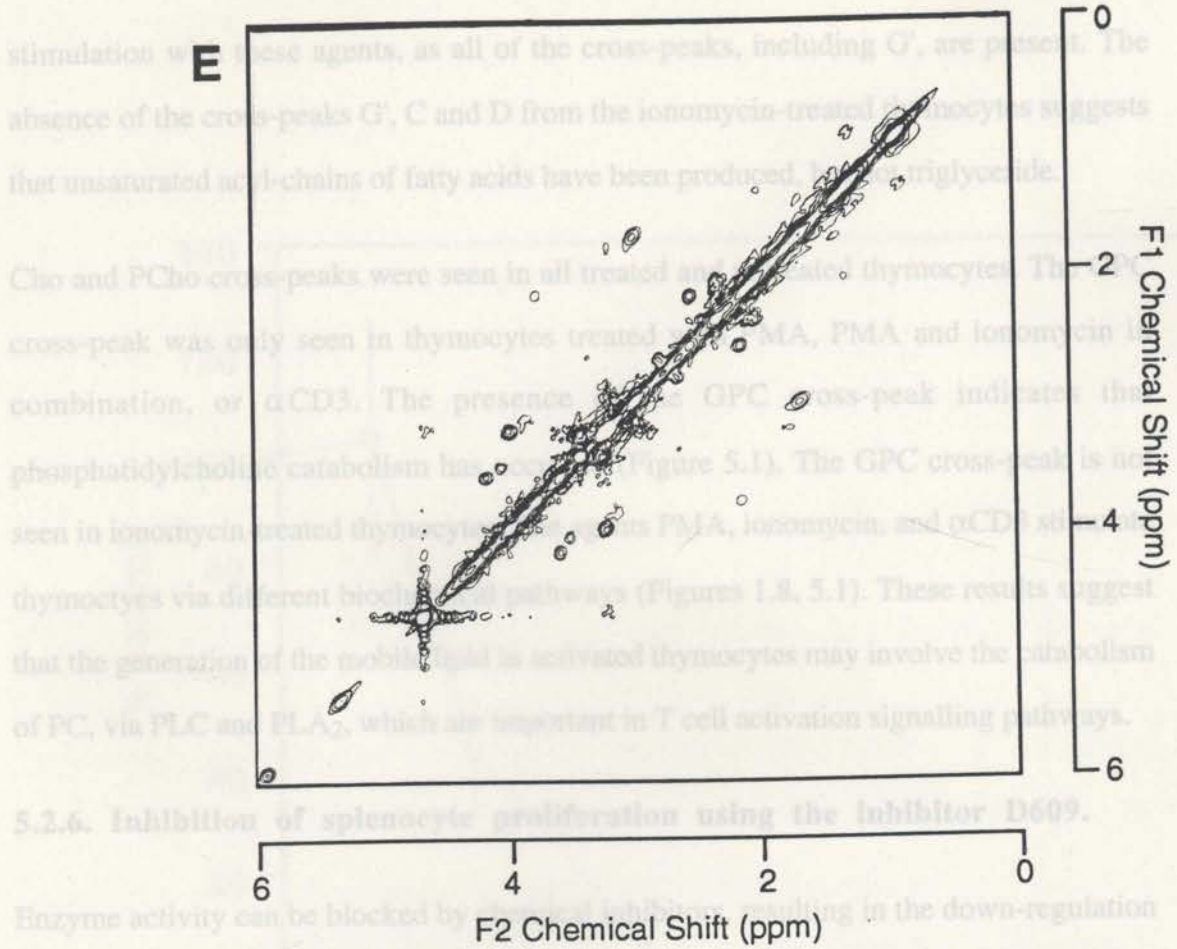
F2 Chemical Shift (ppm)

B

F1 Chemical Shift (ppm)

F2 Chemical Shift (ppm)





stimulation with these agents, as all of the cross-peaks, including G', are present. The absence of the cross-peaks G', C and D from the ionomycin-treated thymocytes suggests that unsaturated acyl-chains of fatty acids have been produced, but not triglyceride.

Cho and PCho cross-peaks were seen in all treated and untreated thymocytes. The GPC cross-peak was only seen in thymocytes treated with PMA, PMA and ionomycin in combination, or α CD3. The presence of the GPC cross-peak indicates that phosphatidylcholine catabolism has occurred (Figure 5.1). The GPC cross-peak is not seen in ionomycin-treated thymocytes. The agents PMA, ionomycin, and α CD3 stimulate thymocytes via different biochemical pathways (Figures 1.8, 5.1). These results suggest that the generation of the mobile lipid in activated thymocytes may involve the catabolism of PC, via PLC and PLA₂, which are important in T cell activation signalling pathways.

5.2.6. Inhibition of splenocyte proliferation using the inhibitor D609.

Enzyme activity can be blocked by chemical inhibitors, resulting in the down-regulation of a specific metabolic pathway. This principle can be used to identify essential steps in pathways responsible for the regulation of metabolite levels. PC catabolism may play a role in generating the ¹H-NMR-visible mobile lipid. Therefore, xanthate tricyclodecan-9-yl-xanthogenate (D609), an inhibitor which blocks the catabolism of PC may provide valuable information about the role of this pathway in the synthesis of the mobile lipid. D609 is reported to inhibit the activity of PC-specific PLC (Mueller-Decker *et al.*, 1988; Mueller-Decker, 1989) and has been shown to inhibit the proliferation of T cells (Antonysamy *et al.*, 1995).

The dependence of inhibition of spleen cell proliferation upon the concentration of D609 was determined using ³H-thymidine incorporation (Figure 5.8). D609 and the α CD3 cell culture supernatant were diluted and incubated with spleen cell suspensions as described (Section 2.1.5). The effects of inhibition upon proliferation are presented as the percent of control proliferation of spleen cells incubated with α CD3 alone for 72 h (Section 2.3). The results show that the IC₅₀ of the D609 inhibitor is $\sim 3 \mu\text{g mL}^{-1}$ for α CD3 stimulated

spleen cells. The proliferation of spleen cells was almost completely abolished at a D609 concentration of $6.25 \mu\text{g mL}^{-1}$. A concentration of $6 \mu\text{g mL}^{-1}$ was therefore used in $^1\text{H-NMR}$ studies of both thymocytes and splenocytes.

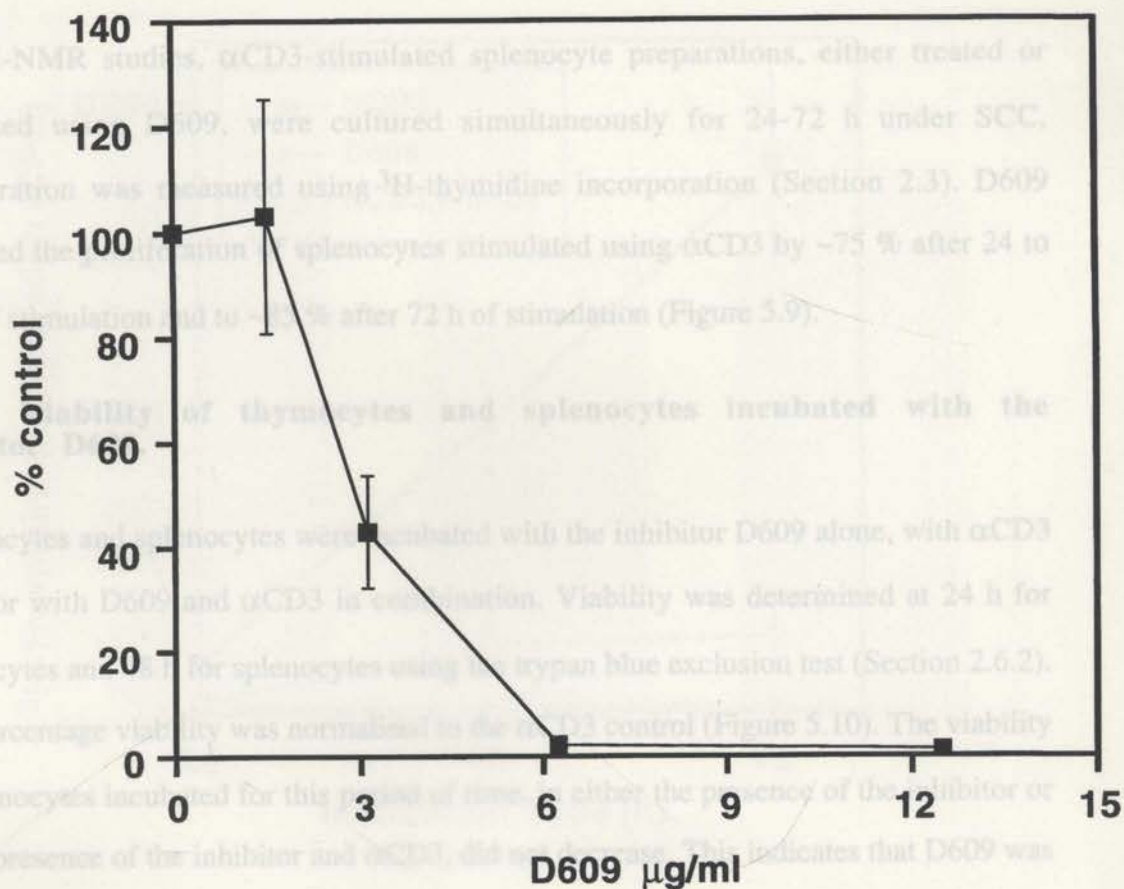


Figure 5.8. Proliferation of spleen cells stimulated with αCD3 for 72 h in the presence of increasing doses of the inhibitor D609.

^3H -thymidine incorporation was measured as CPM and the results are presented as the percentage of the αCD3 stimulated control (mean \pm SEM $n=6$ replicates).

Section 2.6.4 (Figure 5.11). 1D $^1\text{H-NMR}$ spectra of αCD3 stimulated thymocytes (Figure 5.11B) show the characteristic mobile lipid resonances at 5.30 ppm ($-\text{HC}=\text{CH}-$).

spleen cells. The proliferation of spleen cells was almost completely abolished at a D609 concentration of $6.25 \mu\text{g mL}^{-1}$. A concentration of $6 \mu\text{g mL}^{-1}$ was therefore used in $^1\text{H-NMR}$ studies of both thymocytes and splenocytes.

For $^1\text{H-NMR}$ studies, αCD3 -stimulated splenocyte preparations, either treated or untreated using D609, were cultured simultaneously for 24-72 h under SCC. Proliferation was measured using ^3H -thymidine incorporation (Section 2.3). D609 inhibited the proliferation of splenocytes stimulated using αCD3 by ~75 % after 24 to 48 h of stimulation and to ~85 % after 72 h of stimulation (Figure 5.9).

5.2.7. Viability of thymocytes and splenocytes incubated with the inhibitor D609.

Thymocytes and splenocytes were incubated with the inhibitor D609 alone, with αCD3 alone or with D609 and αCD3 in combination. Viability was determined at 24 h for thymocytes and 48 h for splenocytes using the trypan blue exclusion test (Section 2.6.2). The percentage viability was normalised to the αCD3 control (Figure 5.10). The viability of thymocytes incubated for this period of time, in either the presence of the inhibitor or in the presence of the inhibitor and αCD3 , did not decrease. This indicates that D609 was not toxic to the cells and that the inhibition of proliferation was likely to be due to the blockage of a specific biochemical pathway. However, the viability of the splenocyte cultures inhibited with D609 and αCD3 was lower than the thymocyte viability.

5.2.8. $^1\text{H-NMR}$ analysis of thymocytes and splenocytes incubated with the inhibitor D609 and αCD3 .

Thymocytes were cultured for 18-24 h in the presence of the culture supernatant of αCD3 . The inhibitor D609 ($6 \mu\text{g mL}^{-1}$) (Sections 2.6.2 and 5.2.5) was used to inhibit the effects of αCD3 . $^1\text{H-NMR}$ acquisition and analysis were performed as described in Section 2.6.4 (Figure 5.11). 1D $^1\text{H-NMR}$ spectra of αCD3 stimulated thymocytes (Figure 5.11B) show the characteristic mobile lipid resonances at 5.30 ppm ($-\text{HC}=\text{CH}-$),

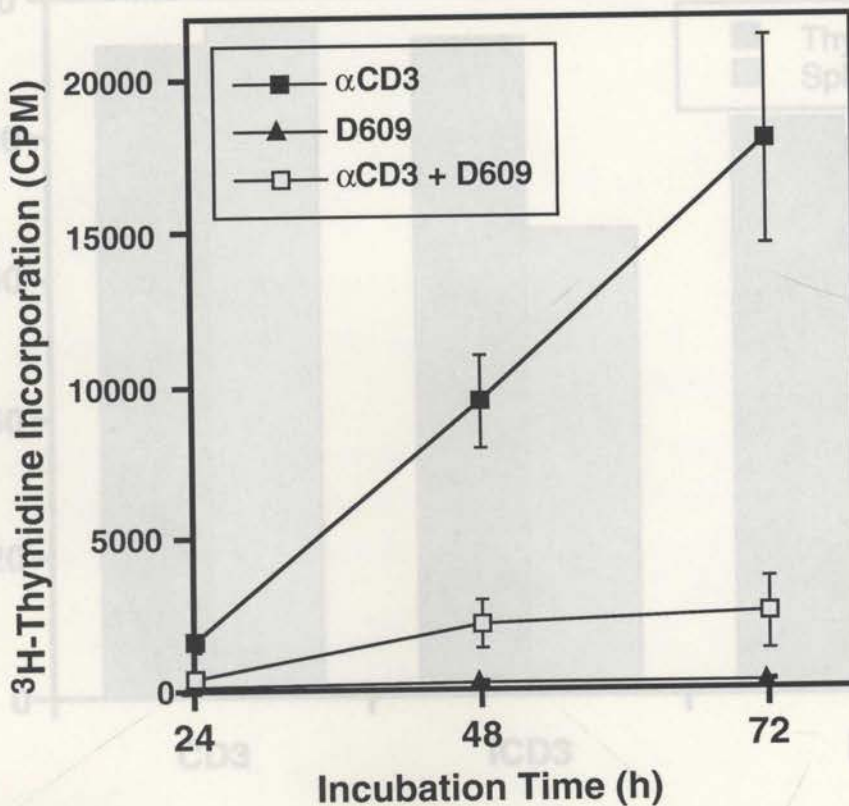


Figure 5.9. The effect of inhibitor D609 on proliferation of splenocytes stimulated using αCD3.

Splenocytes were incubated for 24-72 h with αCD3 culture supernatant (closed squares), the inhibitor D609 alone (triangles), and αCD3 and the inhibitor D609 simultaneously (open squares) (mean±SD, 12 replicates). ³H-Thymidine incorporation of splenocytes incubated for 24-72 h with (i) αCD3 culture supernatant, (ii) the inhibitor D609 alone and (iii) αCD3 and the inhibitor D609 (mean±SD, n = 12 replicates).

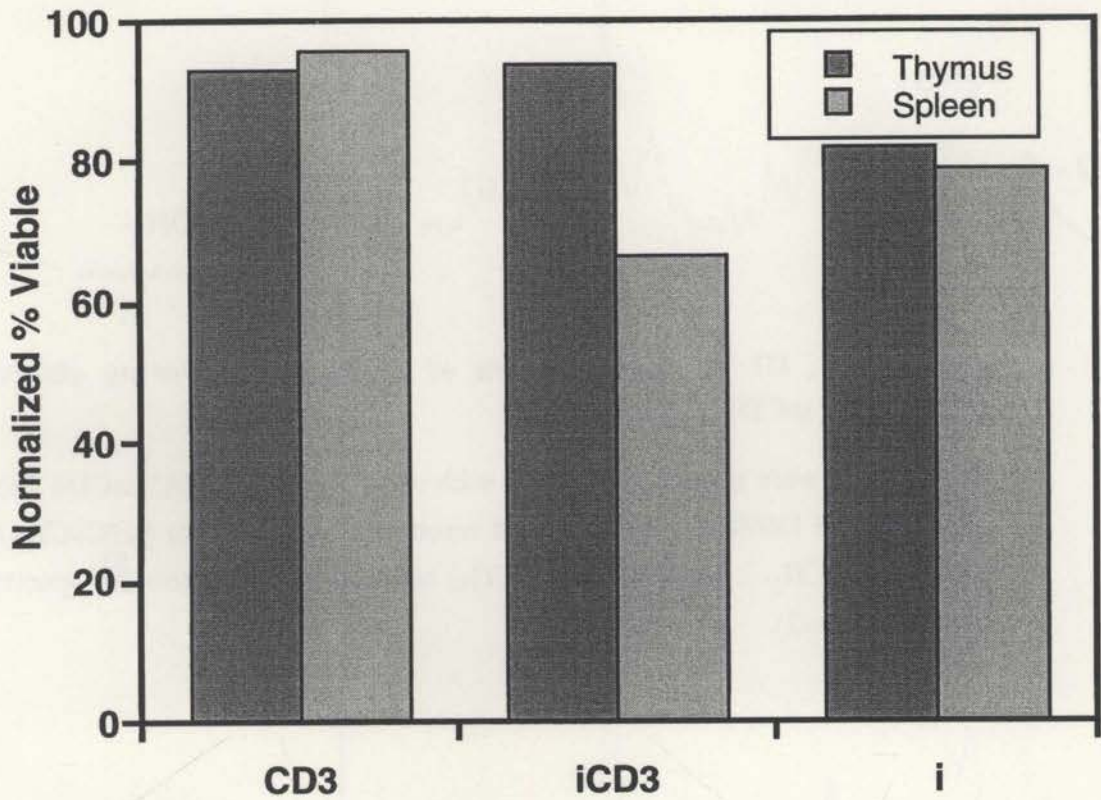


Figure 5.10. Cell viability of cultured thymocytes and splenocytes after α CD3 and D609 treatment.

Thymocyte cell suspensions were incubated for 18-24 h, and splenocyte cell suspensions were incubated for 48 h, with either α CD3 culture supernatant (CD3), α CD3 and the inhibitor D609 ($6 \mu\text{g mL}^{-1}$) (iCD3), the inhibitor D609 alone (i), or control culture supernatants (con), as described previously (Section 2.6.2). Cell viability was measured using the trypan blue dye exclusion method. The results are represented as a normalised percentage of the untreated control cell cultures (n=2).

Figure 5.11. 1D ^1H -NMR spectra of thymocytes showing effects of D609 on αCD3 -stimulation.

Thymocytes were treated for 18-24 h with either control Ab (A), αCD3 (B), or αCD3 and D609 (C). Mobile lipid resonances at 5.30 ppm ($-\text{HC}=\text{CH}-$), 1.30 ppm ($-\text{CH}_2-$), and 0.85 ppm ($-\text{CH}_3$) are shown. Representative spectra are shown (n=2).

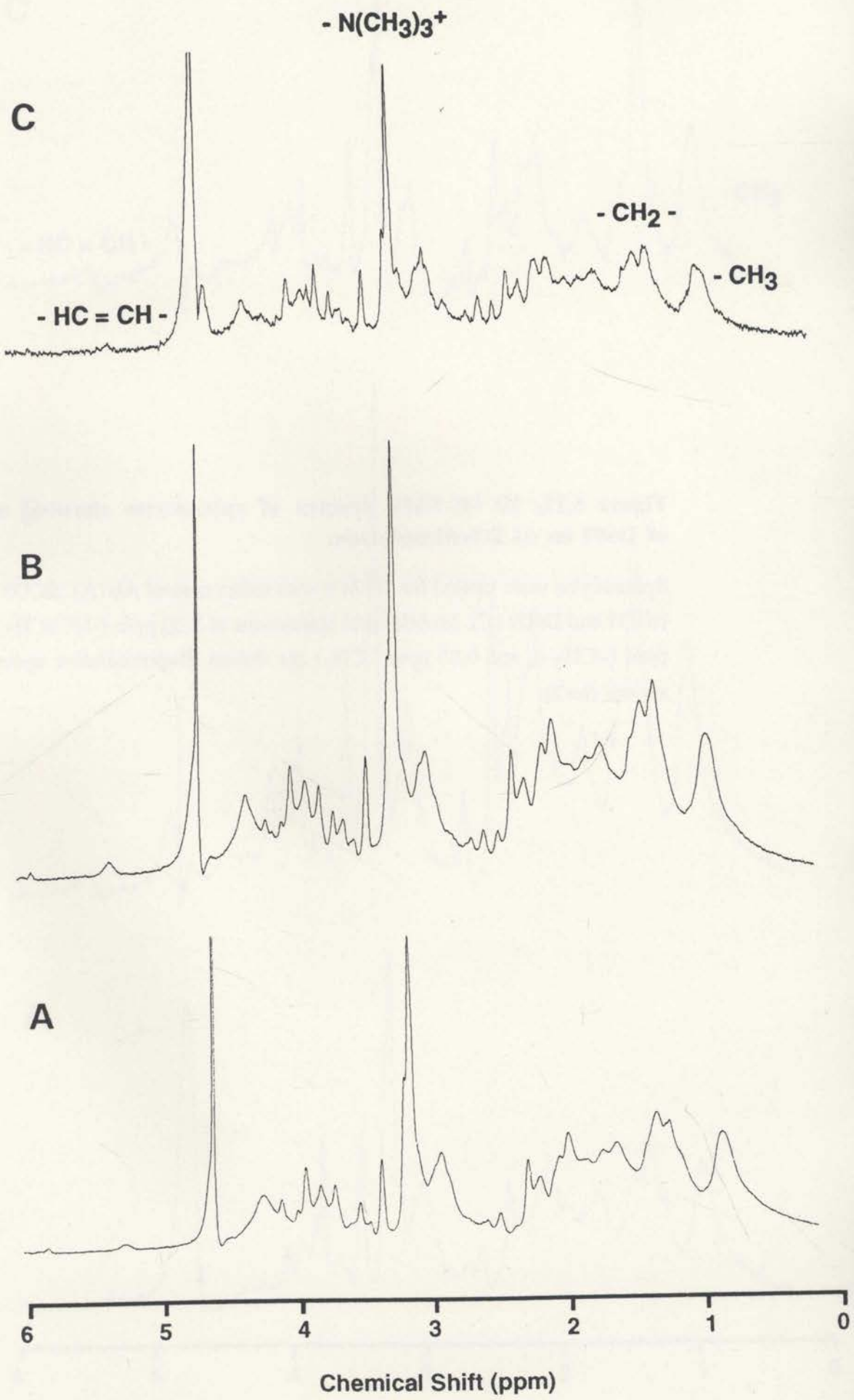
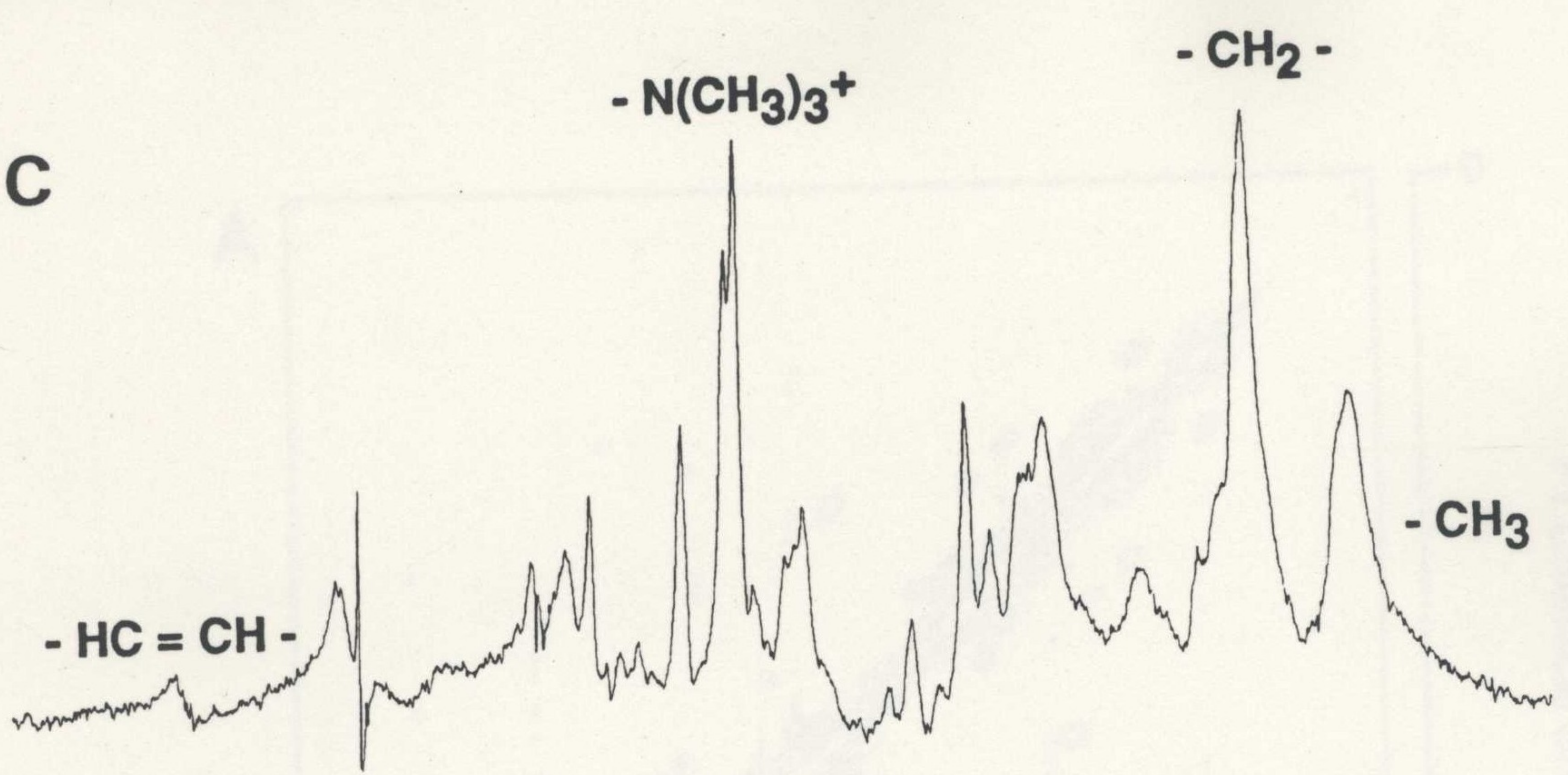


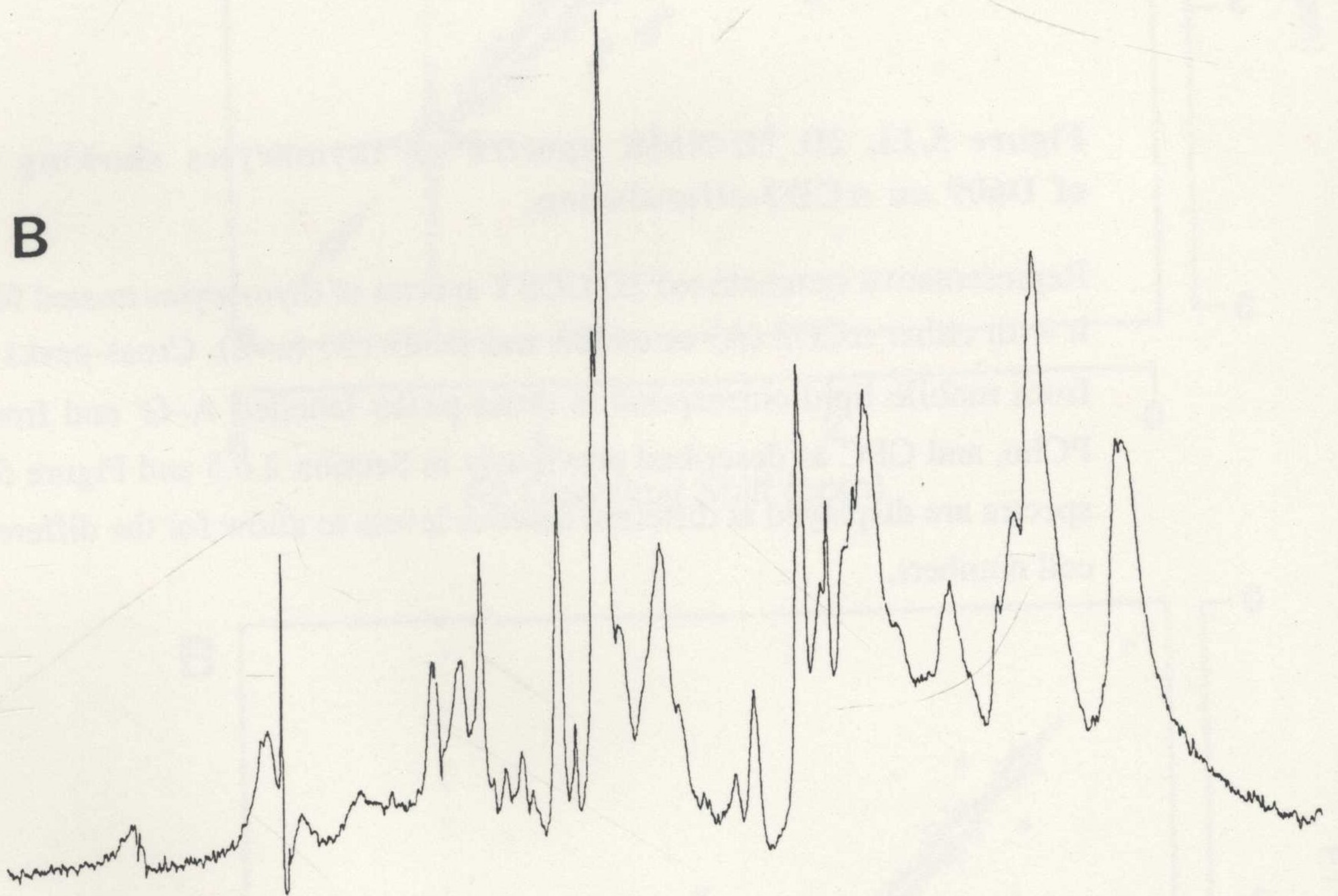
Figure 5.12. 1D ^1H -NMR spectra of splenocytes showing effects of D609 on αCD3 -stimulation.

Splenocytes were treated for 18-24 h with either control Ab (A), αCD3 (B) or αCD3 and D609 (C). Mobile lipid resonances at 5.30 ppm ($-\text{HC}=\text{CH}-$), 1.30 ppm ($-\text{CH}_2-$), and 0.85 ppm ($-\text{CH}_3$) are shown. Representative spectra are shown (n=2).

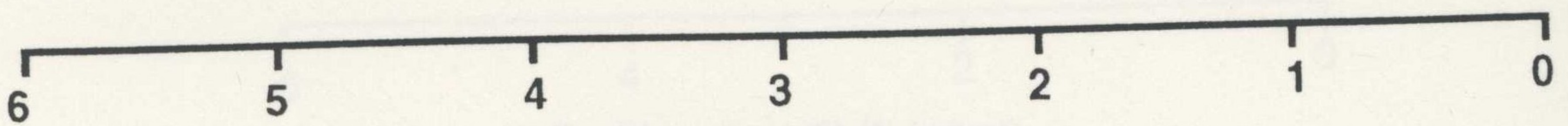
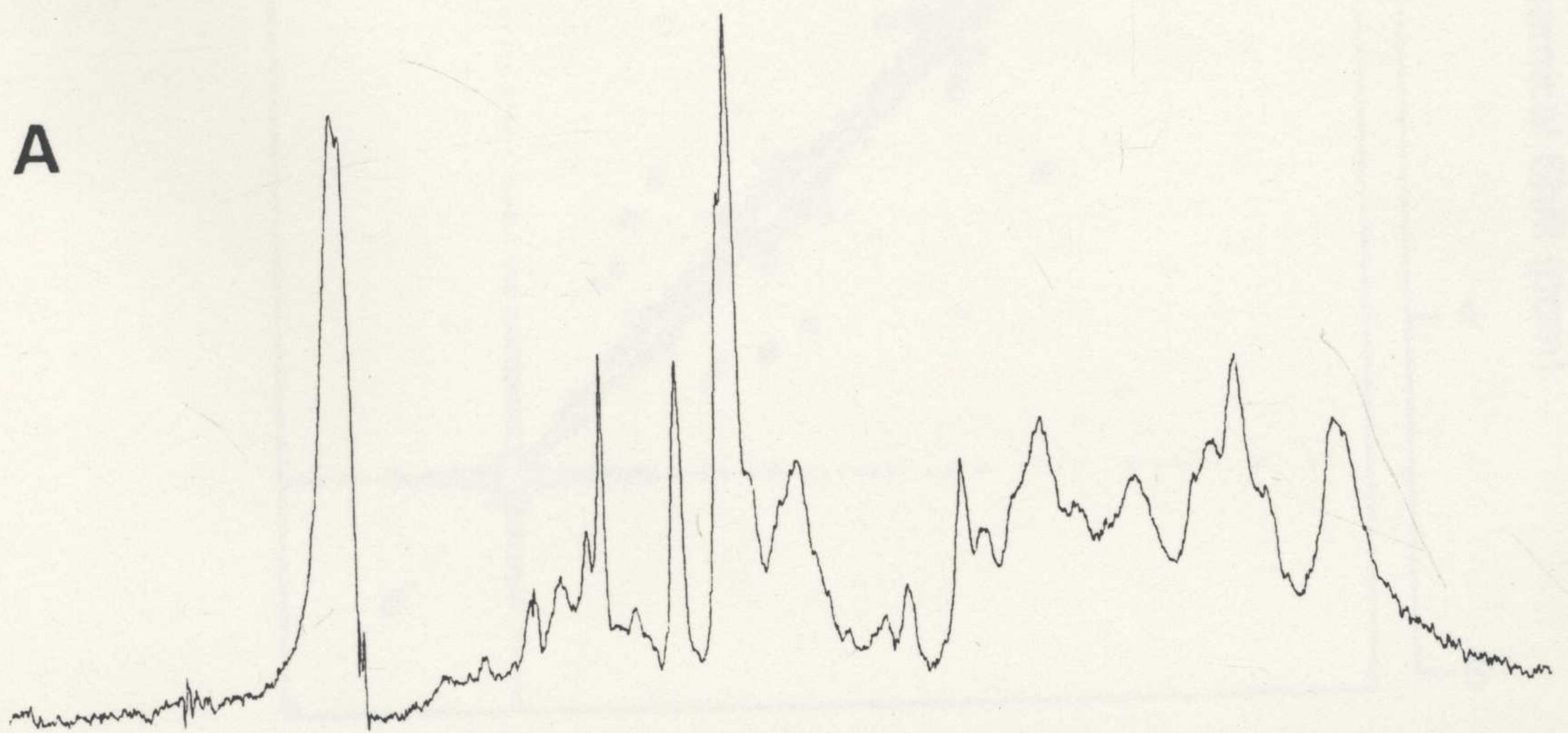
C



B



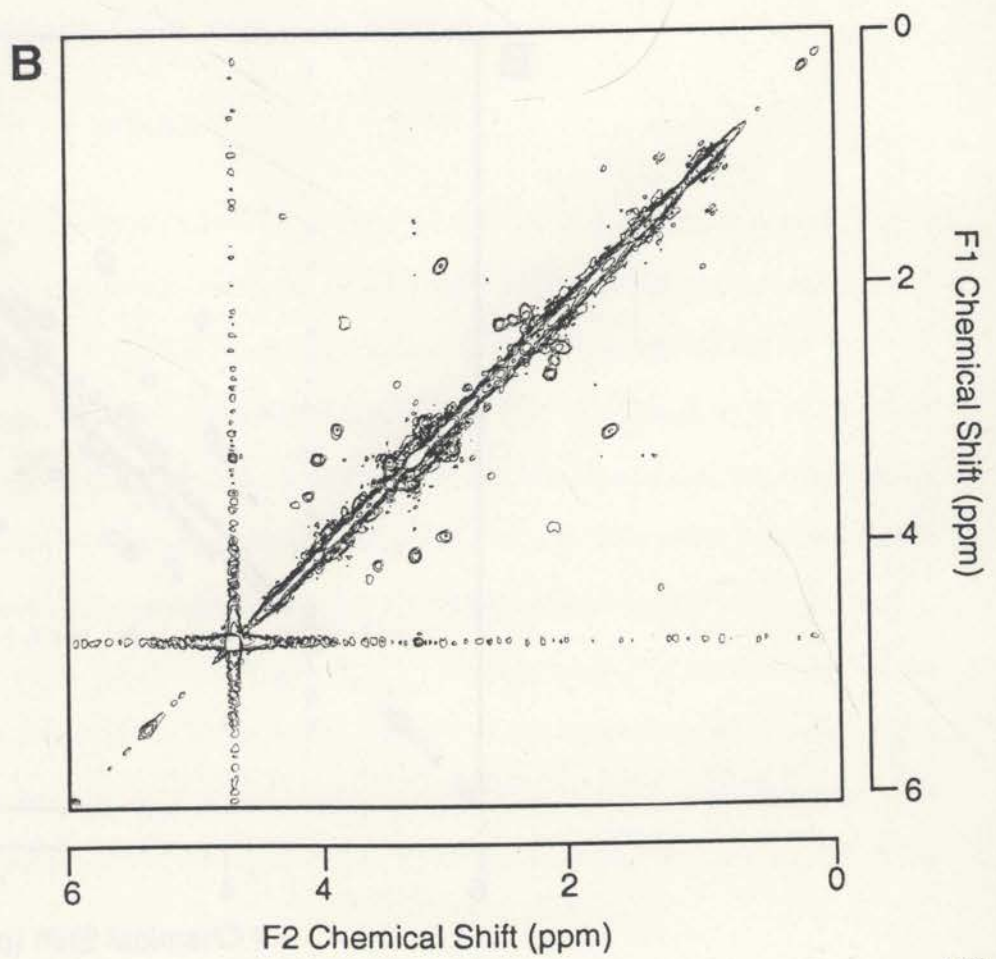
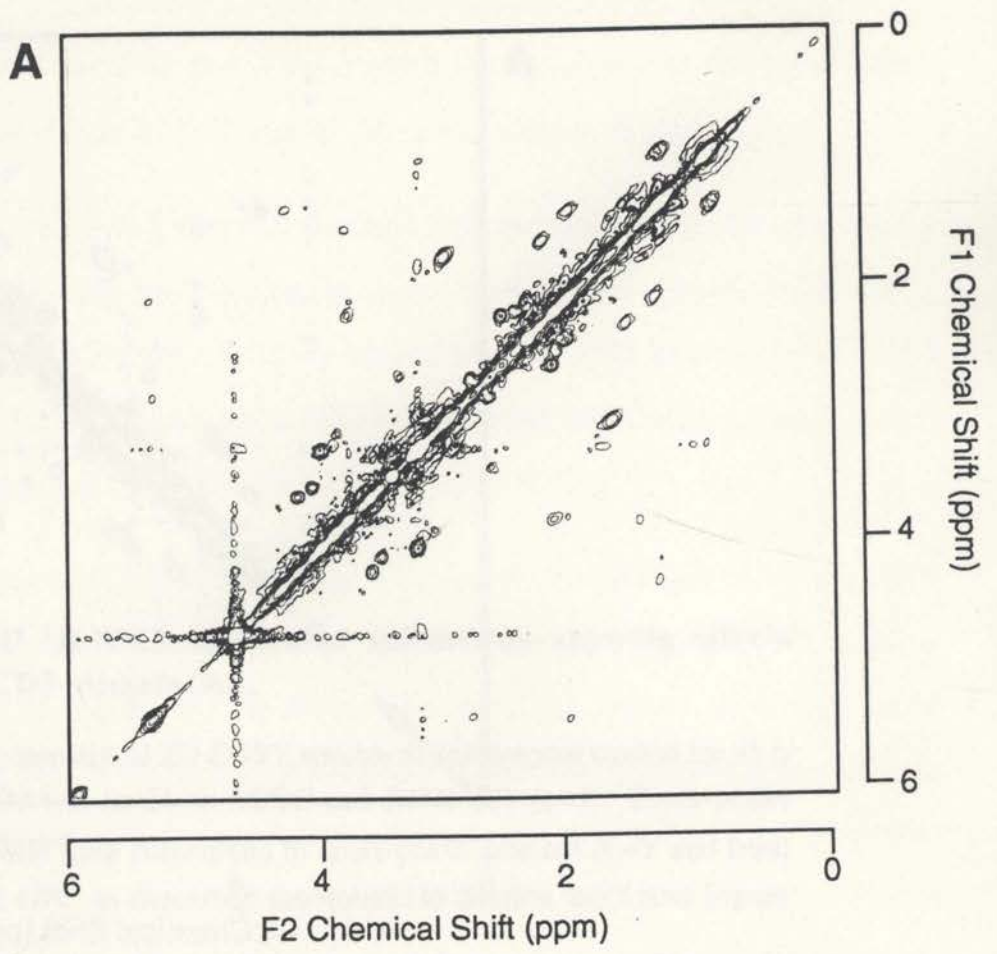
A

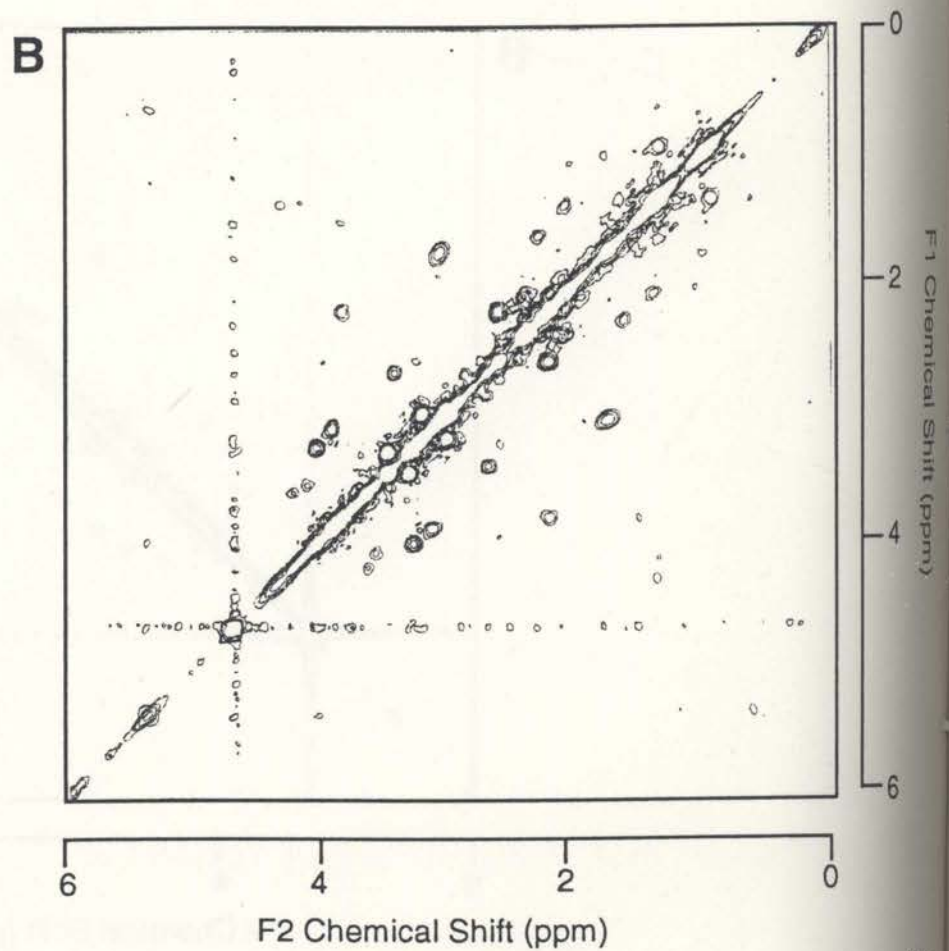
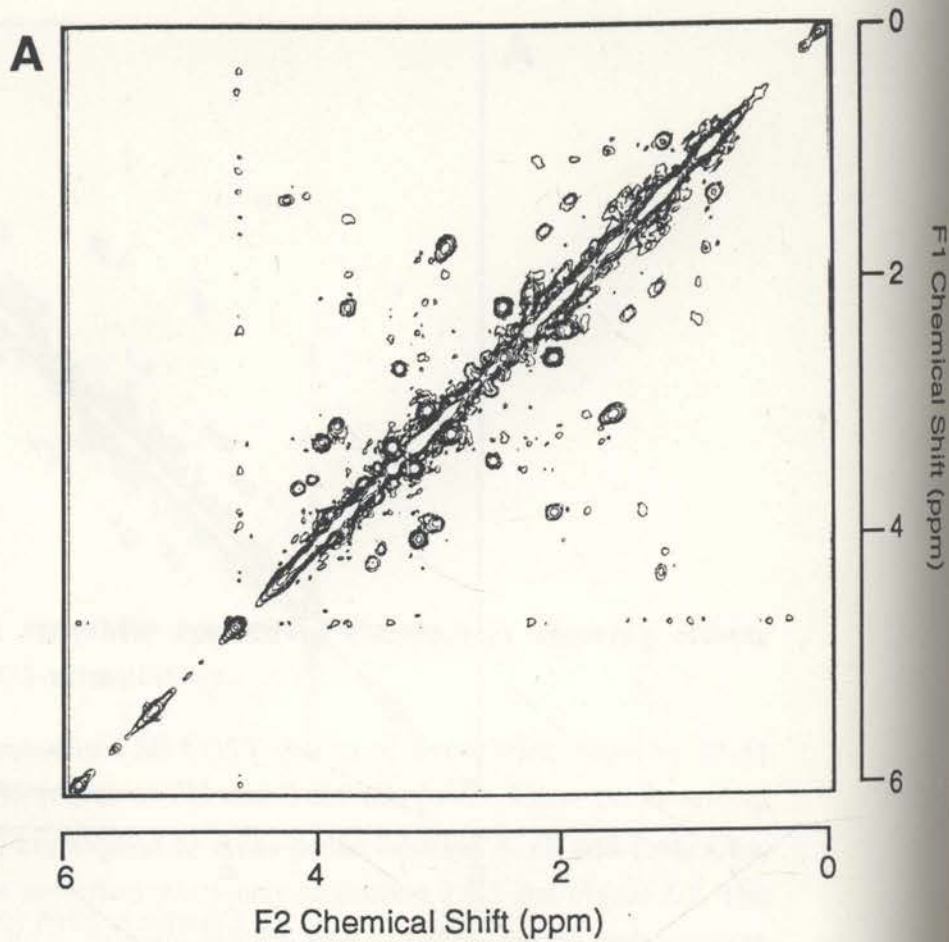


Chemical Shift (ppm)

Figure 5.13. 2D ^1H -NMR spectra of thymocytes showing effects of D609 on αCD3 -stimulation.

Representative symmetrised 2D COSY spectra of thymocytes treated for 18-24 h with either αCD3 (A) or αCD3 and D609 (B) ($n=2$). Cross-peaks arising from mobile lipid correspond to cross-peaks labelled A-G' and from Cho, PCho, and GPC as described previously in Section 2.6.5 and Figure 5.7. The spectra are displayed at different contour levels to allow for the differences in cell numbers.





1.30 ppm ($-\text{CH}_2-$), and 0.85 ppm ($-\text{CH}_3$) which are not present in D609 and αCD3 treated thymocytes (Figure 5.11 C) or in the Ab control cultures (Figure 5.11 A).

Splenocytes cultured for 48 h with αCD3 culture supernatant (Figure 5.12B) also display the characteristic mobile lipid resonances in the 1D $^1\text{H-NMR}$ spectra. However, in contrast to thymocytes, mobile lipid levels increase when the cells are treated with αCD3 and the inhibitor D609 (Figure 5.12C). Splenocytes treated with control antibody did not display the characteristic mobile lipid resonances (Figure 5.12A).

The decrease in the mobile lipid resonances in thymocytes treated with αCD3 and D609

Figure 5.14. 2D $^1\text{H-NMR}$ spectra of splenocytes showing effects of D609 on αCD3 -stimulation.

Representative symmetrised 2D COSY spectra of splenocytes treated for 48 h with either αCD3 (A) (n=3) or αCD3 and D609 (B) (n=1). Cross-peaks arising from mobile lipid correspond to cross-peaks labelled A–G' and from Cho, PCho, and GPC as described previously in Section 2.6.5 and Figure 5.7.

This was despite the inhibition of proliferation shown in Figures 5.8 and 5.9 at the concentration used in the $^1\text{H-NMR}$ experiments (Table 5.2).

5.2.9. Summary of results.

The results presented in this Chapter are summarised in Table 5.2. Stimulation of T cells using PMA and ionomycin resulted in the development of a $^1\text{H-NMR}$ -visible mobile lipid spectrum (Figure 5.6A), IL-2R α upregulation (Figure 5.2), decreases in Thy 1.2 expression (Figure 5.4), and cell proliferation (Table 5.1). Treatment with PMA alone resulted in similar changes except for a lack of proliferation. Ionomycin treatment alone resulted in some IL-2R α upregulation but did not result in proliferation, however, some mobile lipid cross-peaks were observed in the $^1\text{H-NMR}$ spectrum, which corresponded to unsaturated fatty acid acyl-chains (Figure 5.6C). The stimulation of thymocytes via the CD3/TCR complex using the MAb αCD3 resulted in the appearance of a mobile lipid spectrum but not in proliferation or IL-2R α upregulation. A GPC cross-peak was also observed in thymocytes treated with PMA, PMA and ionomycin, and αCD3 . This

1.30 ppm ($-\text{CH}_2-$), and 0.85 ppm ($-\text{CH}_3$) which are not present in D609 and αCD3 treated thymocytes (Figure 5.11 C) or in the Ab control cultures (Figure 5.11 A).

Splenocytes cultured for 48 h with αCD3 culture supernatant (Figure 5.12B) also display the characteristic mobile lipid resonances in the 1D $^1\text{H-NMR}$ spectra. However, in contrast to thymocytes, mobile lipid levels increase when the cells are treated with αCD3 and the inhibitor D609 (Figure 5.12C). Splenocytes treated with control antibody did not display the characteristic mobile lipid resonances (Figure 5.12A).

The decrease in the mobile lipid resonances in thymocytes treated with αCD3 and D609 (Figure 5.13B) compared to αCD3 treated control thymocytes (Figure 5.13A) is shown more clearly in the 2D $^1\text{H-NMR}$ spectra. These results show that D609 significantly reduces the mobile lipid generated in thymocytes stimulated with αCD3 . In contrast, D609 did not effectively reduce the generation of mobile lipid in αCD3 treated splenocytes (Figure 5.14B), compared to αCD3 treated control splenocytes (Figure 5.14A). This was despite the inhibition of proliferation shown in Figures 5.8 and 5.9 at the concentration used in the $^1\text{H-NMR}$ experiments (Table 5.2).

5.2.9. Summary of results.

The results presented in this Chapter are summarised in Table 5.2. Stimulation of T cells using PMA and ionomycin resulted in the development of a $^1\text{H-NMR}$ -visible mobile lipid spectrum (Figure 5.6A), IL-2R α upregulation (Figure 5.2), decreases in Thy 1.2 expression (Figure 5.4), and cell proliferation (Table 5.1). Treatment with PMA alone resulted in similar changes except for a lack of proliferation. Ionomycin treatment alone resulted in some IL-2R α upregulation but did not result in proliferation, however, some mobile lipid cross-peaks were observed in the $^1\text{H-NMR}$ spectrum, which corresponded to unsaturated fatty acid acyl-chains (Figure 5.6C). The stimulation of thymocytes via the CD3/TCR complex using the MAb αCD3 resulted in the appearance of a mobile lipid spectrum but not in proliferation or IL-2R α upregulation. A GPC cross-peak was also observed in thymocytes treated with PMA, PMA and ionomycin, and αCD3 . This

Source of cells	Treatment	Response				
		IL-2R α expression	THY 1.2 expression	Proliferation (^3H thymidine incorporation)	MNL	GPC peak present
Thymus	PMA	+	-	0	+	+
	Ion	+	-	0	+/0	0
	PMA/Ion	++	--	+	++	+
	αCD3	0	--	0	++	+
	D609 & αCD3	ND	ND	0	0	+
	Control	0	++	0	0	0
Spleen	αCD3	ND	ND	++	++	+
	PMA/Ion	ND	ND	++	++	+
	D609 & αCD3	ND	ND	0	++	+ at low contour level*

Table 5.2. Summary of results for Chapter 5.

+ = positive change; 0 = no change; - = negative change; ND = no data.

*Present in data processing (data not shown).

particular isoforms of PKC. Previous reports show that stimulation of human T cells with indicates that PC catabolism has also occurred in these treated cells. Thymocytes treated with ionomycin alone did not display a GPC cross-peak. Thy 1.2 expression was also used to further assess the activation status of the cells (Figure 5.4 and 5.5). All of the treatments, including the treatment with α CD3, resulted in the reduced expression of Thy 1.2. This also showed that the thymocytes had undergone a change in their activation status compared with the untreated control cells.

5.3. Discussion.

In this study, the activation status of T lymphocytes has been correlated with the presence of $^1\text{H-NMR}$ -visible mobile lipid. Previous studies have established an association between mobile lipid and fully activated immune cells. However, this is the first study that combines a range of stimuli to activate the T cells whilst also measuring the activation status of the cell using FCM. This has enabled more detailed examination of the activation requirements for the induction of NMR-visible mobile lipid.

5.3.1. Relationship between cell surface antigen expression and immune cell activation status.

IL-2R α expression and proliferation by stimulated thymocytes.

Treatment of thymocytes with PMA and ionomycin together, or PMA alone, resulted in a significant increase in the expression of the IL-2R α (Figures 5.2 and 5.3), whereas treatment with ionomycin alone resulted in a small change in IL-2R α expression. Previous studies have shown that the IL-2R α is inducible on mature thymocytes (ie., CD4 $^+$ or CD8 $^+$) or CD3 $^+$ double negative thymocytes using phorbol ester and A23187, a calcium ionophore (Boyer *et al.*, 1989). Phorbol ester treatment alone (Depper *et al.*, 1984), but not calcium ionophore, has also been shown to result in the upregulation of the IL-2R α in human peripheral blood lymphocytes (Szamel *et al.*, 1989). The results presented here are consistent with these reports. PMA stimulation, or PMA and ionomycin co-stimulation, of thymocytes is sufficient to induce the expression of IL-2R α . The expression of IL-2R α may be dependent upon the expression of

particular isoforms of PKC. Previous reports show that stimulation of human T cells with both phorbol ester and ionomycin causes elevation of the expression of the α , β and γ isoenzymes of PKC. Phorbol ester stimulation alone for 12 h or more resulted in an increased expression of β but not γ PKC, whereas ionomycin stimulation alone was either inactive or only marginally active in stimulating PKC expression (Altman *et al.*, 1992). It has also been shown previously in CTLL and other mouse and human T cell clones, the addition of phospholipase D (PLD) can result in the upregulation of IL-2R α expression (Cano *et al.*, 1992). PLD is also activated by PKC α and β isoforms in rat fibroblasts (Conricode *et al.*, 1994). These results provide an explanation for the increase in IL-2R α expression seen in the thymocytes stimulated with PMA or the enhanced expression shown with PMA and ionomycin.

In thymocytes stimulated with α CD3 antibody, IL-2R α expression is not increased. Activation via the TCR/CD3 complex results in the activation of different isoforms of PKC from PMA-mediated PKC activation of T cells (Chiaffarino *et al.*, 1994). Stimulation of human T cell lines with α CD3 resulted in the activation of the PKC ζ isoform (Nakanishi *et al.*, 1993; Keenan *et al.*, 1995). The upregulation of this isoform of PKC in addition to α or β may explain the lack of expression of the IL-2R α in these cells. Additional accessory stimulation may be required to activate the appropriate PKC isoforms for increased IL-2R α expression.

Cellular proliferation was not observed following α CD3 stimulation in this study. This is in agreement with other studies (Pierres *et al.*, 1990). Thymocytes did not proliferate in response to the treatment with PMA or ionomycin alone but did, however, proliferate in response to the combined stimulus of PMA and ionomycin (Table 5.1). These results are also confirmed by other studies (Harutoshi *et al.*, 1989; Kizaki *et al.*, 1989; Tadakuma *et al.*, 1990).

Collectively, these results suggest that the stimulation of thymocytes with PMA results in the progression of the cells into the G₁ phase of the cell cycle. Treatment with PMA and ionomycin stimulates the thymocytes to progress into the G₁ phase. This is followed by cell cycle progression and multiple circuits through the cell cycle resulting in proliferation.

Neutral lipids have been shown to be generated in the G₁ phase of the cell cycle (Pierres *et al.*, 1990; Jackowski, 1994; Terce *et al.*, 1994) which is consistent with the results found in this study. The stimulation of murine thymocytes with α CD3 MAb and ionomycin does not result in the expression of the IL-2R α or in cellular proliferation, which suggests that these cells have not progressed to G₁ phase of the cell cycle. However, mobile lipids were generated in these cells, which may be a result of the catabolism of PC via the activation of phospholipases involved in signal transduction.

Thy 1.2 expression in activated thymocytes

There was a reduction in peak intensity of thymocytes staining positively with the fluorescently labelled α Thy 1.2 antibody (Figure 5.4). This strongly suggest that in all of the treatments used PI-PLC was activated (Homans *et al.*, 1988). The greatest reduction in peak intensity resulted from α CD3 stimulation. Stimulation of T cells via the TCR/CD3 complex causes the direct activation of PI-PLC (Figures 1.8, 5.1). Therefore, the reduction of Thy 1.2 expression is consistent with this mode of stimulation. PMA and ionomycin treated thymocytes also showed a similar reduction in peak intensity of Thy 1.2 staining, which may have been due to the influence of PKC and Ca²⁺ on PI-PLC activity (Barrit, 1992). These results show that all of the thymocytes had received an activating signal even though not all of the treatments resulted in proliferation or IL-2R α expression.

5.3.2. The role of the PC cycle in the generation of the mobile lipid spectrum and its relationship to signalling in T lymphocytes.

In thymocytes stimulated with PMA and ionomycin, cellular proliferation occurs (Table 5.1). This involves both the degradation and the biosynthesis of PC to fuel the expanding membrane, and would involve repeated PC cycles (Pelech & Vance, 1989). This explains the appearance of the mobile lipid in proliferating splenocytes, but doesn't explain the appearance of mobile lipid in α CD3-stimulated thymocytes, which do not proliferate.

The PC cycle is responsible for the synthesis and catabolism of PC in the cell (Figure 5.1). It consists of a network of enzyme-catalysed pathways that, when activated, result

in PC turnover and the generation of neutral lipids (Pelech & Vance, 1989; Tronchere *et al.*, 1994). Further to this, PC cycling has been shown to be associated with the cell cycle (Jackowski, 1994). In fact, PC catabolism may be essential for cell cycle progression (Terce *et al.*, 1994). The exact relationship between the PC cycle and cellular signalling is not clearly defined, but the enzymatic pathways and their relationship with PKC activation is clear (Pelech & Vance, 1989; Nishizuka, 1992). The kinetics of activation of signalling phospholipases range from seconds to hours after an initial stimulus (Liscovitch, 1992).

The cross-peak corresponding to GPC is present in thymocytes stimulated with PMA, PMA and ionomycin, or α CD3, but does not appear after stimulation by ionomycin alone or in control cultures (Figure 5.7). This suggests that PC turnover has occurred. The presence of GPC is also associated with the appearance of the mobile lipid in these treated cells. GPC is ultimately a product of phospholipase A₂ hydrolysis of PC, which also produces lysophosphatidylcholine, free fatty acids and may contribute to the generation of DAG (Nishizuka, 1992). The addition of PLA₂ to cells can potentiate the cellular response to diacylglycerol and ionomycin (Asaoka *et al.*, 1991). It is suggested that PC-specific PLC and PLA₂ act in synergy to regulate differentiation and proliferation in T lymphocytes (Asaoka *et al.*, 1991; Szamel & Resch, 1995). Lysophosphatidylcholine has been shown to enhance both IL-2R α expression and thymidine incorporation in human T lymphocytes induced by phorbol esters and ionomycin (Asaoka *et al.*, 1991). The lysophosphatidylcholine accumulates in a time-dependent manner after the stimulation of T lymphocytes with antigen (Nishizuka, 1992). LysoPC can be further degraded to GPC or, in the presence of DAG, can act as an additional second messenger for long-term PKC stimulation (Szamel & Resch, 1995).

The enzymes PLA₂ and LAT are believed to be associated with the TCR/CD3 complex in T cells (Figure 5.1). Stimulation via the TCR/CD3 complex results in the activation of LAT, which incorporates unsaturated fatty acids primarily into PC (Szamel *et al.*, 1989). Subsequent hydrolysis by PLC results in the formation of DAG for the activation of PKC. PC-PLC degradation in signalling occurs several hours after the initial mitogenic

stimulation (Liscovitch, 1992). The mobile lipid has been shown to be detectable in PMA and ionomycin-treated thymocytes using $^1\text{H-NMR}$ after 6 h of stimulation (Dingley *et al.*, 1992). This would be consistent with the degradation of PC which occurs in the G_1 phase of the cell cycle in the first 12 h after stimulation (Jackowski, 1994). Therefore, it is possible that the development of the mobile lipid after stimulation of thymocytes via the TCR/CD3 complex (Figure 5.7F) may be a result of the activation of LAT, PLA_2 , and PLC. The mobile lipid cross-peaks generated in αCD3 stimulated thymocytes are consistent with the generation of unsaturated fatty acids, which may act as a storage pool for TAG.

Ionomycin is thought to potentiate the activity of PKC, but not directly stimulate its activation (Nishizuka, 1992). Ionomycin stimulation alone may potentiate the activity of phospholipases involved in the catabolism of PC, but might not have an effect on the enzymes responsible for the incorporation of unsaturated fatty acids into membrane phospholipids. This may be due to the inability of this agent on its own to activate PKC isoforms (Altman *et al.*, 1992) which are known to influence the activity of PLA_2 , PLC, and PLD (Nishizuka, 1992). This may explain the generation of fatty acids in thymocytes stimulated by ionomycin alone (Figure 5.7). The absence of the GPC cross-peak and mobile lipid cross-peaks G', C, and D, indicate that PLA_2 has not been activated. They also indicate that LAT activity has not been stimulated because the fatty acids generated do not appear to be unsaturated.

5.3.3. Inhibition of the PC-specific PLC with D609.

In this study, D609 was found to block the accumulation of mobile lipids in thymocytes stimulated with soluble αCD3 . D609 specifically inhibits the activity of PC-specific PLC and has been reported to block the proliferation of CTLL cells (Mueller-Decker *et al.*, 1988; Mueller-Decker, 1989; Antonysamy *et al.*, 1995). These results therefore suggest that the accumulation of mobile lipid in αCD3 -stimulated thymocytes results from PC catabolism via the action of PC-specific PLC (Figure 5.12 and 5.13). The reduction in the intensity of the Cho peak (1D spectrum) and the PCho peak (2D spectrum), compared to

the α CD3 stimulated control cells, indicates that this catabolic pathway has been inhibited. The disappearance of the GPC peak in the α CD3-stimulated thymocytes treated with D609 indicates that the activity of PLA₂ has been affected. This supports the proposal that PLA₂ and PC-specific PLC may act in synergy (Asaoka *et al.*, 1991; Szamel & Resch, 1995). These results support previous results suggesting that PC catabolism plays a role in the generation of the ¹H-NMR-visible mobile lipid in cultured fibroblasts (Delikatny *et al.*, 1996a).

In α CD3-treated splenocyte cultures, the generation of the mobile lipid was not inhibited by treatment with D609, in contrast to thymocytes (Figure 5.12). The proliferation of α CD3-stimulated splenocytes was inhibited at 24, 48 and 72 h after stimulation at the concentration of D609 used in the ¹H-NMR experiments (Figure 5.8 and 5.9). A decrease in the peak corresponding to the choline head group was evident at 3.25 ppm in the 1D spectrum from the inhibited thymocytes (Figure 5.11) and splenocytes (Figure 5.12) compared to the α CD3-stimulated control. This indicated that the inhibitor had reduced the level of generation of the catabolic product PCho from PC. In α CD3-treated splenocytes the cells are stimulated to proliferate. This involves the stimulation of the PC cycle, resulting in the biosynthesis and catabolism of PC. Mobile lipid can be generated by a number of enzyme-catalysed pathways which, in splenocytes, may be activated in addition to the catabolism of PC-specific PLC. The stimulation of the splenocyte cultures with α CD3 antibody together with the additional co-stimulation via other interactions between accessory cells and T cells (Figure 1.7) may result in receptor-mediated activation of PLD (Pelech & Vance, 1989; Exton, 1990; Nishizuka, 1992).

Another contribution to the generation of the mobile lipid in the splenocyte cultures may arise from the accessory cells present in the splenocyte cultures. These include macrophages and B cells, which have also been shown to develop ¹H-NMR-visible mobile lipid upon activation (Holmes *et al.*, 1990; King *et al.*, 1991). In macrophages activated using lipopolysaccharide, PC turnover has also been shown to play a role in activation (Grove *et al.*, 1990). The inhibition of PC catabolism via the PLC mechanism may prevent the cells from progressing beyond the G₁ phase of the cell cycle. The

PC-specific PLC has been shown to be important for cell cycle progression beyond the G₁ phase (Terce *et al.*, 1994). This would result in the continued catabolism of PC, which may result in mobile lipid accumulation in the splenocytes stimulated with α CD3 and inhibited with D609.

Apoptosis?

It has been shown that the stimulation of unfractionated thymocytes with α CD3 (Smith *et al.*, 1989; Shi *et al.*, 1991) or PMA or ionomycin alone (Harutoshi *et al.*, 1989), can cause thymocytes to apoptose. It has also been reported, however, that the thymocytes most affected by these treatments are immature thymocytes (Smith *et al.*, 1989). Unfractionated murine thymocytes stimulated with phorbol ester or Ca²⁺-ionophore for 18-24 h resulted in 70%-80% fragmentation of the cellular DNA, leading to cell death. These cells were shown using FCM to consist primarily of immature CD4⁺CD8⁺ double positive cells with a small portion of CD4-CD8⁺ single positive mature cells. In unfractionated thymocytes stimulated with α CD3 antibody for 18-24 h, apoptosis was induced in the subpopulation of CD4⁺CD8⁺ cells, resulting in approximately 60% DNA fragmentation (Tadakuma *et al.*, 1990).

5.3.4. Conclusions.

Although the thymocytes used in these studies were unfractionated, the cells responding to the treatments would have been similar to mature peripheral T cells. All cell preparations for ¹H-NMR analysis were separated over a Ficoll-plaque gradient (Section 2.6.2) to remove non-viable cells. All cells analysed by FCM were gated to only include viable cells in the analysis (Section 2.5.2). The transmembrane signalling via the TCR/CD3 complex in mature thymocytes (ie. CD4⁺ or CD8⁺ single positive cells) is similar to mature peripheral T cells (Sancho *et al.*, 1992). Therefore, the described results using α CD3 stimulation are likely to reflect the response of peripheral T cells (Table 5.2). Therefore, it is not clear from these observations whether apoptosis may be involved.

generation of the ¹H-NMR-detectable mobile lipid spectrum.

Mature thymocytes stimulated with α CD3 may be induced to apoptose via the induction of the expression of Fas and its ligand Fas-L, which is induced in activated mature T cells. Binding of T cells to each other may therefore induce apoptosis (Crispe, 1994).

Apoptotic cells have been shown to have many of the biochemical characteristics of G₁ phase cells (Pardey & Wang, 1995). This may explain the results shown with the inhibitor D609 in both splenocytes and thymocytes. Activated splenocytes have been shown to be the only tissue to express both Fas and its ligand Fas-L. Antigen-presenting cells have been shown to express Fas-L (Crispe, 1994). This would induce apoptosis in other activated splenic T cells and may account for the accumulation of mobile lipid in the D609-treated, growth-arrested splenocytes. This may also account for the lower viability in splenocyte cultures treated with D609 and α CD3. However, as these cells were routinely separated using Ficoll to separate viable from dead cells, the poor viability of the cells alone would not have contributed to the mobile lipid detected in the ¹H-NMR. In thymocytes, the stimulation of the cells with α CD3 alone may be inducing the cells to undergo apoptosis. The inhibition of the stimulating signal via D609 may prevent the induction of this apoptosis. This may explain the accumulation of the mobile lipid in the α CD3 treated thymocytes, and therefore the inhibition of the mobile lipid production in the D609-treated thymocyte cultures, because by inhibiting the signal stimulated via α CD3, the apoptotic signal may therefore be inhibited.

5.3.4. Conclusions.

It is clear from the results presented in this Chapter that the mobile lipid can be generated in thymocytes and splenocytes via the stimulation of cells with the α CD3 antibody, PMA alone, and PMA and ionomycin. The results in this Chapter have shown that the mobile lipid can be generated by the stimulation of PC catabolism via receptor mediated signalling mechanisms. This is consistent with the interactions between receptor mediated signalling mechanisms and the PC cycle. A relationship between the PC cycle and the cell cycle has been established which can affect the activation status of the cell. All of these mechanisms are interrelated and all have an important role to play in immune cell activation and the generation of the ¹H-NMR-detectable mobile lipid spectrum.

Chapter 6.

$^1\text{H-NMR}$ and FCM studies of immune cell activation in an *in vivo* sheep model.

6.1. Introduction.

It has been postulated in the previous Chapters that the mobile lipid detected using $^1\text{H-NMR}$ is generated by phosphatidylcholine cycling, and is associated with immune cell activation and cell cycle status *in vitro* (Veale *et al.*, 1996). There have been a small number of similar studies of activated immune cells after antigen challenge *in vivo* using $^1\text{H-NMR}$ (King *et al.*, 1991; Mountford *et al.*, 1993; May *et al.*, 1994). Previous studies have used $^1\text{H-NMR}$ to investigate immune cell activation at selected time points after antigenic stimulation. However, this will be the first to use FCM to correlate cell surface changes, associated with immune cell activation, with the development of the $^1\text{H-NMR}$ mobile lipid spectrum at various time periods after immune cell activation *in vivo*. Both FCM and $^1\text{H-NMR}$ spectroscopy were used to monitor the immune response in cells from the afferent lymph, efferent lymph and lymph nodes of BCG-primed (Bacille-Calmette-Guerin-primed) sheep, before and after *in vivo* secondary antigen challenge using PPD (purified protein derivative, from BCG).

The cellular compositions of afferent and efferent lymph are different (Hall, 1967). The afferent lymph contains 5-10 fold fewer cells than efferent lymph. The afferent lymph contains predominantly T cells, a few B cells and can contain up to 10% dendritic cells. Efferent lymph, on the other hand, contains a much greater proportion of both B and T cells (Hopkins *et al.*, 1985; Hein *et al.*, 1987; Kimpton *et al.*, 1990; MacKay *et al.*, 1990). In normal, non-immunised sheep there are distinct differences in the distribution of lymphocyte subsets, such as CD4, CD8 and $\gamma\delta$ T cells, in the afferent and efferent lymph and the lymph node (MacKay *et al.*, 1988b; Kimpton *et al.*, 1990). This becomes even more evident in the draining peripheral lymph node after antigen stimulation

(Kimpton *et al.*, 1990; MacKay *et al.*, 1992a). Challenge of previously immunised animals with specific antigen in the skin results in the activation and migration of a variety of immune cells, including T cells and antigen presenting dendritic cells, from the tissue area via the afferent draining lymphatics to the local lymph node (Figures 1.3, 1.4). An increase in the total cell input and output from an antigen-challenged lymph node is also expected after antigen challenge (Hall & Morris, 1965a; Hall, 1967; Hay & Hobbs, 1977). Afferent lymph veiled cells or dendritic cells present antigen to T cells which have migrated from the tissue area into the draining lymph node (Bujdoso *et al.*, 1989a; McKeever *et al.*, 1992). This results in an increase in the total cell input to the lymph node via the afferent lymph vessel after antigen challenge. There is a simultaneous "shut-down" of lymph node cell output to the efferent lymphatic vessels, which occurs for the first 12-24 h after antigenic challenge (Hall & Morris, 1963; Hall & Morris, 1965a; Hall, 1967).

A number of cell surface changes occur in immune cells after antigenic challenge. Animals initially encountering an immunising antigen develop memory cells as a result of antigen-specific activation. Both activated and memory T cells in immune animals show increased expression of the surface adhesion molecules CD2, LFA-3, MHC II and LFA-1. These molecules enhance cell-cell interaction, which are important for passage of T cells between the endothelial cells into the area of antigen challenge and then to the lymph node (Sanders *et al.*, 1988a; Sanders *et al.*, 1989; MacKay *et al.*, 1990). Adhesion molecules also enhance the responsiveness of T cells to activation (Byrne *et al.*, 1988; Sanders *et al.*, 1988b; Sanders *et al.*, 1989; MacKay, 1991). Leucocyte common antigen (CD45) has been recognised as a protein tyrosine phosphatase which is necessary for signalling via the T cell receptor (Pingel & Thomas, 1989; Section 1.4.6). The expression of CD45R, a CD45 isoform (Dutia *et al.*, 1993), can be used to characterise T cell phenotypes (Dianzani *et al.*, 1990). The expression of CD45R has been shown to display different patterns of staining in afferent and efferent lymph (MacKay *et al.*, 1988b). It was therefore postulated that this may indicate the distribution of memory T cells. Naive cells express the CD45R isoform, while memory cells show a reduced expression of this

isoform (MacKay *et al.*, 1990). Therefore, expression levels of CD45R on immune cells may be used as an indication of an immune response.

In this study, however, mixed populations of afferent and efferent cells are used, rather than isolated T cells. Therefore, differences in staining for sheep CD45R may also reflect the different tissue distribution of the types of immune cells found in the afferent and efferent lymph.

Cells with increased expression of adhesion molecules may display a different pattern of recirculation through the lymph node. A higher proportion of memory-type immune cells are found in the tissue area and migrating via the afferent lymphatic vessels to the lymph node. Efferent lymph has a higher proportion of naive cells which have not previously encountered antigen. Naive cells are postulated to migrate into the lymph node via the high endothelial venules from the blood vessels (Figure 1.4). In this study, changes in these cell surface molecules were assessed both before and after antigen challenge, because the proportions of cells expressing the different cell surface molecules may change over time after antigen challenge.

The immune response to antigen challenge was monitored by collecting and isolating cells from the afferent lymph, efferent lymph and lymph nodes of BCG-primed sheep. Before and after secondary antigen challenge using PPD, lymph and lymph nodes were collected. Cells from efferent lymph of naive sheep were also taken. By investigating the $^1\text{H-NMR}$ -detectable mobile lipid associated with immune cells activated specifically with antigen *in vivo*, the possibility of *in vitro* cell culture artefact affecting cellular activation was obviated. This study was performed in sheep (outbred Merino cross) because they are large enough to enable direct cannulation of the afferent and efferent lymph vessels. This cannot be easily performed in smaller animal models. The large number of cells required for $^1\text{H-NMR}$ analysis (King & Kuchel, 1994; Appendix 1) can be collected from a large animal without further culturing. FCM was used to monitor changes in cell phenotype after antigen challenge in order to: (i) determine the changes in expression of cell surface molecules associated with antigen challenge (Kimpton *et al.*, 1990; MacKay

et al., 1992a) to characterise and identify the types of cells present in the afferent and efferent lymph and lymph node, and (ii) to correlate these changes with the occurrence of the $^1\text{H-NMR}$ -detectable mobile lipid spectrum.

It should also be noted that experiments on large animals were logistically difficult to perform, due to the limitations of housing of the animals, and the physical limitations of performing complex cannulation procedures on a large number of animals. Consequently, the numbers of animals used in these studies is small, and meaningful statistical analyses were therefore not possible. Time kinetic studies made using FCM and $^1\text{H-NMR}$ are represented for individual sheep responses in order to enable evaluation of the variation in the responses from these outbred animals.

6.2. Results.

6.2.1. Total cells collected per hour from afferent and efferent vessels of prefemoral lymph nodes of antigen-challenged sheep.

Sheep were immunised with BCG and boosted with PPD prior to surgery to cannulate the prefemoral lymph nodes. The BCG-primed sheep were challenged with PPD 24-48 h after surgery and lymph was collected before and after antigen challenge (Sections 2.7.2 and 2.7.3). The total number of cells collected per hour from the afferent and efferent lymph vessels of the prefemoral lymph nodes were determined using viable cell counting (Figure 6.1). The total input collected from the afferent vessel increased approximately 1.5-3-fold in the first 24 h after antigen challenge (Figure 6.1A). These numbers eventually declined but were still above control levels 72 hours after challenge. In contrast, the total cell output from the lymph node via the efferent lymph vessel tended to decrease immediately after antigen challenge and then increased by 3-6-fold between 24 and 72 h post-antigen challenge. The number of cells then decreased after antigen challenge. These results show an increased migration of cells from the draining tissue area of the antigen challenge via the afferent lymphatic vessels to the lymph node, while early decreased cellular output from the lymph node via the efferent vessels, or "shut-down", is observed in the efferent lymphatics. The increase in the cellular output

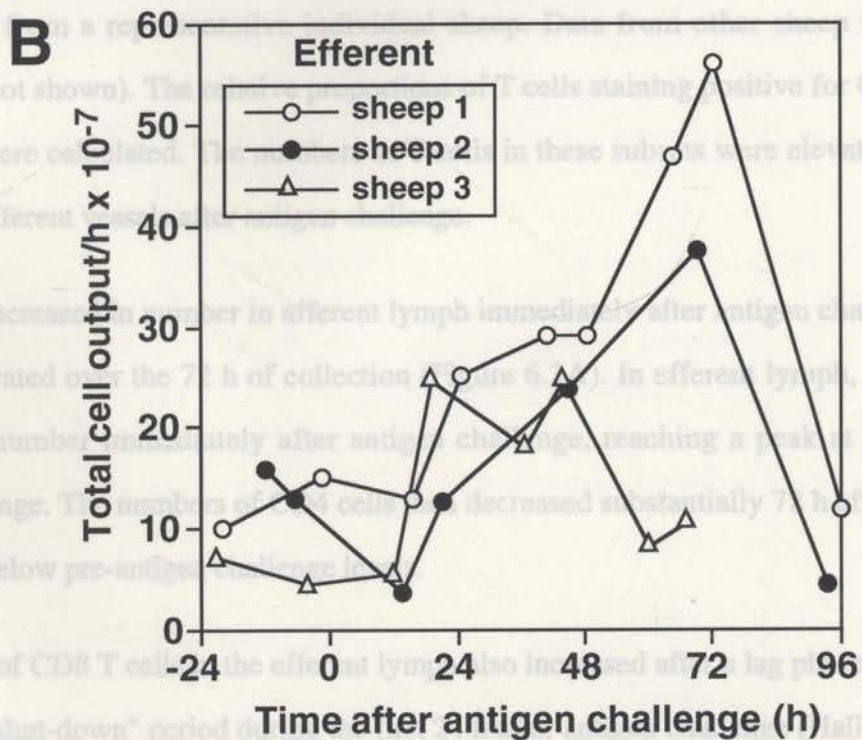
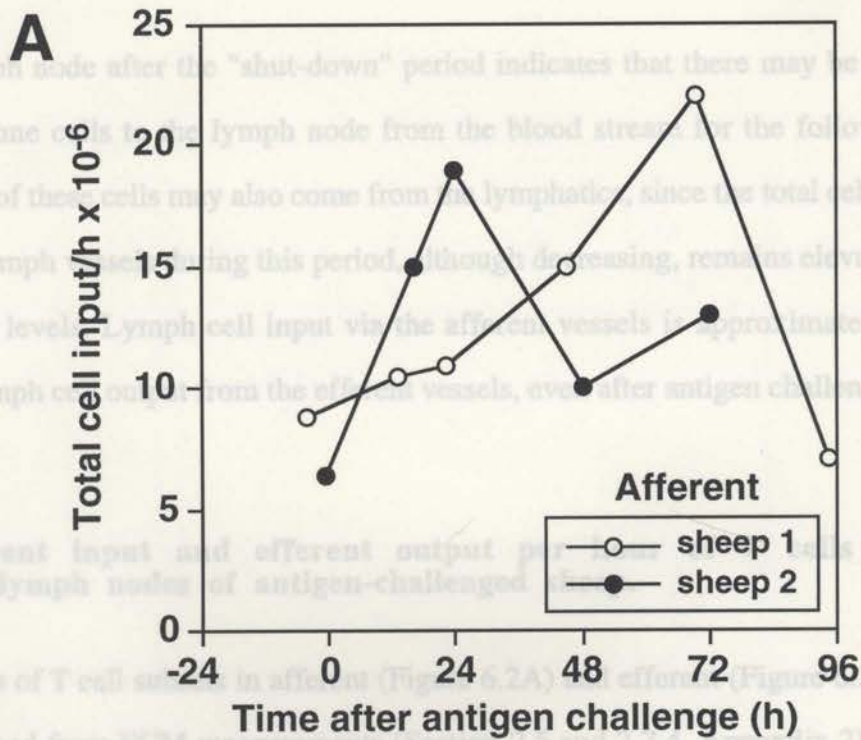


Figure 6.1. Total cell output from the afferent and efferent lymph of antigen-challenged sheep.

Plots of the total lymph cells collected per hour from the afferent (A, $n = 2$) and efferent (B, $n = 3$) vessel of the prefemoral lymph node of a BCG-primed sheep before and after antigen challenge (at time zero) using PPD. Cells were counted on a haemocytometer.

from the lymph node after the "shut-down" period indicates that there may be increased input of immune cells to the lymph node from the blood stream for the following 48 h period. Some of these cells may also come from the lymphatics, since the total cell input via the afferent lymph vessels during this period, although decreasing, remains elevated above pre-challenge levels. Lymph cell input via the afferent vessels is approximately 10-fold lower than lymph cell output from the efferent vessels, even after antigen challenge (Figure 6.1).

6.2.2. Afferent input and efferent output per hour of T cells through prefemoral lymph nodes of antigen-challenged sheep.

Total numbers of T cell subsets in afferent (Figure 6.2A) and efferent (Figure 6.2B) lymph were determined from FCM measurements (Section 2.5 and 2.7.4, Appendix 2). The data presented are from a representative individual sheep. Data from other sheep were very similar (data not shown). The relative proportions of T cells staining positive for CD4, CD8 and $\gamma\delta$ TCR were calculated. The numbers of T cells in these subsets were elevated in both afferent and efferent vessels after antigen challenge.

CD4 T cells increased in number in afferent lymph immediately after antigen challenge and remained elevated over the 72 h of collection (Figure 6.2A). In efferent lymph, CD4 cells increased in number immediately after antigen challenge, reaching a peak at 72 h after antigen challenge. The numbers of CD4 cells then decreased substantially 72 h after antigen challenge to below pre-antigen challenge levels.

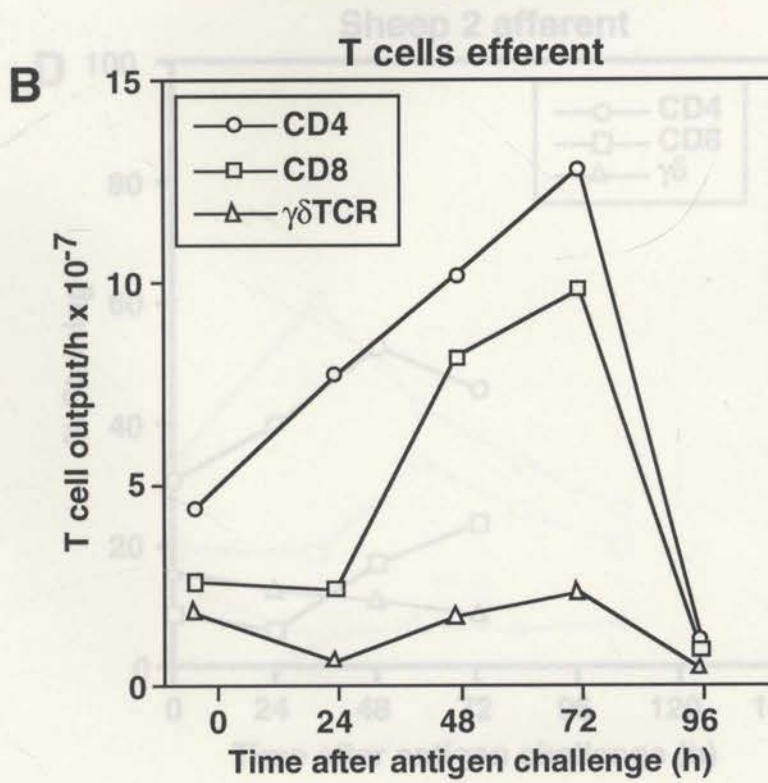
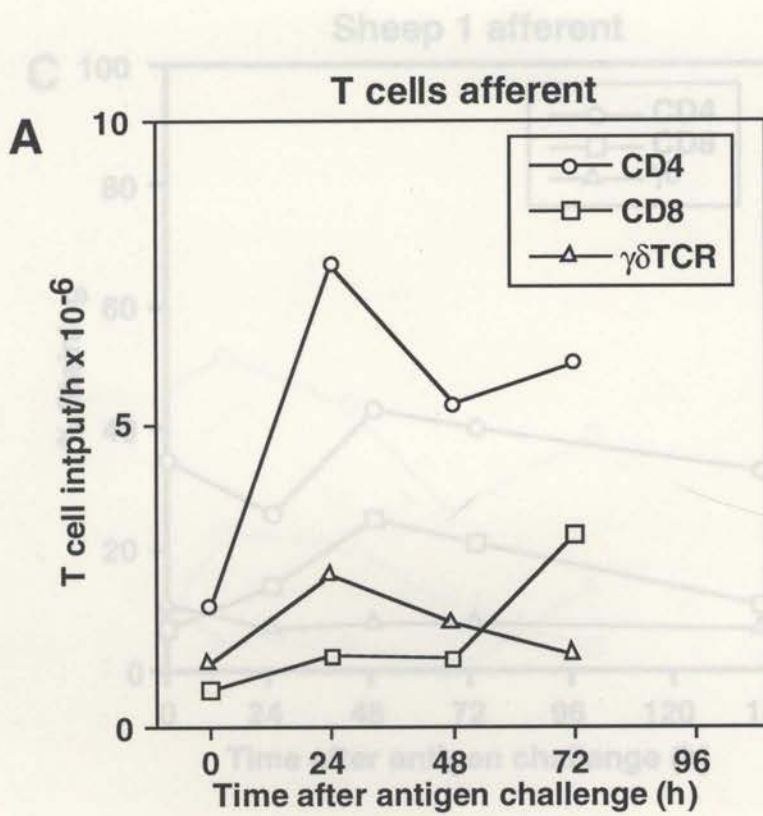
The numbers of CD8 T cells in the efferent lymph also increased after a lag phase due to the lymph node "shut-down" period during the first 24 h after antigen challenge (Hall & Morris, 1965a). Over the remaining 24-72 h period, the occurrence of CD8 T cells in efferent lymph show similar kinetics to those for CD4 cells (Figure 6.2B). However, in the afferent lymph, numbers of CD8 T cells were substantially reduced when compared with CD4 T cells - there was a ~3-fold differences in the cell numbers at 24 h after antigen challenge. The numbers of CD8 T cells in afferent lymph peaked at 24 h and then slowly returned to pre-challenge levels over the next 24-72 h period.

Figure 6.2. Changes in T cell subsets in afferent and efferent lymph and lymph node after antigen challenge.

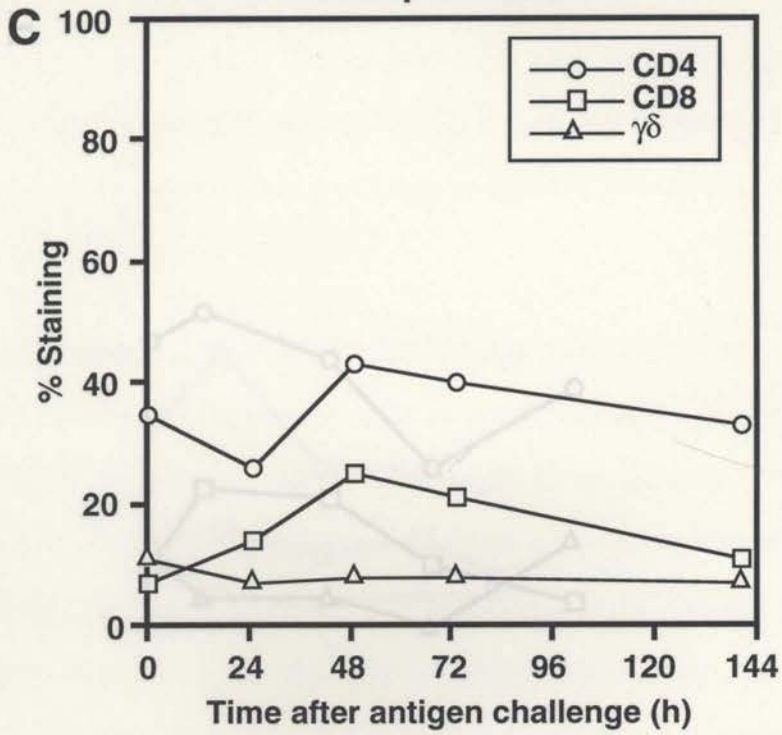
Representative plots of T cell subsets collected from BCG-primed sheep before and after antigen challenge using PPD. Cells were collected from cannulated sheep afferent (A) and efferent (B) prefemoral lymph vessels. Cells were labelled with CD4, CD8 and $\gamma\delta$ TCR MAbs and detected using flow cytometry, as described in Section 2.7.4.

The percentage of T cell subsets from cells collected from the afferent (C & D) and efferent (E, F & G) lymph vessels from individual BCG-primed sheep before and after antigen challenge using PPD.

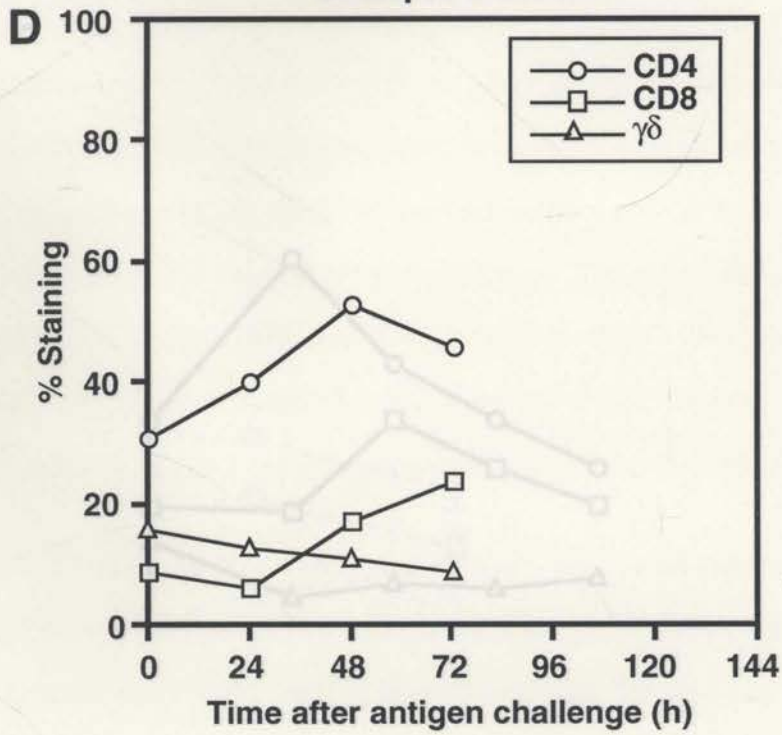
T cell subsets from sheep lymph node (H) before antigen challenge with PPD (n = 1 sheep, 2 lymph nodes), 1 day (n = 1 sheep, 2 lymph nodes) and 3 days after challenge (n = 3 sheep, 6 lymph nodes). The results are represented as mean \pm SEM.



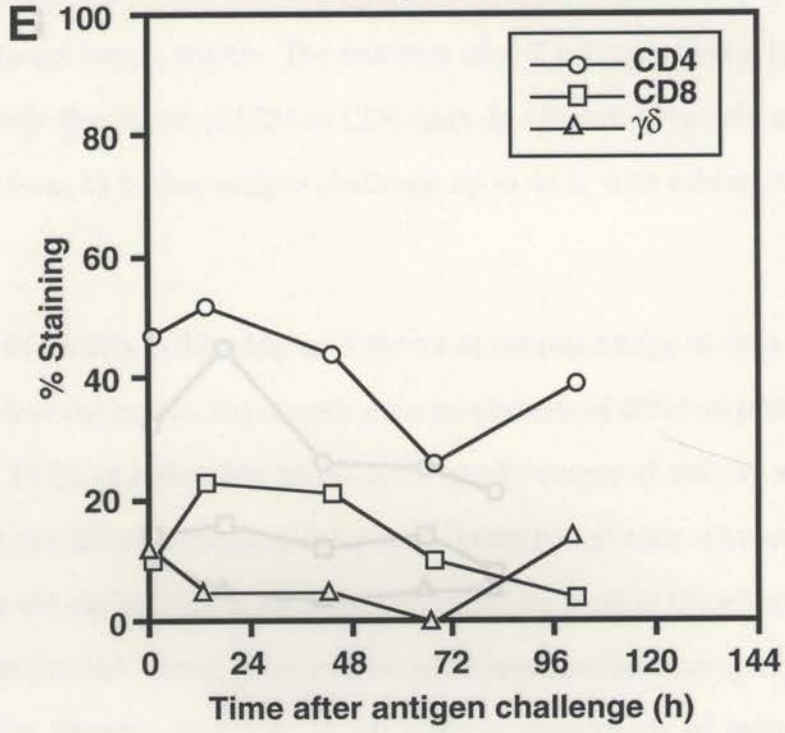
Sheep 1 afferent



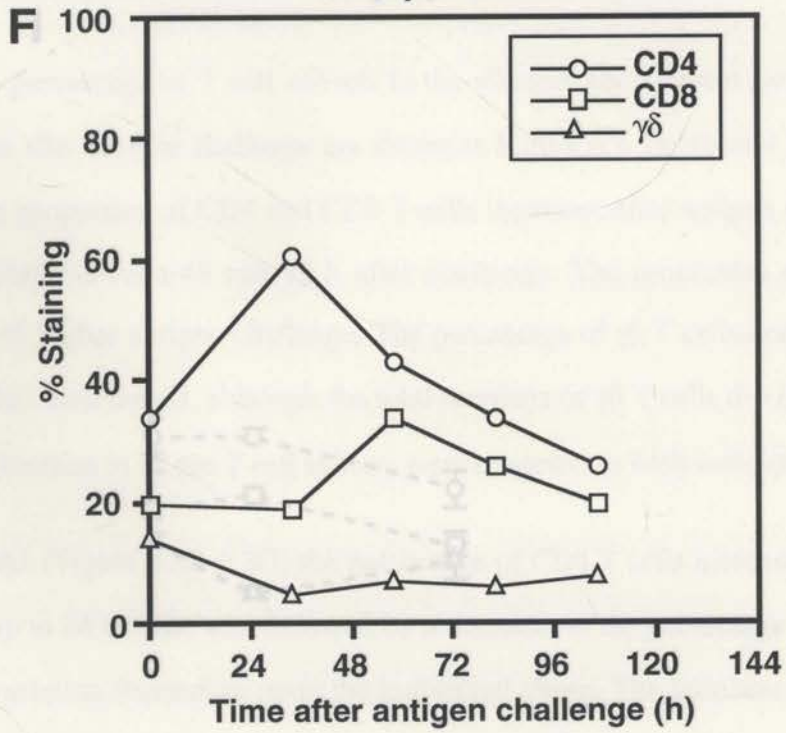
Sheep 2 afferent



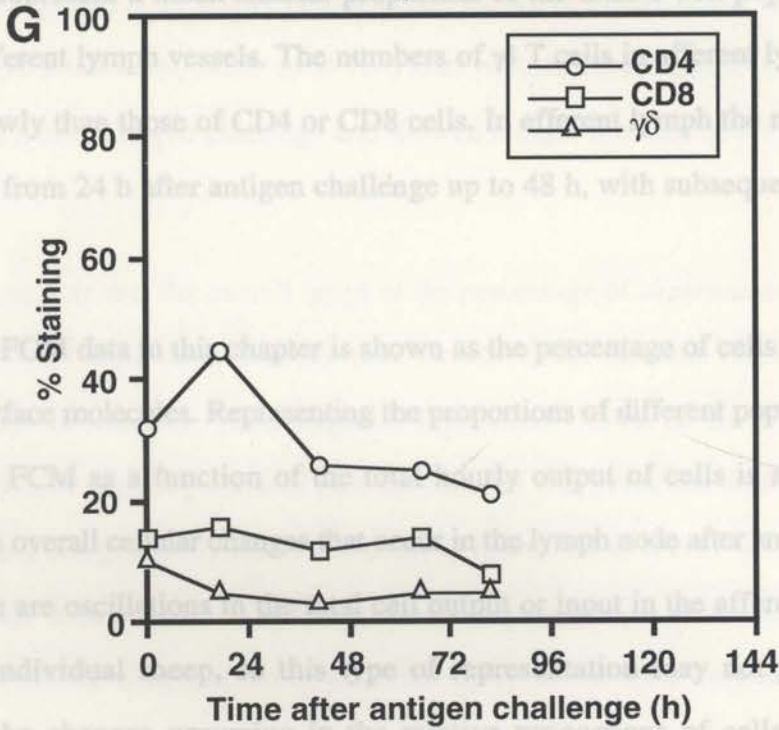
Sheep 1 efferent



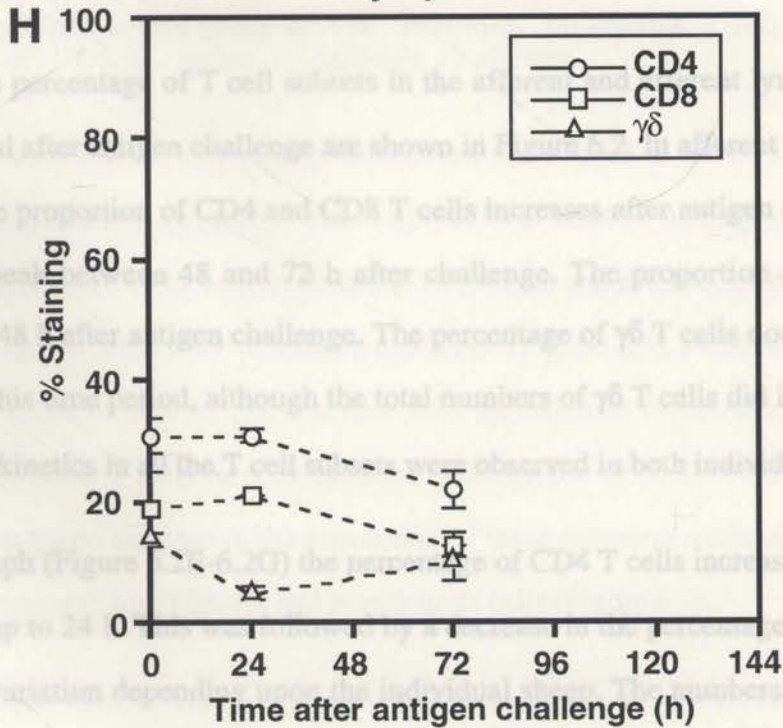
Sheep 2 efferent



Sheep 3 efferent



Lymph node



The percentages of CD4 and CD8 T cells in the lymph node before antigen challenge, at
The $\gamma\delta$ T cells represent a much smaller proportion of the total T cell population in both afferent and efferent lymph vessels. The numbers of $\gamma\delta$ T cells in afferent lymph increased much more slowly than those of CD4 or CD8 cells. In efferent lymph the numbers of $\gamma\delta$ T cells increased from 24 h after antigen challenge up to 48 h, with subsequent decline after 72 h.

It is interesting to note that the overall range of the percentage of expression of CD4, CD8
The remaining FCM data in this chapter is shown as the percentage of cells staining for the specific cell surface molecules. Representing the proportions of different populations of cells detected using FCM as a function of the total hourly output of cells is a useful way of determining the overall cellular changes that occur in the lymph node after antigen challenge. However, there are oscillations in the total cell output or input in the afferent and efferent vessels from individual sheep, so this type of representation may not give a realistic indication of the changes occurring in the relative proportions of cells staining for a particular cell surface molecule.

6.2.3. Cell surface expression of the adhesion molecules CD2, CD44 and LFA-1, and of CD45R, prior to antigen challenge
Changes in the percentage of T cell subsets in the afferent and efferent lymph and lymph node before and after antigen challenge are shown in Figure 6.2. In afferent lymph (Figures 6.2C, 6.2D) the proportion of CD4 and CD8 T cells increases after antigen challenge. CD4 cells reach a peak between 48 and 72 h after challenge. The proportion of CD8 T cells increase up to 48 h after antigen challenge. The percentage of $\gamma\delta$ T cells does not appear to increase over this time period, although the total numbers of $\gamma\delta$ T cells did increase (Figure 6.2B). Similar kinetics in all the T cell subsets were observed in both individual sheep.

6.2.4. Indicated an increase in the expression of these adhesion molecules in afferent lymph cells compared with efferent and lymph node cells (Figure 6.3)
In efferent lymph (Figure 6.2E-6.2G) the percentage of CD4 T cells increased after antigen challenge for up to 24 h. This was followed by a decrease in the percentage between 24-48 h, with some variation depending upon the individual sheep. The numbers of CD8 T cells also showed some variation between individual sheep. However, there was an increased percentage of CD8 T cells in two of the three sheep (Figures 6.2E, 6.2F) before antigen challenge and at 24 or 48 h after antigen challenge. These levels then declined, returning to pre-challenge levels.

The percentages of CD4 and CD8 T cells in the lymph node before antigen challenge, at 24 h after challenge and at 72 h after challenge are shown in Figure 6.2H. The percentage of CD4 and CD8 T cells decreased up to 72 h after antigen challenge. $\gamma\delta$ T cell numbers decreased at 24 h after antigen challenge and showed a slight increase in the percentage of cells at 72 h.

It is interesting to note that the overall range of the percentage of expression of CD4, CD8 and $\gamma\delta$ TCR in the lymph node over the time course of the immune response (Figures 6.2H) generally reflected the percentage of expression shown in the efferent lymph (Figures 6.2E-G). A similar pattern of percent staining was observed with almost every other cell surface antigen analysed in this study (Figures 6.5-6.9, 6.11-6.13, 6.17, 6.18) with the possible exception of LFA-1. There was large variation in the total number of cells isolated from the lymph nodes of different sheep which were unrelated to antigen challenge. Therefore only percent staining data is shown for lymph node cells.

6.2.3. Cell surface expression of the adhesion molecules CD2, CD44 and LFA-1, and of CD45R, prior to antigen challenge.

Expression of a number of cell surface molecules, such as CD2, CD44 and LFA-1, is increased on activated or memory T cells. CD45R was used to distinguish memory T cells from T naive cells. Cells were collected from afferent and efferent lymph, or isolated from immune lymph node prior to antigen challenge (Figure 6.3). FCM was performed for these cell surface markers (see Section 2.5). Histograms representing cells from afferent vessels show a shift in peak channel fluorescence of CD2, CD44 and LFA-1 staining, indicating an increase in the expression of these adhesion molecules in afferent lymph cells compared with efferent and lymph node cells (Figure 6.3).

These results show that afferent lymph cells stain more intensely overall for CD2, CD44 and LFA-1 than do efferent lymph and lymph node cells prior to antigen challenge. However, among efferent lymph and lymph node cells are some of the brightly staining cells from the populations also identified in the afferent lymph cell histogram profiles. The major difference in the pattern of fluorescence staining for CD45R between the

afferent and efferent lymph and lymph node cells, is an absence of a particular population of cells with lower intensity staining in afferent lymph.

CD2.

CD2 histogram profiles for afferent and efferent lymph and lymph node cells are shown in Figures 6.3A, 6.3B and 6.3C. The afferent lymph cells show a uniform distribution of bright fluorescence staining. The efferent and the lymph node cells show two major populations of cells with different intensities of staining for CD2. There was a prominent peak at a lower intensity of fluorescence and a population of cells with high fluorescence intensity staining. The intensity of the staining of the cells in this "shoulder" is similar to those in the afferent lymph cells. The lymph node cells show a lower relative cell number for CD2 staining compared to the afferent and efferent lymph cells.

CD44.

CD44 staining of afferent and efferent lymph and lymph node cells are shown in Figure 6.3D, 6.3E and 6.3F. CD44 staining of afferent lymph cells shows a prominent peak with high fluorescence intensity and a smaller population of cells with very high fluorescence intensity. A majority of the cells in the efferent lymph show lower intensity fluorescence than the afferent lymph cells. However, a small population of very brightly staining cells, similar to those in afferent lymph, is also present. The lymph node shows a larger population of cells with high fluorescence intensity staining than does efferent lymph. These cells in the "shoulder" peak are similar to the main population of afferent lymph cells.

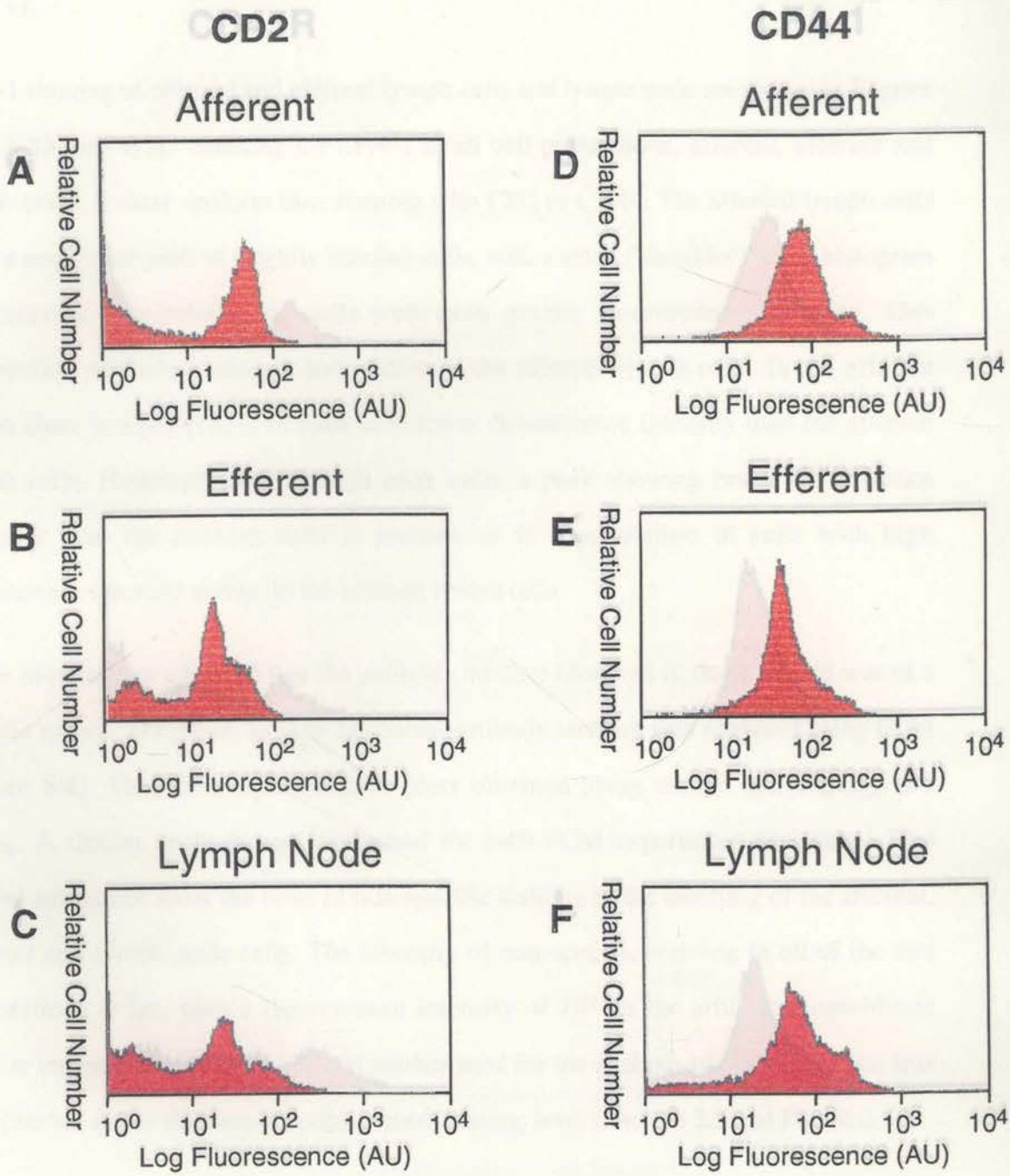
CD45R.

CD45R staining of afferent, efferent and lymph node cells is shown in Figures 6.3G, 6.3H and 6.4I. The staining of afferent lymph cells for CD45R indicates that there is a small population of cells with high fluorescence intensity in the afferent lymph. These cells are also present in both the efferent and the lymph node cells. However, in contrast

Figure 6.3. FCM analysis of CD2, CD44, CD45R and LFA-1 expression.

Representative FCM histogram plots of cells isolated from BCG-primed sheep before antigen challenge. Cells collected from afferent and efferent vessels and lymph node were labelled with the MAbs CD2 (A, B, C), CD44 (D, E, F), CD45R (G, H, I) and LFA-1 (J, K, L) (Section 2.7.3).

Flow Cytometric Analysis of CD2 and CD44 Expression



Flow Cytometric Analysis of CD45R and LFA-1 Expression

to the afferent lymph, efferent lymph and lymph node cells. The intensity of non-specific staining population of cells not present in the afferent lymph cells.

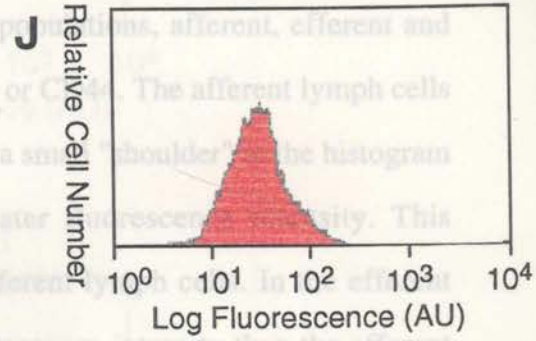
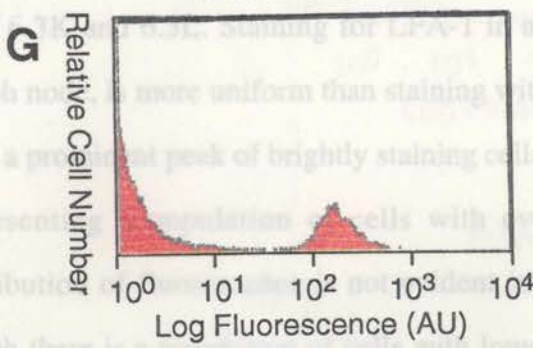
LFA-1.

CD45R

LFA-1

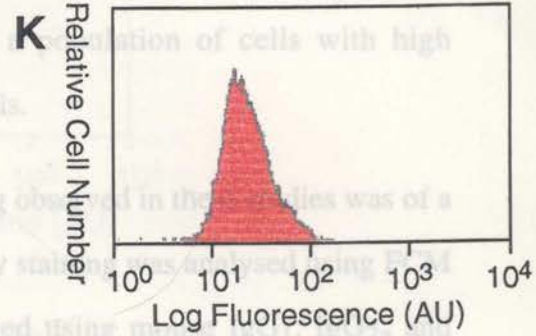
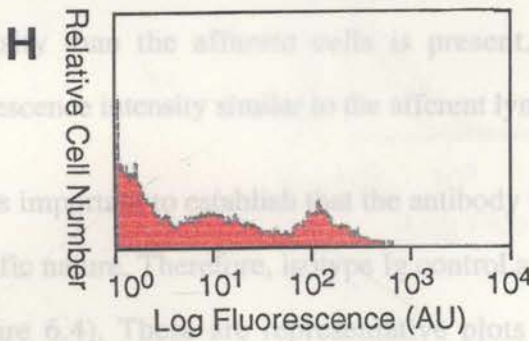
Afferent

Afferent



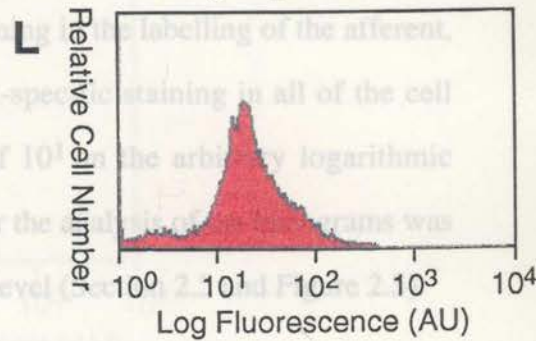
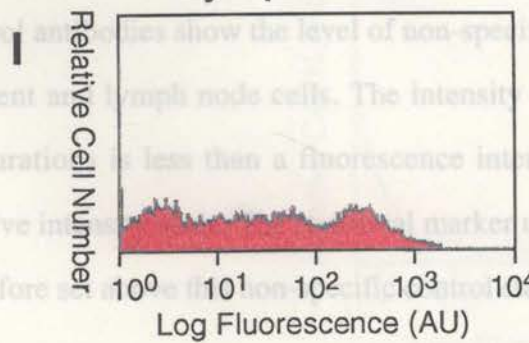
Efferent

Efferent



Lymph Node

Lymph Node



6.2.4. Cell surface expression of CD45R and of the adhesion molecules CD2, CD44 and LFA-1 after antigen challenge.

Changes in the expression of CD2, CD44, LFA-1 and CD45R in afferent and efferent lymph and lymph node cells isolated from BCG-primed sheep prior to and after PPD antigen challenge generally indicated a pronounced antigen responses (Figures 6.5-6.8).

to the afferent lymph, efferent lymph and lymph node cells show a second, less intensely staining population of cells not present in the afferent lymph cells.

LFA-1.

LFA-1 staining of afferent and efferent lymph cells and lymph node are shown in Figures 6.3J, 6.3K and 6.3L. Staining for LFA-1 in all cell populations, afferent, efferent and lymph node, is more uniform than staining with CD2 or CD44. The afferent lymph cells have a prominent peak of brightly staining cells, with a small "shoulder" in the histogram representing a population of cells with even greater fluorescence intensity. This distribution of fluorescence is not evident in the efferent lymph cells. In the efferent lymph there is a population of cells with lower fluorescence intensity than the afferent lymph cells. However, in the lymph node cells, a peak showing lower fluorescence intensity than the afferent cells is present, as is a population of cells with high fluorescence intensity similar to the afferent lymph cells.

It was important to establish that the antibody binding observed in these studies was of a specific nature. Therefore, isotype Ig control antibody staining was analysed using FCM (Figure 6.4). These are representative plots obtained using mouse IgG₁, IgG_{2a} and IgG_{2b}. A similar analysis was performed for each FCM experiment performed. The control antibodies show the level of non-specific staining in the labelling of the afferent, efferent and lymph node cells. The intensity of non-specific staining in all of the cell preparations is less than a fluorescence intensity of 10¹ on the arbitrary logarithmic relative intensity scale. The statistical marker used for the analysis of the histograms was therefore set above this non-specific control staining level (Section 2.5 and Figure 2.5).

6.2.4. Cell surface expression of CD45R and of the adhesion molecules CD2, CD44 and LFA-1 after antigen challenge.

Changes in the expression of CD2, CD44, LFA-1 and CD45R in afferent and efferent lymph and lymph node cells isolated from BCG-primed sheep prior to and after PPD antigen challenge generally indicated a pronounced antigen responses (Figures 6.5-6.8).

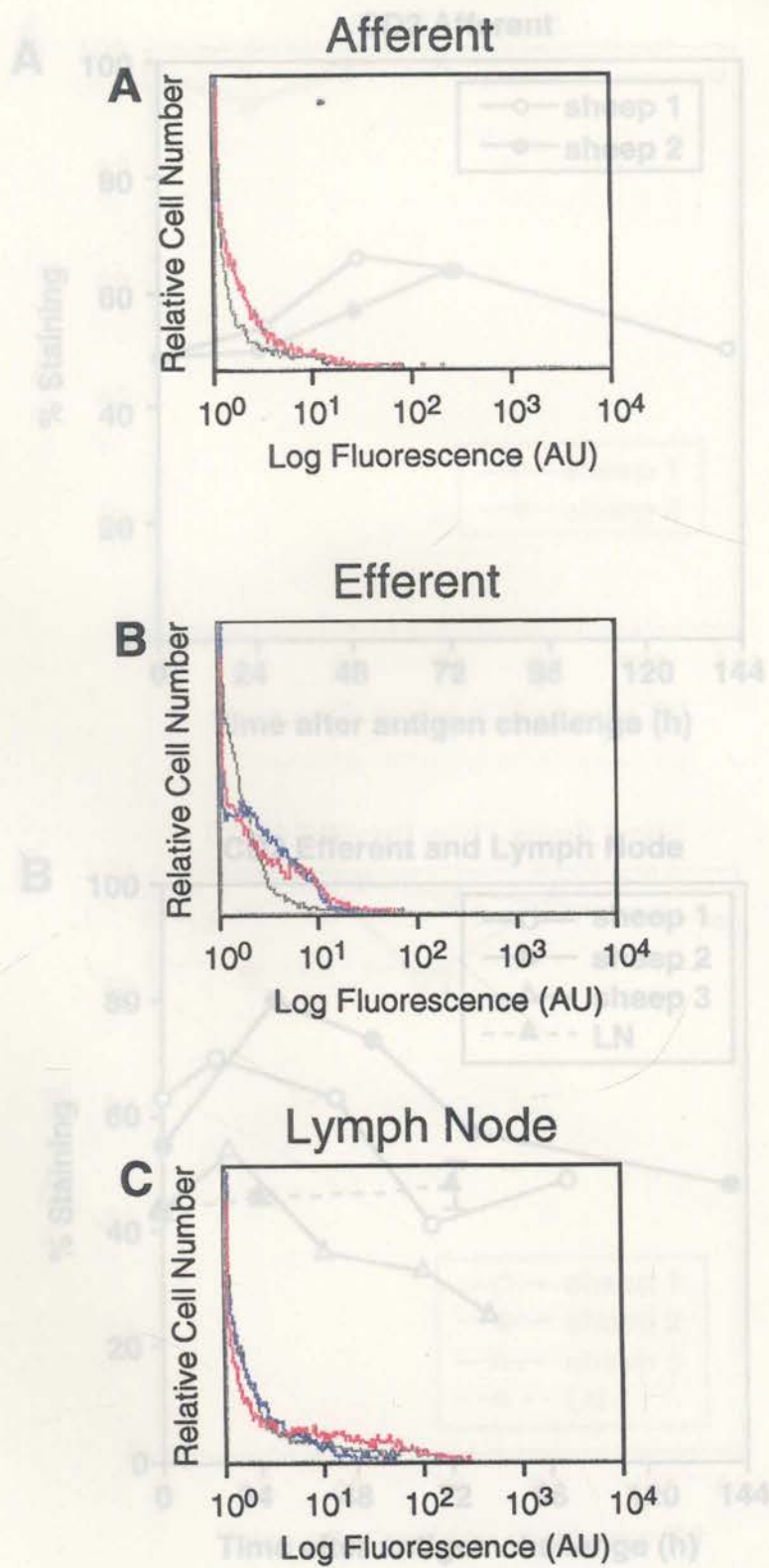


Figure 6.4. FCM histogram plots of mouse control isotype antibodies.
 Cells from sheep (A) afferent lymph, (B) efferent lymph and (C) lymph node were incubated with mouse IgG₁ (black), mouse IgG_{2a} (blue) and mouse IgG_{2b} (red). Counterstain was FITC-labelled sheep α -mouse Ig.

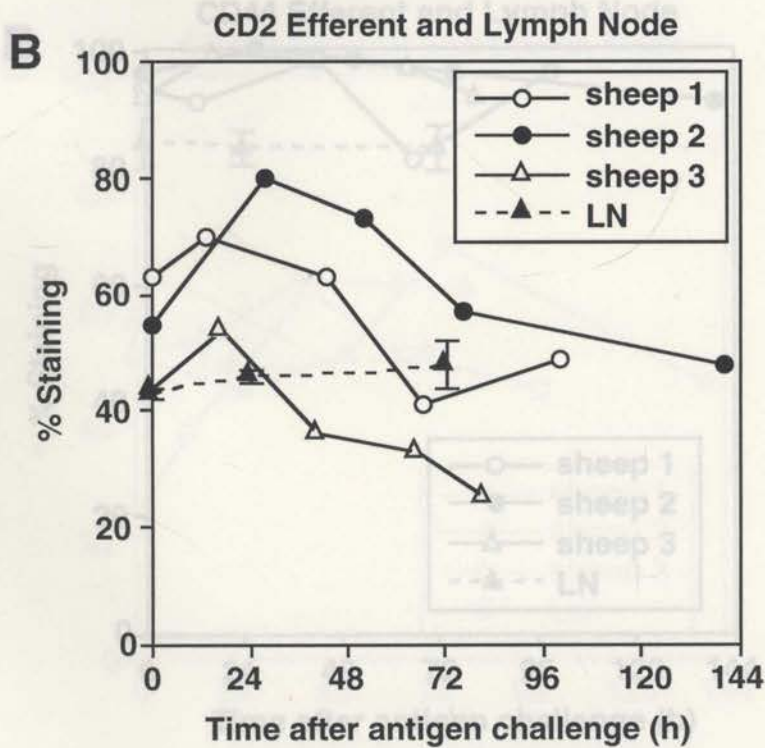
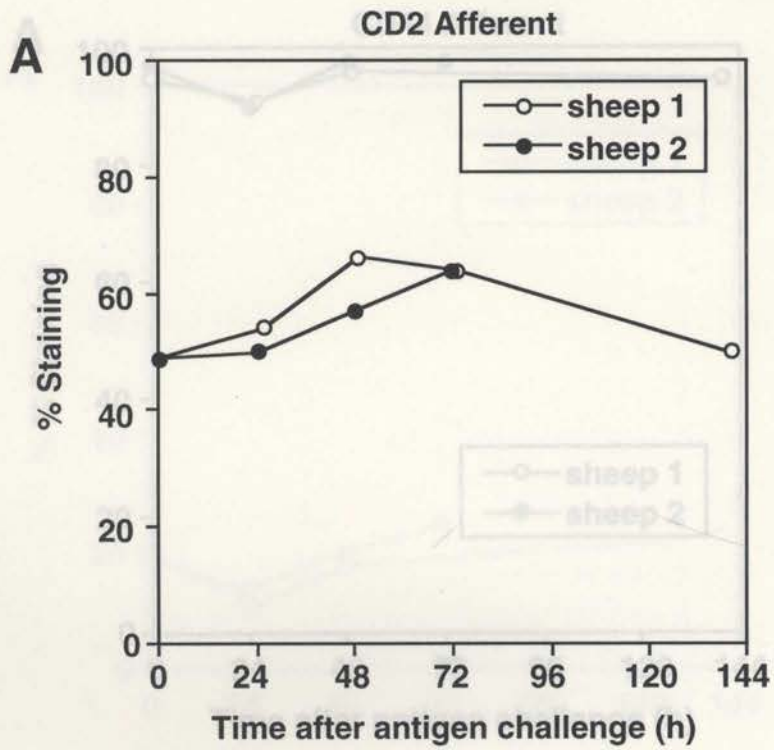


Figure 6.5. CD2 expression on afferent and efferent lymph and lymph node cells.

Cells collected from the afferent (A) and efferent (B) lymph vessels and lymph node cells (B) from BCG-primed sheep were labelled with CD2 MAb. The results represent the percentage of cells expressing CD2 detected using FCM, before after PPD antigen challenge. The results from individual sheep are plotted. Lymph node (LN) (n=1 sheep, 2 lymph nodes) before antigen challenge, day 1 after challenge (n=1 sheep, 2 lymph nodes) and day 3 after challenge (n=3 sheep, 6 lymph nodes, mean \pm SEM).

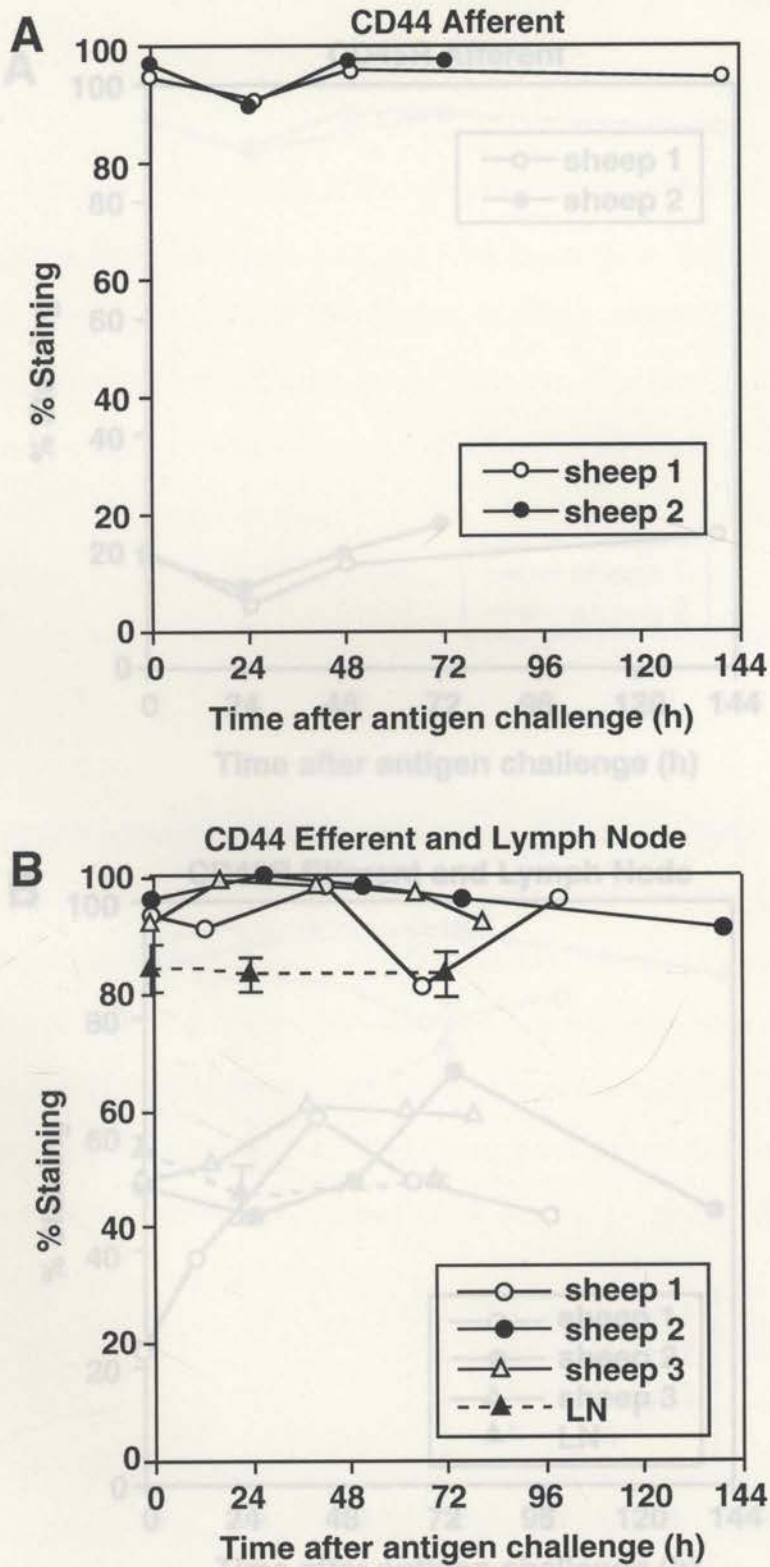


Figure 6.6. CD44 expression on sheep afferent and efferent lymph and lymph node cells.

Cells collected from the afferent (A) and efferent (B) lymph vessels and lymph node cells (B) from BCG-primed sheep were labelled with CD44 MAb. The results represent the percentage of cells expressing CD44 detected using FCM, before after PPD antigen challenge. The results from each sheep are plotted. Lymph node (LN) (n=1 sheep, 2 lymph nodes) before antigen challenge, day 1 after challenge (n=1 sheep, 2 lymph nodes) and day 3 after challenge (n=3 sheep, 6 lymph nodes, mean±SEM).

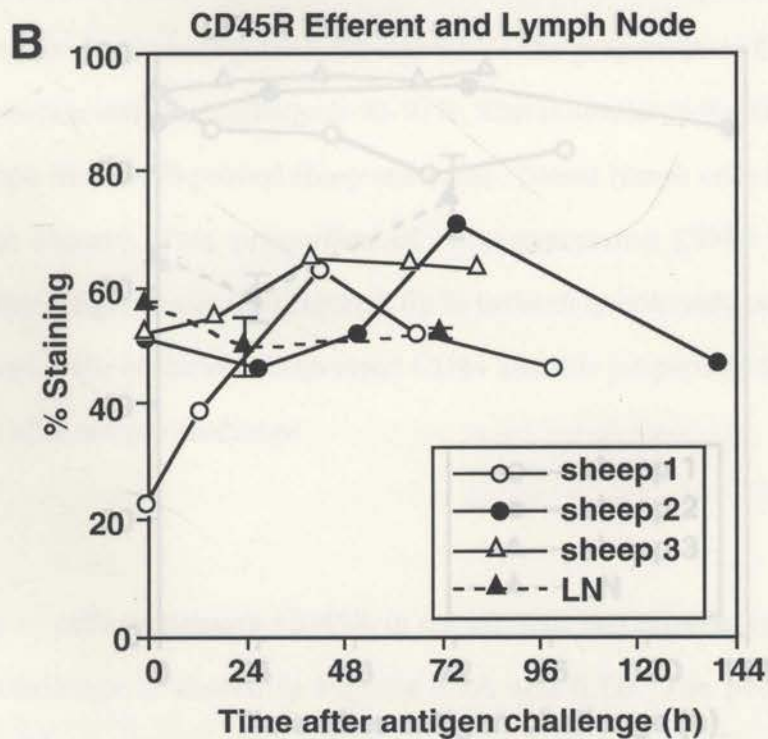
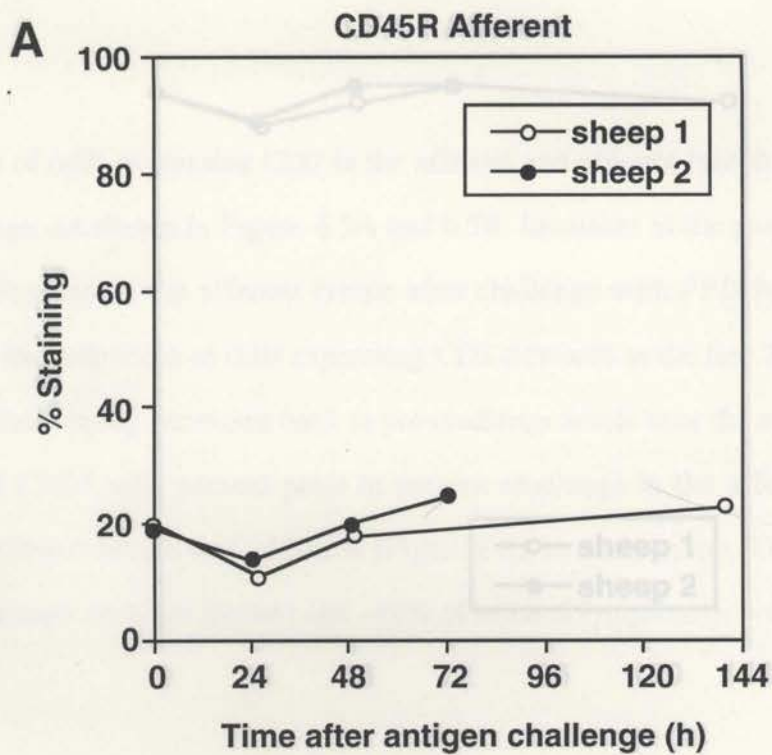


Figure 6.7. CD45R expression on sheep afferent and efferent lymph and lymph node cells.

Cells collected from the afferent (A) and efferent (B) lymph vessels and lymph node cells (B) from BCG-primed sheep were labelled with CD45R MAb. The results represent the percentage of cells expressing CD45R detected using FCM, before and after PPD antigen challenge. The results individual sheep are plotted. Lymph node (n=1 sheep, 2 lymph nodes) before antigen challenge, day 1 after challenge (n=1 sheep, 2 lymph nodes) and day 3 after challenge (n=3 sheep, 6 lymph nodes, mean±SEM).

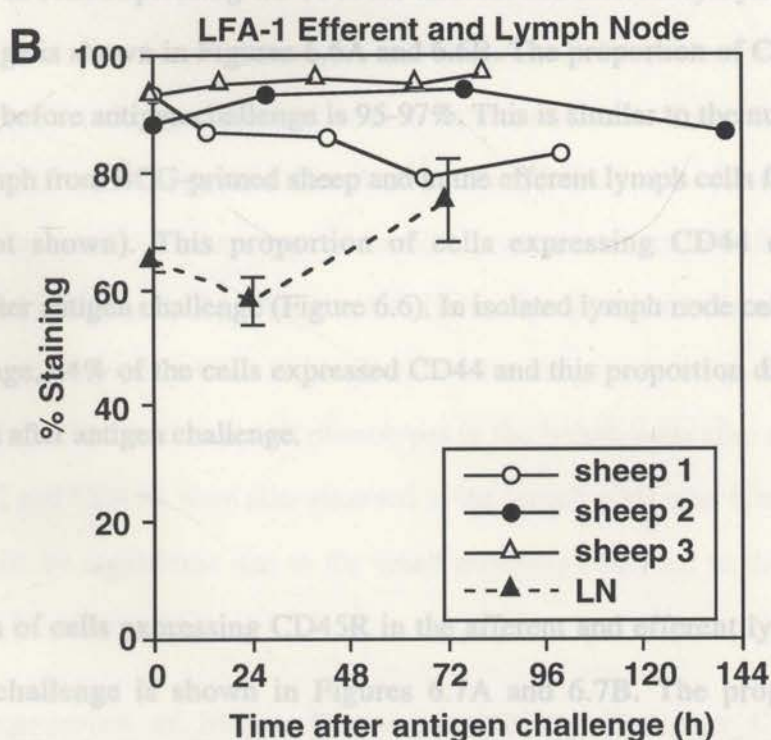
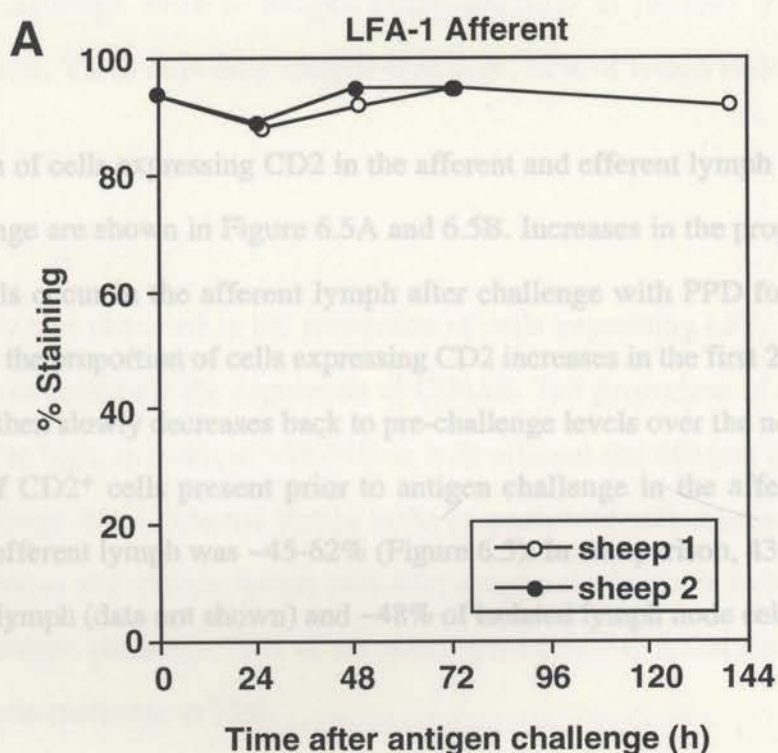


Figure 6.8. LFA-1 expression on sheep afferent and efferent lymph and lymph node cells.

Cells collected from the afferent (A) and efferent (B) lymph vessels and lymph node cells (B) from BCG-primed sheep were labelled with LFA-1 MAb. The results represent the percentage of cells expressing LFA-1 detected using FCM, before and after PPD antigen challenge. The results from individual sheep are plotted. Lymph node (LN) (n=1 sheep, 2 lymph nodes) before antigen challenge, day 1 after challenge (n=1 sheep, 2 lymph nodes) and day 3 after challenge (n=3 sheep, 6 lymph nodes, mean \pm SEM).

after antigen challenge. Prior to antigen challenge, 57% of isolated lymph node cells expressed CD2. Three days after antigen challenge, 52% of lymph node cells expressed CD45R.

The proportion of cells expressing CD2 in the afferent and efferent lymph before and after antigen challenge are shown in Figure 6.5A and 6.5B. Increases in the proportion of CD2-expressing cells occur in the afferent lymph after challenge with PPD for up to 72 h. In efferent lymph the proportion of cells expressing CD2 increases in the first 24 h after antigen challenge and then slowly decreases back to pre-challenge levels over the next 72-96 h. The percentages of CD2⁺ cells present prior to antigen challenge in the afferent lymph was ~50%, and in efferent lymph was ~45-62% (Figure 6.5). In comparison, 43% of the cells in naive efferent lymph (data not shown) and ~48% of isolated lymph node cells were CD2⁺.

CD44. Prior to antigen challenge to 75%.

The proportion of cells expressing CD44 in the afferent and efferent lymph before and after antigen challenge is shown in Figures 6.6A and 6.6B. The proportion of CD44 cells in the afferent lymph before antigen challenge is 95-97%. This is similar to the number of cells in the efferent lymph from BCG-primed sheep and in the efferent lymph cells from naive sheep (95%, data not shown). This proportion of cells expressing CD44 did not change substantially after antigen challenge (Figure 6.6). In isolated lymph node cells taken prior to antigen challenge, 84% of the cells expressed CD44 and this proportion did not change in the lymph node after antigen challenge.

CD45R.

The proportion of cells expressing CD45R in the afferent and efferent lymph before and after antigen challenge is shown in Figures 6.7A and 6.7B. The proportion of cells expressing CD45R prior to antigen challenge among the afferent lymph cells was generally lower (20%) than in efferent lymph (23-55%). In comparison, 48% of efferent lymph cells from naive sheep expressed CD45R (data not shown). In afferent lymph, the proportion of cells expressing CD45R does not change substantially after antigen challenge. However, in efferent lymph cells the proportion of cells expressing CD45R increases during the ~72 h

after antigen challenge. Prior to antigen challenge, 57% of isolated lymph node cells expressed CD45R. Three days after antigen-challenge, 52% of lymph node cells expressed CD45R.

LFA-1.

A similar result was observed in the proportion of cells expressing LFA-1 (Figures 6.8A and 6.8B) as was found for the expression of CD45R. The proportion of cells expressing LFA-1 was quite high, at levels of ~88-94% in both afferent and efferent lymph cells prior to antigen challenge. No substantial change in the proportion of cells staining for LFA-1 was observed in afferent and efferent lymph cells after antigen challenge. In isolated lymph node cells prior to antigen challenge, 65% of the cells expressed LFA-1, and this increased three days after antigen-challenge to 75%.

These results show that the proportion of cells in afferent and efferent lymph expressing CD2 and CD45R surface markers changes in BCG-primed sheep after antigen challenge. However, no similar changes were seen in lymph node cells after antigen challenge, although a change in the proportion of cells expressing LFA-1 was observed. The results indicate either changes in the phenotype of the cells present or changes in the distribution of particular cell populations in the afferent and efferent lymph after antigen challenge. The changes in the expression of LFA-1 in lymph node after antigen challenge may also indicate a change in cellular distribution or cell phenotypes in the lymph node after challenge. Small changes in CD2 and CD45R were also observed in the lymph node after challenge, but these changes may not be significant due to the small numbers observed in the control lymph nodes.

6.2.5. The expression of Major Histocompatibility Complex Class II (MHC II).

Cells collected from the afferent (A) and efferent (B) lymph vessels and lymph node cells (B) from BCG-primed sheep were labelled with MHC II MAbs. The results represent the The proportion of cells expressing MHC II in afferent and efferent immune cells after antigen challenge was monitored using FCM (Figure 6.9A & 6.9B). Antigen challenge resulted in substantial changes in the proportion of cells expressing MHC II in both

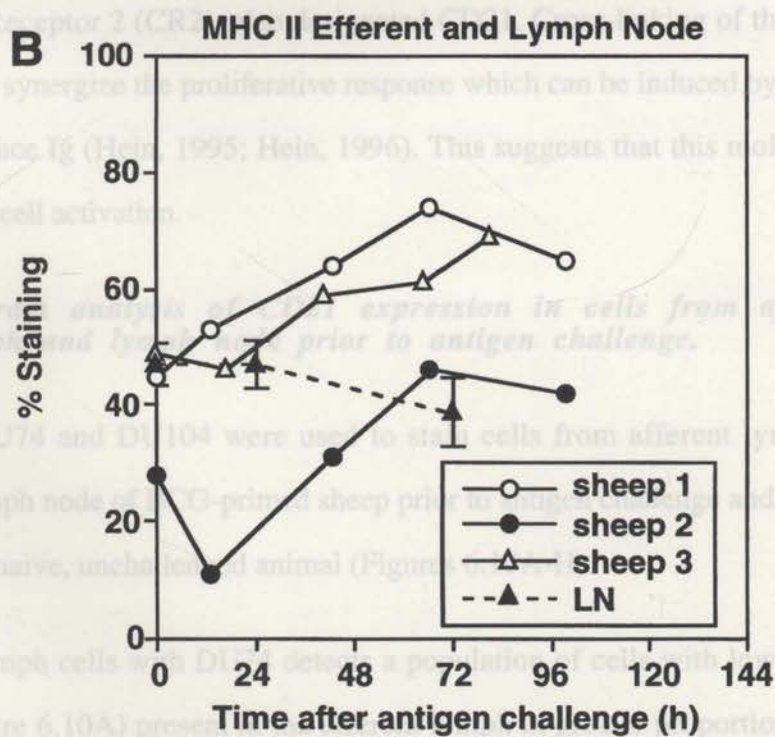
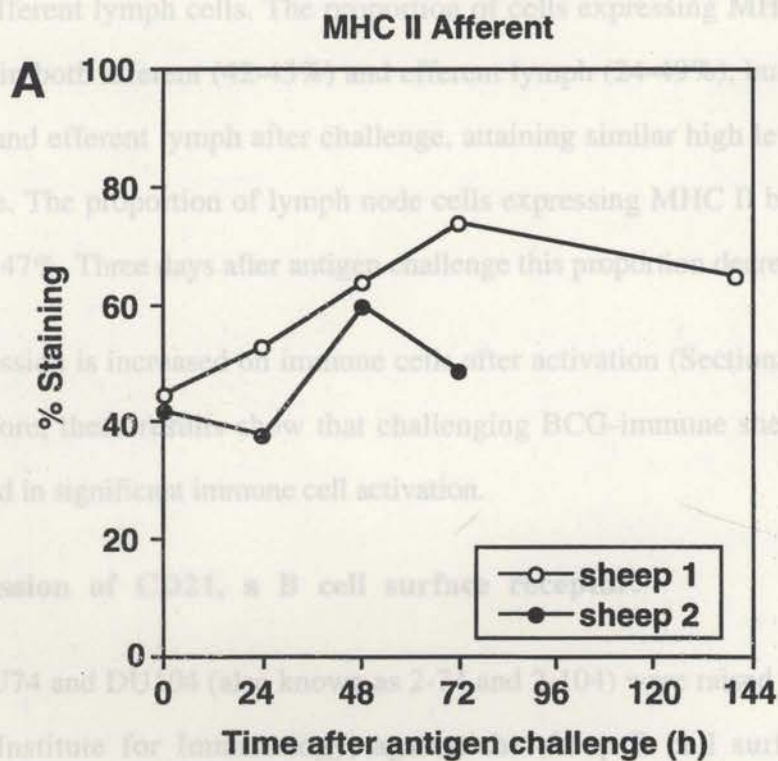


Figure 6.9. MHC II expression on sheep afferent and efferent lymph cells. Cells collected from the afferent (A) and efferent (B) lymph vessels and lymph node cells (B) from BCG-primed sheep were labelled with MHC II MAbs. The results represent the percentage of cells expressing MHC II detected using FCM, before and after PPD antigen challenge. The results from individual sheep are plotted. Lymph node (LN) (n=1 sheep, 2 lymph nodes) before antigen challenge, day 1 after antigen challenge (n=1 sheep, 2 lymph nodes) and day 3 after challenge (n=3 sheep, 6 lymph nodes, mean \pm SEM).

(Figure 6.10C).

afferent and efferent lymph cells. The proportion of cells expressing MHC II was low pre-challenge in both afferent (42-45%) and efferent lymph (24-49%), but increased in both afferent and efferent lymph after challenge, attaining similar high levels by day 3 after challenge. The proportion of lymph node cells expressing MHC II before antigen challenge was 47%. Three days after antigen challenge this proportion decreased to 39%.

MHC II expression is increased on immune cells after activation (Sections 1.2.1, 1.4.1, 1.4.2). Therefore, these results show that challenging BCG-immune sheep with PPD antigen resulted in significant immune cell activation.

6.2.6. Expression of CD21, a B cell surface receptor.

The MAbs DU74 and DU104 (also known as 2-74 and 2-104) were raised by Dr Wayne Hein, Basel Institute for Immunology, against the sheep B cell surface receptor Complement Receptor 2 (CR2), also designated CD21. Cross-linking of the isoforms of CD21 strongly synergize the proliferative response which can be induced by the co-cross-linking of surface Ig (Hein, 1995; Hein, 1996). This suggests that this molecule may be important in B cell activation.

FCM histogram analysis of CD21 expression in cells from afferent and efferent lymph and lymph node prior to antigen challenge.

The MAbs DU74 and DU104 were used to stain cells from afferent lymph, efferent lymph and lymph node of BCG-primed sheep prior to antigen challenge and from efferent lymph from a naive, unchallenged animal (Figures 6.10A-H).

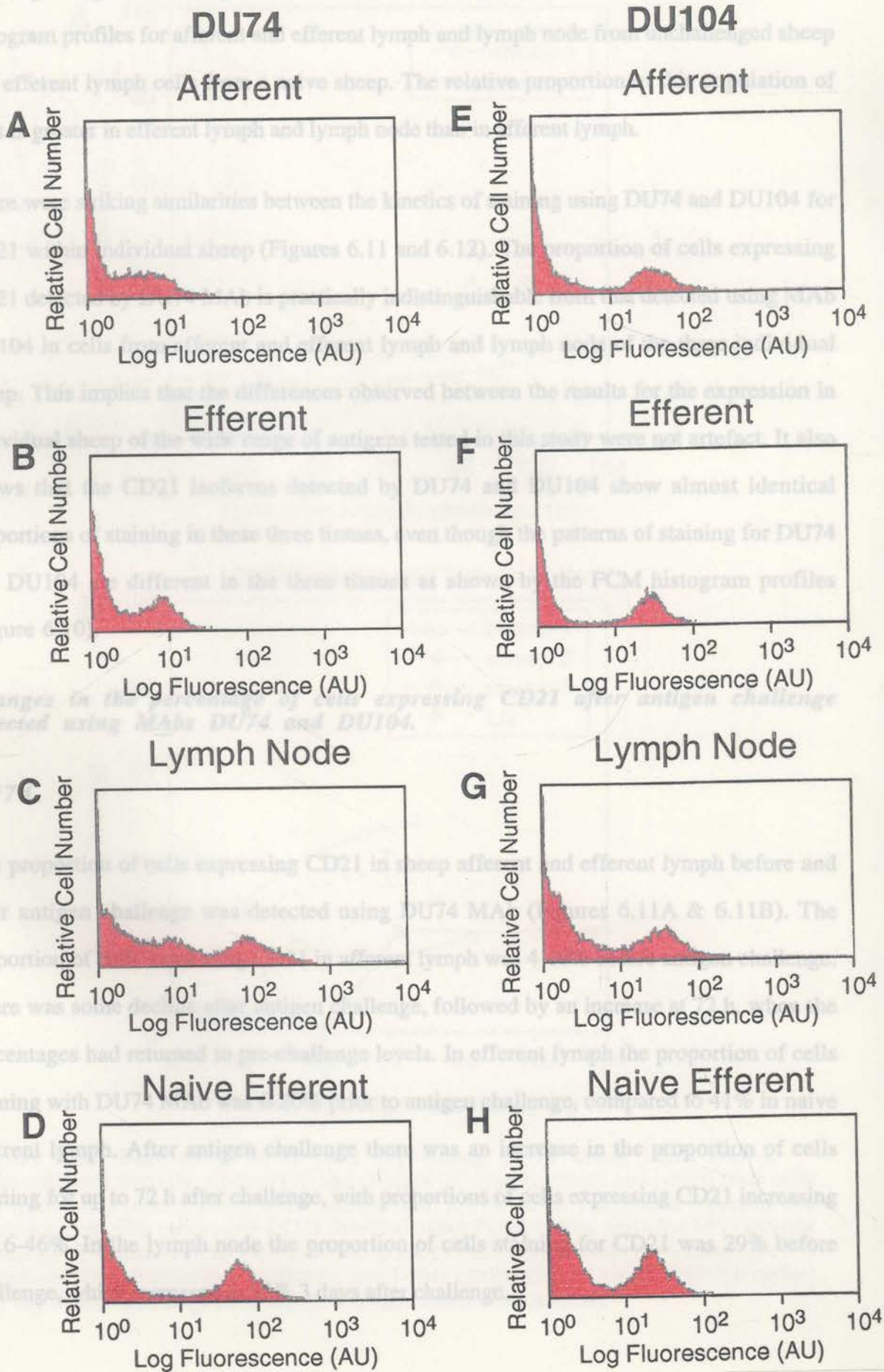
Staining of lymph cells with DU74 detects a population of cells with low fluorescence intensity (Figure 6.10A) present in the efferent lymph in greater proportions than in the afferent lymph (Figure 6.10B). This population was not present in the naive efferent lymph, but a brighter staining population of cells with higher fluorescence intensity was present. This population was also present in unchallenged lymph node, which also contained cells from the lower intensity staining population present in the efferent lymph (Figure 6.10C).

Figure 6.10. FCM analysis of CD21 expression.

Representative FCM histogram plots of cells isolated from BCG-primed sheep before antigen challenge and from naive sheep. Cells collected from afferent and efferent vessels and lymph node were labelled with the MAbs DU74 (A, B, C, D) and DU104 (E, F, G, H) (Section 2.7.3).

Flow Cytometric Analysis of CD21 Expression

Staining using DU104 (Figure 6.10B-H) found a single population of cells in all of the histogram profiles for afferent lymph and lymph node from challenged sheep and efferent lymph cells from naive sheep. The relative proportions of cells in efferent lymph and lymph node that stain for CD21 are similar. There were striking similarities between the kinetics of staining using DU74 and DU104 for CD21 in individual sheep (Figures 6.11 and 6.12). The proportion of cells expressing CD21 in cells in efferent lymph and lymph node from naive sheep stained with DU104 is similar to that in efferent lymph and lymph node from challenged sheep. This implies that the differences observed between the results for the expression in individual sheep of the CD21 isoforms detected by DU74 and DU104 are not significant. It also shows that the CD21 isoforms detected by DU74 and DU104 show almost identical patterns of staining for DU74 and DU104 in cells in efferent lymph and lymph node from naive sheep. The FCM histogram profiles (Figure 6.10A-H) for the expression of CD21 in efferent lymph and lymph node from naive sheep. Changes in the proportion of cells expressing CD21 after antigen challenge detected using MAbs DU74 and DU104.



Staining using DU104 (Figure 6.10E-H) found a single population of cells in all of the histogram profiles for afferent and efferent lymph and lymph node from unchallenged sheep and efferent lymph cells from a naive sheep. The relative proportion of this population of cells is greater in efferent lymph and lymph node than in afferent lymph.

There were striking similarities between the kinetics of staining using DU74 and DU104 for CD21 within individual sheep (Figures 6.11 and 6.12). The proportion of cells expressing CD21 detected by DU74 MAb is practically indistinguishable from that detected using MAb DU104 in cells from afferent and efferent lymph and lymph node of the three individual sheep. This implies that the differences observed between the results for the expression in individual sheep of the wide range of antigens tested in this study were not artefact. It also shows that the CD21 isoforms detected by DU74 and DU104 show almost identical proportions of staining in these three tissues, even though the patterns of staining for DU74 and DU104 are different in the three tissues as shown by the FCM histogram profiles (Figure 6.10).

Changes in the percentage of cells expressing CD21 after antigen challenge detected using MAbs DU74 and DU104.

DU74.

The proportion of cells expressing CD21 in sheep afferent and efferent lymph before and after antigen challenge was detected using DU74 MAb (Figures 6.11A & 6.11B). The proportion of cells expressing CD21 in afferent lymph was 4-10% before antigen challenge. There was some decline after antigen challenge, followed by an increase at 72 h, when the percentages had returned to pre-challenge levels. In efferent lymph the proportion of cells staining with DU74 MAb was 6-20% prior to antigen challenge, compared to 41% in naive efferent lymph. After antigen challenge there was an increase in the proportion of cells staining for up to 72 h after challenge, with proportions of cells expressing CD21 increasing to 16-46%. In the lymph node the proportion of cells staining for CD21 was 29% before challenge, which increased to 38% 3 days after challenge.

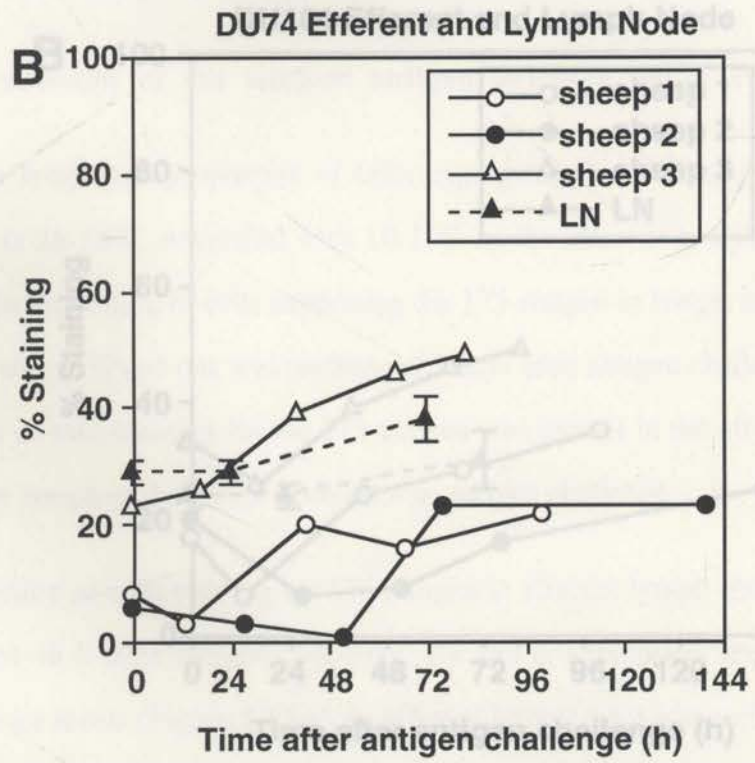
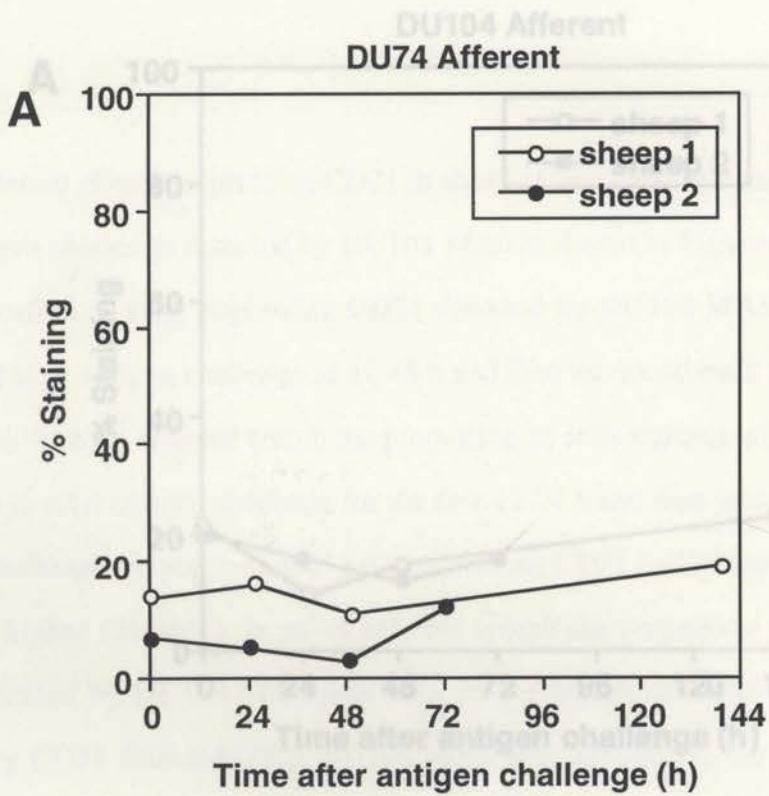


Figure 6.11. Percentage of B cells expressing CD21 using MAb DU74. Cells collected from the afferent (A) and efferent (B) lymph vessels and lymph node cells (B) from BCG-primed sheep were labelled with DU74 MAb. The results represent the percentage of cells expressing CD21 detected using FCM, before and after PPD antigen challenge. The results from individual sheep are plotted. Lymph node (LN) (n=1 sheep, 2 lymph nodes) before antigen challenge, day 1 after challenge (n=1 sheep, 2 lymph nodes) and day 3 after challenge (n=3 sheep, 6 lymph nodes, mean±SEM).

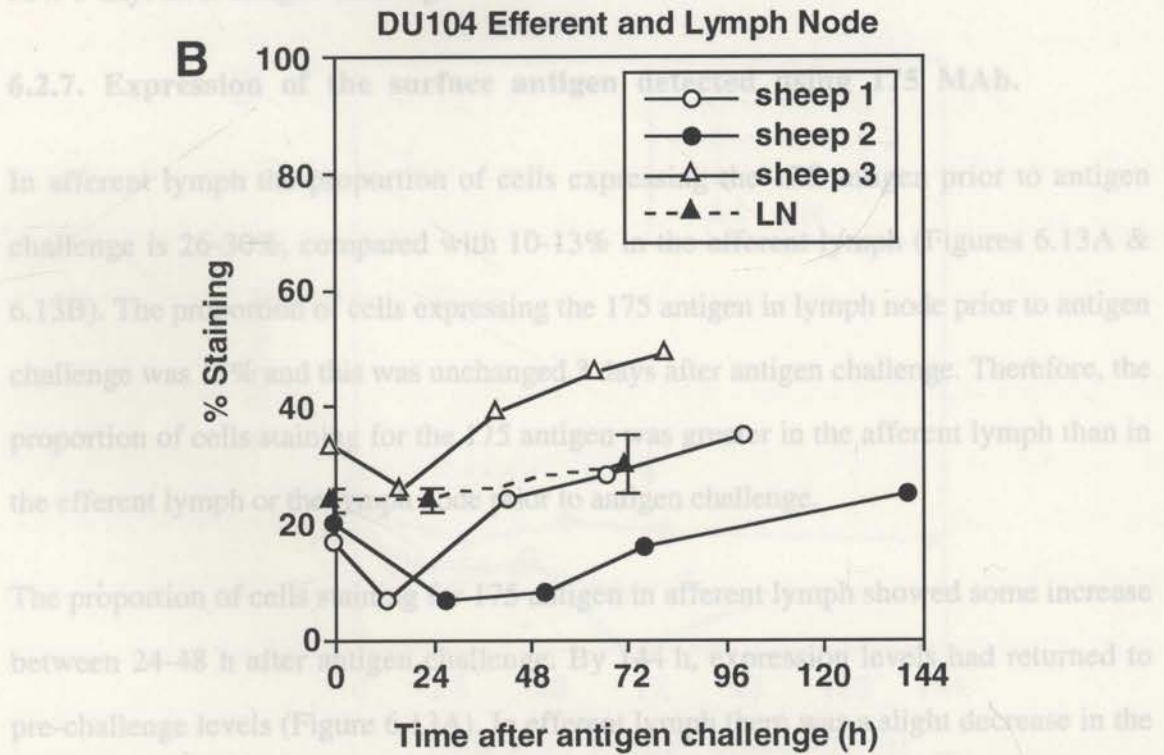
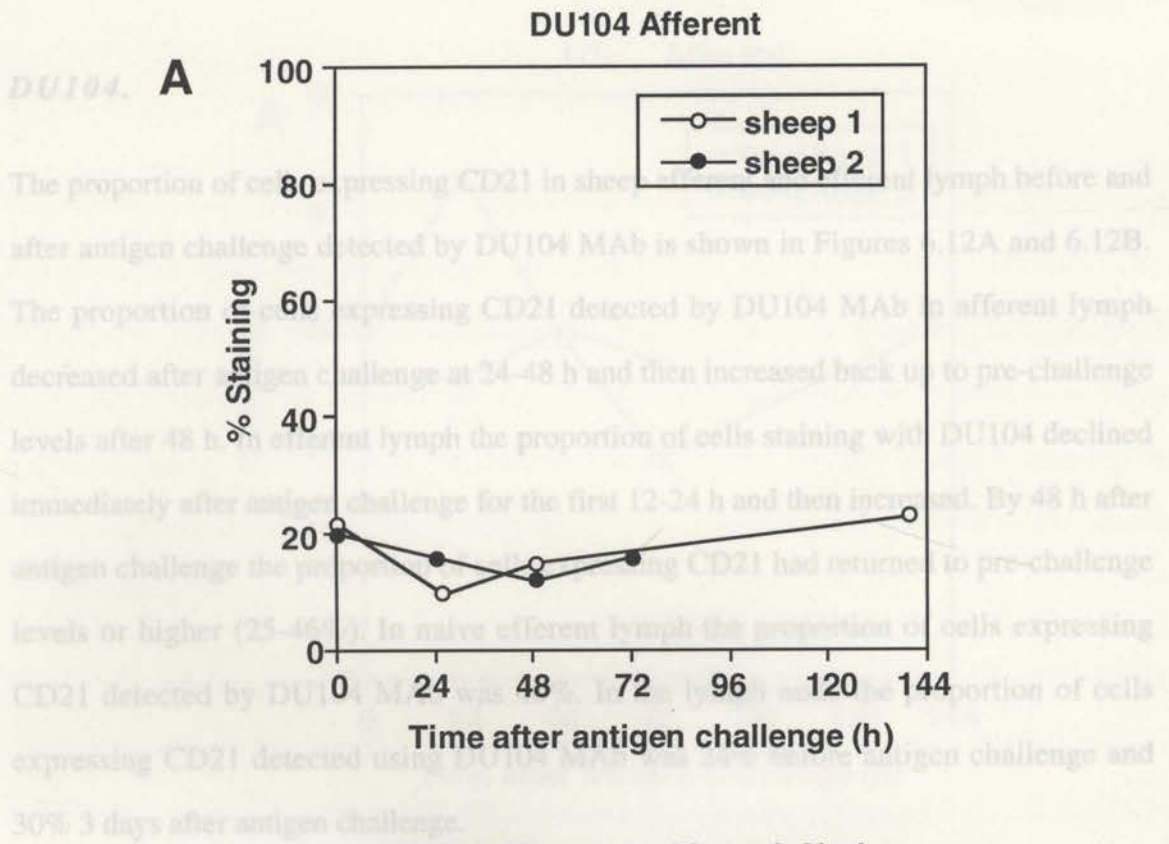


Figure 6.12. Percentage of B cells expressing CD21 using MAb DU104. Cells collected from the afferent (A) and efferent (B) lymph vessels and lymph node (B) from BCG-primed sheep were labelled with DU104 MAb. Results represent percentage of cells expressing CD21 detected using FCM, before and after PPD antigen challenge. Data from individual sheep are plotted. Lymph node (LN) (n=1 sheep, 2 lymph nodes) before antigen challenge, day 1 after challenge (n=1 sheep, 2 lymph nodes) and day 3 after challenge (n=3 sheep, 6 lymph nodes, mean±SEM).

DU104.

The proportion of cells expressing CD21 in sheep afferent and efferent lymph before and after antigen challenge detected by DU104 MAb is shown in Figures 6.12A and 6.12B. The proportion of cells expressing CD21 detected by DU104 MAb in afferent lymph decreased after antigen challenge at 24-48 h and then increased back up to pre-challenge levels after 48 h. In efferent lymph the proportion of cells staining with DU104 declined immediately after antigen challenge for the first 12-24 h and then increased. By 48 h after antigen challenge the proportion of cells expressing CD21 had returned to pre-challenge levels or higher (25-46%). In naive efferent lymph the proportion of cells expressing CD21 detected by DU104 MAb was 40%. In the lymph node the proportion of cells expressing CD21 detected using DU104 MAb was 24% before antigen challenge and 30% 3 days after antigen challenge.

6.2.7. Expression of the surface antigen detected using 175 MAb.

In afferent lymph the proportion of cells expressing the 175 antigen prior to antigen challenge is 26-30%, compared with 10-13% in the efferent lymph (Figures 6.13A & 6.13B). The proportion of cells expressing the 175 antigen in lymph node prior to antigen challenge was 15% and this was unchanged 3 days after antigen challenge. Therefore, the proportion of cells staining for the 175 antigen was greater in the afferent lymph than in the efferent lymph or the lymph node prior to antigen challenge.

The proportion of cells staining for 175 antigen in afferent lymph showed some increase between 24-48 h after antigen challenge. By 144 h, expression levels had returned to pre-challenge levels (Figure 6.13A). In efferent lymph there was a slight decrease in the proportion of cells staining for 175 at 12 h and a return back to pre-challenge levels between 48-96 h after antigen challenge (Figure 6.13B). Therefore, the expression of the 175 antigen was uniformly higher in afferent lymph than in efferent lymph or lymph node, both before and after antigen challenge.

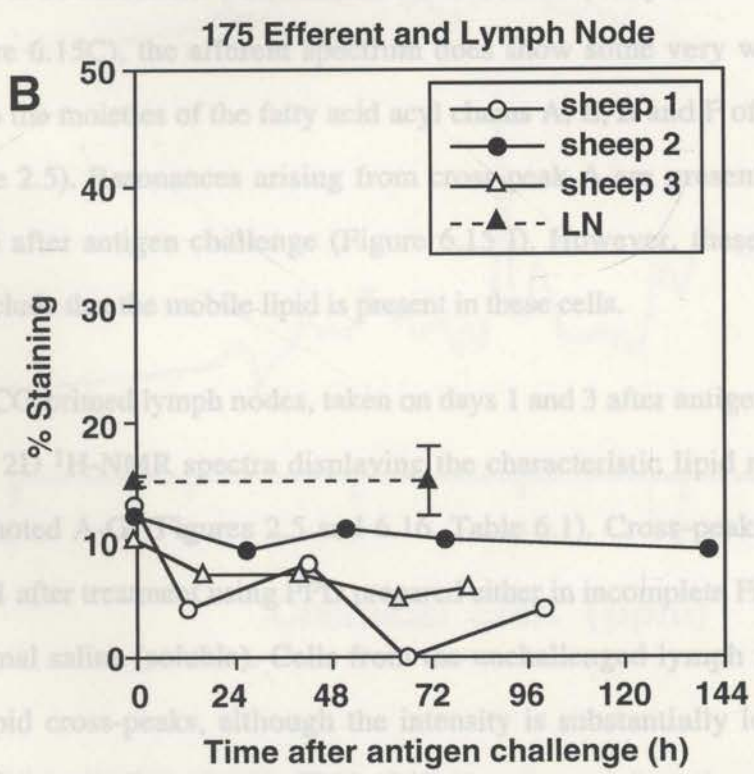
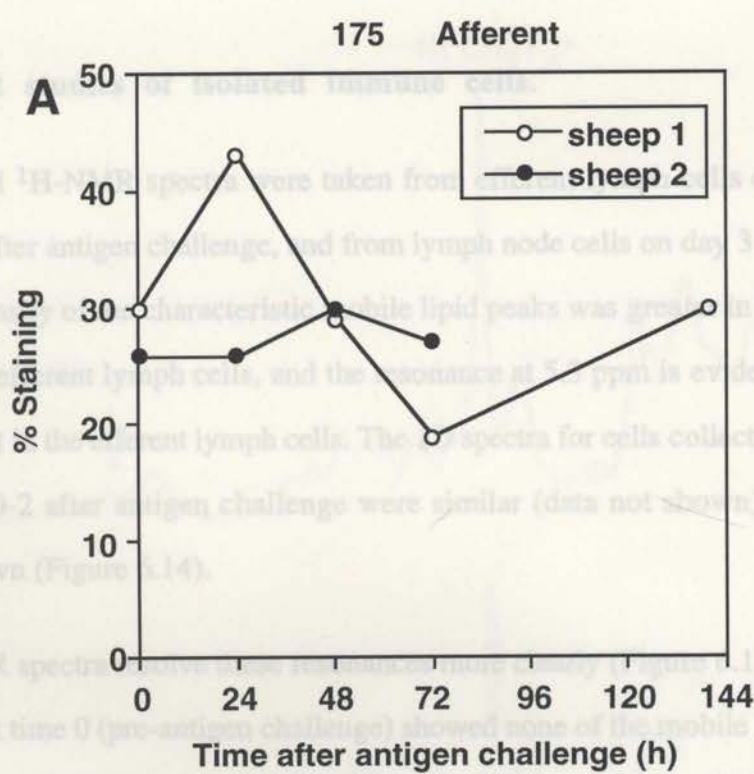


Figure 6.13. The percentage of cells expressing the 175 antigen. Cells collected from the afferent (A) and efferent (B) lymph vessels and lymph node cells (B) from BCG-primed sheep were labelled with 175 MAb. The results represent the percentage of cells expressing 175 detected using FCM, before and after PPD antigen challenge. The results from individual sheep are plotted. Lymph node (LN) (n=1 sheep, 2 lymph nodes) before antigen challenge, day 1 after challenge (n=1 sheep, 2 lymph nodes) and day 3 after challenge (n=3 sheep, 6 lymph nodes, mean±SEM).

6.2.8. $^1\text{H-NMR}$ studies of isolated immune cells.

One-dimensional $^1\text{H-NMR}$ spectra were taken from efferent lymph cells of BCG-primed sheep 0-2 days after antigen challenge, and from lymph node cells on day 3 after challenge. The relative intensity of the characteristic mobile lipid peaks was greater in the lymph node cells than in the efferent lymph cells, and the resonance at 5.3 ppm is evident in the lymph node cells but not in the efferent lymph cells. The 1D spectra for cells collected from afferent lymph on days 0-2 after antigen challenge were similar (data not shown) to the efferent lymph cells shown (Figure 6.14).

The 2D $^1\text{H-NMR}$ spectra resolve these resonances more clearly (Figure 6.15). Afferent and efferent lymph at time 0 (pre-antigen challenge) showed none of the mobile lipid resonances previously found to be associated with immune cell activation (Chapters 3-5). At day 1 after challenge (Figure 6.15C), the afferent spectrum does show some very weak resonances corresponding to the moieties of the fatty acid acyl chains A, E, B and F of the triglyceride structure (Figure 2.5). Resonances arising from cross-peak A are present in the efferent lymph on day 6 after antigen challenge (Figure 6.15 I). However, these results are not sufficient to conclude that the mobile lipid is present in these cells.

Cells from all BCG-primed lymph nodes, taken on days 1 and 3 after antigen challenge with PPD, generated 2D $^1\text{H-NMR}$ spectra displaying the characteristic lipid resonances from mobile lipid denoted A-G' (Figures 2.5 and 6.16, Table 6.1). Cross-peaks C and D were present on days 1 after treatment using PPD prepared either in incomplete Freund's adjuvant (IFA) or in normal saline (soluble). Cells from the unchallenged lymph node do display some mobile lipid cross-peaks, although the intensity is substantially lower than those collected from antigen-challenged cells (Table 6.1).

Representative 1D $^1\text{H-NMR}$ symmetrised spectra of lymph cells collected from sheep BCG-primed: efferent lymph cell control at day 0 ($n=3$) (A); and (B) efferent cells 2 days after BCG antigen challenge ($n=3$); (C) lymph node cells isolated 3 days after PPD antigen challenge ($n=6$).

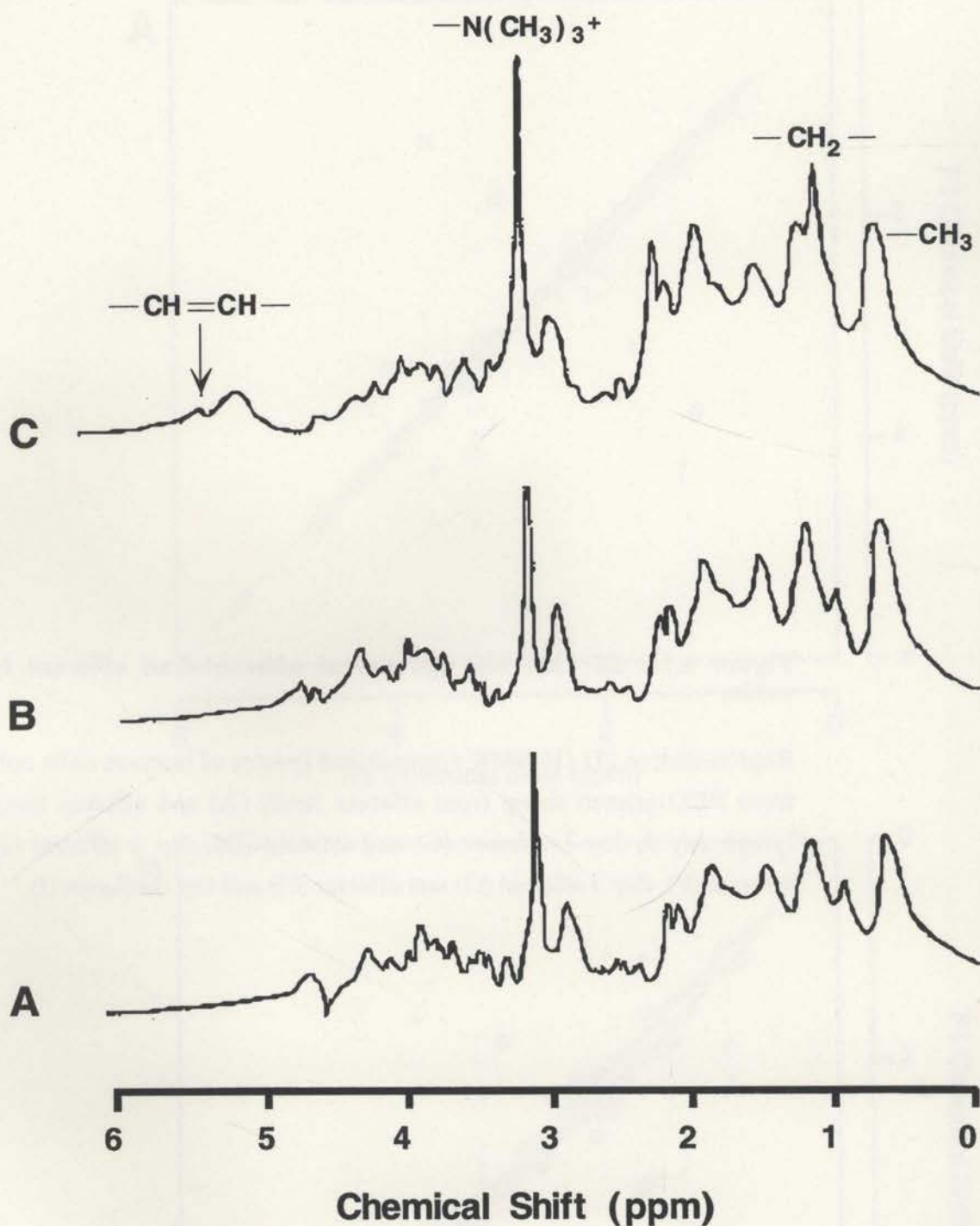
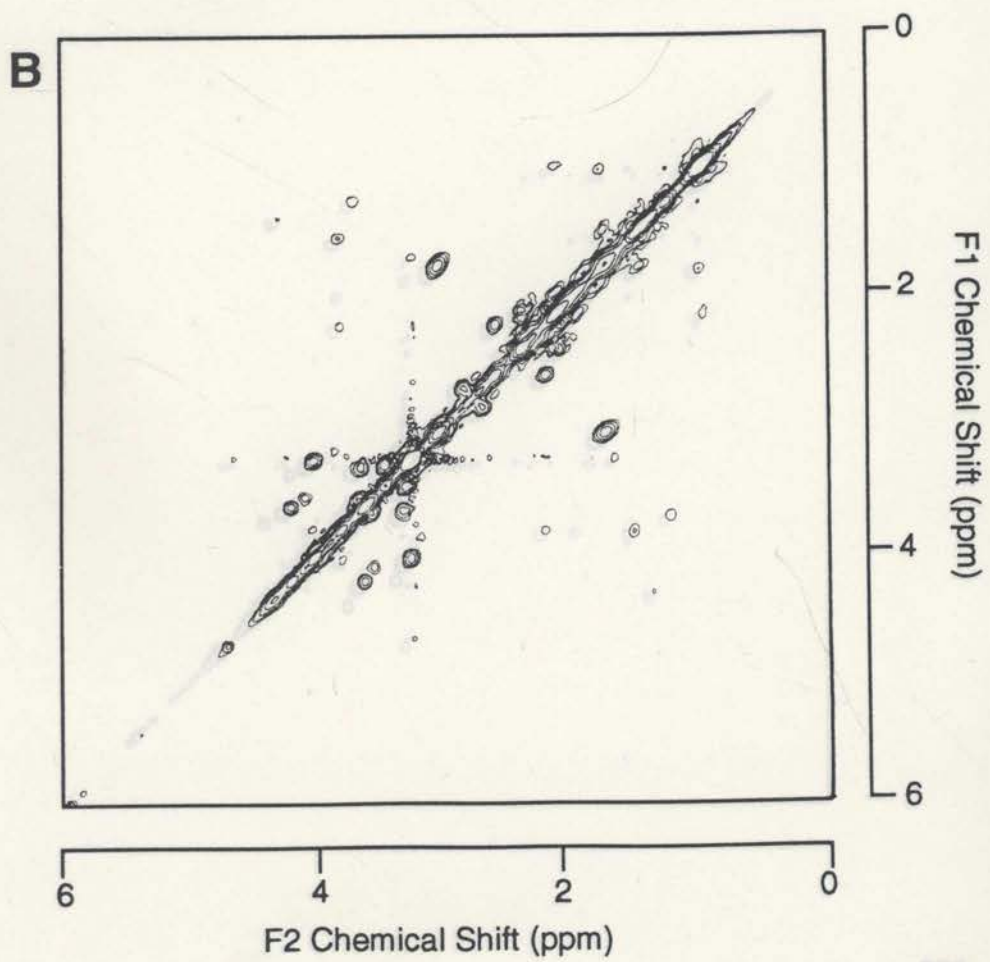
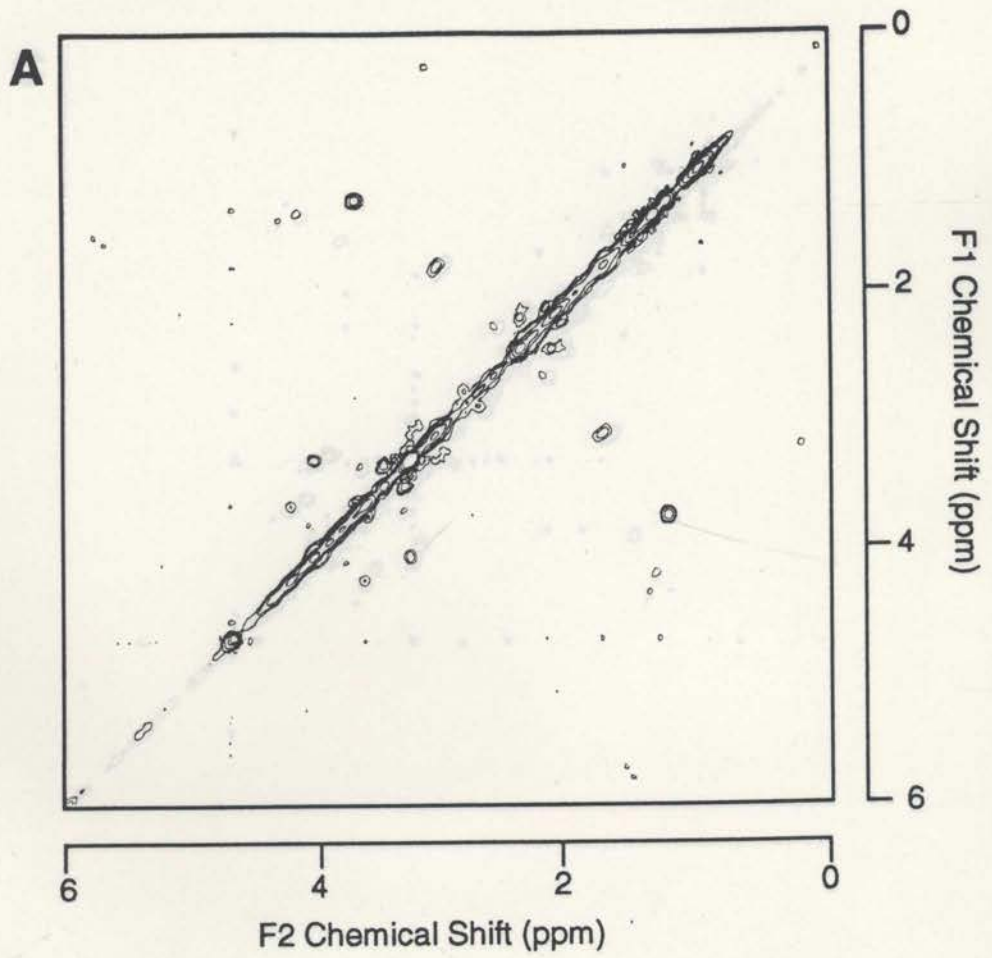


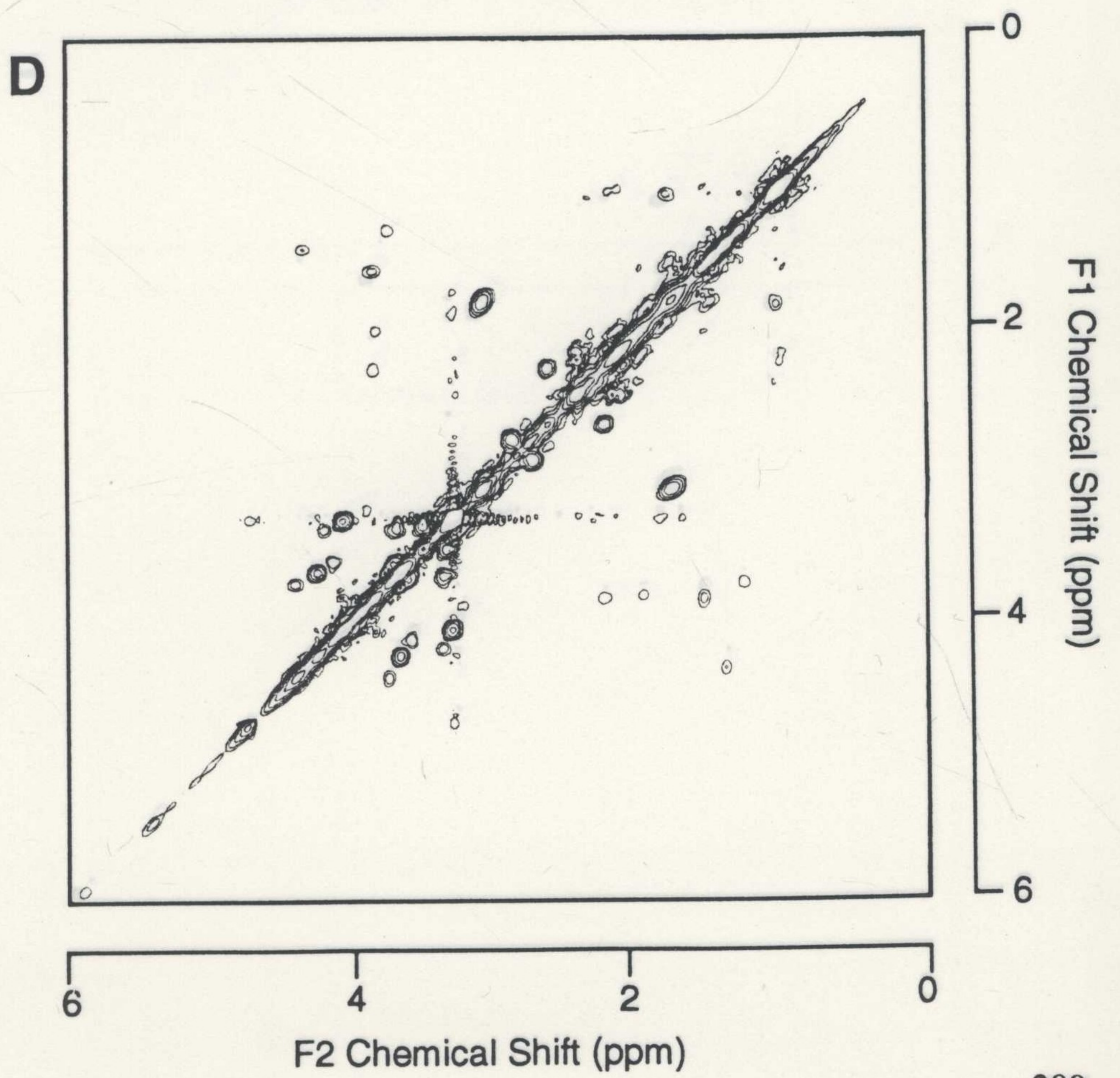
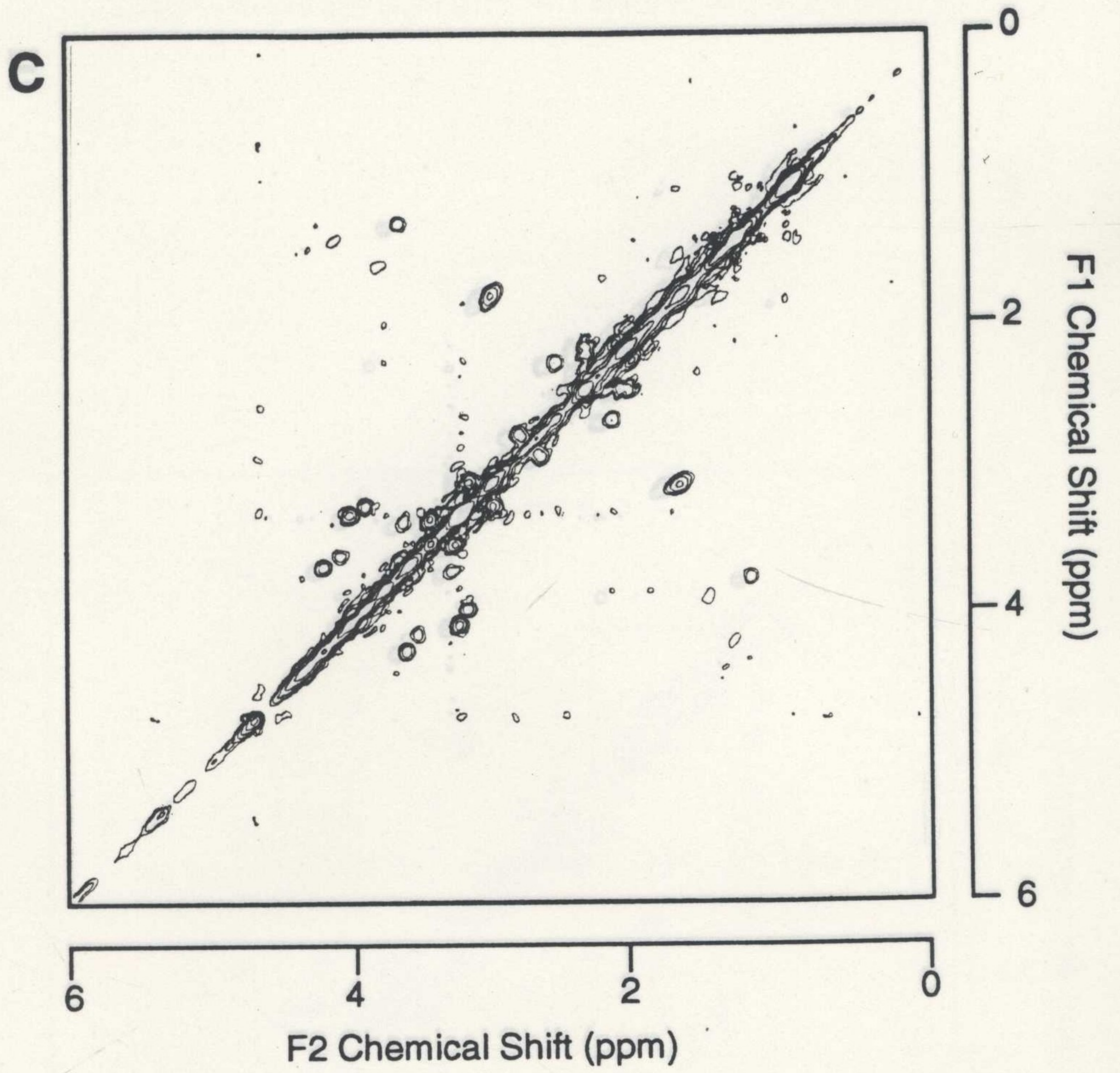
Figure 6.14. 1D ^1H -NMR spectra of lymph and lymph node cells.

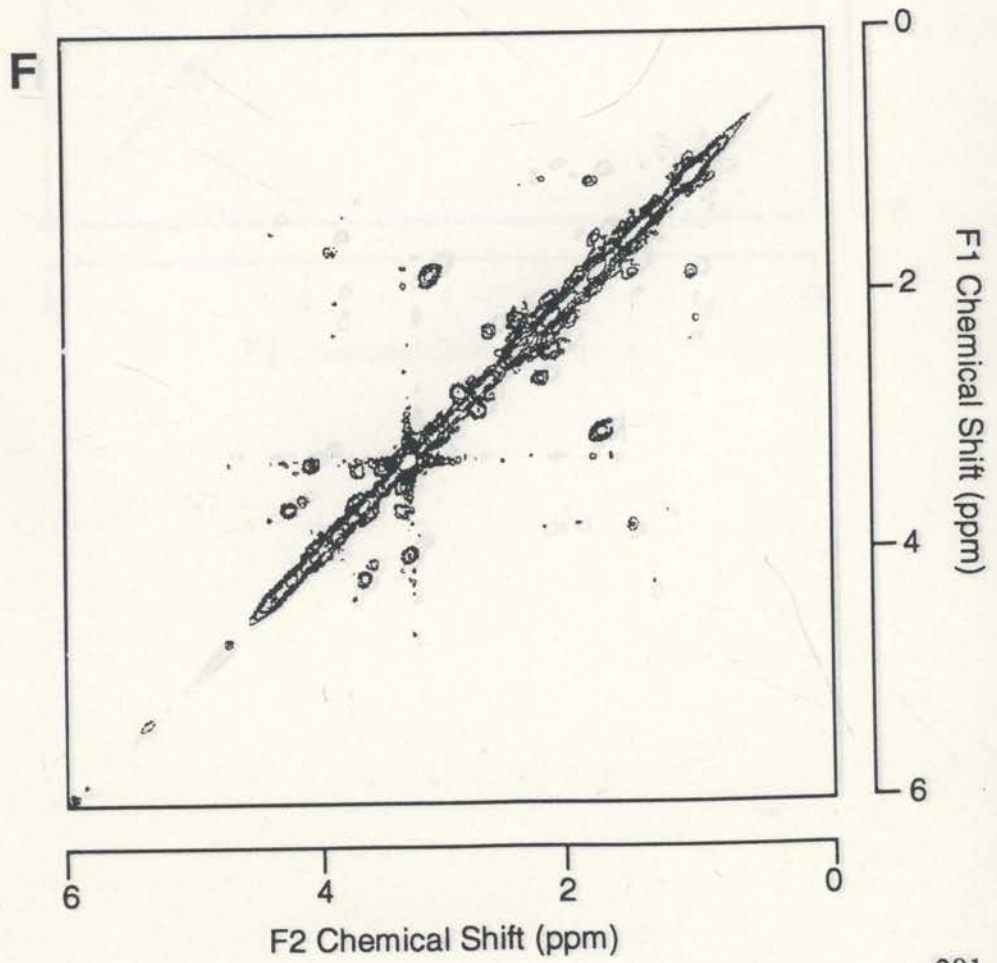
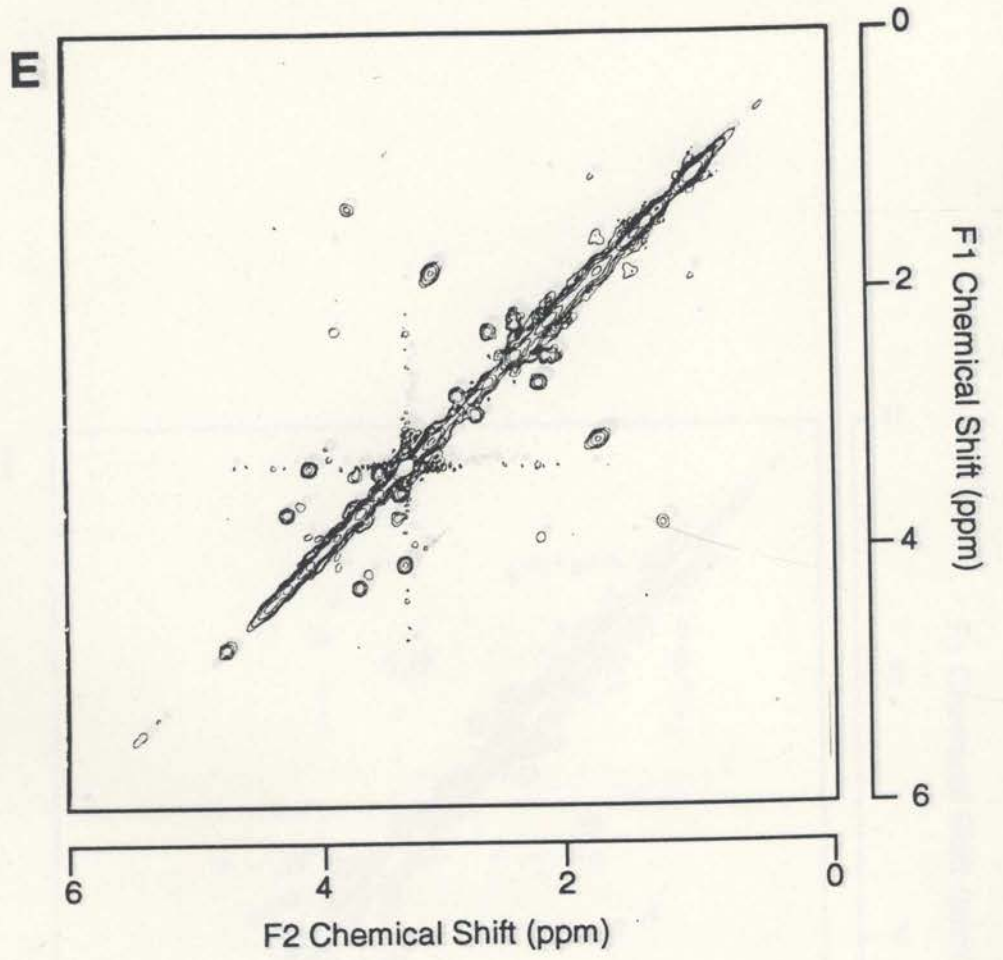
Representative 1D ^1H -NMR symmetrised spectra of lymph cells collected from sheep BCG-primed: efferent lymph cell control at day 0 ($n=3$) (A); and (B) efferent cells 2 days after BCG antigen challenge ($n=3$); (C) lymph node cells isolated 3 days after PPD antigen challenge ($n=6$).

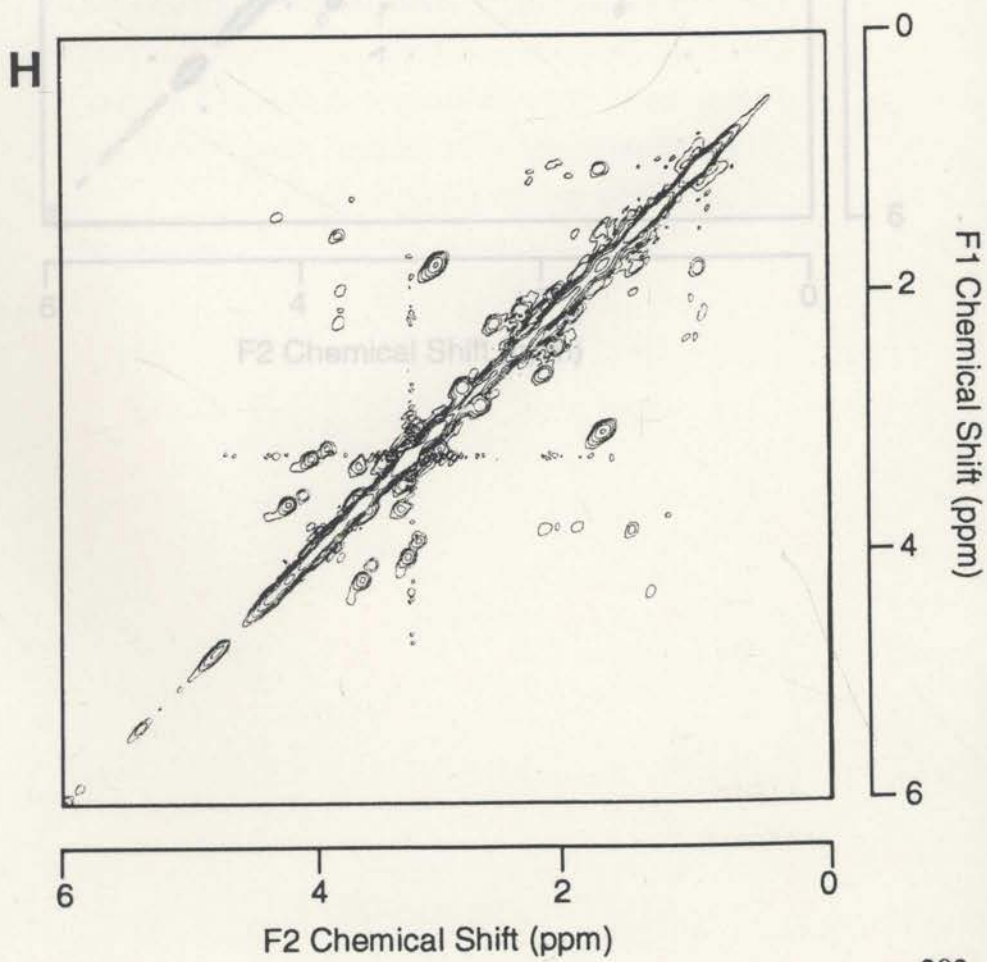
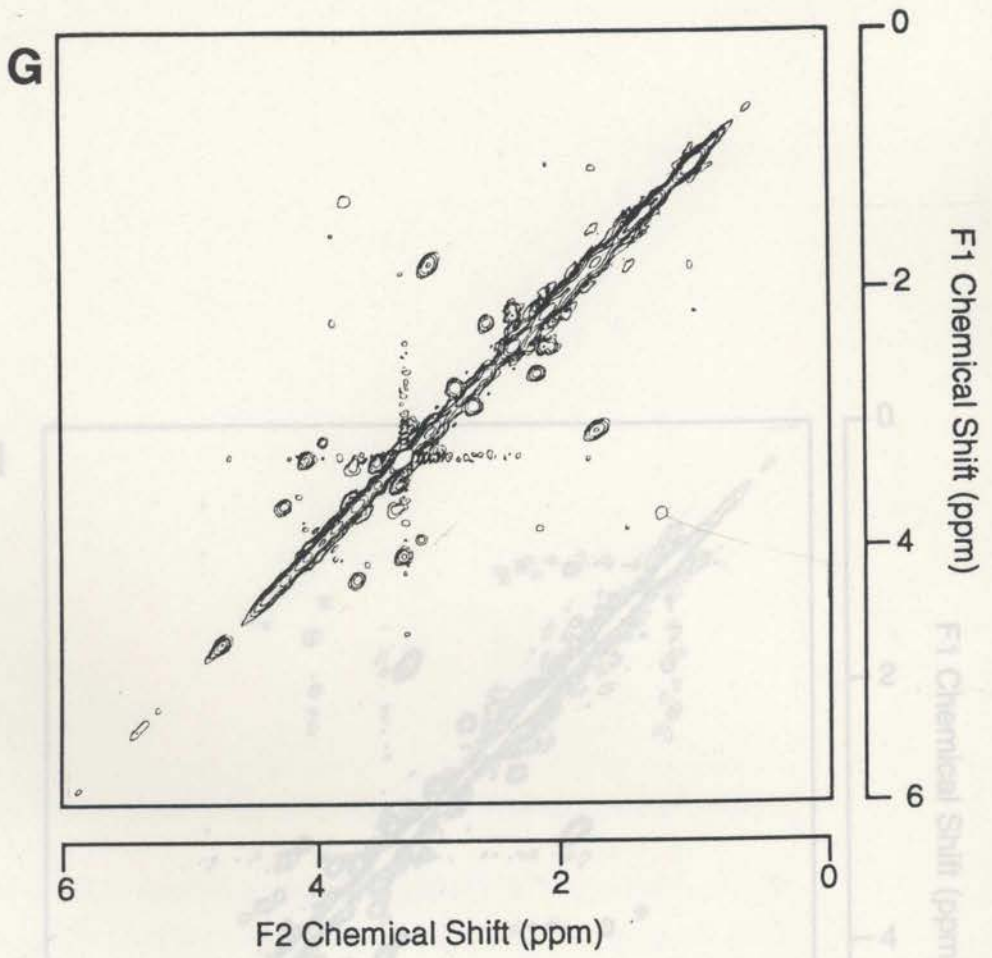
Figure 6.15. 2D $^1\text{H-NMR}$ spectra of afferent and efferent lymph cells.

Representative 2D $^1\text{H-NMR}$ symmetrised spectra of immune cells collected from BCG-primed sheep from afferent (n=2) (A) and efferent (n=3) (B) lymph day 0, day 1 afferent (C) and efferent (D), day 2 afferent (E) and efferent (F), day 3 afferent (G) and efferent (H) and day 6 efferent (I).









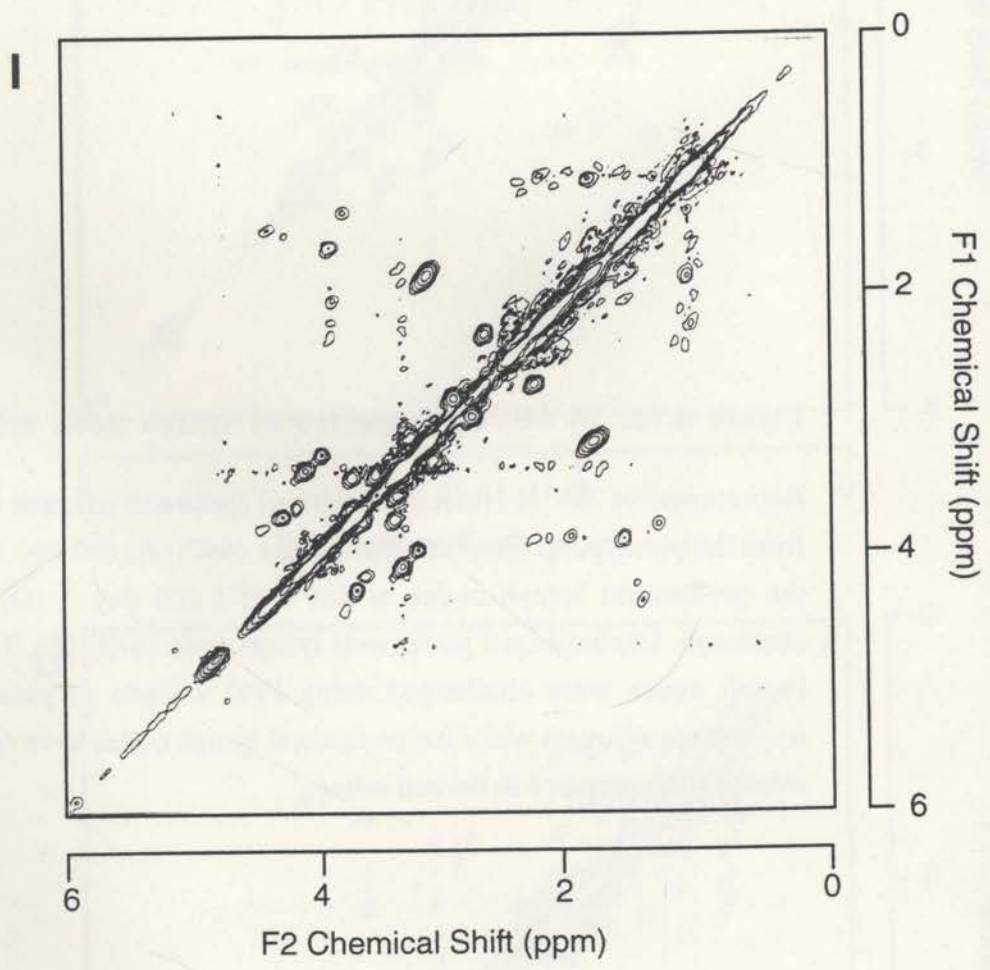
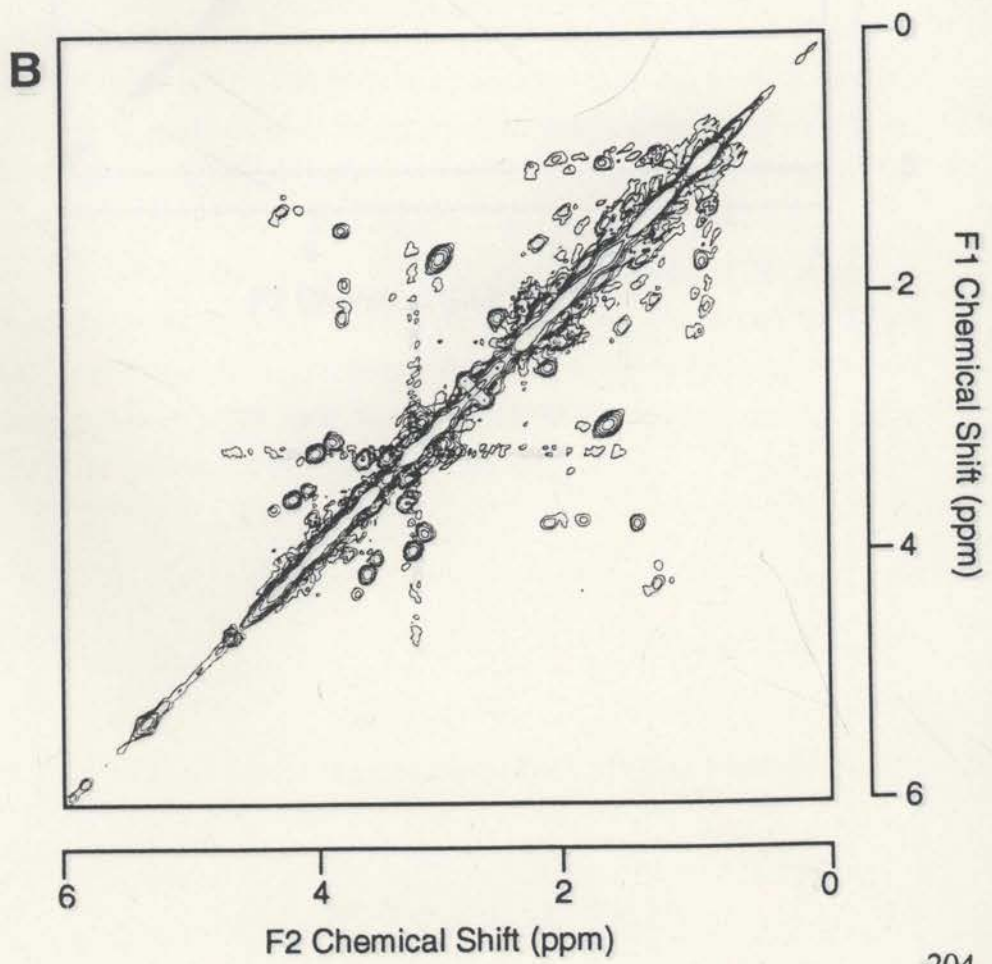
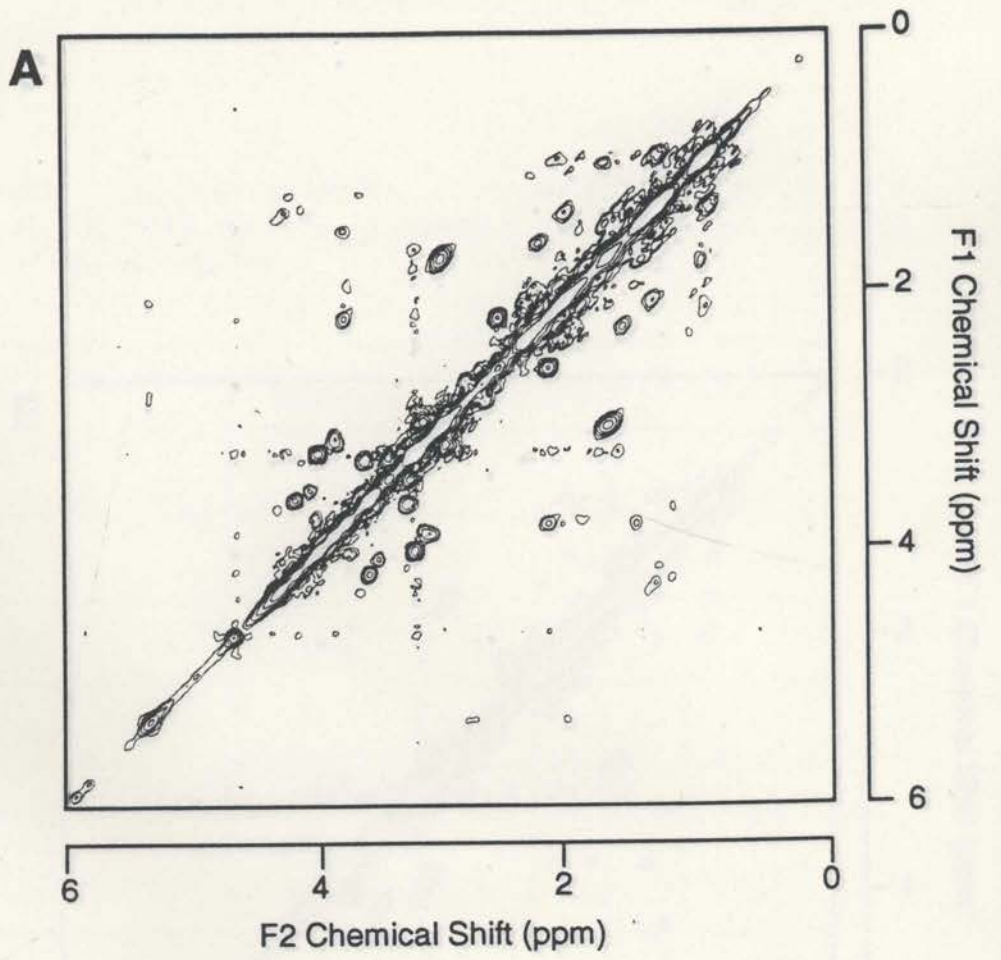


Figure 6.16. 2D ^1H -NMR spectra of lymph node cells.

Representative 2D ^1H -NMR symmetrised spectra of immune cells separated from the prescapular lymph nodes at day 1 (n=2) (A) and day 3 (n=2) (B) and the prefemoral lymph nodes at day 1 (C) and day 3 (D) after antigen challenge. Unchallenged prefemoral lymph node (n=2) (E). The prescapular lymph nodes were challenged using PPD antigen prepared in Freund's incomplete adjuvant while the prefemoral lymph nodes were challenged with soluble PPD prepared in normal saline.



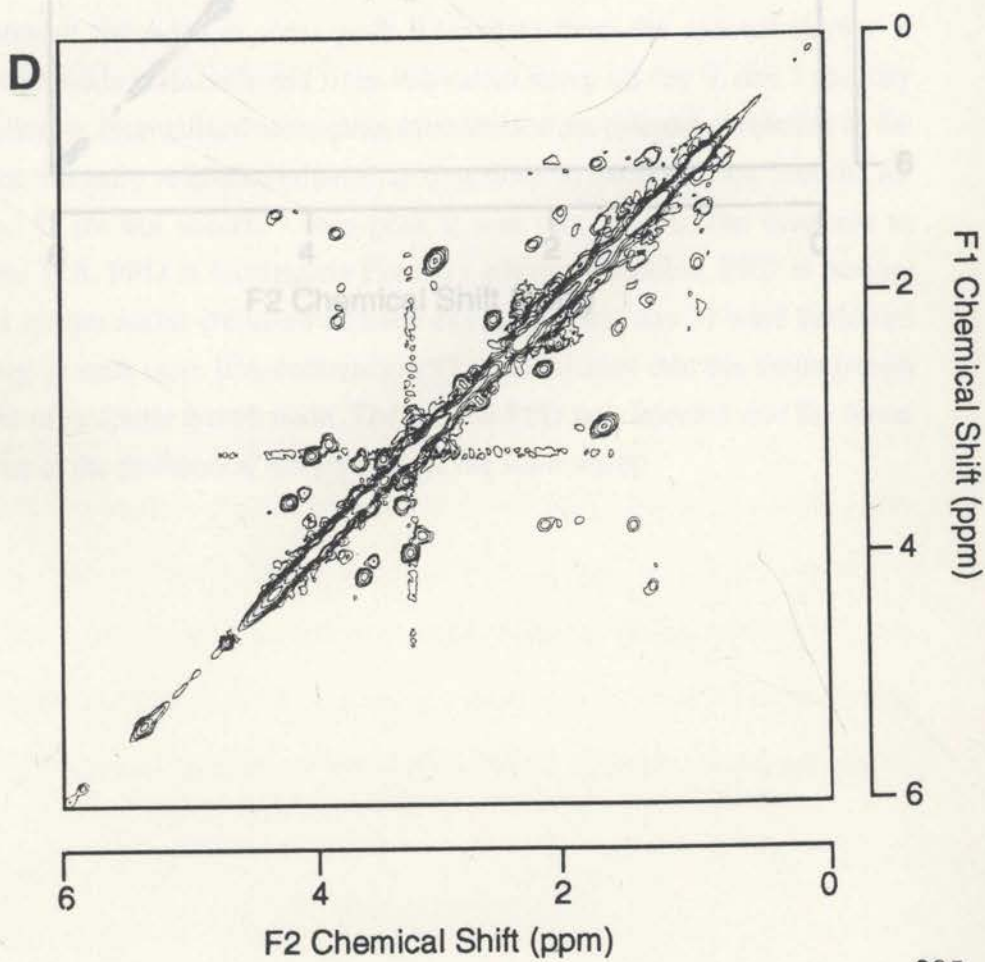
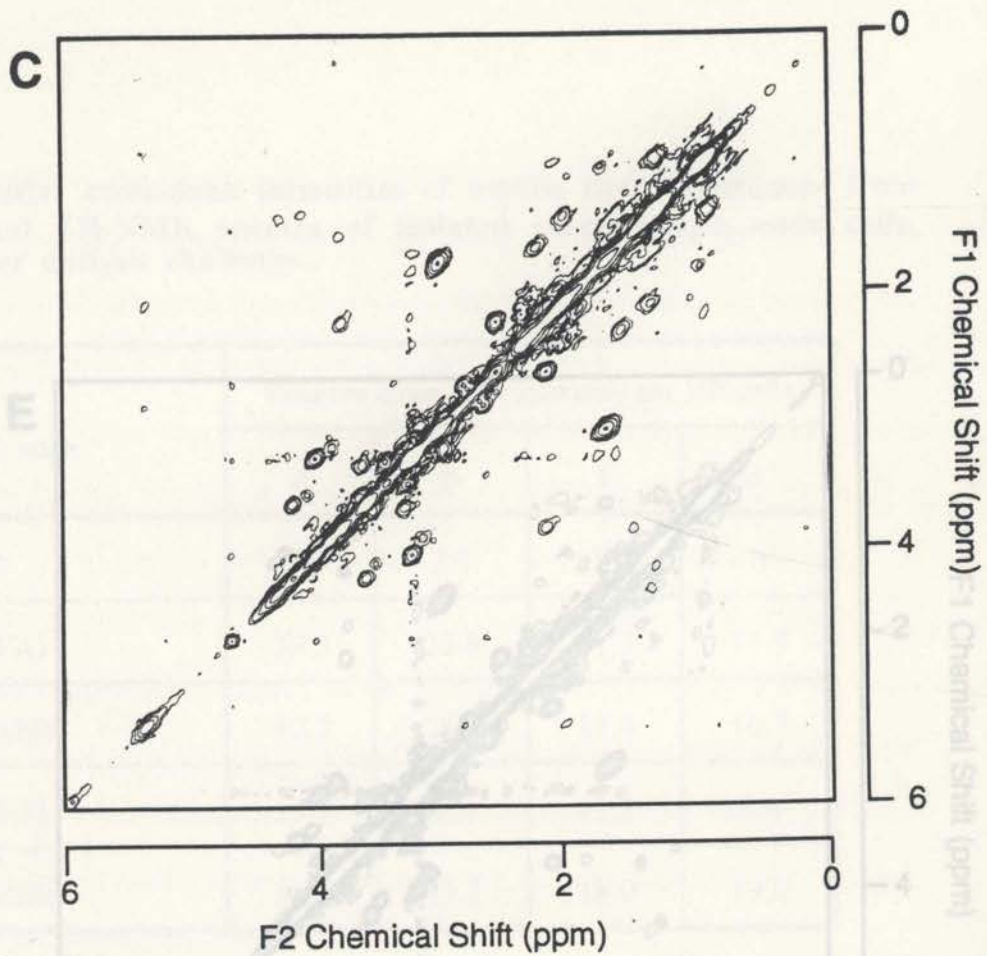
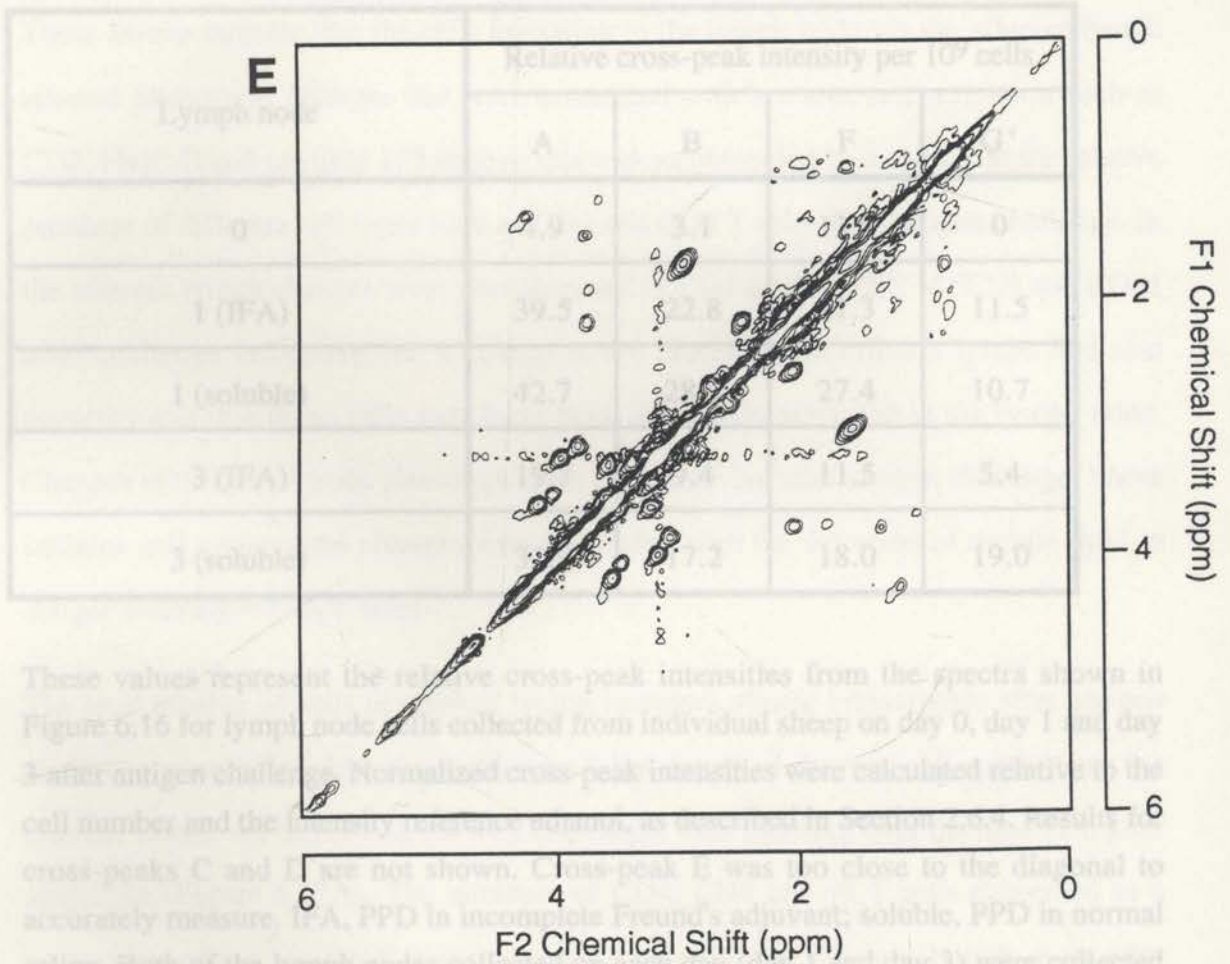


Table 6.1. Relative cross-peak intensities of mobile lipid resonances from two-dimensional ^1H -NMR spectra of isolated sheep lymph node cells, before and after antigen challenge.



These values represent the relative cross-peak intensities from the spectra shown in Figure 6.16 for lymph node cells collected from individual sheep on day 0, day 1 and day 3 after antigen challenge. Normalized cross-peak intensities were calculated relative to the cell number and the intensity of the internal standard as described in Section 2.3.4. Results for cross-peaks C and D are not shown. Cross-peak B was too close to the diagonal to accurately measure. IFA, PPD in incomplete Freund's adjuvant; soluble, PPD in normal saline. Both of the lymph nodes collected on each day (day 1 and day 3) were collected from the same sheep in each case. IFA containing PPD was injected into the tissue lymph draining area of the prescapular lymph node. The soluble PPD was injected into the tissue lymph draining area of the prefemoral lymph node of the same sheep.

6.2.9. Summary of Results.

Table 6.1. Relative cross-peak intensities of mobile lipid resonances from two-dimensional $^1\text{H-NMR}$ spectra of isolated sheep lymph node cells, before and after antigen challenge.

Lymph node	Relative cross-peak intensity per 10^9 cells			
	A	B	F	G'
0	4.9	3.1	13.0	0
1 (IFA)	39.5	22.8	21.3	11.5
1 (soluble)	42.7	28.9	27.4	10.7
3 (IFA)	19.7	9.4	11.5	5.4
3 (soluble)	31.9	17.2	18.0	19.0

These values represent the relative cross-peak intensities from the spectra shown in Figure 6.16 for lymph node cells collected from individual sheep on day 0, day 1 and day 3 after antigen challenge. Normalized cross-peak intensities were calculated relative to the cell number and the intensity reference ethanol, as described in Section 2.6.4. Results for cross-peaks C and D are not shown. Cross-peak E was too close to the diagonal to accurately measure. IFA, PPD in incomplete Freund's adjuvant; soluble, PPD in normal saline. Both of the lymph nodes collected on each day (day 1 and day 3) were collected from the same sheep in each case. IFA containing PPD was injected into the tissue lymph draining area of the prescapular lymph node. The soluble PPD was injected into the tissue lymph draining area of the prefemoral lymph node of the same sheep.

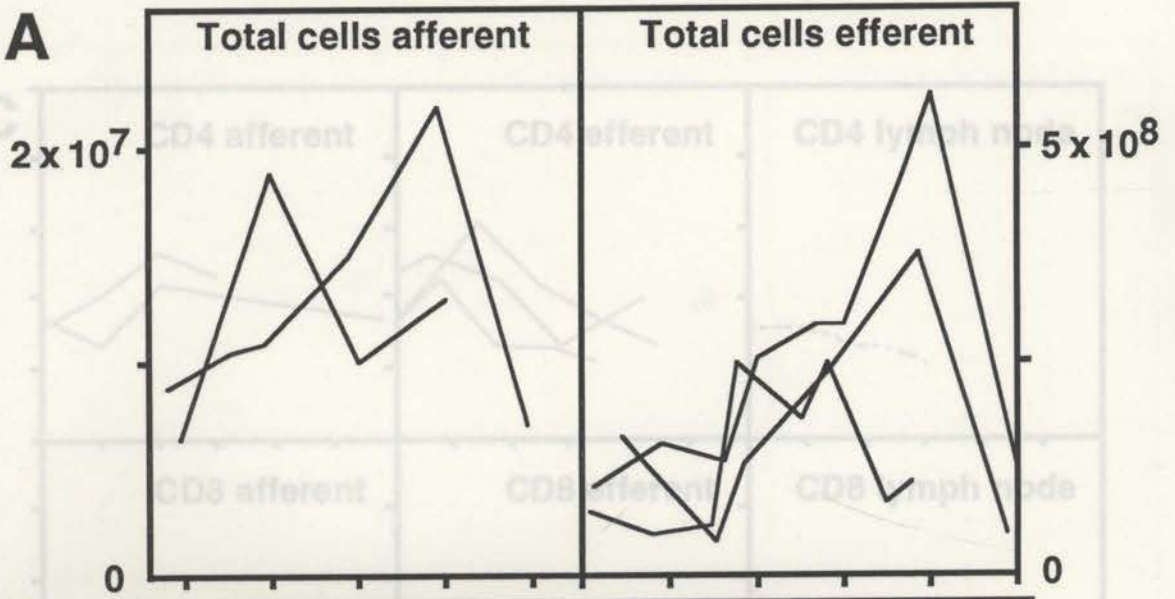
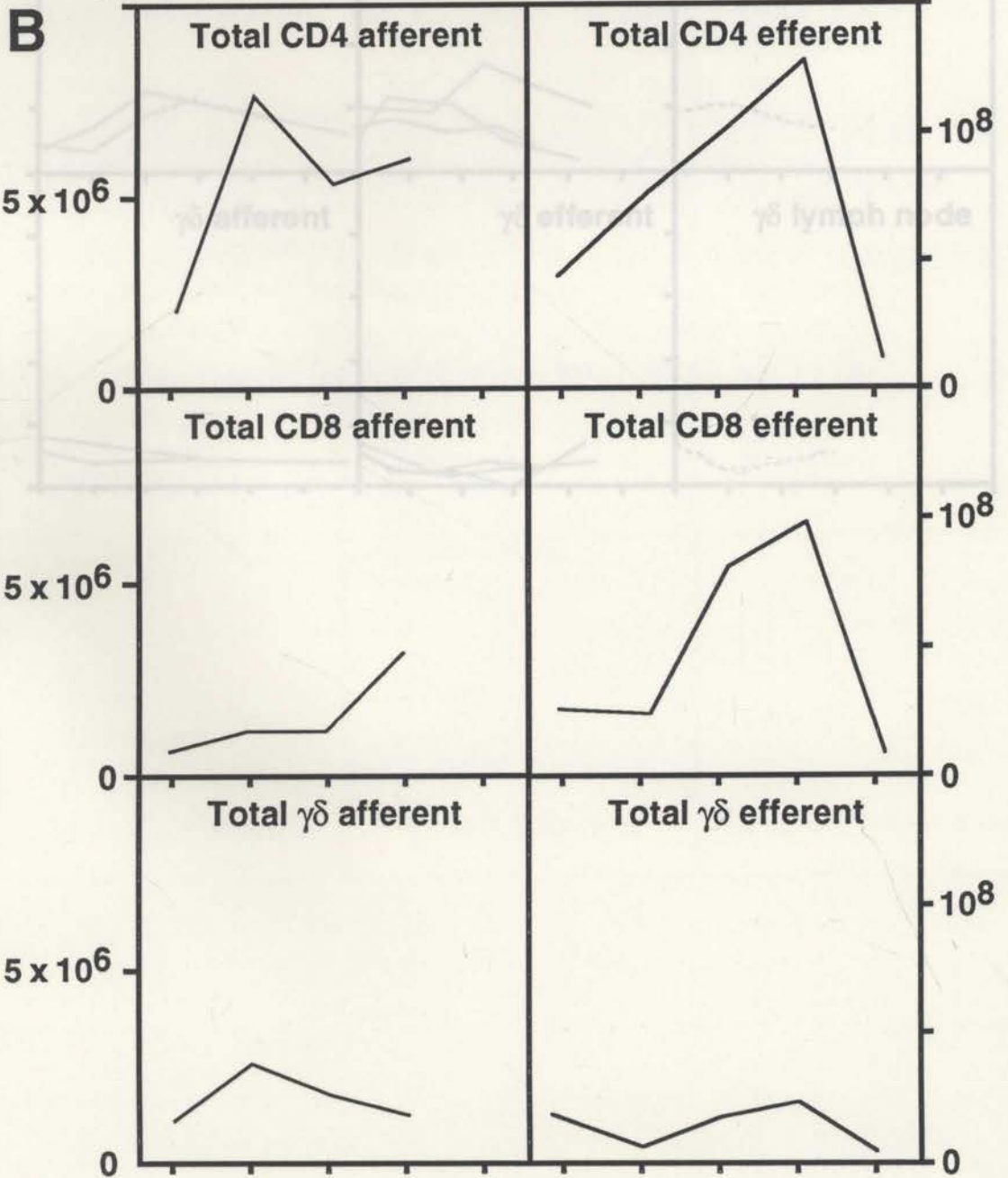
6.2.9. Summary of Results.

The results presented in this Chapter are summarised in Figures 6.17 and 6.18. Results from individual sheep were plotted to show the variations between these outbred animals. In this summary the data for particular phenotypes were plotted together for comparison. These results indicate that the cells migrating to the lymph node via the afferent lymph showed phenotypic changes that were associated with immune cell activation such as CD2, MHC II and possibly 175 antigen this was accompanied by a change in the relative numbers of different cell types such as CD4 and CD8 T cells after antigen challenge. In the efferent lymph changes were also observed in CD2 and CD45R, MHC II and CD21 after challenge indicating that a change in the phenotype in efferent lymph had also occurred and that these cells may have been previously activated in the lymph node. Changes in the lymph node phenotype were also occurring after antigen challenge. These immune cell activation changes were correlated with the detection of mobile lipid in antigen challenged lymph nodes.

The total number of cells in afferent lymph increases almost immediately after antigen challenge, accompanied by a simultaneous "shut down" of the total cell output from the efferent vessel. An increase in the total cell output then followed over the next 72 h after challenge (Figure 6.17A). The numbers of CD4, CD8 and $\gamma\delta$ T cells expressed as a proportion of the total cell output per hour increased in afferent lymph soon after challenge, and after 48-72 h in efferent lymph (Figure 6.17B). The total number of cells increased. The proportion of cells expressing CD4 and CD8 also increased. On the other hand, the increase in the number of cells expressing the $\gamma\delta$ TCR was proportional to the increase in the total number of cells. In the lymph node the proportion of cells expressing CD4 and CD8 declined slightly after antigen challenge, while the proportion of $\gamma\delta$ T cells increased after challenge (Figure 6.17C), although caution is needed when analysing these data because of the small numbers of sheep used and the large individual variation.

Figure 6.17. Summary of effects of antigen challenge upon total numbers of cells and T cell subsets.

Data presented in Figures 6.1 and 6.2 are summarized. (A) Cells were counted using a haemocytometer. Afferent lymph data from 2 sheep and efferent lymph data from 3 sheep are shown. The vertical axes represent cell numbers collected per hour, with different scales on the left and on the right, as indicated. (B) T cell subsets were identified using MAb staining for CD4, CD8 and $\gamma\delta$ TCR, and detected using FCM. All data plotted is from individual sheep, including two sheep which for clarity were not included in Figure 6.2. Vertical axes represent cell numbers collected per hour, with different scales on the left and on the right, as indicated. Horizontal axes represent increments in time of 24 hours. The time of antigen challenge was immediately after the first time point. (C) Percentage of T cell subsets staining for CD4, CD8 and $\gamma\delta$ TCR expression. The proportion of cells in each subset are represented as the percentage of the total number of cells collected per hour. The horizontal axes represent 24 hour increments, beginning immediately after antigen challenge.

A**B**

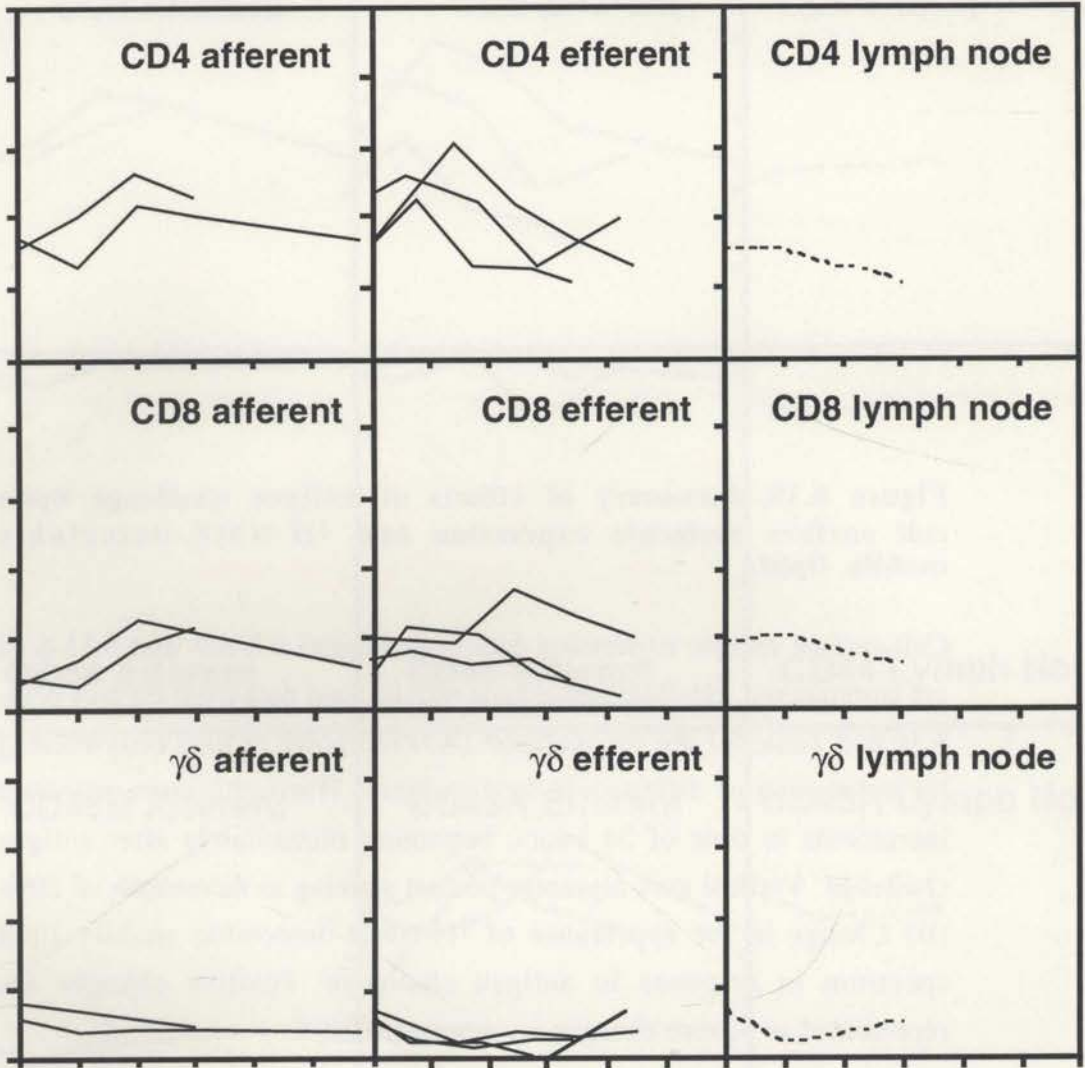
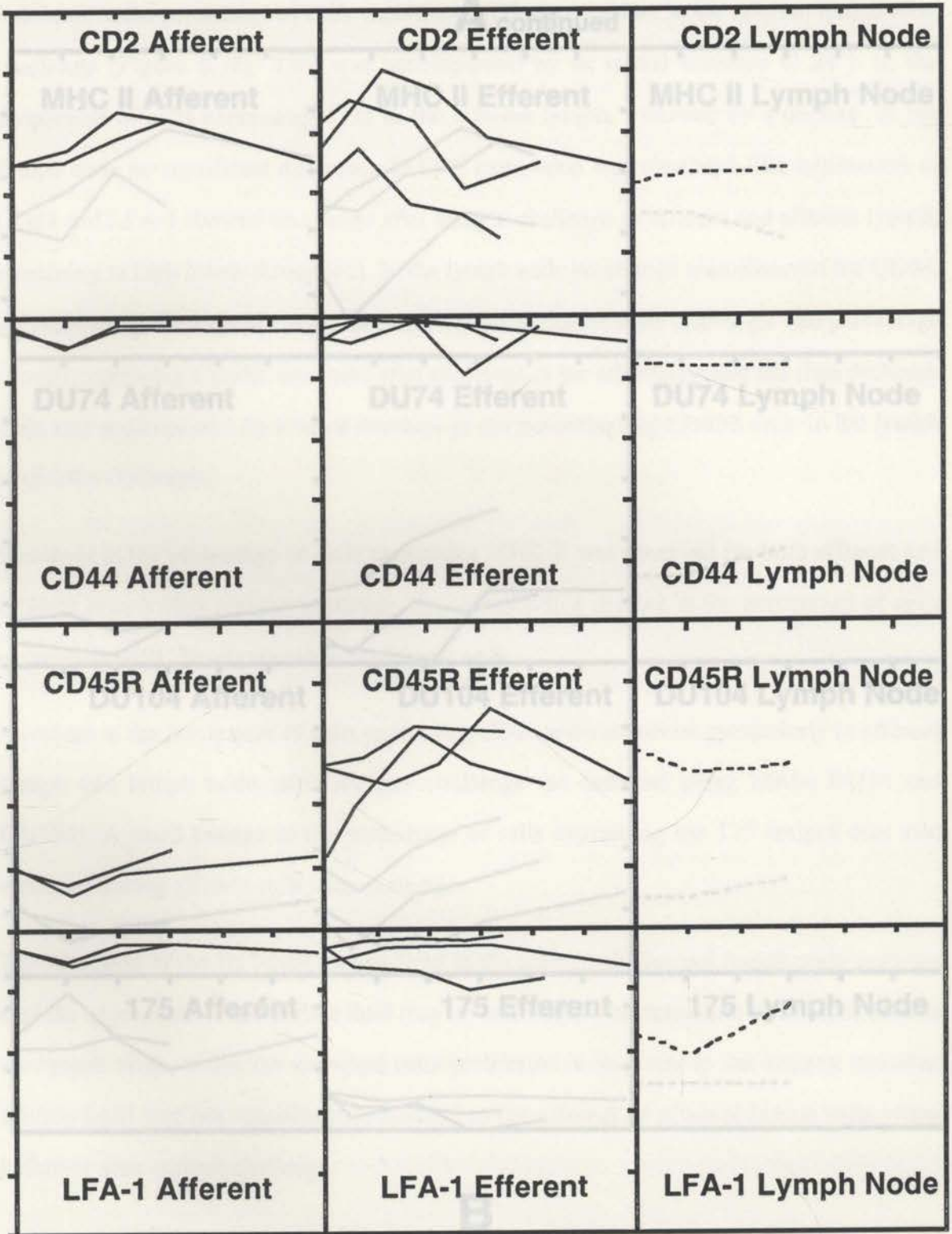
C

Figure 6.18. Summary of effects of antigen challenge upon cell surface molecule expression and ¹H-NMR-detectable mobile lipid.

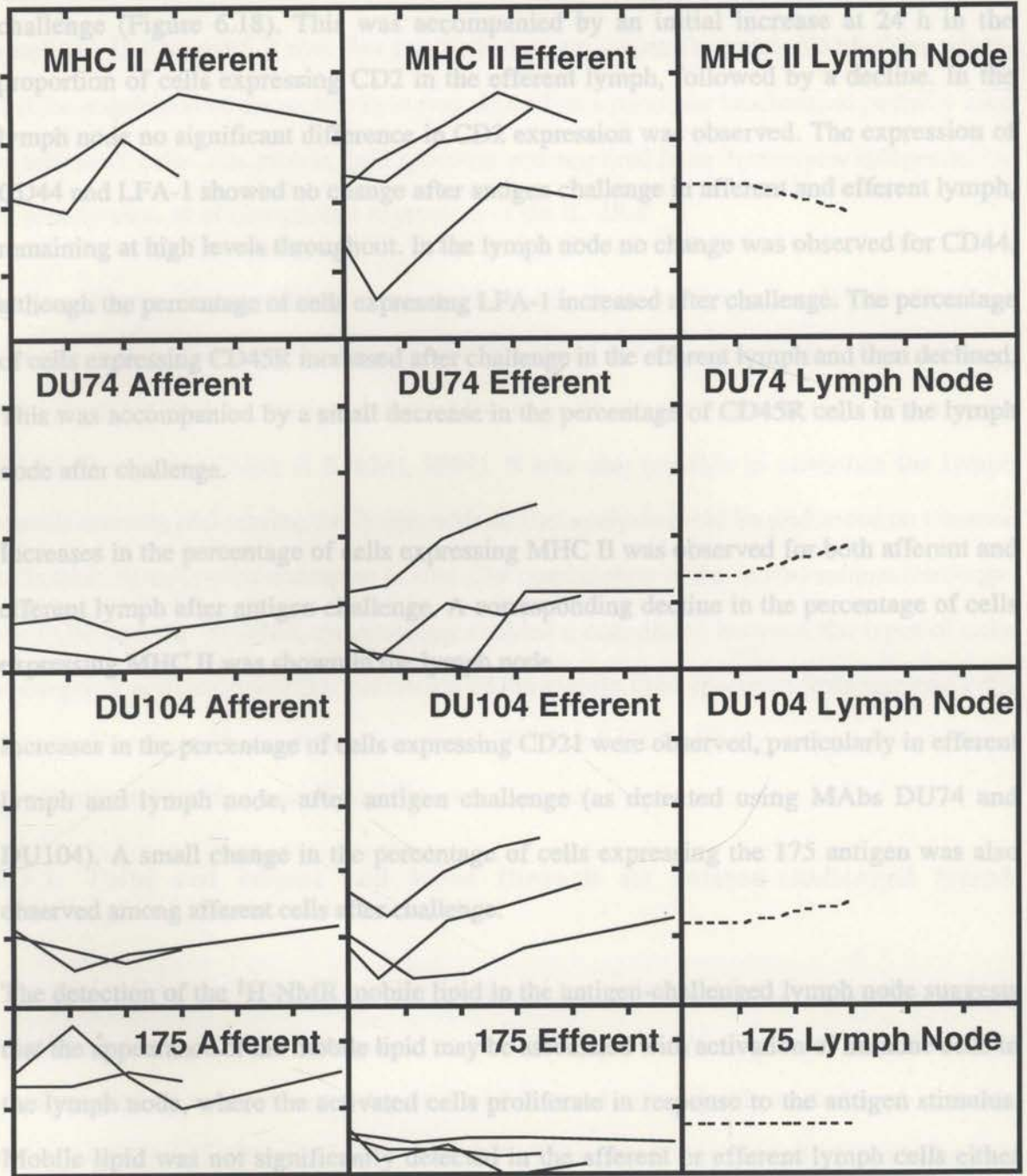
Cell surface antigen expression data from Figures 6.5-6.9. and 6.11-6.13 are summarized. ¹H-NMR-detectable mobile lipid data from Figures 6.14-6.16 and Table 6.1 are summarized. (A) Percentage of total cells staining for expression of different surface antigens. Horizontal axes represent increments in time of 24 hours, beginning immediately after antigen challenge. Vertical axes represent percent staining in increments of 20%. (B) Change in the appearance of ¹H-NMR-detectable mobile lipid spectrum in response to antigen challenge. Positive changes are represented as +, zero changes are represented as 0.

A



Changes in ¹ H-NMR-detectable mobile lipid after antigen challenge		
afferent	efferent	lymph node
0	0	++

A continued



B

Changes in ¹ H-NMR-detectable mobile lipid after antigen challenge		
afferent	efferent	lymph node
0	0	++

Chapter 5 where, for the first time, the activation status of T cells, identified by the increases in the percentage of cells expressing CD2 were evident in the afferent lymph after challenge (Figure 6.18). This was accompanied by an initial increase at 24 h in the proportion of cells expressing CD2 in the efferent lymph, followed by a decline. In the lymph node no significant difference in CD2 expression was observed. The expression of CD44 and LFA-1 showed no change after antigen challenge in afferent and efferent lymph, remaining at high levels throughout. In the lymph node no change was observed for CD44, although the percentage of cells expressing LFA-1 increased after challenge. The percentage of cells expressing CD45R increased after challenge in the efferent lymph and then declined. This was accompanied by a small decrease in the percentage of CD45R cells in the lymph node after challenge.

Increases in the percentage of cells expressing MHC II was observed for both afferent and efferent lymph after antigen challenge. A corresponding decline in the percentage of cells expressing MHC II was shown in the lymph node.

Increases in the percentage of cells expressing CD21 were observed, particularly in efferent lymph and lymph node, after antigen challenge (as detected using MAbs DU74 and DU104). A small change in the percentage of cells expressing the 175 antigen was also observed among afferent cells after challenge.

The detection of the $^1\text{H-NMR}$ mobile lipid in the antigen-challenged lymph node suggests that the appearance of the mobile lipid may be associated with activation of immune cells in the lymph node, where the activated cells proliferate in response to the antigen stimulus. Mobile lipid was not significantly detected in the afferent or efferent lymph cells either before or after antigen challenge.

6.3. Discussion.

In the previous Chapters the presence of the $^1\text{H-NMR}$ -detectable mobile lipid spectrum has been associated with the *in vitro* activation of murine lymphocytes (Chapters 4 & 5). In Chapter 4 the mobile lipid in lymphocytes was suggested to arise from phosphatidylcholine turnover resulting from cellular activation and proliferation. This was investigated further in

Chapter 5 where, for the first time, the activation status of T cells, identified by the expression of the IL-2R α on stimulated T cells, was correlated with the mobile lipid spectrum. In Chapter 5 it was also established, using a specific metabolic blocking agent, that the acquisition of the mobile lipid may depend on a particular biochemical pathway used to activate T cells. The mobile lipid spectrum was acquired from thymocytes independently of proliferation or of upregulated expression of the IL-2R α .

6.3.2. Recirculation of T cells through lymph node before and after antigen challenge.

In this Chapter the correlation between the mobile lipid and immune cell activation was investigated further using a sheep model stimulated *in vivo* with antigen. Using a large animal model enabled the collection of the large number of immune cells required for $^1\text{H-NMR}$ analysis (King & Kuchel, 1994). It was also possible to cannulate the lymph vessels entering and leaving the lymph node so that analysis could be performed on immune cells taken directly after activation *in vivo*. The combination of the *in vivo* antigen challenge, the FCM and the $^1\text{H-NMR}$ spectroscopy enabled a correlation between the types of cells undergoing activation and the generation of the mobile lipid spectrum from immune cells activated *in vivo*. This combination of the FCM and $^1\text{H-NMR}$ has not previously been employed, and enabled unique correlations to be made.

6.3.1. Total cell output and input through an antigen-challenged lymph node.

The total cell input via the afferent lymph vessel to the draining lymph node after antigen challenge was increased compared to pre-challenge levels (Figure 6.1A). This was accompanied by a simultaneous depression of the total cell output from the lymph node via the efferent lymphatic vessels (Figure 6.1B). These results are consistent with the first reports using cannulation techniques of efferent lymphatic vessels and antigen-challenged lymph nodes in sheep, which showed a decrease in the total efferent cell output immediately after antigen challenge (Hall & Morris, 1962; Hall & Morris, 1963). This is described as a "shut down" period after antigen challenge. A "recruitment" phase follows, during which the total cell output increases due to an increase in blood flow to the lymph node (Hay & Hobbs, 1977) and cell traffic through the lymph node in response to antigen challenge (Hall & Morris, 1963; Hall & Morris, 1965a; Cahill *et al.*, 1976; Yirrell *et al.*, 1991; MacKay *et*

et al., 1992a). Such an increase in the cell output occurred 24 h after antigen challenge in this study, with a corresponding increase in the total cell input into the lymph node via the afferent lymphatics (Figures 6.1, 6.17). This response has also been observed in chronically inflamed sheep tissue, where a significantly higher hourly cell output in antigen-stimulated afferent and efferent lymph occurred (Kimpton *et al.*, 1990).

6.3.2. Recirculation of T cells through lymph node before and after antigen challenge.

The percentage of T cell subsets in the afferent and efferent lymph of individual sheep (Figure 6.2C-G) show that, with the exception of $\gamma\delta$ T cells, there were similar increases in the proportion of the different T cell subsets. The percentage of CD4 T cells in the afferent and efferent lymph and lymph node of BCG-primed sheep before antigen challenge were similar (Figure 6.2). The percentage of CD8 T cells was slightly higher in efferent lymph and lymph node than in afferent lymph. Other studies have shown that the pattern of recirculation of the T cell subsets in unchallenged animals had similar proportions of CD4 T cells in the afferent and efferent lymph (Kimpton *et al.*, 1990). A larger proportion of CD8 positive cells are found in the efferent lymph and a greater proportion of $\gamma\delta$ T cells were identified in the afferent lymph (Kimpton *et al.*, 1990; MacKay *et al.*, 1990). However, it was also shown in another previous study that similar levels of CD4 and CD8 T cells in afferent and efferent lymph and lymph node, but a greater proportion of $\gamma\delta$ T cells were present in the afferent lymph (MacKay *et al.*, 1988b).

The CD4 and CD8 T cell subsets were shown to increase rapidly in number and proportion in both afferent and efferent lymph in BCG-primed animals after secondary challenge with PPD antigen (Figure 6.2). Other studies have also shown that in primed-animals the T cell composition of efferent lymph draining from an antigen-stimulated lymph node showed an increase in the numbers of CD4 cells followed by an increase in the number of CD8 cells (Bujdoso *et al.*, 1989b; MacKay *et al.*, 1992a). Mackay *et al.* (1992) have shown that the proportions of CD4 and CD8 T cells in efferent lymph increase for up to 72 h after antigen challenge and then begin to decrease (MacKay *et al.*, 1992a). This is also consistent with the results shown in this study where the numbers of CD4 and CD8 T cells increased in afferent

and efferent lymph at earlier time periods after antigen challenge and then decreased after 72 h of activation (Figure 6.2).

This is clearly an immune activation response. CD4 is expressed on T-helper cells and acts as a co-receptor with the TCR to enhance T cell activation. It also acts as a co-stimulatory molecule for signal transduction (Parnes, 1989; Sleckman *et al.*, 1991). CD8 is expressed on cytotoxic and NK cells and acts to bind to MHC I on target cells. It too enhances T cell activation via signal transduction (Parnes, 1989; Salter *et al.*, 1990).

The numbers of $\gamma\delta$ T cells increased in efferent lymph at 48 and 72 h after antigen challenge. In the afferent lymph the numbers of $\gamma\delta$ T cells increased within the first 24 h and then slowly decreased over 48-72 h. The changes in total $\gamma\delta$ T cell hourly output showed that the number of $\gamma\delta$ T cells followed the pattern of the CD4 and CD8 T cells, in that they increased immediately after challenge in afferent lymph but reflected "shut down" in efferent lymph (Figure 6.2). However, the proportion of $\gamma\delta$ T cells did not substantially change in the afferent and efferent lymph after antigen challenge (Figures 6.2C, 6.2D, and 6.17). This illustrates the need to plot the percentage of cells staining for a cell surface marker rather than only as the proportion of the total cell output/h, because the numbers and proportions of cells after antigen challenge can change differently. $\gamma\delta$ T cells do not express CD4 or CD8. In sheep $\gamma\delta$ T cells have been recognised to express a transmembrane protein T 19 (McClure & Hein, 1989; Evans *et al.*, 1994). These cells can directly bind and respond to bacterial antigens (Evans *et al.*, 1994; Kaufmann, 1996). Thus, the increase in $\gamma\delta$ T cell numbers reflects a response to the bacterial antigen PPD.

6.3.3. Differential cell surface expression of CD2, CD44, CD45R and LFA-1 in afferent and efferent lymph vessels and lymph node, before and after antigen challenge.

The expression of a number of cell surface receptors are altered in memory or activated T cells. Some of the molecules that can be upregulated include CD2 (MacKay *et al.*,

1992b), CD44 and LFA-1 (MacKay *et al.*, 1990). CD45R, an isoform of CD45 (MacKay *et al.*, 1992b), has been shown to have a different pattern of staining on naive and memory T cells. In this study CD2, CD44 and LFA-1 were shown to be upregulated in afferent compared to efferent lymph. CD45R showed different patterns of staining in afferent lymph compared to efferent lymph and lymph node cells. Comparative FCM histograms of afferent lymph, efferent lymph and lymph node cells before antigen challenge show that the overall peak fluorescence is increased for CD2, CD44 and LFA-1 in afferent lymph compared to the lymph node and efferent lymph, possibly indicating an upregulation of these surface molecules in some of the populations of cells. Whether this is due to the proportion of memory T cells present in these mixed cell populations in the afferent lymph or to higher levels of expression on individual cells is difficult to assess. Further studies using double labelling techniques for other T cell markers would need to be done in conjunction with CD2, CD44 and LFA-1 MAb staining. The results obtained certainly highlight the differences in the distribution of cells in the different tissue sites which may reflect the differences in the patterns of recirculation of specific cell types. These patterns of staining will be discussed further together with the other data obtained after antigen challenge.

CD2.

The peak fluorescence staining for CD2 was increased in afferent lymph, although a small proportion of the brightly staining cells in the efferent were also present in the efferent lymph and lymph node (Figure 6.3). This indicates some diversity in the expression of CD2 in the cells in all three tissue locations before antigen challenge. The proportion of cells expressing CD2 in the afferent lymph increased after antigen challenge (Figure 6.5A). While the number of cells in the efferent lymph expressing CD2 increased during the first 12 h after antigen challenge, followed by a decrease in the proportion of cells expressing CD2 over the next 72 h (Figure 6.5B). No significant change was observed in the proportion of CD2 cells in the lymph node after antigen challenge.

These observations may be explained by the differential expression of CD2 on sheep CD4⁺ and CD8⁺ T cells but not on $\gamma\delta$ T cells (Giegerich et al., 1989; MacKay et al., 1990). CD2⁺ T cells adhere to dendritic cells in afferent lymph. The interaction of the ligand LFA-3 with CD2 may provide the mechanism of adherence for the T cell and the antigen presenting dendritic cell which demonstrate CD2 expression and an enhanced LFA-3 expression (MacKay *et al.*, 1988a; Bujdoso *et al.*, 1989a). Consistent with these observations, this study found an increased input of CD4 and CD8 T cells into the lymph node via the afferent lymphatics. This correlated with the reduced proportion of CD4 and CD8 T cells leaving the lymph node via the efferent lymph vessel after an initial increase at 24 h after antigen challenge (Figure 6.2E-G). The differential expression of CD2 on particular T cell subsets and the high expression of LFA-3 on the endothelial cells (Hunig *et al.*, 1986) may contribute to the patterns of recirculation of CD2⁺ T cells from the blood into the lymph node (MacKay *et al.*, 1988a). In addition to this, the stimulation of the T cell via the CD2 antigen binding to its ligand LFA-3 provides an alternative pathway for the activation of T cells (Hunig *et al.*, 1987). CD2 expression has been shown to be increased on activated T cells (MacKay *et al.*, 1990). This is consistent with the view that activated T cells may be migrating to the lymph node after antigen challenge as observed in this study.

CD45R.

The ovine CD45R isoform is functionally equivalent to the CD45RA form found in humans and is expressed on all B cells, NK cells and some naive T cells. CD45R expression may be used to differentiate between naive and memory phenotypes in lymphocytes (Ledbetter *et al.*, 1985; MacKay *et al.*, 1990) although it has been shown that memory cells can revert to a naive phenotype (Bell & Sparshott, 1990). Differential expression of CD45R in afferent, efferent and lymph node cells before antigen challenge was found (Figure 6.3G-I). This may reflect differences in tissue distribution between afferent lymph on the one hand, and efferent lymph and lymph node on the other. The absence of the population with lower staining intensity in afferent lymph compared with the efferent lymph and lymph node may be due to the lower numbers of B cells in afferent

lymph, because a high proportion of cells in the afferent lymph are T cells and antigen-presenting dendritic cells (Bujdoso *et al.*, 1989a). The particular clone of CD45R MAb used in this study, produced by Mackay and colleagues, has been shown to have a particular pattern of staining in afferent and efferent lymph and on activated sheep leucocytes, which is not necessarily conferred by other CD45R-detecting MAbs. The pattern of reactivity obtained in this study for this clone confirms the relative patterns of staining obtained in previous studies. However, further studies are required to define the particular CD45 isoform detected using this MAb (Dutia *et al.*, 1993).

The percentage of cells expressing the CD45R isoform after antigen challenge is different in the efferent lymph and lymph node compared to the afferent lymph (Figures 6.7A, 6.7B). This may be consistent with the increased input of activated or memory CD4 and CD8 T cells into the afferent lymph during this period (Figures 6.2C, 6.2D). These observations would also be consistent with previous observations showing CD45R expression on CD4⁺ T cells but not $\gamma\delta$ T cells (MacKay *et al.*, 1990), and might be consistent with an increased output of B cells in the efferent lymph after antigen challenge (Figure 6.12).

LFA-1.

The pattern of staining for LFA-1 in cells from afferent lymph, efferent lymph and lymph node before antigen challenge are similar (Figure 6.3). However, there is greater fluorescence intensity in afferent lymph compared with efferent lymph and lymph node. This is may be due to the presence of LFA-1 on all leucocytes. A higher expression of LFA-1 in memory T cells was postulated by MacKay *et al.*, (1990). The avidity of this surface molecule changes after activation, which enhances the cell-cell adhesion of the leucocytes. This is essential for immune cell activation events, and is also necessary for the passage of lymphocytes across endothelial cells from the blood to the lymph node (Dustin & Springer, 1989; Dustin & Springer, 1991). The percentage of cells expressing LFA-1 before antigen challenge is ~95 % in both afferent and efferent lymph and this does not change substantially after antigen challenge (Figure 6.8). In lymph node the

expression of LFA-1 was lower than afferent or efferent lymph but this increased after antigen challenge.

MHC II.

MHC II is important for antigen presentation and may also be involved in signal transduction (Davis & Lipsky, 1986; Buus *et al.*, 1987). In this study a marked increase in MHC II expression was observed in afferent and efferent lymph up to 72 h after antigen challenge (Figures 6.9A, 6.9B). This observation is consistent with MHC II expression which was found to increase in cells collected from efferent lymph of sheep following inoculation with Orf virus epidermally in the skin lymph node draining area (Yirrell *et al.*, 1991). There was an increase in the percentage of MHC II positive lymph-borne cells from lymph nodes stimulated *in vivo* with PPD and ovalbumin antigens described by Hopkins and colleagues (1986). The increased expression of MHC II is reported to occur upon stimulation of antigen presenting dendritic cells and activated T cells that express MHC II (Hopkins *et al.*, 1986; Bujdoso *et al.*, 1989a; Hopkins *et al.*, 1989). These results contrast with those by Kimpton *et al.*, (1990) who observed that the percentage of cells staining positive for MHC II was greatest in afferent lymph compared to efferent lymph. This was attributed to the large number of T cells in afferent lymph (Kimpton *et al.*, 1990). In antigen primed animals it has previously been reported that antigen challenge with PPD *in vivo* can have a profound effect on dendritic antigen presenting cells by increasing the relative number of MHC II binding sites per cell compared with T cells. The percentage of T cells expressing MHC II increases significantly whereas the percentage of CD1⁺ dendritic cells and B cells in afferent lymph remains fairly constant (Hopkins *et al.*, 1989). The increase in MHC II expression in lymph after PPD challenge observed in this study might be attributed to activated T cells and dendritic cells in the afferent lymph and activated T cells and B cells in the efferent lymph (Figure 6.9). Cells expressing CD1 were detected in afferent lymph in this study using FCM and immunohistochemical staining of cell smears prepared from afferent lymph (data not shown). The proportion of cells expressing MHC II in the lymph node

decreases 3 days after antigen challenge. This may result from the increased output in the proportion of cells expressing MHC II from the lymph node via the efferent lymph after antigen challenge (Figure 6.9B).

CD44.

Prior to antigen challenge, the fluorescence intensity of staining for CD44 on cells in the afferent lymph is higher than in efferent lymph (Figure 6.3D, E). This may be supported by a previous study which showed that CD4⁺ and some CD8⁺ T cells in afferent lymph are CD44^{hi} compared with efferent lymph (MacKay *et al.*, 1990). These results may be consistent with the function of CD44, which mediates binding of lymphocytes to endothelial venules, thus assisting with the passage of lymphocytes into the lymph node (Aruffo *et al.*, 1990). CD44 has been identified on sheep leucocytes and has been shown to stain positively on >95% of sheep efferent lymphocytes and macrophages, monocytes and granulocytes (MacKay *et al.*, 1988c). These observations are consistent with the results obtained in this study which show that generally ~>85% of afferent and efferent lymph and lymph node stained positive for the CD44 antigen both before and after antigen challenge (Figure 6.6).

DU74 and DU104.

The monoclonal antibodies DU74 and DU104 bind to the complement receptor 2 (CD21) on B cells which binds to the ligand C3d. There are two isoforms of CD21 recognised, gp150 and gp190 that has a ubiquitin attached covalently to the cytoplasmic region (Hein, 1995; Hein, 1996). The staining pattern for DU74 and DU104 from BCG-primed sheep prior to antigen challenge is different in afferent and efferent lymph and lymph node compared to the cells from naive efferent lymph (Figure 6.10). This may be consistent with the observations that these MAbs detect the same antigen but can stain differently in some samples (Hein, 1996). The differences in the patterns of staining are possibly due to a difference in the external conformation of the antigen, i.e., DU74 and DU104 might label different isoforms of CD21. The other possibility is that dimerization of the antigen CR2 occurs and that DU74 detects dimerized forms whereas DU104 MAb detects any form of the antigen (Hein, 1996).

In the lymph node it has also been reported that the two isoforms of CR2 are more heterogeneous than in blood and lymph (Hein, 1995). This is illustrated in this study in unchallenged lymph node from BCG-primed sheep, particularly with the MAb DU74 (Figure 6.11). Previous studies indicate that the proportion of cells expressing DU74 and DU104 was similar (~40%) in efferent lymph from naive sheep, because both isoforms were co-expressed in these cells (Hein, 1995; Hein, 1996). This has been confirmed in this study (data for % staining not shown). After antigen challenge the percentage of cells expressing DU74 and DU104 increases in the efferent lymph after an initial lag phase (Figure 6.10 & 6.11). This coincides with an increase in both DU74 and DU104 after antigen challenge in the lymph node. These are the first studies using DU74 and DU104 to identify changes in CD21 expression in response to antigen challenge.

175. *175* antigen in lymph nodes and afferent and efferent lymph.

The surface antigen detected with the MAb 175 has recently been identified as a serine protease that is membrane-bound and believed to play a role in the regulation of the immune response (Deane et al., 1995). It is part of a family of membrane associated protease enzymes associated with haematopoietic differentiation. The functional role of these enzymes may be to help regulate the immune system by inhibiting the cell response to a peptide or protein substrate (Shipp & Look, 1993).

The proportion of cells staining positive for 175 antigen before antigen challenge in afferent lymph is higher (26-30%) than in efferent lymph (~12%) and lymph node (~15%) (Figure 6.13). Macrophage-like cells have been reported to comprise 10-20% of the cells in the afferent lymph (MacKay *et al.*, 1988b). After antigen challenge the proportion of cells expressing the antigen 175 increases in the afferent lymph at 24-48 h after antigen challenge. This is followed by a decline in the proportion of cells expressing 175 antigen, which returns to pre-challenge levels (Figure 6.13). The changes in the expression of 175 antigen fluctuate in the efferent lymph but do not change after antigen challenge (Figure 6.13).

Previous studies have shown positive staining for the surface antigen 175 in normal peripheral afferent lymph (Hein *et al.*, 1987). The surface antigen 175 is expressed on myeloid and erythroid cells during differentiation (Miyasaka *et al.*, 1985; Deane *et al.*, 1995) and has recently been shown to have serine protease activity (Deane *et al.*, 1995). However, 175 has also been shown to be expressed on activated CD5⁺ CD4 and CD8 T cells (McClure, 1996).

These results (Figure 6.13) show that a greater proportion of cells of myeloid origin, such as macrophages, neutrophils and activated T cells, are present in the afferent lymph than in efferent lymph both before and after challenge. These cells are located at tissue sites of inflammation and would migrate to the draining lymph node via the afferent lymphatics (Hall & Morris, 1963; Hall, 1967). The proportion of 175 antigen expressing cells in the lymph node does not change after antigen challenge.

6.3.4. ¹H-NMR studies of lymph nodes and afferent and efferent lymph.

The 1D ¹H-NMR spectra of cells isolated from efferent lymph (Figure 6.14) show that the cells collected prior to antigen challenge and after day 2 from the efferent lymphatic vessel are very similar. The 1D ¹H-NMR spectra for the afferent lymphatics were also very similar (data not shown). This is also illustrated in the 2D ¹H-NMR spectra of afferent and efferent lymph, prior to and after antigen challenge (Figure 6.15). Mobile lipid peaks at 0.89, 1.33 and 5.3 ppm are evident in the 1D ¹H-NMR spectrum from isolated lymph node cells 3 days after antigen challenge (Figure 6.14). Mobile lipids are more clearly displayed by the 2D ¹H-NMR of the isolated lymph node cells (Figure 6.16). The appearance of mobile lipid resonances in the lymph node 24 h after antigenic challenge may be due to the passage of activated cells and antigen to the draining lymph node, which can stimulate an antigen-induced immune response in the lymph node.

These observations are consistent with the uptake of antigen from the tissue site after intra-dermal or subcutaneous injection. In previously immune animals, subsequent antigen challenge results in most of the antigen being carried to the lymph node via the afferent lymph within the first 24 h, associated largely with afferent veiled dendritic cells (Hall &

Morris, 1963; Hall & Robertson, 1983). The remaining antigen is carried to the lymph node as large molecular weight immune complexes and this occurs within the first 24 h after soluble antigen injection in immunised animals (Beh & Lascelles, 1985).

Bovine afferent veiled or dendritic cells are reported to rapidly process antigen and migrate from the tissue site in antigen-primed animals within 30 mins of antigen challenge (McKeever *et al.*, 1992). Further to this, ovine afferent lymph veiled cells collected 24 h after inoculation of antigen into the lymph draining area were able to induce the proliferation of T cells from the same sheep (Bujdoso *et al.*, 1989a).

The mobile lipids were detected in the lymph node regardless of the use of the adjuvant IFA, which primarily consists of an oil emulsion, in the preparation of the PPD antigen. This shows that the detection of mobile lipids in the lymph node on day 1 after challenge correlates with the immune response as a result of challenge with antigen alone.

There is evidence that in the afferent lymph of unchallenged sheep there is a higher proportion than in efferent lymph of cells that have previously progressed through the cell cycle (MacKay *et al.*, 1990), but this is likely to have occurred at the tissue site or within the lymph node. In this study, ¹H-NMR-detectable mobile lipid is present in isolated sheep lymph node cells after secondary antigen challenge of BCG-primed sheep. An immune response is occurring in the lymph node which corresponds with the passage of antigen and the traffic of cells through the lymph node. The most intense mobile lipid resonances occur in isolated lymph node cells from antigen challenged lymph node. Some resonances are present in the unchallenged lymph node this are probably due to the low level of cell cycling of immune cells occurring in the normal peripheral lymph nodes (McClure *et al.*, 1988).

It is important to note that the results presented in this Chapter were collected from isolated lymph node cells with the fat cells removed. Mountford and colleagues have previously used ¹H-NMR to detect mobile lipid resonances in tissue slices from normal human lymph nodes, lymph nodes from patients with malignancies and antigen stimulated rat lymph node tissue (Mountford *et al.*, 1993). These studies found intense resonances corresponding

to the mobile lipid in all of the examined tissue, including the normal lymph node. The authors suggested that the appearance of the lipid resonances in the stimulated and normal lymph nodes may be attributed to the fatty tissue that was present in the whole tissue sample. In this study, the cross-peak intensity of mobile lipid in antigen-challenged lymph node cells and unstimulated lymph node cells are different (Figure 6.16). In challenged lymph node the cross-peak intensities are higher. These results suggest that the activated and proliferating lymph node cells do contribute to the mobile lipid resonances which are present in the lymph node and that these resonances in whole tissue are not entirely due to fatty deposits.

6.3.5. Conclusions.

The changes that occur in the activation status of cells migrating from and into the lymph node and in the lymph node itself after antigen challenge indicate that an immune response to antigen has occurred in the lymph node. The phenotyping of the different cell types also indicates that the relative proportions of distinctly different immune cells, which have previously been recognised to be present in these lymphatic vessels, also undergo a change after antigen challenge.

The appearance of the mobile lipid resonances therefore coincides with the passage of antigen and activated immune cells from the tissue area to the lymph node. These results therefore suggest that the mobile lipid spectra can occur in activated, rapidly proliferating or growth arrested immune cells at particular tissue sites. The lack of mobile lipid detected in the afferent or efferent lymph cells suggests that the initial activating stimulus may not be adequate for the cells to accumulate lipid which can be detected using $^1\text{H-NMR}$. This is consistent with the results shown in Chapter 4 and 5 of this thesis showing that the generation of the mobile lipid in stimulated immune cells may arise from phosphatidylcholine degradation, involved in phosphatidylcholine cycling. The catabolism of phosphatidylcholine occurs in the G_1 phase of the cell cycle. Phosphatidylcholine catabolism can occur as a result of cellular proliferation, immune cell activation, during cellular growth arrest or even apoptosis. All of these cellular processes occur in the cells in

the lymph node and may be responsible for the increased generation of the $^1\text{H-NMR}$ -detectable mobile lipid after lymph node antigen challenge. Future experiments using the double labeling FCM technique may be useful to determine which type of immune cells are activated. It would also be useful to use separation techniques to enrich for particular immune cell types so that sufficient cells could be obtained and analysed in the $^1\text{H-NMR}$ spectrometer.

A $^1\text{H-NMR}$ mobile lipid spectrum is seen in a number of different cell types, including immune cells in different metabolic states. In this study the nature and origin of the $^1\text{H-NMR}$ mobile lipid spectrum from T cells was investigated. Murine T cells were activated *in vitro* using the mitogenic agents PMA and ionomycin, or by the direct stimulation of the TCR/CD3 complex with αCD3 monoclonal antibodies. Immune cells were stimulated *in vivo* with a specific antigen, PPD, in sheep. This approach enabled the preliminary investigation of the biochemical pathways necessary for the generation of the mobile lipid in T cell activation. It had been shown previously that the mobile lipid was associated with the activation of a variety of immune cell types. However, it was not clear whether the development of the mobile lipid was an integral part of the activation process or whether it was a consequence of the increased metabolism of the cells. The studies reported in this thesis suggest that the mobile lipid is associated with phosphatidylcholine turnover, which is an integral part of the activation process in immune cells.

I would like to propose a model which explains the generation of the mobile lipid in stimulated immune cells. My model is based on models proposed by Pelech and Vance, (1989), Jackowski (1994), and Terce *et al.* (1994), who discuss the relationship of the cell cycle and phosphatidylcholine turnover in proliferating or growth arrested cells. In the G_1 phase of the cell cycle both degradation and biosynthesis of PC occurs. At the G_1/S boundary the level of PC synthesis increases and PC catabolism ceases. I propose that the periodic oscillations in the catabolism and synthesis of PC that occur as cells progress through multiple cell cycles are responsible for the generation of the $^1\text{H-NMR}$ -visible mobile lipid spectrum.

Chapter 7

General Discussion

The initiation of T cell proliferation requires two events: an antigenic signal (which can be mimicked by mitogenic agents) and the binding of IL-2 with its receptor, IL-2R α (Farrar *et al.*, 1990). Exposure to antigen or mitogen induces the progression of T cells from G₀ to G₁ phase of the cell cycle and the expression of the IL-2R α . IL-2 binding to IL-2R α stimulates the progression from G₁ to the S phase of the cell cycle, with subsequent DNA synthesis.

A ¹H-NMR mobile lipid spectrum is seen in a number of different cell types, including immune cells in different metabolic states. In this study the nature and origin of the ¹H-NMR mobile lipid spectrum from T cells was investigated. Murine T cells were activated *in vitro* using the mitogenic agents PMA and ionomycin, or by the direct stimulation of the TCR/CD3 complex with α CD3 monoclonal antibodies. Immune cells were stimulated *in vivo* with a specific antigen, PPD, in sheep. This approach enabled the preliminary investigation of the biochemical pathways necessary for the generation of the mobile lipid in T cell activation. It had been shown previously that the mobile lipid was associated with the activation of a variety of immune cell types. However, it was not clear whether the development of the mobile lipid was an integral part of the activation process or whether it was a consequence of the increased metabolism of the cells. The studies reported in this thesis suggest that the mobile lipid is associated with phosphatidylcholine turnover, which is an integral part of the activation process in immune cells.

I would like to propose a model which explains the generation of the mobile lipid in stimulated immune cells. My model is based on models proposed by Pelech and Vance, (1989), Jackowski (1994), and Terce *et al.* (1994), who discuss the relationship of the cell cycle and phosphatidylcholine turnover in proliferating or growth arrested cells. In the G₁ phase of the cell cycle both degradation and biosynthesis of PC occurs. At the G₁/S boundary the level of PC synthesis increases and PC catabolism ceases. I propose that the periodic oscillations in the catabolism and synthesis of PC that occur as cells progress through multiple cell cycles are responsible for the generation of the ¹H-NMR-visible mobile lipid spectrum.

7.1. Mobile lipid in activated immune cells.

The initiation of T cell proliferation requires two events: an antigenic signal (which can be mimicked by mitogenic agents) followed by the interaction of IL-2 with its receptor, IL-2R α (Farrar *et al.*, 1990). Exposure to antigen or mitogen induces the progression of T cells from G₀ to G₁ phase of the cell cycle and the expression of the IL-2R α . IL-2 binding to IL-2R α initiates the progression from G₁ to the S phase of the cell cycle, with subsequent DNA synthesis resulting in cellular proliferation (Cantrell & Smith, 1984). After the initial stimulation of peripheral blood lymphocytes with mitogens and α CD3 antibodies, unsaturated fatty acids are readily taken up by the lymphocytes and incorporated into plasma membrane phospholipids (Goppelt-Strube & Resch, 1987; Szamel *et al.*, 1989). Increased uptake of lipoproteins in activated T cells also occurs via the upregulation of the lipoprotein receptors on the cell surface, which is enhanced after culture in serum free conditions or after mitogenic stimulation (Cuthbert & Lipsky, 1984, 1986, 1989; Jurgens *et al.*, 1989; Szamel *et al.*, 1989; Traill *et al.*, 1990). This may provide an exogenous source of cholesterol and fatty acids necessary for cell proliferation (Cuthbert & Lipsky, 1986).

Phosphatidylcholine can be catabolised by phospholipases such as PLC, PLA₂, and PLD. This yields catabolic lipid products that are involved in immune cell activation and proliferation. These include the formation of DAG and other free fatty acids which are responsible for the long-term activation of PKC, which is necessary for cellular proliferation (Berry *et al.*, 1990; Nishizuka, 1992; Exton, 1994b; Szamel & Resch, 1995). These events are related to the phosphatidylcholine cycles which have been proposed by Pelech and Vance (1989), in which cycles of phosphatidylcholine synthesis and degradation may play a role in the overall activation process and also play a role in the cell cycle status of dividing cells (Pelech & Vance, 1989; Jackowski, 1994; Terce *et al.*, 1994).

A comparison was made between the mobile lipid accumulated in splenic (peripheral, mature) and thymic (mostly immature) T cells activated with PMA and ionomycin for

activation periods from 0-120 h (Chapter 4; Veale *et al.*, 1996). This extended previous studies by our laboratory indicating that the mobile lipid accumulated in a time dependent manner with increasing activation time in murine thymic T cells activated using PMA and ionomycin (Dingley *et al.*, 1992). At time periods of 72-120 h after activation with PMA and ionomycin, ¹H-NMR detection of mobile lipid increased significantly, particularly in splenic T cells (Chapter 4). Cho and PCho levels were elevated between 12-48 h after activation and then decreased to below resting levels, while GPC levels increased after 12 h and remained elevated. These results can be explained in the light of the phosphatidylcholine cycles, as proposed by Pelech and Vance (1989) and modified by Veale *et al.* (1996). In this cycle the mobile lipid may be generated as cells progress through PC cycles as a function of phospholipid turnover associated with activation signalling events and cell cycle progression (Figure 4.1).

The simultaneous changes in the choline metabolites between 72 and 120 h was accompanied by a decrease in cell size in both thymic and splenic T cells, with no loss of cell viability. Choline deficiency has been shown to arrest cells in the G₀/G₁ phase of the cell cycle (Terce *et al.*, 1994). In medium deficient in choline, cells can decrease in size due to the catabolism of phosphatidylcholine (which makes up a large part of the membrane) and this can result in a decrease in cell mass of up to 35%, even though the cells can remain viable (Terce *et al.*, 1994). Phosphatidylcholine catabolism via phospholipases occurs in the late G₁ phase of the cell cycle (Jackowski, 1994; Terce *et al.*, 1994). These observations may explain the results presented in Chapter 4 which show that the activation of murine T cells is initiated by the simultaneous use of PMA and ionomycin. This treatment can stimulate the activity of phospholipase C and D enzymes, possibly mediated by PKC (Nishizuka, 1992). This event would initiate the progression of the cells from the G₀ (quiescent) phase of the cell cycle into the G₁ (commitment and progression) phase (Figure 1.14). In addition, phorbol esters such as PMA are known to activate the enzyme CT, which is the rate-limiting enzyme for PC synthesis (Pelech & Vance, 1989; Nishizuka, 1992). This may drive the cells into the S phase where the activity of CT is greatest and phospholipid accumulation due to biosynthesis of phospholipids occurs (Jackowski, 1994).

Cell division occurs in the G₂/M phase and the daughter cells re-enter the G₁ phase where another round of catabolism of PC occurs.

Several cell cycles may occur until the metabolites of PC synthesis become rate limiting and the cells arrest in G₀/G₁, where PC catabolism continues as indicated by the production of GPC. The continued catabolism of PC would result in the accumulation of mobile lipids, as shown at 96 and 120 h after activation (Chapter 4), because fatty acyl chains of the lipids would no longer be required for incorporation into newly synthesised PC. A similar phenomenon occurs when CSF-1 stimulated macrophages are blocked in the G₁ phase. In these cells, fatty acids which result from PC catabolism accumulate as triacylglycerol (Jackowski, 1994). Previously our laboratory has shown that blocking ConA-stimulated lymphocytes in the G₁ phase of the cell cycle did not inhibit the ¹H-NMR-detectable mobile lipid spectrum (Holmes *et al.*, 1990). The G₁ phase of the cell cycle has also been shown to correlate with an increase in the mobile lipids in transformed fibroblast cells (Delikatny *et al.*, 1996a). These NMR observations in murine thymocytes confirm previous biochemical analysis of proliferating rat thymocytes stimulated with PHA and IL-2. Here, fatty acids and phospholipid levels increased for up to 48 h after activation. After this fatty acid levels decreased but remained above resting levels 96 h after stimulation (Gross *et al.*, 1988). These results confirm that activated thymocytes accumulate lipids and phospholipids during cell cycle progression as illustrated by the results in Chapter 4.

Together, these results clearly show that the mobile lipid can be generated using PMA and ionomycin stimulation, resulting in cellular proliferation and cell cycle progression, as illustrated by ³H-thymidine incorporation by the T cells (Chapter 4). These studies were extended to include stimulation of thymocytes with PMA and ionomycin alone, or via the TCR/CD3 complex using a monoclonal antibody, α CD3 (Chapter 5).

The activation of cells with PMA directly stimulates PKC, and this can affect the activity of phospholipases and the enzyme CT. Thymocytes stimulated by PMA alone developed a ¹H-NMR-detectable mobile lipid spectrum (Figure 5.7B), displaying all of the 2D cross

peaks previously identified as triglyceride (May *et al.*, 1986). These cells also displayed an upregulation of the IL-2R α as shown using FCM (Figure 5.2C), which indicates that the thymocytes had moved into G₁ (Cantrell & Smith, 1984). However, these cells do not continue to proliferate (Table 5.1), indicating that cell cycle progression past the commitment point is not complete.

Stimulation of thymocytes with ionomycin alone causes a Ca²⁺ flux which can potentiate the effect of PKC but does not result in PKC activation (Nishizuka, 1984). Ionophores such as ionomycin may have an effect upon phospholipases and this may explain the lipid cross-peaks that appeared in the ¹H-NMR spectrum via the PKC-mediated mechanism (Figure 5.7C). However, these cells did show a small increase in the expression of the IL-2R α but did not proliferate (Figure 5.2D, Table 5.1), indicating that the cells did not progress beyond the G₁ phase. The lipid cross-peaks that did appear upon treatment of the cells with ionomycin corresponded to the production of fatty acids rather than triglycerides. The cells treated with the combination of PMA and ionomycin produced a characteristic distinct mobile lipid spectrum (Figure 5.7A). The cells showed a substantial upregulation of IL-2R α and proliferated (Figure 5.1B, Table 5.1). The treatment of thymocytes with α CD3 antibody resulted in the development of a mobile lipid spectrum which included all of the triglyceride cross-peaks (Figure 5.7F), although α CD3 antibody treatment did not induce proliferation or the upregulation of the IL-2R α in thymocytes (Figure 5.2E, Table 5.1). In contrast, treatment of splenocytes (mixed population of T cells and accessory cells) with α CD3 antibody resulted in cell proliferation and the acquisition of a mobile lipid spectrum similar to the spectrum obtained from PMA and ionomycin-stimulated thymocytes.

Together, these results confirm that the mobile lipid spectrum can be acquired independently of cell cycle progression, without the use of cell cycle blocking agents. They also show that agents that can induce the up-regulation of different PKC isoforms, such as PMA used alone or PMA and ionomycin in combination, yield a very similar mobile lipid spectrum after 24 h. Thymocytes treated with PMA alone do not progress beyond the G₁ phase of the cell cycle. PMA and ionomycin-treated cells would have completed at least one cell cycle and be re-entering G₁ at 24 h. These results are consistent with the results shown in Chapter

4 in both splenic and thymic T cells that undergo multiple cell cycle circuits and phosphatidylcholine cycles.

These conclusions are further confirmed by results obtained from the stimulation of splenocytes with the monoclonal antibody α CD3, even though the mode of activation and the biochemical pathways leading to signal transduction are different from those invoked using PMA and ionomycin. The stimulation of unfractionated thymocytes with the α CD3 monoclonal antibody resulted in mobile lipid acquisition, but did not result in proliferation or IL-2R α upregulation. The stimulation of T cells via the CD3 complex mimics the binding of antigen to the TCR, but without the accessory cells or additional signals to initiate co-stimulation of the T cells they will not proliferate in response to α CD3 stimulation (Cantrell & Smith, 1984). However, the biochemical signalling pathway that has been invoked by stimulation via TCR/CD3 initiates the catabolism of PC via the stimulation of PC-specific phospholipase C, resulting in the formation of DAG which activates PKC (Szamel *et al.*, 1993). This may result in the generation of the mobile lipid in these cells, even though they do not progress into G₁.

Further to this, the mobile lipid was shown to be inhibited in α CD3 stimulated thymocytes by the use of a PC-specific PLC inhibitor D609 (Chapter 5). These results show that the generation of the mobile lipid in α CD3-stimulated thymocytes results from the hydrolysis of PC via a PLC-dependent mechanism. In contrast, splenocytes stimulated with the α CD3 antibody accumulated mobile lipid uninhibited by D609 treatment. In fact, an increase in the mobile lipid was evident. These results are not surprising and are consistent with the mechanisms proposed in this Chapter. Firstly, the stimulated splenocytes contained a variety of accessory cells including monocytes, dendritic cells and B cells (Chapter 3), which can all act to stimulate T cells via cell surface adhesion molecules, thus providing additional co-stimulatory signals to the T cells. This may result in the cell surface receptor-mediated activation of other enzymes such as PLA₂ and PLD that can catabolise PC. It would also block the cells in G₁ phase of the cell cycle (as shown by the inhibition of proliferation) when phosphatidylcholine catabolism is enhanced, resulting in the accumulation of DAG and fatty acids which may be stored as triglyceride. The continued incorporation of

lipoproteins may also contribute to the observed accumulation of lipids, because the expression of the lipoprotein receptors occurs after the mitogen-stimulation of lymphocytes. The accumulation of the lipids occurs because the cells are not synthesising new phospholipids for incorporation into the daughter cell membranes. This is because the cells do not progress into the S phase where PC biosynthesis is maximal (Jackowski, 1994). The catabolism of PC via PC-specific PLC is believed to be a necessary step in the progression of cells into the S phase of the cell cycle (Terce *et al.*, 1994) and this may explain the inhibition of proliferation observed in the splenocyte suspension.

These *in vitro* studies of murine T cells have shown that there is a relationship between the mobile lipid, phosphatidylcholine turnover and cellular signalling. These processes have been linked and associated with cell cycle status (Jackowski, 1994). This model can also be applied to the results obtained from immunised sheep which were challenged with antigen *in vivo*.

Single sheep lymph nodes were cannulated and lymph cells were collected from the afferent lymph vessels draining the regional tissue area, and from the efferent lymph vessels leading out from the lymph node and back into the blood and the regional tissue area. After antigen challenge of the lymph node the total cell input to the draining lymph node increased and the T cell subsets, particularly CD4 cells, also increased in number, particularly during the first 24 h after antigen challenge. At the same time there was a "shut down" period observed in the efferent cell output from the lymph node for the first 12 h followed by an increase in total cells and T cell subsets. These results are confirmed by similar studies which indicated that an immune response occurs as a result of antigen challenge *in vivo* using PPD antigen challenge of lymph nodes (MacKay *et al.*, 1992b). The change in cell surface molecules observed in immune cells after antigen challenge can indicate whether or not the cells have been previously activated by antigen. Characteristic up-regulation of expression of particular cell surface molecules, such as MHC II, CD2, CD44, LFA-1 and the expression of CD45 isoforms, can indicate an activated or memory phenotype. These changes function to enhance the cell-cell interactions by altering the affinity of the adhesion molecule and enhance the responsiveness to antigen (Sanders *et al.*, 1988a; MacKay, 1991; Picker *et al.*, 1993b). The

changes observed in the cell surface molecule expression in the cells entering the lymph node via the afferent lymphatic vessels, and leaving the node via the efferent lymphatic vessel, indicated not only that changes had occurred in the phenotype of the cell but also that the distribution of cell types varied during the experimental period after antigen challenge of the lymph node. The change in phenotype would occur after activation, which implies that cell cycle progression from G_0 to G_1 or progression through the entire cell cycle may be necessary for these phenotypic cell surface changes to occur. Many of the cell surface changes which appear in activated immune cells *in vitro* occur 24 h following activating stimuli (Biselli *et al.*, 1992). Cells that are migrating through endothelial cells have been shown to have been activated previously as demonstrated by BrdU incorporation into the DNA of migrating cells (Masuyama *et al.*, 1992). However, the number of cells migrating from the lymph node that have specifically reacted with antigen would be small in comparison with the large number of cells circulating through the lymph node after antigenic challenge. The number of activated antigen-specific cells that are migrating out from the lymph node does not appear to be sufficient to induce ^3H thymidine incorporation when stimulated with antigen *in vitro* until approximately 6-7 days after the *in vivo* antigen challenge (Data not shown; S.J. McClure, personal communication).

Antigen stimulation and cell cycle progression of antigen-specific immune cells would occur in the draining lymph node of the antigen-challenged tissue area. The antigen-specific cells would proliferate in the lymph node in preparation for release into the periphery. Therefore, the greatest abundance of dividing cells would occur in challenged lymph node. This would be consistent with the ^1H -NMR results observed in Chapter 6, where the only significant levels of mobile lipid were detected in isolated lymph node cells. These observations would be consistent with the notion that phosphatidylcholine cycles, which correlate with the phases of the cell cycle, generate the accumulation of mobile lipid in isolated lymph node cells after antigen challenge. In unchallenged lymph nodes some lipid resonances are visible (Chapter 6, Figure 6.15). This would be consistent with cell cycle kinetics in unchallenged sheep lymph nodes, where cell cycle turnover is evident in a very small number of cells (McClure *et al.*, 1988).

7.2. Model for the origin of mobile lipid in activated immune cells.

I would like to summarise the model I am proposing to explain the observations made in this thesis on the origin of mobile lipid in activated T cells and other associated immune cells. The model has drawn on work in this thesis, and previous work from our laboratory and other laboratories.

I propose that the mobile lipid results from cell cycle oscillations of phosphatidylcholine degradation and synthesis (Pelech & Vance, 1989; Jackowski, 1994). It is established that the degradation of phosphatidylcholine occurs in the G₁ phase of the cell cycle (Habenicht *et al.*, 1985; Pelech & Vance, 1989; Jackowski, 1994). This correlates with the development of the mobile lipid in cells independent of further cell cycle progression and proliferation in cells arrested in G₁ (Holmes *et al.*, 1990; King *et al.*, 1991; 1994; Delikatny *et al.*, 1996a; Chapter 5).

This notion is also consistent with the results presented in Chapters 4, 5 and 6, showing that rapid cell division resulted in the accumulation of mobile lipids as the cells moved through multiple cell cycle circuits (Jackowski, 1994; Figure 1.15) at ~24-h intervals. Lipoproteins may also contribute to the accumulation of mobile lipids in cells arrested in the G₁ phase of the cell cycle. This coincides with the expression of lipoprotein receptors after activation of immune cells.

Part of this model has been tested in Chapter 5 using a PC-specific phospholipase C inhibitor, D609. The accumulation of mobile lipid was inhibited in thymocytes stimulated via the TCR/CD3 complex. Cell cycle arrest in splenocytes stimulated via the TCR/CD3 complex occurred after treatment with D609, and an increase in mobile lipid was observed. These results are also consistent with the model because PC-specific PC degradation is required for cell cycle progression (Terce *et al.*, 1994). The accumulation of lipid in the D609-treated splenocytes would result from additional PC catabolism from other phospholipases stimulated by accessory cells and possibly lipoprotein uptake. The model

could be further tested using other phospholipase inhibitors and correlating the cell cycle status of the cell with the $^1\text{H-NMR}$ mobile lipid analysis.

This model provides a link between phospholipid metabolism and mobile lipid accumulation in cells which may be rapidly proliferating or differentiating (Podo *et al.*, 1992; Ferretti *et al.*, 1993; Veale *et al.*, 1996), in necrotic (Kuesel *et al.*, 1994b) or growth arrested (Delikatny *et al.*, 1996a) states, or in immune cells in primed, activated states (King *et al.*, 1991; Dingley *et al.*, 1992; May *et al.*, 1993). Apoptosis may also be involved. This is the first time that a model has been proposed that offers a universal explanation for the accumulation of mobile lipid in a wide variety of divergent cellular states.

- Abeana, J.M. & Fearon, D.T. (1989). Structure and function of the complement receptors, CR1 (CD35) and CR2 (CD21). *Advances in Immunology* 46, 183-219.
- Alberts, B., Bray, D., Lewis, J., Raff, M., Roberts, K. & Watson, J.D. (1994). *Molecular biology of the cell*. (3rd ed.). Garland Publishing Inc., New York. 1294 pp.
- Altman, A., Mally, M.L. & Iakov, N. (1992). Phorbol ester synergizes with Ca^{2+} ionophore in activation of protein kinase C (PKC) alpha and PKC beta isozymes in human T cells and in induction of related cellular functions. *Immunology* 76, 465-71.
- Anderson, C.L. (1980). The murine macrophage Fc receptor for IgG2b is lipid dependent. *Journal of Immunology* 125, 538-40.
- Anderson, K.B., Whitton, D.S. & Mueller, G.C. (1985). Role of fatty acid structure in the reversible activation of phosphatidylcholine synthesis in lymphocytes. *Biochimica et Biophysica Acta* 835, 360-8.
- Ansell, G.B. & Spanger, S. (1982). Phosphatidylserine, phosphatidylethanolamine and phosphatidylcholine. In *Phospholipids*. (1st ed.), Edited by J.N. Hawthorne & G.B. Ansell. Elsevier Biomedical, Amsterdam, pp. 1-41.
- Antonyan, M.A., Medzka, E.J. & Runkumar, V. (1995). Adenosine acts as an endogenous modulator of IL-2-dependent proliferation of cytotoxic T lymphocytes. *Journal of Immunology* 155, 2813-21.
- Areuzana-Seisdedos, P., Fernandez, B., Dominguez, I., Jacque, J.M., Thomas, D., Diaz-Meco, M.T., Moscat, J. & Virelizier, J.L. (1993). Phosphatidylcholine hydrolysis activates NF- κB and increases human immunodeficiency virus replication in human monocytes and T lymphocytes. *Journal of Virology* 67, 6596-604.
- Aruffo, A., Stamenkovic, I., Melnick, M., Underhill, C.B. & Seed, B. (1990). CD44 is the principal cell surface receptor for hyaluronate. *Cell* 61, 1303-13.
- Azaka, Y., Okazaki, M., Yoshida, K. & Nishizuka, Y. (1991). Lysophosphatidylcholine as a possible second messenger synergistic to diacylglycerol and calcium ion for T lymphocyte activation. *Biochemical and Biophysical Research Communications* 178, 1378-85.
- Azzi, A., Boscoboinik, D. & Hensey, C. (1992). The protein kinase C family. *European Journal of Biochemistry* 208, 547-57.

References.

- Bacon, K.B., Flores-Romo, L., Life, P.F., Taub, D.D., Premack, B.A., Arkininstall, S.J., Wells, T.N., Schall, T.J. & Power, C.A. (1995). IL-9-induced signal transduction in T lymphocytes involves receptor-mediated activation of phospholipases C and D. *Journal of Immunology* **154**, 3654-66.
- Bartley, A.N., Birkeland, M.L., Brown, M.H., Beyers, A.D., Davis, S.J., Samoja, C. & Abbas, A.K., Lichtman, A.H. & Pober, J.S. (1994). *Cellular and molecular immunology*. (2nd ed.). W.B. Saunders Company, Philadelphia. 457 pp.
- Acuto, O., Hussey, R.E., Fitzgerald, K.A., Protentis, J.P., Meuer, S.C., Schlossman, S.F. & Reinherz, E.L. (1983). The human T cell receptor: appearance in ontogeny and biochemical relationship of alpha and beta subunits on IL-2 dependent clones and T cell tumors. *Cell* **34**, 717-26.
- Adam, W.R., Craik, D.J., Kneen, M. & Wellard, R.M. (1989). Effect of magnesium depletion and potassium depletion and chlorothiazide on intracellular pH in the rat, studied by ^{31}P NMR. *Clinical and Experimental Pharmacology and Physiology* **16**, 33-40.
- Adebodun, F. & Post, J.F.M. (1994). ^{31}P NMR characterization of cellular metabolism during dexamethasone induced apoptosis in human leukemic cell lines. *Journal of Cellular Physiology* **158**, 180-6.
- Ahearn, J.M. & Fearon, D.T. (1989). Structure and function of the complement receptors, CR1 (CD35) and CR2 (CD21). *Advances in Immunology* **46**, 183-219.
- Alberts, B., Bray, D., Lewis, J., Raff, M., Roberts, K. & Watson, J.D. (1994). *Molecular biology of the cell*. (3rd ed.). Garland Publishing Inc., New York. 1294 pp.
- Altman, A., Mally, M.I. & Isakov, N. (1992). Phorbol ester synergizes with Ca^{2+} ionophore in activation of protein kinase C (PKC) alpha and PKC beta isoenzymes in human T cells and in induction of related cellular functions. *Immunology* **76**, 465-71.
- Anderson, C.L. (1980). The murine macrophage Fc receptor for IgG2b is lipid dependent. *Journal of Immunology* **125**, 538-40.
- Anderson, K.E., Whitlon, D.S. & Mueller, G.C. (1985). Role of fatty acid structure in the reversible activation of phosphatidylcholine synthesis in lymphocytes. *Biochimica et Biophysica Acta* **835**, 360-8.
- Ansell, G.B. & Spanner, S. (1982). Phosphatidylserine, phosphatidylethanolamine and phosphatidylcholine. In *Phospholipids*. (1st ed.). Edited by J.N. Hawthorne & G.B. Ansell. Elsevier Biomedical, Amsterdam. pp. 1-41.
- Antonyamy, M.A., Moticka, E.J. & Ramkumar, V. (1995). Adenosine acts as an endogenous modulator of IL-2-dependent proliferation of cytotoxic T lymphocytes. *Journal of Immunology* **155**, 2813-21.
- Arenzana-Seisdedos, F., Fernandez, B., Dominguez, I., Jacque, J.M., Thomas, D., Diaz-Meco, M.T., Moscat, J. & Virelizier, J.L. (1993). Phosphatidylcholine hydrolysis activates NF- κB and increases human immunodeficiency virus replication in human monocytes and T lymphocytes. *Journal of Virology* **67**, 6596-604.
- Aruffo, A., Stamenkovic, I., Melnick, M., Underhill, C.B. & Seed, B. (1990). CD44 is the principal cell surface receptor for hyaluronate. *Cell* **61**, 1303-13.
- Asaoka, Y., Oka, M., Yoshida, K. & Nishizuka, Y. (1991). Lysophosphatidylcholine as a possible second messenger synergistic to diacylglycerol and calcium ion for T lymphocyte activation. *Biochemical and Biophysical Research Communications* **178**, 1378-85.
- Azzi, A., Boscoboinik, D. & Hensey, C. (1992). The protein kinase C family. *European Journal of Biochemistry* **208**, 547-57.

- Bacon, K.B., Flores-Romo, L., Life, P.F., Taub, D.D., Premack, B.A., Arkininstall, S.J., Wells, T.N., Schall, T.J. & Power, C.A. (1995). IL-8-induced signal transduction in T lymphocytes involves receptor-mediated activation of phospholipases C and D. *Journal of Immunology* **154**, 3654-66.
- Barclay, A.N., Birkeland, M.L., Brown, M.H., Beyers, A.D., Davis, S.J., Somoza, C. & Williams, A.F. (1993). *The leucocyte antigen facts book*. (1st ed.). Academic Press, London. 424 pp.
- Barclay, A.N. & Mayrhofer, G. (1981). Bone marrow origin of Ia-positive cells in the medulla of rat thymus. *Journal of Experimental Medicine* **153**, 1666-71.
- Barrit, G.J. (1992). *Communication within animal cells*. (1st ed.). Oxford University Press, Melbourne. 343 pp.
- Beh, K.J. & Lascelles, A.K. (1985). The effect of adjuvants and prior immunization on the rate of uptake of antigen into afferent popliteal lymph from sheep. *Immunology* **54**, 487-95.
- Bell, E.B. & Sparshott, S.M. (1990). Interconversion of CD45R subsets of CD4 T cells *in vivo*. *Nature* **348**, 163-66.
- Bell, R.M. & Coleman, R.A. (1980). Enzymes of glycerolipid synthesis in eukaryotes. *Annual Review of Biochemistry* **49**, 459-87.
- Bell, R.M. & Coleman, R.A. (1983). Enzymes of triacylglycerol formation in mammals. In *The enzymes, Volume 16. Lipid enzymology*. (2nd ed.). Edited by P.D. Boyer. Academic Press Inc., London. pp. 87-111.
- Bental, M. & Deutsch, C. (1993). Metabolic changes in activated T cells: An NMR study of human peripheral blood lymphocytes. *Magnetic Resonance in Medicine* **29**, 317-26.
- Bental, M. & Deutsch, C. (1994). On-line studies of activation events in primary human T lymphocytes. *ImmunoMethods* **4**, 148-62.
- Berditchevski, F., Bazzoni, G. & Hemler, M.E. (1995). Specific association of CD63 with VLA-3 and VLA-6 integrins. *Journal of Biological Chemistry* **270**, 17784-90.
- Berry, N., Ase, K., Kishimoto, A. & Nishizuka, Y. (1990). Activation of resting human T cells requires prolonged stimulation of protein kinase C. *Proceedings of the National Academy of Sciences U.S.A.* **87**, 2294-8.
- Besterman, J.M., Duronio, V. & Cuatrecasas, P. (1986). Rapid formation of diacylglycerol from phosphatidylcholine: a pathway for generation of a second messenger. *Proceedings of the National Academy of Sciences U.S.A.* **83**, 6785-89.
- Bierer, B.E., Peterson, A., Barbosa, J., Seed, B. & Burakoff, S.J. (1989). Synergistic T cell activation via the physiological ligands for CD2 and the T cell receptor. *Journal of Experimental Medicine* **168**, 1145-56.
- Billah, M.M. & Anthes, J.C. (1990). The regulation and cellular functions of phosphatidylcholine hydrolysis. *Biochemical Journal* **269**, 281-91.
- Biselli, R., Matricardi, P.M., D'Amelio, R. & Fattorossi, A. (1992). Multiparametric flow cytometric analysis of the kinetics of surface molecule expression after polyclonal activation of human peripheral blood T lymphocytes. *Scandinavian Journal of Immunology* **35**, 439-47.
- Bishop, J.F., McGrath, K., Wolf, M.M., Mathews, J.P., De Luise, T., Holdsworth, R., Yuen, K., Veale, M., Whiteside, M.G., Cooper, I.A. & Szer, J. (1988). Clinical factors influencing the efficacy of pooled platelet transfusions. *Blood* **71**, 383-7.
- adhesion induced through the common beta 1 subunit. *European Journal of Immunology* **22**, 3111-9.

- Bishop, W.R. & Bell, R.M. (1988). Assembly of phospholipids into cellular membranes: Biosynthesis, transmembrane movement and intracellular translocation. *Annual Review of Cell Biology* **4**, 579-610.
- Boarder, M.R. (1994). A role for phospholipase D in control of mitogenesis. *Trends in Pharmacological Sciences* **15**, 57-62.
- Boggs, K.P., Rock, C.O. & Jackowski, S. (1995). Lysophosphatidylcholine and 1-*O*-Octadecyl-2-*O*-Methyl-*rac*-Glycero-3-Phosphocholine inhibit the CDP-choline pathway of phosphatidylcholine synthesis at the CTP:Phosphocholine cytidylyltransferase step. *Journal of Biological Chemistry* **270**, 7757-64.
- Boyer, P.D., Diamond, R.A. & Rothenberg, E.V. (1989). Changes in inducibility of IL-2 receptor α -chain and T cell receptor expression during thymocyte differentiation in the mouse. *Journal of Immunology* **142**, 4121-30.
- Brown, J.H., Jardetzky, T., Saper, M.A., Samraoui, B., Bjorkman, P.J. & Wiley, D.C. (1988). A hypothetical model of the foreign antigen binding site of class II histocompatibility molecules (erratum *Nature* **333**, 786 (1988)). *Nature* **332**, 845-50.
- Brown, S.C., Mullis, K., Levenson, C. & Shafer, R.H. (1984). Aqueous solution structure of an intercalated actinomycin D-dATGCAT complex by two-dimensional and one-dimensional proton NMR. *Biochemistry* **23**, 403-8.
- Bujdoso, R., Hopkins, J., Dutia, B.M., Young, P. & McConnell, I. (1989a). Characterization of sheep afferent lymph dendritic cells and their role in antigen carriage. *Journal of Experimental Medicine* **170**, 1285-302.
- Bujdoso, R., Young, P., Hopkins, J., Allen, D. & McConnell, I. (1989b). Non-random migration of CD4 and CD8 T cells: changes in the CD4: CD8 ratio and interleukin 2 responsiveness of efferent lymph cells following *in vivo* antigen challenge. *European Journal of Immunology* **19**, 1779-84.
- Burgess, K.E., Odysseos, A.D., Zalvan, C., Druker, B.J., Anderson, P., Schlossman, S.F. & Rudd, C.E. (1991). Biochemical identification of a direct physical interaction between CD4: p56lck and Ti(TCR)CD3 complexes. *European Journal of Immunology* **21**, 1663-8.
- Buttke, T.M., Van Cleave, S., Steelman, L. & McCubrey, J.A. (1989). Absence of unsaturated fatty acid synthesis in murine T lymphocytes. *Proceedings of the National Academy of Sciences U.S.A.* **86**, 6131-7.
- Buus, S., Sette, A., Colon, S.M., Miles, C. & Grey, H.M. (1987). The relation between major histocompatibility complex (MHC) restriction and the capacity of Ia to bind immunogenic peptides. *Science* **235**, 1353-8.
- Byrne, J.A., Butler, J.L. & Cooper, M.D. (1988). Differential activation requirements for virgin and memory T cells. *Journal of Immunology* **141**, 3249-57.
- Cahill, R.N.P., Frost, H. & Trnka, Z. (1976). The effects of antigen on the migration of recirculating lymphocytes through single lymph nodes. *Journal of Experimental Medicine* **143**, 870-88.
- Callies, R., Sri-Pathmanathan, R.M., Ferguson, D.Y.P. & Brindle, K.M. (1993). The appearance of neutral lipid signals in the ^1H NMR spectra of a myeloma cell line correlates with the induced formation of cytoplasmic lipid droplets. *Magnetic Resonance in Medicine* **29**, 546-50.
- Campanero, M.R., Arroyo, A.G., Pulido, R., Ursa, A., de Matias, M.S., Sanchez-Mateos, P., Kassner, P.D., Chan, B.M., Hemler, M.E. & Corbi, A.L. (1992). Functional role of $\alpha 2/\beta 1$ and $\alpha 4/\beta 1$ integrins in leukocyte intercellular adhesion induced through the common $\beta 1$ subunit. *European Journal of Immunology* **22**, 3111-9.

- Campisi, J. & Pardee, A.B. (1984). Post-transcriptional control of the onset of DNA synthesis by an insulin-like growth factor. *Molecular and Cellular Biology* **4**, 1807-14.
- Cano, E., Angeles Munoz-Fernandez, M. & Fresno, M. (1992). Regulation of interleukin-2 responses by phosphatidic acid. *European Journal of Immunology* **22**, 1883-89.
- Cantrell, D.A. & Smith, K.A. (1984). The interleukin-2 T cell system: a new cell growth model. *Science* **224**, 1312-6.
- Castagna, M., Takai, Y., Kaibuchi, K., Sano, K., Kikkawa, U. & Nishizuka, Y. (1982). Direct activation of calcium-activated, phospholipid-dependent protein kinase by tumour-promoting phorbol esters. *Journal of Biological Chemistry* **257**, 7847-51.
- Chan, A.C., Irving, B.A., Fraser, J.D. & Weiss, A. (1991). The ζ chain is associated with a tyrosine kinase and upon T-cell antigen receptor stimulation associates with ZAP-70, a 70kDa tyrosine phosphoprotein. *Proceedings of the National Academy of Sciences U.S.A.* **88**, 9166-70.
- Chan, A.C., Iwashima, M., Turck, C.W. & Weiss, A. (1992). Zap-70: a 70kd protein-tyrosine kinase that associates with the TCR ζ chain. *Cell* **71**, 649-62.
- Chen, S.G., Kulju, D., Halt, S. & Murakami, K. (1992). Phosphatidylcholine-dependent protein kinase C activation. Effects of cis-fatty acid and diacylglycerol on synergism, autophosphorylation and Ca²⁺-dependency. *Biochemical Journal* **284**, 221-6.
- Chen, Y. & Rabinovitch, P.S. (1989). Platelet-derived growth factor, epidermal growth factor, and Insulin-like growth factor I regulate specific cell-cycle parameters of human diploid fibroblasts in serum-free culture. *Journal of Cellular Physiology* **140**, 59-67.
- Chen, Y. & Rabinovitch, P.S. (1990). Mitogen response and cell cycle kinetics of Swiss 3T3 cells in defined medium: differences from human fibroblasts and effects of cell density. *Experimental Cell Research* **190**, 145-50.
- Chestnut, R.W. & Grey, H.M. (1981). Studies on the capacity of B cells to serve as antigen presenting cells. *Journal of Immunology* **126**, 1075-9.
- Chiaffarino, F., Biffi, M., Luciano, A., Gromo, G. & Leoni, F. (1994). Involvement of multiple protein kinases in CD3-mediated activation of human T lymphocytes. *Cellular Immunology* **153**, 39-51.
- Chin, Y.-H., Carey, G.D. & Woodruff, J.J. (1982). Lymphocyte recognition of lymph node high endothelium. IV. Cell surface structures mediating entry into lymph nodes. *Journal of Immunology* **129**, 1911-5.
- Choy, P.C. & Arthur, G. (1989). Phosphatidylcholine synthesis from lysophosphatidylcholine. In *Phosphatidylcholine metabolism*. (1st ed.). Edited by D.E. Vance. CRC Press, Boca-Raton Florida. pp. 87-102.
- Clevers, H., Alarcon, B., Wileman, T. & Terhorst, C. (1988). The T cell receptor/ CD3 complex: A dynamic protein ensemble. *Annual Review of Immunology* **6**, 629-62.
- Coats, S., Flanagan, W.M., Nourse, J. & Roberts, J.M. (1996). Requirement of p27Kip1 for restriction point control of the fibroblast cell cycle. *Science* **272**, 877-80.
- Cohen, S.M. (1987). *Physiological NMR spectroscopy: from isolated cells to man..* The New York Academy of Sciences, New York. 537 pp.
- Coleman, R.A. & Haynes, E.B. (1984). Hepatic monoacylglycerol acyltransferase. Characterization of an activity associated with the suckling period of rats. *Journal of Biological Chemistry* **259**, 8934-38.

- de Fougerolles, A.R. & Springer, T.A. (1992). Intracellular adhesion molecule 3, a third adhesion counter-receptor for lymphocyte function-associated molecule 1 on resting T cells. *Journal of Cell Biology* **117**, 101-110.
- Collins, T.L., Kassner, P.D., Bierer, B.E. & Burakoff, S.J. (1994). Adhesion receptors in lymphocyte activation. *Current Opinion in Immunology* **6**, 385-93.
- Conricode, K.M., Smith, J.L., Burns, D.J. & Exton, J.H. (1994). Phospholipase D activation in fibroblast membranes by the α and β isoforms of protein kinase C. *FEBS Letters* **342**, 149-53.
- Cornell, R.G.L., Grove, G.H., Rothblat, G.H. & Horowitz, A.F. (1977). Lipid requirement for cell cycling. The effect of selective inhibition of lipid synthesis. *Experimental Cell Research* **109**, 299-307.
- Corrigan, A., O'Kennedy, R. & Smyth, H. (1979). Lymphocyte membrane alterations caused by nylon wool column separation. *Journal of Immunological Methods* **31**, 177-82.
- Crispe, I.N. (1994). Fatal interactions: Fas-induced apoptosis of mature T cells. *Immunity* **1**, 347-9.
- Cross, K.J., Holmes, K.T., Mountford, C.E. & Wright, P.E. (1984). Assignment of acyl chain resonances from membranes of mammalian cells by two-dimensional NMR methods. *Biochemistry* **23**, 5895-7.
- Crowley, M., Inaba, K. & Steinman, R.M. (1990). Dendritic cells are the principal cell in mouse spleen bearing immunogenic fragments of foreign proteins. *Journal of Experimental Medicine* **172**, 383-6.
- Cuthbert, J.A. & Lipsky, P.E. (1984). Immunoregulation by low density lipoproteins in man: Inhibition of mitogen-induced T lymphocyte proliferation by interference with transferrin metabolism. *Journal of Clinical Investigation* **73**, 992-1003.
- Cuthbert, J.A. & Lipsky, P.E. (1986). Promotion of human T lymphocyte activation and proliferation by fatty acids in low density and high density lipoproteins. *Journal of Biological Chemistry* **261**, 3620-27.
- Cuthbert, J.A. & Lipsky, P.E. (1989). Lipoproteins may provide the fatty acids necessary for human lymphocyte proliferation by both low density lipoprotein receptor-dependent and -independent mechanisms. *Journal of Biological Chemistry* **264**, 13468-74.
- Daly, P.F. & Cohen, J.S. (1989). Magnetic resonance spectroscopy of tumors and potential *in vivo* clinical applications: a review. *Cancer Research* **49**, 770-9.
- Daly, P.F., Lyon, R.C., Faustino, P.J. & Cohen, J.S. (1987). Phospholipid metabolism in cancer cells monitored by ^{31}P NMR spectroscopy. *Journal of Biological Chemistry* **262**, 14875-78.
- Davies, D.R. & Metzger, H. (1983). Structural basis of antibody function. *Annual Review of Immunology* **1**, 87-117.
- Davis, L. & Lipsky, P.E. (1986). Signals involved in T cell activation. II. Distinct roles of intact accessory cells, phorbol esters and interleukin 1 in activation and cell cycle progression of resting T lymphocytes. *Journal of Immunology* **136**, 3588-96.
- Davis, L.S. & Lipsky, P.E. (1989). T cell activation induced by anti-CD3 antibodies requires prolonged stimulation of protein kinase C. *Cellular Immunology* **118**, 208-21.
- Davis, M.M. (1988). T cell antigen receptor genes. In *Molecular immunology*. (1st ed.). Edited by B.D. Hames & D.M. Glover. IRL Press, Oxford. pp. 61-79.
- de Carvalho, M.G., Garritano, J. & Leslie, C.C. (1995). Regulation of lysophospholipase activity of the 85-kDa phospholipase A2 and activation in mouse peritoneal macrophages. *Journal of Biological Chemistry* **270**, 20439-46.

- de Fougerolles, A.R. & Springer, T.A. (1992). Intercellular adhesion molecule 3, a third adhesion counter-receptor for lymphocyte function-associated molecule 1 on resting lymphocytes. *Journal of Experimental Medicine* **175**, 185-90.
- Deane, D., Inglis, L. & Haig, D. (1995). The 175 antigen expressed on myeloid and erythroid cells during differentiation is associated with serine protease activity. *Blood* **85**, 1215-19.
- Dekker, L.V. & Parker, P.J. (1994). Protein kinase C - a question of specificity. *Trends in Biochemical Sciences* **19**, 73-7.
- Delikatny, E.J., Hull, W.E. & Mountford, C.E. (1991). The effect of altering time domains and window functions in two-dimensional proton COSY spectra of biological specimens. *Journal of Magnetic Resonance* **94**, 563-73.
- Delikatny, E.J., Ladner, C.M., Jeitner, T.M., Hancock, R. & Mountford, C.E. (1996a). Modulation of MR-visible mobile lipid levels by cell culture conditions and correlations with chemotactic response. *International Journal of Cancer* **65**, 238-45.
- Delikatny, E.J., Roman, S.K., Hancock, R., Jeitner, T.M. & Lander, C.M. (1996b). Tetraphenylphosphonium chloride induced MR-visible lipid accumulation in a malignant human breast cell line. *International Journal of Cancer* **67**, 72-9.
- Delikatny, E.J., Russell, P., Hunter, J.C., Hancock, R., Atkinson, K., van Haaften-Day, C. & Mountford, C.E. (1993). Proton magnetic resonance and human cervical neoplasia. Ex vivo spectroscopy allows distinction of invasive carcinoma of the cervix from carcinoma *in situ* and other preinvasive lesions. *Radiology* **188**, 791-6.
- Depper, J.M., Leonard, W.J., Kronke, M., Noguchi, P.D., Cunningham, R.E., Waldman, T.A. & Greene, W.C. (1984). Regulation of interleukin 2 receptor expression: effects of phorbol diester, phospholipase C and re-exposure to lectin or antigen. *Journal of Immunology* **133**, 3054-61.
- Derome, A.E. (1989). *Modern NMR techniques for chemistry research*. (1st ed.). Pergamon Press, Oxford. 280 pp.
- Deslauriers-Boisvert, N., Mercier, G. & Lafleur, L. (1982). The nylon wool adherence marker of the B cell lineage appears at the resting pre-B cell stage. *European Journal of Immunology* **12**, 285-9.
- Dianzani, U., Luqman, M., Rojo, J., Yagi, J., Baron, J.L., Woods, A., Janeway, C.A. & Bottomly, K. (1990). Molecular associations on the T cell surface correlate with immunological memory. *European Journal of Immunology* **20**, 2249-57.
- Dingley, A.J., King, N.J.C. & King, G.F. (1992). An NMR investigation of the changes in plasma membrane triglyceride and phospholipid precursors during the activation of T-lymphocytes. *Biochemistry* **31**, 9098-106.
- Dingley, A.J., Veale, M.F., King, N.J.C. & King, G.F. (1994). Two-dimensional ¹H-NMR studies of membrane changes during the activation of primary T lymphocytes. *ImmunoMethods* **4**, 127-38.
- DiSalvo, C.V., Zhang, D. & Jacobberger, J.W. (1995). Regulation of NIH-3T3 cell G1 phase transit by serum during exponential growth. *Cell Proliferation* **28**, 511-24.
- Doyle, A., Griffiths, J.B. & Newell, D.G. (1994). *Cell and tissue culture: laboratory procedures*. (1st ed.). John Wiley & Sons, Chichester. 2 Volumes.
- Driscoll, P.C., Cyster, J.G., Campbell, I.D. & Williams, A.F. (1991). Structure of domain 1 of rat T lymphocyte CD2 antigen. *Nature* **353**, 762-5.
- Drobnik, W., Mollers, C., Resnik, T. & Schmitz, G. (1995). Activation of phosphatidylinositol-specific phospholipase C in response to HDL3 and LDL is markedly reduced in cultured fibroblasts from Tangier. *Arteriosclerosis, Thrombosis & Vascular Biology* **15**, 1369-77.

- Dulbecco, R., Bologna, M. & Unger, M. (1980). Control of differentiation of a mammary cell line by lipids. *Proceedings of the National Academy of Sciences U.S.A.* **77**, 1551-55.
- Dumont, F.J., Fischer, P. & Sirotna, A. (1995). Increased LFA-1-mediated homotypic cell adhesion is associated with the G1 growth arrest induced by rapamycin in a T cell lymphoma. *Experimental Cell Research* **219**, 146-58.
- Dustin, M.L. & Springer, T.A. (1989). T-cell receptor cross-linking transiently stimulates adhesiveness through LFA-1. *Nature* **341**, 619-24.
- Dustin, M.L. & Springer, T.A. (1991). Role of lymphocyte adhesion receptors in transient interactions and cell locomotion. *Annual Review of Immunology* **9**, 27-66.
- Dutia, B.M., Ross, A.J. & Hopkins, J. (1993). 6.9 Comparison of workshop CD45R monoclonal antibodies with OvCD45R monoclonal antibodies in sheep. *Veterinary Immunology and Immunopathology* **39**, 121-8.
- Eichholtz, T., Janlink, K., Fahrenfort, I. & Moolenaar, W.H. (1992). Lysophosphatidic acid: A bioactive phospholipid with growth factor like properties. *Review of Physiological and Biochemical Pharmacology* **119**, 48-65.
- Emery, D.L. & Davey, R.J. (1995). An analysis, using monoclonal antibodies, of the role of interferon-gamma in ovine immune responses. *Immunology and Cell Biology* **73**, 146-52.
- Epand, R.M., Epand, R.F. & Lancaster, C.R.D. (1988). Modulation of the bilayer to hexagonal phase transition of phosphatidylethanolamines by acylglycerols. *Biochimica et Biophysica Acta* **945**, 161-6.
- Epand, R.M. & Leon, B.T.-C. (1992). Hexagonal phase forming propensity detected in phospholipid bilayers with fluorescent probes. *Biochemistry* **31**, 1550-54.
- Esko, J.D. & Raetz, C.H. (1980). Autoradiographic detection of animal cell membrane mutants altered in phosphatidylcholine synthesis. *Proceedings of the National Academy of Sciences U.S.A.* **79**, 1698-702.
- Evans, C.W., Lund, B.T., McConnell, I. & Bujdoso, R. (1994). Antigen recognition and activation of ovine $\gamma\delta$ T cells. *Immunology* **82**, 229-37.
- Exton, J.H. (1990). Signalling through phosphatidylcholine breakdown. *Journal of Biological Chemistry* **265**, 1-4.
- Exton, J.H. (1994a). Messenger molecules derived from membrane lipids. *Current Opinion in Cell Biology* **6**, 226-9.
- Exton, J.H. (1994b). Phosphatidylcholine breakdown and signal transduction. *Biochimica et Biophysica Acta* **1212**, 26-42.
- Farrar, W.L., Linnekin, D., Brini, A.T., Kelvin, D.J. & Michiel, D.F. (1990). The interleukin-2 receptor complex: structure, gene regulation, and signal transduction. In *Ligands, receptors, and signal transduction of lymphocyte function* ed.). Edited by J.C. Cambier. American Society for Microbiology, Washington D.C. pp. 267-95.
- Fearon, D.T. & Locksley, R.M. (1996). The instructive role of innate immunity in the acquired immune response. *Science* **272**, 50-4.
- Ferretti, A., Podo, F., Carpinelli, G., Chen, L., Borghi, P. & Masella, R. (1993). Detection of neutral active phosphatidylcholine-specific phospholipase C in friend leukemia cells before and after erythroid differentiation. *Anticancer Research* **13**, 2309-18.

- Fingerman, E. & Hemler, M.E. (1988). Regulation of proteins in the VLA cell substrate adhesion family: influence of cell growth conditions on VLA-1, VLA-2, and VLA-3 expression. *Experimental Cell Research* **177**, 132-42.
- Fink, P.J. & Bevan, M.J. (1978). H-2 antigens of the thymus determine lymphocyte specificity. *Journal of Experimental Medicine* **148**, 766-75.
- Flores, I., Casaseca, T., C., M.-A., Kanoh, H. & Merida, I. (1996). Phosphatidic acid generation through interleukin 2 (IL-2)-induced alpha-diacylglycerol kinase activation is an essential step in IL-2-mediated lymphocyte proliferation. *Journal of Biological Chemistry* **271**, 10334-40.
- Florin-Christensen, J., Florin-Christensen, M., Delfino, J.M., Stegman, T. & Rasmussen, H. (1992). Metabolic fate of plasma membrane diacylglycerols in NIH 3T3 fibroblasts. *Journal of Biological Chemistry* **267**, 14783-89.
- Freire-Moar, J., Cherwinski, H., Hwang, F., Ransom, J. & Webb, D. (1991). Expression of protein kinase C isoenzymes in thymocyte subpopulations and their differential regulation. *Journal of Immunology* **147**, 405-9.
- Frelinger, J.A., Niederhuber, J.E. & Shreffler, D.C. (1975). Inhibition of immune responses in vitro by specific antisera to Ia antigens. *Science* **188**, 268-70.
- Freudenthal, P.S. & Steinman, R.M. (1990). The distinct surface of human blood dendritic cells, as observed after an improved isolation method. *Proceedings of the National Academy of Sciences U.S.A.* **87**, 7698-702.
- Fu, T., Okano, Y. & Nozawa, Y. (1992). Differential pathways (phospholipase C and phospholipase D) of bradykinin-induced biphasic 1,2-diacylglycerol formation in non-transformed and K-ras-transformed NIH-3T3 fibroblasts. Involvement of intracellular Ca²⁺ oscillations in phosphatidylcholine breakdown. *Biochemical Journal* **283**, 347-54.
- Furuya, Y., Berges, R.S., Lundmo, P. & Isaacs, J.T. (1994). Proliferation independent activation of programmed cell death as a novel therapy for prostate cancer. In *Apoptosis*. (1st ed.). Edited by E. Mihich & R.T. Schimke. Plenum Press, New York. pp. 137-55.
- Gallatin, W.M., Weissman, I.L. & Butcher, E.C. (1983). A cell-surface molecule involved in organ-specific homing of lymphocytes. *Nature* **304**, 30-4.
- Geilen, C.C., Weider, T., Boremski, S., Wieprecht, M. & Orfanos, C.E. (1996). c-Ha-ras oncogene expression increases choline uptake, CTP:phosphocholine cytidyltransferase activity and phosphatidylcholine biosynthesis in the immortalized human keratinocyte cell line HaCaT. *Biochimica et Biophysica Acta* **1299**, 299-305.
- Geng, J.-G., Bevilacqua, M.P., Moore, K.L., McIntyre, T.M., Prescott, S.M., Kim, J.M., Bliss, G.A., Zimmerman, G.A. & McEver, R.P. (1990). Rapid neutrophil adhesion to activated endothelium mediated by GMP-140. *Nature* **343**, 757-60.
- Geppert, T.D., Davis, L.S., Gur, H., Wacholtz, M.C. & Lipsky, P.E. (1990). Accessory cell signals involved in T-cell activation. *Immunological Reviews* **117**, 5-65.
- Gerson, D.F., Kiefer, H. & Eufe, W. (1982). Intracellular pH of mitogen-stimulated lymphocytes. *Science* **216**, 1009-10.
- Giegerich, G.W., Hein, W.R., Miyasaka, M., Tiefenthaler, G. & Hunig, T. (1989). Restricted expression of CD2 among subsets of sheep thymocytes and T lymphocytes. *Immunology* **66**, 354-61.
- Goding, J.W. (1976). The chromic chloride method of coupling antigens to erythrocytes: definition of some important parameters. *Journal of Immunological Methods* **10**, 61-6.

- Haig, D.M., Thomson, J. & Dawson, A. (1991). Reactivity of the workshop monoclonal antibodies to phospholipids and mast cell lines.
- Goppelt, M., Kohler, L. & Resch, K. (1985). Functional role of lipid metabolism in activated T-lymphocytes. *Biochimica et Biophysica Acta* **833**, 463-72.
- Goppelt-Strube, M. & Resch, K. (1987). Polyunsaturated fatty acids are enriched in the plasma membranes of mitogen-stimulated T-lymphocytes. *Biochimica et Biophysica Acta* **904**, 22-8.
- Gowans, J.L. & Knight, E.J. (1964). The route of recirculation of lymphocytes in the rat. *Proceedings of the Royal Society of London Series B* **159**, 257-82.
- Greenspan, P., Mayer, E.P. & Fowler, S.D. (1985). Nile red: a selective fluorescent stain for intracellular lipid droplets. *Journal of Cell Biology* **100**, 965-73.
- Gross, G., Danzl, M., Fischer, W. & Brand, K. (1988). Alterations of cellular lipids in rat thymocytes during cell cycle progression. *Biochimica et Biophysica Acta* **962**, 220-6.
- Grove, R.I., Allegretto, N.J., Kierner, P.A. & Warr, G.A. (1990). Lipopolysaccharide (LPS) alters phosphatidylcholine metabolism in elicited peritoneal macrophages. *Journal of Leukocyte Biology* **48**, 38-42.
- Guidoni, L., Mariutti, G.M., Rampelli, G.M., Rosi, A. & Viti, V. (1987). Mobile phospholipid signals in NMR spectra of cultured human adenocarcinoma cells. *Magnetic Resonance in Medicine* **5**, 578-85.
- Gumperz, J.E. & Parham, P. (1995). The enigma of the natural killer cell. *Nature* **378**, 245-8.
- Guy, G.R. & Murray, A.W. (1982). Tumor promoter stimulation of phosphatidylcholine turnover in HeLa cells. *Cancer Research* **42**, 1980-85.
- Ha, K.-S. & Exton, J.H. (1993a). Activation of actin polymerization by phosphatidic acid derived from phosphatidylcholine in IIC9 fibroblasts. *Journal of Cell Biology* **123**, 1789-96.
- Ha, K.-S. & Exton, J.H. (1993b). Differential translocation of protein kinase C isozymes by thrombin and platelet-derived growth factor. A possible function for phosphatidylcholine-derived diacylglycerol. *Journal of Biological Chemistry* **268**, 10534-39.
- Haagsman, H.P. & van Golde, L.M.G. (1981). Synthesis and secretion of very low density lipoproteins by isolated rat hepatocytes in suspension: role of diacylglycerol acyltransferase. *Archives of Biochemistry and Biophysics* **208**, 395-402.
- Habenicht, A.J.R., Glomset, J.A., Goerig, M., Gronwald, R., Grulich, J., Loth, U. & Schettler, G. (1985). Cell cycle-dependent changes in arachidonic acid and glycerol metabolism in Swiss 3T3 cells stimulated by platelet-derived growth factor. *Journal of Biological Chemistry* **260**, 1370-3.
- Habenicht, A.J.R., Salbach, P., Goerig, M., Zeh, W., Janssen-Timmen, U., Blatter, C., King, W.C. & Glomset, J.A. (1990). The LDL receptor pathway delivers arachidonic acid for eicosanoid formation in cells stimulated by platelet-derived growth factor. *Nature* **345**, 634-6.
- Hahn, W.C., Menu, E., Bothwell, A.L.M., Sims, P.J. & Bierer, B.E. (1992a). Overlapping but not identical binding sites on CD2 for CD58 and a second ligand CD59. *Science* **256**, 1805-7.
- Hahn, W.C., Rosenstein, Y., Calvo, V., Burakoff, S.J. & Bierer, B.E. (1992b). A distinctive cytoplasmic domain of CD2 regulates ligand avidity and T-cell responsiveness to antigen. *Proceedings of the National Academy of Science USA* **89**, 7179-83.

- Haig, D.M., Thomson, J. & Dawson, A. (1991). Reactivity of the workshop monoclonal antibodies with ovine bone marrow-derived monocyte-macrophage and mast cell lines. *Veterinary Immunology and Immunopathology* **27**, 135-45.
- Haig, D.M., Thomson, J. & Percival, A. (1992). Purification and adhesion receptor phenotype of ovine bone marrow-derived haemopoietic colony-forming cells. *Veterinary Immunology and Immunopathology* **33**, 223-36.
- Hall, J.B. & Morris, B. (1965a). The immediate effect of antigens on the cell output of a lymph node. *British Journal of Experimental Pathology* **46**, 450-54.
- Hall, J.B. & Morris, B. (1965b). The origin of cells from the efferent lymph from a single lymph node. *Journal of Experimental Medicine* **121**, 901-10.
- Hall, J.G. (1967). Studies of the cells in the afferent and efferent lymph of lymph nodes draining the site of skin homografts. *Journal of Experimental Medicine* **125**, 737-54.
- Hall, J.G. & Morris, B. (1962). The output of cells in lymph from the popliteal node of sheep. *Quarterly Journal of Experimental Physiology and Cognate Medical Sciences* **47**, 360-69.
- Hall, J.G. & Morris, B. (1963). The lymph-borne cells of the immune response. *Quarterly Journal of Experimental Physiology and Cognate Medical Sciences* **48**, 235-47.
- Hall, J.G. & Robertson, D. (1983). Phagocytosis, in vivo, of immune complexes by dendritic cells in the lymph of sheep. *International Archives of Allergy and Applied Immunology* **73**, 155-61.
- Halstead, J., Kemp, K. & Ignatz, R.A. (1995). Evidence for involvement of phosphatidylcholine-phospholipase C and protein kinase C in transforming growth factor-beta signaling. *Journal of Biological Chemistry* **270**, 13600-3.
- Hames, B.D. & Rickwood, D. (1994). *Gel electrophoresis of proteins*. (2nd ed.). IRL press, New York. 383 pp.
- Hamilton, J.A. (1989). Interactions of triglycerides with phospholipids: incorporation into bilayer structure and formation of emulsions. *Biochemistry* **28**, 2514-20.
- Hamilton, J.A. & Small, D.M. (1981). Solubilization and localization of triolein in phosphatidylcholine bilayers: A ^{13}C NMR study. *Proceedings of the National Academy of Sciences U.S.A.* **78**, 6878-82.
- Hamilton, J.A., Small, D.M. & Park, J.S. (1983). ^1H NMR studies of lymph chylomicra and very low density lipoproteins from nonhuman primates. *Journal of Biological Chemistry* **258**, 1172-79.
- Hart, D.N. & McKenzie, J.L. (1988). Isolation and characterization of human tonsil dendritic cells. *Journal of Experimental Medicine* **168**, 157-70.
- Harutoshi, K., Tadakuma, T., Odaka, C., Muramatsu, J. & Ishimura, Y. (1989). Activation of a suicide process of thymocytes through DNA fragmentation by calcium ionophores and phorbol esters. *Journal of Immunology* **143**, 1790-94.
- Haskill, S., Beg, A.A., Tompkins, S.M., Morris, J.S., Yurochko, A.D., Sampson-Johannes, A., Mondal, K., Ralph, P. & Baldwin, A.S.J. (1991). Characterization of an immediate-early gene induced in adherent monocytes that encodes I kappa B-like activity. *Cell* **65**, 1281-9.
- Haskill, S., Johnson, C., Eierman, D., Becker, S. & Warren, K. (1988). Adherence induces selective mRNA expression of monocyte mediators and proto-oncogenes. *Journal of Immunology* **140**, 1690-4.
- Hodgkin, P.D. & Kelsoy, M.R. (1992). The mechanism of T and B cell collaboration. *Immunology and Cell Biology* **70**, 153-8.

- Holmes, K.T., Lean, C., Hunt, N. & King, N.J.C. (1990). Development of the "Activated" high resolution ^1H MR spectrum in murine T cells and B cells occurs in G_1 .
- Hatch, G.M., Jamil, H., Utal, A.K. & Vance, D.E. (1992). On the mechanism of the okadaic acid-induced inhibition of phosphatidylcholine biosynthesis in isolated rat hepatocytes. *Journal of Biological Chemistry* **267**, 15751-58.
- Havran, W.L., Poenie, M., Kimura, J., Tsien, R., Weiss, A. & Allison, J.P. (1987). Expression and function of the CD3-antigen receptor on murine CD4+8+ thymocytes. *Nature* **330**, 170-3.
- Hay, J.B. & Cahill, R.N.P. (1982). Lymphocyte migration patterns in sheep. In *Animal models of immunological processes*. (1st ed.). Edited by J.B. Hay. Academic Press, New York. pp. 97-134.
- Hay, J.B. & Hobbs, B.B. (1977). The blood flow to lymph nodes and its relation to lymphocyte traffic and the immune response. *Journal of Experimental Medicine* **145**, 31-44.
- He, Q., Beyers, A.D., Barclay, A.N. & Williams, A.F. (1988). A role in transmembrane signaling for the cytoplasmic domain of the CD2 T lymphocyte surface antigen. *Cell* **54**, 979-84.
- Hecker, J.F. (1986). *The sheep as an experimental model*. (1st ed.) Academic press, London. 216pp.
- Hein, W.R. (1995). Basel Institute for Immunology Annual Report. Basel Institute for Immunology, Basel, Switzerland.
- Hein, W.R. (1996). Basel Institute for Immunology, Basel, Switzerland. Personal communication.
- Hein, W.R., Dudler, L. & Morris, B. (1990). Differential peripheral expansion and *in vivo* antigen reactivity of $\alpha\beta$ and $\gamma\delta$ T cells emigrating from the early lamb thymus. *European Journal of Immunology* **20**, 1805-13.
- Hein, W.R., McClure, S.J. & Miyasaka, M. (1987). Cellular composition of peripheral lymph and skin of sheep defined by monoclonal antibodies. *International Archives of Allergy and Applied Immunology* **84**, 241-6.
- Hemler, M.E. (1990). VLA proteins in the integrin family: structures, functions, and their role on leukocytes. *Annual Review of Immunology* **8**, 365-400.
- Hemler, M.E. & Jacobson, J.G. (1987). Cell matrix adhesion-related proteins VLA-1 and VLA-2: regulation of expression on T cells. *Journal of Immunology* **138**, 2941-8.
- Hermans, M.H. & Malissen, B. (1993). The cytoplasmic tail of the T cell receptor ζ chain is dispensable for antigen-mediated T cell activation. *European Journal of Immunology* **23**, 2257-62.
- Hii, C.S.T., Kokke, Y.S., Clark, K.J. & Murray, A.W. (1990). Phorbol esters modulate the turnover of both ether- and ester-linked phospholipids in cultured mammalian cells. *Biochimica et Biophysica Acta* **1052**, 327-32.
- Hirakawa, T., Maruyama, K., Kohl, N.E., Kodama, T. & Ruley, H.E. (1991). Massive accumulation of neutral lipids in cells conditionally transformed by an activated H-ras oncogene. *Oncogene* **6**, 289-95.
- Ho, J.L. (1989). Antimicrobial functions of macrophages. In *Phagocytes and Disease*. (1st ed.). Edited by M.S. Klempner, B. Styrts & J. Ho. Kluwer Academic Publishers, Boston. pp. 59-90.
- Hodgkin, P.D. & Kehry, M.R. (1992). The mechanism of T and B cell collaboration. *Immunology and Cell Biology* **70**, 153-8.

- Holmes, K.T., Lean, C., Hunt, N. & King, N.J.C. (1990). Development of the "Activated" high resolution ^1H MR spectrum in murine T cells and B cells occurs in G₁ phase of the cell cycle. *Magnetic Resonance in Medicine* **16**, 1-8.
- Holmes, K.T. & Mountford, C.E. (1991). Identification of triglyceride in malignant cells. *Journal of Magnetic Resonance* **93**, 407-9.
- Holmes, K.T., Williams, P.G., Bloom, M., Dyne, M., Mountford, C.E., King, N., Karaman, M., Ninham, M. & Blanden, R. (1988). Magnetic resonance study of lymphocytes stimulated with concanavalin A. *Magnetic Resonance in Medicine and Biology* **1**, 75-9.
- Holmes, K.T., Williams, P.G., King, N.J.C., May, G.L., Dyne, M., Bloom, M. & Mountford, C.E. (1987). A comparison of the chemical analyses of cell lipids with their complete proton NMR spectrum. *Magnetic Resonance in Medicine* **4**, 567-74.
- Holt, P.G., Schon-Hegrad, M.A. & McMenamin, P.G. (1990). Dendritic cells in the respiratory tract. *International Review of Immunology* **6**, 139-49.
- Homans, S.W., Ferguson, M.A.J., Dwek, R.A., Rademacher, T.W., Anand, R. & Williams, A.F. (1988). Complete structure of the glycosyl phosphatidylinositol membrane anchor of rat brain Thy-1 glycoprotein. *Nature* **333**, 269-72.
- Hopkins, J., Dutia, B.M., Bujdoso, R. & McConnell, I. (1989). *In vivo* modulation of CD1 and MHC class II expression by sheep afferent lymph dendritic cells. *Journal of Experimental Medicine* **170**, 1303-18.
- Hopkins, J., Dutia, B.M. & McConnell, I. (1986). Monoclonal antibodies to sheep lymphocytes. I. Identification of MHC class II molecules on lymphoid tissue and changes in the level of class II expression on lymph-borne cells following antigen stimulation *in vivo*. *Immunology* **59**, 433-8.
- Hopkins, J., McConnell, I., Bujdoso, R. & Munro, A.J. (1985). Studies of MHC class II products on sheep peripheral and efferent lymph cells. In *Immunology of the sheep*. (1st ed.). Edited by B. Morris & M. Miyasaka. F. Hoffman-La Roche & Co., Basle. pp. 441-59.
- Hourcade, D., Holers, V.M. & Atkinson, J.P. (1989). The regulators of complement activation (RCA) gene cluster. *Advances of Immunology* **45**, 381-416.
- Hudson, L. & Hay, F.C. (1989). *Practical immunology*. (3rd ed.). Blackwell Scientific Publications, Oxford. 507 pp.
- Hug, H. & Sarre, T.F. (1993). Protein kinase C isoenzymes: divergence in signal transduction? *Biochemical Journal* **291**, 329-43.
- Hughes, E.N., Colombatti, A. & August, J.T. (1989). Murine cell surface glycoproteins. Purification of the polymorphic Pgp-1 antigen and analysis of its expression on macrophages and other myeloid cells. *Journal of Biological Chemistry* **258**, 1014-21.
- Hunig, T., Mitnacht, R., Tiefenthaler, G., Kohler, C. & Miyasaka, M. (1985). T11TS, the cell surface molecule binding to the "erythrocyte receptor" of T lymphocytes: cellular distribution, purification to homogeneity and biochemical properties. *European Journal of Immunology* **16**, 1615-21.
- Hunig, T., Tiefenthaler, G., Meyer zum Buschenfelde, K.-H. & Meuer, S.C. (1987). Alternative pathway of activation of T cells by binding CD2 to its cell-surface ligand. *Nature* **326**, 298-301.
- Hunt, S.V. (1986). Preparative immunoselection of lymphocyte populations. In *Cellular immunology*. (4th ed.). Edited by D.M. Weir. Blackwell Scientific Publications, Oxford. pp. 55.1-18.
- Hurn, B.A.L. & Chantler, S.M. (1980). Production of reagent antibodies. *Methods in Enzymology* **70**, 104-42.

- Kato, K., Kiyonagi, M., Okada, H., Takamachi, T., Wong, Y.W., Williams, A.F., Okumura, K. & Yagita, H. (1992). CD48 is a counter-receptor for mouse CD2 and is
- Inaba, K. & Steinman, R.M. (1984). Resting and sensitised T lymphocytes exhibit distinct stimulatory (antigen-presenting cell) requirements for growth and lymphokine release. *Journal of Experimental Medicine* **160**, 1717-35.
- Indiveri, F., Huddlestone, J., Pellegrino, M.A. & Ferrone, S. (1980). Isolation of human T lymphocytes: comparison between nylon wool filtration and rosetting with neuramidase (VCN) and 2-aminoethylisothiuronium bromide (AET)-treated sheep red blood cells (SRBC). *Journal of Immunological Methods* **34**, 107-15.
- Irving, B.A., Chan, A.C. & Weiss, A. (1993). Functional characterisation of a signal transducing motif present in the T cell antigen receptor ζ chain. *Journal of Experimental Medicine* **177**, 1093-103.
- Irving, B.A. & Weiss, A. (1991). The cytoplasmic domain of the T cell receptor ζ chain is sufficient to couple to receptor-associated signal transduction pathways. *Cell* **64**, 891-901.
- Isakov, N. (1993). Activation of murine lymphocytes by exogenous phosphatidylethanolamine- and phosphatidylcholine-specific phospholipase C. *Cellular Immunology* **152**, 72-81.
- Isakov, N. & Altman, A. (1987). Human T lymphocyte activation by tumour promoters: role of protein kinase C. *Journal of Immunology* **138**, 3100-7.
- Itohara, S., Farr, A.G., Lafaille, J.J., Boneville, M., Takagaki, Y., Haas, W. & Tonegawa, S. (1990). Homing of a gamma delta thymocyte subset with homogeneous T-cell receptors to mucosal epithelia. *Nature* **343**, 754-7.
- Jackowski, S. (1994). Coordination of membrane phospholipid synthesis with the cell cycle. *Journal of Biological Chemistry* **269**, 3855-67.
- Janeway, C.A.J. (1993). How the immune system recognizes invaders. *Scientific American* **269**(3), 72-9.
- Jefferies, W.A., Brandon, M.R., Hunt, S.V., Williams, A.F., Gatter, K.C. & Mason, D.Y. (1984). Transferrin receptor on endothelium of brain capillaries. *Nature* **312**, 162-3.
- Julius, M.H., Simpson, E. & Herzenberg, L.A. (1973). A rapid method for the isolation of functional thymus-derived murine lymphocytes. *European Journal of Immunology* **3**, 645-9.
- Jurgens, G., Xu, Q.-B., Huber, L.A., Bock, G., Howanietz, H., Wick, G. & Traill, K.N. (1989). Promotion of lymphocyte growth by high density lipoproteins (HDL). Physiological significance of the HDL binding site. *Journal of Biological Chemistry* **264**, 8549-56.
- Kannagi, R., Kino, M., Saito, K. & Masuda, T. (1982). Phospholipid acyl chain metabolism during the differentiation of murine leukemia cell lines. On the redistribution of polyunsaturated acyl chains. *Biochimica et Biophysica Acta* **712**, 161-8.
- Kaplan, O. & Cohen, J.S. (1991). Lymphocyte activation and phospholipid pathways: ^{31}P magnetic resonance studies. *Journal of Biological Chemistry* **266**, 3688-94.
- Kaplan, O. & Cohen, J.S. (1994). Lymphocyte activation - ^{31}P Magnetic resonance studies of energy metabolism and phospholipid pathways. *ImmunoMethods* **4**, 139-47.
- Kappler, J., Kubo, R., Haskins, K., Hannum, C., Marrack, P., Pigeon, M., McIntyre, B., Allison, J. & Trowbridge, I. (1983). The major histocompatibility complex-restricted antigen receptor on T cells in mouse and man: identification of constant and variable peptides. *Cell* **35**, 295-302.

- Kato, K., Koyanagi, M., Okada, H., Takanashi, T., Wong, Y.W., Williams, A.F., Okumura, K. & Yagita, H. (1992). CD48 is a counter-receptor for mouse CD2 and is involved in T cell activation. *Journal of Experimental Medicine* **176**, 1241-50.
- Kaufmann, S.H.E. (1996). $\gamma\delta$ and other unconventional T lymphocytes: What do they see and what do they do? *Proceedings of the National Academy of Sciences U.S.A.* **93**, 2272-79.
- Keenan, C., Kelleher, D. & Long, A. (1995). Regulation of non-classical protein kinase C isoenzymes in a human T cell line. *European Journal of Immunology* **25**, 13-7.
- Kennedy, E.P. (1956). The synthesis of cytidine diphosphate choline, cytidine diphosphate ethanolamine, and related compounds. *Journal of Biological Chemistry* **222**, 185-91.
- Kikkawa, U., Takai, Y., Tanaka, Y., Miyake, R. & Nishizuka, Y. (1983). Protein kinase C as a possible receptor protein of tumour-promoting phorbol esters. *Journal of Biological Chemistry* **258**, 11442-45.
- Kim, H.R., Upadhyay, S., Li, G., Palmer, K.C. & Deuel, T.F. (1995). Platelet-derived growth factor induces apoptosis in growth-arrested murine fibroblasts. *Proceedings of the National Academy of Sciences U.S.A.* **92**, 9500-4.
- Kimpton, W.G., Washington, E.A. & Cahill, R.N.P. (1989). Recirculation of lymphocyte subsets (CD5+, CD4+, CD8+, SBU-T19+ and B cells) through gut and peripheral lymph node. *Immunology* **66**, 69-75.
- Kimpton, W.G., Washington, E.A. & Cahill, R.N.P. (1990). Nonrandom migration of CD4+, CD8+ and $\gamma\delta$ +T19+ lymphocyte subsets following in vivo stimulation with antigen. *Cellular Immunology* **130**, 236-43.
- King, G.F. & Kuchel, P.W. (1994). Theoretical and practical aspects of NMR studies of cells. *ImmunoMethods* **4**, 85-97.
- King, G.F. & Mackay, J.P. (1996). Protein structure determination using NMR spectroscopy. In *NMR in Drug Design*. Edited by D.J. Craik CRC series in Analytical Biotechnology CRC Press. pp 101-200.
- King, N.J.C., Delikatny, E.J. & Holmes, K.T. (1994). ¹H Magnetic resonance spectroscopy of primary human and murine cells of the myeloid lineage. *ImmunoMethods* **4**, 188-98.
- King, N.J.C., Ward, M.H. & Holmes, K.T. (1991). Magnetic resonance studies of murine macrophages. Proliferation is not a prerequisite for acquisition of an "activated" high resolution spectrum. *FEBS Letters* **287**, 97-101.
- Kiss, Z. & Anderson, W.B. (1989). Phorbol ester stimulates the hydrolysis of phosphatidylethanolamine in leukemic HL-60, NIH 3T3 and baby hamster kidney cells. *Journal of Biological Chemistry* **264**, 1483-87.
- Kiss, Z. & Tomono, M. (1995). Compound D609 inhibits phorbol ester-stimulated phospholipase D activity and phospholipase C-mediated phosphatidylethanolamine hydrolysis. *Biochimica et Biophysica Acta* **1259**, 105-8.
- Kizaki, H., Tadakuma, T., Odaka, C., Muramatsu, J. & Ishimura, Y. (1989). Activation of a suicide process of thymocytes through DNA fragmentation by calcium ionophores and phorbol esters. *Journal of Immunology* **143**, 1790-4.
- Knopf, J.L., Lee, M.-H., Sultzman, L.A., Kriz, R.W., Loomis, C.R., Hewick, R.M. & Bell, R.M. (1986). Cloning and expression of multiple protein kinase C cDNAs. *Cell* **46**, 491-502.
- Knowles, P.F., Marsh, D. & Rattle, H.W.E. (1976). *Magnetic resonance of biomolecules. An introduction to the theory and practice of NMR and ESR in biological systems.* (1st ed.). John Wiley & Sons, London.

- Kochs, G., Hummel, R., Meyer, D., Hug, H., Marme, D. & Sarre, T.F. (1993). Activation and substrate specificity of the human protein kinase C α and ζ isoenzymes. *European Journal of Biochemistry* **216**, 597-606.
- Kolanus, W., Romeo, C. & Seed, B. (1993). T cell activation by clustered tyrosine kinases. *Cell* **74**, 171-83.
- Kolesnick, R.N. & Paley, A.E. (1987). 1,2-Diacylglycerols and phorbol esters stimulate phosphatidylcholine metabolism in GH3 pituitary cells. Evidence for separate mechanisms of action. *Journal of Biological Chemistry* **262**, 9204-10.
- Koller, C.A., King, G.W., Hurtubise, P.E., Sagone, A.L. & LoBuglio, A.F. (1973). Characterisation of glass adherent human mononuclear cells. *Journal of Immunology* **111**, 1610-12.
- Korman, A.J., Boss, J.M., Spies, T., Sorrentino, R., Okada, K. & Strominger, J.L. (1985). Genetic Complexity and expression of human class II histocompatibility antigens. *Immunological Reviews* **85**, 45-86.
- Kruijer, W., Cooper, J.A., Hunter, T. & Verma, I.M. (1984). Platelet-derived growth factor induces rapid but transient expression of the *c-fos* gene and protein. *Nature* **312**, 711-6.
- Kruse, P.F.J. & Patterson, M.K.J. (1973). *Tissue culture: methods and applications*. (1st ed.). Academic Press, New York. 868 pp.
- Kuchel, P.W. (1989). Biological applications of NMR. In *Analytical NMR*. (1st ed.). Edited by L.D. Field & S. Sternhell. John Wiley and Sons, Inc, New York. pp. 157-219.
- Kuesel, A.C., Grasczew, G., Hull, W.E., Lorenz, W. & Thielmann, H.W. (1990). ^{31}P NMR studies of cultured human tumor cells. Influence of pH on phospholipid metabolite levels and the detection of cytidine 5'-diphosphate choline. *NMR in Biomedicine* **3**, 78-89.
- Kuesel, A.C., Donnelly, S.M., Halliday, W., Sutherland, G.R. & Smith, I.C.P. (1994a). Mobile lipids and metabolic heterogeneity of brain tumours as detectable by ex vivo ^1H MR spectroscopy. *NMR in Biomedicine* **7**, 172-80.
- Kuesel, A.C., Sutherland, G.R., Halliday, W. & Smith, I.C.P. (1994b). ^1H MRS of high grade astrocytomas: mobile lipid accumulation in necrotic tissue. *NMR in Biomedicine* **7**, 149-55.
- Kumagai, K., Itoh, K., Hinuma, S. & Tada, M. (1979). Pretreatment of plastic Petri dishes with fetal calf serum. A simple method for macrophage isolation. *Journal of Immunological Methods* **29**, 17-25.
- Kupfer, A. & Singer, S.J. (1989). The specific interaction of helper T cells and antigen-presenting B cells. IV. Membrane and cytoskeletal reorganisations in the bound T cell as a function of antigen dose. *Journal of Experimental Medicine* **170**, 1697-713.
- Kuzumaki, T., Matsuda, A. & Ito, K. (1996). Cell adhesion to substratum and activation of tyrosine kinases are essentially required for G1/S phase transition in BALB/c 3T3 fibroblasts. *Biochimica et Biophysica Acta* **1310**, 185-92.
- Kyoizumi, S., Kannagi, R. & Masuda, T. (1981). Membrane expression of Fc-Receptors in cultured leukemic cell lines. I. Induction of Fc-receptor in undifferentiated types of cells after modulation of lipid viscosity. *Journal of Immunology* **127**, 2252-56.
- Laemmli, U.K. (1970). Cleavage of structural proteins during the assembly of the head of bacteriophage T4. *Nature* **227**, 680-5.

- Lands, W.E.M. & Crawford, C.G. (1976). Enzymes of membrane phospholipid metabolism in animals. In *The enzymes of biological membranes, Volume 2. Biosynthesis of cell components*. (1st ed.). Edited by A. Martonosi. Plenum Press, New York. pp. 3-85.
- Larrodera, P., Cornet, M.E., Diaz-Laviada, I., Gudda, P.H., Johansen, T. & Moscat, J. (1990). Phospholipase C-mediated hydrolysis of phosphatidylcholine is an important step in PDGF-stimulated DNA synthesis. *Cell* **61**, 1113-20.
- Larson, R.S. & Springer, T.A. (1990). Structure and function of leukocyte integrins. *Immunological Reviews* **114**, 181-217.
- Lascelles, A.K. & Morris, B. (1961). Surgical techniques for the collection of lymph from unanaesthetised sheep. *Quarterly Journal of Experimental Physiology* **46**, 199-205.
- Lean, C.L., Mackinnon, W.B., Delikatny, E.J., Whitehead, R.H. & Mountford, C.E. (1992). Cell-surface fucosylation and magnetic resonance spectroscopy characterization of human malignant colorectal cells. *Biochemistry* **31**, 11095-105.
- Ledbetter, J.A., Rose, L.M., Spooner, P.G., Beatty, P.G., Martin, P.J. & Clark, E.A. (1985). Antibodies to leucocyte common antigen p220 influence human T cell proliferation by modifying the IL-2 receptor expression. *Journal of Immunology* **135**, 1819-25.
- Lerique, B., Lepetit-Thevenin, J., Verine, A., Delpero, C. & Boyer, J. (1994). Triacylglycerol in biomembranes. *Life Sciences* **54**, 831-40.
- Letourneur, F. & Klausner, R.D. (1992). Activation of T cells by a tyrosine kinase activation domain in the cytoplasmic tail of CD3- ϵ . *Science* **255**, 79-82.
- Levy, G.C. & Craik, D.J. (1981). Recent developments in nuclear magnetic resonance spectroscopy. *Science* **214**, 291-9.
- Liscovitch, M. (1992). Crosstalk among multiple signal-activated phospholipases. *Trends in the Biochemical Sciences* **17**, 393-9.
- Lloyd, D., Poole, K.R. & Edwards, S.W. (1982). *The cell division cycle. Temporal organization and control of cellular growth and reproduction*. (1st ed.). Academic Press, London. 523 pp.
- Lopez-Villegas, D., Lenkinski, R.E., Wehrli, S.L., Ho, W.Z. & Douglas, S.D. (1995). Lactate production by human monocytes/macrophages determined by proton MR spectroscopy. *Magnetic Resonance in Medicine* **34**, 32-8.
- Low, M.G. & Kincade, P.W. (1985). Phosphatidylinositol is the membrane-anchoring domain of the Thy-1 glycoprotein. *Nature* **318**, 62-4.
- Lu, K. & Campisi, J. (1992). Ras proteins are essential and selective for the action of insulin-like growth factor 1 in the G1 phase of the cell cycle in BALBC/c murine fibroblasts. *Proceedings of the National Academy of Sciences U.S.A.* **89**, 3889-93.
- Luciani, A.M., Rosi, A., Maggiorella, M.T., Federico, M., Sulli, N., Verani, F., Rossi, G.B., Viti, V. & Guidoni, L. (1991). Interaction of HIV-1 with susceptible lymphoblastoid cells: ^1H NMR studies. *FEBS Letters* **285**, 11-6.
- MacDonald, H.R., Howe, R.C., Pedrazzini, T., Lees, R.K., Budd, R.C., Schneider, R., Liao, N.S., Zinkernagel, R.M., Louis, J.A., Raulet, D.H., Hengartner, H. & Miescher, G. (1988). T-cell lineages, repertoire selection and tolerance induction. *Immunological Reviews* **104**, 157-82.
- Mackay, C.R. (1991). T-cell memory: the connection between function, phenotype and migration pathways. *Immunology Today* **12**, 189-92.
- May, G.L., Szelma, X. & Scovell, T.C. (1994). The presence of cytoplasmic lipid droplets is not sufficient to account for neutral lipid signals in the ^1H MR spectra of neutrophils. *Magnetic Resonance in Medicine* **31**, 212-7.

- Mackay, C.R., Hein, W.R., Brown, M.H. & Matzinger, P. (1988a). Unusual expression of CD2 in sheep: implications for T cell interactions. *European Journal of Immunology* **18**, 1681-88.
- Mackay, C.R., Kimpton, W.G., Brandon, M.R. & Cahill, R.N.P. (1988b). Lymphocyte subsets show marked differences in their distribution between blood and the afferent and efferent lymph of peripheral lymph nodes. *Journal of Experimental Medicine* **167**, 1755-65.
- Mackay, C.R., Maddox, J.F., Wijffels, G.L., Mackay, I.R. & Walker, I.D. (1988c). Characterisation of a 95,000 molecule on sheep leucocytes homologous to murine Pgp-1 and human CD44. *Immunology* **65**, 93-9.
- Mackay, C.R., Marston, W. & Dudler, L. (1992a). Altered patterns of T cell migration through lymph nodes and skin following antigen challenge. *European Journal of Immunology* **22**, 2205-10.
- Mackay, C.R., Marston, W.L. & Dudler, L. (1990). Naive and memory T cells show distinct pathways of lymphocyte recirculation. *Journal of Experimental Medicine* **171**, 801-17.
- Mackay, C.R., Marston, W.L., Dudler, L., Spertini, O., Tedder, T.E. & Hein, W.R. (1992b). Tissue-specific migration pathways by phenotypically distinct subpopulations of memory T cells. *European Journal of Immunology* **22**, 887-95.
- Mackinnon, W.B., Dyne, M., Holmes, K.T., Mountford, C.E. & Gupta, R.S. (1989). Further evidence that the narrow ^1H magnetic resonance signals from malignant cells do not arise from intracellular lipid droplets. *NMR in Biomedicine* **2**, 161-4.
- Makar, R.S., Lipsky, P.E. & Cuthbert, J.A. (1994). Non-sterol regulation of low density lipoprotein receptor gene expression. *Journal of Lipid Research* **35**, 1888-95.
- Manolios, N., Letourneur, F., Bonifacino, J.S. & Klausner, R.D. (1991). Pairwise, cooperative and inhibitory interactions describe the assembly and probable structure of the T-cell antigen receptor. *EMBO Journal* **10**, 1643-51.
- Marion, D. & Wüthrich, K. (1983). Application of phase sensitive two-dimensional correlated spectroscopy (COSY) for measurements of ^1H - ^1H spin-spin coupling constants in proteins. *Biochemical and Biophysical Research Communications* **113**, 967-74.
- Marlin, S.D. & Springer, T.A. (1987). Purified intercellular adhesion molecule-1 (ICAM-1) is a ligand for lymphocyte function-associated antigen (LFA-1). *Cell* **51**, 813-9.
- Marrack, P. & Kappler, J. (1987). The T cell receptor. *Science* **238**, 1073-79.
- Masuyama, J.-I., Berman, J.S., Cruikshank, W.W., Morimoto, C. & Center, D.M. (1992). Evidence for recent as well as long term activation of T cells migrating through endothelial cell monolayers *in vitro*. *Journal of Immunology* **148**, 1367-74.
- Mathews, C.K. & van Holde, K.E. (1990). *Biochemistry*. (1st ed.). The Benjamin/Cummings Publishing Company, Redwood City. 1129 pp.
- May, G.L., Dunlop, L.C., Sztelma, K., Berndt, M.C. & Sorrell, T.C. (1992). GMP-140 (P-selectin) inhibits human neutrophil activation by lipopolysaccharide: analysis by proton magnetic resonance spectroscopy. *Biochemical and Biophysical Research Communications* **183**, 1062-69.
- May, G.L., Sztelma, K., Paul, M.L. & Sorrell, T.C. (1993). Proton magnetic resonance spectroscopy of polymorphonuclear leukocytes from patients with serious bacterial infections. *Journal of Infectious Diseases* **168**, 386-92.
- May, G.L., Sztelma, K. & Sorrell, T.C. (1994). The presence of cytoplasmic lipid droplets is not sufficient to account for neutral lipid signals in the ^1H MR spectra of neutrophils. *Magnetic Resonance in Medicine* **31**, 212-7.

- Miyasaka, M., Beya, M.F., Dudler, L., Pariset, R., Ezaki, T. & Truka, Z. (1985). Studies
- May, G.L., Sztelma, K., Sorrell, T.C. & Mountford, C.E. (1991). Comparison of human polymorphonuclear leukocytes from peripheral blood and purulent exudates by high resolution ^1H MRS. *Magnetic Resonance in Medicine* **19**, 191-8.
- May, G.L., Wright, L.C., Holmes, K.T., Williams, P.G., Smith, I.C.P., Wright, P.E., Fox, R.M. & Mountford, C.E. (1986). Assignment of methylene proton resonances in NMR spectra of embryonic transformed cells to plasma membrane triglyceride. *Journal of Biological Chemistry* **261**, 3048-53.
- Maziere, C., Auclair, M., Mora, L. & Maziere, J.-C. (1990). Modification of phospholipid polar head group with monoethylethanolamine and dimethylethanolamine decreases cholesteryl ester and triacylglycerol synthesis in cultured human fibroblasts. *Lipids* **25**, 311-5.
- McClure, S.J. (1996). Division of Animal Production, CSIRO, NSW, Australia. Personal communication.
- McClure, S.J., Dudler, L., Thorpe, D. & Hein, W.R. (1988). Analysis of cell division among subpopulations of lymphoid cells in sheep. II. Peripheral lymphocytes. *Immunology* **65**, 401-4.
- McClure, S.J. & Hein, W.R. (1989). Functional characteristics of 197+ CD4-CD8- sheep T lymphocytes: expansion and differentiation of peripheral T cells. *Immunology and Cell Biology* **67**, 223-31.
- McClure, S.J., Hein, W.R., Yamaguchi, K., Dudler, L., Beya, M.F. & Miyasaka, M. (1989). Ontogeny, morphology and tissue distribution of a unique subset of CD4-CD8-sheep T lymphocytes. *Immunology and Cell Biology* **67**, 215-21.
- McGrath, K., Holdsworth, R., Veale, M.F., Bishop, J. & Wolf, M. (1988a). Detection of HLA antibodies by platelet crossmatching techniques. *Transfusion* **28**, 214-6.
- McGrath, K., Wolf, M., Bishop, J., Veale, M., Ayberk, H., Szer, J., Cooper, I. & Whiteside, M. (1988b). Transient platelet and HLA antibody formation in multitransfused patients with malignancy. *British Journal of Haematology* **68**, 345-50.
- McKeever, D.J., Awino, E. & Morrison, W.I. (1992). Afferent lymph veiled cells prime CD4+ T cell responses in vivo. *European Journal of Immunology* **22**, 3057-61.
- McKinney, M.M. & Parkinson, A. (1987). A simple, non-chromatographic procedure to purify immunoglobulins from serum and ascites fluid. *Journal of Immunological Methods* **96**, 271-8.
- McPhail, L.C., Clayton, C.C. & Snyderman, R.A. (1984). A potential second messenger role for unsaturated fatty acids: activation of a Ca^{2+} -dependent protein kinase. *Science* **224**, 622-5.
- Merchant, T.E., Meneses, P., Gierke, L.W., Den Otter, W. & Glonek, T. (1991). ^{31}P Magnetic resonance phospholipid profiles of neoplastic human breast tissues. *British Journal of Cancer* **63**, 693-8.
- Meridith, J., Takada, Y., Fornaro, M., Languino, L.R. & Schwartz, M.A. (1995). Inhibition of cell cycle progression by the alternatively spliced integrin beta 1C. *Science* **269**, 1570-2.
- Mishell, B.B., Shiigi, S.M., Henry, C., Chan, E.L., North, J., Gallily, R., Slomich, M., Miller, K., Marbrook, J., Parks, D. & Good, A.H. (1980). Preparation of mouse cell suspensions. In *Selected methods in cellular immunology*. (1st ed.). Edited by B.B. Mishell & S.M. Shiigi. W.H. Freeman & Company, San Francisco. pp. 3-27.

- Miyasaka, M., Beya, M.F., Dudler, L., Parisot, R., Ezaki, T. & Trnka, Z. (1985). Studies on lymphocyte differentiation and migration in sheep by the use of monoclonal antibodies. In *Immunology of the Sheep*. (1st ed.). Edited by B. Morris & M. Miyasaka. F. Hoffman-La Roche & Co., Basle. pp. 68-87.
- Miyasaka, M. & Morris, B. (1988). The ontogeny of the lymphoid system and immune responsiveness in sheep. *Progress in Veterinary Microbiology & Immunology* **4**, 21-55.
- Moingeon, P., Chang, P.C., Sayre, P.H., Clayton, L.K., Alcover, A., Gardner, P. & Reinherz, E.L. (1989). The structural biology of CD2. *Immunological Reviews* **111**, 111-44.
- Mosmann, T.R., Schumacher, J.H., Street, N.F., Budd, R., O'Garra, A., Fong, T.A.T., Bond, M.W., Moore, K.W.M., Sher, A. & Fiorentino, D.F. (1991). Diversity of cytokine synthesis and function of mouse CD4+ T cells. *Immunological Reviews* **123**, 209-29.
- Mountford, C.E., Grossman, G., Holmes, K.T., Hampson, A.W. & Reid, G.H. (1981). Interaction of influenza virus with chicken fibroblasts: a proton magnetic resonance study. *Biochemical and Biophysical Research Communications* **100**, 1183-8.
- Mountford, C.E., Grossman, G., Reid, G. & Fox, R.M. (1982). Characterisation of transformed cells and tumours by proton nuclear magnetic resonance spectroscopy. *Cancer Research* **42**, 2270-76.
- Mountford, C.E., Lean, C.L., Hancock, R., Dowd, S., Mackinnon, W.B., Tattersall, M.H.N. & Russell, P. (1993). Magnetic resonance spectroscopy detects cancer in draining lymph nodes. *Invasion and Metastasis* **13**, 57-71.
- Mountford, C.E. & Mackinnon, W.B. (1994). Proton magnetic resonance spectroscopy of lymphocytes: An historical perspective. *Immunomethods* **4**, 98-112.
- Mountford, C.E. & Wright, L. (1988). Organization of lipids in the plasma membranes of malignant and stimulated cells: a new model. *Trends in Biochemical Sciences* **13**, 172-7.
- Mountford, C.E., Wright, L.C., Holmes, K.T., MacKinnon, W.B., Gregory, P. & Fox, R.M. (1984). High-resolution proton nuclear magnetic resonance analysis of metastatic cancer cells. *Science* **226**, 1415-18.
- Mueller, H.W., O'Flaherty, J.T., Greene, D.G., Samuel, M.P. & Wykle, R.L. (1984a). 1-O-alkyl-linked glycerophospholipids of human neutrophils: distribution of arachidonate and other acyl residues in the ether-linked and diacyl species. *Journal of Lipid Research* **25**, 383-8.
- Mueller, R., Bravo, R., Buckhardt, J. & Curran, T. (1984b). Induction of *c-fos* gene and protein by growth factors precedes activation of *c-myc*. *Nature* **312**, 716-20.
- Mueller-Decker, K. (1989). Interruption of TPA-induced signals by an antiviral and antitumoral xanthate compound: inhibition of a phospholipase C-type reaction. *Biochemical and Biophysical Research Communications* **162**, 198-205.
- Mueller-Decker, K., Doppler, C., Amtmann, E. & Sauer, G. (1988). Interruption of growth signal transduction by an antiviral and antitumoral xanthate compound. *Experimental Cell Research* **177**, 295-302.
- Murphy, E.J., Brindle, K.M., Rorison, C.J., Dixon, R.M., Rajagopalan, B. & Radda, G.K. (1992). Changes in phosphatidylethanolamine metabolism in regenerating rat liver as measured by ³¹P-NMR. *Biochimica et Biophysica Acta* **1135**, 27-34.
- Parker, P.J., Coulens, L., Totty, N., Rice, L., Young, S. & Chen, E. (1986). The complete primary structure of protein kinase C - the major phorbol ester receptor. *Science* **233**, 853-9.
- Parnes, J.R. (1989). Molecular biology and function of CD4 and CD8. *Advances in Immunology* **44**, 265-311.

- Musgrove, E., Seaman, M. & Hedley, D. (1987). Relationship between cytoplasmic pH and proliferation during exponential growth and cellular quiescence. *Experimental Cell Research* **172**, 65-75.
- Music, L., Mueller-Decker, K., Amtmann, E. & Sauer, G. (1989). Mechanistic aspects of the synergistic antiviral effect of xanthates and monocarbonic acids. *Biochemical Pharmacology* **38**, 1941-5.
- Nakanishi, H., Brewer, K.A. & Exton, J.H. (1993). Activation of the ζ isozyme of protein kinase C by phosphatidylinositol 3,4,5-triphosphate. *Journal of Biological Chemistry* **268**, 13-16.
- Nauseef, W.M. (1989). Ontogeny of phagocytes. In *Phagocytes and Disease*. (1st ed.). Edited by M.S. Klempner, B. Styrk & J. Ho. Kluwer Academic Publishers, Boston. pp. 1-23.
- Nishihira, J., Isibashi, T., Sawamura, Y. & Hosokawa, M. (1994). The role of ether-linked glycerophospholipids in cytotoxic T lymphocytes. *Biochemistry and Molecular Biology International* **33**, 137-46.
- Nishizuka, Y. (1984). The role of protein kinase C in cell surface signal transduction and tumour promotion. *Nature* **308**, 693-7.
- Nishizuka, Y. (1992). Intracellular signaling by hydrolysis of phospholipids and activation of protein kinase C. *Science* **258**, 607-14.
- Nossal, G.J.V. (1993). Life, death and the immune system. *Scientific American* **269**(3), 52-62.
- Okamura, H., Tsutsi, H., Komatsu, T., Yutsudo, M., Hakura, A., Tanimoto, T., Torigoe, K., Okura, T., Nukada, Y. & Hattori, K. (1995). Cloning of a new cytokine that induces IFN-gamma production by T-cells. *Nature* **378**, 88-91.
- Ortega, G., Robb, R.J., Shevach, E.M. & Makek, T.R. (1984). The murine IL-2 receptor I monoclonal Abs that define distinct functional epitopes on activated T cells and react with activated B cells. *Journal of Immunology* **133**, 1970-5.
- Ouchterlony, O. (1968). *Handbook of immunodiffusion and immunoelectrophoresis*. (1st ed.). Ann Arbor Science Publishers, Inc., Ann Arbor. 215 pp.
- Ouchterlony, O. & Nilsson, L.A. (1986). Immunodiffusion and immunoelectrophoresis. In *Handbook of experimental immunology, Volume 1. Immunochemistry*. (4th ed.). Edited by D.M. Weir, L.A. Herzenberg, C. Blackwell & L.A. Herzenberg. Blackwell Scientific Publications, Oxford. pp. 32.1-50.
- Pahl, H.L. & Baeuerle, P.A. (1995). Expression of influenza virus hemagglutinin activates transcription factor NF- κ B. *Journal of Virology* **69**, 1480-4.
- Pardee, A.B. (1989). G₁ events and regulation of cell proliferation. *Science* **246**, 603-8.
- Pardey, S. & Wang, E. (1995). Cells en route to apoptosis are characterised by the upregulation of c-fos, c-myc, c-jun, cdc2 and RB phosphorylation, resembling events of early cell cycle traverse. *Journal of Cellular Biochemistry* **58**, 135-50.
- Parish, C.R., Kirov, S.M., Bowern, N. & Blanden, R.V. (1974). A one-step procedure for separating mouse T and B lymphocytes. *European Journal of Immunology* **4**, 808-15.
- Parker, P.J., Coussens, L., Totty, N., Rhee, L., Young, S. & Chen, E. (1986). The complete primary structure of protein kinase C - the major phorbol ester receptor. *Science* **233**, 853-9.
- Parnes, J.R. (1989). Molecular biology and function of CD4 and CD8. *Advances in Immunology* **44**, 265-311.

- Patarroyo, M., Yogeewaran, G., Biberfeld, P., Klein, E. & Klein, G. (1982). Morphological changes, cell aggregation and cell membrane alterations caused by phorbol 12,13-dibutyrate in human blood lymphocytes. *International Journal of Cancer* **30**, 707-17.
- Pavli, P., Woodhams, C.E., Doe, W.F. & Hume, D.A. (1990). Isolation and characterisation of antigen-presenting dendritic cells from the mouse intestinal lamina propria. *Immunology* **70**, 40-7.
- Pelech, S.L. & Vance, D.E. (1984). Regulation of phosphatidylcholine biosynthesis. *Biochimica et Biophysica Acta* **779**, 217-51.
- Pelech, S.L. & Vance, D.E. (1989). Signal transduction via phosphatidylcholine cycles. *Trends in Biochemical Sciences* **14**, 28-30.
- Pernis, B. & Weber, D. (1989). Cell biology of antigen presentation by B cells. In *B lymphocytes: function and regulation*. (1st ed.). Edited by P. Del Guercio & J.M. Cruse. Karger, Basel. pp. 27-42.
- Petty, H.R. (1993). *Molecular Biology of Membranes*. (1st ed.). Plenum Publishing, New York. 404 pp.
- Pfeffer, L.M., Strulovici, B. & Saltiel, A.R. (1990). Interferon- α selectively activates the beta isoform of protein kinase C through phosphatidylcholine hydrolysis. *Proceedings of the National Academy of Science USA* **87**, 6537-41.
- Phillips, W.A., Mosmann, H. & Ferber, E. (1986). Changes in the incorporation of free fatty acids upon the stimulation of human polymorphonuclear leukocytes. *Journal of Leukocyte Biology* **39**, 267-84.
- Picker, L.J., Treer, J.R., Ferguson-Darnell, B., Collins, P.A., Bergstresser, P.R. & Terstappen, L.W.M.M. (1993a). Control of lymphocyte recirculation in man. II. Differential regulation of the cutaneous lymphocyte-associated antigen, a tissue-selective homing receptor for skin-homing T cells. *Journal of Immunology* **150**, 1122-36.
- Picker, L.J., Treer, J.R., Ferguson-Darnell, B., Collins, P.A., Buck, D. & Terstappen, L.W.M.M. (1993b). Control of lymphocyte recirculation in man. I. Differential regulation of the peripheral lymph node homing receptor L-selectin on T cells during the virgin to memory transition. *Journal of Immunology* **150**, 1105-21.
- Pierce, C.W. & Kapp, J.A. (1976). The role of macrophages in antibody responses *in vitro*. In *Immunobiology of the macrophages*. Edited by D.S. Nelson. Academic Press, New York. pp. 1-33.
- Pierres, A., Cerdan, C., Lopez, M., Mawas, C. & Olive, D. (1990). "CD3low" human thymocyte populations can readily be triggered via the CD2 and/or CD28 activation pathways whereas the CD3 pathway remains nonfunctional. *Journal of Immunology* **144**, 1202-7.
- Pigott, R. & Power, C. (1993). *The adhesion molecule facts book*. (1st ed.). Academic Press, London. 190 pp.
- Pingel, J.T. & Thomas, M.L. (1989). Evidence that the leukocyte-common antigen is required for antigen-induced T lymphocyte proliferation. *Cell* **58**, 1055-65.
- Pleiman, C.M., D'Ambrosio, D. & Cambier, J.C. (1994). The B-cell antigen receptor complex: structure and signal transduction. *Immunology Today* **15**, 393-9.
- Podo, F., Carpinelli, G., Ferretti, A., Borghi, P., Prioietti, E. & Belardelli, F. (1992). Activation of glycerophosphocholine phosphodiesterase in Friend leukemia cells upon *in vitro* induced erythroid differentiation. ^{31}P and ^1H NMR studies. *Israel Journal of Chemistry* **32**, 291-8.

- Ponec, M. (1991). Lipid metabolism in cultured keratinocytes. *Advances in Lipid Research* **24**, 83-118.
- Poston, R.N. (1974). A buffered chromic chloride method of attaching antigens to red cells: use in haemagglutination. *Journal of Immunological Methods* **5**, 91-6.
- Ratnam, S. & Kent, C. (1995). Early increase in choline kinase activity upon induction of the H-ras oncogene in mouse fibroblast cell lines. *Archives of Biochemistry & Biophysics* **323**, 313-22.
- Raulet, D.H., Garman, R.D., Saito, H. & Tonegawa, S. (1985). Developmental regulation of T-cell receptor gene expression. *Nature* **314**, 103-7.
- Ravichandran, K.S., Lee, K.K., Songyang, Z., Cantley, L.C., Burn, P. & Burakoff, S.J. (1993). Interaction of the *Shc* with the ζ chain of the T cell receptor upon T cell activation. *Science* **262**, 902-5.
- Reinherz, E.L., Kung, P.C., Goldstein, G. & Schlossman, S.F. (1979). Separation of functional subsets of human T cells by a monoclonal antibody. *Proceedings of the National Academy of Sciences U.S.A.* **76**, 4061-5.
- Reinherz, E.L., Meuer, S.C., Fitzgerald, K.A., Hussey, R.E., Hodgdon, J.C., Acuto, O. & Schlossman, S.F. (1983). Comparison of T3-associated 49- and 43-kilodalton cell surface molecules on individual human T-cell clones: evidence for peptide variability in T-cell receptor structures. *Proceedings of the National Academy of Sciences U.S.A.* **80**, 4104-08.
- Ricciolini, R., Miccheli, A., Peluso, G., Delfini, M. & Conti, F. (1991). ^{31}P and ^1H NMR studies of ethanolamine-linked phosphoglycerides metabolism in human T lymphocytes. *Cellular and Molecular Biology* **37**, 705-11.
- Rock, C.O., Cleveland, J.L. & Jackowski, S. (1992). Macrophage growth arrest by cyclic AMP defines a distinct checkpoint in the mid-G1 stage of the cell cycle and overrides constitutive c-myc expression. *Molecular and Cellular Biology* **12**, 2351-58.
- Rode, H.N., Szamel, M., Schneider, S. & Resch, K. (1982). Phospholipid metabolism of stimulated lymphocytes. Preferential incorporation of polyunsaturated fatty acids into plasma membrane phospholipid upon stimulation with concanavalin A. *Biochimica et Biophysica Acta* **688**, 66-74.
- Roehm, N., Herron, L., Cambier, J., Diguisto, D., Haskins, K., Kappler, J. & Marrack, P. (1984). The major histocompatibility complex-restricted antigen receptor on T cells: distribution on thymus and peripheral T cells. *Cell* **38**, 577-84.
- Roitt, I. (1991). *Essential immunology*. (7th ed.). Blackwell Scientific, Melbourne. 356 pp.
- Romeo, C., Amiot, M. & Seed, B. (1992). Sequence requirements for induction of cytolysis by the T cell antigen/Fc receptor ζ -chain. *Cell* **68**, 889-97.
- Rosales, C., O'Brien, V., Kornberg, L. & Juliano, R. (1995). Signal transduction by cell adhesion receptors. *Biochimica et Biophysica Acta* **1242**, 77-98.
- Rosoff, P.M., Savage, N. & Dinarello, C.A. (1988). Interleukin-1 stimulates diacylglycerol production in T lymphocytes. *Cell* **54**, 73-81.
- Royer, H.D., Acuto, O., Fabbi, M., Tizard, R., Ramachandran, K., Smart, J.E. & Reinherz, E.L. (1984). Genes encoding the T β subunit of the antigen/MHC receptor undergo rearrangement during intrathymic ontogeny prior to surface T3-T β . *Cell* **39**, 261-66.
- Royer, H.D., Ramarli, D., Acuto, O., Campen, T.J. & Reinherz, E.L. (1985). Genes encoding the T-cell receptor alpha and beta subunits are transcribed in an ordered manner during intrathymic ontogeny. *Proceedings of the National Academy of Sciences U.S.A.* **82**, 5510-14.

- Rudd, C.E., Janssen, O., Yun-Cai, C., da Silva, A.J., Raab, M. & Prasad, K.V.S. (1994). Two-step TCR ζ /CD3-CD4 and CD28 signaling in T cells: SH2/SH3 domains, protein-tyrosine and lipid kinases. *Immunology Today* **15**, 225-34.
- Salter, R.D., Benjamin, R.J., Wesley, P.K., Buxton, S.E., Garrett, T.P.J., Clayberger, C., Krensky, A.M., Norment, A.M., Littman, D.R. & Parham, P. (1990). A binding site for the T-cell co-receptor CD8 on the α_3 domain of HLA-A2. *Nature* **345**, 41-6.
- Salzman, G.C., Crowell, J.M., Martin, J.C., Trujillo, T.T., Romero, A., Mullaney, P.F. & LaBauve, P.M. (1975). Cell classification by laser light scattering: identification and separation of unstained leukocytes. *Acta Cytologica* **19**, 374-7.
- Sancho, J., Silverman, L.B., Castigli, E., Ahern, D., Laudano, A.P., Terhorst, C., Geha, R.S. & Chatila, T.A. (1992). Developmental regulation of transmembrane signaling via the T cell antigen receptor/CD3 complex in human T lymphocytes. *Journal of Immunology* **148**, 1315-21.
- Sanders, M.E., Makgoba, M.W., June, C.H., Young, H.A. & Shaw, S. (1989). Enhanced responsiveness of human memory T cells to CD2 and CD3 receptor-mediated activation. *European Journal of Immunology* **19**, 803-8.
- Sanders, M.E., Makgoba, M.W., Sharrow, S.O., Stephany, D., Springer, T.A., Young, H.A. & Shaw, S. (1988a). Human memory T lymphocytes express increased levels of three adhesion molecules (LFA-3, CD2 and LFA-1) and three other molecules (UCHL1, CDw29 and Pgp-1). *Journal of Immunology* **140**, 1401-7.
- Sanders, M.E., Makgoba, M.W. & Shaw, S. (1988b). Human naive and memory T cells: reinterpretation of helper-inducer and suppressor-inducer subsets. *Immunology Today* **9**, 195-9.
- Santini, M.T., Guidoni, L., Viti, V. & Indovina, P.L. (1992). Localized and transient changes in plasma membrane fluidity during *in vitro* myoblast fusion: An $^1\text{H-NMR}$ study. *Physiological Chemistry and Physics and Medical NMR* **24**, 89-96.
- Sasaki, Y., Asaoka, Y. & Nishizuka, Y. (1993). Potentiation of diacylglycerol-induced activation of protein kinase C by lysophospholipids. Subspecies difference. *FEBS Letters* **320**, 47-51.
- Schaeffer, B.E. & Curtiss, A.S.G. (1977). Effects on cell adhesion and membrane fluidity of changes in plasmalemmal lipids in mouse L929 cells. *Journal of Cell Science* **26**, 47-55.
- Schmitz, G., Fischer, H., Beuck, M., Hoecker, K.P. & Robenek, H. (1990). Dysregulation of lipid metabolism in Tangier monocyte-derived macrophages. *Arteriosclerosis* **10**, 1010-9.
- Schnittman, S.M., Psallidopoulos, M.C., Lane, H.C., Thompson, L., Baseler, M. & Massari, F. (1987). The reservoir for HIV-1 in human peripheral blood is a T cell that maintains expression of CD4. *Science* **245**, 305-8.
- Schuler, G. & Steinman, R.M. (1985). Murine epidermal Langerhans cells mature into potent immunostimulatory dendritic cells *in vitro*. *Journal of Experimental Medicine* **161**, 526-46.
- Schulman, R.G. (1983). NMR spectroscopy of living cells. *Scientific American* **248**(1), 77-84.
- Schutze, S., Potthoff, K., Machieidt, T., Berkovic, D., Wiegmann, K. & Kronke, M. (1992). TNF Activates NF- $\kappa\beta$ phosphatidylcholine-specific phospholipase C-induced "acidic" sphingomyelin breakdown. *Cell* **71**, 765-76.

- Scollay, R., Hall, J. & Orlans, E. (1976). Studies of the lymphocytes of sheep. II. Some properties of cells in various compartments of the recirculating lymphocyte pool. *European Journal of Immunology* **6**, 121-5.
- Scollay, R. & Shortman, K. (1985). Cell traffic in the adult thymus: Cell entry and exit, cell birth and death. In *Recognition and regulation in cell-mediated immunity*. (1st ed.). Edited by J.D. Watson & J. Marbrook. Marcel-Dekker, New York. pp. 3-30.
- Scollay, R., Wilson, A., D'Amico, A., Kelly, K., Egerton, M., Pearse, M., Wu, L. & Shortman, K. (1988). Developmental status and reconstitution potential of subpopulations of murine thymocytes. *Immunological Reviews* **104**, 81-120.
- Seguin, F. & Le Pape, A. (1994). ³¹P and ¹³C nuclear magnetic resonance studies of macrophages. *ImmunoMethods* **4**, 179-87.
- Selvaraj, P., Plunkett, M.L., Dustin, M., Sanders, M.E., Shaw, S. & Springer, T.A. (1987). The T lymphocyte glycoprotein CD2 binds the cell surface ligand LFA-3. *Nature* **326**, 400-3.
- Shapiro, H.M. (1981). Flow cytometric estimation of DNA and RNA content in intact cells stained with Hoechst 33342 and pyronin Y. *Cytometry* **2**, 143-50.
- Shapiro, H.M. (1995). *Practical flow cytometry*. (3rd ed.). Wiley-Liss, New York. 542 pp.
- Shaw, D. (1984). *Fourier transform N.M.R. spectroscopy*. (2nd ed.). Elsevier, Amsterdam. 344 pp.
- Shaw, S., Luce, G.E.G., Quinones, R., Gress, R.E., Springer, T.A. & Sanders, M.E. (1986). Two antigen-independent adhesion pathways used by human cytotoxic T cell clones. *Nature* **323**, 262-4.
- Shi, Y.F., Bissonnette, R.P., Parfrey, N., Szalay, M., Kubo, R.T. & Green, D.R. (1991). *In vivo* administration of monoclonal antibodies to the CD3 T cell receptor complex induces cell death (apoptosis) in immature thymocytes. *Journal of Immunology* **146**, 3340-6.
- Shipp, M.A. & Look, A.T. (1993). Hematopoietic differentiation antigens that are membrane-associated enzymes: cutting is the key! *Blood* **82**, 1052-70.
- Shortman, K. & Scollay, R. (1985). Cortical and medullary thymocytes. In *Recognition and regulation in cell-mediated immunity*. (1st ed.). Edited by J.D. Watson & J. Marbrook. Marcel-Dekker, New York. pp. 31-60.
- Singer, S.J. (1972). A fluid lipid-globular protein mosaic model of membrane structure. *Annals of the New York Academy of Sciences* **195**, 16-23.
- Singer, S.J. & Nicolson, G.L. (1972). The fluid mosaic model of the structure of cell membranes. *Science* **175**, 720-31.
- Siu, G., Clark, S.P., Yoshikai, Y., Malissen, M., Yanagi, Y., Strauss, E., Mak, T.W. & Hood, L. (1984). The human T-cell antigen receptor is encoded by variable, diversity, and joining gene segments that rearrange to generate a complete V gene. *Cell* **37**, 393-401.
- Sivaraja, M., Turner, C., Souza, K. & Singer, S. (1994). *Ex vivo* two-dimensional proton nuclear magnetic resonance spectroscopy of smooth muscle tumors: advantages of total correlated spectroscopy over homonuclear J-correlated spectroscopy. *Cancer Research* **54**, 6037-40.
- Sleckman, B.P., Rosenstein, Y., Igras, V.E., Greenstein, J.L. & Burakoff, S.J. (1991). Glycolipid-anchored form of CD4 increases intercellular adhesion but is unable to enhance T cell activation. *Journal of Immunology* **147**, 428-31.

- Slivka, S.R., Meier, K.E. & Insel, P.A. (1988). Alpha 1-adrenergic receptors promote phosphatidylcholine hydrolysis in MDCK-D1 cells. A mechanism for rapid activation of protein kinase C. *Journal of Biological Chemistry* **263**, 12242-6.
- Smaby, J.M. & Brockman, H.L. (1987). Regulation of cholesteryl oleate and triolein miscibility in monolayers and bilayers. *Journal of Biological Chemistry* **262**, 8206-12.
- Smith, C.A., Williams, G.T., Kingston, R., Jenkinson, E.J. & Owen, J.J.T. (1989). Antibodies to CD3/T-cell receptor complex induce death by apoptosis in immature T cells in thymic cultures. *Nature* **337**, 181-3.
- Smith, J.B., McIntosh, G.H. & Morris, B. (1970). The traffic of cells through tissues: a study of peripheral lymph in sheep. *Journal of Anatomy* **107**, 87-100.
- Spencer, S.C. & Fabre, J.W. (1990). Characterisation of interstitial dendritic cell as distinct leukocytes normally resident in the connective tissue of the rat heart. *Journal of Experimental Medicine* **171**, 1841-51.
- Sprent, J. (1977). Recirculating lymphocytes. In *The lymphocyte: structure and function*. (1st ed.). Edited by J.J. Marchalonis. Marcel Dekker, New York. pp. 43-112.
- Sprent, J. & Webb, S.R. (1987). Function and specificity of T cell subsets in the mouse. *Advances in Immunology* **41**, 39-133.
- Springer, T.A. (1980). Cell-surface differentiation in the mouse. In *Monoclonal antibodies. Hybridomas: a new dimension in biological analyses*. (1st ed.). Edited by R.H. Kennett, T.J. McKearn & K.B. Bechtol. Plenum Press, New York. pp. 185-217.
- Stals, H.K., Top, W. & Declercq, P.E. (1994). Regulation of triacylglycerol synthesis in permeabilized rat hepatocytes. Role of fatty acid concentration and diacylglycerol acyltransferase. *FEBS Letters* **343**, 99-102.
- Stamenkovic, I., Amiot, M., Pesando, J.M. & Seed, B. (1989). A lymphocyte molecule implicated in lymph node homing is a member of the cartilage link protein family. *Cell* **56**, 1057-62.
- Stanworth, D.R. & Turner, M.W. (1978). Immunochemical analysis of immunoglobulins and their sub-units. In *Handbook of Experimental Immunology*. Edited by D.M. Weir. Blackwell Scientific Publications, Oxford. pp. 6.1-102.
- Staunton, D.E., Dustin, M.L. & Springer, T.A. (1989). Functional cloning of ICAM-2, a cell adhesion ligand for LFA-1 homologous to ICAM-1. *Nature* **339**, 61-4.
- Steinman, R.M. (1991). The dendritic cell system and its role in immunogenicity. *Annual Review of Immunology* **9**, 271-96.
- Straus, D.B. & Weiss, A. (1993). The CD3 chains of the T cell receptor associate with the Zap-70 tyrosine kinase and are tyrosine phosphorylated after receptor stimulation. *Journal of Experimental Medicine* **178**, 1523-30.
- Streuli, M., Hall, L.R., Saga, Y., Schlossman, S.F. & Saito, H. (1990). Differential usage of three exons generates at least five different mRNAs encoding human leukocyte common antigens. *Journal of Experimental Medicine* **166**, 1548-66.
- Strulovici, B., Daniel-Isskani, S., Baxter, G., Knopf, J., Sultzman, L., Cherwiniski, H., Nestor, J.J., Webb, D.R. & Ransom, J. (1991). Distinct mechanisms of regulation of protein kinase C epsilon by hormones and phorbol diesters. *Journal of Biological Chemistry* **266**, 168-73.
- Stubbs, C.D., Tsang, W.M., Belin, J., Smith, A.D. & Johnson, S.M. (1980). Incubation of exogenous fatty acids with lymphocytes. Changes in fatty acid composition and effects on the rotational relaxation time of 1,6-diphenyl-1,3,5-hexatriene. *Biochemistry* **19**, 2756-62.

- Suda, T., Takahashi, T., Goldstein, P. & Nagata, S. (1993). Molecular cloning and expression of the Fas ligand, a novel member of the tumour necrosis factor family. *Cell* **75**, 1169-78.
- Swain, S.L. (1983). T cell subsets and the recognition of MHC class. *Immunological Reviews* **74**, 129-42.
- Szamel, M., Bartels, F. & Resch, K. (1993). Cyclosporin A inhibits T cell receptor-induced interleukin-2 synthesis of human T lymphocytes by selectively preventing a transmembrane signal transduction pathway leading to sustained activation of a protein kinase C isoenzyme, protein kinase C β . *European Journal of Immunology* **23**, 3072-81.
- Szamel, M., Kracht, M., Krebs, B., Hubner, U. & Resch, K. (1990). Activation signals in human lymphocytes: Interleukin 2 synthesis and expression of high affinity interleukin 2 receptors require differential signalling for the activation of protein kinase C. *Cellular Immunology* **126**, 117-28.
- Szamel, M., Rehmann, B., Krebs, B., Kurrle, R. & Resch, K. (1989). Activation signals in human lymphocytes: incorporation of polyunsaturated fatty acids into plasma membrane phospholipids regulates IL-2 synthesis via sustained activation of protein kinase C. *Journal of Immunology* **143**, 2806-13.
- Szamel, M. & Resch, K. (1995). T-cell antigen receptor-induced signal-transduction pathways: activation and function of protein kinases C in T lymphocytes. *European Journal of Biochemistry* **228**, 1-15.
- Sze, D.Y. & Jardetzky, O. (1990a). Characterization of lipid composition in stimulated human lymphocytes by $^1\text{H-NMR}$. *Biochimica et Biophysica Acta* **1054**, 198-206.
- Sze, D.Y. & Jardetzky, O. (1990b). Determination of metabolite and nucleotide concentrations in proliferating lymphocytes by $^1\text{H-NMR}$ of acid extracts. *Biochimica et Biophysica Acta* **1054**, 181-97.
- Sze, D.Y. & Jardetzky, O. (1994). High-resolution proton NMR studies of lymphocyte extracts. *ImmunoMethods* **4**, 113-26.
- Tadakuma, T., Kizaki, H., Odaka, C., Kubota, R., Ishimura, Y., Yagita, H. & Okamura, K. (1990). CD4+CD8+ thymocytes are susceptible to DNA fragmentation induced by phorbol ester, calcium ionophore and anti-CD3 antibody. *European Journal of Immunology* **20**, 779-84.
- Takai, Y., Kishimoto, A., Inoue, M. & Nishizuka, Y. (1977). Studies on a cyclic nucleotide-independent protein kinase and its proenzyme in mammalian tissues. I. Purification and characterisation of an active enzyme from bovine cerebellum. *Journal of Biological Chemistry* **252**, 7603-09.
- Tanner, J., Weis, J., Fearon, D., Whang, Y. & Kieff, E. (1987). Epstein-Barr virus gp350/220 binding to the B lymphocyte C3d receptor mediates adsorption, capping, and endocytosis. *Cell* **50**, 203-13.
- Taylor, I.W. & Hodson, P. (1984). Cell cycle regulation by environmental pH. *Journal of Physiology* **121**, 517-25.
- Terada, N., Or, R., Szepesi, A., Lucas, J.J. & Gelfand, E.W. (1993). Definition of the roles for iron and essential fatty acids in cell cycle progression of normal human T lymphocytes. *Experimental Cell Research* **204**, 260-7.
- Terce, F., Brun, H. & Vance, D.E. (1994). Requirement of phosphatidylcholine for normal progression through the cell cycle in C3H/10T1/2 fibroblasts. *Journal of Lipid Research* **35**, 2130-42.
- Uranus, E.R. & Allen, P.M. (1987). The basis for the immunoregulatory role of macrophages and other accessory cells. *Science* **236**, 551-7.

- Tessner, T.G., Rock, C.O., Kalmar, G.B., Cornell, R.B. & Jackowski, S. (1991). Colony-stimulating factor 1 regulates CTP:phosphocholine cytidyltransferase mRNA levels. *Journal of Biological Chemistry* **266**, 16261-64.
- Testi, R., Pulcinelli, F., Frati, L., Gazzaniga, P.P. & Santoni, A. (1990). CD69 is expressed on platelets and mediates platelet activation and aggregation. *Journal of Experimental Medicine* **172**, 701-7.
- Thomas, M.L. (1989). The leukocyte common antigen family. *Annual Review of Immunology* **7**, 339-69.
- Tijburg, L.B.M., Geelen, M.J.H. & Van Golde, L.M.G. (1989). Regulation of the biosynthesis of triacylglycerol, phosphatidylcholine and phosphatidylethanolamine in the rat liver. *Biochimica et Biophysica Acta* **1004**, 1-19.
- Toothill, V.J., Van Mourik, J.A., Niewenhuis, H.K., Metzelaar, M.J. & Pearson, J.D. (1990). Characterization of the enhanced adhesion of neutrophil leukocytes to thrombin-stimulated endothelial cells. *Journal of Immunology* **145**, 283-91.
- Townsend, A.R.M., Rothbard, J., Gotch, F.M., Bahadur, G., Wraith, D. & McMichael, A.J. (1986). The epitopes of influenza nucleoprotein recognised by cytotoxic T lymphocytes can be defined with short synthetic peptides. *Cell* **44**, 959-68.
- Traill, K.N., Huber, L.A., Wick, G. & Jurgens, G. (1990). Lipoprotein interactions with T cells: an update. *Immunology Today* **11**, 411-7.
- Traill, K.N., Jurgens, G., Bock, G. & Wick, G. (1987). High density lipoprotein uptake by freshly isolated human peripheral blood T lymphocytes. *Immunobiology* **175**, 447-54.
- Traill, K.N. & Wick, G. (1984). Lipids and lymphocyte function. *Immunology Today* **5**, 70-6.
- Triggiani, M., D'Souza, D.M. & Chilton, F.H. (1991). Metabolism of 1-acyl-2-acetyl-sn-glycero-3-phosphocholine in the human neutrophil. *Journal of Biological Chemistry* **266**, 6928-35.
- Triggiani, M., Oriente, A. & Marone, G. (1994). Differential roles for triglyceride and phospholipid pools of arachidonic acid in human lung macrophages. *Journal of Immunology* **152**, 1394-403.
- Tronchere, H., Planat, V., Record, M., Terce, F., Ribbes, G. & Chap, H. (1995). Phosphatidylcholine turnover in activated human neutrophils. Agonist-induced cytidyltransferase translocation is subsequent to phospholipase D activation. *Journal of Biological Chemistry* **270**, 13138-46.
- Tronchere, H., Record, M., Terce, F. & Chap, H. (1994). Phosphatidylcholine cycle and regulation of phosphatidylcholine biosynthesis by enzyme translocation. *Biochimica et Biophysica Acta* **1212**, 137-51.
- Tse, A.G., Barclay, A.N., Watts, A. & Williams, A.F. (1985). A glycopospholipid tail at the carboxyl terminus of the Thy-1 glycoprotein of neurons and thymocytes. *Science* **230**, 1003-8.
- Tsien, R.Y., Pozzan, T. & Rink, T.J. (1972). T-cell mitogens cause early changes in cytoplasmic free Ca^{2+} and membrane potential in lymphocytes. *Nature* **295**, 68-71.
- Tuveson, D.A., Ahearn, J.M., Matsumoto, A.K. & Fearon, D.T. (1991). Molecular interactions of complement receptors on B lymphocytes: a CR1/CR2 complex distinct from the CR2/CD19 complex. *Journal of Experimental Medicine* **173**, 1083-9.
- Unanue, E.R. & Allen, P.M. (1987). The basis for the immunoregulatory role of macrophages and other accessory cells. *Science* **236**, 551-7.

- van Blitterswijk, W.J., Hilkmann, H., de Widt, J. & van der Bend, R.L. (1991a). Phospholipid metabolism in bradykinin-stimulated human fibroblasts. I. Biphasic formation of diacylglycerol from phosphatidylinositol and phosphatidylcholine, controlled by protein kinase C. *Journal of Biological Chemistry* **266**, 10337-43.
- van Blitterswijk, W.J., Hilkmann, H., de Widt, J. & van der Bend, R.L. (1991b). Phospholipid metabolism in bradykinin-stimulated human fibroblasts. II. Phosphatidylcholine breakdown by phospholipases C and D; involvement of protein kinase C. *Journal of Biological Chemistry* **266**, 10344-50.
- Van der Giessen, M., Postma, S. & The, T.H. (1985). Isolation of highly purified lymphocyte subsets for functional studies by means of an indirect rosette technique. *Scandinavian Journal of Immunology* **22**, 41-9.
- Vance, D.E. (1986). Phospholipid metabolism in eucaryotes. In *Biochemistry of lipids and membranes*. (1st ed.). Edited by D.E. Vance & J.E. Vance. Benjamin-Cummings, Menlo Park, California. pp. 242-70.
- Veale, M.F., Dingley, A.J., King, G.F. & King, N.J.C. (1996). ¹H-NMR visible mobile neutral lipids: relationship to phosphatidylcholine cycling. *Biochimica et Biophysica Acta*, **1303**, 215-221.
- Veis, N. & Hamilton, J.A. (1991). Colony stimulating factor-1 stimulates diacylglycerol generation in murine bone marrow-derived macrophages, but not in resident peritoneal macrophages. *Journal of Cellular Physiology* **147**, 298-305.
- Von Boehmer, H., Karjalainen, K., Pelkonen, J., Borgulya, P. & Rammensee, H.-G. (1988). The T-cell receptor for antigen in T-cell development and repertoire selection. *Immunological Reviews* **101**, 21-37.
- Waldman, T.A. (1989). The multi-subunit interleukin-2 receptor. *Annual Review of Biochemistry* **58**, 875-911.
- Watkins, J.D. & Kent, C. (1991). Regulation of CTP:phosphocholine cytidyltransferase activity and subcellular location by phosphorylation in Chinese hamster ovary cells. The effect of phospholipase C treatment. *Journal of Biological Chemistry* **266**, 21113-7.
- Wegner, A.M., Letourneur, F., Hoeveler, A., Brocker, T., Luton, F. & Malissen, B. (1992). The T cell receptor/CD3 complex is composed of at least two autonomous transduction modules. *Cell* **68**, 83-95.
- Weiss, A. (1989). T lymphocyte activation. In *Fundamental Immunology*. (2nd ed.). Edited by W.E. Paul. Raven Press, New York. pp. 359-84.
- Weiss, A., Iwashima, M., Irving, B., van Oers, N.S.C., Kadlecsek, T.A., Straus, D. & Chan, A. (1994). Molecular and genetic insights into T cell antigen receptor signal transduction. In *Mechanisms of lymphocyte activation and immune regulation V: molecular basis of signal transduction*. (1st ed.). Edited by S. Gupta, W.E. Paul, A. De Franco & R. Perlmutter. Plenum Press, New York. pp. 53-62.
- Weller, P.F., Ryeom, S.W., Picard, S.T., Ackerman, S.J. & Dvorak, A.M. (1991). Cytoplasmic lipid bodies of neutrophils: Formation induced by *cis*-unsaturated fatty acids and mediated by protein kinase C. *The Journal of Cell Biology* **113**, 137-46.
- Whiteside, T.L. & Herberman, R.B. (1994). Role of human natural killer cells in health and disease. *Clinical and Diagnostic Laboratory Immunology* **1**, 125-33.
- Whitlon, D.S., Anderson, K.E. & Mueller, G.C. (1985). Analysis of the effects of fatty acids and related compounds on the synthesis of phosphatidylcholine in lymphocytes. *Biochimica et Biophysica Acta* **835**, 369-77.
- Williams, A.F. & Gagnon, J. (1982). Neuronal cell Thy-1 glycoprotein: homology with immunoglobulin. *Science* **216**, 696-703.

- Wright, L.C., May, G.L., Dyne, M. & Mountford, C.E. (1986). A proteolipid in cancer cells is the origin of their high-resolution NMR spectrum. *FEBS Letters* **203**, 164-8.
- Wright, L.C., May, G.L., Gregory, P., Dyne, M., Holmes, K.T., Williams, P.G. & Mountford, C.E. (1988). Inhibition of metastatic potential by fucosidase: an NMR study identifies a cell surface metastasis marker. *Journal of Cellular Biochemistry* **37**, 49-59.
- Wüthrich, K., Billeter, M. & Braun, W. (1984). Polypeptide secondary structure determination by nuclear magnetic resonance observation of short proton-proton distances. *Journal of Molecular Biology* **180**, 715-40.
- Xu, X.-X., Tessner, T.G., Rock, C.O. & Jackowski, S. (1993). Phosphatidylcholine hydrolysis and *c-myc* expression are in collaborating mitogenic pathways activated by colony-stimulating factor 1. *Molecular and Cellular Biology* **13**, 1522-33.
- Yamaguchi, H., Hosokawa, K., Jiang, Z.L., Takahashi, A., Ikehara, T. & Miyamoto, H. (1993). Arrest of cell cycle progression of HeLa cells in the early G1 phase in K⁺-depleted conditions and its recovery upon addition of insulin and LDL. *Journal of Cellular Biochemistry* **53**, 13-20.
- Yang, W. & Jackowski, S. (1995). Lipid activation of CTP:phosphocholine cytidyltransferase is regulated by the phosphorylated carboxyl-terminal domain. *Journal of Biological Chemistry* **270**, 16503-6.
- Yewdell, J.W. & Bennink, J.R. (1990). The binary logic of antigen processing and presentation to T cells. *Cell* **62**, 203-6.
- Yirrell, D.L., Reid, H.W., Norval, M., Entrican, G. & Miller, H.R.P. (1991). Response of efferent lymph and popliteal lymph node to epidermal infection of sheep with Orf virus. *Veterinary Immunology and Immunopathology* **28**, 219-35.
- Yoshikai, Y., Clark, S.P., Taylor, S., Sohn, U., Wilson, B.I., Minden, M.D. & Mak, T.W. (1985). Organization and sequences of the variable, joining and constant region genes of the human T-cell receptor alpha-chain. *Nature* **316**, 837-40.
- Zinkernagel, R.M., Callahan, G.N., Klein, J. & Dennert, G. (1978). Cytotoxic T cells learn specificity for self H-2 during differentiation in the thymus. *Nature* **336**, 73-6.

When compounds or cells are placed in the magnetic field of an NMR spectrometer, two non-degenerate energy levels are created for nuclei with spin quantum number $I=1/2$ (Figure A3.1). The lower energy level (α) corresponds to nuclear spins aligned with the magnetic field, while the higher energy level (β) corresponds to nuclear spins aligned against the magnetic field. The transition from the lower to the higher energy level is achieved by the absorption of rf waves at a characteristic nuclear resonance frequency which corresponds to the energy difference between the α and β states.

The resonance frequency depends on the type of nucleus. NMR spectroscopy can therefore be used to identify different types of nuclei. Almost all biological samples have NMR-receptive nuclei which can be monitored without the use of radiochemically labelled tracer

Appendix 1.

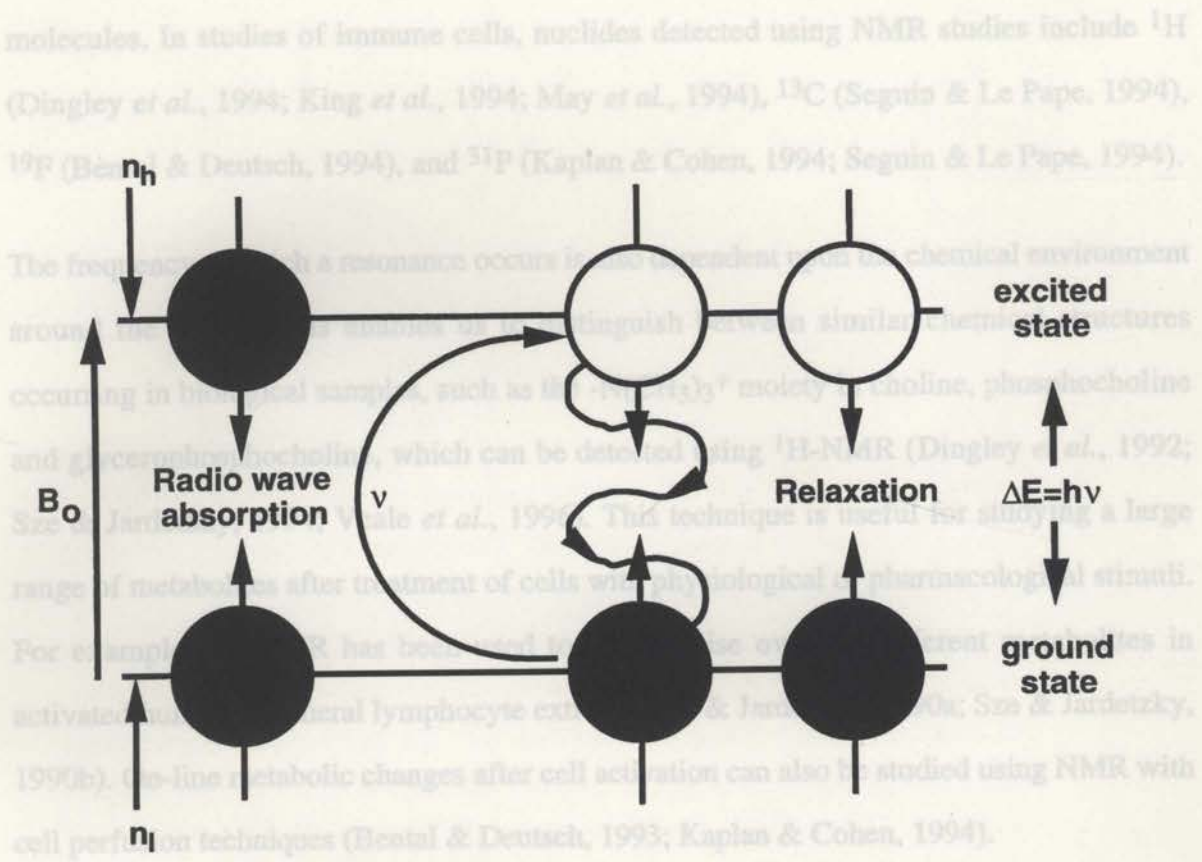
The theory of nuclear magnetic resonance (NMR) spectroscopy.

A1.1. Introduction.

Nuclear magnetic resonance (NMR) spectroscopy is a method used to detect the chemical environment around atomic nuclei. NMR occurs when the nuclei in a sample, placed in a magnetic field of particular field strength, absorb electromagnetic radiation in a particular radio frequency (rf) range (Figure A1.1). NMR can be used to determine chemical structures, to identify chemicals, and to monitor changes in the environment around molecules. Chemical, biophysical, and metabolic changes occurring in biological samples, such as proteins, cells or whole organisms, can therefore be monitored (Knowles *et al.*, 1976; Levy & Craik, 1981; Schulman, 1983; Cohen, 1987; Adam *et al.*, 1989; King & Kuchel, 1994). NMR differs from other forms of spectroscopy in that it uses the absorption of radio waves, which have long wavelengths, to detect these changes.

When compounds or cells are placed in the magnetic field of an NMR spectrometer, two non-degenerate energy levels are created for nuclei with spin quantum number $I=1/2$ (Figure A1.1). The lower energy level (α) corresponds to nuclear spins aligned with the magnetic field, while the higher energy level (β) corresponds to nuclear spins aligned against the magnetic field. The transition from the lower to the higher energy level is achieved by the absorption of rf waves at a characteristic nuclear resonance frequency which corresponds to the energy difference between the α and β states.

The resonance frequency depends on the type of nucleus. NMR spectroscopy can therefore be used to identify different types of nuclei. Almost all biological samples have NMR-receptive nuclei which can be monitored without the use of radiochemically labelled tracer



A1.2. Theory of Fourier transform NMR spectroscopy.

Quantum mechanical description.

Figure A1.1. Thermal population of energy levels and spin-lattice relaxation from the excited energy level.

made by Pauli in 1924. The spinning nuclei generate a dipolar magnetic field and the Absorption of radiofrequency radiation can promote nuclei from the ground state to the excited state, but this can only occur if there is an excess of nuclei in the ground state. Although the ratio n_h/n_l at equilibrium is close to unity, the ground state is slightly more energetically favourable, rendering net absorption possible in an NMR experiment. The number of nuclei in the high energy state (n_h) compared with the number in the low energy state (n_l) at equilibrium is determined by the Boltzmann distribution (see text). Adapted from Knowles *et al.* (1976).

the effect of gravity upon a spinning top which wobbles as it spins. This precession (or wobbling) can be described by the following relationship known as the Larmor equation (Shaw, 1984):

$$\omega_0 = -\gamma B_0$$

molecules. In studies of immune cells, nuclides detected using NMR studies include ^1H (Dingley *et al.*, 1994; King *et al.*, 1994; May *et al.*, 1994), ^{13}C (Seguin & Le Pape, 1994), ^{19}F (Bental & Deutsch, 1994), and ^{31}P (Kaplan & Cohen, 1994; Seguin & Le Pape, 1994).

The frequency at which a resonance occurs is also dependent upon the chemical environment around the nuclei. This enables us to distinguish between similar chemical structures occurring in biological samples, such as the $-\text{N}(\text{CH}_3)_3^+$ moiety in choline, phosphocholine and glycerophosphocholine, which can be detected using ^1H -NMR (Dingley *et al.*, 1992; Sze & Jardetzky, 1994; Veale *et al.*, 1996). This technique is useful for studying a large range of metabolites after treatment of cells with physiological or pharmacological stimuli. For example, ^1H -NMR has been used to characterise over 50 different metabolites in activated human peripheral lymphocyte extracts (Sze & Jardetzky, 1990a; Sze & Jardetzky, 1990b). On-line metabolic changes after cell activation can also be studied using NMR with cell perfusion techniques (Bental & Deutsch, 1993; Kaplan & Cohen, 1994).

A1.2. Theory of Fourier transform NMR spectroscopy.

Quantum mechanical description.

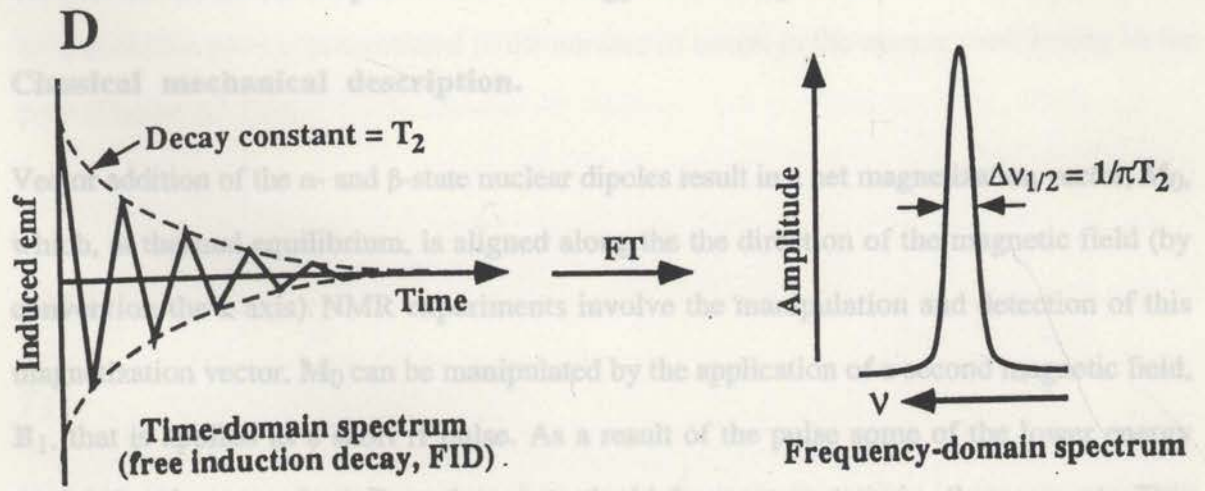
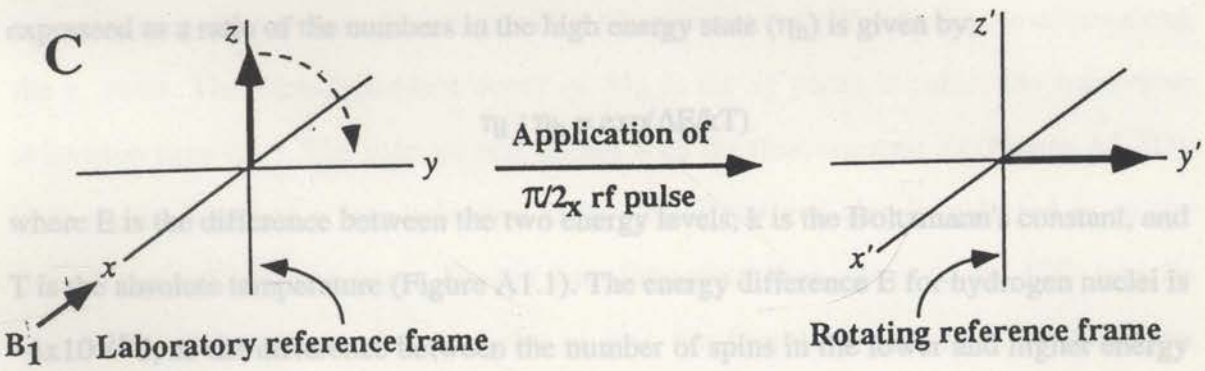
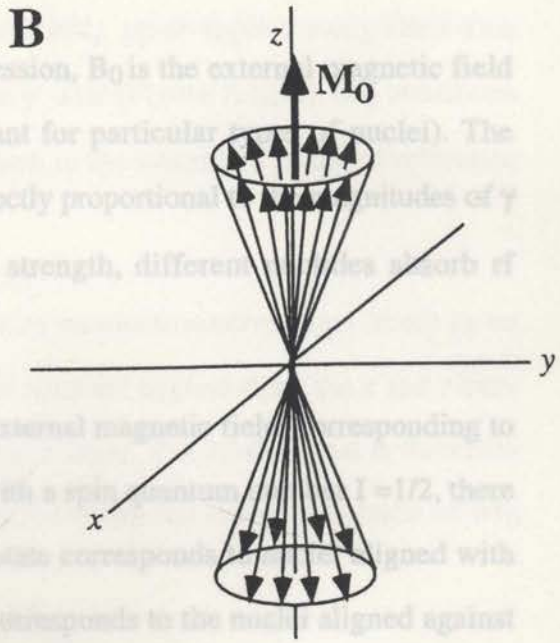
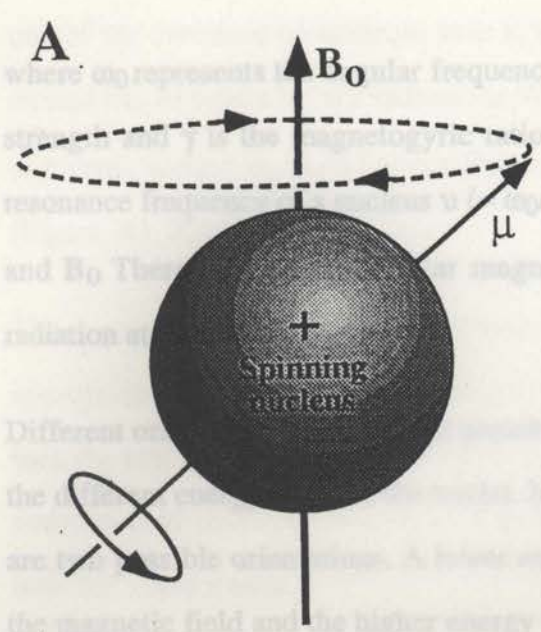
The observation that particular nuclei spin and therefore possess angular momentum was made by Pauli in 1924. The spinning nuclei generate a dipolar magnetic field and the magnetic dipole is denoted as μ in Figure A1.2A. Magnetic nuclei can be thought of as bar magnets possessing angular momentum.

When a nucleus is placed in a magnetic field (B_0) it aligns in the direction of B_0 and precesses, i.e., its axis of rotation rotates around the direction of B_0 . This can be likened to the effect of gravity upon a spinning top which wobbles as it spins. This precession (or wobbling) can be described by the following relationship known as the Larmor equation (Shaw, 1984);

$$\omega_0 = -\gamma B_0$$

Figure A1.2. Proton spin and angular momentum.

(A) A spinning nucleus with associated magnetic dipole moment, μ , precessing around the axis of the external magnetic field, \mathbf{B}_0 . (B) A collection of nuclei in a magnetic field. The spins align with \mathbf{B}_0 (low energy state) or against \mathbf{B}_0 (high energy state). A net magnetization vector \mathbf{M}_0 results from the excess of spins in the low energy state. (C) The application of an rf pulse along the x axis causes the magnetization to nutate onto the y axis in the rotating frame of reference. (D) The precessing magnetization after the rf pulse is stopped, induces an emf in the receiver coil and generates a time domain NMR spectrum called a free induction decay (FID). This oscillates cosinusoidally and decays with a time-constant T_2 . Fourier transformation of the FID results in a frequency domain spectrum, where the peak linewidth ($\Delta \nu_{1/2}$) at half height is $1/\pi T_2$ (from King & Kuchel, 1994).



where ω_0 represents the angular frequency of precession, B_0 is the external magnetic field strength and γ is the magnetogyric ratio (a constant for particular types of nuclei). The resonance frequency of a nucleus ν ($= \omega_0/2\pi$) is directly proportional to the magnitudes of γ and B_0 . Therefore, at a particular magnetic field strength, different nuclides absorb rf radiation at different frequencies.

Different orientations of nuclei are possible in the external magnetic field, corresponding to the different energy states of the nuclei. In nuclei with a spin quantum number $I = 1/2$, there are two possible orientations. A lower energy (α) state corresponds to nuclei aligned with the magnetic field and the higher energy (β) state corresponds to the nuclei aligned against the magnetic field (Figure A1.2B). The Boltzmann equation gives a ratio of the number of nuclei in the two energy spin states. The number of nuclei in the low energy state (η_l) expressed as a ratio of the numbers in the high energy state (η_h) is given by;

$$\eta_l / \eta_h = \exp(\Delta E/kT)$$

where E is the difference between the two energy levels, k is the Boltzmann's constant, and T is the absolute temperature (Figure A1.1). The energy difference E for hydrogen nuclei is $\sim 4 \times 10^{-25}$ J, so the difference between the number of spins in the lower and higher energy states is very small. Therefore, NMR is an inherently insensitive spectroscopic technique because the net excess of spins in the low energy state is very small.

Classical mechanical description.

Vector addition of the α - and β -state nuclear dipoles result in a net magnetization vector, \mathbf{M}_0 , which, at thermal equilibrium, is aligned along the the direction of the magnetic field (by convention the z axis). NMR experiments involve the manipulation and detection of this magnetization vector. \mathbf{M}_0 can be manipulated by the application of a second magnetic field, \mathbf{B}_1 , that is applied as a short rf pulse. As a result of the pulse some of the lower energy nuclei absorb energy from \mathbf{B}_1 and move to the higher-energy state, ie., they resonate. This causes \mathbf{M}_0 to nutate around \mathbf{B}_1 . The angle of the nutation of \mathbf{M}_0 is determined by the magnitude and duration of the \mathbf{B}_1 pulse. In most experiments the rf pulse is applied along

one of the cartesian co-ordinate axes x , y , $-x$, or $-y$. A $\pi/2_x$ pulse applied along the x axis causes \mathbf{M}_0 to nutate by $\pi/2$ radians, or 90° , onto the y axis (Figure A1.2C). \mathbf{M}_0 continues to precess around \mathbf{B}_0 at its Larmor frequency as shown in the laboratory frame of reference (Figure A1.2C).

The precession of \mathbf{M}_0 in the transverse plane induces an electromotive force (emf) in an appropriately positioned receiver coil. If two receiver coils are aligned along the x and y axes then the emf induced will be 90° out of phase with each other. The NMR signal is therefore composed of two components, M'_x and M'_y , which correspond to the projection of \mathbf{M}_0 onto the x and y axes.

After a $\pi/2_x$ pulse, M'_y is maximal and then declines to zero. The rate at which the signal in the receiver coils declines is dependent upon the rate of nuclear relaxation. Longitudinal relaxation time (T_1) reflects the rate at which \mathbf{M}_0 returns to equilibrium (i.e., re-aligns along the z axis). The time-dependent decay of \mathbf{M}_0 in the xy plane is called the transverse relaxation time (T_2). The induced emf decays with the time constant T_2 (Figure A1.2D). This signal is called a free induction decay (FID) and can also be referred to as the time-domain NMR spectrum. Fourier transformation then converts the FID into its component amplitudes and frequencies to give the frequency-domain NMR spectrum (Figure A1.2D). The frequency of a peak or resonance is dependent upon the chemical environment of the nucleus and can therefore be used for identification. The peak height or area under the peak is proportional to the number of nuclei in the sample contributing to the peak (Figure A1.2D).

Chemical Shift.

NMR Relaxation.

T_1

The chemical shift is characteristic for a particular chemical group and occurs at the Larmor frequency expressed in parts per million (ppm) relative to an internal reference standard. T_1 is the longitudinal relaxation time. It is a measure of the time taken by the magnetisation to return to thermal equilibrium. The signal decays due to the transfer of energy from the

excited or resonating nuclei to other surrounding nuclei. T_1 is also known as spin-lattice relaxation, where the term lattice refers to the network of surrounding nuclei.

The magnetization M at a time τ after an rf pulse is described by the following equation;

$$M = M_p \exp(\tau / T_1) + M_0[1 - \exp(\tau / T_1)]$$

Linewidth is measured in Hertz at half the peak height ($\Delta\nu_{1/2}$). It is related to the transverse relaxation time by the equation where M_p is the magnetization immediately after the pulse and M_0 is the equilibrium magnetization. Therefore, in experiments where the peaks are used to quantify metabolites, an intertransient delay of $\sim 5 \times T_1$ is used to ensure that equilibrium is almost completely recovered before the next transient is acquired.

T_2 peak area is obtained by computer integration and is proportional to the number of nuclei contributing to the resonance.

T_2 is the transverse relaxation time. It describes the rate of loss of the NMR signal in the transverse (xy) plane. T_2 is also known as the spin relaxation time as it also involves the coupled flipping of nuclei in opposite directions between high and low energy states (Knowles *et al.*, 1976; Derome, 1989).

A1.3. The NMR spectrum.

The five essential features of an NMR spectrum are chemical shift, linewidth, peak area, multiplicity and phase. In order to distinguish the spectrum from electrical noise, signal averaging must be done. These features are discussed below (Knowles *et al.*, 1976).

Chemical Shift.

Note that chemical shift is B_0 -independent, thus enabling resonance frequencies to be compared at different magnetic field strengths.

The chemical shift is characteristic for a particular chemical group and occurs at the Larmor frequency expressed in parts per million (ppm) relative to an internal reference standard:

$$\text{Chemical shift (ppm)} = \left(\frac{\text{sample frequency} - \text{reference frequency}}{\text{reference frequency}} \right) \times 10^6$$

Linewidth.

Linewidth is measured in Hertz at half the peak height ($\Delta\nu_{1/2}$). It is related to the transverse relaxation time by the equation

$$\Delta\nu_{1/2} = 1/\pi T_2.$$

Area of Peak.

A1.4. Two-dimensional NMR spectroscopy.

The peak area is obtained by computer integration and is proportional to the number of nuclei contributing to the resonance.

Peak Multiplicity.

The multiplicity, or "splitting", of NMR spectral peaks is due to J coupling, or spin-spin coupling. It results from the influences of local magnetic fields from adjacent nuclei. The separation of the split peaks is measured in Hertz (Hz) and is called the coupling constant (J). J -coupling effects only exert an influence upon nuclei within 3-4 chemical bonds of each other. A peak arising from a spin 1/2 nucleus, separated from n adjacent spin 1/2 nuclei by ≤ 3 chemical bonds, will be split into $n + 1$ peaks.

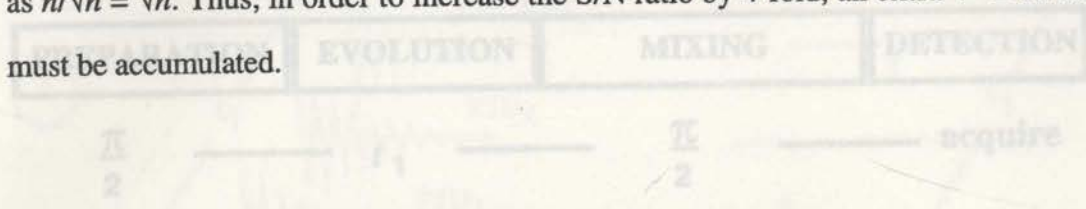
Phase.

Phase describes whether the peak is upright or inverted or dispersive (both upright and inverted). Usually peaks are in the upright position but in some cases where multiple pulse experiments are used the spectra can display inverted or dispersive peaks.

Sensitivity and Signal Averaging.

NMR is a relatively insensitive form of spectroscopy, as it only detects a very small excess of nuclear spins in the lower energy state (Figure A1.2B). This makes it difficult to visualise the peaks above the electrical noise arising from a number of electrical components of the

spectrometer. The signal-to-noise ratio can be improved by collecting a large number of transients and adding these signals together before FT to give the spectrum. The number of scans or transients corresponds to the number of FIDs acquired. The intensity of the signal is proportional to the number of transients n , and increases as n . However, noise adds destructively and its intensity only increases as \sqrt{n} . Thus, the signal-to-noise ratio increases as $n/\sqrt{n} = \sqrt{n}$. Thus, in order to increase the S/N ratio by 4-fold, an extra $4^2 = 16$ transients must be accumulated.



A1.4. Two-dimensional NMR spectroscopy.

In one-dimensional ^1H -NMR spectra there are a large number of overlapping peaks, unlike most ^{13}C and ^{31}P NMR of biological samples. This is due to the presence of ^1H protons in almost all biological molecules. The resonance overlap can be extensive in ^1H -NMR spectra, which makes identification and integration of peaks for the assignment of resonances and the quantitation of metabolites difficult. By extension of the NMR experiment into a second frequency dimension the resolution can be improved. Two-dimensional (2D) NMR was developed in the 1970s by Professor Richard Ernst, who was awarded the Nobel Prize for his achievements in 1992.

There are a number of different types of 2D experiments, with two of the most common being COSY (CORrelated SpectroscopY) and NOESY (Nuclear Overhauser Effect SpectroscopY) (Marion & Wüthrich, 1983; Brown *et al.*, 1984; Wüthrich *et al.*, 1984). In this thesis COSY experiments are shown. The basis of a 2D COSY NMR experiment is illustrated in Figure A1.3. The second frequency dimension is created by introducing an incremental delay period, t_1 sandwiched between two pulses. A schematic diagram of the way in which such a pulse can be used to generate a second frequency dimension is shown in Figure A1.4. The value of t_1 is incrementally increased from zero to several milliseconds over a number of experiments (Figure A1.4A). As t_1 increases, \mathbf{M} evolves and results in the 1D spectra from each of the experiments showing the same resonances but with variable

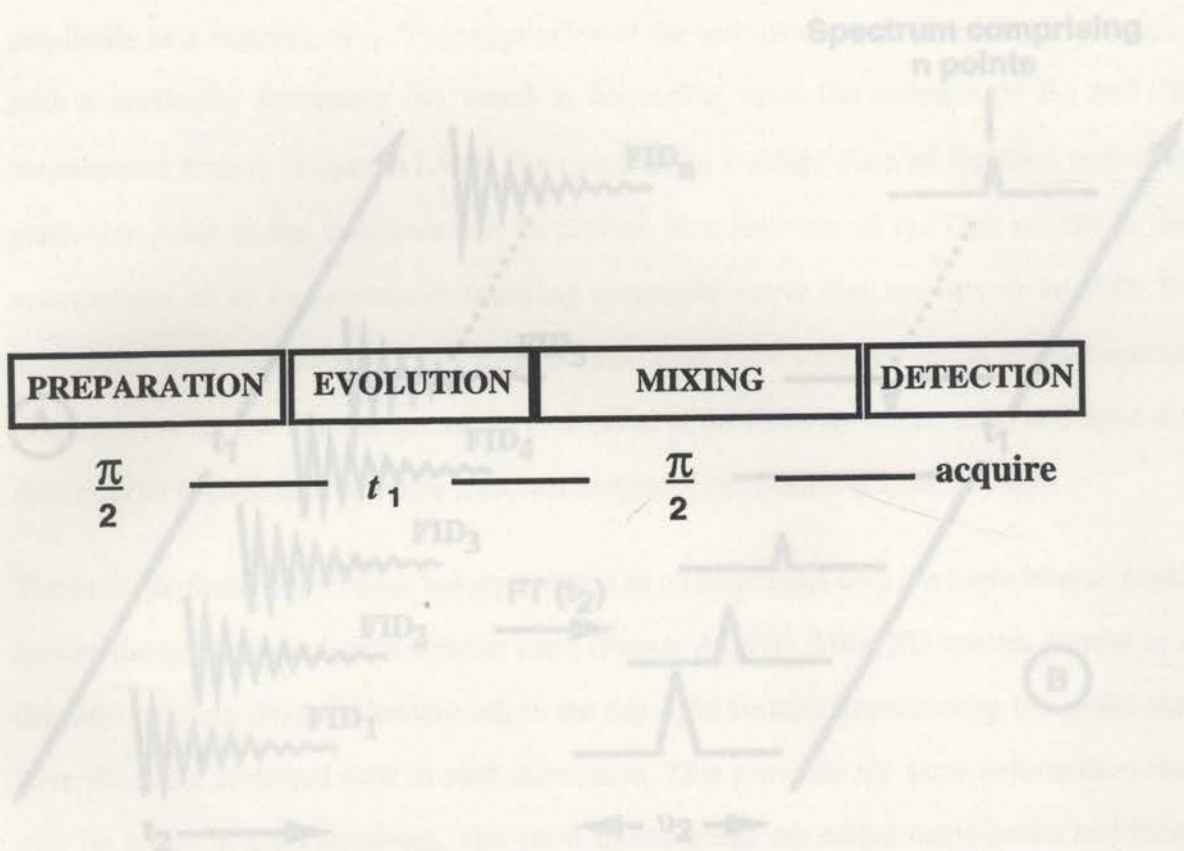


Figure A1.3. The general philosophy of 2D COSY experiment.

Adapted from Derome (1989).

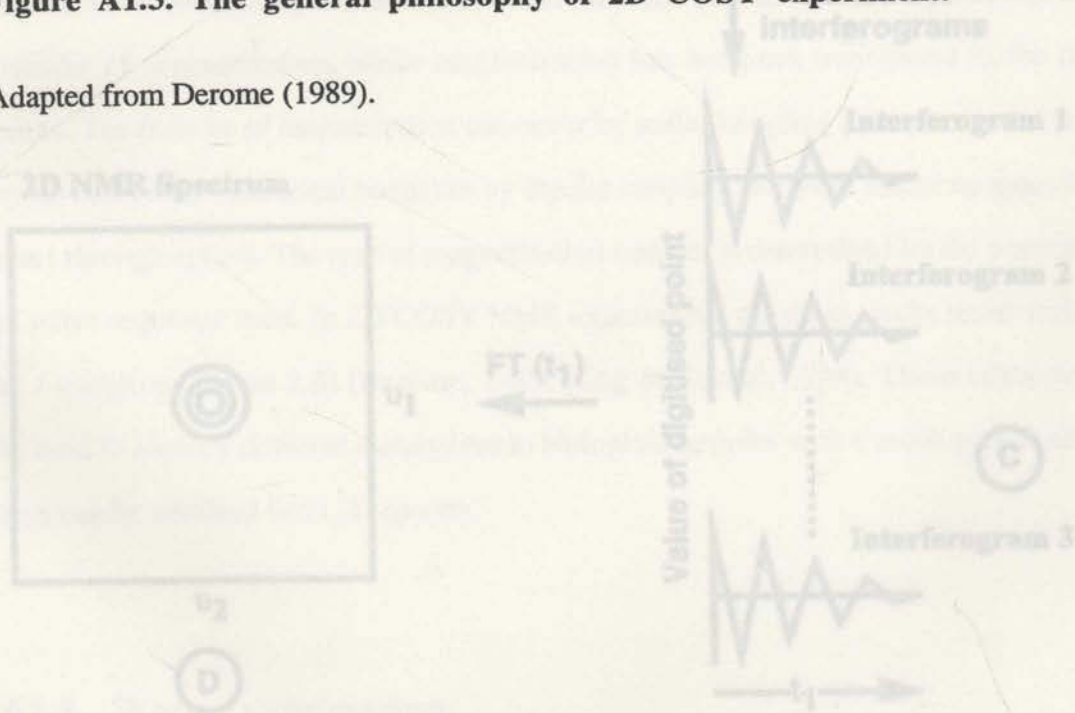


Figure A1.4. Schematic representation of the general 2D NMR experiment.

Adapted from King and Mackay (1996). See text for details.

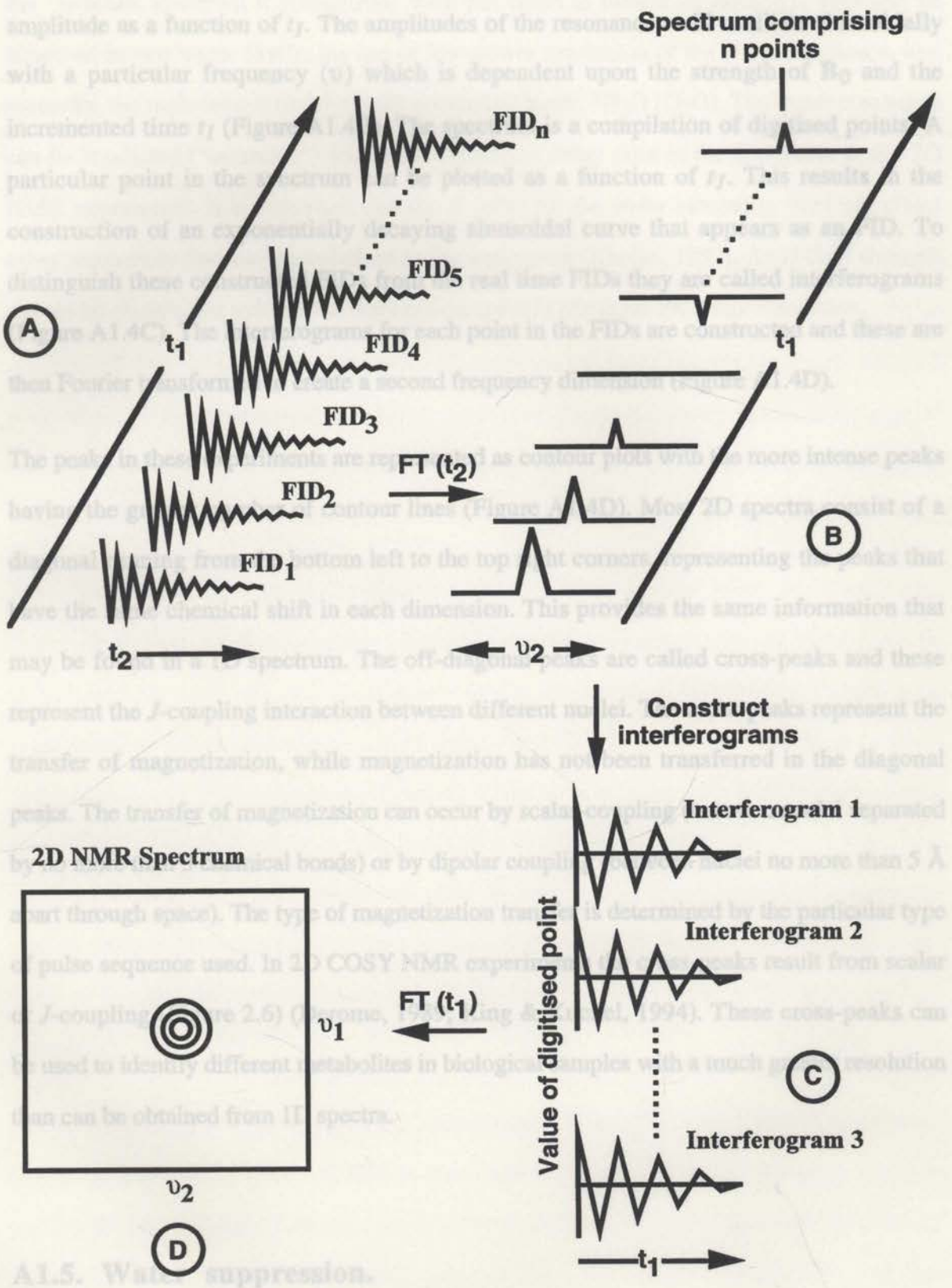


Figure A1.4. Schematic representation of the general 2D NMR experiment.

Adapted from King and Mackay (1996). See text for details.

amplitude as a function of t_1 . The amplitudes of the resonances will oscillate sinusoidally with a particular frequency (ν) which is dependent upon the strength of B_0 and the incremented time t_1 (Figure A1.4B). The spectrum is a compilation of digitised points. A particular point in the spectrum can be plotted as a function of t_1 . This results in the construction of an exponentially decaying sinusoidal curve that appears as an FID. To distinguish these constructed FIDs from the real time FIDs they are called interferograms (Figure A1.4C). The interferograms for each point in the FIDs are constructed and these are then Fourier transformed to create a second frequency dimension (Figure A1.4D).

The peaks in these experiments are represented as contour plots with the more intense peaks having the greater number of contour lines (Figure A1.4D). Most 2D spectra consist of a diagonal running from the bottom left to the top right corners, representing the peaks that have the same chemical shift in each dimension. This provides the same information that may be found in a 1D spectrum. The off-diagonal peaks are called cross-peaks and these represent the J -coupling interaction between different nuclei. The cross-peaks represent the transfer of magnetization, while magnetization has not been transferred in the diagonal peaks. The transfer of magnetization can occur by scalar-coupling (between nuclei separated by no more than 3 chemical bonds) or by dipolar coupling (between nuclei no more than 5 Å apart through space). The type of magnetization transfer is determined by the particular type of pulse sequence used. In 2D COSY NMR experiments the cross-peaks result from scalar or J -coupling (Figure 2.6) (Derome, 1989; King & Kuchel, 1994). These cross-peaks can be used to identify different metabolites in biological samples with a much greater resolution than can be obtained from 1D spectra.

A1.5. Water suppression.

The concentration of pure water (55 M) is much greater than that of the metabolites of interest (in the mM range) that one is usually trying to detect using ^1H -NMR. This creates a significant problem as the extremely strong resonance from water protons would dominate

the $^1\text{H-NMR}$ spectrum if precautions were not taken to reduce its intensity. This can be achieved in two ways: firstly, the use of low-power irradiation of the water resonance, and secondly, the replacement of $^1\text{H}_2\text{O}$ with deuterated water, $^2\text{H}_2\text{O}$ (D_2O). The water resonance can be irradiated ("saturated") during the relaxation delay prior to the first pulse in the 2D NMR experiment. It is important that the rf pulse for the water saturation does not affect other resonances that are located close to the water peak (Kuchel, 1989). An rf field strength should be chosen that reduces but does not completely eliminate the water resonance.

particles in fluid in a single stream past a laser beam of light. The chemical and physical properties are monitored by their optical properties. Flow cytometry has a wide range of uses which can be applied to the analysis and preparation of cells. Usually the properties of 10,000 cells per sample are counted, which is much more efficient than microscopy.

Flow cytometry enables the quantitation of cell fluorescence intensity from cells stained with fluorescent dyes or fluorescently labelled antibodies. Fluorescence intensity can be quantitated for each cell and the intensity of the fluorescence distribution in particular populations of cells in the sample can be determined. Biochemical properties such as DNA and RNA content can be monitored by direct labelling of nucleic acids with Hoechst 33342 (DNA) and pyronin Y (RNA), thus facilitating cell cycle analysis (Shapiro, 1993). Cell surface antigens, such as receptors and other ligands, can be detected using fluorescently labelled antibodies against the antigen (Reinherz *et al.*, 1979). In this case, fluorochromes such as fluorescein isothiocyanate (FITC) are covalently attached to the antibody (see Chapter 2).

On the basis of light scattering, physical properties such as cellular complexity (the number of organelles) and cell size can also be measured (Shapiro, 1995). For example, the flow cytometer can be used to identify monocytes, lymphocytes, and neutrophils in a mixed population on the basis of complexity and size. The cells can then be sorted by the flow cytometer on this basis (Salzman *et al.*, 1975). Light scatter and fluorescence emission from a fluorochrome can be measured simultaneously.

Appendix 2.

The theory of flow cytometry.

A2.1. Introduction.

Cytometry is the measurement of a range of chemical or physical characteristics of cells or subcellular particles. Flow cytometry measures cellular parameters by passing the cells or particles in fluid in a single stream past a laser beam of light. The chemical and physical properties are monitored by their optical properties. Flow cytometry has a wide range of uses which can be applied to the analysis and preparation of cells. Usually the properties of 10,000 cells per sample are counted, which is much more efficient than microscopy.

Flow cytometry enables the quantitation of cell fluorescence intensity from cells stained with fluorescent dyes or fluorescently labelled antibodies. Fluorescence intensity can be quantitated for each cell and the intensity of the fluorescence distribution in particular populations of cells in the sample can be determined. Biochemical properties such as DNA and RNA content can be monitored by direct labelling of nucleic acids with Hoechst 33342 (DNA) and pyronin Y (RNA), thus facilitating cell cycle analysis (Shapiro, 1981). Cell surface antigens, such as receptors and other ligands, can be detected using fluorescently labelled antibodies against the antigen (Reinherz *et al.*, 1979). In this case, fluorochromes such as fluorescein isothiocyanate (FITC) are covalently attached to the antibody (see Chapter 2).

On the basis of light scattering, physical properties such as cellular complexity (the number of organelles) and cell size can also be measured (Shapiro, 1995). For example, the flow cytometer can be used to identify monocytes, lymphocytes, and neutrophils in a mixed population on the basis of complexity and size. The cells can then be sorted by the flow cytometer on this basis (Salzman *et al.*, 1975). Light scatter and fluorescence emission from a fluorochrome can be measured simultaneously.

Other applications of the flow cytometer include the detection of lipids associated with cells (Greenspan *et al.*, 1985), changes in intracellular pH (Gerson *et al.*, 1982) and measurement of Ca²⁺ fluxes (Tsien *et al.*, 1972).

A2.2. The flow cytometer.

The basic features of the flow cytometer are shown in Figure A2.1. Essentially, individual cells in buffer are passed through the incident laser beam (argon-ion laser usually set at 488 nm). Light scatter and fluorescence emission can be measured simultaneously using an array of lenses designed to allow passage of both scattered incident light and emitted fluorescence, which are of different wavelengths. The scattered incident light and emitted fluorescence light are collected by a series of band-pass filters and mirrors and detected by photomultipliers.

A2.3. Light scatter.

The light can then be scattered in different ways depending upon the inherent properties of the cell. Forward scatter (FSC) and 90° side scatter (SSC) can be analysed (Hudson & Hay, 1989; Shapiro, 1995). These optical features can be used to identify individual cells in mixed populations of cells.

Forward-angle light scatter (FSC).

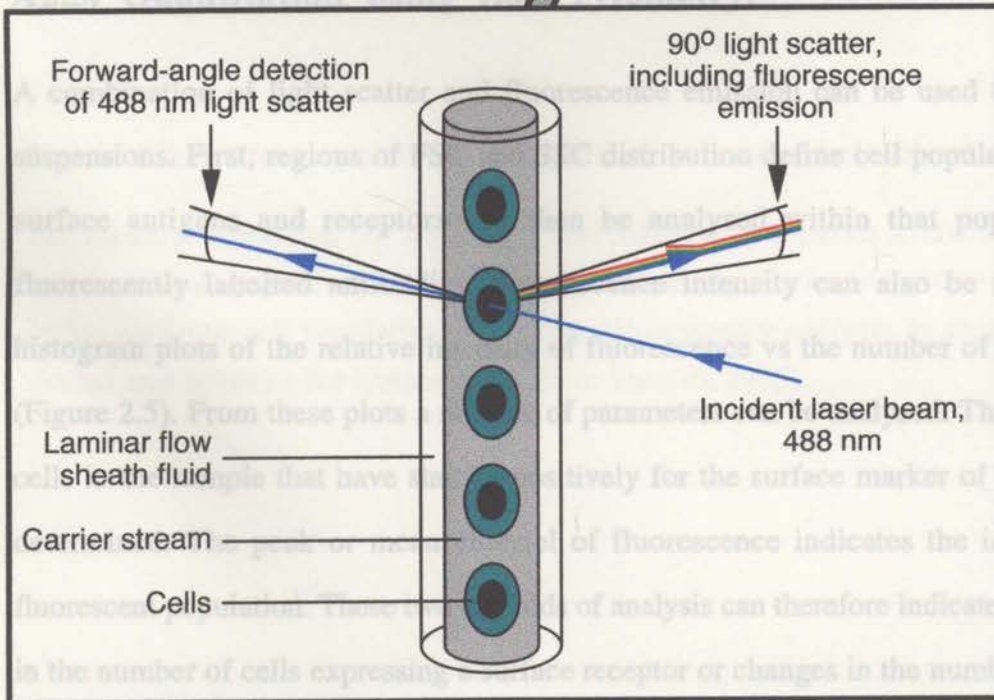
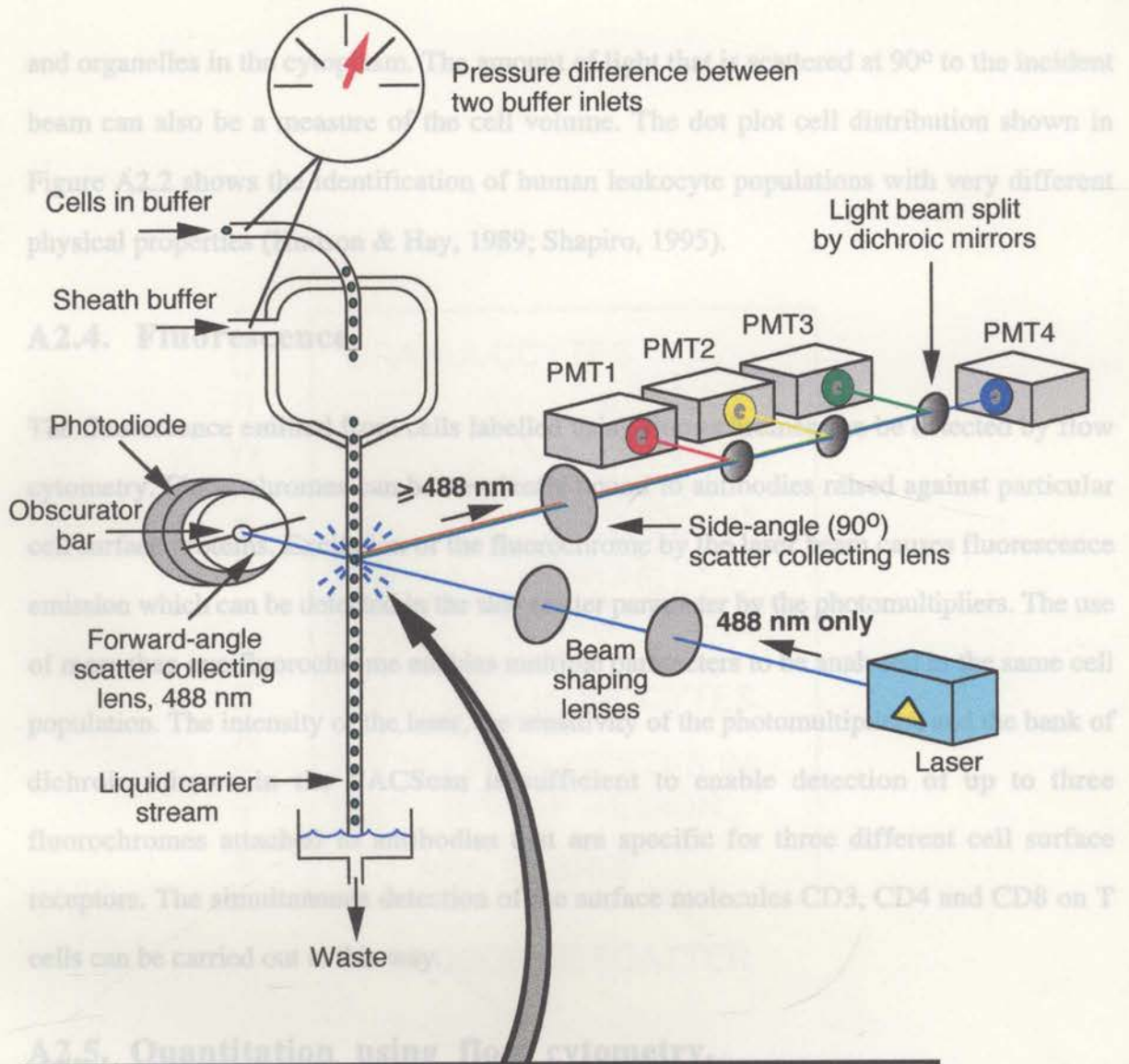
In a spherical cell the amount of fluorescence in FSC is proportional to the cell volume. FSC can therefore be used to determine cell size. Even the cells that are not fluorescently labelled can be sorted on the basis of size and this parameter can be used to count the number of events or cells to be collected in the sample. FSC can also be used to determine cell viability. Viable cells generate more FSC than dead cells.

Ninety-degree side scatter (SSC).

SSC is affected by cellular complexity. The cellular organelles that can contribute to these inherent optical properties include cell surface topographical features, such as microvilli or membrane blebs, the nucleus:cytoplasm ratio and the presence of intracellular granules

Figure A2.1. The flow cytometer.

Cells suspended in a dilute solution are taken up into a nozzle through which a stream of sheath fluid flows (isotonic solution). The cell and the sheath buffer inlets are at different pressures and the buffer streams emerging from the nozzle run at different rates and therefore do not mix. This confines the cells to the centre of the stream in single file. An argon-ion laser light passes through a set of lenses to produce a beam which is aimed at the cell buffer stream. The optical system is arranged and aligned so that only after the laser light hits a cell is it recorded by the instrument, because the obscurator bar prevents any light which has *not* passed through a cell from being collected. The cell acts as a spherical lens dispersing light in all directions. The light is detected by forward angle light scatter and 90° light scatter detectors. If the cell is labelled with one or more fluorochromes, the emitted light is resolved from in the side scatter parameter from the light of excitation (the emitted fluorescent light will have a longer wavelength) by a series of dichroic mirrors and filters which direct the light to a set of photomultipliers, PMT1, PMT2, and PMT3. Light scatter and fluorescence can be measured and stored simultaneously. The integral of the electrical impulse generated can be stored or analysed by the attached computer (adapted from Hudson & Hay, 1989; Shapiro, 1995).



and organelles in the cytoplasm. The amount of light that is scattered at 90° to the incident beam can also be a measure of the cell volume. The dot plot cell distribution shown in Figure A2.2 shows the identification of human leukocyte populations with very different physical properties (Hudson & Hay, 1989; Shapiro, 1995).

A2.4. Fluorescence.

The fluorescence emitted from cells labelled using fluorochromes can be detected by flow cytometry. Fluorochromes can be covalently bound to antibodies raised against particular cell surface proteins. Excitation of the fluorochrome by the laser beam causes fluorescence emission which can be detected in the side scatter parameter by the photomultipliers. The use of more than one fluorochrome enables multiple parameters to be analysed in the same cell population. The intensity of the laser, the sensitivity of the photomultipliers, and the bank of dichroic mirrors in the FACScan is sufficient to enable detection of up to three fluorochromes attached to antibodies that are specific for three different cell surface receptors. The simultaneous detection of the surface molecules CD3, CD4 and CD8 on T cells can be carried out in this way.

A2.5. Quantitation using flow cytometry.

A combination of light scatter and fluorescence emission can be used to analyse cell suspensions. First, regions of FSC and SSC distribution define cell populations. The cell surface antigens and receptors can then be analysed within that population using fluorescently labelled antibodies. Fluorescence intensity can also be represented as histogram plots of the relative intensity of fluorescence vs the number of cells or events (Figure 2.5). From these plots a number of parameters can be analysed. The proportion of cells in the sample that have stained positively for the surface marker of interest can be determined. The peak or mean channel of fluorescence indicates the intensity of the fluorescent population. These two methods of analysis can therefore indicate either changes in the number of cells expressing a surface receptor or changes in the number of receptors expressed per cell (Hudson & Hay, 1989; Shapiro, 1995).

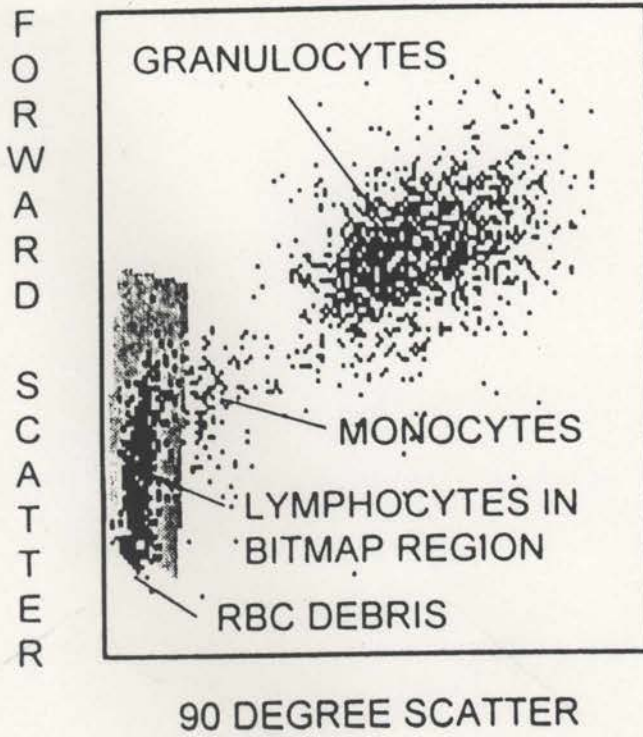


Figure A2.2. Flow cytometry dot plot of a lysed whole blood sample.

The forward scatter and 90° scatter (or side scatter) can separate a mixed population of leukocytes based on size and intracellular complexity. Gates or regions can be used to define particular cell populations for immunofluorescence analysis, as shown by the grey shaded area selecting for lymphocytes (from Shapiro, 1995).